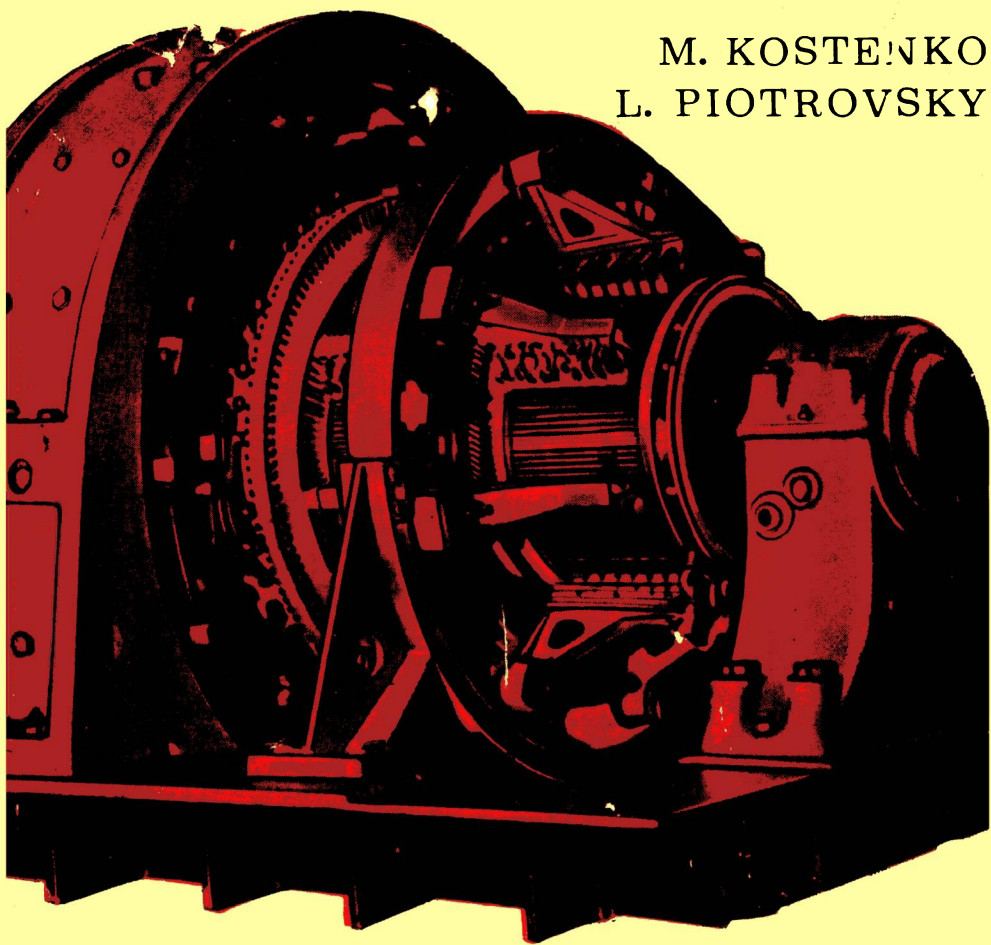


M. KOSTENKO
L. PIOTROVSKY



ELECTRICAL MACHINES

VOLUME I

MIR PUBLISHERS

M.KOSTENKO and L.PIOTROVSKY

ELECTRICAL MACHINES

IN TWO PARTS

PART ONE

FOREIGN LANGUAGES PUBLISHING HOUSE
Moscow

TRANSLATED FROM THE RUSSIAN
BY ADOLPH E. TCHERNUKHIN, EL. ENG.

PREFACE

This text-book is the result of an extensive programme in which the Department of Electrical Machines of the Kalinin Polytechnical Institute in Leningrad has been engaged for some years, namely, the compiling of text-books and manuals for power engineering schools.

In 1944, the first part of the book *Electrical Machines* by Professor M. P. Kostenko was published. It was followed in 1949 by a second, so-called special, part. Also in 1949, there was published and in 1950 reprinted, the text-book *Electrical Machines* written for higher schools by Professor L. M. Piotrovsky. To facilitate training of the students, the authors have found it desirable to publish a joint text-book on the subject.

In this text-book the subject-matter covered is arranged in the order the lecture course is treated at the Electromechanical Faculty of the Institute, viz.: direct current commutator machines, transformers, general problems of alternating current machine theory, synchronous machines, induction machines and alternating current commutator machines. The main part is prefaced by an introduction in which the major stages of development of the electrical machine-industry are discussed and information of a general nature is given.

From the standpoint of practical convenience this text-book is published in two parts. The first part covers direct current machines and transformers, the second part is devoted entirely to alternating current machines.

Though the first part in the main was written by Professor L. M. Piotrovsky, and the second, by Academician M. P. Kostenko, there has been achieved, it is hoped, an overall unity of presentation.

Several of the sections have been revised both from the point of view of method and the subject proper, as, for example, the problems of sudden short circuits in synchronous machines, d. c. and a. c. machines windings, etc.

The fundamental units employed throughout the book belong to MKSA practical system of units. Since, however, this system has not yet universally been adopted by Soviet electrical machine-building works, some quantities as, for instance, flux density, flux, force, etc., are defined both in the MKSA system and the mixed system of units.

The authors

CONTENTS

Preface	3
Introduction	11
1-1. Principal Stages in Electrical Machine-Building Development . .	11
1-2. Development of Soviet Electrical Machine-Engineering	18
1-3. Basic Quantities and Systems of Units	20
1-4. Rationalisation of Electromagnetic Field Equations	21
1-5. Materials Used in Electrical Machine-Building	22

SECTION ONE

DIRECT CURRENT MACHINES

<i>Chapter One. The Fundamental Type of Direct Current Machine and Its Design Elements</i>	30
1-1. Brief Outline of Direct Current Machine Development	30
1-2. Fundamental Type of Direct Current Machine	31
1-3. Conversion of Alternating Current into Direct Current by Means of a Commutator	32
1-4. Main Structural Elements of a Direct Current Machine	37
1-5. Ratings	42
<i>Chapter Two. The D. C. Machine Magnetic Circuit on No-Load</i>	43
2-1. Introduction	43
2-2. Magnetic Circuit of a Direct Current Machine. Determination of Main M.M.F.	45
2-3. Air-Gap, Air-Gap Flux Density Distribution Curve	47
2-4. Reduction Method. The Calculated Pole Arc Value	49
2-5. Calculated Armature Length	50
2-6. M.M.F. of Air-Gap for a Smooth Armature	51
2-7. M.M.F. of Slotted Armature Gap	51
2-8. Air-Gap Data	53
2-9. M.M.F. of Tooth Section	53
2-10. M.M.F. of Armature Core Section	57
2-11. M.M.F. of Poles and Yoke	57
2-12. Magnetisation Curve	60
2-13. Numerical Example	61
<i>Chapter Three. Windings and E. M. F. of Direct Current Machine Armature</i>	64
3-1. Introduction	64
3-2. Classification of Armature Windings	64

3-3. Formulas for Assembling Ring-Type Armature Simple Windings and Their Fundamental Characteristics	65
3-4. Simple Lap Winding for Ring-Type Armature	67
3-5. Simple Wave Winding for a Ring Armature	78
3-6. E.M.F. of Ring Armature	81
3-7. Drum-Type Winding Assembling Principles	83
3-8. Features of Drum Armature Winding	85
3-9. Winding Pitches	89
3-10. Examples of Simple Lap Winding	91
3-11. Simple Wave Winding for a Drum Armature	101
3-12. Special Types of Wave Windings	104
3-13. Multiplex Lap Winding	106
3-14. Multiplex Wave Winding	111
3-15. Conditions for Armature Winding Symmetry	113
3-16. Equalisers	114
3-17. Special Armature Windings of the Composite Type	123
3-18. Comparison of Different Winding Characteristics	127
3-19. E.M.F. of Drum Armature Windings	128
Chapter Four. Armature Reaction	129
4-1. M.M.F. of Machine on Load	129
4-2. Armature Cross- and Direct-Axis M. M. F.	133
4-3. Armature Reaction in a Generator	135
4-4. Effect of Direct-Axis Armature Reaction on Machine E.M.F.	141
4-5. Armature Reaction in a Motor	142
Chapter Five. Commutation	143
5-1. Introduction. Standard Sparking Scale	143
5-2. Commutation Process	143
5-3. E.M.F. of Circuit Undergoing Commutation	146
5-4. Commutation Equation when $b_{br}=b_c$	146
5-5. Resistance Commutation	147
5-6. Commutation with E.M.F.s e_L and e_c Acting	149
5-7. Commutation when $b_{br}=b_c$, $2r_w+r_c=0$ and $e_L+e_c \neq 0$	150
5-8. Determination of E.M.F. of Self-Induction e_L for $b_{br}=b_c$	152
5-9. The Coil Section Commutating E.M.F. e_c	155
5-10. Commutation when Brush Width Is $b_{br}>b_c$	155
5-11. Commutation Armature Reaction	159
5-12. Electromagnetic Sources of Sparking	160
5-13. Potential Causes of Sparking	161
5-14. Mechanical Causes of Sparking	165
5-15. Contemporary Conceptions on Nature of Commutation Process	165
Chapter Six. Means of Improving Commutation and Methods of Its Investigation	168
6-1. Means for Mitigating Sparking of Electromagnetic Origin	168
6-2. Reduction of the Reactive E.M.F. e_r	169
6-3. Creation of a Commutating Field by Shifting the Brushes from Neutral	169
6-4. Creation of a Commutating Field by Means of Commutating Poles	171
6-5. Effect of Commutating Poles on the Main Field	175
6-6. Effect of Commutating Poles Saturation on Commutation	175
6-7. Compensation Winding	177
6-8. Additional Methods of Protection Against Flashovers	180

6-9. Brushes and Their Characteristics	181
6-10. The Nature of Brush Contact	186
6-11. Experimental Methods of Analysis and Adjustment of Commutation	187

Chapter Seven. Energy Losses and Efficiency of Electrical Machines 192

7-1. Preliminary	192
7-2. Classification of Losses	193
7-3. Mechanical Losses	194
7-4. Principal Core Losses	197
7-5. Principal Copper Losses	201
7-6. Additional Losses	203
7-7. Total Losses in D. C. Machines and Their Efficiency	204

Chapter Eight. Direct Current Generators 205

8-1. Preliminary	205
8-2. Classification of D. C. Generators According to Method of Field Excitation	206
8-3. The Energy Conversion Process in the D. C. Generator	207
8-4. Equation of Generator E.M.F. at $n=\text{const}$	208
8-5. The Electromagnetic Torque of the Generator	208
8-6. Generator Torque Equation	211
8-7. The Fundamental Characteristics of a D. C. Generator	211
8-8. Characteristics of the Separately Excited Generator	212
8-9. Characteristic Curves of Shunt Generators	222
8-10. The Series Generator	227
8-11. Compound Generator	228

Chapter Nine. Parallel Operation of D. C. Generators 231

9-1. General Considerations	231
9-2. Parallel Operation of Shunt Generators	232
9-3. Parallel Operation of Compound Generators	235

Chapter Ten. Direct Current Motors 237

10-1. Reversibility Principle of Electrical Machines	237
10-2. Classification of D. C. Motors	238
10-3. The Energy Process and Energy Diagram of D. C. Motors	239
10-4. Equation for Motor E. M. F.	239
10-5. Motor Torque Equation	241
10-6. Motor Characteristics	243
10-7. Methods of Starting D. C. Motors	244
10-8. Non-Rheostatic Start of Motor	244
10-9. Rheostatic Starting Method. Starting Rheostats	246
10-10. Starting Motors with the Help of Special Units	249
10-11. Motor Performance Characteristics	249
10-12. Mechanical Characteristics of D. C. Motors: $n=f(M)$	256
10-13. Braking Characteristics of D. C. Motors	260
10-14. Speed Control Characteristics of D. C. Motors	264
10-15. Motor Speed Regulation by a Rheostat in the Armature Circuit	265
10-16. Motor Speed Regulation by Variable Excitation	267
10-17. Motor Speed Regulation by Varying the Voltage Applied to the Circuit	273

Chapter Eleven. Fundamental and Special Types of D. C. Machines and Their Future Development	276
11-1. Preliminary	276
11-2. Fundamental Types of D. C. Machines	276
11-3. Special Types of D. C. Machines	282

SECTION TWO

TRANSFORMERS

Chapter Twelve. Fundamentals and Construction Elements of Transformers	297
12-1. Progress in Transformer Engineering	297
12-2. Fundamental Definitions	299
12-3. Basic Types of Transformers	300
12-4. Transformer Ratings	301
12-5. Basic Construction Elements of Transformers	302
Chapter Thirteen. Physical Conditions of Transformer Operation	315
13-1. Principle of Operation	315
13-2. M. M. F. and E. M. F. Transformer Equations	316
13-3. Transformation Ratio of Transformer E. M. F.	318
13-4. M. M. F. and E. M. F. Equations for Sine-Wave Variation of Voltages and Currents	319
13-5. The Reduced Transformer	320
13-6. M. M. F. and E. M. F. Equations for the Reduced Transformer	322
13-7. Transformer Equivalent Circuit	323
Chapter Fourteen. Transformer on No-Load	326
14-1. Preliminary	326
14-2. No-Load Operation of a Single-Phase Transformer	326
14-3. No-Load Operation of an Elementary Transformer	327
14-4. No-Load Operation of a Commercial Single-Phase Transformer	332
14-5. No-Load Transformer Losses	334
14-6. The Effect of Voltage-Curve Shape on Steel Losses	336
14-7. No-Load Transformer Equivalent Circuit	337
14-8. No-Load Transformer Test	337
Chapter Fifteen. Classification of Magnetic Systems and Winding Connections for Three-Phase Transformers. E.M.F.s of Three-Phase Transformers	339
15-1. Classification of Three-Phase Transformer Magnetic Systems	339
15-2. Methods of Connecting Three-Phase Transformer Windings	341
15-3. Three-Phase Winding E.M.F.s	342
15-4. Star-Connected Three-Phase Winding	343
15-5. Delta-Connected Three-Phase Winding	345
15-6. Zigzag-Connected Three-Phase Winding	347
15-7. Standard Methods of Connecting Three-Phase Transformer Windings	347
15-8. Winding Diagrams and Connection Groups	348
15-9. Application of Various Winding Connection Methods	353
Chapter Sixteen. No-Load Operation of Three-Phase Transformer	354
16-1. Transformer on No-Load with Y/Y_0 -12 Winding Connection	354
16-2. Transformer on No-Load with Δ/Y Winding Connection	358
16-3. Transformer on No-Load with Y/Δ Winding Connection	358

16-4. Y_0/Y_0 -12 Connection with a Tertiary Winding	359
16-5. Characteristic Data for No-Load Transformer Operation	359
Chapter Seventeen. Short-Circuit Operation of Transformers. Magnetic Leakage in Transformers	360
17-1. Preliminary	360
17-2. Impedance Voltage	361
17-3. Physical Conditions of Transformer Operation at Short Circuit	361
17-4. Short-Circuit Diagram of Reduced Transformer	363
17-5. Equivalent Circuit of Transformer on Short Circuit	364
17-6. Transformer Short-Circuit Triangle	364
17-7. Short-Circuit Losses	365
17-8. Determination of Short-Circuit Parameters	367
17-9. Short Circuit of Three-Phase Transformers	368
17-10. Leakage in Transformers with Concentric and Sandwich Windings	368
Chapter Eighteen. Transformers on Load	375
18-1. Preliminary	375
18-2. Elementary Transformer on Load	375
18-3. Real Transformer on Load	376
18-4. Vector Diagrams of the Equivalent Transformer	378
18-5. Simplified Vector Diagrams of the Transformer	378
18-6. The Relationship U_2-f ($\cos\phi_2$)	380
18-7. Determination of Secondary Voltage Variation ΔU	381
18-8. Transformer External Characteristics	383
18-9. Transformer Efficiency	383
18-10. Numerical Example	386
Chapter Nineteen. Unbalanced Conditions in Three-Phase Transformers.	386
19-1. Preliminary	386
19-2. Symmetrical Component Analysis	387
19-3. Assumptions Used for Unbalanced Short-Circuit Analysis	389
19-4. Single-Phase Short Circuit of Transformer with Y/Y_0 Connected Windings	389
19-5. Diagram of Single-Phase Short Circuit of Transformer with Y/Y_0 Connected Windings	394
19-6. Determination of Zero-Sequence Resistance	395
19-7. Unbalanced Loading of Transformer with Y/Y_0 Connected Windings	396
19-8. Single-Phase Short Circuit of Transformer with Δ/Y_0 Connected Windings	398
19-9. Two-Phase Short Circuit of Transformer with Y/Y Connected Windings	398
19-10. Unbalanced Loading of Transformer with Y/Y Connected Windings	400
19-11. Transformer Operation with Open-Delta Connection	401
Chapter Twenty. Parallel Operation of Transformers	404
20-1. Stipulations for Parallel Operation of Transformers	404
20-2. Parallel Operation of Transformers with Unequal Transformation Ratios	405
20-3. Parallel Operation of Transformers Belonging to Different Groups	410
20-4. Parallel Operation of Transformers with Unequal Impedance Voltages	410

Chapter Twenty-One. Transient Phenomena in Transformers	413
21-1. Classification of Transients	413
21-2. Overcurrents	414
21-3. Short-Circuit Thermal Phenomena	420
21-4. Mechanical Stresses Accompanying Sudden Short Circuits	420
21-5. Cause and Nature of Overvoltages in Transformers	423
21-6. Transformer Equivalent Circuit for Overvoltages	425
21-7. Initial Voltage Distribution Along Transformer Windings	427
21-8. Transfer Process and Final Voltage Distribution	430
21-9. Transformer Overvoltage Protection	433
 Chapter Twenty-Two. Special Types of Transformers	 437
22-1. General	437
22-2. Autotransformers	437
22-3. Three-Circuit Transformers	441
22-4. Transformers with Voltage Regulation Under Load	450
22-5. Transformers with Continuous Voltage Regulation	453
22-6. Transformers for Mercury Arc Rectifiers (Rectifier Transformers)	454
22-7. Test Transformers	463
22-8. Welding Transformers	466
22-9. Brief Information on Various Types of Transformers	467

INTRODUCTION

1-1. Principal Stages in Electrical Machine-Building Development

The most important of the laws of electromagnetism for electrical machine-building is the law of electromagnetic induction discovered by Michael Faraday in 1831. That this fundamental discovery met the needs of the times may be seen from the fact that already a year later, in 1832, an unknown inventor (known only as M. P.), the brothers Pixii and then in 1833 the physicist Richey suggested the first designs for rectified-current electrical generators, based on the laws of electromagnetic induction.

The first electric motor with continuous armature rotation was proposed in 1834 by the Russian scientist and member of the Petersburg Academy of Sciences B. S. Jacobi, its rating being subsequently brought up to 500 watts. In 1838 this Jacobi motor was installed on a launch and tested under practical electric haulage conditions on the river. The source of power was a galvanic battery mounted on the launch; the motor was fitted with a device which was a prototype of the modern commutator. The launch travelled not only down the Neva River but also against the current and strong head wind. This was the first electrically powered ship in the world, and though at that time further development was not encouraged, it proved the possibility of converting electrical energy into mechanical energy. It brought up many new problems including one of major importance, viz.: of substituting the heavy inefficient and unreliable galvanic battery by an electrical generator of the electromagnetic type.

After a series of developments and refinements (for more details see § 1-1) the direct-current machine had already by the middle eighties attained all the fundamental features of modern

design. For further particulars on the development of the direct current machine and some information on Soviet electrical machine-building see § 1-2.

As the use of electric energy increased and its field of utilization continuously expanded, the disadvantages of direct current energy distribution became more and more pronounced. Consequently, in the early 70s attempts were made to use electric energy in the form of alternating current. These attempts were strongly opposed by specialists; this, of course, may be explained, to some extent, by the insufficient knowledge of alternating-current circuit phenomena. Thus, for instance, Edison, one of the greatest authorities of those times, stated that the laying of alternating current cables in the town street ducts was tantamount to laying dynamite mines under the roadway.

All the more remarkable then is the courageous initiative of the Russian scientist P. N. Yablochkov who in 1878 built the first commercial plant for feeding a new type of electric lamp invented by him and known as the "Yablochkov candle." For this power plant, Yablochkov developed together with the Gramme Engineering Works in France a synchronous generator, which was the prototype of modern synchronous alternators; and then, to improve the work of the installation, invented also a transformer which had an open magnetic circuit. Though the priority of this invention was disputed, the patents granted to Yablochkov in 1876 and 1877, the evidence in Fontaine's report on the illumination of the World Exhibition in Paris and the statement issued by the French Company of Electrical Illumination leave no doubt that Yablochkov is the inventor of the most important apparatus in the history of electrical engineering—the transformer—and was the first engineer to use it in a commercial plant.

The valuable properties of the transformer were so obvious, that alternating current lighting plants incorporating transformers and also the transformer proper very rapidly attained wide development. Already in 1882, at the All-Russian Industrial Exhibition, I. F. Usagin, using the Yablochkov transformers, demonstrated that not only could alternating current energy be used for lighting purposes but that it was possible to convert it into mechanical and thermal energy. This new issue gave great impetus to further development of alternating current engineering.

To improve the performance of the transformer, the engineers Deri, Blathy and Zipernowski (of Ganz Ltd. in Budapest) developed and in 1885 patented single-phase dry-type transformers with closed cores made up of insulated wires. After this the further development of transformer construction proceeded at a

rapid pace. In 1891, the Russian engineer M. O. Dolivo-Dobrovolsky working on the problems of the three-phase current system, which he had at that time developed, suggested a three-phase transformer construction with the nowadays conventional arrangement of the transformer core legs in one plane.

In the same year Brown, the manager of the Oerlikon Works in Switzerland, constructed the first 30 kV oil-immersed transformer, which was a rather high voltage for those days. Since then, practically every electric power installation uses only oil-immersed transformers.

Between 1875 and 1890, single-phase alternating current engineering reached a very developed state. However its further evolution was hindered by the absence of a single-phase motor with the necessary performance characteristics. A solution was found along entirely new lines by M. O. Dolivo-Dobrovolsky, who by inventing the three-phase current system shaped the entire future development of all branches of electrical engineering.

In electrical machine-building an outstanding service rendered by Dolivo-Dobrovolsky was the invention of a commercial-type three-phase induction motor, employing the principle of the rotary magnetic field, created by a multiphase current system. The magnetic rotating field principle was first discovered in 1885 by the Italian physicist G. Ferraris. Ferraris in Italy, and later Tesla in 1886 in the U.S.A., constructed their first models of two-phase induction motors. However, owing to many flaws in the design they were of no practical use. Dolivo-Dobrovolsky was the first to develop and in 1889 to manufacture on a commercial scale induction motors both with phase-wound and squirrel-cage rotors of such design that the fundamental features are retained in all modern induction machines.

Dolivo-Dobrovolsky's three-phase system and his induction motor gave a tremendous impetus to the development of electric power engineering. The first three-phase current installation (which included a 200 kW electric plant erected at Lauffen, 170 km from the exhibition site, a three-phase 15 kV transmission line and two step-down substations at the exhibition site, one of them feeding a three-phase induction motor of approximately 75 kW) was demonstrated in 1891 at the Frankfort-on-the-Maine International Electrical Engineering Exhibition.

The tests on this installation proved not only the applicability of the three-phase current system for bulk transmission of electric energy with a high efficiency, but also the excellent

performance of the three-phase induction motor. The advantages of the three-phase current system proved so conclusive, that after overcoming the brief resistance of the adherents of direct and single-phase current it had by the beginning of the current century attained universal acknowledgement, and began to develop rapidly.

Since then, the general development of electrical power engineering was of a composite nature, this being due, mainly, to wide electrification of various industrial enterprises and many branches of national economy (illumination, transport, metallurgy, metal-working, coal industry, etc.). This stimulated an increase in the output of central power stations and individual generator units, in power lines and voltages of electric-transmission and distribution systems. Under these conditions further development of electrical machine-building became of prime importance.

More detailed information on the development of separate types of machines is given in the appropriate sections of the text-book; here we mention only the major stages of electrical machine and transformer development.

Of tremendous importance for electrical machine-building as a whole was the invention, at the beginning of the current century, of the alloyed electrical sheet steel, i. e. steel containing a certain percentage of silicon. This steel has much better magnetic properties than ordinary steel. Its application has allowed a considerable reduction in the overall dimensions and weight of electrical machines with an accompanying increase of efficiencies (see efficiency data for transformers in § 12-1). Recently, further development of electrical machine-building was made possible, especially for transformers, by the invention of cold-rolled grain-oriented sheet steel, which, compared with conventional hot-rolled electrical sheet, possesses much better magnetic properties in the direction of roll.

In power generation by means of three-phase synchronous alternators, a new era began during the first decade of the century as a result of technical development of steam turbines with speeds greatly exceeding those of the steam machines used hitherto. In accordance with this new trend the efforts of electrical machine-building works were directed to making so-called *turbogenerators*, i.e., generators designed for direct coupling to the steam turbine. These efforts were crowned by success: by 1920 a 25,000 kVA turbogenerator for 3,000 r.p.m. and a 60,000 kVA turbogenerator for 1,000 r.p.m. were already constructed. Later came air-cooled steam turbogenerators for outputs of 100,000 kW at

3,000 r.p.m. and 60,000 kW at 3,600 r.p.m. which is practically the limit for air-cooled machines.

Subsequent development of steam turbogenerator design largely depended on the utilisation of hydrogen as a cooling medium. Hydrogen cooling was first applied in 1928 for cooling synchronous condensers. In 1937 its application was extended to turbogenerators. With this new system of cooling it became possible to build turbogenerators for outputs of 150,000 kW at 3,000 r.p.m. and 200,000 kW at 3,600 r.p.m. Hydrogen cooling of the hollow rotor windings and also gas or liquid cooling of the stator are among the very recent cooling methods used. These methods are so effective that turbogenerators are now being constructed with an output of 500,000 kW and there are designs for 800,000 kW and larger units.

Parallel with new steam turbogenerator development, *hydro-generators* were also developed, though of smaller speed than the steam turbogenerators, but of much greater size and weight (see Part II). For the Lenin Hydroelectric Plant (near Kuibyshev) the Leningrad Elektrosila Works has manufactured hydrogenerators of 123,500 kVA output at 68.2 r.p.m. with diameters exceeding 18 m and a total weight of 1,650 tons. The Angara Hydroelectric Plant is to use hydrogenerators of 250,000 to 300,000 kVA output.

The development of new transformers was due in particular to the rapid growth of central power plant capacities and to the larger units employed, and also to longer transmission lines and higher voltages (see § 12-1). Among the problems that have arisen in connection with the above-mentioned factors, of tremendous importance was the problem of transformer overvoltage protection. Work in this field brought about the development of the *non-resonating* or *surge-proof* transformer first designed in 1929 with complete capacitor protection and then later in 1937 at the Moscow Transformer Works with partial capacitor protection. More recently, wide use has been made of the so-called foliated winding for the highest voltage, which offers the same overvoltage protection as the capacitor protection.

Simultaneously with the creation of the power transformer for electrical systems, work was in progress on the development of many types of special transformers, some of the most important of which are described in Chapter 22.

In the field of utilisation of electric energy the major role is played by the electric motor. The last decade of the past century saw widespread industrial use of the three-phase induction motor. But along with very valuable advantages these motors showed some inherent disadvantages, among the most important of which

are: a) worse, when compared with direct current motors, regulation characteristics, especially for drives with wide-range speed regulation, b) decrease in circuit power factor ($\cos \varphi$), as the motor magnetising current necessary for the creation of the revolving magnetic field lags in phase on the mains voltage almost by 90° .

In the period from 1900 to 1915 of prime importance was the first of the above-mentioned disadvantages. The steps taken by the electric machine industry to cope with this problem was the development of: a) alternating current commutator motors, b) cascade control arrangements of induction machines and c) converter units for supplying power to direct current motors with a wide variation in speed.

The basic idea of the a.c. commutator motors—single-phase and three-phase—was that they should be the synthesis of an asynchronous induction machine and a d.c. machine. Special attention was paid to developing a single-phase series commutator motor for single-phase electric traction on trunk railways. Since 1904 such railways were constructed in Germany and other European countries with a reduced frequency of $16\frac{2}{3}$ c.p.s. and 25 c.p.s. in the U.S.A.

Recently the Oerlikon Works in Switzerland in collaboration with French engineers have developed a single-phase series motor to be energised from the commercial 50 c.p.s. supply network, thus dispensing with special converting plants for reducing the frequency.

This problem is of prime importance to the U.S.S.R., as, in accordance with the general plan of railway electrification, during the next 15 to 20 years a total of 40,000 kilometres of railways is to be electrified.

During the period from 1900 to 1915 various types of series and shunt commutator motors were developed for small and average capacity stationary drive installations with speed regulation. These included the most important of them all, the Schrage-Richter shunt-wound three-phase motor invented in 1914 for regulating the speed in the range of 1 : 3. Unfortunately, the alternating current commutator machine has also a number of deficiencies, mainly due to much higher cost compared with the conventional induction motor. Nowadays this type of machine is used mainly for special installations.

For large-capacity stationary installations with a relatively narrow range of adjustable speed (1 : 1.5 to 1 : 1.8) various cascade connected induction motors were developed. These include, first of all, the Kraemer (1900) and Scherbius (1910) systems (see

Part II) which later were developed with many modifications. Their practical applications, however, are comparatively limited due to the fact that modern industrial requirements are that the adjustable speeds of large-power installations should be in the range of 1 : 2 and more. In such plants, as also in smaller installations but where a very wide range of speed control (up to 1 : 40 = 1:50) is necessary, the Ward-Leonard system, both in its fundamental form and in its various modifications, has found wide application.

The next major step in the development of electrical machinery took place during World War I and after. The industrial needs of the war period necessitated a tremendous increase in the use of induction motors, the power of which greatly exceeded the actual rating of the installation drive. This brought about an abrupt drop in power factor ($\cos \varphi$) of the power supply system—in some cases down to 0.5 and even lower. To counteract it, besides the introduction of double rates for active and reactive power, various machines and apparatus were developed for $\cos \varphi$ compensation such as static condensers, phase compensators introduced into the rotor circuit of the low power factor induction motors, and also synchronous compensators. But of greatest interest was the development during the period 1915-16 of the synchronous motor.

The synchronous motor was, of course, known before but the starting process was so difficult that up to the year 1915 this type of motor was considered impractical. But at the same time it was known that a synchronous motor could operate not only at $\cos \varphi = 1$, but also with a so-called leading $\cos \varphi$, thus representing a capacitor in respect to the power supply source. The major improvements that were carried out concerned the improvement of the starting characteristics of the synchronous motor, naturally, without deteriorating the performance characteristics. This problem was first studied and solved in the U.S.A., and now the synchronous motor with an induction asynchronous start is widely used, in many types of non-adjustable drive it has successfully substituted the induction motor.

During the period mentioned and especially immediately following World War I, the driving shaft system in the metal-working industry was replaced, for reasons of greater efficiency, by the individual motor drive. This brought about the widespread introduction of the squirrel-cage induction motor in its two main modifications: the deep-slot motor and the double-cage motor, superseding the previously used phase-wound rotor motors.

Due to continuous growth of the capacity of electrical supply systems, both industrial and municipal, wide use was made of the across-the-line start squirrel-cage motors (viz., practically without starting devices). This application greatly increases the efficiency of the installation, especially of low-power units and facilitates their maintenance.

The more recent period of electrical machinery development is connected mainly with transition from the contactor-controlled electrical drives to the continuous-controlled units and introduction of automatic control into technological processes.

To make continuous drive control efficient by means of available electrical machines, at the end of the 30s of the current century, several types of rotating amplifiers (amplidynes) were developed, viz., machines with cross-field excitation (termed metadynes), with self-excitation, with regulating exciters, etc. These systems, especially the cross-field system, have found the widest application in modern industry.

Introduction of automation and remote control into industrial technology has necessitated the production of miniature electrical machines rated at several watts, the so-called fractional horsepower machines. The number of types of these machines is enormous and their design, testing and maintenance greatly differ from machines in conventional power systems. This field of electrical machine-building is at present rapidly developing.

I-2. Development of Soviet Electrical Machine-Engineering

The foreign ownership that prevailed in most of the important branches of the industry of pre-revolutionary Russia, including electrical machine-building, was not interested in the development of this branch of industry. The small electrical machine-building factories that existed prior to the Great October Revolution, viz., the Siemens-Schuckert and Duffon-Constantinovitch in Petersburg, the Volta in Revel, the General Electric Company in Riga and others, were more like custom-working assembly shops than industrial enterprises designated to carry out independent manufacturing. Such conditions did not facilitate creative effort, and new electrical engineering ideas did not find fertile soil in pre-revolutionary Russia, and Russian electrical engineers, notwithstanding their exceptional technical initiative, could not carry out developmental work on a broad footing.

The situation changed radically after the Great October Socialist Revolution. In a very short time large electrical machine-build-

ing works were created, which have been successfully coping with the most intricate and responsible tasks of the country's developing economy. Workers and specialists were trained and research was taken up by factory and high school laboratories and by the growing number of research institutions.

Soviet electrical machine-engineering development was part of the magnificent plan of electrification of the U.S.S.R. declared the order of the day by the Communist Party and the Government immediately after the termination of the Civil War. The main principles of Soviet electrical power progress are as follows:

- 1) Planned development integrated with the state plans for the development of the national economy;

- 2) Centralised production of electrical energy at large regional power plants;

- 3) Construction of electrical plants for the utilisation of local and low-grade fuels and also of large hydroelectric plants;

- 4) Construction and development of electric power grids interconnected by high voltage transmission systems. These were the basic principles of the historical GOELRO¹⁾ plan drawn up in 1920 at the initiative of V. I. Lenin and further developed and realised during the five-year plans prior to World War II.

According to the GOELRO plan, in a period of 10 to 15 years 30 electric plants were to be constructed with a total installed capacity of 1,700,000 kW. This plan called by V. I. Lenin the Second Programme of the Party was fundamental for the development of the planned economy of the country and the beginning of the great epoch of socialist reconstruction of the entire economy.

Under the leadership of the Communist Party the GOELRO plan was fulfilled ahead of schedule, by the 1st of January, 1931. Total capacity of all electric stations was increased threefold, and the energy produced, fourfold compared with 1913.

During that same period, up to the thirties, the Soviet electrical machine-building industry made its first steps in the field of large electrical machinery construction and mastered the production of many new types of machines or completely modernised the old ones left over from pre-revolutionary times.

Soviet electrical machine engineering continued to develop at a very rapid pace and already by the forties had reached the level of the foremost industrial countries of Europe and the U.S.A.

¹⁾ The State Plan for the Electrification of Russia.— *Ed.*

Data on the development of various types of machines are given in the various chapters of the book.

In connection with the tremendous influx of automatic and remote-control devices into industrial processes, there have been developed along with electrical machines for power installations, very important fractional horsepower and miniature types of control machines.

The successes gained by the Soviet electrical machine-industry are very great. But new immense tasks have been set by the Twenty-Second Congress of the Communist Party of the U.S.S.R. both for the development of new products and an increase in quality. New materials, new types of insulation and durable varnishes, etc., will facilitate many new important improvements in the design and the technology of electrical machines.

The high level attained by Soviet electrical machine-engineering, the large body of continuously growing qualified personnel and the strong ties that exist between industry and research, form a reliable source for new contributions of the electrical industry towards creation in the U.S.S.R. of the material basis of a communist society.

I-3. Basic Quantities and Systems of Units

For various engineering problems and, in particular, for practical design computations in electrical machine-engineering practice, the proper choice of basic quantities and the system of measurement units are of tremendous importance. The main requirement of a system of units is that it should be a *coherent* system in which all derivatives are determined by means of the basic units on the condition that parasitic multiples like 10^{-8} , 9.81, etc., should disappear from the equations.

Equations and formulas written in the coherent form, are applicable without introducing any additional factors for any logically developed system of units. If, in one of the formulas, the quantities were to be substituted by units of any other coherent system, the quantity received will also be in units of the accepted system. With this method of writing equations there is no need each time to stipulate the units of measurements, and this, in turn, eliminates difficulties when making computations.

To describe and study all electromagnetic phenomena it is necessary to introduce four fundamental quantities. In 1935 the International Electrotechnical Commission recommended that preparations be made for the transition to a system of units sug-

gested by Giorgi in which the basic units were: unit of length—the metre, unit of mass—the kilogram and unit of time—the second; as for the fourth unit, it was initially proposed to assume the value of magnetic permeability of free space μ_0 , for which the basic practical units, for example the volt, watt, henry, etc., hold (the MKS μ_0 system). This idea did not receive universal recognition and instead it was suggested that the fourth basic unit was to be the ampere. Thus the system became denoted MKSA.

When used for practical purposes, all the existing systems have some disadvantages. This has given rise to a wide use of mixed systems of units, thus leading to the appearance in the equations of parasitic factors valid only for the given *mixed* system. Thus, for example, the expression for e. m. f. constantly met with in technical literature is in the form of $e = Blv \cdot 10^{-8}$; to obtain by means of this formula the e. m. f. in conventional units, i. e., in volts, it is necessary to substitute flux density B in gauss, the length l —in cm and linear rotation speed v in cm/sec; if, then, the expression for the e. m. f. is written in the coherent form, i. e., $e = Blv$, the quantities B, l, v denoting the same units as before, the e. m. f. will be expressed as a nameless unit of the CGS μ_0 system.

To obtain the e. m. f. in volts by the MKSA system and without introducing any parasitic factors it is necessary to express B in webers per sq. cm, l in metres (m) and v in metres per second. Naturally, any system of units, as also the MKSA system, may use both fractions and multiple values of the basic units; thus, for example, current density may be expressed in the MKSA system as A/mm² in the same manner as in the system CGS μ_0 where the centimetre has been assumed as the unit of length. But in that case the formula expressing current density would contain the necessary conversion factor.

I-4. Rationalisation of Electromagnetic Field Equations

By rationalisation of the equations of the electromagnetic field is understood a reducing of the system of relationships (connecting electrical and magnetic quantities) to a symmetric form with simultaneous transfer of the factor 4π into expressions referring to cases of spherical symmetry. [B.5]

It must be noted that the rationalisation of equations is not connected with the adoption of any definite measurement units and

is carried out only by means of changing the concepts of certain of the electrical and magnetic quantities.

Table I-1 gives the relations existing between units of the MKSA and CGS μ_0 systems; the conversion factors in the last vertical column hold true regardless of whether the equations of the electromagnetic field are written in a rationalised or non-rationalised form. The dashes in the columns mean that the unit has no name.

In factory practice the mixed system of units is more favoured and the electromagnetic equations are written in the non-rationalised form.

In this case it must be borne in mind that the concepts of some quantities, specifically those of magnetic field intensity and magnetomotive force, change. The formulas for these quantities have the factor 4π ; the magnetomotive force, for example, is written in the rationalised system of units as $F=iw$, and in the non-rationalised system as $F=4\pi iw$.

On the other hand, the factor 4π appears also in the quantities of magnetic permeability and dielectric permeability; for example, in the rationalised CGS μ_0 system the magnetic permeability of free space $\mu_0=4\pi$, and in the non-rationalised system $\mu_0=1$; correspondingly, in the MKSA system $\mu_0=4\pi \cdot 10^{-7}$ and $\mu_0=10^{-7}$.

Thus, the factor 4π is removed from some expressions and introduced in others; therefore, in technical computations, the rationalisation of electromagnetic field equations does not appreciably simplify anything other than the writing of the principle, more frequently used equations.

From the 1st of January, 1957, the State Standard (ГОСТ) 8033-56 officially introduced the MKSA system as the basic system of units for measuring electrical and magnetic quantities in the U.S.S.R., the use of the CGS μ_0 system also being allowed.

I-5. Materials Used in Electrical Machine-Building

Materials used in electrical machine-engineering may be divided into the following three classes:

- A) Structural materials;
- B) Active materials—conducting and magnetic;
- C) Insulation materials.

A. Structural materials. Structural materials are those used for manufacturing machine components, the main function of which is the transmission and absorption of mechanical loads and stresses.

Table I-1

Relationship Between Units of MKSA and CGS μ , Systems

Quantity	Designation and abbreviation of units in MKSA system		Designation and abbreviation of units in CGS μ system		1 unit MKSA contains CGS μ units
Time	second	sec	second	sec	1
Frequency	cycles per sec, hertz	hz, c.p.s.	hertz, cycles per sec	hz, c.p.s.	1
Length	metre	m	centimetre	cm	10^2
Speed	metre per second	m/sec	centimetre per second	cm/sec	10^2
Acceleration	metre per second squared	m/sec ²	centimetre per second squared	cm/sec ²	10^2
Mass	kilogram	kg	gram	g	10^3
Mechanical force	newton	newton	dyne	dyne	10^5
Work and energy	joule	joule	erg	erg	10^7
Power	watt	W	erg/sec	erg/sec	10^7
Quantity of electricity	coulomb	C	—	—	10^{-1}
Electric current	ampere	A	—	—	10^{-1}
Magnetomotive force	ampere, ampere-turn	A, At	gilbert	gilbert	10^{-1}
Intensity of magnetic field	—	A/m	oersted	oersted	10^{-3}
Magnetic flux	weber	weber	maxwell, lines	maxwell	10^8
Magnetic flux density	—	weber/m ²	gauss	gauss	10^4
Electrical capacitance	farad	F	—	—	10^{-9}
Electrical resistance	ohm	ohm	—	—	10^9
Inductance	henry	H	—	—	10^9
Magnetic intensity	—	henry/m	—	—	10^7

Among the structural materials used in electrical machine-engineering are: 1) gray-iron castings (including special dynamo-frame castings), malleable and non-magnetic steel castings; 2) carbon steel and alloyed steel both for obtaining high mechanical strength, and non-magnetic properties; 3) non-ferrous metals and their alloys; 4) plastics.

The mechanical properties of materials are usually classified by the following data: 1) ultimate strength; 2) elastic limit; 3) yield point; 4) percentage elongation; 5) modulus of resilience.

When a machine is in operation the material used is subjected to many complex, periodically changing stresses, and the determination of necessary safety factors in respect to the proportional limit and yield point is a very responsible problem, especially for high-speed machines (steam turbogenerators), and for machines which during the period of their operation may be subjected to large increases in speed (hydrogenerators). The term "safety factor" usually refers to the ratio $k_s = \frac{f_m}{f}$ where f_m is the stress at which part of the mechanism is destroyed or so deformed that its further utilisation becomes impossible; f is the computed stress in the given part of the mechanism. As suggested by I. A. Oding, the k_s coefficient may be assumed for malleable steel from 1.0 to 1.35; for cast steel, 1.1-1.5; for cast iron, 1.0 to 2.3.

B. Active materials. Active materials are conductors and magnetic materials serving to create the most favourable conditions for the electromagnetic processes taking place in the machine.

1. *Conductor materials.* Of all conductor materials, the most important for electrical machine-engineering are copper and aluminium.

Copper has a very small specific resistance compared with other metals (excluding silver), resists corrosion better than steel, and is readily welded and fused.

Aluminium as a conductor is inferior to copper, but it is approximately 3.5 times lighter, this being its most important advantage. Lately aluminium has proved in many cases a successful substitute for copper.

The main properties of copper are: specific gravity $\gamma = 8.89$ kg per cu dm; resistivity at 15°C $\rho_{15} = 1/57 = 0.0175$ ohm sq. mm per m; average temperature coefficient of resistance in the 0 to 100°C range $\alpha = 0.00393 \frac{1}{\text{degree}}$; average thermal capacity in the 0 to 100°C range $C = 393$ watt sec per degree kg; thermal conductivity $\lambda = 3.85$ watts per cm degree.

The corresponding figures for aluminium are: $\gamma = 2.7$ kg per cu dm; $\rho_{15} = 0.0283$ ohm sq. mm per metre; $\alpha = 0.004 \frac{1}{\text{degree}}$; $C = 910$ watts sec per degree kg; $\lambda = (2 \text{ to } 2.1)$ watts per cm degree.

2. *Magnetic materials.* Of all existing magnetic materials the most important for electrical machine-building are silicon electrical steel of various grades, cast steel and cast iron.

The fundamental electromagnetic characteristics of these materials are the relation of the magnetic flux density B to the magnetic

field intensity or magnetising force, H , i. e., $B=f(H)$ and also the relation of losses in the steel p_s (also called iron losses) to flux density B and frequency f , i. e., $p_s=f(B, f)$.

Electrical sheet steel. The magnetic circuits of all modern electrical machines and transformers are made up of *alloyed* electrical steel, which contains a certain percentage (by weight) of silicon added to the iron; this increases the resistivity of the steel almost in direct proportion to the silicon content, thus decreasing eddy-current losses in the steel when the latter is subjected to an alternating magnetic field. An admixture of silicon above 1.8 per cent markedly increases the magnetic permeability of steel in weak magnetic fields, but somewhat decreases it in stronger fields. Silicon also abates ageing of steel (ageing is expressed by increased steel losses with time), but at the same time it impairs the mechanical properties of the alloy, in particular its machinability; if, for example, electrical steel sheet grades E11, E12 and E21, 0.5 mm thick must endure without damage not less than 10 bends, the E41 or E42 grades of the same thickness can withstand only one bend.

From the metal-working standpoint we nowadays discern: *hot-rolled* steel and *cold-rolled grain-oriented* steel. The latter, as compared with the former, has better magnetic properties (see Table I-2), but only when the magnetic flux is oriented in the direction of the rolling; in the direction across the rolling the magnetic properties of the cold-rolled steel are much worse; in other words, this steel possesses a sharply defined anisotropy. For this reason it is used chiefly in transformer manufacture, but lately it has found use also in electrical machines.

The silicon content and average specific gravity of steel conform to the following values of the State Standard (ГОСТ 802-54):

Steel alloy grade	Silicon content, %	Average specific gravity
Low alloy	from 0.8 to 1.8	7.8
Average alloy	1.8 to 2.8	7.75
Above-average alloy		
a) hot-rolled	2.8 to 4.0	7.65
b) cold-rolled	2.5 to 3.5	7.65
High alloy	4.0 to 4.8	7.55

The electrical machine industry uses mainly the following grades of steel: E11, E12, E21, E31, E310, E320, E330, E41, E42, E43.

Here the letter E designates electrical steel; the figures immediately following the letter denote the grade of silicon alloy: 1—denotes a low alloy, 2—average alloy, 3—above average alloy, 4—high alloy.

The second figure after the letter denotes the quality of the given grade in respect to specific losses in the steel, i. e., losses per 1 kg of steel at a given flux density and frequency. The figures in sequence (1, 2, 3) denote steel with normal, average and low specific losses at a frequency of 50 c/s (see Table I-2).

The third figure, 0, means that the steel is cold-rolled and grain-oriented. For example, E320 denotes above-average alloy, cold-rolled grain-oriented steel with less than the average specific losses at 50 c/s frequency.

The conventional dimensions of electrical sheet steel are (width by length): 750×1,500 mm and 1,000×2,000 mm; sheets of other dimensions are also being manufactured, for example, 600×1,200 mm, 210×1,500 mm, etc.

Table I-2

U.S.S.R. Standard Sheet Steel Grades

Sheet steel grade	Standard sheet thickness, mm	Flux density, weber/m ² for magnetising force, ampere-turns per cm					Specific losses, watts per kg		
		B ₁₀	B ₂₅	B ₅₀	B ₁₀₀	B ₃₀₀	p _{1.0/50}	p _{1.5/50}	p _{1.7/50}
		not less than					not over		
E11	1.0	—	1.50	1.62	1.75	1.97	5.80	13.4	—
E11	0.50	—	1.50	1.62	1.75	1.97	3.30	7.90	—
E12	0.50	—	1.49	1.61	1.74	1.96	2.80	6.80	—
E21	0.50	—	1.48	1.59	1.73	1.94	2.50	6.10	—
E31	0.50	—	1.46	1.57	1.70	1.90	2.00	4.50	—
E31	0.35	—	1.46	1.57	1.70	1.90	1.60	3.60	—
E41	0.50	1.30	1.45	1.56	1.68	1.88	1.60	3.60	—
E42	0.50	1.29	1.44	1.55	1.67	1.87	1.40	3.20	—
E43	0.50	1.28	1.43	1.54	1.66	1.87	1.25	2.90	—
E41	0.35	1.30	1.45	1.56	1.68	1.88	1.35	3.20	—
E42	0.35	1.29	1.44	1.55	1.67	1.87	1.20	2.80	—
E43	0.35	1.28	1.43	1.54	1.66	1.87	1.05	2.50	—
E310	0.50	1.57	1.70	1.80	1.90	1.98	1.25	2.80	3.80
E320	0.50	1.65	1.80	1.87	1.92	2.00	1.15	2.50	3.50
E330	0.50	1.70	1.85	1.90	1.95	2.00	1.05	2.30	3.20
E310	0.35	1.57	1.70	1.80	1.90	1.98	1.00	2.20	3.20
E320	0.35	1.65	1.80	1.87	1.92	2.00	0.90	1.90	2.90
E330	0.35	1.70	1.85	1.90	1.95	2.00	0.80	1.70	2.60

The standard sheet thicknesses are 0.5 and 0.35 mm. The E11 grade is also made 1 mm thick; for machines of higher frequencies sheets are made 0.2, 0.15 and 0.1 mm thick. Sheets 0.42 and 0.3 mm thick can be made by special order.

The flux density and specific steel losses for the grades mentioned are given in Table I-2. Here the subscripts of B show magnetic field intensity in ampere-turns per cm, which corresponds to the given value of flux density. The numerator of the fractional subscript of p denotes the flux density (in webers per sq m), the denominator, the frequency for which the specific loss was obtained. In Figs. I-1 and I-2 are given curves of B as a function of H [$B=f(H)$] for silicon steel, cast steel and cast iron.

B. Insulation materials. A great number of diverse insulation materials are used for the insulation of current-carrying parts in electrical machines. The fundamental requirement for all of these is high dielectric strength. But since the machine insulation comes into contact with heated parts and is subjected to the effect of voltage, atmospheric moisture, etc., besides dielectric strength it must also possess proper heat-proof, waterproof and corrosion-proof properties and be sufficiently durable mechanically. Table I-3 gives data characterising

Table I-3

Insulation Materials

Material	Specific weight	Dielectric strength	Rupturing strength, kV per cm	Permissible operating temperature, °C	Thermal conductivity, watt per cm 1°	Thermal capacity, watt sec per g 1°
Paper	0.7-1.0	2.5-3.0	80-90	90	0.0013	1.5
Presspahn	1.16	—	13.5	90	0.0017	—
Electrical cardboard	0.9-1.5	3.0	90-130	90	0.0014-0.0025	—
Varnished cloth	1.0	3.0-4.0	240-650	150	0.0025	—
Asbestos	2.5	—	20	450	0.0018	0.82
Mica (Muscovite)	2.8	6.7	1,000	500	0.0036	0.70
Micanite	2.0-2.4	—	30-36	—	0.0012-0.0015	0.92
Transformer oil	0.89	2.2	70-120	95	0.0012-0.0017	1.8
Porcelain	2.4	5.5-6.0	100-200	—	0.01	—
Air	0.00121	1.0	30	—	0.00025	1.5

the main insulation materials used in electrical machine-building.

The reliability of the machines in service to a great extent depends on varnish impregnation dipping and baking and also vac-

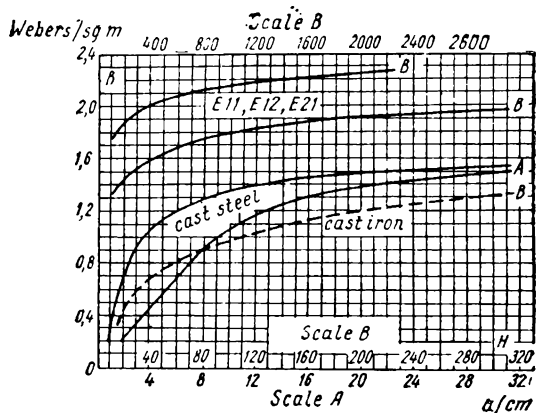


Fig. I-1. Magnetisation curves for electrical steel, cast-iron, cast steel

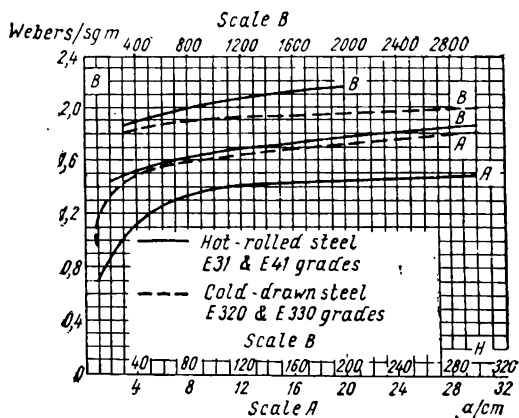


Fig. I-2. Magnetisation curves for electrical sheet steel

uum compound-filling both of the assembled winding and of the separate insulating materials.

The varnish and compounds commercially used for this purpose are of great variety. They should all conform to the following

basic requirements: 1) the varnish should have a sufficient dielectric strength; 2) it should properly impregnate the insulation materials; 3) the varnish film should be water- and corrosion-resistant; 4) the varnish should be heat-resistant and at normal service temperatures should not crack and lose its elasticity.

In a number of cases the varnish must also have good adhesive properties. To meet all the stipulated requirements is of course very difficult. The most important insulation materials for the windings used in electrical machine-engineering are: a) oil varnishes used chiefly as impregnating varnish; b) asphalt varnishes used as compounds for impregnating the windings under vacuum; c) varnishes with volatile solvents, used as surface lacquer or for impregnation—shellac, bakelite varnish, or heat-resistant silicon varnish, etc.

For insulation of transformer windings and for better cooling the so-called transformer oil is used. The main requirement for transformer oil is high dielectric strength, achieved by careful refining, purifying and dehydrating the oil. The properties of transformer oil are given in Table I-3 and also later in Part II. [Bibl. 1,2,3]

SECTION ONE
DIRECT CURRENT MACHINES

Chapter One

**THE FUNDAMENTAL TYPE OF DIRECT CURRENT
MACHINE AND ITS DESIGN ELEMENTS**

1-1. Brief Outline of Direct Current Machine Development

The history of electrical machine development, beginning with Faraday's discovery of the laws of electromagnetic induction in 1831 and up to the eighties of the last century is, in fact, the history of the development of the direct current machine. During this period it passed through four major stages of development, namely: 1) as a magnetoelectric machine with permanent magnets; 2) as an electromagnetic type of machine with separate or external excitation; 3) as an electromagnetic machine with self-excitation and an elementary type of armature, and 4) as a multipole type of machine with an improved armature.

The first stage of direct current machine development, covering the period from 1831 to 1851, is closely linked with the names of the Russian scientists Lentz and Jacobi whose contribution to science was already mentioned in the introduction. Gradually developing, the magnetoelectric machine attained the peak of its perfection in the designs of the French Alliance Company in 1855. It was much used in lighthouses, in illumination of buildings and for electrochemical plants.

The second and third stages of the d. c. machine development which embrace the period from 1851 to 1871 are characterised by the trend towards electromagnetic machines, first with external excitation and later with self-excitation. In 1860, Pacinotti (Italy) invented the slotted armature with a ring-type winding, which was the prototype of modern slotted armatures and slot windings. This invention of Pacinotti was of tremendous importance, but due to the very low general level of engineering development in Italy at that time, it could not find commercial use. Though the Pacinotti machine operated with external excitation, as early as 1867 the principle of self-excitation known for some time

previously was already practically developed and theoretically explained (Hiort 1851).

During the fourth stage of development, from 1871 to 1886, the d. c. machine had attained all the main features of modern design. There were developed and commercially manufactured the self-excitation machine of Gramme, who was the first to introduce commercially the Pacinotti ring-type armature; the nowadays standard type of drum armature (Hefner-Alteneck 1871); armatures and poles assembled of sheet steel (Edison 1880, Craig 1883); the fundamental modifications of various types of winding; the equaliser connections (Mordey 1883), commutating poles and compensation windings (Maître and Menges 1885).

Parallel with development in design of d. c. machines, intensive theoretical work and research were being carried out. Of especial importance was the fundamental research carried out by the Russian scientist G. Stoletov who investigated the magnetic properties of ferromagnetic materials; the results of his tests are basic for rational computation methods for the magnetic circuit of electrical machinery (1872). Soon after new theories were developed: the theory of armature windings, the theory of the commutation phenomena; also an analysis of transient phenomena was given; the computation of electrical machines was elaborated and greatly improved, etc.

1-2. Fundamental Type of Direct Current Machine

All previous considerations pertaining to the d. c. machine relate to the *commutator*-type machine. This, as a matter of fact, is an *alternating current* machine, but furnished with a special device—the commutator, which under certain specific conditions converts alternating current into direct current.

The commutator naturally greatly complicated the machine's performance and therefore at the beginning of the current century an attempt was made to develop the non-collector or homopolar direct current machine. Practice has since nevertheless proved, that the homopolar machine has no advantages compared with the commutator machine, moreover as during the first decade of the current century a direct current commutator machine was developed, which could meet the most stringent demands of practically any heavy-duty performance. Nowadays, therefore, the *fundamental d. c. machine is of the commutator type*, the homopolar machine being used only in certain special cases.

The field of industrial direct current usage being very wide, d. c. machines are produced both as generators and motors for a large

range of output, voltage, speed, etc. But closer acquaintance with various types of direct current machines reveals that the fundamental design elements and the processes taking place have much in common. This allows us to distinguish the main properties and types and then (at the end of this section) discuss some of the more special types of d. c. machines.

1-3. Conversion of Alternating Current into Direct Current by Means of a Commutator

To make clear a. c. to d. c. conversion in the commutator machine, consider first the operation of an elementary alternating current machine. Assume that it works as a generator, i. e., that the a. c. machine is driven by an engine and converts the applied mechanical energy into electrical energy.

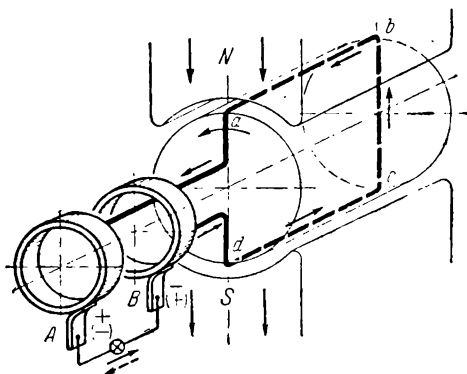


Fig. 1-1. A. c. machine operation diagram

Fig. 1-1 shows a machine the magnetic system of which comprises two poles, *N* and *S*, stationary in space. They create a magnetic flux of constant magnitude. According to the general rule, the magnetic lines in the space between the *N-S* poles are directed from the north pole *N* to the south pole *S*. Into this space an armature is inserted, with a single turn of wire *ab-cd* on its periphery in the diametrical plane; the ends of this turn are connected to two rings, fixed onto a shaft. The copper rings make contact with the two brushes *A-B* which are connected to an external circuit consisting of various power consumers.

Let us bring the armature into rotation with constant speed and in a given, say, anticlockwise, direction. As both conductors ab and cd are in similar conditions: one in respect to pole N , the other in respect to pole S , it is sufficient to consider the process of creation of electromotive force (e.m.f.) only in one conductor, for instance, in the conductor ab . Suppose that along the entire active length of a conductor, i. e., that part which cuts the lines of the magnetic field, the magnetic flux density is of constant value. If v is the rotation speed of the conductor in relation to the magnetic field then, according to Faraday's law of electromagnetic induction, the instantaneous e.m.f. induced in the conductor with the armature in motion is determined by the formula:

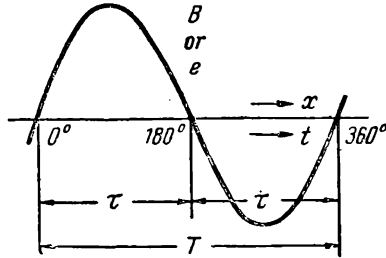


Fig. 1-2. Sine-wave of flux density or e.m.f.

$$e = Blv. \quad (1-1)$$

As l and v are given constants, formula (1-1) may be rewritten as:

$$e = \text{const} \times B. \quad (1-1a)$$

Thus, for given conditions, the change in e. m. f. induced in the conductor with time is completely defined by the magnetic flux density distribution under the pole.

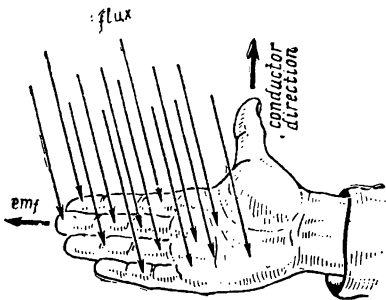


Fig. 1-3. Right-hand (palm) rule

Let us agree to call the line which passes through the armature centre, exactly midway between the poles N and S , the *geometrical* or *mechanical neutral*, and that part of the armature periphery τ corresponding to one pole, the *pole pitch*. The machine shown in Fig. 1-1 has two pole pitches corresponding to one pair of poles.

The distribution of magnetic flux density under the poles of a workable machine is of a complex nature (see § 2-3). But by using the Fourier method of analysis and after expanding the peri-

odic functions into a series of harmonic components it is possible to separate the first or fundamental harmonic. It may then be assumed that the magnetic flux density under the N and S poles is sine-wave distributed (Fig. 1-2). In this case the e. m. f. induced in the conductor varies with time also as a sine-wave function.

The direction of the induced e. m. f. may be easily determined by the so-called *right-hand palm rule*: If the right-hand palm is

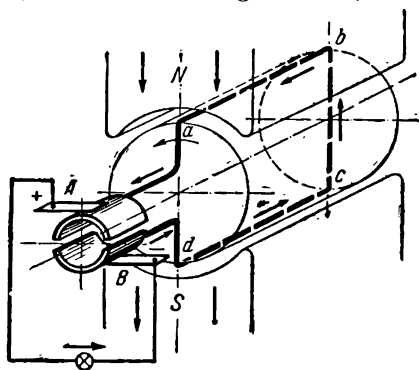


Fig. 1-4. D. c. machine operation diagram

arranged in the magnetic field so that, figuratively speaking, the lines of flux enter the palm and the thumb is set in the palm plane 90° to the other fingers and points in the direction of conductor motion (Fig. 1-3), the other fingers will indicate the direction of the e. m. f. induced in the conductor ¹.

Applying this rule to conductor ab in Fig. 1-1 it may be seen that when the conductor passes under the north pole, an e.m.f. is induced

therein directed from the page towards the reader, and when the conductor passes under the south pole, the e. m. f. direction is reversed and passes from the reader into the page. Thus, an alternating *with time* e.m.f. is induced in conductor ab , and changes its direction twice for each revolution of armature. The time T , during which one complete variation of e.m.f. takes place, is called the e.m.f. *cycle*. The number of cycles per one second is called the *frequency* and is measured in hertz ², or in cycles per sec (c/s). If we consider the general case, when a machine has p pairs of poles, the frequency of the induced e.m.f. increases proportional to p , i. e.,

$$f = pn, \quad (1-2)$$

where n is the rotational speed measured in revolutions per second.

¹ An alternate rule is the *right-hand rule*: If the forefinger of the right hand is pointed in the direction of the flux and the thumb then pointed in the direction of the motion of the conductor through the flux, then the middle finger will indicate the direction of induced voltage. The thumb, forefinger and middle finger should be held at right angles to each other when applying the rule.

² Standard frequency unit in the U.S.S.R.— Tr .

Usually n is measured in revolutions per minute; in this case:

$$f = \frac{pn}{60}. \quad (1-2a)$$

Considering Fig. 1-1, we may see, that each brush is connected through a ring only with one conductor, namely, brush A with conductor ab and brush B with conductor cd . Therefore, across the terminals of the external circuit an alternating with time voltage is impressed and in the circuit an alternating current is set up with a frequency of f .

To compel this current to flow through the external circuit in one stipulated direction, in other words, to rectify the current, the machine is furnished with a special device called the *commutator* which functions as follows.

The ends of the turn $ab-cd$ are connected to two copper segments—bars of the commutator, insulated from each other and from the shaft onto which these bars are fixed (Fig. 1-4). Two stationary brushes $A-B$, connected

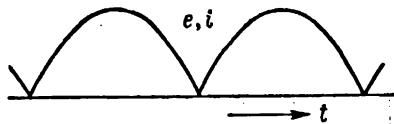


Fig. 1-5. Rectified e.m.f. or current

to the external circuit contact the commutator. In this case, however, the location of the brushes is of essential importance, contrary to that in the case of the rings in Fig. 1-1 where brush location is entirely arbitrary.

To rectify the alternating current completely, it is necessary to arrange the brushes as shown in Fig. 1-4, viz., so that the e.m.f. induced in the turn is zero at the instant when the brush passes over from one bar to another.

When the armature rotates an alternating e.m.f. will be induced as before, in the turn $ab-cd$, but *each of the brushes will contact only that commutator bar and its corresponding conductor, which are under the pole of given polarity*. For example, brush A always contacts the bar to which the conductor lying under the north pole is connected; and conversely, brush B is in contact with the conductor which is under the south pole. Hence the current in the external circuit will flow only in one direction, namely, from brush A to brush B ; in other words, *the induced alternating e.m.f. and the corresponding alternating current are rectified in the turn $ab-cd$ into a pulsating e. m. f. and a pulsating current at the brushes and, consequently, in the external part of the circuit too* (Fig. 1-5). If, as it was assumed previously, the machine works as a generator, the brush A , from which the current flows into the external circuit, is assumed as positive and denoted by

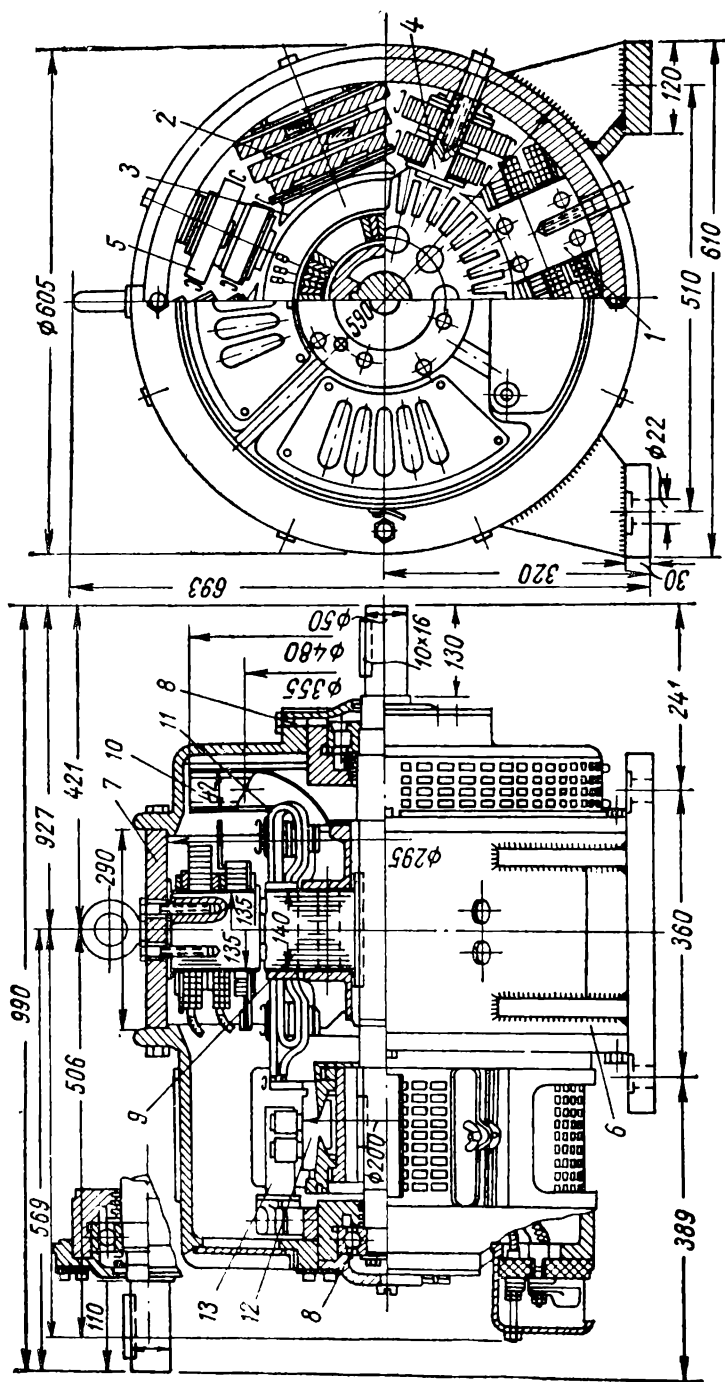


Fig. 1-6. Cross-sections of a d.c. machine

1 — main pole core; 2 — main pole coil; 3 — pole shoe; 4 — commutating pole core; 5 — commutating pole shoe; 6 — frame; 7 — yoke; 8 — frame bearing; 9 — armature core; 10 — fan; 11 — armature winding; 12 — commutator; 13 — brush stud

the "plus" sign, whereas brush *B*, through which the current returns to the machine, is regarded as negative and denoted by the "minus" sign.

The current pulsations in Fig. 1-5 occur in a range from the maximum value to zero, i.e., the pulsations are very prominent.

Later it will be shown (Chapter 3) that the e.m.f. pulsations may be smoothed out if a multi-conductor winding specially arranged on the armature and connected to the commutator is used.

1-4. Main Structural Elements of a Direct Current Machine

The direct current machine consists of two main parts: 1) the stationary part, designated mainly for producing the magnetic flux, and 2) the rotating part, called the *armature* where the process of conversion of mechanical energy into electrical (the electrical generator), or conversely electrical energy into mechanical (the electric motor) takes place. The stationary and rotating parts are separated from each other by the *air-gap*.

The stationary part of a direct current machine comprises: A) the *main poles*, designed to create the main magnetic flux; B) the *commutating poles* interposed between the main poles, designed to ensure sparkless operation of the brushes at the commutator (in very small machines commutating poles are not used); C) the *frame*.

The armature is a cylindrical body, rotating in the space between the magnetic poles and comprising: D) a *slotted armature core*; E) a *winding* inserted in the armature slot; F) the *commutator* and G) the *brush gear*.

Following is a short description of the main design elements of direct current machines.

A. Main field poles. In the process of d. c. machine development the magnetic system design has undergone many changes. The axial and cross-section drawings of a modern machine are given in Fig. 1-6.

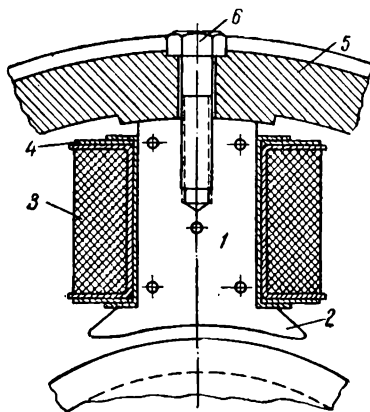


Fig. 1-7. Main pole

The main field is shown in Fig. 1-7. It consists of laminated pole 1 with 1 mm electrical grade sheets assembled on studs. At the end directed towards the armature, the pole core widens into pole shoe 2 which facilitates the passage of the magnetic flux through the air-gap. Mounted onto the core is field coil 3, energised by direct current passing through it. The coil is wound on frame 4, made of 1-2 mm sheet steel lined with cardboard glued on 2 to 3 mm thick or plastic or bakelised paper. To reduce the hygroscopicity and increase the heat-conducting capacity of the coils, they are compound-treated or subjected to a series of impregnations in hot varnish, with subsequent baking in furnaces. For better cooling the field coil may be subdivided

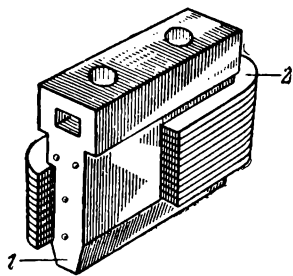


Fig. 1-8. Commutating pole
1 — core; 2 — pole coil

width in between. The poles are bolted to yoke 5 with the help of special bolts 6.

B. Commutating poles. (Fig. 1-8). The commutating pole is similar to the main pole in that it consists of core 1 with a pole shoe at the end, of various forms, and a wound coil 2 set on the core. The commutating poles are arranged strictly midway between the main poles and are bolted to the yoke. Commutating poles are usually made of solid steel, but for machines operating on abruptly varying loads they are made of sheet steel. For further discussion of the functions of the commutating poles and their importance see § 6-4.

C. Frame. The frame is the name given to the stationary part of the machine to which are fixed the main and commutating poles and by means of which the machine is bolted to its bedplate. The ring-shaped portion, that serves as the path for the main and commutating pole fluxes, is called the yoke (7 in Fig. 1-6). The frame of modern machines is made of cast iron or steel. Depending on the type and efficiency of the machine two types of frames were formerly in use, viz., 1) the split frame, 2) the solid frame, but present-day practice uses only the solid frame. If the armature diameter does not exceed 35 to 45 cm, then besides the poles

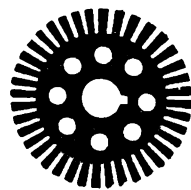


Fig. 1-9. Drum armature steel sheet punching with axial duct ventilation system

the shields or frame-heads which support the shield bearings (8 in Fig. 1-6) are also attached to the frame. When the machine diameter exceeds 1 m, it is common practice to use pedestal bearings, mounted separately on the machine bedplate outside the frame.

The shield bearings and sometimes the pedestal bearing housings are fitted with ball or roller bearings, the pedestal bearings being more frequently of the friction type.

In machines with large diameter armatures the *brush-yoke* is frequently fixed to the frame.

D. The armature. The former types of solid armatures—the T-type, disc and ring types are now of historical interest. Only slotted drum-type armatures assembled of 0.5 mm steel sheet laminations are used in present-day practice for the normal number of armature magnetic reversals in d. c. machines, i. e., 20 to 60 c/s. The steel laminations are assembled axially and to reduce eddy-current losses the sheets are insulated with a thin layer of varnish or layers of paper 0.03 to 0.05 mm thick. Small-output d. c. machines are usually constructed with an axial system of ventilation (Fig. 1-9), larger output machines have a radial system of ventilation (see Fig. 2-4). In the latter case the armature core consists of two or more packets, the length of each packet being 4 to 10 cm and the width of the ventilation ducts 8 to 10 mm. The armature core is pressed from both sides by clamping devices either specially fixed onto the shaft or tightened by bolts. To improve the cooling of small machines they are usually fitted with vanes; the larger machines have a special ventilator fan mounted on the shaft (Fig. 1-6).

E. Armature winding. Along with other machine elements the d. c. armature winding has also undergone a series of changes. All modern d. c. machines employ the drum-wound armature; that is, the winding is laid entirely on the outside of the armature core or drum periphery. The winding is built up in sections wound on special moulds and then laid in the armature core slots. The main features of the armature winding are discussed in § 3-8.

F. The commutator. The ends of all armature coils are joined to the commutator, which is of diverse design depending mainly on

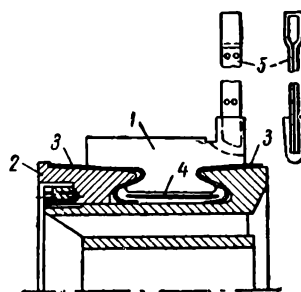


Fig. 1-10. Axial cross-section of a cylinder-type commutator

1 — commutator bar; 2 — clamping cones; 3 — insulating cups; 4 — insulating gasket; 5 — riser

machine output and speed. In Fig. 1-10 is shown a simple, cylindrical-type commutator. The commutator consists of a number of small wedge-shaped segments of hard drawn or drop-forged copper, which when assembled together form a cylinder. The copper bars are separated from each other by sheet mica and are insulated from their supporting rings by means of mica cones and gaskets. The bars are dovetail-fixed and after a series of hot pressings the commutator is lathe-turned to make its surface an exact cylinder. The armature winding is joined to the commutator in various ways. If the armature

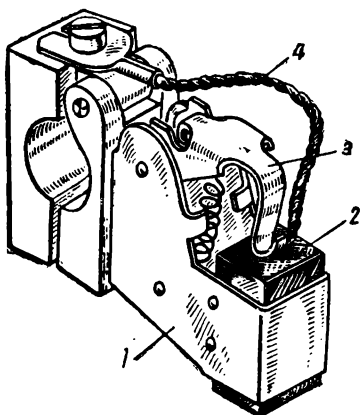


Fig. 1-11. Brush-holder
1 — brush-holder box; 2 — brush; 3 — pressure spring; 4 — current shunt (brush pigtail)

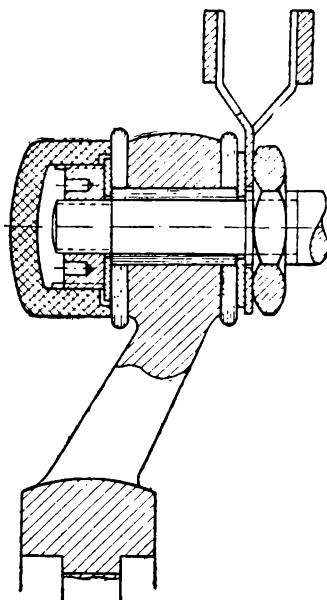


Fig. 1-12. Mounting of brush studs in brush-rocker

and commutator diameters do not differ considerably, the winding ends are directly soldered to the commutator bars. When the difference is great the connection is carried out with the help of commutator *lugs* or *risers*, one of the forms of which is shown in Fig. 1-10.

Machines of large output with normal r.p.m. often employ a *double* or *divided* commutator. Such a commutator consists of two halves, clamped together by bolts and joined by copper strips which act also as supplementary fan vanes.

In high-speed machines with an output from 15 to 25 kW and more, when the periphery speed is 3,000 r.p.m. and more,

the commutator is additionally reinforced with shrink rings, so as to eliminate bulging of commutator bars due to centrifugal forces and to heating of commutator. In special cases, to eliminate brush vibration at high periphery speeds instead of a cylindrical commutator, a butt or side-disk type of commutator is used, its contact surface perpendicular to the rotation axis with the brushes arranged for side contact.

G. Brush-gear. To collect the current off a rotating commutator or to lead the current to it brush-gear is used which consists of: a) brushes, b) brush-holders, c) brush studs or brush-holder arms, d) brush-yoke, e) the current-collecting busbars.

One of the typical brush-holder designs for d.c. machines is shown in Fig. 1-11. The brushes employed in practically all

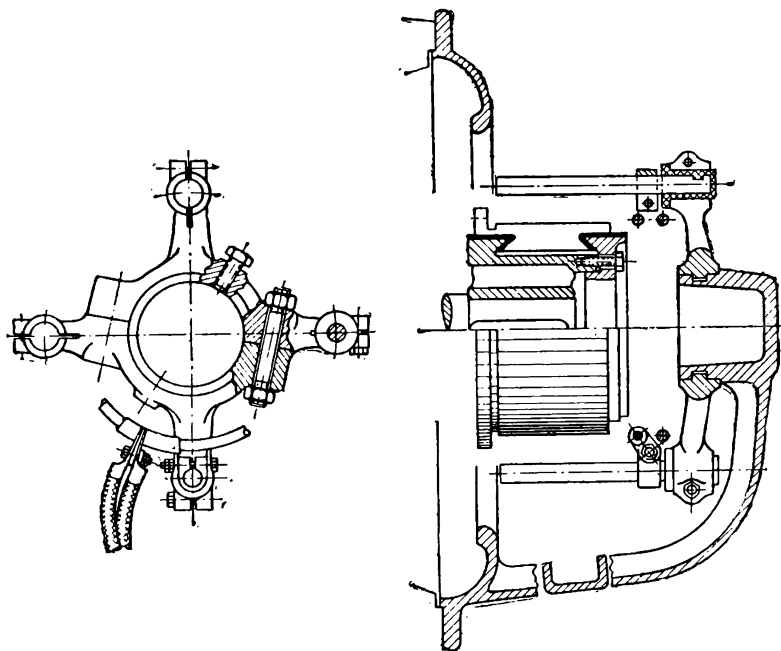


Fig. 1-13. Mounting of brush-rocker on bearing

modern machines are solely compositions of carbon and graphite or carbon and copper, the latter used for low-voltage commutator d.c. machines. The brush is inserted into the brush-holder where a spring presses it against the commutator with a force of

1.5 to 2.5 newtons per sq. cm (approximately 150 to 250 grams per sq. cm). The brush-holder is mounted on a stud which maintains the brush in a definite position in relation to the commutator. The most common type of brush-holder is the design in which the brush occupies a radial position and can move vertically in its brush-box. The current from the brush is led to the stud by means of a special flexible lead. Each brush stud usually carries two or more brushes working in parallel. The brush-holder studs are of a cylindrical or prismatic form and are fixed to the brush-yoke and insulated from it by insulation bushes. One method of fixing the brush studs to the brush-yoke is shown in Fig. 1-12. In small and average power machines the brush-yoke is mounted on the bearings (Fig. 1-13) but in large machines it is usually bolted to the yoke. All brushes of the same polarity are interconnected by busbars with leads to the machine terminals.

1-5. Ratings

The *rated performance* of an electrical machine is the duty assigned by the maker under certain specified conditions.

The rated performance is defined by values given on the machine's nameplate, and termed *rated values*, as, for instance: *rated output or load*¹, *rated voltage*, *rated current*, *rated r.p.m.*, etc.

But the term "rated" may be applied not only to values inscribed on the machine nameplate, but also to its performance parameters, as, for example, rated torque, rated efficiency, etc.

The *rated capacity* of a d. c. machine is:

a) When operating as a generator—the electrical power delivered into the external circuit and measured in watts (W) or in kilowatts (kW);

b) When operating as a motor—the useful mechanical power at the shaft and measured in the same units as in a).

Rated values should not be confused with normal values. If, for example, the rated voltage of the motor is 220 V, in actual working conditions a voltage may fluctuate and be more or less than the rated value. If we take the average value of voltage for a long enough period then it may arbitrarily be called the *normal* or *operating* voltage of the machine. Hence it follows from the above that in the general case normal (operating) values are not equal to rated values.

¹ *Output* has reference, more commonly, to the generation of electric power and *load* to its consumption.

Chapter Two

THE D. C. MACHINE MAGNETIC CIRCUIT ON NO-LOAD

2-1. Introduction

The following chapter is devoted to methods for the determination of the magnetomotive force (m.m.f.) of the main poles, necessary for the creation of the main magnetic flux.

The main magnetic flux of a d. c. machine is the flux in the air-gap Φ_0 which passes through an area corresponding to one pole-pitch τ when the machine is on no-load.

Fig. 2-1 schematically represents part of a four-pole direct current machine and gives a picture of the magnetic flux set up by the main poles (the commutating poles are not shown so as not to obscure the diagram). Because of complete symmetry of the machine and since all the field poles are structurally duplicates, the flux set up by each of the poles may be divided with respect to the axial line into two identical magnetic circuits symmetrically disposed on both sides of the axial line of the given pole. The number of circuits will then amount to the number of field poles, but for the computation of the m.m.f. it is common practice to confine the calculations to only one of the circuits.

That part of the main flux, which corresponds to one-half of pole is arbitrarily depicted on Fig. 2-1 by two heavy broken lines, that define the external and internal boundaries of the circuit, and by one continuous line passing through the middle of the circuit.

The main flux constitutes only part of the total flux established by the pole. The other part of the flux, called the *leakage flux*, branches off into the space between the poles and therefore does not penetrate into the armature core and take part in the creation of the e.m.f. In Fig. 2-1 the leakage flux is depicted by two thin broken lines 1 and 2.

If Φ_m is the total flux set up by the pole, and Φ_0 is the leakage flux, then

$$\Phi_m = \Phi_0 + \Phi_s = \Phi_0 \left(1 + \frac{\Phi_s}{\Phi_0} \right) = \Phi_0 k_s. \quad (2-1)$$

The factor $k_s = 1 + \frac{\Phi_s}{\Phi_0}$ is referred to as the *leakage coefficient of the main poles*. Usually $k_s = 1.12$ to 1.25 .

The m.m.f. F_0 , required to produce the main magnetic flux Φ_0 , we shall call the *main m.m.f.*

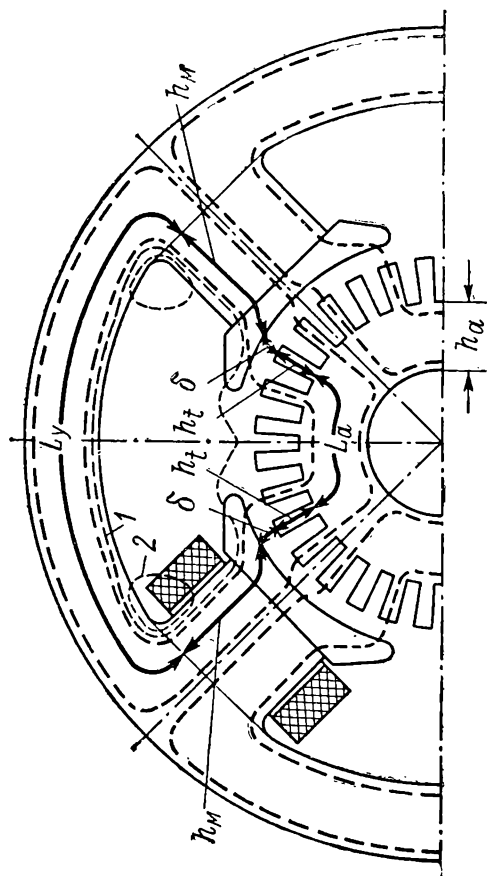


Fig. 2-1. Magnetic circuit of the main poles of a d.c. machine

2-2. Magnetic Circuit of a Direct-Current Machine. Determination of Main M.M.F.

From the diagram in Fig. 2-1 it may be seen that each line of the magnetic flux passes through successive sections that together form the *magnetic circuit* of the machine; each section differs both in geometric dimensions and in physical properties. In this case to assess the required m. m. f. it is necessary to proceed from the basic law of the magnetic circuit in its generalised form, viz.,

$$d\Phi = \frac{F}{R_\mu} = \frac{i\omega}{\oint \frac{1}{\mu} \frac{dl}{dS}},$$

hence:

$$F = d\Phi \oint \frac{dl}{\mu dS}.$$

In these formulas:

$F = i\omega$ is the m. m. f. along the magnetic circuit;

R_μ is the magnetic reluctance of the circuit;

$d\Phi$ — the flux of an elementary tube within the magnetic field of the circuit under consideration;

dl — the element of tube length;

μ — the magnetic permeability of the body or medium which constitutes the given section;

dS — the cross-section of the elementary tube, perpendicular to its axis.

For calculating the main m.m.f. of the machine F_0 we may divide the magnetic circuit of the machine into a series of sections so that it may be safely assumed that within the boundaries of each of them the magnetic flux of the tube, its permeability and cross-section remain constant along the entire length l of the tube. We may then consider the magnetic flux of each area as consisting of several identical elementary tubes, each having the length l and evenly distributed over the cross-section area S . There are five main sections of the magnetic circuit: 1) air-gap, 2) tooth, 3) armature core, 4) pole core including the pole shoe, and 5) yoke. The characteristic values for each section of the magnetic circuit are given in Table 2-1. It should be taken into consideration that the lengths of the elementary tubes (magnetic lines) of such sections as the yoke and the armature core are not the same; therefore the calculation of the m.m.f. of each of these sections is carried *along a middle magnetic line length* (the thick continuous line in Fig. 2-1). The main m.m.f. of the machine calculated for a

pair of poles may then be written in the following form:

$$F_o = \Phi_o \frac{2\delta}{\mu_o S_\delta} + \Phi_o \frac{2h_t}{\mu_t S_t} + \frac{\Phi_o}{2} \frac{L_a}{\mu_a S_a} + k_o \Phi_o \frac{2h_m}{\mu_m S_m} + k_o \frac{\Phi_o}{2} \frac{L_y}{\mu_y S_y}. \quad (2-2)$$

Since, according to the fundamental assumption, the magnetic flux is evenly distributed across each section area, then

$$\frac{\Phi_{sec}}{S_{sec}} = B_{sec} = \mu_{sec} H_{sec}. \quad (2-3)$$

Table 2-1

D. C. Machine Magnetic Circuit

Section No.	Section	Flux	Induction	Cross-section	Magnetic field voltage	Path length per pair of poles	M.m.f. per pair of poles
1	Air-gap Tooth	Φ_o	B_δ	S_δ	H_δ	2δ	F_δ
2		Φ_o	B_t	S_t	H_t	$2h_t$	F_t
3	Armature core	$\Phi_a = \frac{\Phi_o}{2}$	B_a	S_a	H_a	L_a	F_a
4	Pole core with pole shoe	$\Phi_m = k_o \Phi_o$	B_m	S_m	H_m	$2h_m$	F_m
5	Yoke	$\Phi_y = \frac{\Phi_m}{2}$	B_y	S_y	H_y	L_y	F_y

For these conditions the equation (2-2) may be rewritten in the following form:

$$\begin{aligned} F_o &= 2 \frac{B_\delta}{\mu_o} \delta + 2 \frac{B_t}{\mu_t} h_t + \frac{B_a}{\mu_a} L_a + 2 \frac{B_m}{\mu_m} h_m + \frac{B_y}{\mu_y} L_y = \\ &= 2H_\delta \delta + 2H_t h_t + H_a L_a + 2H_m h_m + H_y L_y = \\ &= F_\delta + F_t + F_a + F_m + F_y. \end{aligned} \quad (2-4)$$

The equation (2-4) shows, that to determine the total m. m. f. F_o it is necessary to determine for each of the five sections the corresponding field strength H and multiply it by the length of the section path. Since $H = \frac{B}{\mu}$, the field strength of each section depends on the flux density value and magnetic permeability of

the materials of each section. If the flux values and the dimensions of all sections are given, this is sufficient to compute the flux density in the section [see formula (2-3)]. The magnetic permeability of the section depends on the magnetic properties of the materials comprising it. For non-magnetic materials, as, for instance, the air-gaps, we have (see Table I-1): $\mu_0 = 4\pi \times 10^{-7}$ henry per m in the rationalised MKSA system and $\mu_0 = 4\pi$ in the rationalised CGS μ_0 system.

In factory design practice for such magnetic circuit computations a mixed system of units is preferred, this based on the CGS μ_0 system with the units of voltage, current, power, etc., converted into practical units—volts, amperes, watts, etc.

In this case

$$\mu_0 = 4\pi 10^{-1}.$$

For magnetic materials the magnetic permeability value depends on the flux density, i. e., $\mu = f(B)$; knowing this relation for any given material, it is possible to determine the field strength H and plot the magnetisation curve $H = f(B)$ of the given material. Such curves are shown in Fig. I-1 and I-2.

Let us discuss in detail the methods of determining the m.m.f. for each section of the magnetic circuit.

2-3. Air-Gap. Air-Gap Flux Density Distribution Curve

The air-gap is the main resistance offered to the magnetic flux, and because of this the m.m.f. F_g of the air-gap usually accounts for not less than 60 per cent of the main m.m.f. F_0 . Hence the precision with which the reluctance of the air-gap is calculated, predetermines to a great extent the precision of the entire magnetic circuit computation. To determine this resistance and the corresponding F_g , it is necessary first of all to map out, as precisely as possible, the picture of magnetic field distribution in the space between the pole shoes and the armature. For mapping purposes it is common practice to use the so-called method of the *unit magnetic tubes*. Consider first the simple case of a smooth armature and suppose that its length in the axial direction is very great and therefore we may disregard the fringing influence of the end parts of the armature and of the pole shoes. It may thus be assumed that the magnetic field distribution in all cross-sections perpendicular to the machine axis is the same, and therefore it is possible to map the magnetic field tubes in only one cross-section plane (Fig. 2-2). [Bibl. 8a, 40a].

Presuming the usual flux densities in steel it may be assumed that its permeability is very great, and therefore the surfaces of the armature and pole shoes are equipotential surfaces, penetrated by gap magnetic lines entering at right angles. The middle line drawn between the poles through the neutral point on the armature possesses, due to structural symmetry, the same potential as the armature surface. To map out a magnetic field the space between the equipotential surfaces is divided into unit tubes, so that the

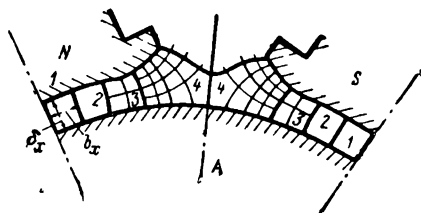


Fig. 2-2. Magnetic field map for a smooth armature air-gap

average width b_x of each tube equals its average length δ_x . In Fig. 2-2 the entire space between the axial lines of the north and south poles is divided roughly into $m=7.5$ unit tubes, i. e., $\frac{m}{2}=3.75$ tubes per each half of pole. If the length of armature is l_a then the magnetic permeance of each such tube is

$$\Lambda_{tube} = \mu_0 \frac{l_a b_x}{\delta_x} = \mu_0 l_a = \text{const},$$

i. e., all *unit tubes*, constructed by the above method have the same *magnetic permeances*.

Let F_{i_0} be the m.m.f. for a smooth armature; since the m.m.f. acts between the equipotential surfaces for all unit tubes, then $F_{i_0} = \text{const}$. Hence,

$$\Phi_{tube} = F_{i_0} \Lambda_{tube} = F_{i_0} \mu_0 l_a,$$

or, in other words: *the magnetic fluxes of all elementary tubes are equal*.

The magnetic flux in the gap may then be expressed as:

$$\Phi_0 = m \Phi_{tube} = m F_{i_0} \mu_0 l_a,$$

hence

$$F_{i_0} = \frac{1 \Phi_0}{\mu_0 m l_a}. \quad (2-5)$$

Of the unit tubes mapped in Fig. 2-2 only tubes 1 and 2 that lie close to the pole axial line approximate square cross-sections. Tube 3 already departs from a square and tube 4 near the edge of the pole shoe represents a pentagon. Such an approximate picture can serve its purpose only as the first approach to the problem.

To make the computation more precise tube 3 is subdivided into four partial tubes, and tube 4 into 16 partial tubes, taking care to observe the same conditions stipulated for mapping the unit tubes. If the unit tubes are sufficiently finely subdivided into partial tubes we obtain a grid that divides the entire space considered (excluding sections, bordering the neutral zone) practically into squares. That is why this field map is often referred to as the *square field map*.

The field map in Fig. 2-2 allows to determine, along with the m.m.f. F_{δ_0} , also the distribution of the normal component of the air-gap flux density. For this purpose it is sufficient to divide the unit tube flux $\Phi_{tube} = F_{\delta_0} \mu_0 l_a$ by the average cross-section area $S_{tube, x} = b_{x av} l_a = \delta_{x av} l_a$ (because the field is divided into squares), hence

$$B_{\delta x} = \frac{\Phi_{tube}}{S_{tube x}} = \frac{F_{\delta_0} \mu_0 l_a}{\delta_{x av} l_a} = \mu_0 \frac{F_{\delta_0}}{\delta_{x av}}. \quad (2-6)$$

Thus, for a given value of m.m.f. F_{δ_0} the flux density $B_{\delta x}$ is inversely proportional to the average length of the tube in the air-gap. Using this method, it is possible to plot a curve of flux density distribution in the gap along a developed armature periphery (Fig. 2-3). It should be noted that the entire construction is carried out, to some extent, by a rule-of-thumb method. Therefore for greater precision it is necessary to plot several versions of field maps, so as to be able to choose the one, where the permeance of the gap and flux therein distributed have the maximum value.

2-4. Reduction Method. The Calculated Pole Arc Value

Considering the curve in Fig. 2-3, we may see that the flux density in the gap varies from point to point round the armature periphery, attaining its maximum value $B_{\delta m}$ in the region adjacent to the middle of pole. To simplify the m. m. f. calculation procedure of the gap F_{δ_0} , without resorting to the plotting of numerous flux density distribution curves, the new conception of the *calculated flux density in the gap* B_{δ_0} is introduced, using for this purpose the so-called *reduction method*.

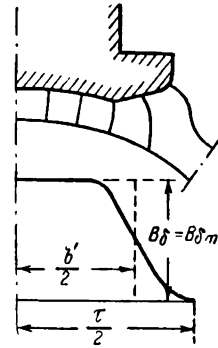


Fig. 2-3. True and reduced map of air-gap in a smooth armature cross-section

The substance of this method, widely used in the theory and for computations of electrical machines is as follows. The *real, and usually complex physical picture of a phenomenon is substituted by reduced conditions which first of all must represent the most simple aspect and secondly, when calculated should yield practically the same quantitative results as the actual picture.*

In the given case the actual trapezoidal curve of flux density distribution in the air-gap over the pole pitch is substituted by a rectangle with a height $B_\delta = B_{\delta m}$ and base b' , which should be so arranged that the areas confined within the boundaries of both curves are congruent. This base b' is referred to as the *calculated pole arc* and the ratio

$$\alpha' = \frac{b'}{\tau} \quad (2-7)$$

is called *the calculated pole arc coefficient*.

This coefficient α' is one of the most important values in electrical machine engineering. For direct current machines without commutating poles, $\alpha' = 0.7$ to 0.8 ; for machines with commutating poles $\alpha' = 0.62$ to 0.72 .

2-5. Calculated Armature Length

The computation carried out previously for field distribution in the air-gap around the periphery of the armature was based on

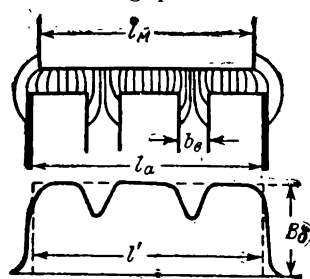


Fig. 2-4. True and reduced map of air-gap field in an axial armature cross-section

the assumption that the field distribution in all planes perpendicular to the machine axis along the entire length of armature is the same. In reality, however, it is necessary to consider the influence of the sides and radial cooling ducts (in machines with a radial system of ventilation) where the fringing of magnetic lines takes place. The corresponding picture of field distribution mapped along the length of the armature is represented in Fig. 2-4. Here l_m is the pole length along the machine axis; l_a is the total length of the armature, which is often made a few millimetres longer than l_m to reduce losses in the steel of the armature sides; b_δ is the width of duct. If n_δ is the number of ducts, then the length

of the armature without the ventilation ducts, i.e., the length of the stacks, is:

$$l = l_a - n_b b_b. \quad (2-8)$$

As above, we then substitute the actual curve of flux density distribution along the armature length by a reduced rectangle, which has the height B_δ and an area equal to the area confined within the actual curve. The base of this rectangle l' is called the *calculated armature length*. With sufficient accuracy it may be assumed that

$$l' = 0.5 (l_m + l). \quad (2-9)$$

2-6. M.M.F. of Air-Gap for a Smooth Armature

Using the calculated values established previously: B_δ , b' and l' , we may express the main magnetic flux of the machine as:

$$\Phi_0 = B_\delta b' l' = B_\delta a' \tau l'. \quad (2-10)$$

Knowing B_δ , it is possible to determine the m. m. f. of the gap for a pair of poles in the case of a smooth armature [formula (2-4)]:

$$F_{i_0} = \frac{2}{\mu_a} B_\delta \delta = \frac{2}{\mu_0} B_\delta \delta. \quad (2-11)$$

2-7. M.M.F. of Slotted Armature Gap

Direct current machine armature windings are assembled in open or semi-closed slots (see Fig. 3-23). Therefore the field in the gap is not uniformly distributed—it is concentrated above the teeth and thins out above the slots (Fig. 2-5). Because of the great density of field tubes above the teeth, the cross-sectional area of each tube decreases, whereas the tubes passing into the tooth from the side of the slot have a relatively large cross-section, but their path length is much greater than δ . As a result the reluctance of the gap is increased. This increase of reluctance may be taken into consideration, if the slotted armature is reduced to a smooth armature by means of increasing the gap to the value:

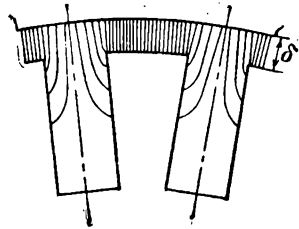


Fig. 2-5. Magnetic flux density in a toothed armature gap

$$\delta' = \delta k_\delta. \quad (2-12)$$

The value δ' is referred to as *the calculated value of the air-gap*, and the coefficient k_δ —as *the coefficient of the air-gap*.

The coefficient of the air-gap may be determined mathematically and is expressed by the formula:

$$k_\delta = \frac{t_1}{t_1 - \gamma \delta}; \quad (2-13)$$

here t_1 is the tooth pitch over the armature periphery, γ is a complex function of the ratio $\frac{b_n}{\delta}$, where b_n is the slot aperture (see dimensions t_1 and b_n in Fig. 2-6). With sufficient approximation it may be assumed that

$$\gamma = \frac{\left(\frac{b_n}{\delta}\right)^2}{5 + \left(\frac{b_n}{\delta}\right)^2}. \quad (2-14)$$

There exist several empirical formulas which simplify the calculation of coefficient k_δ . The most commonly used is the formula:

$$k_\delta = \frac{t_1 + 10\delta}{b_{t1} + 10\delta}, \quad (2-15)$$

where b_{t1} is the dimension (width) of the top part of the tooth along the armature periphery (see Fig. 2-6).

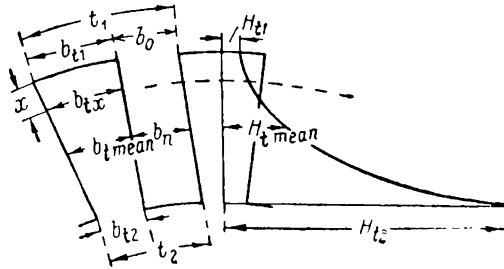


Fig. 2-6. Tooth m.m.f.

When the same flux in the air-gap with a slotted armature is required, as with a smooth armature it is necessary to enhance the m.m.f., by multiplying it by the gap coefficient. Therefore,

$$F_\delta = F_{\delta_0} k_\delta = \frac{2}{\mu_0} B_\delta k_\delta \delta = \frac{2}{\mu_0} B_\delta \delta'. \quad (2-16)$$

2-8. Air-Gap Data

In conventional machines the flux density B_g depends on the output of the machine and varies in the range 0.4 to 0.65 wb/sq.m for small machines (i. e. with outputs up to 10 kW) and reaching 1.0 to 1.05 wb/sq.m in larger machines. The air-gap is 0.7 to 3 mm for machines with outputs up to 50 kW and up to 10 mm for large-power machines; the air-gap coefficient $k_g = 1.05$ to 1.1 for semi-enclosed armature slots and 1.2 to 1.3 for open slots.

2-9. M.M.F. of Tooth Section

After passing through the air-gap, the flux Φ_0 enters the tooth section and here divides along two parallel paths, one part passing through the teeth, and the other through the slots. The relationship between these two parts depends on the relation between the magnetic permeances of tooth and slot. Thus, for example, when the maximum flux density in the tooth $B_{t_2} \leq 1.8$ wb/sq.m the permeance of the tooth is large compared with the slot permeance and we may disregard that part of the flux which branches off into the slot and assume that the entire flux passes only through the tooth. In this case the calculation of tooth m.m.f. is, of course, simplified, but, nevertheless, the typical case is when the flux density $B_g > 1.8$ wb/sq.m and when we cannot disregard the part of the flux that passes into the slot.

It is sufficient, however, to calculate the m.m.f. for one tooth pitch t_1 since all teeth conduct the flux in parallel and are in identical magnetic conditions over pole arc b' in accordance with the flux rectangle in Fig. 2-3.

Consider the calculation of the teeth m.m.f. in the case of a trapezoidal tooth (Fig. 2-6).

The flux in the gap per one tooth pitch is equal to:

$$\Phi_t = B_g t_1 l'.$$

Let us draw a concentric surface within the armature surface at a distance x from the tooth top.

If Φ_{tx} and Φ_{stx} are the fluxes in the tooth and slot, corresponding to this section, then

$$\Phi_t = \Phi_{tx} + \Phi_{stx}.$$

Dividing both parts of the equation by the cross-section area of the tooth in the given section:

$$\frac{\Phi_t}{S_{tx}} = \frac{\Phi_{tx}}{S_{tx}} + \frac{\Phi_{stx}}{S_{tx}}. \quad (2-17)$$

The value $\frac{\Phi_t}{S_{tx}}$ shall be referred to as the *estimated flux density* in the tooth B'_{tx} , i. e., the flux magnitude that would be available in the given tooth section, if the flux Φ_t would pass entirely through the tooth.

The first component on the right-hand side of the (2-17) equation represents the actual tooth flux density B_{tx} in the same tooth section.

The second component we can represent as:

$$\frac{\Phi_{stx}}{S_{tx}} = \frac{\Phi_{stx}}{S_{st}} \frac{S_{st}}{S_{tx}} = B_{stx} k_{tx} = \mu_0 H_{stx} k_{tx}.$$

Here

S_{st} is the cross-section of the slot, for a rectangular slot it is independent of its height;

B_{stx} is the flux density in the given slot section;

$k_{tx} = \frac{S_{st}}{S_{tx}}$ is the tooth coefficient, determined only by the dimensions of the tooth and slot;

H_{stx} is the magnetic field strength in the given slot section.

Suppose the concentric cylindrical surfaces which cut through the teeth and slots at various distances from the tooth top (see the broken line in Fig. 2-6), are also equipotential surfaces.

In this case the magnetizing force drop along the heights of the tooth and slot are equal and, therefore, $H_{stx} = H_{tx}$. Then the equation (2-17) becomes:

$$B'_{tx} = B_{tx} + \mu_0 H_{tx} k_{tx}. \quad (2-18)$$

To be able to use this formula for the calculation of tooth m.m.f. the following procedure is used. The magnetisation curve for the given grade of sheet steel is plotted (curve 1 in Fig. 2-7). The

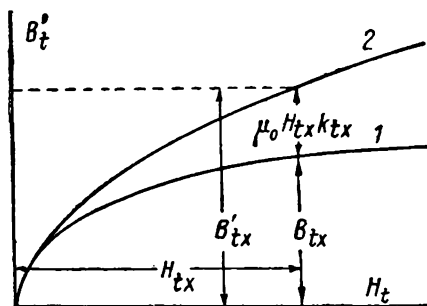


Fig. 2-7. $B'_t = f(H_t)$ curves

dimensions of slot and tooth if known, determine the coefficient k_{tx} . Assuming the actual flux density in the tooth B_{tx} and having found on curve 1 the corresponding value of H_{tx} we find the product $\mu_0 H_{tx} k_{tx}$ and then by means of formula (2-18) the calculated flux density in the tooth B'_{tx} . Having carried out this calculation for various flux densities B_{tx} we can then plot

in Fig. 2-7 the curve 2, which represents the relationship $B'_{tx} = f(H_{tx})$ for the given value of coefficient k_{tx} .

Several such curves for the E11, E12, E21 grades of electrical sheet steel and for values of k_{tx} in the range of $k_{tx}=0$ to $k_{tx}=2.4$ are plotted in Fig. 2-8.

When all these curves are obtained, they can be used in reverse order, i.e., first, for the given cross-section of tooth the calculated flux density B'_{tx} and tooth coefficient k_{tx} are determined, and then by using the corresponding curve on Fig. 2-8, the actual flux density B_{tx} and field density H_{tx} may be found.

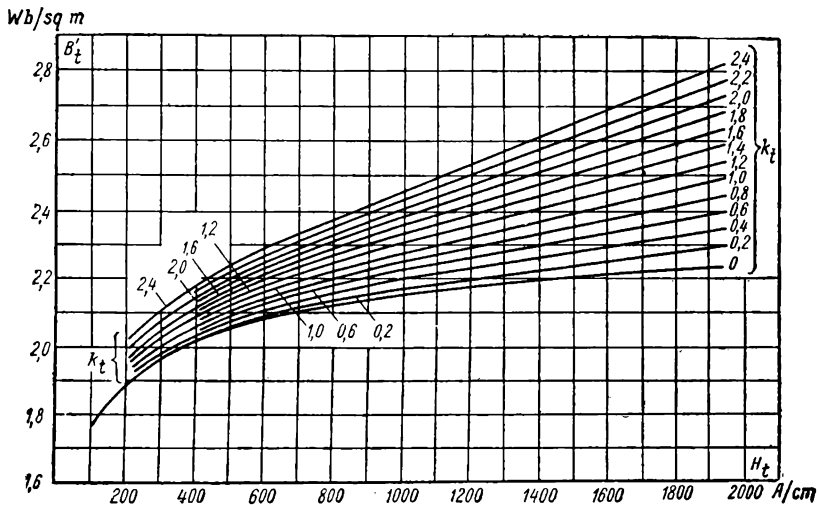


Fig. 2-8. $B'_t = f(H_t)$ curves for E11, E12 and E21 sheet steel grades

In accordance with the considerations mentioned previously, the calculated flux densities are determined by assuming that the flux passes only through the tooth.

Therefore,

$$\Phi_{tx} = \Phi_t$$

or

$$B'_{tx} b_{tx} l k_{st} = B_{\delta} t_1 l'$$

hence

$$B'_{tx} = B_{\delta} \frac{t_1 l'}{b_{tx} l k_{st}}. \quad (2-19)$$

Here b_{tx} is the width of the tooth in the given section; l is the length of all armature stacks and k_{st} is the stacking factor (the ratio of cross-sectional area of iron to cross-sectional area of stack),

that takes into consideration the insulation of the steel sheet laminations. For 0.5 mm steel sheets insulated with paper $k_{st}=0.88$ to 0.90; for varnished sheets $k_{st}=0.91$ to 0.93.

The tooth coefficient is determined by formula:

$$k_{tx} = \frac{S_n}{S_{tx}} = \frac{S_{tx} - S_{tx}}{S_{tx}} = \frac{t_x l'}{l_{tx} l k_{st}} - 1. \quad (2-20)$$

If, by using formula (2-19), we calculate the flux density B'_{tx} for successive points along the height of the tooth, and then determine their corresponding H_{tx} values from the curves in Fig. 2-8, we shall obtain the relation $H_{tx}=f(x)$, which is of a parabolic nature (Fig. 2-6).

For practical purposes it is sufficient to take three points along the height of the tooth—at its top, bottom and middle cross-sections.

Taking into consideration the dimensions in Fig. 2-6, we get:

$$B'_{t1} = B_\delta \frac{t_1 l'}{b_{t1} l k_{st}}; \quad (2-21a)$$

$$B'_{t. av} = B_\delta \frac{t_1 l'}{b_{t. av} l k_{st}}; \quad (2-21b)$$

$$B'_{t2} = B_\delta \frac{t_1 l'}{b_{t2} l k_{st}}. \quad (2-21c)$$

For the same sections we find the tooth coefficients and by using the curves in Fig. 2-8 we may determine the magnetizing force H_{t1} , $H_{t. av}$ and H_{t2} .

The calculated value of the magnetizing force H_t we may find as the mean value for the parabolic curve in Fig. 2-6:

$$H_t = \frac{1}{6} (H_{t1} + 4H_{t. mean} + H_{t2}). \quad (2-22)$$

If h_t is the height of tooth, then the m.m.f. of the teeth per pair of poles will be:

$$F_t = 2H_t h_t. \quad (2-23a)$$

It is common practice to simplify the calculation by determining the flux density and also the corresponding field strength only for one cross-section, taken at the distance $\frac{h_t}{3}$ from the base of the tooth. In this case

$$F_t = 2H_{t1/3} h_t. \quad (2-23b)$$

The results obtained by means of formulas (2-23a) and (2-23b) are numerically always the same. The flux density for direct cur-

rent machines is $B_{t_2}=1.8$ to 2.3 wb/sq.m (18,000 to 23,000 gauss) but in some cases, as, for example, in traction motors, it reaches 2.6 wb/sq.m and higher.

2-10. M.M.F. of Armature Core Section

The flux in the armature core section is not evenly distributed along its height: maximum flux density is observed at points nearer to the tooth, i. e., at the outer armature core surface, the minimum density being at its inner surface. However, the difference between these flux densities is usually small; therefore for practical calculation purposes an average flux density in the armature core B_a is assumed. As the flux in the armature core $\Phi = \frac{\Phi_0}{2}$ (see Table 2-1) and the cross-section of the core is $S_a = h_a l k_{st}$, where h_a is the height of the armature core (Fig. 2-1), then

$$B_a = \frac{\Phi_0}{2S_a} = \frac{\Phi_0}{2h_a l k_{st}}. \quad (2-24)$$

By using the magnetisation curve for steel of the given grade we may find the magnetizing force H_a . Then the m.m.f. of the armature core is

$$F_a = H_a L_a, \quad (2-25)$$

where L_a is the length of the middle magnetic line in the armature core steel.

The flux density B_a is usually chosen in the range from 1.0 to 1.5 wb/sq.m.

2-11. M.M.F. of Poles and Yoke

The calculation procedure for the determination of the m.m.f. of these sections of the magnetic circuit is the same as for the armature, but it should be taken into consideration here that the flux in these sections exceeds the main flux by the value of the leakage flux Φ_l which originates in the space between the poles and at the sides of the poles. [Bibl. 8a, 40b]

In Fig. 2-9 is depicted a magnetic field map of a machine with a smooth armature and commutating poles on no-load. The mapping is carried out by the same method of unit tubes as in the field mapping for the gap in Fig. 2-2. To simplify mapping it is assumed that the field winding of each pole is evenly distributed in a thin layer along the height h_{exc} of the pole core and, consequently,

it practically does not occupy any place in the interpole space (that is why the field winding is not shown in the picture). As the m.m.f. of one pole $F_{exc} = \frac{F_0}{2}$, the linear current loading along the core height, defined as the number of ampere turns per unit of length has the same value, i. e.:

$$A_{exc} = \frac{1}{h_{exc}} \frac{F_0}{2}.$$

Due to the constancy of the linear current loading, the distribution of the m.m.f. along the height of the core is also linear;

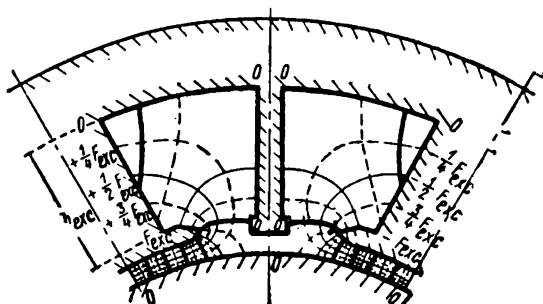


Fig. 2-9. Field map in cross-section of commutating pole machine

if the magnetic permeability of steel is infinitely large, then the pole-shoe surfaces are equipotential surfaces up to the points where the field windings begin. Hence, the m.m.f. of each pole uniformly decreases from the values $\pm F_{exc}$ to zero at points adjacent to the yoke. Of the same, zero, potential are the surfaces of the yoke and armature and, by virtue of pole symmetry, also the middle line drawn between poles through the neutral point on the armature.

If in Fig. 2-9 we shall divide the air-gap under the middle of the pole into four similar parts by three equipotential surfaces, these should terminate at the pole side surface and divide it along its height also into four equal parts. Then we can map out the lines of magnetic field and plot the grid of rectangles and squares in accordance with the method described previously (§ 2-3). The leakage flux in the interpole space is determined by a formula, identical to formula (2-5), namely:

$$\Phi_{oi} = \mu_0 m_o l_m F_0,$$

where

m_o is the number of leakage flux unit tubes;

l_m is the length of the pole-core in the axial direction.

In Fig. 2-10 is shown a map of leakage flux at the pole sides. The calculation procedure for the leakage flux Φ_{o2} at the sides is

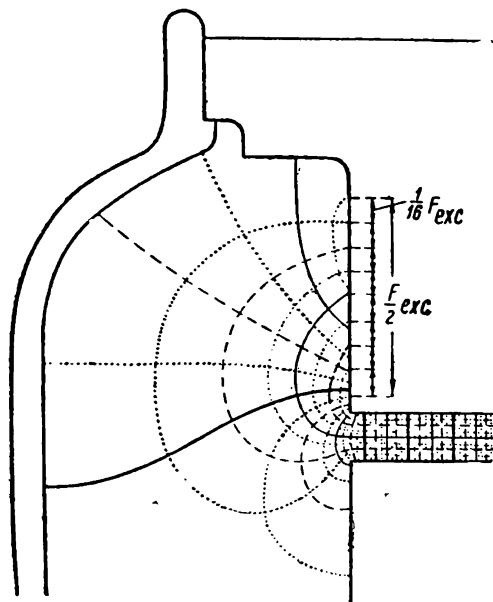


Fig. 2-10. Map for pole side field and equipotential surfaces

identical to the previous calculations. The total leakage flux is the sum of fluxes Φ_{o1} and Φ_{o2} , i. e.,

$$\Phi_o = \Phi_{o1} + \Phi_{o2}.$$

For normal conditions it may be assumed that the pole flux at any cross-section along its length will be:

$$\Phi_m = \Phi_o + \Phi_o = k_o \Phi_o. \quad (2-26)$$

Accordingly, the flux in the yoke is

$$\Phi_y = \frac{\Phi_m}{2} = \frac{1}{2} k_o \Phi_o. \quad (2-27)$$

If the geometrical dimensions of the pole core and the yoke are given, the average flux densities at these sections may be deter-

mined by the formulas:

$$B_m = \frac{\Phi_m}{S_m} \quad (2-28a)$$

and

$$B_y = \frac{\Phi_m}{2S_y} \quad (2-28b)$$

Usually $B_m = 1.2$ to 1.6 wb/sq.m and $B_y = 0.8$ to 1.4 wb/sq.m if the yoke is of steel, and approximately half this value if the yoke is of castiron.

If we use the magnetisation curves to determine the magnetizing forces H_m and H_y corresponding to the flux densities B_m and B_y , we may determine the m.m.f. of the poles and yoke:

$$F_m = 2H_m h_m \quad (2-29a)$$

and

$$F_y = H_y L_y \quad (2-29b)$$

The dimensions h_m and L_y are shown in Fig. 2-1.

It should be noted that a precise determination of the leakage coefficient is a very labour-consuming operation; therefore for practical purposes the leakage coefficient is often assumed, in accordance with the data in Table 2-2, based on experience available.

Table 2-2

2b	Armature diameter D_a , cm	k_a
4	Up to 25	1.28
>4	25-75	1.25
>4	75-150	1.20
>4	>150	1.15

2-12. Magnetisation Curve

Having obtained the m.m.f. of the separate sections of the magnetic circuit, the total m.m.f. per pair of poles can be determined by means of formula (2-4).

Suppose that the rated voltage and rated speed of the machine correspond to the rated value of the main flux $\Phi_0 = 1$. By assuming a series of values for the main flux, for example, 0.5; 0.8; 1.1 and 1.2, we may calculate F_0 for each value. The relation $\Phi_0 = f(F_0)$ plotted in rectangular co-ordinates (Fig. 2-11) is termed *the mag-*

netisation curve of the machine. Here the curves for the separate part of the magnetic circuit may also be plotted.

The initial part of the curve follows practically a straight line, because for small values of the flux Φ_0 the steel of the machine is little saturated and the gap m.m.f. is of major significance here.

By extending the linear part of curve, we may obtain the relationship $F_\delta = f(\Phi_0)$. For values $\Phi_0 = 1$, the m.m.f. F_δ is defined by segment ab in Fig. 2-11.

With an increase in the flux Φ_0 , a still greater part of m.m.f. is required for conducting the flux through the steel. For the given value of flux $\Phi_0 = 1$ this part of the m.m.f. is now defined by segment bc . By means of the ratio $k_\mu = \frac{F_\delta}{F_\delta} = \frac{ac}{ab}$, referred to as

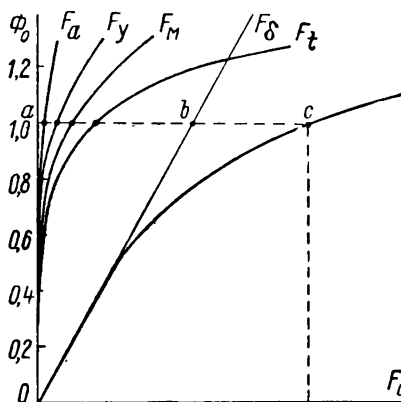


Fig. 2-11. Magnetisation curves of a machine

the *saturation coefficient*, it is possible to judge of the degree of magnetic circuit saturation of the machine at a given value of flux Φ_0 . For conventional-type machines $k_\mu = 1.10$ to 1.35 . Later (Chapter 8) we shall see that various degrees of saturation greatly influence the characteristics of the machine and its performance.

2-13. Numerical Example

Let us calculate the m. m. f. F_0 necessary to set up the magnetic flux $\Phi_0 = 0.638 \times 10^{-2}$ weber $= 0.638 \times 10^6$ maxwell in a ПН-100-type generator. The machine data is as follows: rated power $P_n = 13.3$ kW; rated voltage $U_n = 230$ V; rated current $I_n = 58$ A; rated speed $n = 1,460$ r. p. m.; number of poles $2p = 4$; outside armature diameter $D_a = 245$ mm; inside diameter of armature $D_{a\text{int}} = 60$ mm; length of armature $l_a = 80$ mm; ventilation ducts are axial type; number of armature slots $Z = 35$; slot dimensions: $b_{st} = 8.5$ mm, $h_{st} = 36.2$ mm; the air-gap under the main poles $\delta = 1.5$ mm; dimensions of main pole: axial length $l_m = 80$ mm; width $b_m = 80$ mm; height in the radial direction including pole shoe $h_m = 70$ mm; pole arc coefficient $\alpha' = 0.65$; yoke cross-section (approximately) $S_y = 26 \times 160 \text{ mm}^2 = 41.5 \times 10^{-4} \text{ m}^2$. The pole cores are assembled of E11 grade steel, the armature core of E12 grade steel.

Using given dimensions for armature and slot we may determine (see Fig. 2-1 and 2-6):

$$\begin{aligned}\tau &= \frac{\pi D_a}{2p} = \frac{\pi \times 245}{4} = 192 \text{ mm;} \\ t_1 &= \frac{\pi D_a}{Z} = \frac{\pi \times 245}{35} = 22 \text{ mm;} \\ b_{t1} &= t_1 - b_{st} = 22 - 8.5 = 13.5 \text{ mm;} \\ t_2 &= \frac{\pi(D_a - 2h_t)}{Z} = \frac{(245 - 2 \times 36.2)}{35} = 15.5 \text{ mm;} \\ b_{t2} &= t_2 - b_{st} = 15.5 - 8.5 = 7 \text{ mm;} \\ t_{av} &= \frac{1}{2}(t_1 + t_2) = \frac{1}{2}(22 + 15.5) = 18.75 \text{ mm.} \\ b_{t.av} &= t_{av} - b_{st} = 18.75 - 8.5 = 10.25 \text{ mm.}\end{aligned}$$

As the machine is fitted with an axial ventilation system, we may assume that:

$$l' = l = l_a = 80 \text{ mm.}$$

We shall carry out the calculation using both the MKSA basic system of units and the mixed system. On the basis of formula (2-10) we find:

$$B_\delta = \frac{\Phi_0}{\alpha' \tau l'} = \frac{0.638 \times 10^{-2}}{0.65 \times 192 \times 10^{-2} \times 80 \times 10^{-2}} = 0.64 \text{ webers per sq. m,}$$

or

$$B_\delta = \frac{\Phi_0}{\alpha' \tau l'} = \frac{0.638 \times 10^8}{0.65 \times 192 \times 10^{-1} \times 80 \times 10^{-1}} = 6,400 \text{ gaussess.}$$

The air-gap factor is determined by formula (2-15):

$$k_\delta = \frac{t_1 + 10\delta}{b_{t1} + 10\delta} = \frac{22 + 10 \times 1.5}{13.5 + 10 \times 1.5} = 1.30.$$

The air-gap m. m. f. will then be [formula (2-16)]:

$$\begin{aligned}F_\delta &= \frac{2}{\mu_0} B_\delta \delta' k_\delta = \frac{2}{4\pi \times 10^{-7}} 0.64 \times 1.5 \times 10^{-2} \times 1.30 = \\ &= \frac{2}{4\pi \times 10^{-1}} 6,400 \times 1.5 \times 10^{-1} \times 1.30 = 1,990 \text{ A.}\end{aligned}$$

To determine the flux density in the tooth we assume a stacking factor $k_{st} = 0.9$; then, by using formula (2-21a), we find:

$$B'_{t1} = \frac{B_\delta t_1 l_1}{k_\delta b_{t1} l} = \frac{0.64 \times 22 \times 10^{-2}}{0.9 \times 13.5 \times 10^{-2}} = 1.16 \text{ wb/sq.m} = 11,600 \text{ gaussess.}$$

The flux density over the height of tooth varies inversely as the width of tooth; accordingly we may write:

$$B'_{t.av} = B'_{t1} \frac{b_{t1}}{b_{t.av}} = 1.16 \frac{13.5}{10.25} = 1.53 \text{ wb/sq.m} = 15,300 \text{ gaussess,}$$

$$B'_{t2} = B'_{t1} \frac{b_{t1}}{b_{t2}} = 1.16 \frac{13.5}{7.0} = 2.24 \text{ wb/sq.m} = 22,400 \text{ gaussess.}$$

By using the curves for E12 grade steel in Fig. 1-1 we find $H_{t1} = 5.4$ amperes per cm and $H_{t,av} = 29$ amperes per cm. By using formula (2-20) we may determine coefficient $k_t = 1.46 \approx 1.5$ and by using the corresponding curve in Fig. 2-8 we find $H_{t2} = 690$ amperes per cm.

As $h_t = h_{st} = 36.2$ mm, then by means of formulas (2-22) and (2-23) we obtain:
 $H_t = 135$ A/cm and $F_t = 2H_t h_t = 2 \times 135 \times 3.62 = 980$ A. The height of armature core

$$h_a = \frac{D_a - 2h_t - D_{a,int}}{2} \leq \frac{245 - 2 \times 36.2 - 60}{2} = 56 \text{ mm.}$$

The flux density in the armature core [formula (2-24)]

$$B_a = \frac{\Phi_0}{2h_a l k_{st}} = \frac{0.638 \times 10^{-2}}{2 \times 56 \times 10^{-3} \times 80 \times 10^{-3} \times 0.9} = 0.8 \text{ wb/sq.m} = 8,000$$

gausses.

The magnetic field strength corresponding to this flux density is $H_a = 2.3$ A/cm. The length of the middle magnetic line in the armature core we determine as $1/4$ of the circumference of a circle, having a diameter $D_a - 2h_t - h_a = 24.5 - 2 \times 3.62 - 5.6 = 11.66$ cm; therefore,

$$L_a = \frac{\pi 11.66}{4} = 9.2 \text{ cm and } F_a = 2.3 \times 9.2 = 21 \text{ A.}$$

To determine the m. m. f. of the pole and yoke we assume a leakage factor $k_s = 1.25$ see (Table 2-2); then

$$\Phi_m = k_s \Phi_0 = 1.25 \times 0.638 \times 10^{-2} = 0.8 \times 10^{-2} \text{ webers} = 0.8 \times 10^8 \text{ maxwells.}$$

The flux density in the pole core

$$B_m = \frac{\Phi_m}{S_m} = \frac{0.8 \times 10^{-2}}{80 \times 10^{-3} \times 80 \times 10^{-3}} = 1.25 \text{ wb/sq.m} = 12,500 \text{ gauss.}$$

From curve A in Fig. 1-1 we determine $H_m = 6.7$ A/cm; then

$$F_m = 2H_m h_m = 2 \times 6.7 \times 7 = 94 \text{ A.}$$

For the yoke we obtain:

$$B_y = \frac{\Phi_m}{2 \times S_y} = \frac{0.8 \times 10^{-2}}{2 \times 41.5 \times 10^{-4}} = 0.96 \text{ wb/sq.m} = 9,600 \text{ gauss.}$$

Accordingly $H_y = 3.3$ A/cm.

We assume the length L_y of the middle magnetic line in the yoke as $1/4$ of the circumference with the diameter

$$D_a + 2\delta + 2h_m + h_y = 245 + 2 \times 1.5 + 2 \times 70 + 26 = 414 \text{ mm} = 41.4 \text{ cm;}$$

hence:

$$L_y = \frac{41.4}{4} = 32.5 \text{ cm and } F_y = H_y L_y = 3.3 \times 32.5 = 107 \text{ A.}$$

The m. m. f. per pair of poles, required for the creation of the main flux of $\Phi_0 = 0.638 \times 10^{-2}$ webers, is:

$$F_0 = F_\delta + F_t + F_m + F_a + F_y = 1,990 + 980 + 94 + 21 + 107 = 3,200 \text{ A.}$$

The other points of the magnetisation curve may be calculated in the same way.

Chapter Three

WINDINGS AND E.M.F. OF DIRECT CURRENT MACHINE ARMATURE

3-1. Introduction

The armature winding is a very important element of the machine, as it directly takes part in the process of conversion of energy from one form into another. The requirements specified for a winding are diverse and often of a conflicting nature. Of these requirements the following are of major importance: A) the winding must be constructed with the most advantageous utilisation of material in respect to weight and efficiency; B) the winding should provide the necessary mechanical, thermal and electrical strength of the machine to ensure a service life of 16-20 years; C) for d. c. machines proper current collection at the commutator (i. e., absence of detrimental sparking) is a basic requirement.

We shall begin the study of d. c. machine armature windings with the *ring-type windings*, even though nowadays the *drum-type windings* have completely superseded them. This is done because there is no essential difference between the ring and drum windings; but the ring winding, though technically inadequate, is much simpler than the drum-type. Therefore it is more convenient to study first of all the simplest ring types of windings and then the more complex drum windings; practice has proved that for the beginner this is of greater advantage.

It was already mentioned previously (§ 1-3), that an alternating e.m.f. is induced in the d.c. machine armature winding. To facilitate the analysis of this e.m.f. the method of plotting *e.m.f. vector stars* and *potentials* or *e.m.f. polygons* are used. This method is utilised also to discuss alternating current machine windings and consequently is of singular importance for the theoretical study of electrical machines. In many cases it is the only reliable method by which it is possible to analyse and understand the intricate nature of a winding and obtain a clear notion of the e.m.f. induced in them.

While discussing ring-type windings we shall not consider their manufacture, as this at present is practically of no interest.

3-2. Classification of Armature Windings

Regardless of type of armature, whether it is a ring or drum type, there exist the following types of direct current armature windings:

- A) Simple lap;
- B) Simple wave;
- C) Multiplex lap;
- D) Multiplex wave.

The simple windings always form only one closed upon itself circuit, whereas the multiplex windings may consist of either one or several such circuits. In the first case we shall refer to the multiplex winding as *single closed*, in the latter case as *multiple closed*.

In the early stages of d. c. machine development the so-called open windings gained some import, but at present they are of historical interest only.

3-3. Formulas for Assembling Ring-Type Armature Simple Windings and Their Fundamental Characteristics

The principal element of any type of d.c. machine armature winding is the *coil section*. A coil section is part of an armature winding, consisting of one, two or, in the general case, of several conductor turns connected to two adjoining commutator bars, in accordance with the winding diagram. For simplicity only single-turn windings will be depicted.

Fig. 3-1 shows three coil sections of a simple lap winding. The distinctive features of these coils are that the *start and finish of each coil section are connected to two consecutive commutator bars*, for example, coil section 1 is connected to bars 1 and 2, coil section 2—to bars 2 and 3, and so on. To assemble the winding as a closed on itself circuit, the *start of each subsequent coil section is connected to the finish of the preceding coil section*. For example, the finish of coil section 1 and the start of coil section 2 are connected to bar 2, to bar 3—the finish of coil section 2 and the start of coil section 3, and so on. The lead that connects the winding to the commutator is brought out to the middle of the commutator bar which arbitrarily is assumed as the starting point for counting the commutator divisions. Here and in further discussions we shall refer to a commutator division as *the commutator bar together with the insulation* dividing it from the adjacent bar.

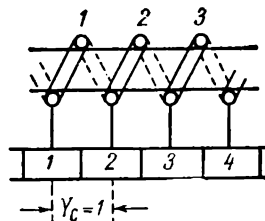


Fig. 3-1. Simple lap winding coil section for ring armature

The distance y_c between the commutator divisions to which the coil section is joined, measured by the number of commutator divisions spanned, is called the winding pitch over the commutator or simply the commutator pitch. For a simple lap winding, the commutator pitch is equal to one commutator division, i. e.,

$$y_c = 1. \quad (3-1)$$

Fig. 3-2 shows sections 1, 6, 11 and 16 of a simple wave winding; To complete this winding we have to make the rounds

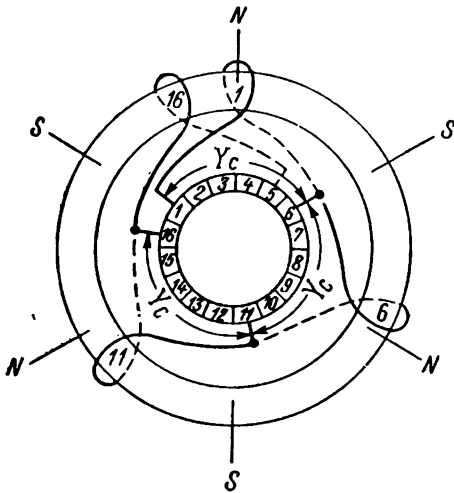


Fig. 3-2. Single-turn coil sections for armature with simple wave winding

of the entire armature and accordingly of the commutator, arranging on the armature under each pair of poles one coil section, and spanning one commutator pitch y_c . The fundamental requirement for the simple wave winding is that after completing one round of the armature and commutator we must arrive at the commutator division, adjacent to the one we started from left or right of it.

If a machine has p pairs of poles and the commutator consists of K commutator divisions, after one round we assemble on the armature p coil sections, and span py_c commutator divisions. According to stipulated conditions,

$$\begin{aligned} \text{hence} \quad py_c &= K \mp 1, \\ y_c &= \frac{K \mp 1}{p}. \end{aligned} \quad (3-2)$$

Let, for instance, the machine in Fig. 3-2 have $p=3$ and $K=16$; then

$$y_c = \frac{16 - 1}{3} = 5.$$

Suppose, the first coil section is laid under the middle of the north pole and the first pitch $y_c=5$ is spanned joining division 1 with divisions $1+5=6$. The second coil section following the first in accordance with the winding diagram, is laid approxi-

mately under the middle of the second north pole, spanning a second commutator pitch $y_c=5$ and joining division 6 with division $6+5=11$. Finally, we arrange the third coil section following the second according to the winding diagram, approximately under the middle of the third north pole and, spanning the third commutator pitch $y_c=5$, arrive at division $11+5=16$ which lies next to the initial division, but set apart by one commutator division. But if $p=3$ and $K=14$, we would have obtained the former pitch $y_c=5$, surpassing the first commutator division by one division ($y_c = \frac{14+1}{3} = 5$).

Comparing coil sections of the simple lap and wave windings (Fig. 3-1 and 3-2), we may observe that the main difference between them is that the former has a pitch $y_c=1$, i. e., much less than a pole pitch, while the pitch of the latter is $y_c \approx \frac{K}{p}$, i. e., almost equal to double the pole pitch, measured by the number of commutator divisions spanned.

Since for any of the winding types the start of one coil section and the finish of the next section is connected to each commutator bar, each armature winding coil section corresponds to one commutator division. If the number of sections is S and the number of commutator divisions is K , then

$$S=K. \quad (3-3)$$

All the relationships established here (3-1), (3-2) and (3-3) for simple ring-type armature windings may then be used also for any of the drum-type armature simple windings.

3-4. Simple Lap Winding for Ring-Type Armature

The assembling of a simple lap winding on a ring armature lap is a very simple process. Assume, for example, $2p=4$ and $S=K=14$ (Fig. 3-3, *a*, *b*). Let us arrange the coil sections uniformly round the armature periphery and then number them consecutively in one direction, say, clockwise. Let us then connect the start of coil section 1 to the bar which we also denote by figure 1 and number all the commutator bars in the same order as the armature coil sections. To construct a simple lap winding, it is sufficient to join all the 14 sections consecutively, in the order of their arrangement on the armature, spanning a commutator pitch of $y_c=1$ each time a coil section is laid.

When such a winding is rotated in a magnetic field, set up by the main poles, an e.m.f. is induced in it. To understand the nature

of this process, we should first consider the e.m.f. of one coil section.

The distinctive feature of a ring-type armature coil section is that it has *only one active side* lying on the external surface of the armature, whereas the other side of the section, embedded in the hollow of the armature, is non-active because no magnetic flux passes here. For this reason we may speak of the e.m.f., bearing in mind that it is the e.m.f. of its active side only.

Previously (see Fig. 2-3) we saw, that the magnetic flux distribution curve in the air-gap under the pole is of a trapezoidal

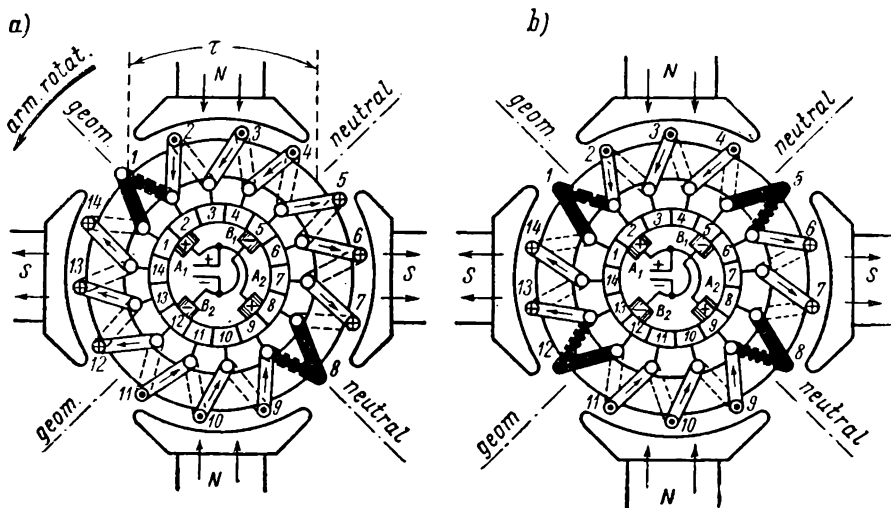


Fig. 3-3. Radial scheme for ring armature simple lap winding: $2p=4$; $S=K=14$

form, and for calculation purposes it was substituted by a rectangle. Fig. 3-4 shows two such rectangles corresponding to one pair of poles. We may resolve them in a harmonic series, composed of a fundamental or first harmonic curve and of higher order components (in Fig. 3-4 are shown the fifth and seventh harmonic components). Disregarding the higher order, we may assume, that the flux density in the air-gap under the poles is sinusoidally distributed. In this case to each pair of poles, i. e., to a double pole pitch 2τ , corresponds one complete sine-wave of the flux density distribution curve in the air-gap. If the machine has p pairs of poles then the armature periphery accommodates p sine-wave. The machine in Fig. 3-3 has $p=2$; hence the armature periphery can accommodate two magnetic flux

density sine-waves (Fig. 3-5, a). Using angular measures, a complete sine-wave corresponds to 2π radians or 360° . Thus the armature circumference that conforms to a *geometric* angle of 2π or 360° , *electrically* corresponds to an angle of $p \times 2\pi$ or $p \times 360^\circ$. For this reason the angles $p \times 2\pi$ and $p \times 360^\circ$ are referred to as *electrical angles* and accordingly the terms *electrical radians* or *electrical degrees* are also used. From the above considerations it

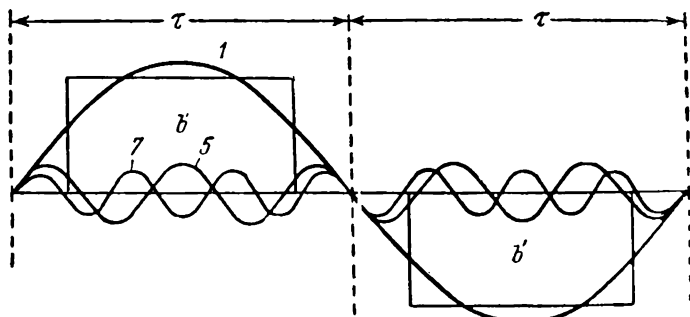


Fig. 3-4. Calculated flux density curve resolved into fundamental and higher harmonics

follows, that one geometric radian or degree corresponds to p electrical radians or p electrical degrees. In all further discussions, unless otherwise mentioned, we shall express angles only in *electrical radians* or in *electrical degrees*.

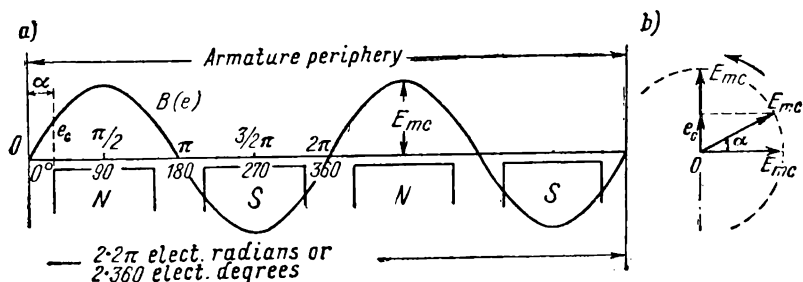


Fig. 3-5. Electrical angle concept (a) and vector method of depicting sine-wave e.m.f. (b)

When an armature rotates in a sinusoidal field an e.m.f. that varies also with time sinusoidally is induced in a coil section [formula (1-1a)]. Thus, the sine curve depicted in Fig. 3-5, a, that determines the flux density distribution in the air-gap under the poles, i. e., in space, at the same time is the curve depicting the variation with time of the e.m.f. induced in the coil section. From

alternating current theory we know that any sine curve, specifically a sinusoidal e.m.f., may be represented as a *vector, equal in magnitude to the e.m.f. amplitude*—in our case to the coil section e.m.f. amplitude E_{mc} and *rotating counterclockwise* with an angular frequency of $\omega = 2\pi f = 2\pi pn$ (Fig. 3-5, *b*). The projection of vector E_{mc} onto the ordinate axis gives the instantaneous value of the coil section e.m.f. e_c .

Let us now examine the process of e.m.f. induction in the case of the armature winding in Fig. 3-3. Since armature winding sections are evenly distributed round the periphery, each section is displaced in respect to its adjacent coil section by an angle

$$\text{or} \quad \alpha = \frac{p \times 2\pi}{S} \text{ electrical radians} \quad (3-4a)$$

$$\alpha = \frac{p \times 360^\circ}{S} \text{ electrical degrees.} \quad (3-4b)$$

In our case (Fig. 3-3) $p=2$ and $S=14$, therefore,

$$\alpha = \frac{2 \times 360^\circ}{14} = 51 \frac{3}{7}^\circ.$$

At the instant shown in Fig. 3-3, *a*, the armature occupies a position where section 1 is in line with the geometrical neutral. Hence the e.m.f. of this section is $e_1=0$ and is represented on the vector diagram by vector 1, superposed on the abscissa axis (Fig. 3-6, *a*).

For a counterclockwise direction of armature rotation, coil section 2 follows coil section 1, then coil section 3 follows section 2 and so on. Therefore the e.m.f. of sections 2, 3, etc., lag on the e.m.f. of sections 1, 2, etc., by angle $\alpha = 51 \frac{3}{7}^\circ$. Hence in the vector diagram we should depict the e.m.f. of coil section 2 by means of a vector 2 displaced in respect to vector 1 by an angle $\alpha = 51 \frac{3}{7}^\circ$ *against the direction of vector rotation*; accordingly, the e.m.f. of section 3 given by vector 3, is again displaced in the same direction by another $51 \frac{3}{7}^\circ$ angle and so on. Making thus a round of the first seven winding coil sections, we obtain a regular seven-ray star of e.m.f.s consisting of vectors 1, 2, 3..., 7. If we were to continue the round of the winding, vector 8 will be superposed on vector 1, vector 9—on vector 2 and so on. This means that in the coil sections 8, 9, 10..., 14 e.m.f.s of the same magnitude and direction are induced as in sections 1, 2..., 7. As a result of this we obtain a second star of e.m.f.s superposed on the first star and differing from it only by the numbers allotted to the coil sections.

Since all armature winding coil sections are connected in series, so that the finish of the preceding coil section is joined to the start

of the next, the e.m.f.s induced in the sections may be added geometrically. This is done by plotting from the end of vector *1*, parallel to the e.m.f. star vector *1* (Fig. 3-6, *a*), vector *2*, equal and parallel to the e.m.f. star vector *2*, then, from the end of vector *2*—a vector equal and parallel to vector *3* of the e.m.f. star and so on. As a result of this we obtain two equal heptagons, which for clarity are depicted in Fig. 3-6, *a*, *b*, *c* separately.

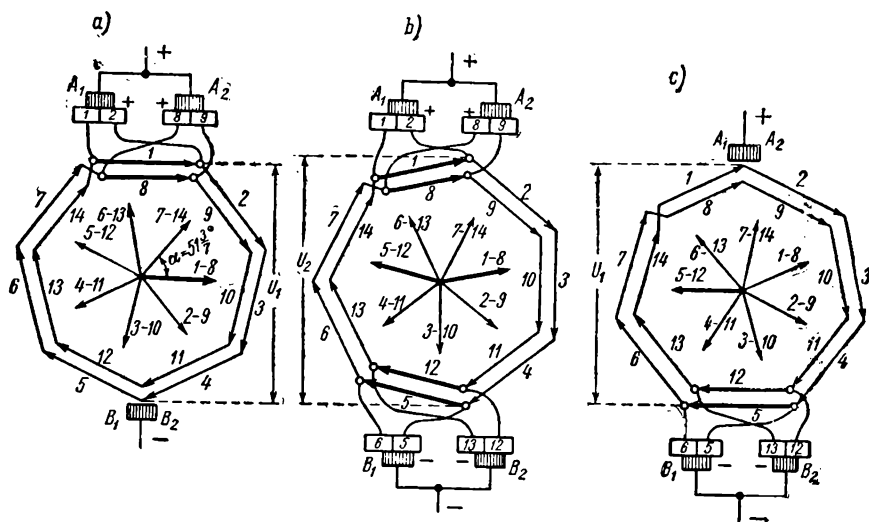


Fig. 3-6. Stars and polygons of the winding e.m.f.s in Fig. 3-3 for three different instances

To obtain maximum voltage across the brushes, they should be set on the commutator in line with the geometric neutrals. The width of the brushes in Fig. 3-3 is assumed equal to one commutator division. In the position of the armature given in Fig. 3-3, *a*, brushes *A*₁ and *A*₂ short-circuit sections *1* and *8*. Vectors *1* and *8* of the e.m.f. star and polygon in Fig. 3-6, *a* corresponding to these sections are depicted by heavy lines. To show the relation existing between the e.m.f. polygon and the commutator, the beginning and end of vectors *1* and *8* in Fig. 3-6, *a* are joined to bars *1-2* and *8-9*, to which are connected the start and finish of sections *1* and *8* in Fig. 3-3, *a*.

When the armature is turned $\frac{\alpha}{4} = 12.7^\circ$ (Fig. 3-3, *b*) the star and polygon of e.m.f.s will turn the same angle in direction of vector rotation (Fig. 3-6, *b*). In the considered position of armature,

sections 1-8 and 5-12 are short-circuited by the brushes A_1 - A_2 and B_1 - B_2 . As before, the vectors 1-8 and 5-12 are depicted in Fig. 3-6, *b* by heavy lines and joined to the corresponding commutator bars.

When the armature is turned $\frac{\alpha}{4}$, both the e.m.f. star and polygon assume the position shown in Fig. 3-6, *c*. Here only sections 5 and 12 prove to be short-circuited by brushes B_1 and B_2 . When the armature is turned further besides the sections 5-12 coil sections 2-9 will also be short-circuited (the corresponding e.m.f. polygon is not shown) and so on.

By analysing the e.m.f. polygons for different positions of armature, we arrive at several conclusions of considerable import for understanding d.c. machine windings construction and their operation.

A. The e.m.f. of a given part of winding. Previously (Fig. 3-5, *a*) we saw that with sinusoidal distribution of flux density under the

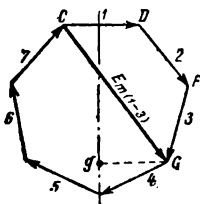


Fig. 3-7. E.m.f.s for group of coil sections

poles, the e.m.f. of the armature winding coil sections also varies with time sinusoidally. But this is true also in respect to any group of coil sections, or in other words, refers to any part of the armature winding. Take, for example, the group of coil sections 1, 2, 3 of the armature winding in Fig. 3-3, *a*; the corresponding e.m.f.s are shown in Fig. 3-7 by vectors \overline{CD} , \overline{DF} and \overline{FG} . Since each vector of the polygon represents the amplitude of the e.m.f. of the corresponding coil section, then by adding together geometrically the vectors \overline{CD} , \overline{DF} and \overline{FG} we obtain the closing line \overline{CG} , which is the amplitude of the resultant e.m.f. $E_{m(1-3)}$ of the considered group of sections. The instantaneous value of the e.m.f. of this group e_{1-3} for a given moment of time is represented by the projection of the resultant e.m.f. onto the ordinate axis. When the armature rotates, the polygon and consequently the vector of the resultant e.m.f. \overline{CG} also rotate with an angular speed of $\omega = 2\pi f$ counterclockwise; the instantaneous value of e.m.f., e_{1-3} , varies with time sinusoidally, passing through zero when \overline{CG} is perpendicular to the ordinate axis and attaining maximum at the moment when vector \overline{CG} is parallel to the ordinate.

B. Number of current paths for a simple lap winding. The winding diagram in Fig. 3-3, *a* may be represented as an electrical diagram of connections, depicted in Fig. 3-8. We see in

this case that the armature winding consists of four parts which we shall refer to as *current paths* or *paths*. Within the range of each path, the coil sections are connected *in series* and are located between two adjacent brushes of different polarity; thus for example, the path made up of sections 2-3-4 is located between brushes A_1 and B_1 , the path with sections 5-6-7 is located between brushes B_1 and A_2 and so on. If the brushes are set on the neutral then e.m.f.s of all coil sections forming the path are similarly directed (Fig. 3-3, *a*) and therefore may be added to form the e.m.f. of the path E'_a . Taken round the winding circuit, the e.m.f.s of any two adjacent paths *oppose* each other and are mutually balanced, if the e.m.f.s E'_a of both paths are equal in magnitude. But, in respect to the external circuit all winding paths operate in parallel, viz., through brushes A_1 and A_2 and then into the external circuit passes a current $2i_a + 2i_a = 4i_a$, where i_a is the current flowing through one path. From the external circuit the current $4i_a$ returns to the machine through brushes B_1 and B_2 . Considering Fig. 3-6 we may see, that the e.m.f. vectors of coil sections 1, 2, 3..., 7, lying under one pair of poles and constituting one pair of parallel paths, make up one e.m.f. polygon, while sections 8, 9, 10..., 14 lying under the second pair of poles make up the second pair of parallel paths and accordingly the second e.m.f. polygon.

This deduction may be generalised for the case of a machine having p pairs of poles. Reasoning along the same line, we may find that in *d. c. machines with a simple lap winding* the number of pairs of current paths " a " of the armature winding, defined by the number of e.m.f. polygons, is equal to the pole pairs p of

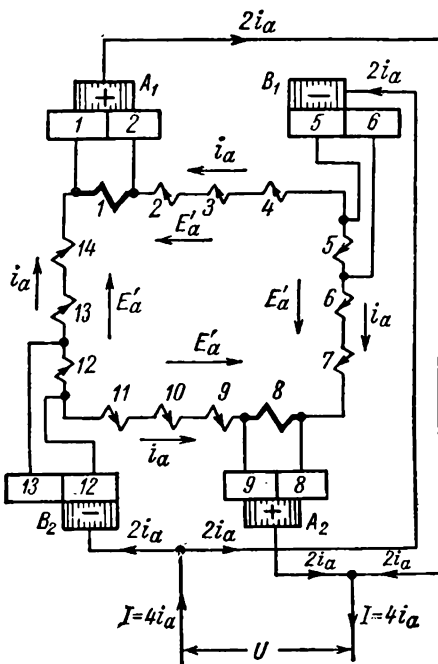


Fig. 3-8. Electrical diagram for winding in Fig. 3-3, *a*

the machine. Thus:

$$a=p \text{ or } 2a=2p. \quad (3-5)$$

This relation is one of the most important characteristics of a simple lap winding.

Conforming to the number of pairs of paths $a=p$ or number of e.m.f. polygons, as many pairs of brushes (brush studs) should be arranged at the commutator of a simple lap winding as there are pole pairs, all brushes of the same polarity being connected together electrically. If as before E'_a and i_a are the e.m.f. and current of one path, and E_a and I_a the e.m.f. and current, delivered to the external circuit by the machine or fed to it from the mains, then

$$E_a = E'_a \quad (3-6a)$$

and

$$I_a = 2ai_a. \quad (3-6b)$$

C. Voltage pulsations at the brushes. With a limited number of armature coil sections the voltage across the brushes will vary within a certain range, depending on the position of the armature

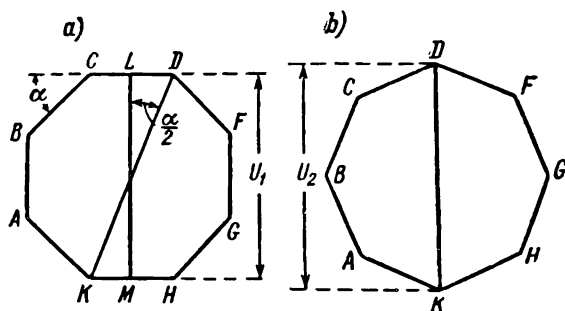


Fig. 3-9. Voltage pulsations at the brushes for an even number of coil sections in the armature winding paths

in the magnetic field. This is easy to deduct if the e.m.f. polygon in Fig. 3-6, *a*, *b*, *c* is considered. It is apparent that the voltage across the brushes varies (pulsates) within the range from U_1 in Fig. 3-6, *a* to U_2 in Fig. 3-6, *b*; then again it reaches the value of U_1 in Fig. 3-6, *c* and so on.

The pulsation of voltage across the brushes occurs in a much wider range, when the e.m.f. polygon consists of an even number of sides

(for example, eight, in Fig. 3-9, *a*, *b*). From the plotted drawing, it may be seen that

$$LM = U_1 = DK \cos \frac{\alpha}{2} = U_2 \cos \frac{\alpha}{2}.$$

The average voltage across the brushes is equal to half the sum of the U_1 and U_2 voltages, i. e.,

$$U_{av} = \frac{1}{2} U_2 \left(1 + \cos \frac{\alpha}{2} \right).$$

This voltage exceeds the U_1 voltage, but is less than the U_2 by the value $\Delta U = \frac{1}{2} U_2 \left(1 - \cos \frac{\alpha}{2} \right)$. The e.m.f. pulsations are defined by the ratio

$$\frac{\Delta U}{U_{av}} = \frac{\frac{1}{2} U_2 \left(1 - \cos \frac{\alpha}{2} \right)}{\frac{1}{2} U_2 \left(1 + \cos \frac{\alpha}{2} \right)} = \tan^2 \frac{\alpha}{4}. \quad (3-7)$$

It should be recalled [formula (3-4a)], that

$$\alpha = \frac{p2\pi}{S} = \frac{\pi}{S/2p},$$

where $\frac{S}{2p} = \frac{K}{2p}$ is the number of coil sections or commutator divisions per pole.

In Table 3-1 are given the values of $\frac{\Delta U}{U_{av}} \times 100 = f \left(\frac{K}{2p} \right)$. We may see, that already for $\frac{K}{2p} = 8$ the voltage pulsations are less than 1 per cent, i. e., they are practically negligible:

$$\frac{\Delta U}{U_{av}} \times 100 = f \left(\frac{K}{2p} \right). \quad (3-8)$$

Table 3-1

$K/2p$	1	2	3	5	8	15	30
$\frac{\Delta U}{U_{av}} \times 100$	100	17	7.2	2.5	0.97	0.28	0.07

If the e.m.f. polygon consists of an odd number of sides as in Fig. 3-6, then, reasoning along the same lines, we may find that the pulsation voltage has decreased almost fourfold $\left(\tan^2 \frac{\alpha}{8} \right)$.

The performed calculations of $\frac{\Delta U}{U_{av}}$ were based on using the fundamental harmonic only, but a more detailed analysis shows that for the usual values of the pole arc coefficient ($a' \approx \frac{2}{3}$), higher-order harmonics practically do not influence the e.m.f. pulsations.

If the armature is of the slotted type, the e.m.f. of the winding may include additional pulsations, caused by cross or longitudinal fluctuations of the magnetic flux.

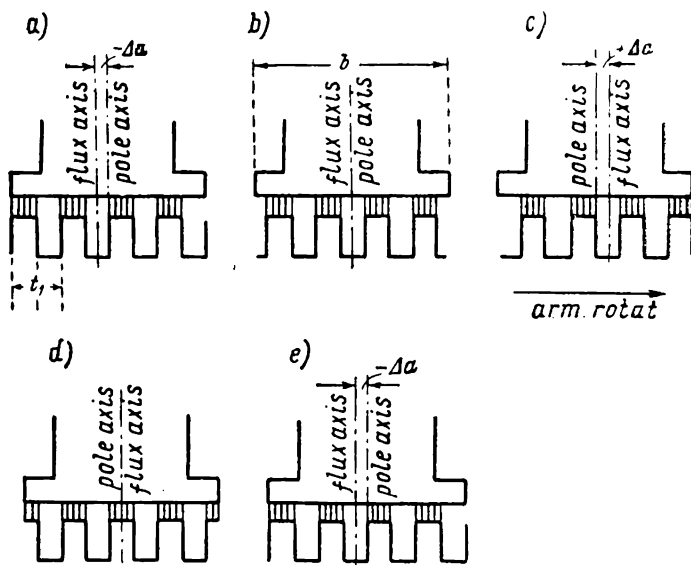


Fig. 3-10. Cross fluctuations of magnetic flux

Assume, that the pole shoe width b spans an *integral number* of tooth pitches t_1 , for example, $b=4t_1$ (Fig. 3-10). At the instant considered in Fig. 3-10, *a*, the flux axis is displaced in respect to the pole axis by a magnitude Δa against the direction of armature rotation ($-\Delta a$). For other consecutive instants, corresponding to the armature turning one tooth pitch (Fig. 3-10, *b, c, d, e*) the magnetic flux axis accomplishes one complete oscillation in the direction *across* the pole axis ($-\Delta a, +\Delta a, -\Delta a$). Such cross oscillations of flux cause additional pulsations of e.m.f. superposed onto the main e.m.f. of the machine and with a frequency of $f_t = Zn$. To weaken these pulsations it is recommended to skew either the armature slots per one tooth pitch along the axis of pole shoe, or the pole shoe edges leaving the armature teeth straight.

Suppose now that the tooth pitch cannot be integrally accommodated within the limits of the pole arc b , let for example $b = 3.5 t_1$ (Fig. 3-11). By comparing the two extreme positions of the armature in Fig. 3-11, a and b , we may see that when the armature rotates the axis of the magnetic flux occupies a permanent position in space, but the reluctance of the air-gap is continuously changed since under the pole shoe appear alternately four, and three, teeth. This causes *longitudinal* fluctuations of the magnetic flux to arise and corresponding e.m.f. pulsations with the same as in the previous case frequency, $f_t = Zn$. To decrease the longitudinal flux oscillations and the corresponding e.m.f. of the armature it is advisable to choose an odd number of slots per pairs of poles, since a change in magnetic reluctance under one pole is partially compensated by a change of reluctance under the other pole.

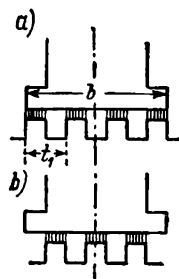


Fig. 3-11. Axial pulsations of magnetic field

D. Symmetry conditions for the ring-type armature winding. Considering the e.m.f. polygon in Fig. 3-6, a , we may observe that the geometrical sum of e.m.f. of each polygon is equal to zero. Physically this may be explained by the fact, that in each pair of paths lying under poles of different polarity, e.m.f.s equal in magnitude and opposing each other are induced in the winding circuit. This holds true for any position of armature in respect to the poles. In other words, with a symmetrical magnetic field, the e.m.f.s inside the winding are mutually balanced, independent of position of the armature in the magnetic field. As a result of this no circulating currents appear in the winding and for this reason such windings are called *balanced* or *symmetrical* windings.

From the above considerations it follows, that all path pairs of a symmetrical winding should comprise the same and also integral number of coil sections, i.e.,

$$\frac{S}{a} = \frac{K}{a} = \text{integer.}$$

This condition is of great importance, because if it is not fulfilled the various path pairs consist of different numbers of coil sections, and as a result of this e.m.f.s of various magnitudes would be induced, causing a circulating current to appear in the armature thus greatly complicating the operation of the machine.

3-5. Simple Wave Winding for a Ring Armature

Let $2p=4$ and $S=K=15$ (Fig. 3-12, a). According to formula (3-2) it follows that:

$$y_c = \frac{15 \pm 1}{2} = 7 \text{ or } 8.$$

Let us consider the first case and construct an e.m.f. star. The angle between two adjacent sections on the armature is determined by the formula (3-4 b):

$$\alpha = \frac{2 \times 360^\circ}{15} = 48^\circ.$$

This is also the angle of displacement of the e.m.f. vectors induced in coil sections 1, 2, 3, ..., 15 (Fig. 3-12, b).

To facilitate plotting of the e.m.f. star, we can make up a table of sections or commutator pitches, assuming that at the given instant, section 1 is in the neutral zone (Table 3-2).

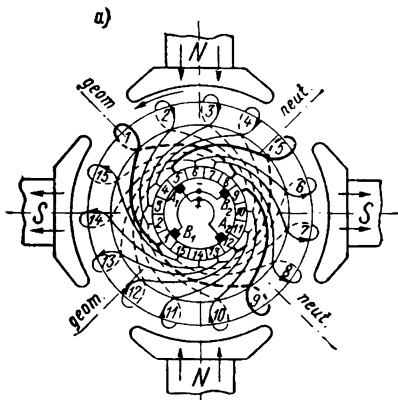


Fig. 3-12a. Radial scheme of simple-wave winding for a ring armature:
 $2p=4$; $S=K=15$

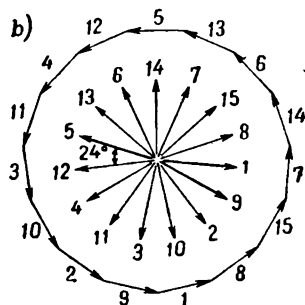


Fig. 3-12b. E.m.f. star and polygon for the winding in
Fig. 3-12 a

From this table it can be seen, that the e.m.f. star comprises 15 rays, each displaced from the one adjacent by 24° (Fig. 3-12, b). To assemble a simple wave winding it should be wound in the same sequence as the rays are plotted in the e.m.f. star. Let us assume coil section 1 as the initial coil and set it at the neutral so that its end connections are symmetrical in respect to the coil section. We shall denote the bar to which the start of section 1 is joined also by figure 1; then we must connect the finish of the coil section 1 to bar $1+7=8$, spanning a commutator pitch $y_c=7$. To bar 8 we join the start of coil section 8, which is under the right-hand south pole; spanning the next commutator pitch, we arrive

at bar $8+7=15$ and join to it the start of section 15, lying under the left-hand south pole next to coil section 1; continuing thus the assembling of the winding we connect in series first all coil sections arranged under both south poles, and then those under both north poles, closing the winding upon the initial section. The order in which the winding sections and the appropriate commutator divisions are connected is given in Table 3-3.

Table 3-2

Number of coil section and commutator bar	1	2	3	4	5	6	7	8
Angle of displacement (in electrical degrees)	0	48	96	144	192	240	288	336
Number of coil section and commutator bar	9	10	11	12	13	14	15	1
Angle of displacement (in electrical degrees)	$336+48=360+24$	72	120	168	216	264	312	0

Table 3-3

Sequence of Connections of Wave Winding Coil Sections and Commutator Bars

Under both south poles

Under both north poles

1—8—15—7—14—6—13—5—12—4—11—3—10—2—9—1

In accordance with the order in which the coil sections are connected we plot a regular, closed on itself, 15-sided polygon of e.m.f. (Fig. 3-12,*b*). Arranging the brushes on the geometrical neutrals (Fig. 3-12,*a*), we may represent the winding in Fig. 3-12,*a* as the electrical winding diagram of Fig. 3-13,*a*. We then see that the group of coil sections 12-4-11-3-10-2, lying under the north poles on the right-hand part of the e.m.f. polygon, forms one armature winding path, while the other group of coil sections —13-6-14-7-15-8, under the south poles of the left-hand part of the e.m.f. polygon forms the second armature winding path. Thus, in our case, the number of pairs of parallel paths, defined by the e.m.f. polygons is $a=1$, whereas the number of poles is $2p=4$. But the accepted method does not depend on the number of poles since with any number of poles all the sections under the poles of similar polarity are interconnected in series, thus forming one path, while the other path, also connected in series,

is made up of sections under all poles of the opposite polarity. Thus, *a simple wave winding has, independent of the number of poles, always only one pair of armature winding current paths and accordingly only one e.m.f. polygon.* Hence,

$$a=1 \text{ or } 2a=2.$$

This property of the simple wave winding is one of its most important features.

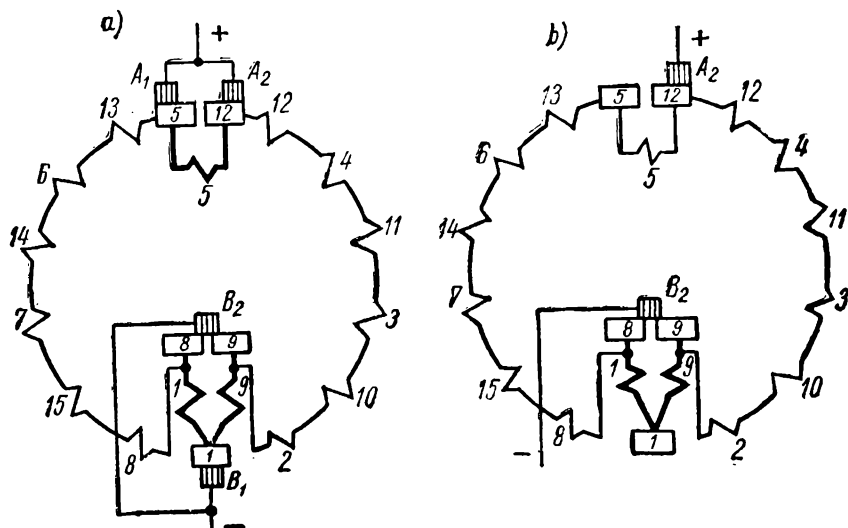


Fig. 3-13. Electric diagrams for the winding in Fig. 3-12 a

In accordance with the number of winding current paths we could limit the number of brushes to be arranged on the commutator to only two, for example the A_1 and B_1 . But nevertheless, a complete set of brushes (brush-holder arms), is usually arranged equal to the number of poles, as shown in Fig. 3-12, a.

Though this is usually done to distribute the current over a larger number of brushes and thus decrease the active length of the commutator, the main reason is to provide symmetry of both current paths. Actually, when arranging a complete number of brushes (Fig. 3-13, a) we have three coil sections, short-circuited by the brushes: sections 1 and 9 are short-circuited via brush B_2 , and section 5 by brushes A_1 and A_2 via the connection bus (in Fig. 3-12, a and 3-12, b the short-circuited sections and their e.m.f. are depicted by heavy lines). From the drawing it can be observed

that both winding current paths consist of six coil sections each, i.e., they are symmetrical.

If we would arrange only two brushes, say, A_2 and B_2 (Fig. 3-13,b), sections 1 and 9 would remain short-circuited, whereas section 5 would then belong to the left-hand winding path bringing the number of its coil sections to seven. This makes the paths non-symmetrical and their e.m.f. non-equal. It should also be taken into consideration that with a complete set of brushes coil sections 1 and 9, short-circuited by the brushes B_1 and B_2 , would be connected in parallel, but with only one brush B_2 they would be connected in series. In the latter case the commutation conditions would be aggravated (see § 5-9), this being wholly undesirable. For these reasons in machines with a simple wave winding only complete sets of brushes are used, with an exception only in those cases when insufficient place does not allow them one as, for instance, in small traction motors.

From the diagram in Fig. 3-13 it follows that for machines with a simple wave winding as for those with a simple lap winding, the voltage across the brushes is determined by the e.m.f. of only one current path, and the current delivered by the machine to the mains is the summated current of both paths [formulas (3-6a) and (3-6b)].

3-6. E.M.F. of Ring Armature

From previous considerations in § 3-4 and 3-5 it follows that independent of the type of winding, the voltage across brushes of different polarity is fixed by the sum of e.m.f.s of all coil sections

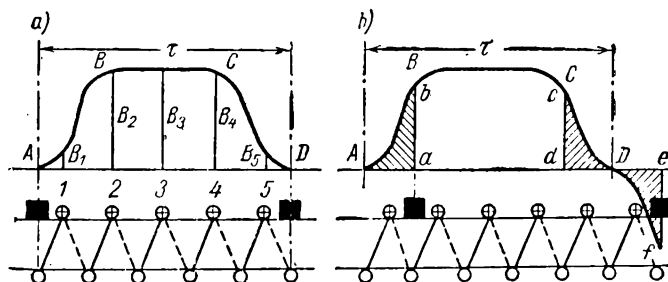


Fig. 3-14. E.m.f. of path for two cases:
a — brushes on neutral, b — brushes shifted from neutral

that make up, at the given instant, any one winding current path. Let us assume that the brushes are in line with the geometrical

neutrals (Fig. 3-14, *a*) and that the voltage across the machine terminals is of constant magnitude, since with a sufficiently large number of winding coil sections the voltage pulsations at the brushes are negligible.

When an armature rotates in a magnetic field, in any of the arbitrarily taken armature conductors an e.m.f. $e_x = B_x lv$ [formula (1-1)] is induced. If the winding consists of N conductors and makes up $2a$ current paths, then each winding path will consist of $N/2a$ conductors connected in series; for a lap winding these conductors are all located under one pole (Fig. 3-3), and for a wave winding are distributed under all like poles (Fig. 3-12*a*).

To obtain the voltage across the brushes E_a , it is necessary to add together the e.m.f.s of all conductors, constituting the winding current path. Thus,

$$\begin{aligned} E_a &= e_1 + e_2 + e_3 + \dots + e_{\frac{N}{2a}} = \sum_1^{\frac{N}{2a}} e_x = \\ &= \left(B_1 + B_2 + B_3 + \dots + B_{\frac{N}{2a}} \right) lv = \sum_1^{\frac{N}{2a}} B_x lv. \end{aligned} \quad (3-9)$$

With a sufficiently large number of coil sections $\sum_1^{\frac{N}{2a}} B_x = B_{av} \frac{N}{2a} = \text{const}$, where the average value of the flux density is

$$B_{av} = \frac{1}{\tau} \int_0^{\tau} B_x dx.$$

Then

$$E_a = B_{av} \frac{N}{2a} lv.$$

The armature speed is

$$v = \pi D n = 2\rho \frac{\pi D}{2\rho} n = 2\rho \pi n.$$

Hence,

$$E_a = B_{av} \frac{N}{2a} l 2\rho \pi n$$

or, as $B_{av} l \tau = \Phi$, we have finally:

$$E_a = p n \frac{N}{a} \Phi. \quad (3-10)$$

Here the flux Φ is the *useful magnetic flux*, i. e., the flux utilised in the armature for the creation of an e.m.f. If the brushes are set on neutral, as in Figs. 3-3, 3-12, *a* or 3-14, *a*, the useful flux is equal to the main flux, i. e., $\Phi = \Phi_0$. If we shift the brushes from the

neutrals (Fig. 3-14,*b*) the winding current path is made up of coil sections with e.m.f.s of different signs, and this is equivalent to a reduction in useful magnetic flux, by the value of the hatched areas Aab and $Ddc=Def$. The portion of the flux that is utilised is left unhatched (Fig. 3-14,*b*). It is obvious that if we had shifted the brushes half a pole pitch $\frac{\tau}{2}$, the useful flux Φ and the corresponding voltage across the machine terminals would become equal to zero.

3-7. Drum-Type Winding Assembling Principles

All modern d. c. machines employ the drum-wound armature, where the winding is arranged entirely on the outside of the iron armature core or drum. This type has completely superseded the earlier ring-wound type, because of greater efficiency and ease of manufacture. In the ring winding, over 50 per cent of the armature copper is ineffective in the production of voltage and the cooling is difficult, especially of the internal conductors. *To change a ring armature into a drum-type armature it is necessary, while maintaining the order of the connections between each of the coil sections and with the commutator, to bring the non-active sides, located inside the ring armature, to the outside surface in such an arrangement that both section sides cut the magnetic lines of flux.* Fig. 3-15 shows one drum-type armature winding coil section. Let us call the coil section parts lying in the slots the *active parts*, and those parts by means of which the active parts are joined together to the commutator as the *end connections* of the coil section or the overhang.

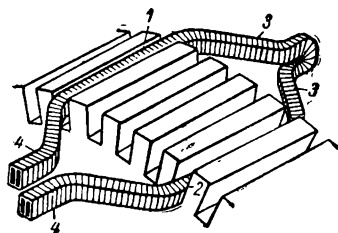


Fig. 3-15. Arrangement of drum armature winding coil section

Thus, the drum armature coil sections have *two* active sides, whereas the ring armature sections have only one active side. But since the winding connection order for the drum armature remains the same as for the ring winding, the fundamental winding types, i. e., the simple lap and simple wave windings and their characteristic features are the same in both cases. Therefore, the drum-type armature winding repeats the ring-type armature winding, but with better performance, and particularly, with better utilisation of the copper.

Let us consider the method of laying a coil section on the drum armature surface to obtain the best results from the point of view of e.m.f. creation.

In Fig. 3-16 are shown three section coils ab , ac and ad . The width of the first coil section is $y_1 = \tau$, of the second is $y_1 < \tau$ and of the third coil $y_1 > \tau$. The outline of the first coil section embraces the entire flux Φ , corresponding to the area denoted by $ABCD$, and the outlines of the second and third sections embrace only

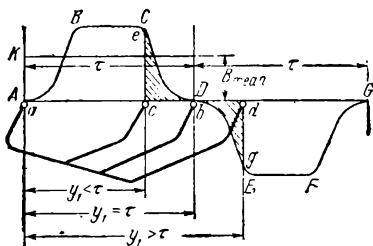


Fig. 3-16. Drum armature coil sections with full, short-chord and long-chord pitches

part of the flux, corresponding to the non-hatched part of the area $ABCD$. Hence the e.m.f. of section ab attains, with other conditions being equal, a maximum value, i.e., $e_{ac} < e_{ab} > e_{ad}$. Thus, the active sides of the drum winding coil sections should each be located at a distance equal, or approximately equal, to the pole pitch.

But in practice, only those windings are used that have either a full or diametrical pitch ($y_1 = \tau$) or a fractional or short-pitch (short-chord) ($y_1 < \tau$). Windings with a lengthened pitch are used only in rare cases, since they create the same e.m.f. as a short-pitch winding but call for more copper in the end connections.

Since on approaching the neutral zone the flux density in the air-gap abruptly decreases a small reduction (or increase) in pitch has a very small effect both on the diminution of the flux penetrating the section outline and on the winding e.m.f. But, at the same time, as we shall find out from a later chapter, such windings have a marked advantage in respect to current commutation (§ 5-10).

The second outstanding feature of the drum winding is that it is arranged as a *double-layer* winding, i. e., in which one active side of each coil section is located in the upper part of the slot, the other in the lower part (Fig. 3-15). If we were to arrange both section sides in one plane, then in such a single-layer winding the coil end connections would intersect, and this would necessitate bending them, which from design standpoint is very undesirable.

We refer to the layer nearer to the armature periphery as the *top* layer and the other as the *bottom* layer. Transition from one layer to the other takes place in the middle of the end connection, as shown in Fig. 3-15.

Thus the transition from a ring armature winding to a drum armature winding consists in withdrawing the inside non-active coil side of the ring armature and laying it on the outside surface of the drum armature at a distance equal, or approximately equal, to the pole pitch so that one side of the coil section occupies a place in the top slot layer, and the other in the bottom layer. This allows us to consider the drum winding as a ring winding which for a given number of coil sections has a double number of active sides.

3-8. Features of Drum Armature Winding

The main element of a d.c. machine drum type armature winding, as also of the ring armature, is the coil section. Let us recall that a coil section is that part of the winding which spans two successive, according to the winding diagram, commutator segments (3-3).

In the general case a section may comprise $w_s > 1$ turns and, each side may contain $w_s > 1$ conductors.

In Fig. 3-17, *a, b* two-turn coil sections for lap and wave windings are shown schematically, each coil side consisting of two

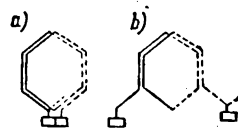


Fig. 3-17. Two-turn coil sections of windings:
a - simple lap; *b* - simple wave

conductors. The most simple are coil sections of one turn, widely used in machines of average and large output. When representing the diagrams we shall, as before, consider only one-turn coil sections and show the coil sides, in the top layer by thick lines, and in the bottom layer—by broken lines.

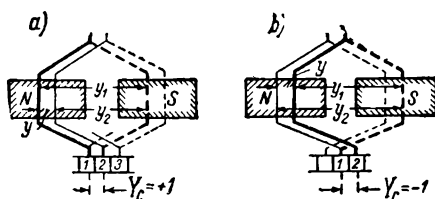


Fig. 3-18. Simple lap winding:
a - R.H. or progressive; *b* - L.H. or retrogressive

following the first is laid to the right side of the first coil and in the latter case to the left side. Therefore the winding in Fig. 3-18, *a* is often referred to as a *right-hand lead* winding or simply a *right-hand* (R.H.) winding and the winding in Fig. 3-18, *b* as a *left-hand lead* or *left-hand* (L.H.) winding.

The end connections may be of the *intersecting* or *non-intersecting* types. In Fig. 3-18, *a* and *b* both types of lap winding coil sections are shown. In the first case, the second section

To find out the type of wave winding it is necessary to make a complete round of the armature core and also of the commutator.

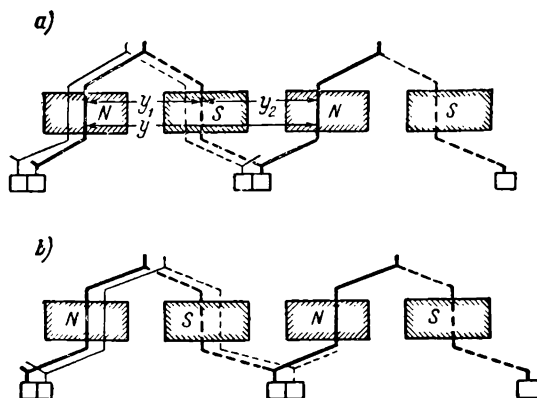


Fig. 3-19. Simple-wave winding:

a — L.H. or and *b* — R.H.

If then we arrive at the initial bar (Fig. 3-19,*a*), then the winding is of a non-intersecting type and if we pass the initial bar, the winding is of the intersecting type. The former is called a L. H. wave winding, the latter a R. H. wave winding.

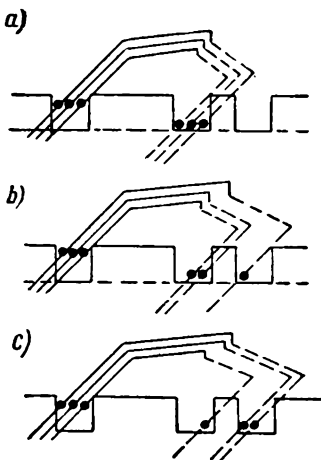


Fig. 3-20. Equisectional and stepped windings

As a rule, preference is given to the non-intersecting windings as they call for less copper to make up the end connections.

Depending on the method of making the end connections we distinguish windings: *a*) *equisectional* in which all coil sections are of equal dimensions (Fig. 3-20,*a*) and *b*) *stepped* windings in which the starts of any two sections are placed into one slot, whereas the ends occupy different slots and, consequently, the section end connections are alternately of different dimensions (Fig. 3-20, *b*, *c*).

The coil sections of the windings are made of round or rectangular cross-section copper conductors insulated with cotton tape, enamel, silk, etc.

When the number of coil sections is large but the number of slots is relatively small (machines of small and medium output), two, three and, in the general case, n coil sections are combined into a coil with a common, in respect to the slot, insulation.

Fig. 3-21 shows a lap winding coil, comprising three single-turn sections. Transposition from top to bottom layer is effected by bending the conductors at the centre of the coil end connections. The winding assembled in this manner is called a *coil winding*.

With large cross-section conductors the bending of the end connections is often very difficult. In this case a *bar winding* is used, each coil of which consists of two half-coils. When arranged in the slots the top and bottom sides of the half-coils are joined at the end connections by means of special soldered clamps. Fig. 3-22, *a* and *b* shows the half-coils, consisting of two single-turn lap and wave winding half-sections of the bar type.

To provide the proper shape of the coils, they are usually assembled on special coil forms.

The coils are laid in semi-closed oval or rectangular slots (Fig. 3-23, *a*, *b*). Fig. 3-23, *b*, *c* shows the way the 500 V coil slot part and end connection are insulated.

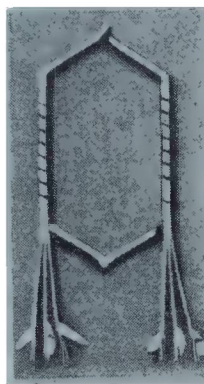


Fig. 3-21. Coil, consisting of three single-turn sections

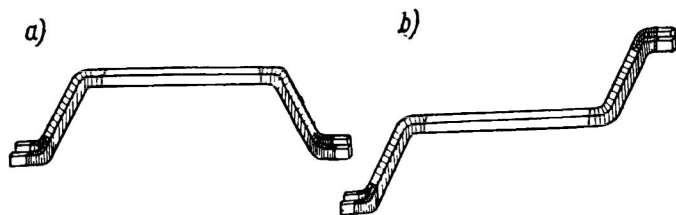


Fig. 3-22. Half-coils of bar-type winding:
a – lap winding; *b* – wave winding

The winding in the slot is braced either: *a*) with the help of wedges made out of hard wood (beech) or of insulation material, for instance, pressboard, or *b*) by means of steel wire bands laid

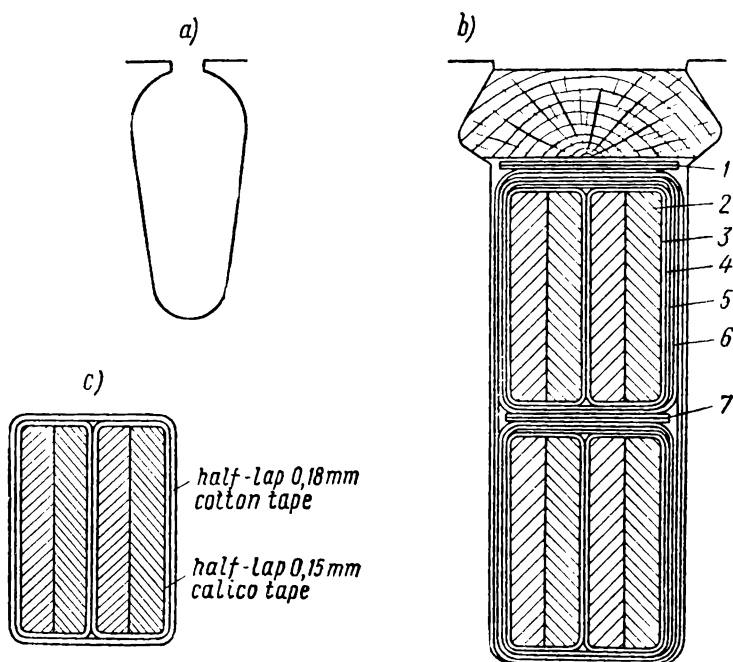


Fig. 3-23. Slot forms and armature coil insulation:
 1 — pressboard; 2 — copper; 3 — mica tape; 4 — mica foil; 5 — telephone paper; 6 and 7 — pressboard

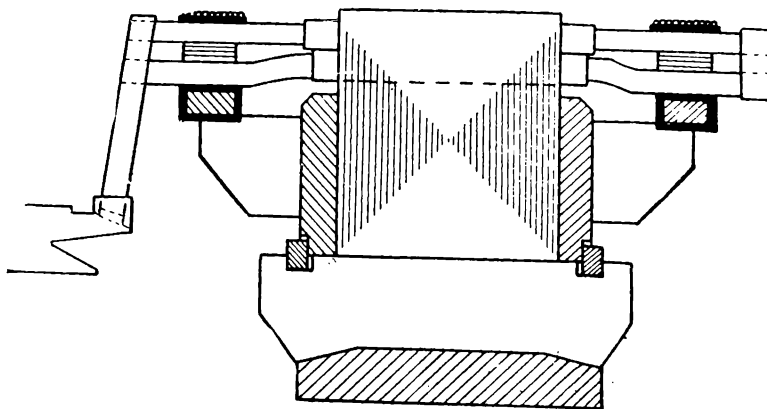


Fig. 3-24. Fixing of armature winding end connections

in special grooves provided in the armature steel stacking, so that the banding wire is flush with the armature core surface.

The end connections of the armature winding are fastened with the help of wire bandages (Fig. 3-24) that press the overhang toward the supporting surface. The part that holds the end connection is called the *winding-holder*.

3-9. Winding Pitches

To correctly assemble the armature winding in the armature slots and then join it to the commutator, it is necessary to know the pitches of the armature winding and the commutator.

A. Front winding pitch of armature. *The front winding pitch of the armature* or, in short, the front pitch y_1 is the distance between the first and second active coil sides of the same coil section (Figs. 3-18 and 3-19). According to the drum winding formulas this pitch should be equal or approximately equal to the pole pitch. In practice the pitch y_1 is generally defined by the number of real slots contained between two active coil section sides.

But for preliminary discussion of windings, however, it is more convenient to measure y_1 in so-called *elementary slots*, an elementary slot being termed a slot with two active coil sides in it (Fig. 3-25, a). Such slot assemblies are generally used in machines with a large path current i_a . If a real slot contains 4, 6, ..., $2u$ active sides, it may be divided into 2, 3, ..., u , elementary slots (Fig. 3-25, b and c). Since two active coil sides per slot, i. e., one elementary slot, corresponds to one coil section or one commutator division, then

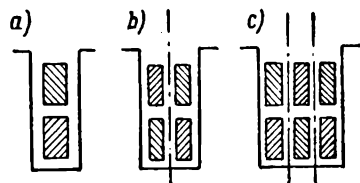


Fig. 3-25. Armature slots consisting of:

a — one, b — two, c — three elementary slots

to measure y_1 in so-called *elementary slots*, an elementary slot being termed a slot with two active coil sides in it (Fig. 3-25, a). Such slot assemblies are generally used in machines with a large path current i_a . If a real slot contains 4, 6, ..., $2u$ active sides, it may be divided into 2, 3, ..., u , elementary slots (Fig. 3-25, b and c). Since two active coil sides per slot, i. e., one elementary slot, corresponds to one coil section or one commutator division, then

$$S = K = Z_e, \quad (3-11)$$

where Z_e is the number of elementary slots.

One pole pitch contains $\frac{Z_e}{2p}$ elementary slots. But it often happens that $\frac{Z_e}{2p}$ cannot be divided by $2p$ without a remainder, whereas the assumed method of measuring the pitch y_1 requires that it must be equal to an integral number of elementary slots. To meet this requirement, we may shorten or lengthen the section pitch in

respect to the pole pitch by a fraction of an elementary slot so that:

$$y_1 = \frac{Z_e}{2p} \mp \epsilon = \text{integer.} \quad (3-12)$$

Since formula (3-12) ensues from a general formula for drum-type winding assembly, it holds good for any type of drum winding.

B. Back winding pitch of armature. The back pitch of an armature winding, or in short the back pitch y_2 is the *distance between the second active coil section side and the first active section side following the first, according to the diagram* (Figs. 3-18 and 3-19). The back pitch is also measured by the number of elementary slots spanned.

C. Winding pitch of the armature. The total winding pitch of the armature winding or in short the winding pitch y is the *distance measured in elementary slots between corresponding active sides* (i.e., sides lying either in the top or the bottom layers) *of two consecutive coil sections of the winding according to the diagram* (Figs. 3-18 and 3-19).

Between the front and back pitches and the winding pitch there exists a common, for both types of winding, relationship:

$$y_2 = y - y_1. \quad (3-13)$$

D. Commutator pitch. All deductions from previous discussion of the commutator pitch y_c for ring windings (§ 3-3) hold true for all drum-type windings. Hence,

A) for a simple lap winding (Fig. 3-18, *a*, *b*)

$$y_c = \pm 1; \quad (3-14)$$

B) for a simple wave winding (Fig. 3-19, *a*, *b*)

$$y_c = \frac{K \pm 1}{p}. \quad (3-15)$$

The top signs in the (3-14) and (3-15) formulas apply to non-intersecting windings, the bottom signs to intersecting windings.

Between the commutator pitch y_c and the total pitch y exists a direct relationship, resulting from the requirement that the *lead of the winding over the commutator periphery should correspond to the lead of the armature winding*. From the winding diagrams in Figs. 3-18 and 3-19 we may see, that in laying a coil section we make a throw, i.e., we span y_c commutator divisions over the commutator periphery and then at the same time pass a pitch, i.e., span y elementary slots over the armature periphery. To assemble a winding correctly these pitches must be in mutual alignment, i.e.,

the lead of the winding over the commutator should not lag or lead on the winding spanning the armature slots.

Since one elementary slot corresponds to one commutator division pitch [formula (3-11)] to obtain complete correspondence of the y_c and y pitches it is necessary that they should be numerically equal, i. e.,

$$y_k = y. \quad (3-16)$$

This formula, along with formula (3-12), holds true for any type of drum winding.

Let us consider some examples of simple drum-armature windings. The winding diagrams will be depicted in the developed form as this method is both simple and illustrative.

3-10. Examples of Simple Lap Winding

Example 1. To compare the ring and drum-type windings let us assemble a simple lap drum-type winding for the same data as stipulated for the ring armature in Fig. 3-3, viz., number of poles $2p=4$; number of armature coil sections and commutator divisions $S=K=14$. The number of true slots into which the winding is laid is $Z=14$; number of active sides laid across slot width is $u=1$; hence the number of elementary slots is $Z_e=Z=14$.

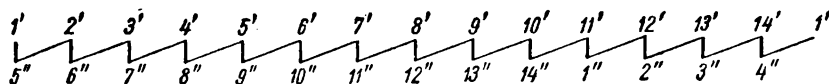
Assuming that the winding is R. H. with a lengthened pitch we have according to formulas (3-14), (3-16), (3-12) and (3-13):

$$y_c = y = +1; \quad y_1 = \frac{Z_e}{2p} \pm \varepsilon = \frac{14}{4} + \frac{2}{4} = 4; \quad y_2 = -3.$$

When assembling the winding we shall refer to the active coil section side in the top layer, i. e., the layer nearest to the armature periphery, as the *top section side* or its *start*, and the section side in the bottom layer as the *bottom section side* or its *finish*. The top section sides we shall depict by heavy lines, the bottom—by broken lines. In the same manner we shall denote by the same figures the numbers allotted to the coil sections, to the slot in which the top side of a coil section is laid and to the commutator bar to which the start of the coil section is joined. As there are two active sides lying in each slot, one in the top, the other in the bottom layer, we shall denote the top side by a number with a prime, the bottom side by the same number with a double prime, for example, the active sides in slot 5 will be denoted by numbers 5' and 5".

Let us begin assembling the winding with coil section 1, the start of which 1' we shall arrange, as stipulated, in slot 1 (Fig. 3-26). Let slot 1, at the considered instant, be at the south pole axis. We shall number the slots consecutively, from left to right. Since the pitch is $y_1=4$, the second, bottom side of coil 1 should be laid in slot $1+4=5$ and be denoted by number 5". The start of coil section 1 we shall connect to bar 1 and then number the commutator bars in the same consecutive order as the slots of the armature. The finish 5" of coil section 1 we shall join to bar 2 ($y_c=+1$) and this will terminate the laying of coil section 1 on the armature. The start 2' of coil 2 we then connect to bar 2 and lay into slot 2, and the finish 6" of this coil is joined to bar 3. In the same order we join up all other coil sections (Table 3-4).

Table 3-4



The active coil section sides and the end connections are usually arranged symmetrically in respect to the commutator bars to which the coil sections are joined but in machines of small output it is more convenient from the design standpoint to arrange the end connections at the commutator side non-symmetrically.

The brushes are arranged on the commutator the same way as in the case of the ring armature, along the *geometrical neutrals spaced at a precise uniform distance from each other*, i.e., in our case, a span of 3.5 commutator divisions (Fig. 3-26). But it should be noted that with a drum armature the neutrals at the armature and at the commutator are positioned differently. Thus, for example, in Fig. 3-26 the active sides of coil section 6 are located along the armature neutrals, whereas the neutral at the commutator, defined by the position of bars 6 and 7 to which the coil section is connected, is at the S pole axis or near it.

Now let us plot the e.m.f. star and the polygon of e.m.f. for the coil section active sides of Fig. 3-26. First we shall show the method of constructing the e.m.f. vectors of only one coil section, say, section 1 with sides 1' in slot 1 under the south pole and 5" in slot 5 under the north pole (Fig. 3-27, a). At the given moment side 1' lies exactly at the south pole axis. Therefore a maximum e.m.f. is induced in it, directed along the coil circuit from the commutator upwards. We shall denote this value by vector 1', that coincides with the positive direction of the co-ordinate axes (Fig. 3-27, b). In the second side of the coil section an e.m.f. is induced in the

direction along the coil circuit towards the commutator and downwards and if the coil section would have a full pitch, i.e., $y_1 = \tau$, then we would have to denote the e.m.f. of this side by a vector

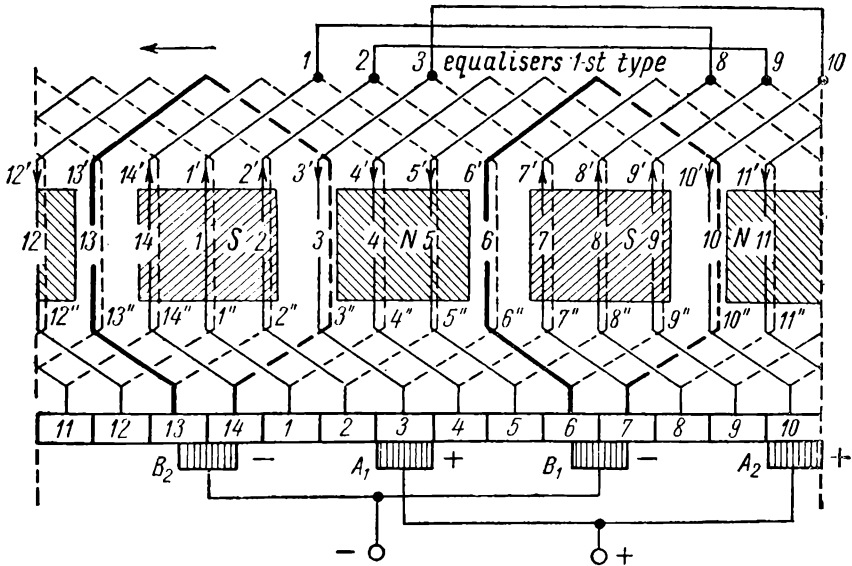


Fig. 3-26. Developed diagram of simple-lap winding: $2p = 4$; $S = K = 14$; $u = 1$; $Z_e = Z = 14$

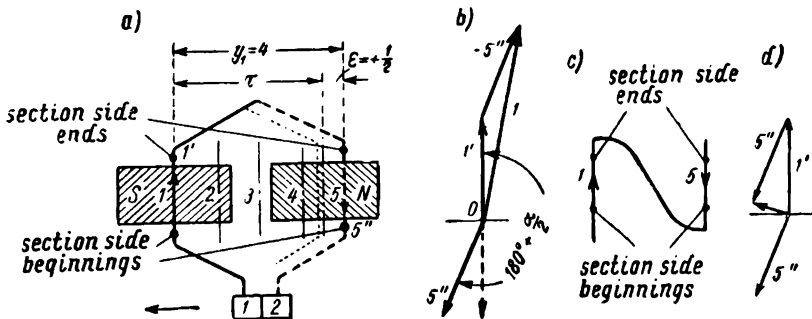


Fig. 3-27. Vector representation of coil section I sides e.m.f. for the winding in Fig. 3-26

equal in magnitude to vector $1'$, but set in the negative direction of the ordinate axis (the broken line in Fig. 3-27,b). Actually this coil section has a pitch lengthened by the value $\epsilon = \frac{1}{2}$, i.e., by

one-half of an elementary slot. Since the angle between two elementary slots, expressed in electrical degrees, amounts to

$$\alpha = \frac{p \times 360^\circ}{Z_e} = \frac{2 \times 360^\circ}{14} = 51\frac{3}{7}^\circ,$$

the distance between the active sides of the coil sections in slots 1 and 5 is determined by the angle:

$$4\alpha = 4 \times \frac{2 \times 360^\circ}{14} = 180^\circ + 25\frac{3}{7}^\circ = 180^\circ + \frac{\alpha}{2}.$$

Therefore the e.m.f. vector 5" should be turned by the same angle in respect to vector 1' in the direction against vector rotation (Fig. 3-27,b).

The procedures used with the e.m.f. vectors 1' and 5" to obtain the resultant coil section e.m.f. will depend on the way the sides of the coil section are connected. In electrical machines the coil sides are always connected as shown in Fig. 3-27,a, i. e., so that to the *finish* of the first side 1' is connected the *finish* of the second side 5"; in this case, when making the round of the coil we change the direction of the round, since we first pass from the start of coil side 1' to its *finish*, and then from the *finish* of coil side 5" to its *start*. Such a change in the making of the round of the coil corresponds to the procedure of geometrical subtraction of e.m.f. vectors 1' and 5" in Fig. 3-27,b; for this purpose we turn vector 5" by 180° and draw the vector 5" from the end of vector 1'; the closing line 1 is the resultant vector of the e.m.f. of coil section 1 and is equal to approximately double the value of the e.m.f. of a coil side for the case of concurrent action around the coil circuit of both coil side e.m.f.s.

If we were to connect the section sides in slots 1 and 5, as shown in Fig. 3-27,c, then when making a round of the section coil we would not change the direction of the round (*start* and *finish* of the first side and *start* and *finish* of the second side). In this case the procedure of geometrical summation of vectors carried out would mean that from the end of the first vector 1' (Fig. 3-27,d) a vector is drawn equal and parallel to the second vector 5". The closing line (resultant) obtained is very small in magnitude this conforming to the opposing action in the coil circuit of both coil sides of the e.m.f.

Referring to the method for connecting coil sides shown in Fig. 3-27,a we may plot the winding e.m.f. star of Fig. 3-26. The elementary slot 1 contains two active sides 1' and 1", in which e.m.f.s are induced equal in magnitude and coinciding in phase. Since at the instant considered slot 1 is exactly under the middle of the pole, the e.m.f. vectors 1' and 1" of these sides should

coincide with the ordinate axis (Fig. 3-28,a). For the assumed direction of armature rotation coil section 2 follows section 1, section 3 follows section 2 and so on. Therefore the e.m.f.s of these coil sections lag in phase on the e.m.f.s of section 1 and vectors $2'-2''$, $3'-3''$, etc., in the slot sides 2, 3 and so on should be turned in

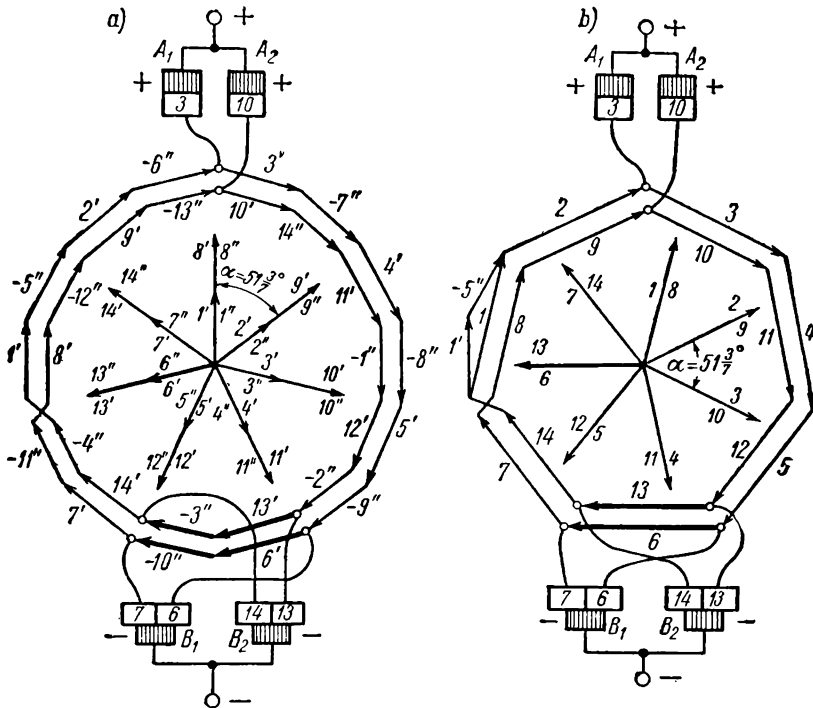


Fig. 3-28. Star and polygon of the winding e.m.f.s in Fig. 3-26:
a — coil section sides; b — coil sections

respect to vectors $1'-1''$ by an angle $\alpha = 51 \frac{3}{7}^\circ$ against the direction of vector rotation. Continuing the plotting we will obtain a seven-ray star of e.m.f.s of the active coil section sides first under the first pair of poles ($1'-1''$, $2'-2''$..., $7'-7''$), and then under the second pair ($8'-8''$, $9'-9''$..., $14'-14''$).

In accordance with the e.m.f. star we construct two polygons of e.m.f.s. of 14 sides each, each side successively displaced by an angle $\frac{\alpha}{2} = 25 \frac{3}{7}^\circ$. For convenience the polygons are drawn similar, though their sides should be equal. In plotting the polygon

we carry out the same procedure of geometrical subtraction for each coil as previously for coil 1 in Fig. 3-27,b; as a result we obtain vectors $1'$ and $-5''$, $2'$ and $-6''$, ..., $8'$ and $-12''$ and so on. Here also, depicted by thick lines, are given the vectors of the e.m.f.s of sections 6 and 13, short-circuited by brushes B_1 and B_2 (see winding diagram in Fig. 3-26).

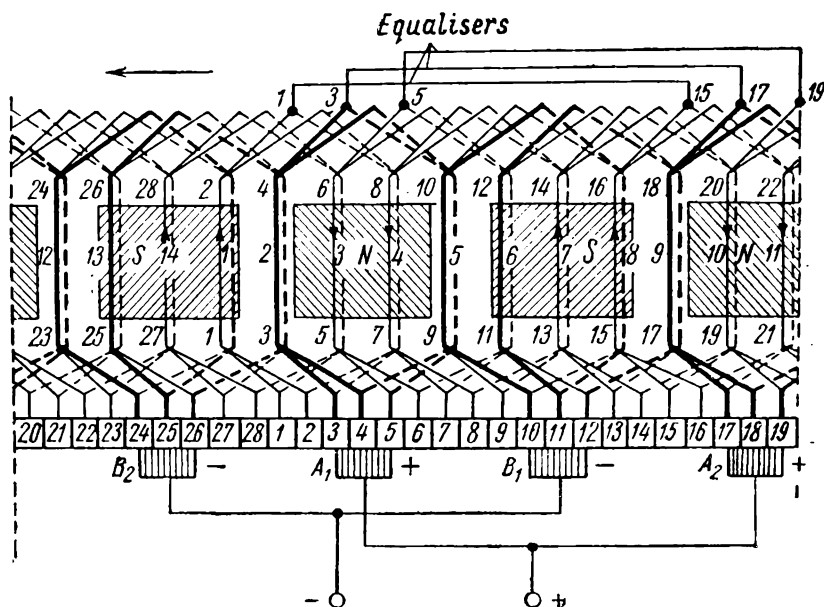


Fig. 3-29. Developed diagram of simple-lap equisectional winding: $2p = 4$; $S = K = Z_e = 28$; $u = 2$; $Z = 14$

From the e.m.f. polygon in Fig. 3-28,a we then arrive at the same conclusions, as from the analogous polygon in Fig. 3-6 for the ring armature. We see that the winding in Fig. 3-26 has two pairs of parallel current paths, i. e., $a = 2$ conforming to the number of polygons, each of the four paths consisting of three coil sections. The resultant e.m.f.s of all four paths are equal to each other and therefore there are no circulating currents within the closed upon itself winding; in other words the winding is a balanced winding.

It is possible to simplify the plotting of the star and e.m.f. polygon if we were to limit the procedure to depicting only the e.m.f. of the coil sections. In Fig. 3-28,b the plotting of vector 1 of section e.m.f. 1 given in Fig. 3-27,b is repeated. The vectors

2, 3 and so on, of the e.m.f. of the corresponding coil sections are each turned in respect to that of the adjacent coil by the angle $\alpha = 51 \frac{3}{7}^\circ$ in the direction against vector rotation. A 7-ray star is then obtained for sections 1, 2, ..., 7 onto which is superposed a second similar star for sections 8, 9, ..., 14. In conformance with the e.m.f. star, two e.m.f. septagons are plotted with each side consecutively turned by the angle $\alpha = 51 \frac{3}{7}^\circ$. Sections 6 and 13, short-circuited by brushes B_1 and B_2 , are distinguished by thick lines. This method of depicting only the coil section e.m.f.s has the advantage of simplicity and clarity.

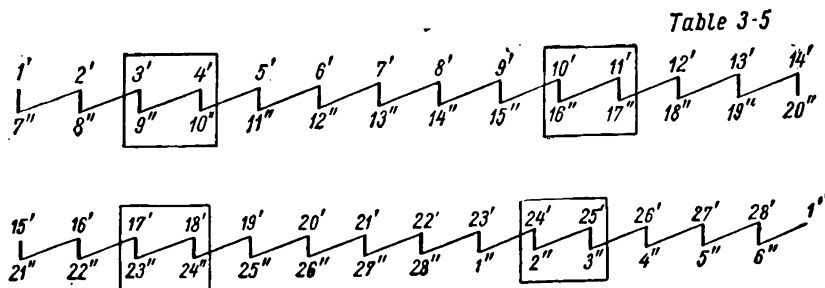
Example 2. Using the same notations as in example one, let us assemble a simple lap winding with the following data: $2p=4$; $S=K=Z_e=28$; $u=2$; $Z=14$.

If in each slot we lay side by side two or more active sides, the winding may be constructed as: a) equisectional, i. e., all sections of which are of equal dimensions (Fig. 3-20,a) or b) stepped when has the starts of two sections in one slot, and their finishes—in different slots (Fig. 3-20,b and 3-20,c).

We shall make our winding a R. H. equisectional, and fractional-pitch winding. In accordance with the winding formulas for a simple lap winding (§ 3-9) we have:

$$y_c = y = +1; \quad y_1 = \frac{Z_e}{2p} \mp e = \frac{28}{4} - \frac{4}{4} = 6; \quad y_2 = -5.$$

The developed winding diagram is given in Fig. 3-29. The figures in the middle horizontal row refer to numbers of true slots; the figures placed at the top and bottom of each true slot correspond to the numbers of the coil sections laid in the slot, or to the numbers of the elementary slots. Section sides are joined according to Table 3-5, in which the figures encompassed by rectangles correspond to the short-circuited coils.



The width of the brush is assumed equal to two commutator divisions.

Since the winding is equisectional, two coil sections, the top sides of which are in any one of the slots, have the bottom sides also in one slot (Fig. 3-20, *a*). Therefore the e.m.f.s of both of these coil sections are not only of the same magnitude, but also in phase.

We will restrict ourselves to the construction of the star and polygon e.m.f. only for the coil sections. At the instant con-

sidered, the top side 13' of coil section 13 lies in elementary slot 13 (true slot 7) exactly under the middle of the south pole; therefore we should depict the e.m.f. of this coil side by vector 13', superposed with the ordinate axis (Fig. 3-30, *a*). The second side of coil section 13 lies in the 13+6=19 elementary slot and is accordingly designated by the figure 19". As the angle of displacement of two adjacent elementary slots is

$$\alpha = \frac{p \times 360^\circ}{Z_e} = \frac{2 \times 360^\circ}{28} = 25 \frac{1}{7}^\circ,$$

the e.m.f. vector 19" should be turned in respect to vector 13' by $6 \times 25 \frac{1}{7}^\circ = 154 \frac{1}{7}^\circ = 180^\circ - 25 \frac{1}{7}^\circ = 180^\circ - \alpha$ against vector

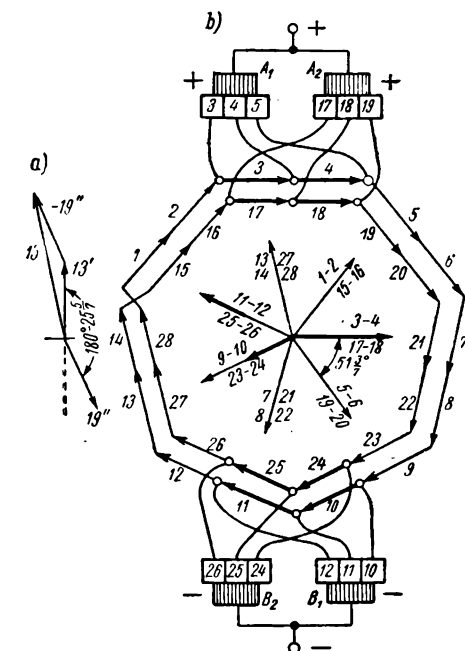


Fig. 3-30. Diagram of section e.m.f.s, star and polygon for the winding e.m.f. in Fig. 3-29

rotation. Carrying out the procedure of geometrical subtraction of e.m.f.s vectors 13' and 19", we obtain vector 13 as the resultant e.m.f. of the 13th coil section. After this we construct the star for section e.m.f.s. Vector 13 in Fig. 3-30, *b* we draw parallel to vector 13, Fig. 3-30, *a* (at a reduced scale). We superpose vector 13 onto vector 14, because coil sections 13 and 14 lie in the same slot. Coil section groups 15-16, 17-18 and so on, adjacent to sections 13-14 are each displaced in the direction against the rotation of vectors, by an angle corresponding to one true slot or two elementary ones, i. e., by $2\alpha = 51 \frac{1}{7}^\circ$. A 7-ray star of e.m.f. for the first pair of poles is thus obtained. Continuing the construc-

tion we obtain a similar star for the second pair of poles, superposed onto the first star.

In conformance with the e.m.f. stars we may plot two e.m.f. polygons, with each of its seven sides displaced by the angle $2\alpha = 51^\circ$ (Fig. 3-30, *b*). Sections 3-4 and 17-18 short-circuited by brushes A_1 and A_2 and sections 10-11 and 24-25 short-circuited by brushes B_1 and B_2 , are as before depicted by thick lines and shown joined to their respective commutator bars. The completed winding has two pairs of current paths corresponding to the two e.m.f. polygons, each path comprising five series-connected coil sections. The winding is balanced, because the resultant e.m.f.s of all four paths are equal.

Example 3. With the same data as in example 2, viz., $2p=4$, $S=K=Z_e=28$, $u=2$, $Z=14$ let us construct a R. H. simple full-pitch lap winding. In this case we have:

$$y_c = y = +1; \quad y_1 = \frac{28}{4} = 7; \quad y_2 = -6.$$

The developed winding diagram is shown in Fig. 3-31. The figures in the middle, bottom and top horizontal rows have the same

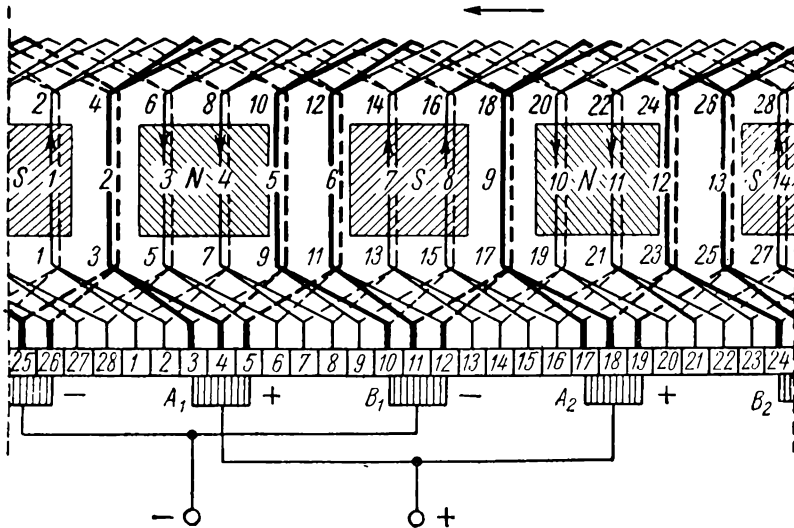
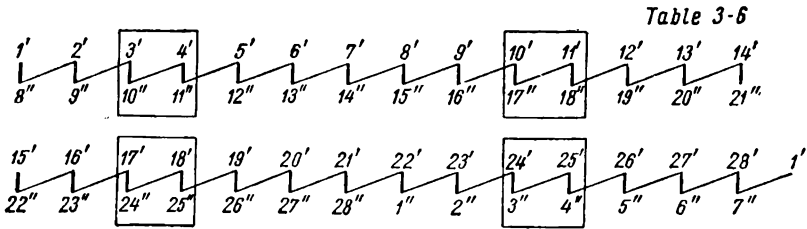


Fig. 3-31. Developed diagram of simple-lap stepped winding: $2p=4$; $S=K=Z_e=28$; $u=2$; $Z=14$

meaning as in the 2nd example. The section sides are joined up according to Table 3-6. The width of the brushes is assumed equal to two commutator divisions.



Let us plot the e.m.f. diagram for a pair of coil sections the top sides of which are laid in one of the true slots, for example, for coil sections 13 and 14, lying in the 7th true slot (Fig. 3-23,a). The

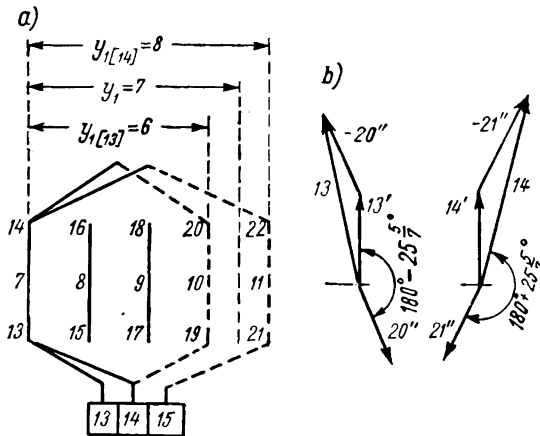


Fig. 3-32. Diagram of stepped winding coil section e.m.f.s

bottom coil section sides 13 and 14 must lie: the former in the 13+7=20 elementary slot or in the 10th true slot, the latter in the 14+7=21 elementary or the 11th true slot. Thus, we obtain a stepped winding, the pitch $y_{1(13)}$ of the 13th coil section of which is equal to three true slots, and the pitch $y_{1(14)}$ of the 14th coil section—to four true slots. As the angle between two adjacent true slots is

$$\alpha_{true} = \frac{p \times 360^\circ}{Z} = \frac{2 \times 360^\circ}{14} = 51 \frac{1}{7}^\circ,$$

the second, bottom section side 13 is displaced in respect to its top side by an angle $3 \times 51 \frac{1}{7}^\circ = 180^\circ - 25 \frac{1}{7}^\circ = 180^\circ - \frac{\alpha_{true}}{2}$,

and the second section side 14 by an angle $4 \times 51 \frac{1}{7}^\circ = 180^\circ + 25 \frac{1}{7}^\circ$. Conforming to this, the e.m.f. diagram of sections 13 and 14 (Fig. 3-32,b) is plotted in the usual way. Comparing the vectors of resultant e.m.f.s of coil sections 13 and 14, we may see that they are each displaced in respect to the other by an angle $\frac{\alpha_{true}}{2} = 25 \frac{1}{7}^\circ$.

The above conclusions may be extended to other coils, and then the star and polygons of section e.m.f. may be plotted (Fig. 3-33). The star has 14 rays, each ray consecutively displaced by an angle $\frac{\alpha_{true}}{2} = 25 \frac{1}{7}^\circ$. The polygons are accordingly of 14 sides (compare with 7 rays of the star, and 7 sides of the polygon for the e.m.f. of the equisectional winding in Fig. 3-30,b). The vectors of the e.m.f. of the coils short-circuited by the brushes, are depicted by thick lines. The conclusions that may be drawn from the e.m.f. polygon are the same as in the former example ($a=2$, with the winding balanced).

A stepped winding is from the design standpoint more complicated than the equisectional one, but its e.m.f. polygon more closely approximates a circle, and this facilitates better commutation. Therefore the stepped winding is used in d.c. machines of comparatively large output and with single-turn bar coil sections.

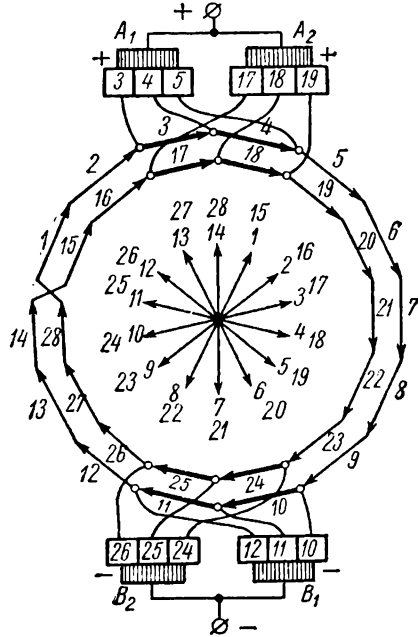


Fig. 3-33. Star and polygon of the winding coil section e.m.f. s in Fig. 3-31

3-11. Simple Wave Winding for a Drum Armature

All previously discussed pertaining to ring-type armatures also holds good for simple wave winding drum armatures (§ 3-5). It should be recalled, that when a drum-type armature winding is assembled the joining-up procedure remains the same

as for a ring winding; hence the second active coil section side may be considered as a complement to the first section and improving its performance without introducing substantial changes.

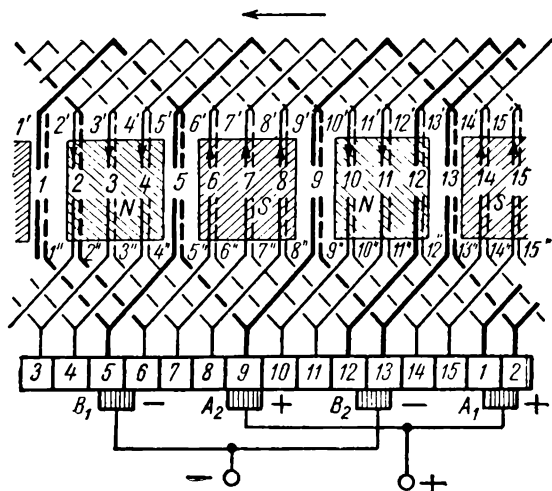


Fig. 3-34. Developed diagram of simple-wave winding: $2p=4$; $S=K=Z_e=15$; $u=1$; $Z=15$

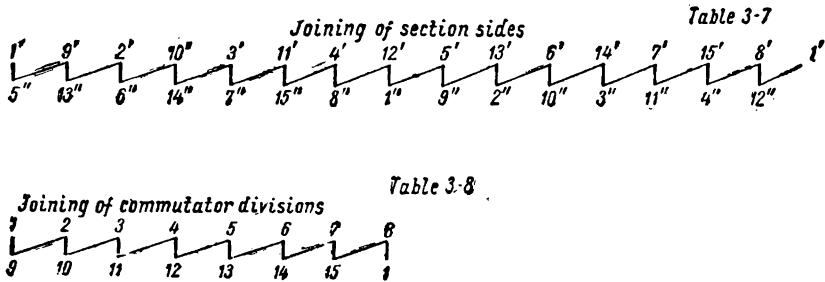
Let us assemble a simple wave R. H. (intersecting) winding with the same data as for the ring armature: $2p=4$, $S=K=Z_e=15$, $u=1$, $Z=15$ (Fig. 3-34). According to the formulas (3-16), (3-17), (3-12) and (3-14) we have:

$$y_c = y = \frac{K \mp 1}{p} = \frac{15 \mp 1}{2} = 8;$$

$$y_1 = \frac{Z_e}{2p} \mp \epsilon = \frac{15}{4} \mp \frac{1}{4} = 4;$$

then $y_2 = y - y_1 = 8 - 4 = 4$.

Let us start assembling the winding with the commutator bar 1, to which we shall join the start, i. e., the top side 1' of section 1, laid in slot 1. The second, bottom coil section side we lay into slot $1 + y_1 = 1 + 4 = 5$ and denoting it by figure 5'', we join the finish of the coil section to bar $1 + y_c = 1 + 8 = 9$; to this point we also join the start, i. e., the top side 9' of the adjacent (according to winding diagram) section 9, so that having spanned a commutator pitch y_c equal to eight commutator divisions the winding will span an armature pitch y equal to eight elementary slots. The further connection of section sides and commutator divisions is carried out according to Tables 3-7 and 3-8.



The brushes are set on the geometrical neutrals; the brush width is assumed equal to one commutator bar.

To construct the e.m.f. star let us plot the preliminary diagram of the e.m.f. of one coil section, say 7.

As the angle between two adjacent slots is $\alpha = \frac{2 \times 360^\circ}{15} = 48^\circ$, the second section side is displaced in respect to the first side by

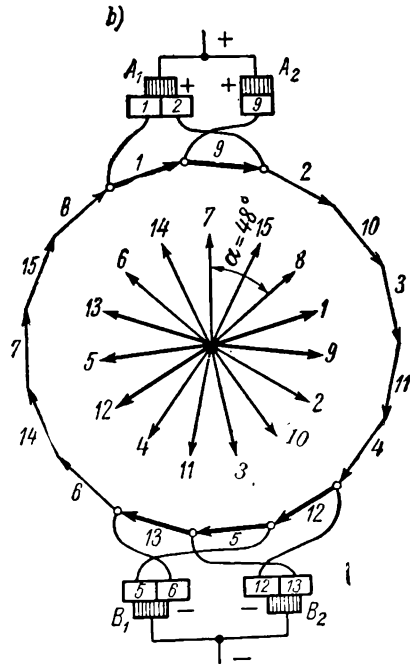
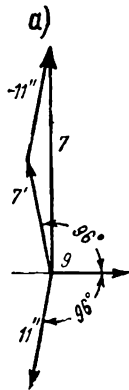


Fig. 3-35. Diagram of section e.m.f., star and polygon of the winding e.m.f. sections in Fig. 3-34

an angle $4 \times 48^\circ = 180^\circ + 12^\circ = 180^\circ + \frac{\alpha}{4}$. At the instant considered, slot 9 lies exactly on the geometric neutral line, and the slots

7 and 11, in which section 7 has been laid, are located symmetrically in respect to slot 9 each displaced in respect to this slot by an angle $2\alpha = 2 \times 48^\circ = 90^\circ + 6^\circ$. Hence, the diagram of section 7 e. m. f. has the form shown in Fig. 3-35, *a*.

The e.m.f. star and coil section e.m.f. polygon are built accordingly (Fig. 3-35, *b*).

Since the drum armature windings do not differ essentially from the ring armature windings (see § 3-7), all the deductions which were made in § 3-5 concerning the simple wave winding of the ring armature, refer in full to the simple drum-type armature winding. In particular, such a winding has only one pair of current paths independent of the number of poles, conforming to one e.m.f. polygon, i.e., $a=1$ or $2a=2$.

Also hold true the deductions pertaining to the number of brushes to be set on the commutator.

3-12. Special Types of Wave Windings

A. Wave windings with dead coils. From the formula $y_c = \frac{K \pm 1}{p}$ for a simple wave winding commutator pitch it can be seen, that for an even number of poles the number of commutator divisions K and consequently the number of coil sections S should be odd. If, however, it is of an even number of coils a simple wave winding with a so-called *dead* coil section is used.

Assume $S=20$ and $p=2$; if in this case we had $K=S=20$, then $y_c = \frac{20 \pm 1}{2}$ = fraction, and therefore, this winding is impracticable. To be able to arrange such a winding we leave $S=20$, but take $K=19$. In this case $y_c = y = \frac{19-1}{2} = 9$, $y_1=4$ and $y_2=y-y_1=9-4=5$. When assembling this winding (Fig. 3-36) 19 coil sections are joined in accordance with the commutator pitch $y_c=9$, but for the 20th coil, its ends are cut a short distance from the commutator and taped. The dead section 20 is indicated in the figure by a thick line.

B. Artificially-closed wave winding. It is given that $S=K=20$ and $2p=4$. To compute the pitches for an artificially closed wave winding we assume that S and K are one digit larger, i. e., $S=K=21$; hence $y_c = y = \frac{21-1}{2} = 10$, $y_1=5$ and $y_2=5$. In accordance with the pitch values obtained, make the first round of the commutator and of the armature (Fig. 3-37): bar 1—top side of coil section 1 in slot 1—bottom

side of the same section in slot 6—bar $1+10=11$ —top side of coil section 11 in slot 11—bottom side of the same section in slot 16; proceeding with the assembly of the winding we would have to come to bar $11+10=21$ which, however, does not exist. In this case we substitute the missing bar and its corresponding section by a conductor with the help of which we connect the bottom side of section 11 in slot 16 with commutator bar 10, adjacent to bar 11. After this the assembling of the winding is continued as usual but with one essential difference, that the commutator pitches and

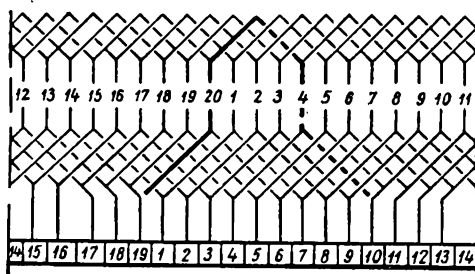


Fig. 3-35. Simple-wave winding with dead coil section

the resultant armature pitches are not equal, viz., $y_{c1}=10$ and $y_{c2}=9$; these pitches alternate, when the complete round of the armature and commutator is made.

C. Multiplex Single, Double and Triple Windings. In cases when it is necessary that the armature shall carry a very heavy current more than one winding may be used on the armature with an equal number of commutator bars for each. Both lap and wave windings may be so laid with one, two, or more entirely separate windings. Each brush must be thick enough to always touch two or more commutator bars so that all windings will always be connected to the brushes and deliver or receive current uniformly.

Meaning of the Term Re-entrant. A winding is often said to be single or double reentrant. In the case of a single winding, this means that the winding closes on itself or returns to the beginning point after being traced through all the coils upon passing once round the armature core. A winding is doubly reentrant if it only reenters itself after making two passages around the coils of the armature. A single winding may be either single reentrant or double reentrant.

In the case of double and triple windings, the term reentrant is sometimes used in an improper sense. For this reason it is ad-

visible to specify types of armature winding by the number of separate windings used. Thus a single winding should be specified as a single closed; two windings as double closed and three

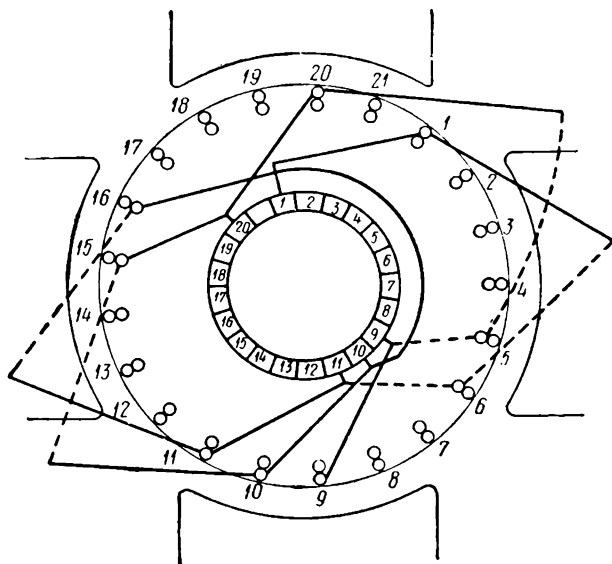


Fig. 3-37. Artificially-closed simple wave winding

windings as triple closed, etc. A winding made up of two single windings, each of which reenters itself, will therefore be a double-closed winding not a "double-reentrant" one.

3-13. Multiplex Lap Winding

A multiplex lap winding is a winding the commutator pitch of which is $y_c = m$, where $m = 2, 3, \dots$ and so on (integer). In practice, however, only those multiplex lap windings are used for which $m = y_c = \pm 2$.

In accordance with the principle of conformity of the direction of winding for both commutator and armature (§ 3-9, *D*) we have:

$$y = y_c = \pm 2. \quad (3-17)$$

Here y is the resultant armature winding pitch, measured, as in the case of a simple lap winding, by the number of elementary slots spanned.

According to the formula for assembling a drum winding, the front pitch of any type of winding, in particular a multiplex lap winding, should be equal or approximately equal to the pole pitch.

Hence,

$$y_1 = \frac{Z_e}{2p} \mp \epsilon. \quad (3-18)$$

The back pitch of the winding is $y_2 = y - y_1$. (3-19)

If the commutator comprises an even number of commutator divisions, then for $y_c = 2$ we get two similar independent windings. Consider $K = 20$; beginning the assembly of the winding with division 1 we join together only the odd commutator divisions 1-3-5 ... 19-1 and then close the winding, arranging it into the odd armature elementary slots.

Then we assemble the second winding, joining together only the even-numbered commutator divisions and close the winding, using only the even-numbered armature slots. Such a winding is a *multiplex double-closed winding*.

With K an odd number, for instance $K = 19$, the order of winding assembly is: 1-3-5 ... 19-2-4 ... 18-1, i.e., we first connect all the odd-numbered commutator divisions and make the first round of the commutator and then, without a break in the winding, make a second round of the commutator and then close the winding by joining together all even-numbered commutator divisions. Such a winding is a *multiplex single-closed winding*. Until quite recently the former type was generally preferred because it met the requirement of winding symmetry (see § 3-15). But recent practice has shown that the multiplex single-closed windings used in large machines give quite satisfactory service, notwithstanding their asymmetry.

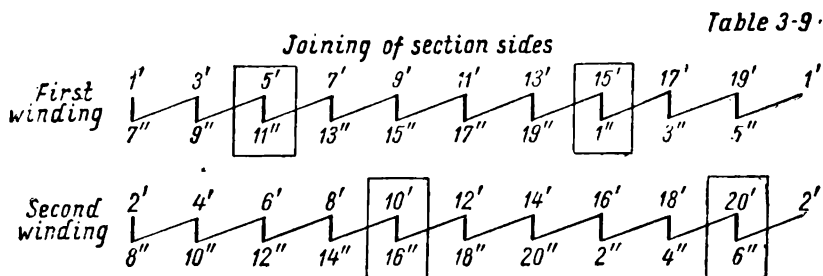
Consider two examples of the multiplex lap winding.

Example 1. Let us assemble a multiplex lap winding for the following data: $2p = 4$, $S = K = Z_e = 20$, $u = 1$, $Z = 20$. We assume a R. H. winding with a lengthened pitch.

According to the previously discussed formulas we have:

$$y_c = y = +2; y_1 = \frac{Z_e}{2p} \mp \epsilon = \frac{20}{4} + 1 = 6; y_2 = -4.$$

The winding diagram is shown in Fig. 3-38. This diagram shows the slot numbers and the corresponding coil sections 1, 2, 3 ..., 20, but the slot active sides, as, for instance, 1'-1" in slot 1 or 2'-2" in slot 2 and so on, are not shown for clarity sake. Coil section sides are joined together in the order given in Table 3-9. The brush thickness is equal to two commutator divisions.



Since at the instant considered, the slots 3 and 13 are under the centres of the corresponding north poles, the e. m. f. vectors $3'-3''$ and $13'-13''$ coincide with the ordinate axis

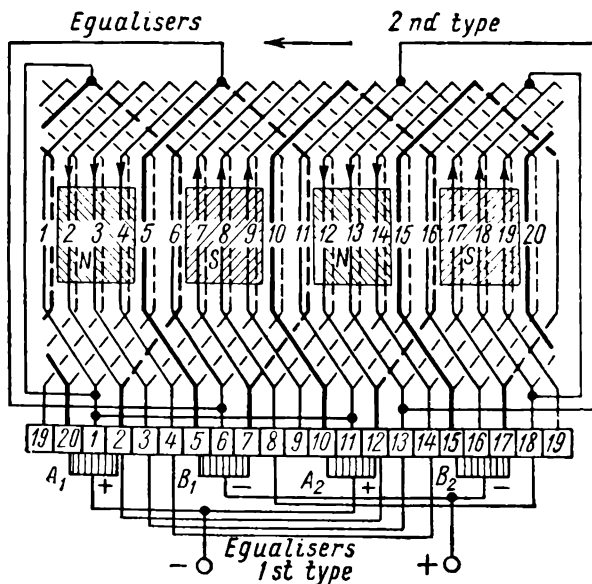


Fig. 3-38. Complex lap double-closed winding with long-chord pitch: $2p=4$; $S=K=Z_c=20$; $u=1$; $Z=20$

(Fig. 3-39, a). For the given direction of armature rotation the e. m. f. vectors follow each other in the order 1-2-3 and so on. The second star corresponding to slots 11-20 is superposed onto the first e. m. f. star corresponding to slots 1-10;

The e. m. f. diagram of one coil section, for example, coil section 3, is shown in Fig. 3-39, b. The construction is carried out as

usual, provided that the displacement angle between two adjacent slots $\alpha = \frac{p \times 360^\circ}{Z_e} = \frac{2 \times 360^\circ}{20} = 36^\circ$ and the second — lower — side of section 3 is in slot $3+6=9$, i. e., is shifted relative to the upper side of the same section by $6\alpha = 6.36^\circ = 180^\circ + 36^\circ$.

The e.m.f. polygons of the coil sections are shown in Fig. 3-39, c. The construction procedure is the same as that previously discussed (see Fig. 3-28, a). Two polygons correspond to each winding: the two outside ones of the first winding which is composed of the odd-numbered coil sections, and the two inner ones pertaining to the second winding, comprising the even-numbered

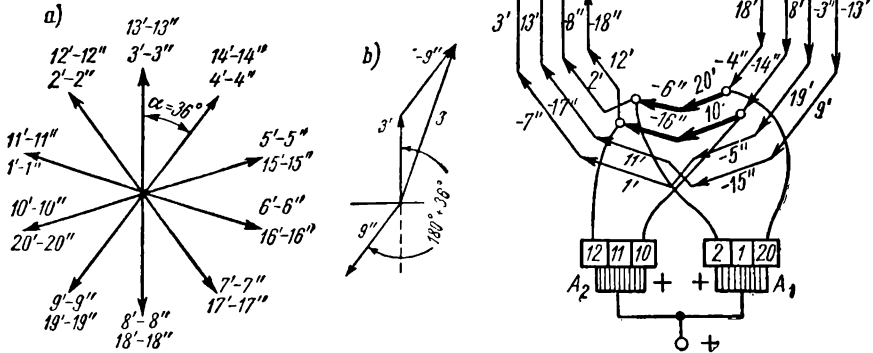


Fig. 3-39.

a — star of section side e.m.f.s; b — diagram of section coil e.m.f.s; c — polygon of the winding section sides e.m.f.s in Fig. 3-38

coil sections. Since to each e.m.f. polygon corresponds one pair of armature winding current paths, in respect to the brushes there are eight parallel current paths. Thus, in comparison with a simple lap winding, the number of paths of a multiplex double-closed lap winding with a commutator pitch of $y_c=2$ is doubled, i. e.,

$$a=2p \quad \text{or} \quad 2a=2 \times 2p. \quad (3-20)$$

It is this relationship, a special feature of the multiplex winding, that allows it to be utilised in large-current machines, such as those used, for example, in electrolysis techniques.

Considering the e.m.f. polygons in Fig. 3-39, *c*, we may see that the resultant e.m.f.s of all paths are equal both in magnitude and in direction; hence with a symmetrical magnetic field there are no circulating currents in the winding, in other words, the winding is balanced.

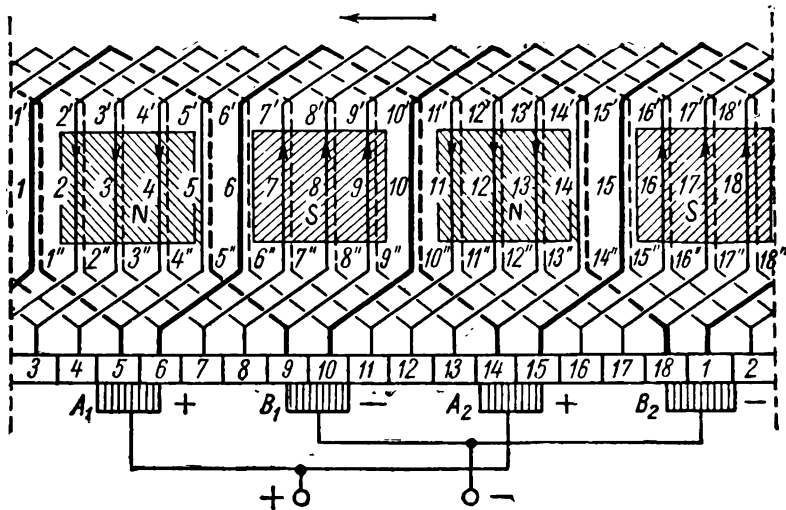


Fig. 3-40. Complex lap double-closed full pitch winding: $2p=4$; $S=K=Z_e=20$; $u=1$; $Z=20$

Example 2. Let us assemble a R. H. multiplex lap winding with the same data as in the first example: $2p=4$, $S=K=Z_e=20$, $u=1$ and $Z=20$, but for a full pitch.

In this case we have,

$$y_c = y = 2; \quad y_1 = \frac{Z_e}{2p} \mp \epsilon = \frac{20}{4} = 5; \quad y_2 = -3.$$

The winding diagram is depicted in Fig. 3-40 for the same time instant as in the first example. The diagram of section 3 e.m.f. in this case is as given in Fig. 3-41, *a*; the coil section side e.m.f. star is the same as in Fig. 3-39, *a*. The e. m. f. polygon construction is given in Fig. 3-41, *b*; it is then necessary only to number the sides of the polygon, denoting the coil sections. We may see then, that two polygons correspond to each winding, but the po-

lygons of both windings are displaced in respect to each other by an angle:

$$\alpha = \frac{2 \times 360^\circ}{20} = 36^\circ.$$

Comparing the polygons in Fig. 3-39, *c* and 3-41, *b*, we see that in the first case the polygons of both windings are similarly positioned in respect to each other, whereas in the second case they are positioned differently. This gives winding in Fig. 3-38 such a marked advantage in current distribution between the armature paths, that the winding in Fig. 3-40 becomes unsuitable in practice (§ 3-16, C).

3-14. Multiplex Wave Winding

In a multiplex wavewinding after making one round of the commutator we arrive at the commutator division not adjacent to the initial division, but removed from it by 2, 3 ..., m divisions. In this case we may obtain 2, 3 ..., m windings, each of which is a simple wave winding with $a=1$ current paths. Hence, all the m windings have $a=m$ pairs of paths. Reasoning, as in § 3-3, we have:

$$y_c = \frac{K \mp m}{p} = \frac{K \mp a}{p}. \quad (3-21)$$

In accordance with formulas (3-16), (3-12) and (3-13) we may determine the armature pitches:

$$y = y_c; \quad (3-22a)$$

$$y_1 = \frac{Z_e}{2p} = \mp \varepsilon; \quad (3-22b)$$

$$y_2 = y - y_1. \quad (3-22c)$$

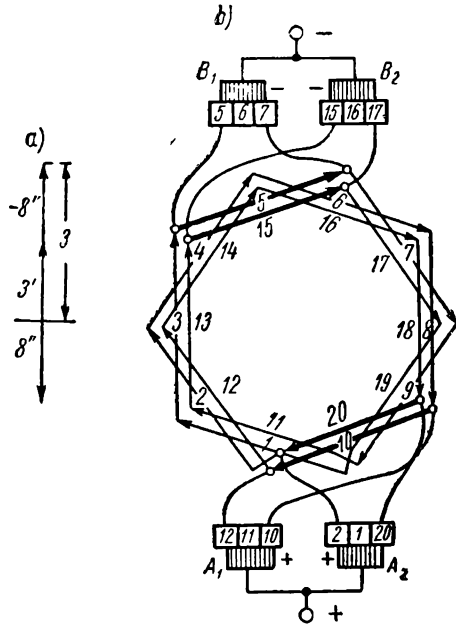


Fig. 3-41. *a* — diagram of coil section e.m.f.;
b — polygon of coil section e.m.f.

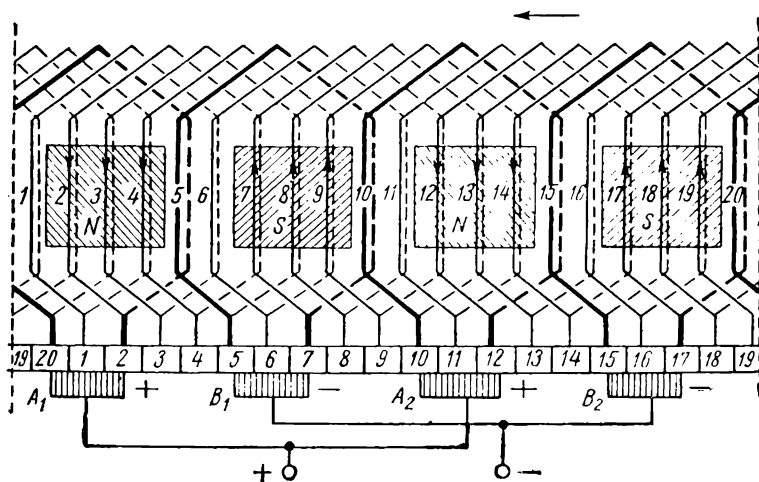


Fig. 3-42. Developed diagram of complex double-closed wave winding with short-chord pitch: $2p = 4$; $S = K = Z_e = 18$; $u = 1$; $Z = 18$

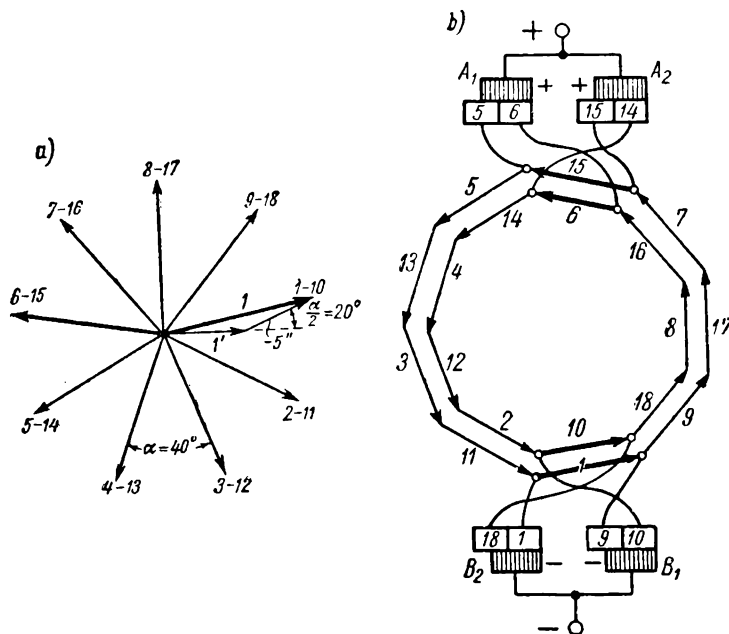


Fig. 3-43. Star (a) and polygon (b) for the winding sections in Fig. 3-42

A multiplex wave winding, like the multiplex lap winding, may be a multi-closed or single-closed winding. The former is the case when the pitch y_c and pairs of paths $a=m$ have a greatest common measure t ; the winding may then be decomposed into t single-closed windings. The second case is when both y_c and $a=m$ are mutually prime numbers, i.e., when their greatest common measure is $t=1$. For example, let us assemble a multiplex wave double-closed progressive winding with the following data: $2p=4$, $S=K=Z_e=18$, $u=1$, $Z=18$, $a=m=2$.

With the help of the previously given formulas we may obtain:

$$y_c = y = \frac{K \mp a}{p} = \frac{18 - 2}{2} = 8;$$

$$y_1 = \frac{Z_e}{2p} \mp \epsilon = \frac{18}{4} - \frac{2}{4} = 4;$$

$$y_2 = y - y_1 = 8 - 4 = 4.$$

The winding diagram is represented in Fig. 3-42. The section sides are joined up in the order shown in Table 3-10.

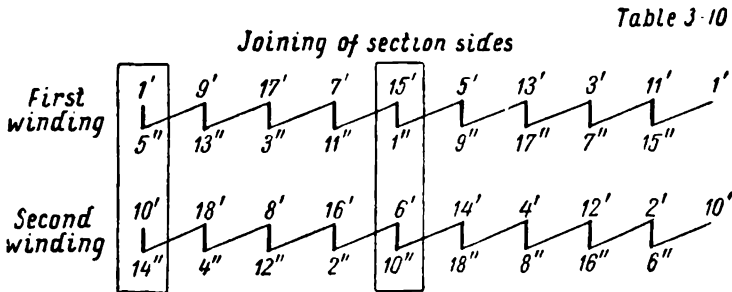


Fig. 3-43, *a, b* shows the coil section e.m.f. star and polygons. For coil section sides *1* the e.m.f. diagram is plotted as usual, assuming at the considered instant that the slot *1* is on the geometrical neutral and the armature rotation is in the appointed direction of Fig. 3-42. From the e.m.f. polygon it can be seen that there are two pairs of current paths, i.e., that $a=m=2$. The e.m.f. of both windings are identical, therefore the windings are mutually balanced.

3-15. Conditions for Armature Winding Symmetry

Previously (§ 3-4, D) the conditions of symmetry for the ring winding were stated, namely, that all pairs of paths of the winding must be made up of the same integral number of coil sec-

tions, i. e.,

$$\frac{S}{a} = \frac{K}{a} = \text{integer.} \quad (3-23)$$

This condition is applicable also to drum-type windings; but the coil section of a drum armature comprises one turn or two conductors; therefore, the least number of conductors of the armature winding is $N=2S=2K$ and $\frac{S}{a} = \frac{2S}{2a} = \frac{N}{2a}$; in other words, if the condition $\frac{S}{a} = \text{integer}$ is met, each path of the drum-type armature winding comprises the same number of conductors.

The arrangement of the winding in the slots demands one more condition, namely, that the winding paths be symmetrically positioned in the magnetic field. This condition is met if:

$$\frac{Z}{a} = \text{integer}; \quad \frac{2p}{a} = \text{integer.} \quad (3-24)$$

To provide for the symmetry of a simple lap winding it is sufficient that only the first two conditions were met, viz.: $\frac{S}{a} = \text{integer}$ and $\frac{Z}{a} = \text{integer}$, since the third condition $\frac{2p}{a} = \text{integer}$ is fulfilled as a matter of course.

Of all the multiplex lap windings only the double-closed winding with $m=2$ can be symmetrical. When $m>2$ the condition $\frac{2p}{a} = \text{integer}$ is not fulfilled.

The larger the dimensions and output of the machine, the greater the necessity for fulfilling the conditions of armature winding symmetry.

3-16. Equalisers

A. Equalisers of the first type. Equalisers or equipotential connections of the first type are used in simple lap windings for equalising the potentials in the winding paths, lying under like poles. Practice has proved, that even when all conditions for winding symmetry are observed exactly, the e.m.f. of the separate paths may be different. This is due to various reasons, such as inequality of air-gap under various poles, asymmetry in the arrangement of brushes on the commutator, the eccentricity of the armature in respect to rotation axis, flaws in the cast yokes, etc.

This inequality of the e.m.f. in the separate paths produces a circulating current that flows through the winding from points of higher potential to points of lower potential.

The circulating currents act as additional loads on the winding and brushes, hence the performance is impaired causing additional copper losses, additional heating; the result is lower efficiency of the machine.

Consider a ring armature with a simple lap winding for which $2a=2p=4$.

If all the winding paths operate symmetrically, the same e.m.f., for instance, $E_a=100$ V would be induced in each path and through each path a current of the same magnitude, for example, $i_a=200$ A (Fig. 3-44, *a*) would flow; the corresponding current in each path is then equal to 400 A and the current in the external circuit would total 800 A.

Now, suppose that the air-gap under the top pair of poles has become somewhat larger than under the bottom pair of poles and because of this the e. m. f. s induced in the top and bottom pairs of paths are of different values, for example, across the top pair of paths $E_{a1}=99$ V, and across the bottom pair $E_{a2}=101$ V. Under these conditions the negative brushes will remain equipotential, but between the top and bottom positive brushes there appears a difference in e. m. f. equal to $101-99=2$ V. This e. m. f. difference gives rise to a circulating current which flows in the armature winding in the direction shown in Fig. 3-44, *b* by arrows at the inner side of the armature and will close through the positive brushes and the connecting bus-bar between them. Suppose the resistance of one path of armature winding is $r_a=0.01$

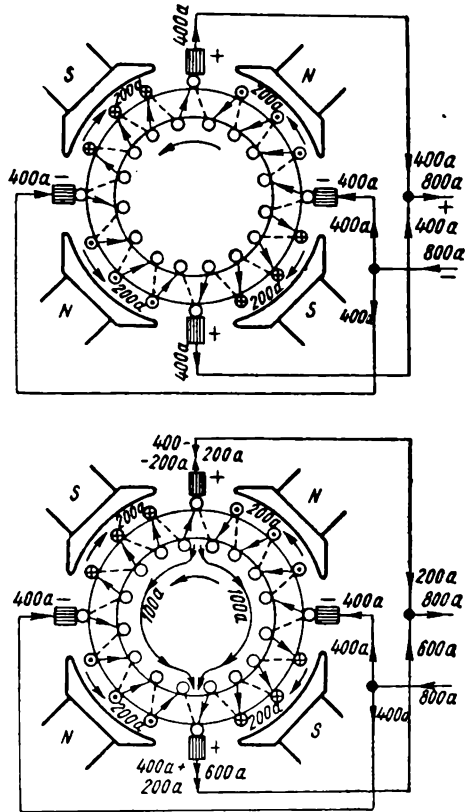


Fig. 3-44. Distribution of current in armature winding:

a — with balanced winding path e.m.f.s; *b* — with unbalanced winding path e.m.f.s

ohm; then the resistance of each half of armature winding through which the current circulates equals $2r_a=0.02$ ohm; hence through each of the winding halves flows a circulating current $i_c = \frac{2}{0.02} = 100$ A, and the circulating current through each positive brush is 200 A. If the machine delivers to the external circuit 800 A, then as may be seen from the diagram in Fig. 3-44, *b*, the circulating current decreases the load of each of the top winding paths down to $200-100=100$ A, and overloads each of the lower paths up to $200+100=300$ A. Accordingly the top brush load falls to $400-200=200$ A, and the bottom brush load is increased to $400+200=600$ A, i. e., 50 per cent overload. This may cause sparking at the commutator. Besides, the winding copper losses increase: in a machine without circulating currents the losses amount to $4 \times 200^2 \times 0.01 = 1,600$ W and when circulating currents appear, the losses attain a value of $2 \times 100^2 \times 0.01 + 2 \times 300^2 \times 0.01 = 2,000$ W. This creates unfavourable heating conditions of the machine and reduces its efficiency.

To eliminate, at least to some extent, these undesirable phenomena it is necessary to compel the circulating currents to close within the armature winding proper, without allowing them to pass into the brushes and brush connection bus-bars. To achieve this it is first necessary to find inside the armature winding points of theoretically equal potentials and connect them together by conductors of the least possible resistance. It is important to note that when we speak of the equipotential points we have in view only such spots which are more or less easily accessible. These are either the ends of coil sections connected to the commutator bars, or the end connections of the winding on the side opposite to the commutator, since other points of equal potential at those portions of the coil sections which are laid in the slots are practically inaccessible. The actual layout of equalisers will be shown further in Fig. 3-48, *a*, *b*, *c*.

The equaliser connections may be employed only when the simple lap winding is designed with all conditions of symmetry, formulated previously in § 3-15, fulfilled. In this case $a=p$ of similar e. m. f. polygons are obtained, each having only one point of a given potential. Hence, the number of equal potential points, which we may find in a symmetrical winding are always equal to $a=p$. The distance between two adjacent equipotential points is determined by the so-called potential pitch y_p , measured by the number of coil sections or commutator divisions

corresponding to one pair of paths, i.e.,

$$y_p = \frac{S}{a} = \frac{K}{a} = \frac{K}{p}. \quad (3-25)$$

Thus, for example, the winding in Fig. 3-26 is symmetrical because all requirements of symmetry have been met (§ 3-15), viz.:

$$\begin{aligned} \frac{S}{a} = \frac{K}{a} = \frac{14}{2} = 7 &= \text{integer}; \\ \frac{Z}{a} = \frac{14}{2} = 7 &= \text{integer and} \\ \frac{2p}{a} = \frac{4}{2} &= 2. \end{aligned}$$

In accordance with the given winding data the potential pitch $y_p = \frac{S}{a} = \frac{K}{a} = 7$. Therefore, the equipotential coil sections are 1— $-(1+7=8)$, then 2— $(2+7=9)$ and so on. The same may be seen also from the e.m.f. polygon of the coil section in Fig. 3-28, *b*. Fig. 3-26 shows a group of equalisers 1-8, 2-9, 3-10 and so on, arranged on the side opposite to the commutator.

Let us examine the role of the equalisers of the first type, by considering the ring armature in Fig. 3-44. According to data: $2p=4$, $S=K=16$, $2a=2p=4$ we obtain the potential pitch $y_p = \frac{S}{a} = \frac{K}{a} = 8$, i. e., points (or coil sections) of equal potential are those positioned along the armature diameter.

Suppose that due to inequality of air-gaps a difference in fluxes is set up, the lower pair of poles give the larger flux, depicted in Fig. 3-45, *a* by five lines, while the flux of the top pair is smaller and depicted by three lines. This flux non-uniformly distributed under the poles may be considered as containing two superposed fluxes, i. e., flux Φ_1 , uniformly distributed under all four poles, shown in Fig. 3-45, *b* by four broken lines, and flux Φ_2 , setting up only two poles, depicted in the same figure by two thick lines. Each flux induces an e. m. f. in the armature winding. The e. m. f. created by flux Φ_1 is of a conventional for a 4-pole machine nature and is shown in Fig. 3-45, *a*; the e. m. f. created by flux Φ_2 corresponds to a 2-pole machine and is depicted in Fig. 3-45, *b*.

We see, that for each winding path between points *a* and *b* which are located along the vertical diametrical line and which are theoretically the equipotential points, the flux Φ_2 induces an e.m.f. of one sign—in the left-hand side of the winding—denoted by the “point” sign and on the right-hand side denoted by the “cross”

sign; therefore between the points a and b there is a maximum difference of potentials u_{ab} . After the armature has turned 180° , the points a and b exchange places and the voltage across them again reaches its highest value, but already is of a different sign.

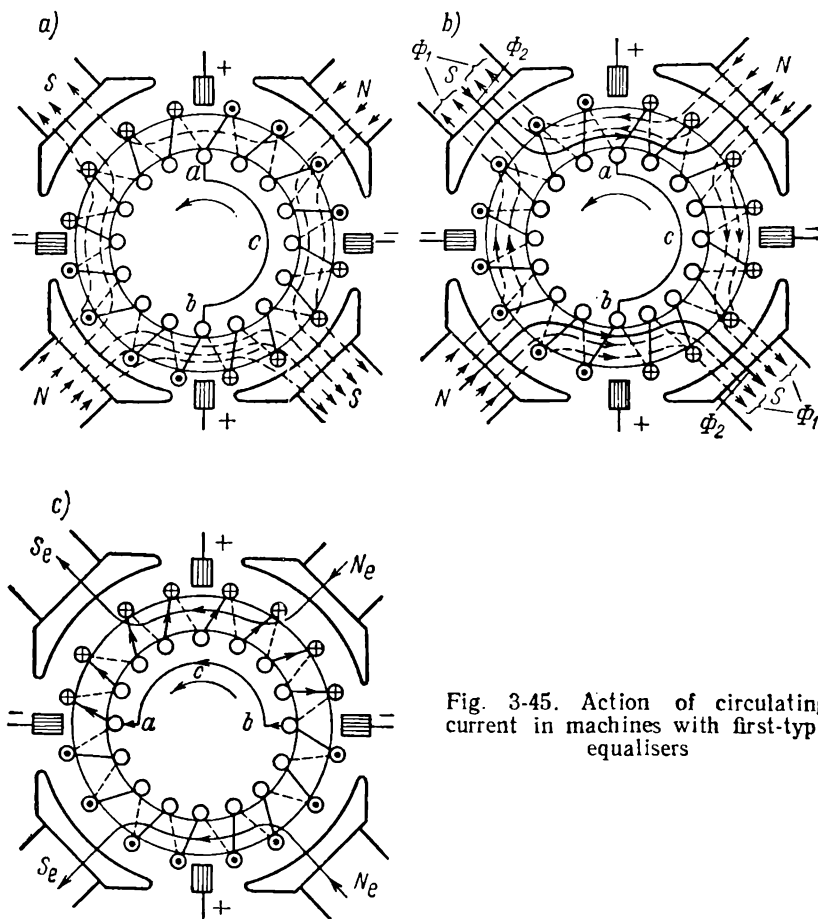


Fig. 3-45. Action of circulating current in machines with first-type equalisers

With a further turning of armature by another 180° the picture will repeat itself. Hence during one complete turn of armature a complete wave of voltage u_{ab} is obtained.

If we were to connect points a and b by means of an equalising conductor, then, due to this alternating voltage, through both halves of armature windings, which are divided in points a and b , an alternating current i_e will flow, closing through the

equaliser circuit acb . As the reactive resistance of the armature winding is much greater than its resistance to direct current, the current i_e will lag on the voltage u_{ab} almost by 90° . Therefore current i_e will attain its maximum value after the armature has turned 90° in the direction of rotation, i. e., at the instant when points a and b will set along the horizontal diametrical line (Fig. 3-45, c). At this moment the maximum value will also be reached by the magnetic flux Φ_e , set up by current i_e (depicted by two thin continuous lines in Fig. 3-45, c).

Comparing the direction of flux Φ_2 in Fig. 3-45, b with that of flux Φ_e in Fig. 3-45, c , we may see that they are opposed to each other, so that if flux Φ_e would be equal in magnitude to that of flux Φ_2 , the non-symmetry of the magnetic flux could be completely eliminated. Actually, however, the flux Φ_e only partially smooths out this non-symmetry, intensifying the flux under those poles where it is weakened and weakening it where it has been strengthened. This deduction may be generalised and therefore *an equaliser of the first type and the circulating current serve for the creation of such a flux Φ_e , which, being superposed on to the non-symmetrical flux of the machine, tends to smooth out the magnetic non-symmetry under the influence of which it was created.*

One equaliser cannot produce the necessary effect and therefore their number of equalisers has to be increased. The maximum possible number of equalisers is $\frac{K}{a}$, as each commutator bar and consequently each of the coil sections within the limits of one pair of paths may be joined to the corresponding bars and section coils within the limits of the remaining $a-1$ pair of paths. Such machines are referred to as machines *with a full number of equaliser connections*. But this case calls for excessive copper and also complicates the design and manufacture of the machine; hence, the number of equalising connections is usually decreased, especially for machines with relatively easy commutation conditions. For example, with equal-section windings it is sufficient to arrange one equaliser per slot. Fig. 3-29 shows a group of equalising connections from the rear side of the machine; since for this winding the pitch $y_p = \frac{S}{a} = \frac{28}{2} = 14$, it is possible to join sections 1-15, 3-17 and so on. In the same way the equalising connections are laid for a stepped winding.

The circulating current in the equalising connections causes additional losses and increased heating of the armature winding. Nevertheless, this is not so dangerous, as the relatively large reactive resistance of the armature winding lowers the cir-

culating current to only several per cent of the rated value.

B. Equalisers of the second type. *The simple wave windings with one pair of paths, and, therefore, with one e.m.f. polygon, do not have any two points of equal potential, hence there cannot be any equalisers.* But for multiplex wave windings $a > 1$, and therefore such windings permit equalisers to be used. But, compared

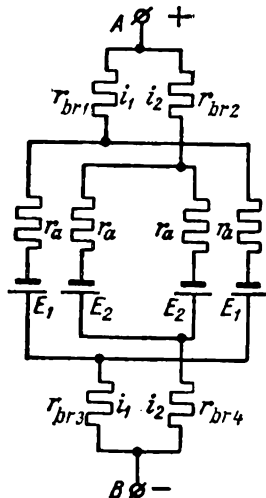


Fig. 3-46. Equivalent diagram for the winding in Fig. 3-42

with simple lap windings the role of these equalisers is different and they are distinguished as *equalisers of the second type*. Indeed, in wave windings the coil sections of each pair of paths are arranged under all the poles of the machine; therefore the possible magnetic non-symmetry of the machine would in a similar manner affect all winding paths and therefore the e.m.f.s of all paths may be assumed as practically balanced. But even in cases of complete equality of e.m.f.s for all paths there may be a non-uniform distribution of currents between the separate paths of the multiplex wave winding. Let us examine the phenomena taking place by considering an example of multiplex wave double-closed winding, the diagram of which is represented in Fig. 3-42. The winding may be substituted by the diagram of Fig. 3-46. Here r_a is the resistance of one armature winding branch; $r_{br1} \dots r_{br4}$ are the resistances of brush contacts; E_1 and E_2 are the e.m.f. in the armature winding paths, it being assumed that $E_1 = E_2$; i_1 and i_2 are the currents in each of the windings that constitute the total winding of the armature.

The voltage across the terminals A and B is equal to:

$$u_{AB} = E_1 - i_1 \left(r_{br1} + r_{br3} + \frac{1}{2} r_a \right) = E_2 - i_2 \left(r_{br2} + r_{br4} + \frac{1}{2} r_a \right), \text{ or, as } E_1 = E_2,$$

then

$$\frac{i_1}{i_2} = \frac{r_{br2} + r_{br4} + \frac{1}{2} r_a}{r_{br1} + r_{br3} + \frac{1}{2} r_a}.$$

It follows that the currents are distributed equally between the windings only in case when the sums of the resistances $r_{br1} + r_{br3} = r_{br2} + r_{br4}$ are also equal.

As this equation never takes place in practice it is always possible that a non-uniform distribution of currents will exist both between the windings and in the region of the short-circuited circuits, this involving a non-uniform distribution of voltage between adjacent commutator bars and impairing the machine's performance. To eliminate this trouble equaliser connections of the second type are used: with the help of these the points in both simple windings, theoretically of the same potential, are connected. From the polygon of e.m.f. in Fig. 3-43, *b* it follows that bar 2 should be joined to bar 11, bar 6 with bar 15 and so on. In other words it is necessary to join bars that are at a distance equal to the potential pitch $y_p = \frac{S}{a} = \frac{K}{a} = \frac{18}{2} = 9$. Thus *equalisers of the first and second type differ in functions: the equalisers of the first type smooth out the non-symmetry of the magnet system of the machine, whereas equalisers of the second type reduce the non-symmetry of potential distribution over the commutator.*

C. Equalisers in multiplex lap windings. Both types of equalisers are used in machines with multiplex lap windings, the first type being necessary in each of the simple lap windings, whereas the second type is used for levelling the potentials over the commutator and providing uniform distribution of currents between the separate simple windings, since they are connected together only by the brushgear, as is also the case with multiplex wave windings.

For example, consider the multiplex lap double-closed winding in Fig. 3-33. One of its simple windings is joined to the odd-numbered commutator bars and comprises all the odd-numbered coil sections, the other simple winding being joined to the even-numbered bars and containing the even-number coil sections. Accordingly, the two outside e.m.f. polygons in Fig. 3-39, *c* belong to the first winding, and the two inside polygons—to the second winding. From this e.m.f. polygon it may be seen that when arranging equalisers of the first type we must join the coil sections on the commutator side or on the rear side of the machine which span a distance equal to the potential pitch

$$y_p = \frac{S}{a} = \frac{K}{a} = \frac{20}{2} = 10,$$

where a denotes the number of path pairs of one simple winding, i. e., $a = p = 2$; hence we should join coil sections 1-11, 3-13 and so on, comprising the first winding, and coil sections 2-

12, 4-14 and so on, comprising the second winding. Several of these equalisers are shown on the commutator side in Fig. 3-38.

The arrangement of equalisers of the second type is somewhat more complex. Fig. 3-47 shows coil sections 1 and 2 of windings given in Fig. 3-38. The ends of coil section 1 are joined not to adjacent but to alternate bars. Hence, across adjacent commutator bars 1 and 2 there exists a voltage not of a complete coil section, but only of half of it. To provide proper distribution of voltage between adjacent bars, it is necessary to join the middle of coil section 1, which is at the end connection on the side opposite to the commutator, to the intermediate bar 2. In Fig. 3-38 the middle of section 5 is joined to bar 6, the middle of section 12 to bar 13 and so on. Since the other simple winding is also connected to the intermediate bar, equalisers of the second type electrically connect together both simple windings.

Recall, that the winding diagram in Fig. 3-38 is carried out with a long-chord pitch $y_1=6$; this permits equal polygons to

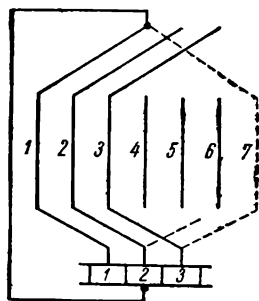


Fig. 3-47. Arrangement of second-type equalisers

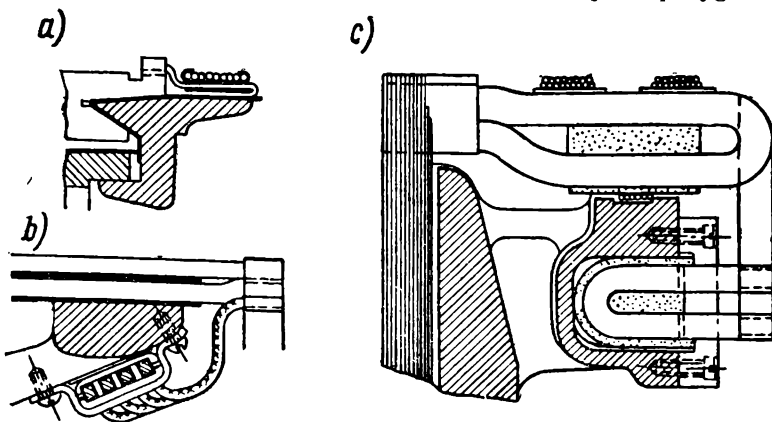


Fig. 3-48. Equalisers: *a* — on the commutator side, *b* and *c* — on the side opposite the commutator in the form of rings and forks

be obtained and provides the possibility of arranging equalisers of the second type. On the other hand for the windings in Fig. 3-40 with a full pitch the e. m. f. polygons of both simple lap

windings are relatively displaced (Fig. 3-41, *b*); therefore, these windings do not have accessible equipotential points and the arrangement of equalisers of the second type in such windings is impossible. Therefore the diagram in Fig. 3-40, contrary to the diagram in Fig. 3-38, does not provide correct performance of a machine and should be acknowledged as unpractical.

Equalisers of the second type, as also those of the first type, are often provided in smaller quantities not more than one per slot for an equisectional winding.

D. Design of equalisers. Equalisers may be arranged both from the commutator side (Fig. 3-48, *a*) and from the rear side;

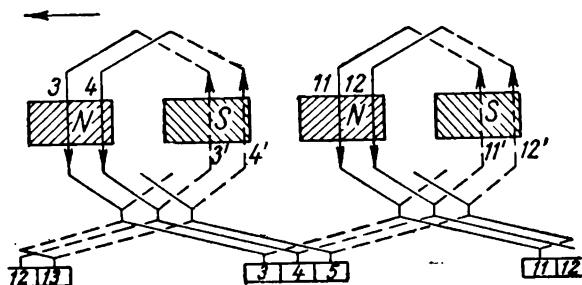


Fig. 3-49. Equaliser connections for large machines

under the end winding connections, in the form of rings (Fig. 3-48, *b*) or forks (Fig. 3-48, *c*). In large machines the equalisers are often designed so that they may act as commutator risers. This is shown by broken lines in Fig. 3-49.

Of the greatest complexity is the arrangement of the second type equalisers for multiplex lap windings (Fig. 3-38), because points located on both sides of the armature have to be joined and this necessitates pulling the equalisers through the openings between the armature core and shaft.

The cross-section of an equaliser is usually $1/4$ to $1/2$ of the armature conductor cross-section.

3-17. Special Armature Windings of the Composite Type

Large-output d. c. machines often employ the so-called *composite* or *frog-leg armature winding* which represents a combination of a simple lap and multiplex wave windings, and which does not need any special equaliser connectors. Both windings are joined to one and the same commutator and since a simple lap

winding has $a=p$ parallel paths, a multiplex wave winding should also be constructed with the same number of parallel paths $a=p$. Moreover, both windings consist of the same number of

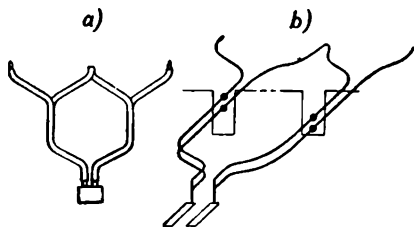


Fig. 3-50.

a—winding coil section of the combined (frog) type; *b*—arrangement of coil section in slots

coil section and the adjacent, according to the diagram, wave winding coil section, form the circuit $abcdefgh$, closed through the brushes and connecting bus between them. To prevent the creation of a circulating current in this circuit it is necessary that the sum of the e. m. f. of all coil sections comprising the circuit should be zero. But in the sides cd and ef laid in one slot, there act e.m.f.s of equal magnitude and opposed to each other along the circuit; hence, it is necessary to obtain a similar effect also in the sides ab and gh ; for this purpose it is necessary to space them at a distance exactly 2τ apart. If, as before, we shall measure the armature winding pitches by the number of elementary slots or by the number of commutator divisions spanned then, as it directly follows from Fig. 3-51,

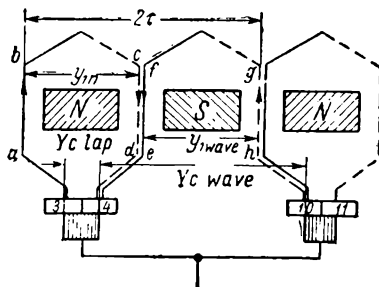


Fig. 3-51. Combined-type winding diagram (frog-type winding)

$$y_{lap} + y_{wave} = \frac{Z_e}{p} = \frac{K}{p}. \quad (3-26)$$

Here the subscripts refer to the lap and wave windings. The commutator pitch should correspond to the armature winding pitch. Hence,

$$y_{lap} + y_{wave} = \frac{K}{p}. \quad (3-27)$$

Furthermore, by taking into consideration formulas (3-16) and (3-13) we may write:

$$y_{c\ lap} = y_{lap} = y_{1\ lap} + y_{2\ lap} \text{ and}$$

$$y_{c\ wave} = y_{wave} = y_{1\ wave} + y_{2\ wave}.$$

Adding together the corresponding members of the latter equations and taking into account (3-26) and (3-27) we find:

$$y_{2\ lap} + y_{2\ wave} = 0, \quad (3-28)$$

i. e., the back pitches of both windings should be of equal (absolute) magnitude.

To investigate the role of each winding in respect to the other, let us construct a composite winding with the following data:

$$2p=4, S=K=Z_e=14,$$

$$u=1, Z=14, 2a=4.$$

The lap winding pitches:

$$y_{c\ lap} = y_{lap} = +1; \quad y_{1\ lap} = \frac{Z_e}{2p} \mp \varepsilon = \frac{14}{4} + \frac{2}{4} = 4;$$

$$y_{2\ lap} = y_{lap} - y_{1\ lap} = 1 - 4 = -3.$$

The wave winding pitches are:

$$y_{c\ wave} = y_{wave} = \frac{K \mp a}{2} = \frac{14 - 2}{2} = 6;$$

$$y_{1\ wave} = \frac{14}{4} - \frac{2}{4} = 3;$$

$$y_{2\ wave} = y_{wave} - y_{1\ wave} = 6 - 3 = 3.$$

The developed winding diagram is given in Fig. 3-52, *a*. The winding data are given as in Table 3-11.

Since the potential pitch of each of the windings is $y_{lap} = \frac{14}{2} = 7$, the bars 4 and 11 in Fig. 3-52 are equipotential and could be joined

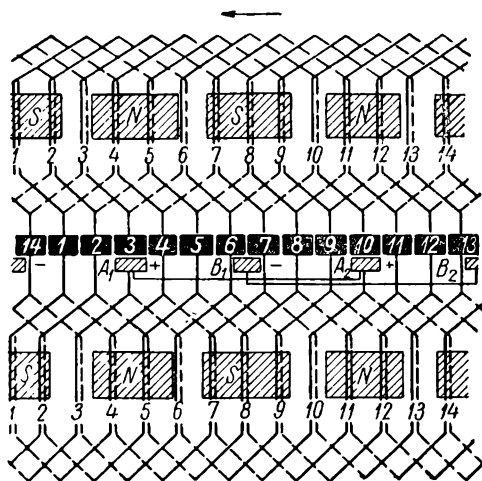
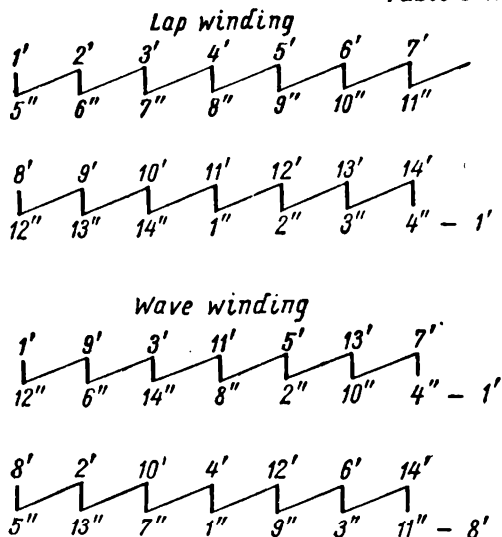


Fig. 3-52. Developed diagram for combined (frog)-type winding: $2p=2a=4$;
 $S=K=Z_e=14, u=1; Z=14$

by a first type equaliser with a pitch $y_{lap}=7$, but instead, bars 4 and 10 are joined by a *wave winding* coil section with a commutator pitch for this winding $y_{c\ wave}=6$ and the bars 10 and 11 are joined together by means of a lap winding coil section with a commutator pitch $y_{c\ lap}=1$ (Fig. 3-51). Since in a wave winding coil section the same e. m. f. is induced as in a lap winding coil section, but of a sign reversed in respect to the latter, then in case

Table 3-11



of a similar distribution of flux density *there will be no circulating current in the wave winding coil sections* under the poles of the signs, and, therefore, it is an *equaliser of the first type in respect to the lap winding*. In the same manner coil sections of the two separate wave winding paths are joined to bars 3 and 4, but these same bars are joined by means of a lap winding coil section which has an equal, but opposite in direction e. m. f.; therefore this *lap winding coil section in respect to the wave winding is an equaliser of the second type*.

Thus, the difference in performance conditions of conventional equaliser connections and of each of the windings acting as equalisers in the composite winding lies solely in the fact, that conventional equalisers connect together points of equal potential, whereas, with the composite type winding only those points are

joined which have a potential difference balanced by an opposite-acting e.m.f. in the equaliser circuit.

Fig. 3-53, *a*, *b*, *c*, shows the e.m.f. diagrams of lap and wave winding coil sections, the star and corresponding polygon of the

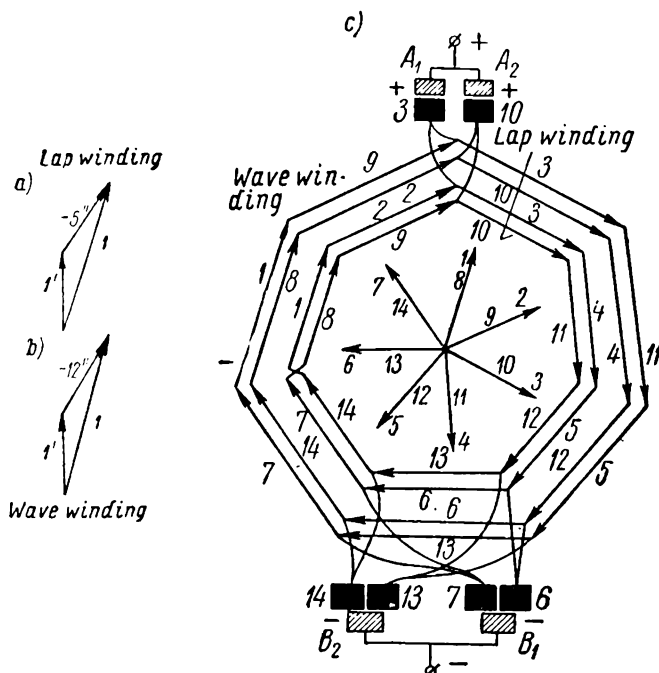


Fig. 3-53. Coil section e.m.f. diagrams for: lap (*a*) and wave (*b*) windings in Fig. 3-52, star and polygon (*c*) of coil section e.m.f.s

coil section e.m.f. constructed by conventional methods. We may see that since the lap and wave winding polygons coincide (in the figure they are similar) and the resultant e.m.f.s of all paths are equal in magnitude and direction the winding is balanced.

3-18. Comparison of Different Winding Characteristics

Table 3-12 gives a summary of all specific data pertaining to the previously discussed windings and shows where they are used. Assume, arbitrarily, that low-output machines are those up to 50 kW, average-output machines are within the range of 50 to 500 kW and large-output machines are from 500 kW upwards. We

also distinguish low-voltage d. c. machines as those operating with voltages up to and including 24 volts, reduced-voltage—from 60 to 80 volts, normal-voltage—from 110 to 220 volts, medium-voltage—from 440 to 600 volts and high-voltage—as those from 750 volts and higher.

3-19. E.M.F. of Drum Armature Windings

Since the drum-type armature in principle does not differ in any respect from the ring-type armature winding, the drum-type armature e.m.f. is determined by the same formula (3-10) as the e.m.f. for the ring armature, viz.:

$$E_a = pn \frac{N}{a} \Phi. \quad (3-29)$$

This formula gives the value of e. m. f. in volts, while the flux Φ is given in webers. If the flux is given in maxwells, then the multiple 10^{-8} is introduced into the formula (1 weber = 10^8 maxwells).

As in the case of the ring armature, the Φ in formula (3-29) should be the *useful flux*. For a given main flux Φ_0 (see definition in § 2-1) the useful flux of the drum-type armature depends: a) on the position of the brushes on the commutator and b) on the

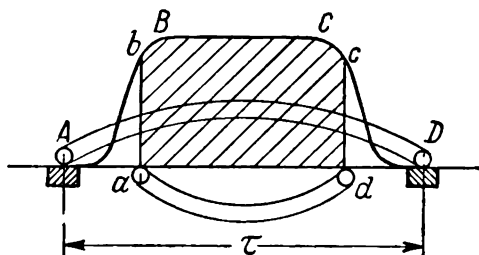


Fig. 3-54. Relation of useful flux to winding pitch

armature winding front pitch y_1 . If $y_1 = \tau$ and the brushes are set on the neutral (Fig. 3-54), then the entire main flux becomes the useful flux, defined by the area of the trapezoid ABCDA. If $y_1 < \tau$, with the brushes set on the neutral, then the useful part is only a portion of the main flux, corresponding to the hatched part of the area ABCDA in Fig. 3-54; the same holds true for the condition $y_1 > \tau$. If we shift the brushes from the neutral, then, as was shown previously in Fig. 3-14, b , the magnetic flux actually used by the armature winding for the creation of an e.m.f. is again decreased. Hence, in machines of standard make the front pitch y_1 should not differ materially from the pole pitch, and the brushes should be set at no-load in line with the geometrical axis.

Since for a manufactured machine the value $p \frac{N}{a} = \text{const} = C_e$, formula (3-29) may be represented in another form:

$$E_a = C_e n \Phi. \quad (3-30)$$

Table 3-12

Winding Characteristics

Name of winding	$y_c = y$	y_1	y_2	Number of path pairs	Main field of use
Simple lap	± 1	$\frac{Z_p}{2p} \mp \varepsilon$	$\pm 1 - y_1$	p	Machines of average output and normal voltage and also large-output medium voltage
Multiplex lap	$\pm m$	$\frac{Z_p}{2p} \mp \varepsilon$	$\pm m - y_1$	mp	Machines of low output and very low voltage and also large-output machines of normal, reduced and low voltage
Simple wave	$\frac{K \pm 1}{p}$	$\frac{Z_p}{2p} \mp \varepsilon$	$y - y_1$	1	Small-output machines of normal voltage and also machines of average output, medium and high voltage
Multiplex wave	$\frac{K \pm a}{p}$	$\frac{Z_p}{2p} \mp \varepsilon$	$y - y_1$	m	Average-output machines of medium voltage
Composite	$\pm 1 \text{ and } \frac{K \mp a}{p}$	$\frac{y_{lap} + y_{wave}}{2} = \frac{K}{p}$	$y_{lap} = -y_{wave}$	p	Large-output machines

Chapter Four

ARMATURE REACTION

4-1. M.M.F. of Machine on Load

When operating on no-load, there exists in the machine only the m.m.f. of the main poles which creates the main flux Φ_{main} .

On load, when a current flows through the armature winding, a m.m.f. is originated which interacts with the main m. m. f. Hence the magnetic flux Φ that exists in the machine when

it operates on load should be considered as the resultant flux created by the resultant m.m.f.

The effect of the armature m. m. f. on the main m. m. f. is termed the *armature reaction*.

To analyse this phenomenon we shall use the *method of superposition*. With this method the maps of the main field and the armature field are plotted separately and then superposed so as

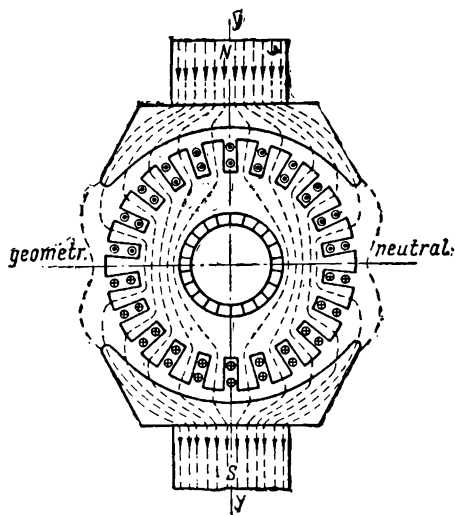


Fig 4-1. Main field

to obtain a map of the resultant magnetic field of the machine. This method gives proper results *if when superposing the parameters of the machine do not undergo any changes*. In the case considered, the parameter is the degree of saturation of the magnetic circuit of the machine, which in future we shall assume as a constant ($\mu = \text{const}$).

A. Main field of machine.

The main field originates when an excited machine is operating on no-load. The picture of this field in a two-pole machine is shown in Fig. 4-1. The field is symmetrical in respect to

the axis of the main poles that occupy a permanent position in space.

When the armature turns counterclockwise, an e.m.f. is induced in the armature winding in the direction shown in Fig. 4-1. The position of the brushes in this case is of no importance.

B. Armature field. Assume that the machine is not excited and is not running ($i_{exc} = 0$, $n = 0$). Set the brushes on the geometrical neutral axis and feed the current to them from some d. c. source so, that the direction of the currents in the winding paths coincides with the direction of the e.m.f. in Fig. 4-1. The field established by these currents is located symmetrically in respect to midpoints of both winding paths (Fig. 4-2). It may easily be noticed, that the R. H. half of the armature obtains the north polarity N_a , whereas the L. H. half obtains the south polarity— S_a , the axis of the armature field coinciding with the line on which the brushes are located.

To be able to analyse the armature field quantitatively it is necessary to determine the m. m. f. of the armature. For this purpose the *real slotted armature is reduced to a smooth armature with a layer of conductors distributed evenly over the armature periphery, but having the same calculated gap δ' as in the real machine.*

If N is the number of winding conductors and i_a is the current in one conductor (one path), then per unit of armature periphery length we have:

$$A = \frac{Ni_a}{\pi D_a}, \quad (4-1)$$

where D_a is the armature diameter.

The value A called the *armature electrical loading*, is one of the most important values in electrical machine-engineering. Since the number of conductors is a dimensionless quantity, the value A may be measured the same way as the value H , i. e., in amperes per unit length. In modern highly specifically loaded d. c. machines, the loading is within the range of 100 A/cm in small-output machines, up to 600 A/cm and sometimes more, in large-capacity machines.

The calculation of armature m. m. f. is carried out per pair of poles under the condition that the brushes are on the geometrical neutrals and the winding pitch is $y_1 = \tau$. In this case the midpoint of each armature current path coincides exactly with the corresponding pole axis (Fig. 4-3,a). The lines (tubes) of the armature field are grouped symmetrically both sides of the midpoint. Let one of these lines be at a distance x from the midpoint. The m. m. f. F_{ax} along the circuit of this line is equal to the total current encompassed by this circuit and therefore constitutes $A \times 2x$ ampere-turns per pair of poles, i. e.,

$$F_{ax} = A \times 2x. \quad (4-2)$$

Receding from the midpoint both ways we may observe that the armature m. m. f. curve represents an open polygon 1-1-1 that intersects the abscissa axis at a point midway between the brushes and that it attains maximum value F_a near each brush, i. e., at $x = \frac{\tau}{2}$. Substituting this value of x into formula (4-2),

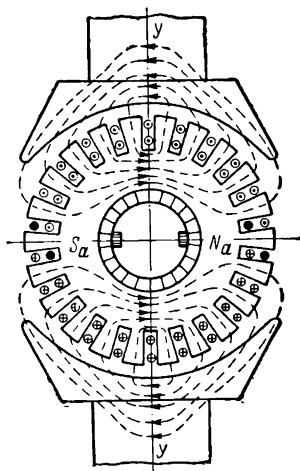


Fig. 42. Armature field

we obtain per pair of poles:

$$F_a = A \times 2x = A \times 2 \frac{\tau}{2} = A\tau. \quad (4-3)$$

Within the pole-shoe limits each magnetic line passes through the gap twice and closes within the armature and pole steel. For

normal saturation values of the steel its magnetic reluctance may be disregarded and we may assume that the reluctance of an armature magnetic reaction line is defined only by the reluctance of a double air-gap. Hence, at any point under the pole-shoe the magnetic flux density B_{ax} will be:

$$\begin{aligned} B_{ax} &= \mu_0 H_{ax} = \\ &= \mu_0 \frac{F_{ax}}{2\delta'} = \mu_0 \frac{A}{\delta'} x. \end{aligned}$$

With a properly chosen scale, the m. m. f. curve in Fig. 4-3, *a* may represent, within the bounds of the pole arc, the curve of magnetic flux density B_{ax} . But in the interpolar space the flux density abruptly decreases due to a large increase in length of the line in the air and consequently a decrease of its reluctance takes place; therefore curve 2 of the flux density B_{ax} is saddle-shaped.

Fig. 4-3, *b* and *c* shows m. m. f. and armature field flux density curves for two cases: 1) when the machine is without

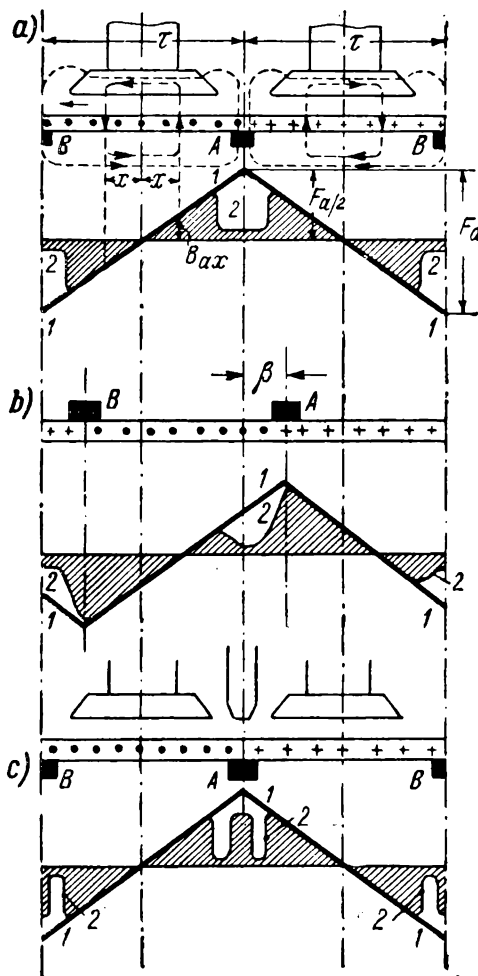


Fig. 4-3. Field and armature m.m.f. curves: *a*—in machines without commutating poles with the brushes on neutral; *b*—the same but with brushes shifted from neutral; *c*—for machines with non-excited commutating poles with brushes on neutral

commutating poles and the brushes have been shifted from the neutral by an angle β and 2) when the machine is fitted with commutating poles and the brushes are on the neutral. The commutating poles and the main poles are not excited.

The m.m.f. and flux density curves in Fig. 4-3 have been plotted with the assumption that the armature is at a standstill. If the armature is brought into rotation and the brushes are on the neutral, the armature field lines are symmetrically disposed in respect to the axis of the poles (Fig. 4-4); therefore an e. m. f. of one sign is induced in one half of the armature winding path and in the other half—of another sign. Hence, the resultant e.m.f. of the path and consequently the voltage at the brushes is equal to zero.

It is possible to arrive at this deduction by another way. Considering the flux density curve in Fig. 4-3, *a* we may see that there are equal and directly opposed portions of the armature field between brushes *A* and *B*; hence, the resultant flux through the portion of the winding between the brushes and the voltage across the brushes equal zero.

When the brushes are shifted from the neutral (Fig. 4-3, *b*) the picture changes. Now the portions of the armature field of different signs, located between brushes *B* and *A*, are not equal, the part below the abscissa axis is larger than the part above it; hence, there appears a voltage across the brushes. If the brushes are shifted the other way in respect to the neutral (angle $-\beta$) direction the voltage across the brushes changes its sign.

The effect of the e.m.f., created by the armature, on the main e.m.f., created by the main field of the machine, depends on the performance of the machine; this problem is considered in the chapters below.

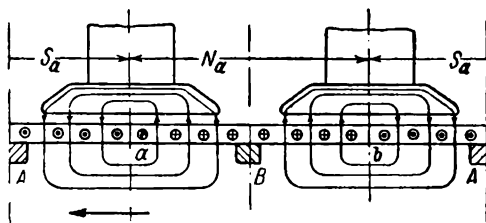


Fig. 4-4. E.m.f. induced in the armature by the armature field

4-2. Armature Cross- and Direct-Axis M.M.F.

If the brushes are set on the geometrical neutral *X-X* (Fig. 4-5, *a*) the armature field is directed *across the axial line of the main poles Y-Y* i. e. at 90° . Therefore this armature field is termed

the *cross* or *quadrature* field and is determined by the *cross* or *quadrature* m.m.f. of the armature F_{aq} .

According to formula (4-3) we have per pair of poles

$$F_{aq} = F_a = A\tau. \quad (4-4)$$

The position of the brushes on the geometrical neutral is their first basic position.

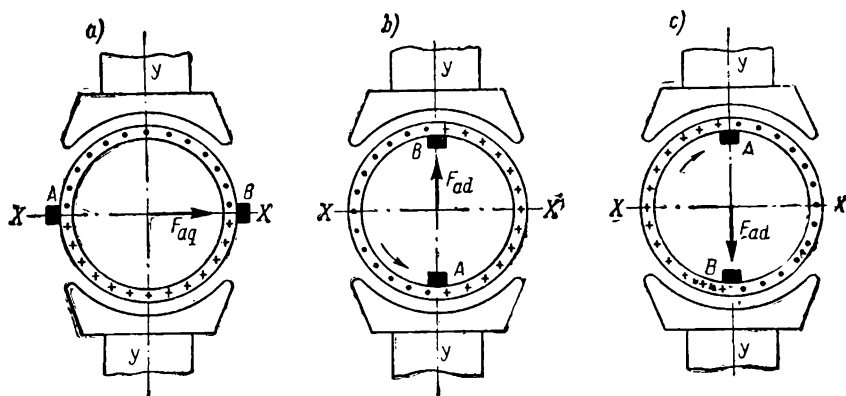


Fig. 4-5. M.m.f. of the quadrature and direct-axis armature reaction

When the brushes are shifted from the neutral $\pm 90^\circ$, the axis of the armature field sets along the pole axis $Y-Y$ above or below the abscissa (Fig. 4-5, *b* and *c*). This armature field is called the *direct-axis* field and is determined by the *armature direct-axis m.m.f.* F_{ad} . Per pair of poles we have:

$$F_{ad} = F_a = A\tau. \quad (4-5)$$

The position of the brushes when they are set along the pole axis is their second basic position.

In the general case the brushes may be shifted from the neutral by an angle β or over the corresponding arc b_c on the armature periphery (Fig. 4-6, *a*, *b*). These conditions make it possible to consider the armature as two superposed electromagnets of which one, created by the portion of the winding within the twin angle 2β , forms the armature direct-axis m.m.f. F_{ad} , and the other one, created by the remainder of the winding over the arc $\tau - 2b_c$, produces the armature quadrature m.m.f. F_{aq} . Since to the brush shift

per unit of length corresponds the m.m.f. $2A$, then for a brush shift equal to b_c , we have per pair of poles for the same unit lengths:

$$F_{ad} = 2Ab_c \quad (4-6a)$$

and

$$F_{aq} = A(\tau - 2b_c). \quad (4-6b)$$

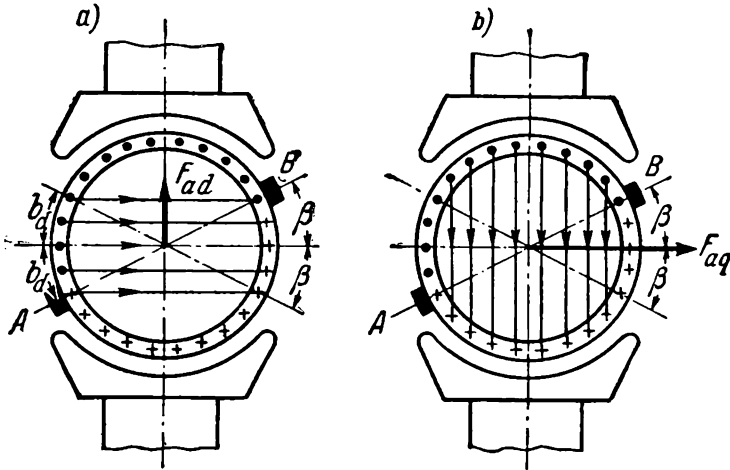


Fig. 4-6. Direct- and quadrature-axis m.m.f. of armature when the brushes are shifted from neutral

4-3. Armature Reaction in a Generator

In a machine working on load the armature m. m. f. interacts with the main pole m. m. f. and produces, together with the latter, the resultant m. m. f. of the machine. But in the general case the resultant flux of the machine depends both on the resultant m.m.f. and on the possible change in reluctance of the machine magnetic circuit.

Let us consider several important cases of armature reaction assuming the machine working as a generator and running counterclockwise with a definite constant speed, commutating poles being absent.

A. The brushes are on the neutral and the magnetic circuit reluctance is independent of load ($\mu = \text{const}$). In Fig. 4-7, *a* the curve *1* depicts the generator main field distribution in the air-gap under one pair of poles.

When the armature rotates in a given direction an e. m. f. is induced directed in the L. H. armature path towards us and in

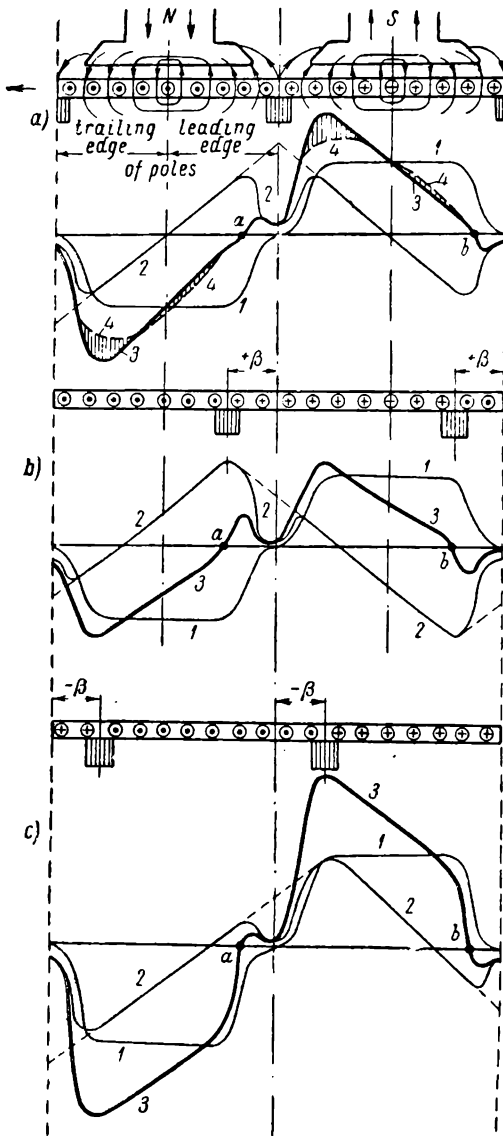


Fig. 4-7. Generator field curves for different positions of brushes

the R. H. part, from us (into the page). The same directions are followed by the currents in the winding. The midpoint of each winding path, around which the armature field lines are formed, lies on the correspondent pole axis. Having determined by conventional methods how the armature field lines are directed, we notice, that *at the leading pole tips the armature field is in opposition to the main pole, i. e., it demagnetises the field, while at the trailing tips, the field is concurrent, i. e., increases field magnetisation.* According to these deductions curve 2 of the armature reaction field is plotted. It is distinguished by the same saddle-like feature as in Fig. 4-3,a.

Since according to stipulation $\mu = \text{const}$, then to obtain the resultant field it is sufficient to add together both component fields by means of adding the ordinates at each point under both poles. The curve 3 obtained in this manner envelopes an area equal to the area enveloped by curve 1, since the demagnetising and magnetising effects along both

sides of the pole axis are mutually compensated. Hence, the resultant flux Φ , determined by the area of curve 3, remains equal to the main flux Φ_0 determined by the area of curve 1.

Thus, in a machine with a non-saturated magnetic circuit, the cross armature reaction distorts the main field, when the brushes are set on the geometrical neutrals, but does not alter the field magnitude.

Fig. 4-8 illustrates the distribution of the generator resultant field, according to considered working conditions of the generator.

The points a and b at which the resultant field curve passes through zero (Fig. 4-7, a) determine the position of the so-called *physical neutral*. At no-load the physical neutral coincides with the geometrical neutral but with load it shifts in the direction of armature rotation by an angle α (Fig. 4-8).

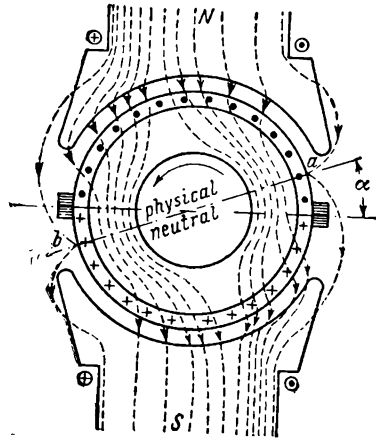


Fig. 4-8. Distribution of machine resultant magnetic field when brushes are on geometrical neutral

This deduction may be generalised, i.e., it holds true independent of pole polarity and direction of armature rotation.

B. The machine works as a generator, the brushes are on the neutral but the magnetic circuit reluctance depends on the load ($\mu \neq \text{const}$). In this case, as in the first one there exists only the cross m.m.f. of the armature. But if the machine possesses a *saturated magnetic circuit* the resultant field cannot be obtained by adding together field components since the reluctance of the saturated magnetic circuit sections, i.e., the trailing tips of the poles (Fig. 4-7, a) is augmented more than it is reduced under the leading pole tips. Therefore the reduction of field in the saturated part (the hatched areas to the left of the pole axis, Fig. 4-7, a) is greater than its increase under the other pole edge (the hatched areas to the right of the pole axis). Because of this the resultant field and the generator e.m.f.s E_a are somewhat reduced even when the brushes are on the geometrical neutral. For this reason it is possible to speak of the *demagnetising effect of the cross armature reaction in a machine with a saturated magnetic circuit*.

To evaluate this effect consider the magnetic circuit of the machine in Fig. 4-9. The m.m.f. acting along the closed path $abcd$ (heavy solid line) may be written as follows:

$$F_0 = F_{ab} + F_{bc} + F_{cd} + F_{da}. \quad (4-7)$$

Here $F_{ab} = F_i + F_t = F_{it.o}$ is the m.m.f. of the air-gap and tooth in the axial pole plane.

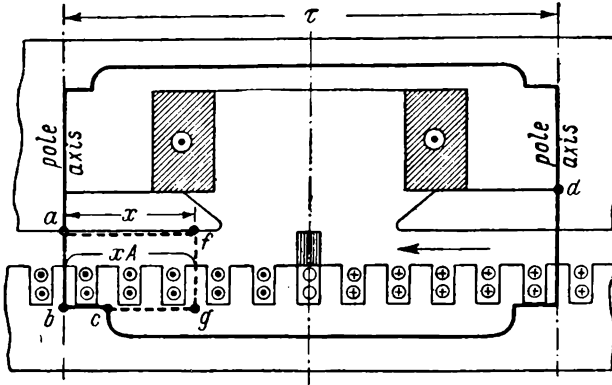


Fig. 4-9. Quadrature re-axis armature reaction effect

If the machine operates on no-load, the m.m.f. $F_{it.o}$ acts at any point under the pole piece. By assuming different values of B_i , we may plot the curve $F_{it.o} = f(B_i)$. This curve is called the *transition characteristic* of the machine (Fig. 4-10, a).

With load, the m.m.f. $F_{it.o}$ acts only in the axial plane along segment ab (Fig. 4-9), whereas in other points other m.m.f.s will act. Consider, for example, point f located at a distance x from the pole axis and arrange in Fig. 4-9 an additional path $afgc$, depicted by the broken line. Then the m.m.f. along the closed path $afgcda$ would be $F_0 \pm Ax$, the plus sign taken when the point f is on the trailing pole tip and minus when on the leading tip. Hence,

$$F_0 \pm Ax = F_{af} + F_{fg} + F_{gc} + F_{cd} + F_{da}. \quad (4-8)$$

Subtracting equation (4-7) from equation (4-8) and disregarding the m.m.f.s F_{af} , F_{bc} and F_{gc} as second order magnitudes we have:

$$F_{fg} = F_{ab} \pm Ax = F_{it.o} \pm Ax.$$

This equation allows us to obtain by means of the transition characteristic the flux density B_{tx} at any point of the gap accord-

ing to assigned operating conditions of the machine under load.

Let us assume that for no-load point A on the transition characteristic (Fig. 4-10, a)¹ defines the gap flux density $B_{\delta_0} = AP$ and correspondingly the m.m.f. $F_{\delta t,0} = OP$.

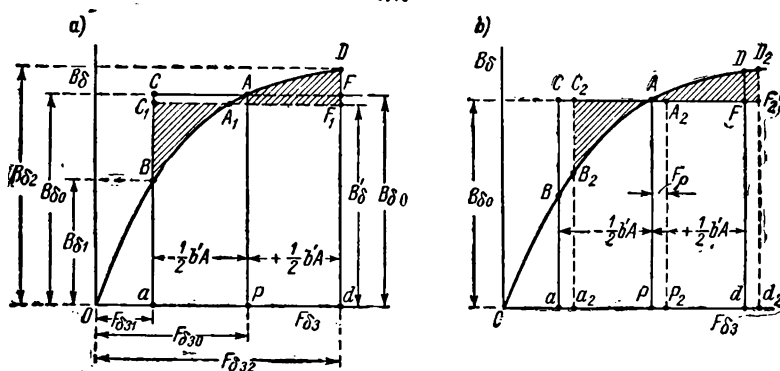


Fig. 4-10. Determination of demagnetising effect of quadrature armature reaction

Let the load of the machine and accordingly the electrical loading A be given. At points, which are at a distance $x = \pm \frac{1}{2} b'$ from the pole axis, we have:

$$F_{\delta t,1} = F_{\delta t,0} - \frac{1}{2} b' A \quad \text{and} \quad F_{\delta t,2} = F_{\delta t,0} + \frac{1}{2} b' A.$$

To obtain these m.m.f.s we lay off in Fig. 4-10, a , to both sides of point P sections $Pa = -\frac{1}{2} b' A$ and $Pd = +\frac{1}{2} b' A$. Hence, $F_{\delta t,1} = Oa$ and $F_{\delta t,2} = Od$; the sections aB and dD then define the flux densities B_{δ_1} , and B_{δ_2} under the leading and trailing edges of the pole piece. Reasoning in the same manner, we may find that the BAD part of the transition characteristic gives the distribution of the flux density in the gap under the pole piece for a given load.

Since rectangle $aCFd$ has a base proportional to arc b' , and a height equal to B_{δ_0} , its area may represent a measure of flux Φ_0 at no-load. In the same manner the area of the curvilinear tetragon $aBDD$ serves as a measure of the flux under load condition. If the machine is saturated then area $ACB > AFD$; therefore for a given excitation the load will bring about a decrease in air-gap flux and accordingly a decrease in machine e.m.f. E_a .

¹ Note: "3" stands for "l" — tooth in Fig. 4-10. — *Tr.*

from the neutral in a generator is not permitted due to commutation reasons; this will be explained in detail in Chapter 5.

The evaluation of the direct-axis armature reaction is performed with the help of the magnetisation curve $\Phi = f(F)$, Fig. 4-12. Suppose that at no-load the m.m.f. $F_0 = OP$ and the flux $\Phi_0 = AP$; then under load conditions we have: $F_1 = F_0 - F_{ad}$ or $F_2 = F_0 + F_{ad}$; in the first case the flux Φ_0 is reduced to value $\Phi_1 = \Phi_0 - \Delta\Phi_1$, in the second case it is increased to the value $\Phi_2 = \Phi_0 + \Delta\Phi_2$.

The direct-axis armature reaction affects only the magnitude of the resultant flux, but does not change its form.

To compensate for the direct-axis armature m.m.f. $\mp F_{ad}$ the excitation current should be so altered that the main m. m. f. is modified by the value $\pm F_{ad}$.

In machines with commutating poles the brushes are set, as close as possible, to the geometrical neutral. Actually, the brushes are always shifted a little off the neutral either due to mounting errors or due to physical properties inherent to the brush contact. The shift may be from 0.3 to 0.5 cm ahead or back of the neutral. Hence,

$$F_{ad} = \pm A \times 2 \times (0.3 \text{ to } 0.5)$$

per pair of poles, i.e., in machines with a large loading the direct-axis m.m.f. may reach a value of several hundred ampere-turns and in certain conditions, as for instance, in case of motors with speed regulation, may appreciably affect the operation of the machine.

4-4. Effect of Direct-Axis Armature Reaction on Machine E.M.F.

Consider the machine, as before, working as a generator with $n = \text{const}$ and $\Phi_0 = \text{const}$. When the brushes are shifted any direction off the neutral the useful flux Φ is reduced (Fig. 3-14, b)

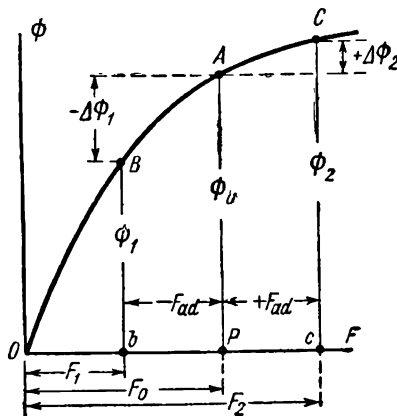


Fig. 4-12. Direct-axis armature reaction effect

and proportionally the e.m.f. E_a is also reduced. At no-load the relationship $E_{ao}=f(\beta)$ is represented in Fig. 4-13 by the sine-wave curve 1. Under load any shifting of the brushes creates a longitudinal demagnetising or magnetising armature reaction. Furthermore, in conventional salient pole d. c. machines there appears another additional demagnetising or magnetising effect due to the armature field portions of different signs, located between adjacent brushes of equal polarity, not being equal in magnitude (Fig. 4-3, b).

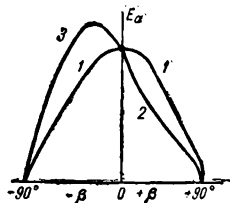


Fig. 4-13. Effect of brush shift on machine e.m.f.

When the brushes are shifted in direction of armature rotation, all the three factors previously mentioned act with the same trend, i.e., to demagnetise the machine; as a result curve 2 of the e.m.f. E_a in Fig. 4-13 falls abruptly. On the contrary, when the brushes are shifted against armature rotation, the first factor acts to decrease the e. m. f., and the remaining two—to increase it. At first the predominating effect is rendered by the two last factors and then later the first factor becomes the predominating one. Therefore curve 3 of the e.m.f. E_a in Fig. 4-13 at first begins to grow and then falls. For $\beta=\pm 90^\circ$ the e. m. f. $E_a=0$.

4-5. Armature Reaction in a Motor

Above we have discussed armature reaction phenomena in a generator. From later considerations (Chapter 10) we shall learn that if the polarity of the main poles and direction of currents in the armature windings are the same as for the generator, then in respect to the latter the motor will run in the opposite direction (G is the generator and M —the motor in Fig. 4-11). This allows us to make the following deductions on armature reaction in motors:

a) When the brushes are on the geometrical neutral the armature cross m. m. f. distorts the main field, weakening it at the trailing tip and augmenting it at the leading pole tip.

b) When the brushes of a motor are shifted ahead or back from the neutral there appears, besides the cross armature reaction, also a direct-axis armature reaction, in the first case—of a magnetising, in the second case—of a demagnetising nature. Nevertheless, shifting of brushes in the direction of armature rotation is not allowed because of commutation considerations.

Chapter Five

COMMUTATION

5-1. Introduction. Standard Sparking Scale

Commutation is the phenomenon pertaining to the reversal of current in a coil short-circuited by the brush when a coil section is switched from one winding path to another. From the physical standpoint the commutation process is of a very complex nature in which various mechanical, thermal, electrochemical and electromagnetic factors are closely interwoven. The quality of commutation is defined mainly according to the sparking effect at the commutator and under the brushes.

The State Standard 183-55 establishes a method of evaluating sparking at the commutator by the degree of sparking under the trailing edge of brush in compliance with the sparking scale (i. e., classes of commutation) given in Table 5-1.

The degree of sparking (or class of commutation) of the commutator machines should be specified in the standards for individual types of machines, and when there are no standards, it should be stipulated in the machine specifications. If the degree of sparking of d. c. commutator is not stipulated, for rated load conditions of the machine it should not exceed the value of $1\frac{1}{2}$.

It should be mentioned, that the degree of sparking stipulated by the State Standard 183-55 is not quite definite.

Sparking at the commutator may originate due to most diverse causes, but the most significant of these are the electromagnetical, potential and mechanical causes. The effect of the first and second causes are considered in the following sections, but their analysis is possible only after the mechanical causes are eliminated.

Therefore, assume that the commutator and brush gear have been perfectly manufactured and from the mechanical standpoint have no effect on the commutation process. [Bibl. 15b, 17a, 22a, 23, 45, 46, 47, 52, 53b]

5-2. Commutation Process

Proceeding from the classical theory of commutation we assume, that: 1) the entire brush surface adjacent to the commutator surface conducts current uniformly; 2) the specific transient resistance of brush contact (viz., the resistance referred to a brush contact unit surface) represents a value which is independent of current density and surface contact dimensions.

Table 5-1

Degree of sparking (class of commutation)	Degree of sparking	Condition of commutator and brushes
1	Absence of sparking (dark commutation)	No blackening of commutator or deposit on brushes
1 1/4	Slight pin-point sparking under a small part of the brush	
1 1/2	Slight sparking under major part of the brush	Black traces appear on commutator, easily removed by rubbing the commutator surface with petrol; deposits appear on brushes
2	Sparking under entire edge of the brush	Black traces which cannot be wiped off with petrol; deposits on brushes
3	Allowed only for short-time intermittent-duty loads and overloads Heavy sparking under entire edge of the brush with large and flying sparks Allowed only momentarily, with on-line starting or reversing, if the commutator and brushes afterwards are in condition allowing further operation	Considerable blackening of commutator that cannot be wiped clean with petrol; burning and destruction of brushes

To simplify the initial analysis of the commutation process, assume that the width of the brush b_{br} is equal to the width of the commutator bar b_c and neglect the width of the insulation strip between the commutator bars.

We shall endeavour to make clear the nature of the commutation process by using the ring armature with a simple lap winding as an example.

Let i_a in Fig. 5-1, a be the current in each armature winding path. At the moment when the brush contacts only bar 2, the currents are distributed as follows: in conductor cd current $i_2 = 2i_a$, in conductor ab current $i_1 = 0$, and in the coil section aKc between bars 1 and 2 a current flows from node a to node c ; this direction we arbitrarily assume as the positive direction, i. e., we will regard at the given instant $i = +i_a$.

After a time period T the brush will run off the bar 2 and settle only on bar 1 (Fig. 5-1, b). At this moment

$$i_1 = 2i_a, \quad i_2 = 0 \quad \text{and} \quad i = -i_a.$$

Thus, during time T , termed the *period (or time) of coil section commutation*, the current in section aKc varies from $+i_a$ to $-i_a$, i.e., by $2i_a$. This process is named *current commutation* and constitutes the essential part of the phenomena which the commutation process comprises.

The position of a brush on bar 2 corresponds to the initial moment of the commutation period $t=0$, and brush position on bar 1 conforms to the final moment of the commutation period $t=T$. The time T is usually small compared with time T_n which it takes the coil section to shift from the given brush to the adjacent brush of the other polarity when the commutation process terminates ($T \approx 0.001$ sec, $T_n \approx 0.02$ sec). Therefore the current variation curve in the coil section with the armature running has an almost rectangular form (Fig. 5-2).

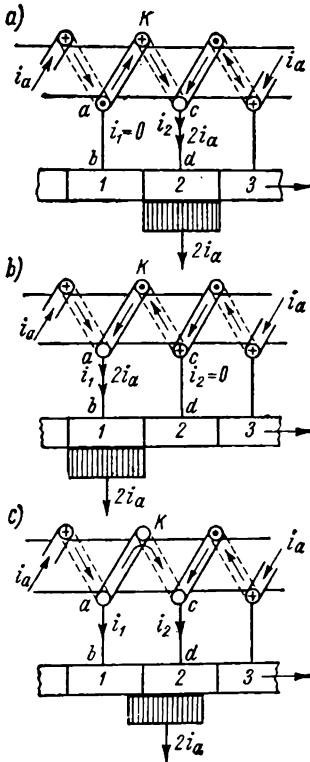


Fig. 5-1. Current commutation for $b_{br} = b_c$

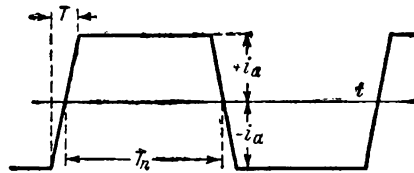


Fig. 5-2. Curve of current change in d. c. machine armature winding conductor

At intermediate moments of the commutation process (Fig. 5-1, c) the brush is partially on bar 1 and partially on bar 2. In this case we have a circuit closed upon itself, made up of the brush, bars 1 and 2 and the coil section aKc connected to them by conductors ab and cd . Applying to this circuit the second law of Kirchhoff we have:

$$\Sigma e = \Sigma ir.$$

5-3. E.M.F. of Circuit Undergoing Commutation

When the armature runs with a finite speed in the coil section undergoing commutation there are induced the following e.m.f.s:

a) **The e. m. f. of self-induction e_L .** Since during the commutation period T the current in the coil section undergoing commutation varies from $+i_a$ to $-i_a$, there is a corresponding change in the flux coupled with this coil section from a value $+\Phi_c$ established by current $+i_a$ at the initial time period, up to value $-\Phi_c$, established by current $-i_a$ at the final moment.

With this change in flux, in the section undergoing commutation an e. m. f. of self-induction $e_L = -\frac{d(L_c i)}{dt}$ is set up; L_c is the inductance of the section. By virtue of its inherent property e_L tends to delay current reversal in the circuit.

b) **E.m.f. of mutual inductance e_M .** In the general case a brush spans several commutator bars. In this case several adjacent coil sections undergo commutation, and each coil induces in the considered coil section a corresponding e. m. f. of mutual induction e_M . This e.m.f., the same as the e.m.f. e_L , tends to delay the reversal of current in the section undergoing commutation.

c) **Commutating e.m.f. e_c .** This e.m.f. originates in the coil section undergoing commutation when its sides are traversed by lines of field flux, that are practically always present in the commutation zone. This field can be established by armature reaction, but more often it is set up with the help of commutating poles. To this type of e.m.f. belong also the e.m.f.s created by the pulsations of the resultant field in the commutation zone caused by cross oscillations of the field due to slots of the armature (Fig. 3-10).

In contrast to the e.m.f. e_L , the e.m.f. e_c may have a sign depending on the polarity of the external field, in which the section undergoing commutation is located. Hence in one case the action of the e.m.f. e_c , is in the same direction as the e.m.f. e_L , and in the other case—in the opposite direction.

5-4. Commutation Equation when $b_{br}=b_c$

Let r_{br1} and r_{br2} be the contact resistances of parts of brushes on bars 1 and 2; r_n —resistance of conductors ab and cd ; r_c —resistance of coil section.

Since for $b_{br}=b_c$ the e.m.f. $e_M=0$, on making a round of the circuit of the coil section undergoing commutation counterclockwise (Fig. 5-1,c) we have

$$i_1 r_{br1} - i_2 r_{br2} - i_2 r_n - i r_c + i_1 r_n = e_L + e_c. \quad (5-1)$$

5-5. Resistance Commutation

We shall start the analysis of the commutation process with the simplest case, when the sum $e_L + e_c = 0$; this is possible either when the e.m.f. e_L and e_c are mutually balanced, or in the case when the speed of the armature is so small ($v_a \approx 0$) and consequently the process of commutation takes place so slowly, that each of the e.m.f.s e_L and e_c may be assumed as equal to zero. In these conditions commutation takes place with only the resistance of the coil section undergoing commutation present and therefore this type of commutation is called *resistance commutation*.

A. First case of resistance commutation: $b_{br}=b_c$; $e_L + e_c = 0$; $r_w = 0$; $r_s = 0$.

With carbon brushes the resistance r_w of conductors ab and cd and the resistance of coil section r_s may be disregarded. Then the equation (5-1) appears as follows:

$$i_1 r_{br1} - i_2 r_{br2} = 0, \quad (5-2)$$

from which follows:

$$\frac{i_1}{i_2} = \frac{r_{br2}}{r_{br1}}. \quad (5-3)$$

Considering nodes a and c in Fig. 5-1 we have according to Kirchhoff's first law,

$$i_1 = i_a - i \quad (5-4a)$$

and

$$i_2 = i_a + i. \quad (5-4b)$$

Let r_{br} be the resistance of brush contact, corresponding to its whole surface S_{br} ; let S_{br1} and S_{br2} be the surfaces of the parts of brush leading onto bar 1 and correspondingly trailing off bar 2; b_{br1} and b_{br2} are the widths of brushes occupying bars 1 and 2; l_{br} is the length of the brush in the axial direction of the machine; v_c is the speed at the periphery of the commutator, then

$$r_{br1} = r_{br} \frac{S_{br}}{S_{br1}} = r_{br} \frac{b_{br} l_{br}}{b_{br1} l_{br}} = r_{br} \frac{v_c T}{v_c l} = r_{br} \frac{T}{l}, \quad (5-5)$$

$$r_{br2} = r_{br} \frac{S_{br}}{S_{br2}} = r_{br} \frac{b_{br} l_{br}}{b_{br2} l_{br}} = r_{br} \frac{v_c T}{v_c (T - t)} = r_{br} \frac{T}{T - t}. \quad (5-6)$$

Therefore the equation (5-3) may be rewritten in the form:

$$\frac{i_a - i}{i_a + i} = \frac{t}{T - t},$$

from which we obtain:

$$i = i_a \left(1 - \frac{2t}{T} \right). \quad (5-7)$$

Thus, in the conditions considered the variation of current i in the coil section undergoing commutation follows a linear with time relationship, i. e., the commutation is linear (Fig. 5-3, a).

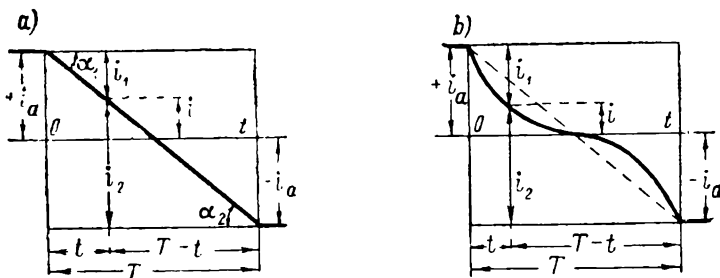


Fig. 5-3. Resistance commutation:
a — linear commutation; b — the general case

With linear commutation the current densities j_{br1} and j_{br2} under the leading and trailing parts of the brush are expressed as follows:

$$j_{br1} = \frac{i_1}{S_{br1}} = \frac{i_1}{b_{br1} l_{br}} = \frac{i_1}{v_c t l_{br}} = \tan \alpha_1, \quad (5-8a)$$

$$j_{br2} = \frac{i_2}{S_{br2}} = \frac{i_2}{b_{br2} l_{br}} = \frac{i_2}{v_c (T - t) l_{br}} = \tan \alpha_2. \quad (5-8b)$$

Here α_1 and α_2 are angles formed with the abscissa axis by tangents drawn from points $t=0$ and $t=T$ through a point corresponding to current i when $t=t$ (Fig. 5-3). With linear commutation $\alpha_1 = \alpha_2 = \alpha$ for the entire length of the straight line $i = f(t)$; therefore, independent of time we have:

$$j_{br1} = j_{br2} = j_{br}, \quad (5-9)$$

i. e., for linear commutation the current densities under the trailing and leading tips of the brush are equal.

B. Second case of resistance commutation:

$$b_{br} = b_c; \quad e_L + e_c = 0; \quad r_w \neq 0; \quad r_s \neq 0.$$

In this case equation (5-1) becomes:

$$i_1 r_{br1} - i_2 r_{br2} - i_2 r_w - i r_s + i_1 r_w = 0. \quad (5-10)$$

Substituting for previously received values of currents i_1 and i_2 and resistances r_{br1} and r_{br2} we have:

$$(i_a - i)r_{br}\frac{T}{t} - (i_a + i)r_{br}\frac{T}{T-t} - (i_a + i)r_w - ir_s + (i_a - i)r_w = 0,$$

or

$$i_ar_{br}T\left(\frac{1}{t} - \frac{1}{T-t}\right) - ir_{br}T\left(\frac{1}{t} - \frac{1}{T-t}\right) - i(r_s + 2r_w) = 0,$$

from where

$$i = i_a \frac{1 - \frac{2t}{T}}{1 - \frac{r_s + 2r_w}{r_{br}} \frac{t}{T} \left(1 - \frac{t}{T}\right)}. \quad (5-11)$$

The curve $i=f(t)$ plotted with the help of formula (5-11) is shown in Fig. 5-3, *b* by a solid line. We may observe, that when the resistance $r_s + 2r_w$ is taken into account the commutation becomes curvilinear. Nevertheless, this case is of no great importance as for conventionally used carbon brushes the resistance r_{br} of the brush contact is much greater than the resistance $r_s + 2r_w$.

5-6. Commutation with the E.M.F.s e_L and e_c Acting

As previously stated, the e.m.f. of self-induction e_L tends to retard current reversal in the circuit and the commutating e.m.f. e_c may act concurrently or in opposition to the e.m.f. e_L depending on field polarity in the commutation zone.

Let us first make clear the effect of the e. m. f. e_L , assuming that $e_c = 0$. As the brush slides more and more onto bar 1 (Fig. 5-4, *a*) current i_1 increases, while current i_2 decreases and the additional commutation current i_c , set up in the short-circuited coil by the e.m.f. e_L is so directed that it is in opposition to current i_1 and concurrent with current i_2 . The current i in the coil undergoing commutation attains the given value later than in

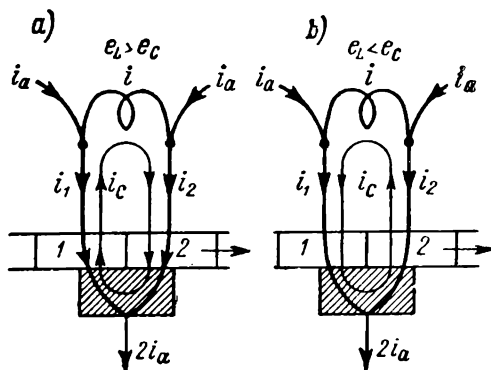


Fig. 5-4. Current i_c for commutation:
a - retarded and *b* - accelerated

case of linear commutation (curve 2 in Fig. 5-5, a) and therefore, the commutation acquires a curvilinear retarded feature.

With this feature of commutation we have:

$$j_{br2} \equiv \tan \alpha_2 > j_{br1} \equiv \tan \alpha_1, \quad (5-12)$$

i. e., with retarded commutation the current density at the trailing edge of the brush is greater than at the leading edge.

If now the e.m.f. e_c were to appear in the coil undergoing commutation, and act concurrently with the e.m.f. e_L , the commutation would acquire a still more retarded character (curve 3 in Fig. 5-5, a). With an abruptly retarded commutation the angle α_2 tends to 90° and therefore j_{br2} tends to infinity. Under these conditions sparking may originate at the trailing edge of the brush (see below § 5-12). With the effect of e_c opposing e_L the current i_c reverses its direction, if $e_c > e_L$ (Fig. 5-4, b). In this case the current i in the coil undergoing commutation will reach the given value earlier than with linear commutation (curves 4 and 5 in Fig. 5-5, a) and therefore commutation acquires a curvilinear accelerated character.

For accelerated commutation we have:

$$j_{br2} \equiv \tan \alpha_2 < j_{br1} \equiv \tan \alpha_1, \quad (5-13)$$

viz., with accelerated commutation the current density at the trailing edge of the brush is less than that at the leading edge. For an abruptly accelerated commutation (curve 5 in Fig. 5-5, a) angle α_1 tends to 90° and current density j_{br1} , therefore, tends to infinity. Under these conditions sparking may appear at the leading edge of the brush.

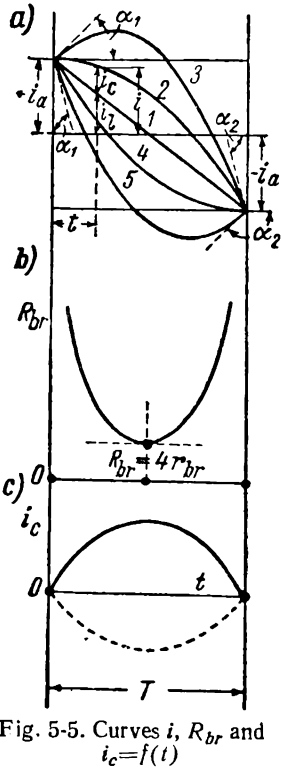


Fig. 5-5. Curves i , R_{br} and $i_c = f(t)$

5-7. Commutation when $b_{br} = b_c$, $2r_w + r_c = 0$ and $e_L + e_c \neq 0$.

In this case the equation for the commutation e.m.f. [formula (5-1)] acquires the form:

$$i_3 r_{br1} - i_2 r_{br2} = e_L + e_c = \Sigma e. \quad (5-14)$$

Substituting in the equation the expressions for currents i_1 and i_2 and resistances r_{br1} and r_{br2} [formulas (5-4a), (5-4b), (5-5) and (5-6)], we get:

$$(i_a - i)r_{br}\frac{T}{t} + (i_a + i)r_{br}\frac{T}{T-t} = \Sigma e,$$

and further

$$i = i_a \left(1 - \frac{2t}{T}\right) + \frac{\Sigma e}{r_{br} \left(\frac{T}{t} + \frac{T}{T-t}\right)} = i_L + i_c, \quad (5-15)$$

here

$$i_L = i_a \left(1 - \frac{2t}{T}\right) \quad (5-16a)$$

and

$$i_c = \frac{\Sigma e}{r_{br} \left(\frac{T}{t} + \frac{T}{T-t}\right)} = \frac{\Sigma e}{R_{br}}, \quad (5-16b)$$

where R_{br} represents the resistance of brush contact to current i_c at each moment.

Thus, for the conditions considered, the commutating current i equals the total of two currents—the current of linear commutation i_L and the superposed onto it additional commutation current i_c , due to the sum of the e.m.f.s

$$e_L + e_c = \Sigma e.$$

For the given value of T and $r_{br} = \text{const}$ the resistance $R_{br} = r_{br} \left(\frac{T}{t} + \frac{T}{T-t}\right) = \infty$ at moments $t=0$ and $t=T$ and passes through a minimum $R_{br} = 4r_{br}$ at $t = \frac{T}{2}$ (Fig. 5-5,b). If in this case the sum $e_L + e_c = \text{const}$ then the curves $i_c = f(t)$ have the form shown in Fig. 5-5,c; the curve above the abscissa axis corresponds to the predominance of self-induction e.m.f. e_L , the curve below the abscissa being the case of e.m.f. e_c predominance.

Comparing both formulas, (5-7) and (5-15), we may observe, that if the e.m.f. e_c is chosen of such magnitude and sign as to make $\Sigma e = e_L + e_c = 0$, then current $i_c = 0$ and there would remain only the linear commutation current $i = i_L$ (Fig. 5-3, a).

If resistances r_w and r_c are to be taken into account, but with the former assumption, that $\Sigma e = e_L + e_c = 0$, the relation $i = f(t)$ will have the form of the curve shown in Fig. 5-3,b.

The coil circuit undergoing commutation, for which $\Sigma e = e_L + e_c = 0$ and for which, consequently, the process of commutation

is definable by active resistances of the circuit, may be considered as *non-inductive*; it closes at $t=0$ and breaks at $t=T$ without sparking. Such commutation, usually known as *dark commutation*, though it provides the best conditions for d.c. machine operation,

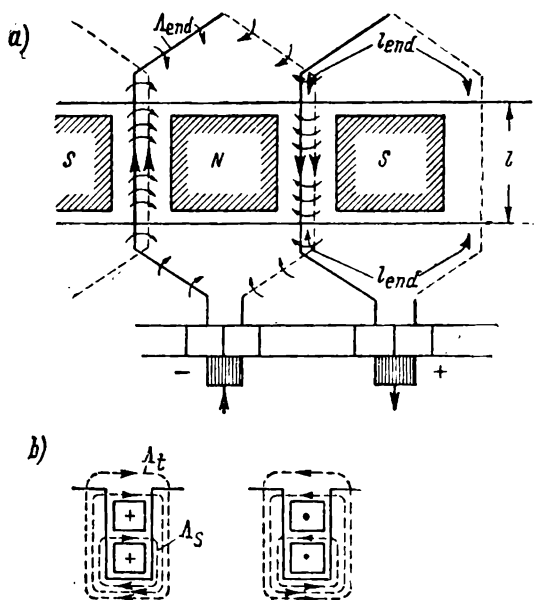


Fig. 5-6. Flux of coil section undergoing commutation

ration, is not absolutely necessary, since the State Standard 183-55, allows for the $1\frac{1}{2}$ degree of sparking at rated conditions when sparking is not stipulated. Such commutation is often termed as "commutation practically without sparking". The operation of a machine with "practically no sparking" is a fundamental requirement for any kind of commutator machine.

5-8. Determination of E.M.F. of Self-Induction e_L for $b_{br}=b_c$

When we speak of the e.m.f. e_L , it is its instantaneous value that we are contemplating. But as the determination of this value is a very complex problem, it is the usual practice to confine oneself to determining the mean value of e.m.f. of self-induction for the commutation period T . During this period the current in

the section undergoing commutation varies from the value $+i_a$ to $-i_a$. Therefore,

$$e_L = \frac{1}{T} \int_{+i_a}^{-i_a} -L_c \frac{di}{dt} = L_c \frac{2i_a}{T} \quad (5-17)$$

Here L_c is the inductance of the section undergoing commutation. Let us recall that the inductance is defined by the flux linkage, i. e., the product of the flux and the number of turns linked with it, when a current of 1 A flows through the coil section.

The definition of L_c is based on the conception of *specific magnetic permeance* Λ which is the number of flux linkages per unit length of coil section consisting of one turn, through which a current of 1 A is flowing.

The flux linked with the coil undergoing commutation is shown in Fig. 5-6, a. It may generally be divided into three parts (Fig. 5-6, b): a) *the slot part*, which consists of flux lines, flowing across the slot from one side to the other; this flux section is distributed along the length $l+l=2l$ of the active part of the coil section; b) *the tooth part*, consisting of flux lines closing between the heads of adjacent teeth; this part of the flux is also distributed along the length $2l$; c) *end connection part*, consisting of flux lines closing round the coil section end connection parts along the length $2l_{end}$ (Fig. 5-6, a).

Thus we have three specific magnetic permeances: slot permeance Λ_s , tooth permeance Λ_t and end connection permeance Λ_{end} . The number of flux linkages along the entire length of section when a current of 1 A flows through it is equal to:

$$2l\Lambda_s + 2l\Lambda_t + 2l_{end}\Lambda_{end} = 2l \left(\Lambda_s + \Lambda_t + \frac{l_{end}}{l} \Lambda_{end} \right) = 2l\Lambda'$$

The value Λ' we shall call the *equivalent specific magnetic permeance of the coil section*.

In the general case a section comprises w_c turns. For a current of 1 A its m.m.f. totals w_c amperes, i. e., compared with the former case it is increased w_c times. Since the flux linked with the coil undergoing commutation flows mainly through the air, it also changes w_c times; accordingly the number of flux linkages increases w_c^2 times. Hence the inductance of such a coil section will amount to:

$$L_c = 2w_c^2 l \Lambda' \quad (5-18)$$

Up till now it was assumed that in the slot considered only one coil side undergoes commutation. But in a full-pitch winding

($y_1 = \tau$) there is in the same slot the side of the other coil section undergoing commutation short-circuited by a brush of the other polarity (Fig. 5-6,a). Between these sides there exists in the slot a very close mutual inductive coupling, while there is no mutual inductance between the end connections. Therefore it may be stated, that the number of flux linkages of each active side along the length l is doubled, while the number of flux linkages of the end connections does not change. Hence, taking into account for L_c also the mutual inductance due to the coil sections undergoing commutation under other poles, it is possible to write:

$$\Lambda' = 2(\Lambda_s + \Lambda_t) + \frac{l_{end}}{l} \Lambda_{end}. \quad (5-19)$$

Substituting the value L_c in the formula (5-17), we get:

$$e_L = 2\omega_c l \Lambda' \frac{2i_a}{T}.$$

But

$$\omega_c = \frac{N}{2S} = \frac{N}{2K}$$

and

$$T = \frac{b_{br}}{v_c} = \frac{b_c}{v_c} = \frac{b_c \frac{D_a}{D_c}}{v_c \frac{D_a}{D_c}} = \frac{b_c \frac{D_a}{D_c}}{v_a}.$$

Here D_a and D_c are the diameters of armature and commutator; v_a and v_c —the linear speeds at the armature and commutator peripheries. Therefore,

$$e_L = 2\omega_c l \Lambda' \frac{N}{2K} \frac{2i_a}{b_c \frac{D_a}{D_c}} v_a$$

or, since $Kb_c = \pi D_c$
then

$$e_L = 2\omega_c l \Lambda' \frac{Ni_a}{\pi D_a} v_a = 2\omega_c v_a l \Lambda' A. \quad (5-20)$$

The formula (5-20) was suggested by Pichelmayer. All values in it may be assumed as known except the permeance Λ' . The estimation of this value may be carried out by methods described in Part II of this book. To determine the e.m.f. e_L preliminarily we may use experimentally obtained values of Λ' .

In the MKSA system of units the permeance Λ is measured in henries per metre. According to data given by Trettina for a ma-

chine with commutating poles the following values of Λ' may be used:

Low-output machines with a winding of round copper wire for $w_c > 1$	$(6 \text{ to } 8) \times 10^{-6}$
Average-output machines with bar windings	$(5 \text{ to } 6) \times 10^{-6}$
Low-speed, large-output machines with short steel cores . . .	$(6 \text{ to } 8) \times 10^{-6}$
Low-speed, large-output machines with long steel cores . . .	$(3.8 \text{ to } 4.5) \times 10^{-6}$
High-speed, large-output machines	$(4 \text{ to } 5) \times 10^{-6}$

Let us note, that when e_L is determined by formula (5-20) the numerical result will not change if instead of units of the MKSA system we shall express the length l in cm and the loading A in amperes per cm.

5-9. The Coil Section Commutating E.M.F. e_c

Consider the winding having a full pitch $y_1 = \tau$. In this case both sides of the coil section undergoing commutation are influenced by the same conditions in respect to the field in the commutation zone (Fig. 5-6, a). If B_c is the flux density in the commutation zone and l_c —the length of that part of conductor which crosses the lines of the commutating field, then

$$e_c = 2\omega_c v_a l_c B_c. \quad (5-21)$$

Usually $l_c \approx l_a$, where l_a is the length of armature.

5-10. Commutation when Brush Width Is $b_{br} > b_c$

Usually a brush covers 2-3 commutator divisions. In such a case several adjacent lying coil sections simultaneously undergo commutation and in each of them the adjacent coil sections, undergoing commutation, would induce the e.m.f. of mutual induction e_M .

The e.m.f.s of self-induction e_L and mutual induction e_M together form the resultant reactive e.m.f. e_r of the section undergoing commutation.

If L_c is the inductance of a coil section, with the mutual inductance from coils undergoing commutation located under other poles, taken into account, and ΣM is the mutual inductance of the given section with all other adjacent sections simultaneously undergoing commutation, the resultant coil section induction will be:

$$L_r = L_c + \Sigma M. \quad (5-22)$$

To determine L_r , we must first find its corresponding magnetic permeance Λ_r . For this purpose we shall use the method of adding specific magnetic permeances of all inductively coupled active sides taking into account the commutation start time lag of each section.

Consider the case of a simple lap winding with full pitch ($y_1 = \tau$), the number of section sides per slot being $2u=8$, so that in each layer there are $u=4$ sides; the width of the brush $b_{br}=2.5b_c$ (Fig. 5-7).

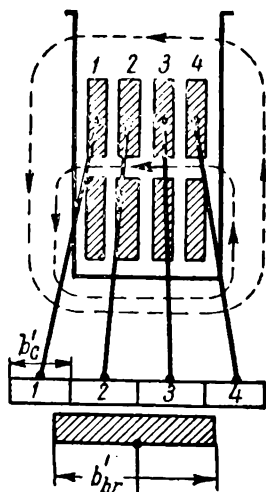


Fig. 5-7. Commutation for a lap winding: $y_1 = \tau$, $u=4$ and $b_{br}=2.5b_c$

In a winding with a full pitch the sides of the top and bottom layers, being short-circuited by brushes of opposite polarity, undergo commutations simultaneously (see Fig. 5-6, a); therefore, when joining each side of the top layer with the corresponding side of the bottom layer, we may speak of commutation of four coil sections.

From the winding diagram in Fig. 5-6, a it may be seen, that inductive interaction exists only between the coil active sides embedded in the slots, whereas their end connection parts are practically not coupled inductively.

Since we accept the e.m.f. e_L as the mean value, i.e., as constant during the commutation period, we may depict the specific magnetic permeance Λ_s of each of the four coil sections per slot by the height of a rectangle, the base of which is proportional to

the brush width $b_{br}' = b_{br} \frac{D_a}{D_c}$, reduced to the armature periphery or, for a given linear speed of armature v_a — the commutation period $T = \frac{b_{br}'}{v_a}$. It is obvious, that four such rectangles correspond to the four coil sections in the slot undergoing commutation plotted one on top of the other, and each displaced in respect to the preceding one by the width of the commutator division reduced to the armature periphery $b_c' = b_c \frac{D_a}{D_c}$ and in the order corresponding to a given armature rotation direction (Fig. 5-8, a).

To obtain the resultant permeance of the given coil section, it is necessary to add together the corresponding ordinates of the four rectangles. The results of the addition for each of the four coil sections are shown in Fig. 5-8, *b, c, d, e*. The resultant permeance of the entire slot is then depicted as a curve in Fig. 5-8, *f*. The base of this curve shows the magnitude of the commutation zone $b_{c.z.}$. In the considered case of a simple full-pitch lap winding we have then:

$$b_{c.z.} = b'_{br} + (u - 1) b'_c. \quad (5-23)$$

Comparing the permeances of separate sections, we may observe that they are different in form and magnitude. In accordance with this, the e.m.f.s induced in each section during the commutation period are also different in form and magnitude; in other words the commutation conditions for the various sections occupying the same slot are different.

In order to determine the mean value of permeance Λ_r for all the four coil sections contained in one slot, it is necessary to determine the mean value of the permeance for each coil section. The mean values of permeance for coil sections 1 and 4 is $\Lambda_{av1} = \Lambda_{av4} = 1.8\Lambda_s$; correspondingly, for coil sections 2 and 3

$$\Lambda_{av2} = \Lambda_{av3} = 2.4\Lambda_s; \text{ hence, } \Lambda_r = \frac{1.8 + 2.4}{2} \Lambda_s = 2.1\Lambda_s, \text{ i.e., the mean}$$

resultant permeance Λ_r , and also, therefore, the mean resultant inductance of the coil section L_r , have increased 2.1 times. On the other hand, the commutation period T of the coil section has increased by the ratio $\frac{b_{br}}{b_c}$,

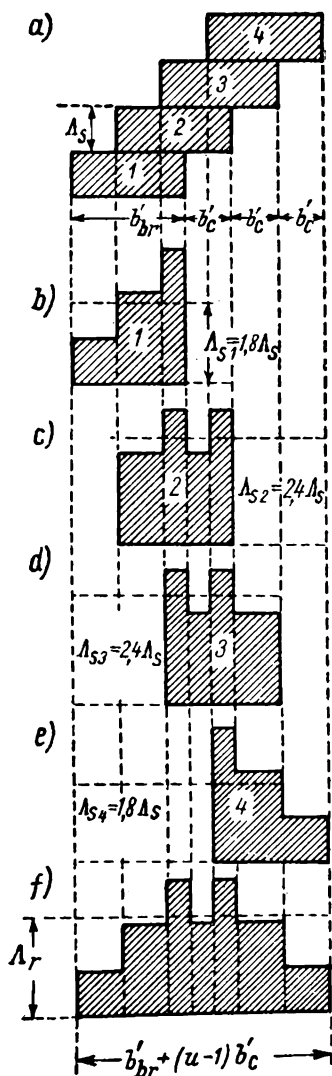


Fig. 5-8. *a, b, c, d, e* — the resultant inductance of coil sections 1, 2, 3, 4 in Fig. 5-7; *e* — resultant inductance of slot in Fig. 5-7

i.e., 2.5 times, and since the e.m.f. $e_r \equiv \frac{L_r}{T} e_L$, then in the given case we have:

$$e_r = \frac{2.1}{2.5} e_L = 0.84 e_L.$$

Thus the reactive e. m. f. e_r has somewhat decreased in comparison with e.m.f. e_L but very little. In the other cases the deductions are analogous. For example, in Fig. 5-9 are given

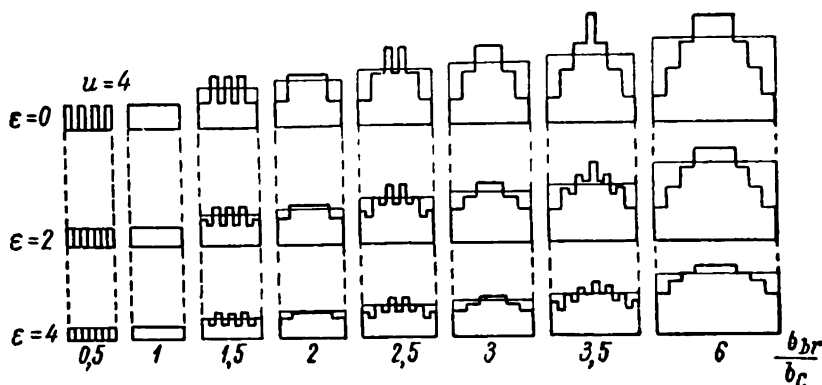


Fig. 5-9. Resultant inductance of coil section undergoing commutation for $u=4$ in relation to degree of winding pitch chording and to relative

width of brushes $\frac{b_{br}}{b_c}$

curves of the resultant inductance for the case of a simple lap winding with $u=4$ active sides per layer in relation to the ratio $\frac{b_{br}}{b_c}$; the top horizontal line refers to full-pitch windings ($\varepsilon=0$); the two other lines refer to windings with a pitch shortened by $\varepsilon=2$ and $\varepsilon=4$, ε being measured by the number of elementary slots (§ 3-9, A). We see, that fractional pitch windings, and the stepped winding in particular, possess valuable properties in respect to commutation, since the maximum value of resultant inductance for such windings is always less than with a full-pitch winding, and besides this, the inductance fluctuations in respect to the mean value are smoothed out.

Very detailed research on the effect of brush width on the magnitude of reactive e. m. f. has been carried out by K. I. Shenfer. He arrived at the conclusion, that if the number of commutator divisions covered by the brush is less than the number of active

sides in the layer or equal to it, i. e., $\frac{b_{br}}{b_c} \leq u$, then it is possible to use the formula (5-20) without any corrections, since in this case the increase in inductance L_r is compensated by a similar increase of the commutation period T . If $\frac{b_{br}}{b_c} > u$, then in formula (5-20) a correction coefficient should be introduced amounting in the average to $0.7 \frac{u}{\frac{b_{br}}{b_c}} + 0.3$.

In ordinary cases the reactive e.m.f. e_r is calculated by formula (5-20) without introducing any corrections, thus obtaining a somewhat exaggerated value of e.m.f. e_r and therefore a certain unfavourable error is allowed to creep in.

5-11. Commutation Armature Reaction

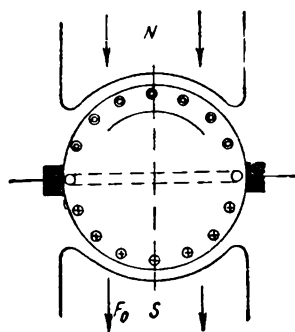
The commutation armature reaction is the effect produced on the main field by the field established by the commutation current.

Consider the machine operating as a generator, the brushes being set on the geometrical neutral and the armature winding pitch $y_1 = \tau$ (Fig. 5-10, *a*). In this case the axis of the circuit undergoing commutation coincides with the axis of the main poles, and therefore the m.m.f. established by the circuit may act either contrary to, i.e., as a demagnetising factor in respect to the m.m.f. of the main poles, or concurrently with it, viz., as a magnetising factor.

Assume the commutation as linear. In this case during the first half of the commutation process, i.e., during the period from $t=0$ to $t=T/2$, the current in the coil undergoing commutation has still the direction it had prior to the beginning of commutation, and during the second half of the commutation process from $t=T/2$ up to $t=T$ the current direction in the section undergoing commutation is reversed (in Fig. 5-10, *b* the brush scale is exaggerated). Hence, during the first half of the commutation process the m.m.f. of commutation F_{cm} has a demagnetising effect on the main field and during the second half a magnetising effect. As a result both effects are mutually compensated and for this reason it may be said, that with linear commutation the commutation current does not effect the main magnetic field. This deduction is also true in the case of the motor.

If the commutation is of a *retarded nature*, then, as may be seen in Fig. 5-10, *c* the demagnetising effect of the circuit under-

going commutation is predominating, and as a result the *main field is weakened*. It is quite easy to show, that if the machine operates as a *motor*, the circuit undergoing commutation renders the same demagnetising effect on the main field but with accelerated commutation.



If, on the contrary, the commutation is of an accelerated nature in a generator or retarded in a motor, the circuit undergoing commutation renders a demagnetising effect on the main field (Fig. 5-10,d).

5-12. Electromagnetic Sources of Sparking

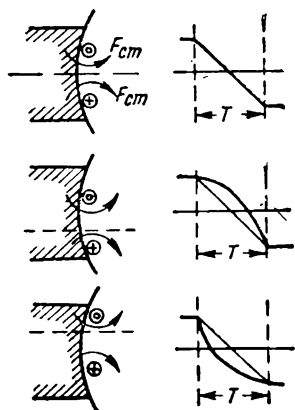


Fig. 5-10. Effect of commutation current on main field

The opinions as to which electromagnetic sources contribute most to sparking have changed with passage of years. First it was suggested (T. Ride) that sparking was due to *excessive current density under the brush*. But tests have proved that if the brush works on the commutator with the coil undergoing commutation possessing a practically active resistance then no sparking is visible even for average current densities of 255 A/cm² per brush and up to 350 to 400 A/cm² under the trailing edge of the brush.

Another suggestion that failed to give proper explanation of this was that the existing *switching voltage* between the brush edge and the commutator trailing bar was quite sufficient to create sparking. But tests carried out by Arnold and La Cour proved that under certain conditions no sparking was visualised even with a voltage up to 10 V. This brought up the idea that sparking originates when the coil short-circuited by the brush at the moment of interruption stores a sufficient amount of *electromagnetic energy* $\frac{1}{2} L_r i_{cm.sh}^2$ where $i_{cm.sh}$ is the additional commutation current when the short-circuited coil is opened. According to Arnold the power released when interrupting such a circuit should not exceed 50 watts per 1 cm length of brush.

Research work carried out by K. I. Shenfer and S. B. Yuditsky allowed to make the deduction that when the reactive e.m.f. e_r predominates in the circuit undergoing commutation, i.e., $e_r - e_c = +\Delta e_c$ the commutation process depends on the value Δe_c , i.e.: if Δe_c is smaller than a certain critical value $\Delta e_{c, crit}$, the resistance R_{br} in formula (5-16b) will vary according to the curve in Fig. 5-5, *b*, i.e., at the moment $t=T$ it tends to infinity while the current i_c tends to zero (Fig. 5-5, *c*). In this case commutation takes place without sparking. If it happens that $\Delta e_c > \Delta e_{c, crit}$ then, beginning with the instant $t = \frac{T}{2}$, the resistance R_{br} almost ceases to increase and, therefore, for $t=T$ the current $i_{c, crit} \neq 0$. The discharge of electromagnetic energy $\frac{1}{2} L i_{c, crit}^2$ corresponding to this current is therefore the cause of sparking at the brush trailing edge, when the circuit with current is interrupted. [Bibl. 52a]

Sparking at the brush leading edge originates in cases of abruptly accelerated commutation due to a significant predomination of e.m.f. of the outer field e_c , the current passing only through a small number of initially originating points of contact between brush and commutator bar. This facilitates a large increase in current density and voltage at these points and if the energy released is sufficiently large, then the leading edge of the brush begins to glow and starts sparking.

Along with stored electromagnetic energy in the coil undergoing commutation, of great importance is the power released in the contact resistance. At overloads and especially when abrupt short-circuits occur, the energy released at the commutator leads to formation of commutation arcs between the brushes and the commutator, and in the extreme case to flashovers. This is discussed in more detail in § 5-13, C.

5-13. Potential Causes of Sparking

Practice shows, that commutation is to a great extent influenced by the distribution of potential over the commutator and, in particular, by the maximum voltage possible between two adjacent commutator bars u_{max} .

A. Distribution of voltage between adjacent commutator bars. Assume that a simple full-pitch lap winding ($y_1 = \tau$) is arranged on the armature. The voltage between two adjacent commutator bars is defined by the e.m.f. $e_x = B_x l v = C B_x$, induced in the coil section connected to these bars, while the magnitude B_x represents the flux density at the point where at

the given instant the coil section is located (Fig. 5-11). With a sufficiently large number of commutator divisions we may assume, that the voltage distribution between adjacent commutator bars

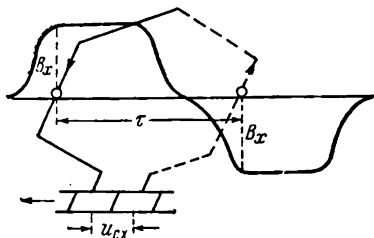


Fig. 5-11. Voltage between adjacent commutator bars

to the flux density curve along the air-gap of the machine.

If U is the voltage between two adjacent brushes of different polarity and K — the number of commutator divisions, then the average voltage between two adjacent commutator bars is:

$$U_{av} = \frac{U}{K/2p} = 2p \frac{U}{K}. \quad (5.24)$$

It is possible to prove that the voltage u_{av} does not depend on the type of winding.

To determine u_{max} it is necessary to take into account, that: a) the machine e.m.f. is created not by all the coil sections S but only by coil sections $\alpha'S = \alpha'K$, and b) the cross armature reaction in machines without a compensation winding greatly distorts the distribution of flux density in the gap, increasing it at the trailing edge of the pole in a generator and at the leading edge in a motor (§ 4-3 and 4-5); the e.m.f. of the coil sections in the places under the poles

corresponds, to a certain scale, to the distribution of flux density over the air-gap of the machine.

In Fig. 5-12, *a* and *b* curves 1 depict voltage distribution between commutator bars for no-load and load conditions of a machine. With a relatively small number of commutator divisions per pole the voltage between the bars is characterised by the stepped curve 2, the middle line of which (curve 1) is proportional

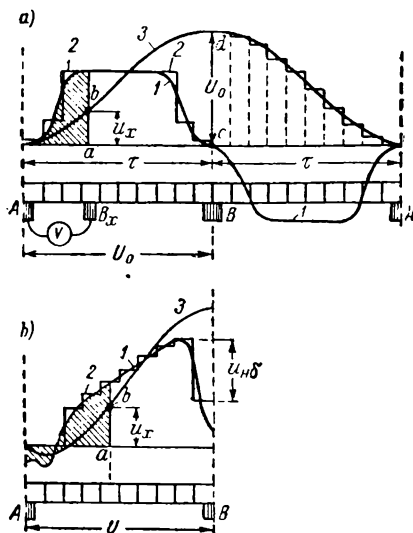


Fig. 5-12. Voltage between adjacent commutator bars and potential curves: *a* — on no-load; *b* — on load (u_{x0} stands for u_{av0})

increases correspondingly; this increase is taken into account by a factor $k_u = 1.3$ to 1.5 . Then,

$$U_{max} = k_u 2\rho \frac{U}{a'K}. \quad (5-25)$$

Tests have proved, that the commutation process proceeds a normal course only when $u_{max} \leq 25$ to 28 V in large machines, 30 to 35 V in medium-power machines and 50 to 60 V in small machines. If the voltage u_{max} exceeds these limits, the insulation strip between two adjacent commutator bars may be spanned by an arc, this fault being facilitated by carbon and metallic dust deposits always present on the commutator. The arc ionises the air thus facilitating the appearance of more powerful arcs which may disrupt the operation of the machine.

B. Commutator potential curves. In close relation to the distribution of voltage between the bars is the curve voltage distribution over the commutator periphery, called the commutator

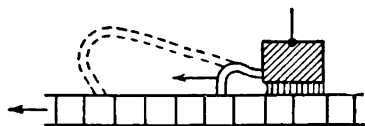


Fig. 5-13. Arcing at commutator

potential curve. To obtain this curve by experimental means, one brush is fixed in respect to commutator, usually the brush which is on the geometrical neutral axis, the other brush being moved round the commutator periphery and voltmeter readings taken of the voltage between these brushes. In Fig. 5-12, *a* and *b* curves 3 depict the potential curves for no-load and load conditions of the machine. The hatched areas of the curves are proportional to the sum of e.m.f.s of all winding coil sections, arranged between brushes *A* and *B_x* and express the voltage value between them. Thus the *potential curve over the commutator represents an integrated curve in respect to the air-gap flux density distribution curve* and therefore in respect to voltage between adjacent commutator bars. With the help of this curve it is possible to obtain the voltage between any commutator bars as the difference between the corresponding ordinates of the potential curves. Thus, for example, the voltage between brushes *A* and *B_x* (Fig. 5-12, *a*) is determined by the ordinate $ab = U_x$, the voltage across brushes *A* and *B* by the ordinate $cd = U_0$ and so on.

C. Commutator flashovers. When abrupt changes in load or sudden short-circuits occur, *flashing or bucking* develops over the commutator, i. e., a long blue spark is drawn out around the surface of the commutator from brush to brush or from brush to frame. The spark is somewhat of the nature of an arc and may

seriously injure the machine. The investigation of this phenomenon and development of methods impeding flashover or eliminating its consequences as quickly as possible are of great practical value. The physical nature of the phenomenon which is of very great complexity was investigated by A. I. Moskvitin and especially by O. B. Bron and V. S. Alexandrov. [Bibl. 50,51]

In the main the process may be described as follows. When an inrush of current takes place in the coil section undergoing commutation the reactive e.m.f. e_r becomes predominating due to which the commutation process acquires an abruptly retarded nature. A large amount of energy is released in the transient brush contact, which brings about an abrupt drop of transient voltage and this causes a powerful commutation arc between the trailing commutator bar and brush tip. Due to commutator rotation this arc is mechanically expanded and under the effect of electro-dynamical forces moves along the commutator at a great speed which sometimes exceeds the commutator periphery speed.

This large current inrush causes also a large distortion of the main field due to the armature reaction effect. Because of this the distribution of potential among the commutator bars established for normal operation becomes upset. This, on the one hand, may lead to the generation of voltaic arcs between some adjacent bars due to an increase of voltage across them, and on the other hand, the distortion of potential distribution causes a very abrupt increase of voltage between the brush and commutator bars when they are running off the trailing edge of the brush. Such an increase of voltage facilitates the propagation of the commutation arc over the commutator periphery, since as it becomes more and more elongated a larger difference of potential is required to keep it burning.

When the arc moves, it is greatly stretched by electro-dynamical forces (Fig.5-13) and, on reaching a certain point of the commutator, it dies out. At this moment a new arc is created and again moves over the commutator. Due to the ionisation of the space over the commutator by the previous arc, burning conditions for each of the consecutive arcs are alleviated and therefore before the arc is extinguished it may move a longer distance round the commutator. This process is repeated many times, becoming a high-frequency process. In this case the commutation arcs are superimposed onto the voltaic arcs thus forming a continuous ring round the commutator. All this is followed by intensive luminous and acoustic effects. Methods for preventing flashing are discussed later in Chapter 6.

5-14. Mechanical Causes of Sparking

These are due, on the one hand, to deficiencies of the commutator and rotating parts, and on the other hand, to brushgear faults. The former may comprise such faults as: eccentricity of commutator on shaft, improper balancing of rotation parts, rough commutator face, high mica between bars (therefore they are usually undercut to a depth of 1 to 1.5 mm), insufficient baking of commutator, high bars, etc. The latter type of faults may include: incorrect fixing of brush-holder on brush-stud, loose mounting of the brush-rocker, incorrect choice of brush grade, etc. Experience shows that the brushgear apparatus greatly influences the quality of the machine's commutation; of especial importance is the brush contact, its nature and characteristics are discussed in Chapter 6.

5-15. Contemporary Conceptions on Nature of Commutation Process

Both concepts of the classic theory of commutation which were formulated previously in § 5-2 are in contradiction with reality. Tests carried out at an early stage by Arnold have shown that in no case will the entire surface of the brush conduct current and that the real commutation period is always less than the calculated period, determined by the width of the brush and speed at the commutator periphery ($T = \frac{b_{br}}{b_c}$). Further tests (V. Styne) have shown, that no change takes place in the curve of contact pressure drop, if we would cut bits off the contact surface of the brush and decrease it to 1/10 of its initial value, without changing the pressure of the brush.

Even less relevant to the actual facts is the second concept of the classical theory of commutation. When solving the equation for e.m.f. in the coil section undergoing commutation [formula (5-14)], the classical theory comes to the conclusion that to obtain non-sparking commutation it is necessary, that $\frac{r_{br}T}{L_r} > 1$ (r_{br} is the contact resistance of the entire brush contact surface, T —the commutation period and L_r —the inductance of the coil section undergoing commutation). But the data established by R. Richter show that many commercial machines work without any sparking with the $\frac{r_{br}T}{L_r}$ values of the order of 0.1, i. e., much less than the stipulated 1. This, naturally, may be explained by

the fact, that if we consider conventional type carbon brushes then the specific contact resistance of brush ρ_{br} varies almost inversely to current density j_{br} , while the transient drop of potential $\Delta U_{br} = \rho_{br} j_{br}$ remains approximately constant. It was on this experimentally established fact, that O. G. Wegner based his analysis of the commutation process from an entirely new point of view. In this case resistance commutation becomes impossible and the current in the coil section undergoing commutation remains constant during a major part of the period T . [Bibl. 56]

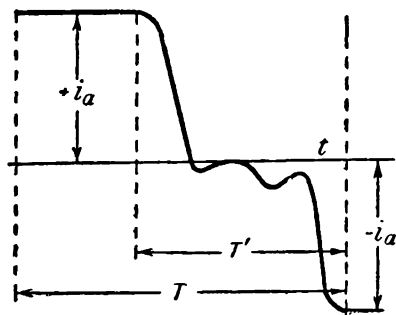


Fig. 5-14. Experimental curve $i=f(t)$ for slow armature rotation

This deduction conforms well with the results of tests carried out by K. I. Shenfer, M. F. Karasyov and also by O. G. Wegner. For illustration Fig. 5-14 shows the curve $i=f(t)$ taken by K. I. Shenfer

for the case of a slowly revolving armature, when it was legitimate to assume, that the commutation process is defined only by the active resistances of the section undergoing commutation. The curve proves that the real commutation period T' is much less than the calculated period $T = \frac{b_{br}}{b_c}$ and that current i varies with two abrupt drops which thus exclude the possibility of assuming a linear commutation. [Bibl. 55]

But if the concept which assumes that $\Delta U_{br} = \text{const}$ is nearer to actual conditions than with $\rho_{br} = \text{const}$ this in itself is yet far from being sufficient.

For a more complete elucidation of the phenomena observed with a brush in operation, a new theory of *point contact* was suggested in conjunction with the conception of the *ionic nature of the processes in the contact layer of the brush*.

In its complete form this theory was developed by I. Neukirchen and later supplemented by investigations carried out at the All-Union Electrical Engineering Institute by M. S. Sosnovskaya and A. I. Moskvitin, then more recently by M. F. Karasyov.

The effect of chemical, thermal and mechanical factors on commutation was analysed in detail from the point of view of the new theory. From the results of this analysis the following basic conclusions could be drawn:

1. With loads, exceeding a certain limited value, depending on the grade of brush, the *brush contact phenomenon is ionic by nature*.

2. The ionic processes taking place under anode- or cathode-polarised brushes are of different nature (the brush is called anode-polarised or anodic when the current flows from the brush to the commutator and cathode-polarised or cathodic when the current flows from the commutator to the brush). In this case the *process of electrolysis* takes place in the contact layer of the brushes of both polarities. But if the brush is polarised cathodically, then with passage of current minute carbon particles are transported onto the commutator and, being burnt in the oxygen of the air, are deposited on the commutator surface in the form of an oxidised film, which protects the commutator from attrition and increases the transient resistance of the brush contact.

If the brush is anodically polarised, no protective film will be formed. The thickness of the film layer and its nature depends on the current density, contact surface and ambient medium properties.

3. Since the greater part of the brush surface does not directly come into contact with the commutator surface, in considering the wear of these machine parts, we distinguish: a) purely mechanical wear, i. e., wear without participation of current; b) mechanical wear due to passage of current, and c) electrical wear without mechanical attrition.

The mechanical wear of commutator and brushes is as a rule insignificant, though there may be cases of abnormal wear of these parts mainly due to the brush structure.

The mechanical wear of commutator and brushes with passage of current is in general *much greater* than wear without current. This may be explained by the fact that the ionic processes taking place in the contact layer with passage of current destroy the smooth surfaces of the commutator and brushes. Especially detrimental is the action rendered by the arc (the so-called rising arc) which appears when the brush and commutator contact surfaces separate as in cases of machine jolting. The wear is of a polar nature. For example, the anode-polarised commutator wears quicker compared with the cathode-polarised commutator. With other conditions equal wear depends on the ambient air; humidity of the air, presence of gases chemically reacting with the commutator and brushes facilitate the wear.

Pure electrical wear of commutator takes place in conditions facilitating arc-forming, for instance, when the brush moves over the high mica spots on the commutator practically without touch-

ing the surface. With cathode polarisation of commutator the cathode arc spot is bound to the commutator, and the copper at the spot evaporates; as a result of this cathodic pulverisation of the commutator copper takes place.

4. With an increase of commutator temperature the contact ionisation occurs at lesser values of load current (according to tests by M. F. Karasyov ionisation of contact began: for a commutator temperature of 8°C—with a current of 12 A, while for a temperature of 43°C—with a current of only 4 A).

As regards temperature effect on sparking, according to the opinion of I. Neukirchen, it is an accompanying factor, but not a must.

The theory of ionic commutation, which presupposes an intermittent-point character of the sliding-surface contact, provides a fuller and more exact explanation of the commutator machine commutation process from physical point of view of this very complex phenomenon, but it still needs further development.

Chapter Six

MEANS OF IMPROVING COMMUTATION AND METHODS OF ITS INVESTIGATION

6-1. Means for Mitigating Sparking of Electromagnetic Origin

In the previous chapter it was shown, that the main cause of sparking of electromagnetic origin was the additional commutation current i_c , it being equal to:

$$i_c = \frac{\Sigma e}{\Sigma r} = \frac{e_r + e_c}{\Sigma r}, \quad (6-1)$$

where Σr is the resistance of the entire circuit undergoing commutation.

From formula (6-1) it follows that current i_c may be reduced or in other words, improved commutation may be obtained: a) by reducing the e.m.f. e_r , since it has a detrimental influence on the commutation; b) by establishing in the commutation zone a commutating field of such magnitude and polarity, that the e. m. f. e_c created by it in the coil section undergoing commutation could balance the e.m.f. e_r ; c) by increasing the resistance of the circuit undergoing commutation by means of selecting a brush with a large transient resistance of the brush contact or by inserting additional resistances into the circuit undergoing commutation.

6-2. Reduction of the Reactive E.M.F. e_r

From formula (5-20) it may be seen, that commutation conditions are more favourable in machines with smaller values of ω_c , v_a , l , Λ' and A . Therefore, the tendency is usually to make a coil section of one turn, i. e., with $\omega_c=1$; from the point of view of reducing magnetic permeance Λ' the slots of smaller height and greater width and stepped short-pitched windings are more advantageous. But a decrease in speed of v_a and of linear load A is unsuitable, as both lead to an increase of overall dimensions and cost of the machine.

In large-output machines slot dampers (Fig. 6-1) are sometimes used, which comprise a system of massive copper conductors laid in the slots along with the conductors, or a series of short-circuited turns enveloping the armature winding coil sections.

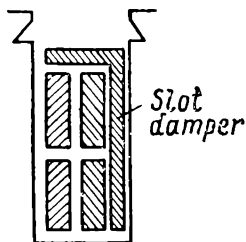


Fig. 6-1. Slot damper

Eddy currents originate in these dampers during commutation which decrease the e.m.f. e_r by 30 to 40 per cent and damp any abrupt changes in the coil section field undergoing commutation, not compensated by the machine commutating field (see below Fig. 6-4).

The slot dampers in the form of copper conductors were first suggested by K. I. Shenfer in 1921. Since they complicate machine design and increase losses this method of improving commutation is used only in exceptional cases. [Bibl. 23]

6-3. Creation of a Commutating Field by Shifting the Brushes from Neutral

In machines without commutating poles, the commutating field necessary to establish the e.m.f. e_c , that balances the e.m.f. e_r , is created by means of shifting the brush off the geometrical neutral.

To show how the brushes are to be shifted, assume that the machine works as a generator G and that the brushes $A-B$ are set on geometrical neutral (Fig. 6-2,a). Depict the e.m.f. e_a induced in the coil section "a" before the beginning of commutation by a segment directed upwards from the abscissa axis (Fig. 6-2,b). When the machine works as a generator, the current i_a coincides in direction with the e.m.f. e_a and establishes in the commutation

zone an armature cross field, shown in Fig. 6-2, *a* by two broken lines. By using the rule of the right palm, we find, that when coil section *a* moves under brush *A* and starts undergoing commutation, then the armature field induces in this coil section an e.m.f. e_{aq} of the same sign as the e.m.f. e_a ; therefore in Fig. 6-2, *b* the e.m.f. e_{aq} is depicted by a segment, directed upwards from the abscissa axis the same way as e.m.f. e_a .

During the commutation period T the current i_a varies from $+i_a$ to $-i_a$, and a reactive e.m.f. e_r is created in the coil undergoing commutation, always opposing the reversal of current i_a

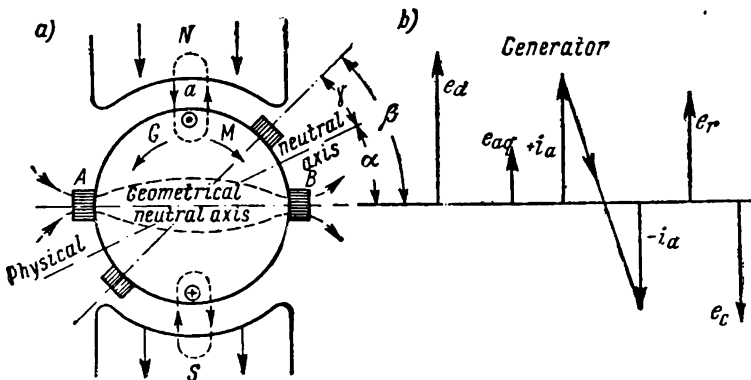


Fig. 6-2. Brush shift to improve commutation in generator

in the coil section; accordingly the e.m.f. should be depicted by a segment, directed upwards from the abscissa axis the same as the e.m.f.s e_a and e_{aq} . We may see, that the e.m.f. e_{aq} acts in the same direction as the e.m.f. e_r , i.e., retards and therefore exerts an unfavourable influence on the commutation. Having shifted the brushes in the direction of armature rotation by an angle α into the position of the physical neutral (Fig. 6-2, *a*), we obtain $e_{aq}=0$. But, besides this, it is still necessary to compensate the reactive e.m.f. e_r , by establishing in the section undergoing commutation an e.m.f. e_c of opposite direction in respect to e.m.f. e_r . Therefore in Fig. 6-2, *b* it should be depicted by a segment, directed downwards from the abscissa axis. Comparing the e.m.f.s e_a and e_c , we see, that they should be of different signs; in other words, if the e.m.f. e_a is created in the field of northern polarity before commutation has begun then the e.m.f. e_c during commutation must be created in the field of southern polarity. To satisfy this requirement, it is necessary to shift the brushes from the phys-

ical neutral by an additional angle γ in the direction of armature rotation.

This deduction is of a general nature, i. e., *for improving the commutation of a machine without commutating poles, working as a generator, it is necessary to shift the brushes from the geometrical neutral in the direction of armature rotation by an angle $\beta = \alpha + \gamma$.*

If the machine works as a motor with the same main pole and polarity, the same direction of current in the armature winding, then, compared with the generator it would rotate in the reverse direction (in Fig. 6-2, a —clockwise). Hence, *for improving commutation when the machine works as a motor it is necessary to move the brushes from the geometrical neutral against the direction of armature rotation.*

The main disadvantage of creating a commutating field by shifting the brushes is that the angle of brush shift must change with load. In a number of cases this is impossible, as for instance, with totally enclosed types of machines or with machines working with abruptly intermittent loads. Therefore in such machines the brushes have to be put in some middle position corresponding to some average load. But in such cases a superfluous commutating field will be obtained for small loads and insufficient for large loads.

With brushes on the geometrical neutral, the permissible value of non-compensated e.m.f. in machines without commutating poles is $e_r + e_{aq} \leq 2$ to 3 V.

When the brushes are shifted into a position which corresponds to half the load, it is possible to permit $e_r + e_{aq} \leq 4$ V.

6-4. Creation of a Commutating Field by Means of Commutating Poles

The most perfect and widely used method of improving commutation is the introduction of commutating poles, suggested by Metre as far back as 1885, but introduced into electrical machine-engineering practice only about 20 years later.

The commutating poles are arranged between the main poles along the geometrical neutrals axes (Fig. 6-3). The brushes are also set on these axes and remain in this position for all loads.

The number of commutating poles is usually equal to the number of the main poles and only in small-power machines their number may be decreased twofold. Thus, for instance, the two-pole machines of ПН-5, ПН-10 and ПН-17.5 types of 0.3 to 3.7 kW output have two main and one commutating poles.

The polarity of the commutating poles is determined by the consideration, that they should carry out the same function as that intended by shifting the brush in machines without commutating poles. Therefore, *if a machine works as a generator, the commutating pole must have the polarity of the leading pole, and in the case of a motor, of the trailing pole.*

To provide mutual compensation of the e.m.f.s e_r and e_c for some load, for example, the rated load, the commutating e.m.f. e_c should coincide as closely as possible in form with curve of

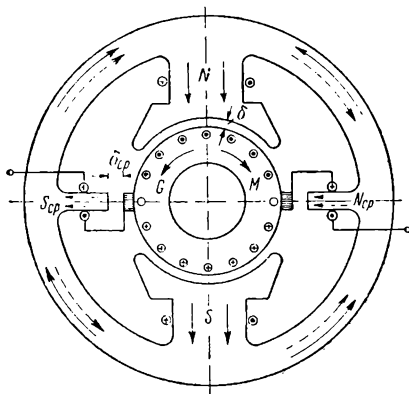


Fig. 6-3. Polarity of commutating poles when the machine works as a generator (G) and as a motor (M)

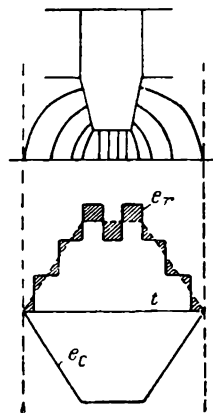


Fig. 6-4. Field curves in the commutation zone

reactive e.m.f. e_r determined by the curve of resultant inductance. This is, however, practically unattainable mainly because the e.m.f. e_r curve has a stepped form (see above the curves in Fig. 5-8). Examples of e_c and e_r curves in relation to time are shown in Fig. 6-4; the hatched areas on this figure correspond to the remaining e.m.f. $e_r + e_c$. Thus, when we speak of mutual compensation of e.m.f.s e_r and e_c it is their *mean values during the commutation period* that we consider, i. e., we assume $e_c = e_r$. Using formulas (5-20) and (5-21) we get:

$$2\omega_c v_a l_c B_c = 2\omega_c v_a l \Lambda' A,$$

whence

$$B_c = \frac{l}{l_c} \Lambda' A. \quad (6-2)$$

To maintain the proportionality between flux density B_c and electric loading A for all duties, *it is necessary to connect the commutating pole winding in series with the armature winding. The mag-*

netic circuit of the commutating poles should in this case be non-saturated, because only then will the flux density B_c vary as the current in the armature, and therefore also as the line load. For this purpose the following steps are taken: a) the gap under the commutating field is increased compared with the gap of the main pole (see Table 11-1); b) the commutating pole core flux density is chosen so as not to exceed 0.8 to 1.0 wb/sq.m at rated current; c) the flux density in the yoke created by the main m.m.f. value is not to exceed 1.2 wb/sq.m considering that the m.m.f.s of the main and commutating poles sum up at some parts of the yoke (Fig. 6-3).

The width of the commutating pole shoe $b_{c,p}$ is determined in relation to the width of the commutation zone $b_{c,z}$. Usually

$$b_{c,p} = (0.9 \text{ to } 1.0) b_{c,z}. \quad (6-3)$$

The width of the commutation zone in the case of a simple lap full-pitch winding is determined by formula (5-23). If a fractional pitch is used short-chorded by $\epsilon = \frac{Z_e}{2p} - y_1 = \frac{S}{2p} - y_1$ elementary slots, then the coil sides that are in the lower slot layer do not start commutation simultaneously with the sides in the top layer of the same slot, but either later or prior to the latter, this depending on the direction of armature rotation. Therefore before the last lower side finishes commutation the armature moves additionally over a distance

$$\left(\frac{S}{2p} - y \right) b_c \frac{D_a}{D_c} = \epsilon b'_c,$$

and, therefore, the commutation zone is increased by the same value, i. e.,

$$b_{c,z} = b'_{br} + (u - 1 + \epsilon) b'_c. \quad (6-4)$$

By analogous reasoning we obtain in the general case:

$$b_{c,z} = b'_{br} + \left(u - \frac{a}{p} + \epsilon \right) b'_c. \quad (6-5)$$

To calculate the magnetic circuit of the commutating poles, let us depict Fig. 6-3 in a developed form and plot separate curves of m.m.f. of the main poles F_o , cross armature reaction F_{aq} , commutating poles $F_{c,p}$, resultant m.m.f. of a machine and the curve of field distribution in the air-gap of a machine with commutating poles working as a generator (Fig. 6-5, a, b, c, d and see also Fig. 4-7, a). We may see, that in the commutation zone the m.m.f. of the commutating poles and armature reaction act in mutual op-

position, and it may readily be proved that this deduction is of a general nature.

Since the magnetic circuit of the commutating poles is not saturated, the reluctance of the steel in this circuit may be disregarded and it may be assumed that

$$F_{c.p} = F_{aq} + F_{\delta c.p} \quad (6-6)$$

where $F_{\delta c.p}$ is the m.m.f. per pair of poles, necessary for conducting the commutating pole flux through the double gap $2\delta_{c.p}$ between the commutating pole and the armature. According to formula (4-4) $F_{aq} = \tau A$, and $F_{\delta c.p}$ may be expressed by a formula, similar to (2-16) for the main pole gap. Hence,

$$F_{c.p} = \tau A + \frac{2}{\mu_0} B_c \delta_{c.p} k_{\delta c.p} \quad (6-7)$$

Here $k_{\delta c.p}$ is the gap factor for the commutating poles, which may be determined by a formula similar to formula (2-15):

$$k_{\delta c.p} = \frac{t_1 + 5\delta_{c.p}}{z_1 + 5\delta_{c.p}} \quad (6-8)$$

Usually

$$\delta_{c.p} > \delta; \quad k_{\delta c.p} \approx k_{\delta};$$

$$\frac{F_{c.p}}{F_{aq}} = 1.15 - 1.30.$$

The mutually opposed action of m.m.f.s $F_{c.p}$ and F_{aq} explains why the leakage of the commutating poles is much greater than that of the main poles. If $\Phi_{c.p}$ is the flux in the commutating pole core and $\Phi_{c.z}$ —the flux in the gap under this pole, then in the machines without compensation windings we have a leakage factor for the commutating poles of:

$$k_{\delta c.p} = \frac{\Phi_{c.p}}{\Phi_{c.z}} = 2 \text{ to } 5.$$

To decrease the leakage of the commutating poles, their winding is arranged as near as possible to the armature and the air-gap is

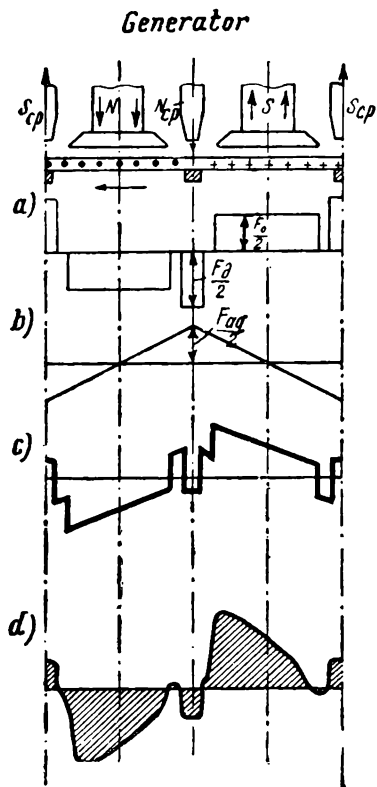


Fig. 6-5. M.m.f. and curve of resultant field of machine with commutating poles but without compensation winding

divided into two parts—the gap between the armature and the shoe of the commutating pole and the gap between the commutating pole core and the yoke, this gap being filled with non-magnetic gaskets.

6-5. Effect of Commutating Poles on the Main Field

With the brushes on the geometrical neutral the commutating poles do not affect the main field in any way, since their demagnetising and magnetising effects, defined by the hatched surfaces in Fig. 6-6, *a*, are mutually neutralised within the limits of a pole division.

If, when the machine works as a generator, we were to shift the brushes from neutral in direction of armature rotation (Fig. 6-6, *b*), then the hatched surfaces of the main and commutating pole fields are of different sign, i. e., in this case the commutating poles demagnetise the machine. The reverse takes place when the brushes are shifted off the neutral against the direction of generator armature rotation, the commutating poles magnetise the machine (Fig. 6-6, *c*). Thus, *the commutating poles render the same effect on the main field as the direct-axis armature reaction*. Therefore very often the effect of the commutating poles is included in the effect of the armature reaction, without specifying it. This deduction may be extended also to motors.

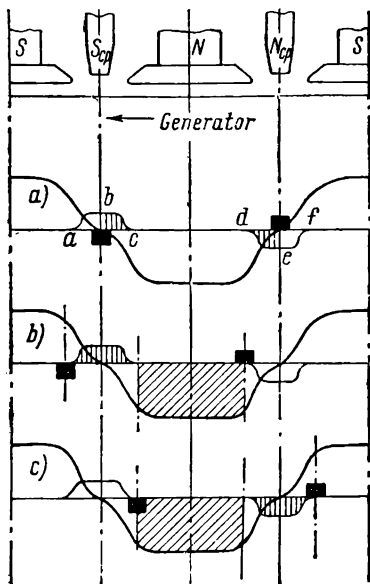


Fig. 6-6. Effect of commutating poles on main field

6-6. Effect of Commutating Poles Saturation on Commutation

Previously (§6-4) we could see that the mutual compensation of the reactive e.m.f. e_r and the commutating e.m.f. e_c is possible with change of load only when the commutating field B_c varies, practically, as the current I_a . [Bibl. 55a]

With a large increase of current I_a above the nominal value the magnetic circuit of the commutating poles may become saturated and the linearity in the relation of $B_c = f(I_a)$ is upset.

In Fig. 6-7, *a* the continuous lines denote the useful commutating flux Φ_c and the broken line—the leakage flux of the commutating pole $\Phi_{ic.p}$. The resultant flux in the commutating pole core $\Phi_{c.p} = \Phi_c + \Phi_{ic.p}$.

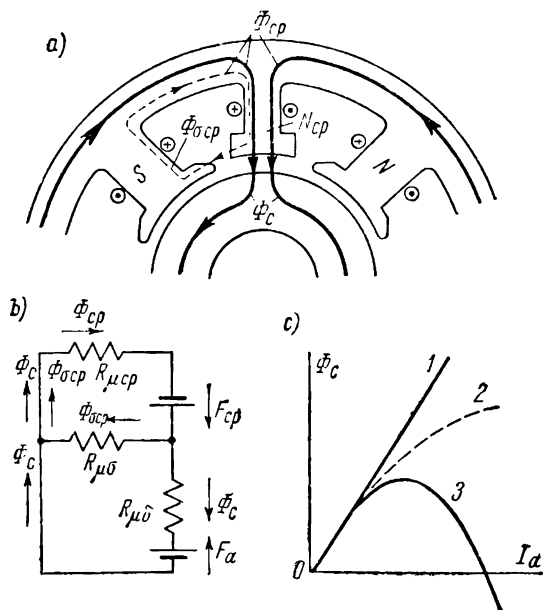


Fig. 6-7. Effect of commutating poles saturation

For one pair of poles, let the commutating poles of a magnetic circuit be represented schematically in the form of an electric current equivalent circuit (Fig. 6-7, *b*). Here $F_{c.p}$ and F_a are the opposing m.m.f.s of the commutating pole and armature; $R_{\mu \delta}$, and $R_{\mu c.p}$ are reluctances along the paths: of the commutating flux Φ_c in the gap under the commutating pole, of the leakage flux $\Phi_{ic.p}$ and resultant flux $\Phi_{c.p}$ in the steel. Then,

$$F_{c.p} - F_a = \Phi_c R_{\mu \delta} + \Phi_{c.p} R_{\mu c.p}, \text{ whence}$$

$$\Phi_c = \frac{(F_{c.p} - F_a) - \Phi_{c.p} R_{\mu c.p}}{R_{\mu \delta}}.$$

In this formula the resistance $R_{\mu_{\delta}}$ may be assumed constant, since it depends only on the gap resistance. With an increase of current I_a the m.m.f.s $F_{c,p}$ and F_a , and consequently their difference $F_{c,p} - F_a$ also increases in proportion to current I_a . If the machine is not saturated, then the resistance $R_{\mu_{c,p}}$ remains constant, and the flux $\Phi_{c,p}$ increases in proportion to current I_a . In these conditions the flux Φ_c also increases proportionally to current I_a and the relation $\Phi_c = f(I_a)$ is a linear function (I in Fig. 6-7, c). But when the magnetic circuit of the commutating pole becomes saturated the increase of reluctance $R_{\mu_{c,p}}$ becomes noticeable, and the relation $\Phi_c = f(I_a)$ no longer follows the straight-line law. If, in this case, there would be no leakage flux $\Phi_{sc,p}$ then this relationship would follow that of the magnetisation curve (curve 2 in Fig. 6-7, c). But in reality the leakage flux of the commutating pole facilitates a more rapid growth of flux $\Phi_{c,p}$ in respect to flux Φ_c ; therefore the product $\Phi_{c,p} R_{\mu_{c,p}}$ increases faster than current I_a and the faster, the more the saturation of the commutating pole. For a certain value of current I_a the flux Φ_c not only stops growing but actually begins to decrease, and then with a further increase of current I_a , passes through zero and even changes its sign, as indicated by curve 3 in Fig. 6-7, c.

From this discussion it follows that overloaded d.c. machines attain a limit when the commutating e.m.f. e_c not only stops compensating the reactive e.m.f. e_r , but begins to act in the same direction as the latter. In these conditions sparkless operation of the machine is, of course, entirely impossible.

6-7. Compensation Winding

The compensation winding suggested by Menges as far back as 1884, is one of the most effective means for the improvement of commutation of machines subjected to abrupt changes of load. The object of the compensation winding is to eliminate as far as possible the distortions of the main magnetic field, caused by armature reaction. For this purpose the compensation winding is laid in slots punched in the pole shoes of the main poles and is arranged according to the scheme in Fig. 6-8. To be able to obtain compensation for any load, it is necessary that the compensation winding be so joined in series with the armature winding that the m.m.f.s of both windings should oppose each other. In Fig. 6-9, a the curves 1 and 2 depict the distribution of m.m.f.s of the armature reaction F_{aq} and of the compensation winding $F_{c,w}$; the curve 3, shown by the rectangle *adeh*, depicts the m.m.f. of the

commutating pole for the case when a machine has no compensation winding.

To reduce to a minimum the main magnetic field distortions, when the machine is loaded, it is necessary to fully compensate within the limits of the pole arc $b' = \alpha' \tau$, the m.m.f. of cross armature reaction F_{aq} ; for this purpose the compensation winding

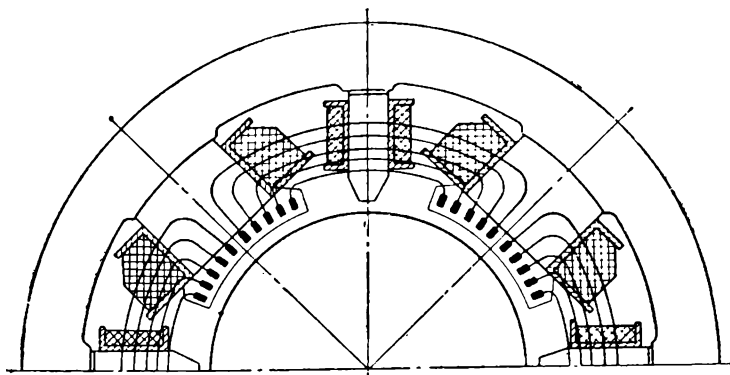


Fig. 6-8. Compensation winding

should be so arranged that the segments $kl = ts = \frac{1}{2} F_{c.w}$ are equal to segments $ml = rs = \frac{1}{2} \alpha' F_{aq}$, i. e., so that

$$F_{c.w} = \alpha' F_{aq} = \alpha' \tau A = b' A. \quad (6-9)$$

With such a distribution of m.m.f.s F_{aq} and $F_{c.w}$ in the interpolar space, a non-compensated (residual) m.m.f. $F_{aq} - F_{c.w}$ remains (in Fig. 6-9, *a* the hatched triangles), which, however, only to a very small extent influences the operation of the machine because the field created by it in the interpolar space is small. When the compensation winding is used the m.m.f. of the commutating poles becomes $F'_{c.p} = F_{c.p} - F_{c.w}$, i. e., it is much smaller, than in machines without compensation windings; in Fig. 6-9, *a* the m.m.f. $F'_{c.p}$ is shown by a rectangle $acfh$, in which the part shown by rectangle $bcfg$ compensates the m.m.f. difference $F_{aq} - F_{c.p}$ remaining in the interpole space, and the rectangle $abgh$ determines the m.m.f. $F_{c.z}$ necessary for the creation of the commutating flux Φ_c .

Fig. 6-9, *b* shows the curve of field distribution in a machine with a compensation winding. We may see that in such a machine the main pole curve is practically independent of the load. This increases the reliability of the machine from the point of view of

commutation, but complicates the design and increases its cost. Therefore, the compensation winding is used for relatively large-output machines, beginning with approximately 150 kW.

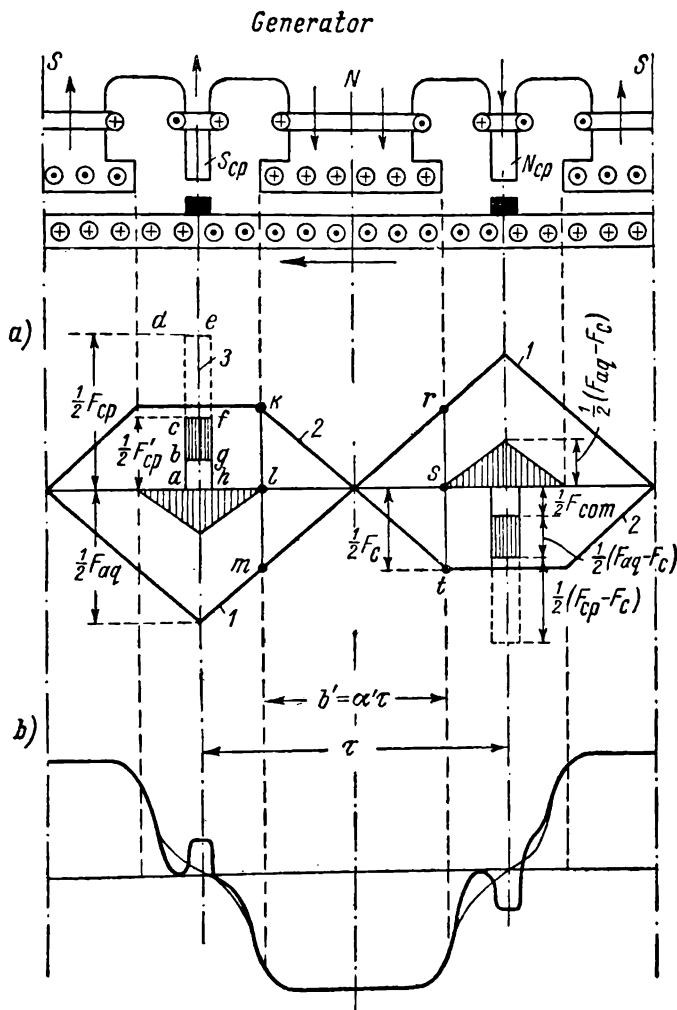


Fig. 6-9. Curves for F_{aq} and $F_{c.w}$ m.m.f.s and curve for resultant field of machine with compensation winding

6-8. Additional Methods of Protection Against Flashovers

Practice shows that with abrupt changes of current flashing may originate even in machines with compensation windings. To make the machine more resistant to flashing the following additional measures are carried out:

A. Special calculations and experimental adjustment of machine commutation. Machines designed for operation in conditions of overload and abrupt

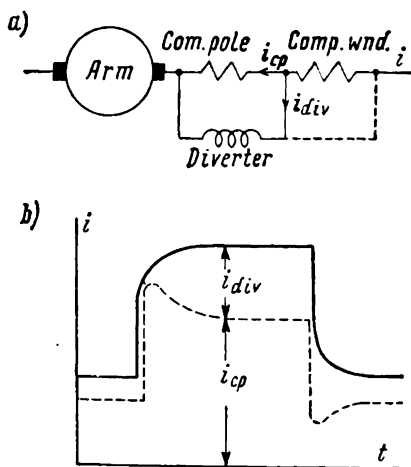


Fig. 6-10. Scheme of inductive shunt connection and curves of i and i_{add} currents change

changes in current are so calculated that for rated operation conditions the commutation would be somewhat accelerated. Though in this case when overloaded it becomes retarded, the calculations should be carried out so that in both cases favourable commutation is obtained.

The experimental adjustment of commutation in a machine is discussed in § 6-13.

B. Inductive shunt. We know that the eddy currents created in the massive parts of the machine magnetic circuit, when abrupt changes of current take place, prevent any such changes in the

magnetic flux of the commutating poles. To eliminate this disadvantage, in some cases an *inductive shunt* (divertor) is used, connected according to the diagram in Fig. 6-10, a across the commutating pole winding CP and, when a compensation winding CW is used, together with the latter. With the active resistance and inductance of the shunt properly selected it is possible to attain conditions when an abrupt change of current i would be followed by a still more abrupt change in commutating pole current $i_{c.p}$ thus accelerating the process of the commutating pole flux change both with an increase or decrease in current i (Fig. 6-10, b). [Bibl. 48]

For steady-state conditions the current in the shunt would be $i_{shunt} \leq 0.1 I_n$.

The main field of application of the inductive shunt is in

large-output machines, working with very abrupt intermittent loads. With the same aim of weakening the screening effect of the eddy currents the cores of the commutating poles are made of sheet steel similar to the main pole cores.

C. Flashover barriers. Screens. High-speed automatic breakers. To check arc propagation between brush-holder arms of different polarity, barriers are arranged around the commutator made of arc-resisting insulation material. To protect the armature winding from arc damage, insulating screens are mounted between the commutator and the risers of the armature winding, i. e., laterally. For the same purpose an air blast is used for blowing the arc towards the bearing, protected by a special cement-asbestos baffle plate. [Bibl. 54]

The conditions which may lead to flashovers are especially favourable when short circuits occur. Therefore in some cases a high-speed automatic breaker is inserted into the armature circuit to break the circuit before the short-circuit current reaches a dangerous value. The automatic breaker developed by A. I. Golubev can interrupt a short-circuit in 0.01 of a second.

D. Improving commutation by increasing the resistance of the circuit undergoing commutation. Commutation conditions may be improved if the resistance Σr of the circuit undergoing commutation is increased by introducing additional active resistances between the armature winding and the commutator. But this method is used only for a.c. commutator machines (see Part II). For d.c. machines the proper choice brush grade is of greater importance.

6-9. Brushes and Their Characteristics

One of the most important characteristics of a brush is its specific contact resistance q_{br} , i. e., its resistance per unit contact surface of brush.

If r_{br} is the resistance of the entire contact surface of brush and S_{br} —the area of this surface, then $r_{br} = \frac{q_{br}}{S_{br}}$. Therefore the voltage drop in the contact layer will be:

$$\Delta U_{br} = I r_{br} = j_{br} S_{br} \frac{q_{br}}{S_{br}} = j_{br} q_{br} \quad (6-10)$$

Here I is the current flowing into the brush or from it, j_{br} is the average current density under the brush.

Studies have proved, that the contact brush resistance and the corresponding contact drop potential depend on several factors,

Summary of Brush

Brush group	Grade	Rated current intensity, A/cm ²	Maximum peripheral speed, m/sec	Specific brush pressure, g/cm ²
Carbon graphite	T2, T6	6	10	200-250
	УГ2	8	15	200-250
	УГ4	7	12	200-250
Graphite	Г 1	7	12	200-250
	Г 2	8	15	200-250
	Г 3	10-11	25	200-250
	Г 6	9	18	200-250
	Г 8	11	25	200-300
	Г58	9	25	175-200
Electrographite	ЭГ 2	10	25	200-250
	ЭГ 4	12	40	150-200
	ЭГ 6	9	—	200-250
	ЭГ 8	10	40	200-400
	ЭГ10	9	—	200-250
	ЭГ14	10-11	40	200-400
	ЭГ83	9	45	175-220
Copper-graphite	M1	15	25	150-200
	M3	12	20	150-200
	M6	15	25	150-200
	M16	12-14	25	150-200
	M20	12	20	150-200
	M22	11-14	25	150-200
	M24	20	15	175-200
	MГ	20	20	180-230
	MГ2	20	20	200-250
	MГ4	15	20	200-250
	MГ6	18	20	200-250
Bronze-graphite	БГ	20	20	170—220

Table 6-1

Characteristics

Electrical resistivity, ohm.mm ² /m	Shore sclerometer hardness	Contact voltage drop per pair of brushes for rated current and speed $V = 15 \text{ m/sec}$ V	Friction coefficient for $V = 15 \text{ m/sec}$	Wear in 50 hours of work at $V = 15 \text{ m/sec}$ not to exceed, mm
40-60 18-30 26-38	45-58 40-60 45-65	2 ± 0.5 2 ± 0.4 2.1 ± 0.5	0.30 0.25 0.25	0.1 0.3 0.3
30-46 25-37 10-20 26-42 10-20 20-30	35-50 40-50 30-40 35-50 20-40 35-50	2.2 ± 0.5 1.7 ± 0.5 1.9 ± 0.4 2.2 ± 0.6 1.9 ± 0.4 —	0.30 0.25 0.25 0.25 0.25 0.25	0.2 0.15 0.20 0.20 0.15 —
20-30 10-16 30-46 40-50 40-56 26-38 35-65	46-60 20-30 47-63 42-55 50-70 40-60 15-32	2.75 ± 0.6 2.0 ± 0.4 2.5 ± 0.6 2.4 ± 0.5 2.4 ± 0.6 2.5 ± 0.5 —	0.20 0.20 0.25 0.25 0.25 0.25 0.25	0.10 0.25 0.15 0.15 0.15 0.15 —
2-6 7-12 2-6 0.5-1.5 5-13 1-4 0.1-0.3 0.05-0.15 0.15-0.35 0.3-1.3 0.3-1.3	26-38 30-40 26-35 20-30 24-36 20-30 — — — 22-32 18-30	1.5 ± 0.5 1.8 ± 0.4 1.5 ± 0.5 0.9 ± 0.3 1.4 ± 0.4 1.2 ± 0.3 0.5 ± 0.2 0.2 ± 0.1 0.5 ± 0.2 1.1 ± 0.5 1.0 ± 0.4	0.25 0.25 0.20 0.25 0.26 0.20 0.25 0.20 0.20 0.20 0.20	0.18 0.15 0.15 0.20 0.20 0.20 0.70 0.80 0.40 0.30 0.50
0.5-0.9	—	0.3 ± 0.1	0.25	0.25

of which of major importance are: a) the material of the brush and the material of the commutator or contact rings; b) current density j_{br} ; c) the direction of current from brush to commutator (or ring) or from commutator to brush; d) chemical condition of contact surface; e) temperature of contact surface; f) brush specific pressure; g) linear speed at commutator periphery; h) mechanical factors.

The grades of brushes used in the U.S.S.R. and their main characteristics are given in Table 6-1.

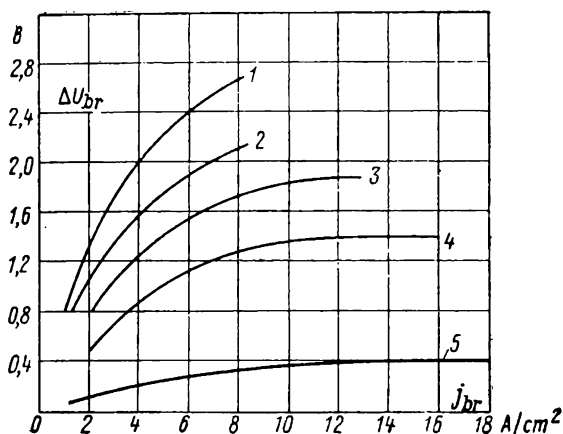


Fig. 6-11. Curves $\Delta U_{br}=f(j_{br})$ for various grades of brushes

The hard carbon-graphite brushes have the greatest specific resistance ρ_{br} ; the graphite and electrographite brushes have less resistance and the soft copper-graphite or bronze-graphite brushes have the least resistance.

Fig. 6-11 shows curves $\Delta U_{br}=f(j_{br})$ for brushes of various grades. Since the voltage drop is greater when the direction of current is from the metal to the carbon brush than when flowing in the reverse direction, ΔU_{br} is assumed to be the sum of the voltage drops for brushes of both polarities. The curves 1 and 2 are plotted for hard brushes, curves 3 and 4 for brushes of average hardness and soft brushes, and curve 5 for bronze-graphite brushes. The notable feature of the curves 3 and 4 is the steep section, where, beginning with a certain current density, $\Delta U_{br} \approx \text{const}$, i. e., the contact resistance varies in this zone almost inversely proportional to j_{br} .

With an increase in temperature the electrical conductivity of the brushes increases and, therefore, the contact resistance is decreases; hence a machine with good commutation when cold may begin to commute perceptibly worse as the temperature rises. From this point of view it is necessary that only one grade of brush be used in a machine and of the same size. Since all brushes of the same polarity are connected in parallel, the more heated brushes having less contact resistance will conduct larger currents if the above requirements are not fulfilled; this would cause a further increase of temperature of these brushes and may lead to the burning out both of the brushes and the cable leads.

The value of the contact resistance is to a significant extent influenced by the chemical condition of the commutator surface. After long operation the commutator surface becomes covered with a thin oxide film very hard and heat-resistant in respect to brush sparking; the film is sometimes of a dark brown hue

(the commutator "polish"). In this case the contact resistance is increased and the commutation becomes more favourable. If the commutator retains its natural colour and the surface is dull then this indicates that the stable conditions ensuring reliable commutation have not yet been attained at the commutator.

With an increase of specific pressure per brush, the voltage drop ΔU_{br} decreases at first rapidly and then slower and slower (Fig. 6-12).

The linear speed at the commutator periphery has very little effect on the value ΔU_{br} . But if with increased speed the brushes begin to vibrate, then the brush resistance may rise rapidly and this unfavourably influences the commutation process.

The values ΔU_{br} given above have been obtained for contact between a brush and ring. For a commutator the value ΔU_{br} is always somewhat higher because of larger irregularities compared with ring surface.

When choosing a grade of brush best adapted for a particular machine it is often necessary to take into account conflicting considerations. Thus, for instance, from the point of view of

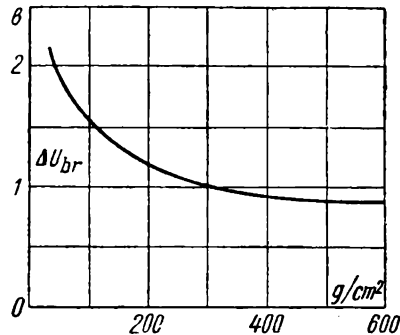


Fig. 6-12. Curve of ΔU_{br} voltage in relation to unit brush pressure

improving commutation it is of greater advantage to use harder brushes with a larger contact resistance. But as these brushes allow less current density, then necessarily the brush contact surface has to be increased, thus necessitating an increase in size of commutator, and hence the losses grow.

On the other hand, the permissible current density under the brush j_{br} increases with decrease of brush contact surface; hence it is more advantageous to have a larger number of smaller brushes, but this makes the design of the machine more complicated and its cost increases.

Usually in conventional types of d.c. machines graphite brushes are used; in machines with difficult conditions of commutation — carbon-graphite or electrographite brushes, and in low-voltage machines up to 30 V—copper-graphite and bronze-graphite brushes are used.

6-10. The Nature of Brush Contact

During the years of studying the properties of sliding contact opinions as to its nature have undergone many a change. One of the first accepted as fundamental in the classical theory of commutation was the *hypothesis of the uninterrupted contact*, i.e., such a contact when the current is evenly distributed over the entire contact surface. But this hypothesis could not explain the nature of the relationship of contact voltage drop to current density (Fig. 6-11). Therefore this hypothesis was subsequently superseded by a new *hypothesis* according to which the *sliding contact* is considered as a *totality of direct contact points*, the actual contact surface of which is many times less than the brush surface. To this actual contact surface borders a wedge-shaped part of the space between the surfaces of the brush and commutator, part of it covered with carbon and metal dust particles that have stuck to the commutator and may yet contact the brush. This part of the wedge-shaped space is called the *dust zone* and conducts the current only when a sufficiently large voltage is impressed between the surfaces of the brush and commutator. Adjacent to the dust zone is the *rupturing zone* through which current is conducted by means of ionic and electronic emission, but only if the friction surfaces are in contact. To supplement in part this hypothesis a third one was suggested according to which the major factor determining the behaviour of the sliding contact is the oxide film on the commutator surface or ring. The film is supposed to be in a state of dynamic equilibri-

um, i. e., a process takes place of simultaneous creation and destruction of the surface film due to the grinding action of brushes; this results in puncturing of the film and in forming conducting paths.

From the point of view of this hypothesis it is easy to explain the form of the curves in Fig. 6-11. Indeed, the film of oxide on the copper ring can withstand only a definite voltage; with an increase of current density the film begins to deteriorate, and the number of points conducting the current increases, bringing about a decrease in contact resistance. In the case of a non-oxidizing ring, as, for example, a ring of graphite, the curves $\Delta U_{br} = f(j_{br})$ would be straight lines.

The brush contact phenomena were investigated in detail by the All-Union Electrotechnical Institute laboratories, and of especial interest were the tests carried out for abruptly changing loads.

Besides brushes of conventional design, a rather large number of specially designed brushes was suggested at different times, as for example, compound, threaded at the sides, brushes with slotted sliding surfaces, etc.

Nevertheless, in the electrical machine-building field brushes of special design are, practically, not used.

6-11. Experimental Methods of Analysis and Adjustment of Commutation

A. General considerations. The theoretical analysis of d. c. machine commutation (Chapter 5) from the standpoint of the classical theory of commutation, as we know, was founded on several assumptions which, though facilitating the analysis, are nevertheless not completely true. Hence the conclusions based on the classical theory, though representing correct qualitative tendencies, do not allow precise quantitative estimations.

As a result, it is impossible to determine the exact number of turns of the commutating pole, to establish the exact gap value under the commutating pole and the form of the pole shoe, etc. All these questions have to be finally solved during experimental investigations of commutation, introducing the necessary corrections into the initial calculation data. This is the reason why the final electrical data of a machine can be established only as a result of combining computation with experimental work.

The most widely used and valuable method of experimental analysis of commutation is the *plotting of curves of the potential*

under the brushes and curves for additional excitation of the commutating poles.

B. Brush potential curves. This method allows to judge of the nature of commutation by the form of the plotted brush potential curve, i.e., to determine if the commutation following a straight-line law is retarded or accelerated.

The brush potential curves are plotted by using the scheme in Fig. 6-13, *a*. The voltmeter should have a scale to enable it to measure voltages from 1.5 to 3V. One voltmeter terminal is connected directly to the brush, while

the other is joined to a thin metal or carbon contact moved over the commutator periphery along the brush-box.

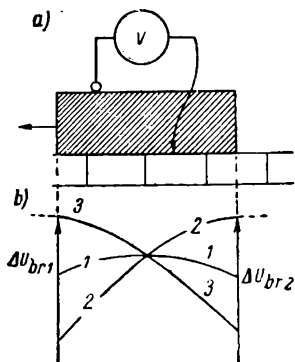


Fig. 6-13. Scheme for plotting brush potential curves and potential curves

If the commutation is linear the current density under the brush is of the same value everywhere [formula (5-9)], therefore, the contact potential drop ΔU_{br} has one and the same value along the entire brush and the brush potential curve represents almost a straight line, parallel to the abscissa axis (curve 1 in Fig. 6-13, *b*).

For retarded commutation the current density and the corresponding contact voltage is larger at the trailing edge of the brush than at the leading edge, i.e., $\Delta U_{br2} > \Delta U_{br1}$.

In this case curve 2 in Fig. 6-13, *b* is obtained. With accelerated commutation curve 3 is obtained.

The method described allows us to judge, with a certain approximation, of the commutating field magnitude since curve 2 in Fig. 6-13, *b* indicates a weak commutating field, and curve 3—an excessively strong field.

The main disadvantages of this method are: a) it is difficult to make a brush-holder which could provide complete uniformity over the entire brush surface, whereas the voltage ΔU_{br} depends on the force with which the brush is pressed against the commutator at a given point; b) the voltage ΔU_{br} is proportional to current density only with small densities, and then increases at a much lesser rate. Therefore, the method of the brush potential curve permits of only a qualitative appraisal of the commutation process.

C. Method of non-sparking zone. The method developed by V. T. Kasyanov [Bibl. 12] and called the method of non-sparking

zone proved to be of utmost effectiveness for the experimental adjustment of commutation. The essence of the method consists in that the commutating pole winding is given an additional or boosting excitation from a special d.c. source and *boost excitation curves* are plotted which allow to discover the non-sparking zone of operation and to determine with the necessary precision the most advantageous number of commutating pole turns and gap $\delta_{c,p}$ value.

The circuit in Fig. 6-14 may be used to plot these additional

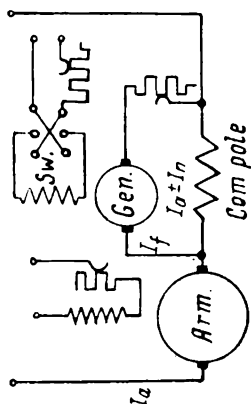


Fig. 6-14. Scheme for plotting boost feed curves

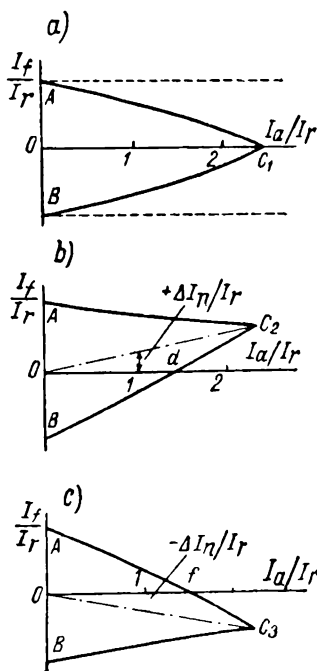


Fig. 6-15. Boost feed curves

excitation curves. Here *Arm* is the armature of the machine undergoing tests, *Com. pole* — the commutating pole winding, *Gen* — a separately excited d. c. generator, used for the boost excitation of the commutating poles, *Sw* is a switch for reversing the current in the excitation circuit and consequently the polarity of the generator. For testing purposes the machine may work both in loaded and short-circuited conditions, because with the same magnitude of current I_a in the machine armature circuit the commutation conditions in both cases are practically the same.

The plotting of the boost excitation curves is begun with no-load ($I_a=0$). In this case the reactive e.m.f. $e_r=0$. By additionally exciting the commutating poles first in one direc-

tion, then in the other, we may establish the value of the current $\Delta I_f = \pm \frac{I_f}{I_n} \times 100$, at which the first noticeable sparking begins. The cause of sparking is the non-compensated (excessive) e.m.f. $\Delta e = \pm e_c$, created in the coil sections undergoing commutation by the field of the commutating poles. If we disregard the hysteresis phenomenon, then the boost excitation currents of both signs, causing the first sparking under the brushes, should at no-load be equal (segments $OA=OB$ in Fig. 6-15). The test shows that the machine starts to spark at $\Delta e=1.0$ to 1.5 V depending mainly on brush grade and brush pressure. In small power machines $\Delta I_f=10$ to 25 per cent, and in average-power and large-power—6 to 10 per cent.

If a d.c. machine could have a commutating field so designed that at all loads it completely compensates the reactive field of commutation, i. e., it would have the same magnitude and form as the latter, then the e.m.f.s e_r and e_c would always be mutually balanced. In this case the boost excitation curves would have the form of two straight lines running parallel to the abscissa line and at the same distance from it both of the positive and negative branches (broken lines in Fig. 6-15, a).

But since complete mutual compensation of e.m.f.s e_r and e_c cannot be achieved in a real machine, the residual e.m. f. e_0 (the hatched areas in Fig. 6-4) increases with an increase of load current I_a and for some definite value of this current, the machine begins to spark even with a quite correctly chosen number of commutating pole turns. In this case the boost excitation of these poles may only increase the discrepancy between the e.m.f.s e_r and e_c and consequently impair the commutation. Thus, in the case of a real machine it is possible to load it to such a limiting current for which no degree of regulation of the commutating poles could give satisfactory commutation.

Hence, in real machines the boost excitation curves are not parallel to the abscissa axis but intersect at points C_1 , C_2 , or C_3 , this depending on the relationship between the e.m.f.s e_r and e_c .

If, for instance, the e.m.f.s e_r and e_c are more or less precisely balanced, i.e., the number of turns of the commutating poles is properly selected, then the excitation curves will intersect at point C_1 on the abscissa axis and the middle line of these curves will coincide with the abscissa axis (Fig. 6-15, a).

If in a machine working without boost excitation the reactive e.m.f. e_r predominates and therefore the commutation is of a retarded nature, it is necessary to additionally excite the

commutating poles in the positive direction, strengthening the field created by it in the commutation zone. In this case the middle line of the curve will pass above the abscissa axis to the intersection point of curves C_2 (Fig. 6-15,b).

On the contrary, if e.m. f. e_c predominates, it is necessary to excite the commutating poles in the negative direction, weakening the field created by them. In this case the middle line of the curve will pass below the abscissa axis at curve intersection C_3 (Fig. 6-15, c).

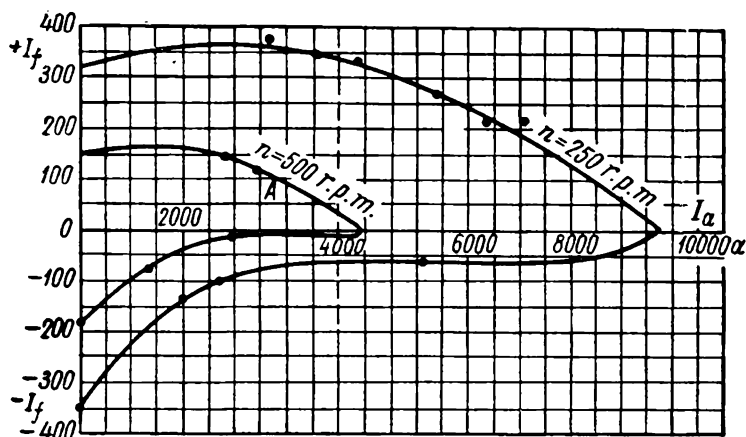


Fig. 6-16. Boost feed curves for 2,000 kW, 500 V, 4,000 A d.c. generator plotted at the Kharkov Electrical Engineering Works for various machine speeds

Comparing the curves in Fig. 6-15, *a*, *b*, *c* we may observe that in the first case the machine can operate without sparking at larger overloads (segment OC_1 in Fig. 6-15,*a*) than in the second and third cases (segments Od and Oj in Fig. 6-15,*b* and *c*), i.e., the curve in Fig. 6-15,*a* is the most favourable.

The boost excitation curves allow to determine the most advantageous number of turns of commutating pole $w_{c.p}$ for a given gap under the commutating pole or the most advantageous gap for a given number of turns $w_{c.p}$. The first method is used mostly for small- and average-power machines, the second for large-output machines with a small number of commutating pole turns.

Besides this, the boost excitation curves allow to predetermine within certain limits the commutation conditions with change in operation conditions of the machine.

Let us suppose that for a given load current I_a the machine speed n has increased. In this case the e.m.f.s e_r and e_c increase in direct proportion to the speed and accordingly both the residual e.m.f. $e_r + e_c$ (Fig. 6-4) and boost commutation current i_c are also increased; as a result of this the non-sparking zone is narrowed.

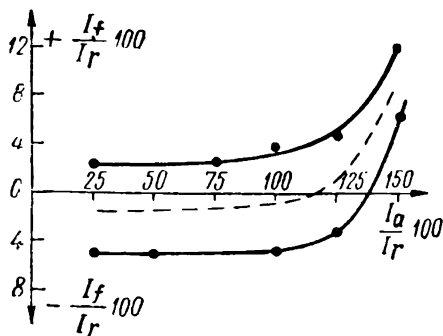


Fig. 6-17. Boost feed curves of a 4.4 kW, 1,430 r.p.m., 220 V, 24 A d.c. machine

Fig. 6-16 represents the boost excitation curves obtained by M. P. Kostenko [Bibl. 53b] for a d.c. generator of the Kharkov Electrical Works of 2,000 kW, 500 V, 4,000 A; the curves were taken for the rated speed $n=500$ r.p.m. and for half of this speed, i.e., $n=250$ r.p.m. It is evident from the comparison of these curves that in the latter case the non-sparking zone of operation has

widened, approximately double, in direction of both axes.

The second essential factor, influencing commutation, is the saturation of the commutation poles. In this case the commutating e.m.f. e_c ceases to increase proportional to the current I_a and the machine begins to work in the zone of retarded commutation. Therefore, to compensate the reactive e.m.f. e_r and obtain non-sparking commutation a larger boost excitation current is needed than for small loads. The corresponding curves for the additional excitation of a d.c. machine of 4.4 kW, 1,430 r.p.m., 220 V, 24 A are shown in Fig. 6-17.

Chapter Seven

ENERGY LOSSES AND EFFICIENCY OF ELECTRICAL MACHINES

7-1. Preliminary

Electrical machines are designed either as machines for converting mechanical energy into electric energy, i.e., generators, or as machines for converting electric energy into mechanical energy, i. e., motors. Obviously, part of the energy consumed by

the machine cannot be *effectively* utilised in the machine proper since, practically, it is dispersed in the form of heat into the air. This part of the energy is called lost energy or simply *losses*.

The losses in electrical machines are comparatively small. If we consider a d.c. machine of average or large output, the losses are not more than 10 to 4 per cent of the input and in the largest possible synchronous alternator machines with hydrogen cooling they constitute only 1 to 2 per cent. Nevertheless, taking into account the colossal amount of energy converted nowadays, the losses problem is of tremendous importance, as each excess per cent of loss corresponds to a very large absolute quantity of energy made unavailable.

On the other hand since all losses are dissipated in the form of heat the machine *must necessarily get heated*. Practice has shown that if reliable operation of a machine is desired during its normal service life (16 to 20 years), the temperatures of the various parts should not exceed certain limits. But the temperatures of the given parts depend not only on the losses but also on the cooling conditions. By proper choice of the ventilation system we may greatly increase the effective utilisation of the active materials of the machine (copper, steel) and therefore be able to make the machine of lower weight and cheaper.

Thus the problem of losses in the machine is closely connected with the problems of its service and economic factors.

It should be especially emphasised that the contents of this chapter refer to all types of electrical machines.

7-2. Classification of Losses

All losses, originating in the machine may be divided into two groups: 1) *principal losses* and 2) *additional losses*.

The principal losses are those which occur as a result of the fundamental processes taking place in the machine, viz., the electromagnetic and mechanical processes. They include the following losses:

A) *Mechanical losses*, viz.: a) bearing friction, b) brush friction, c) air friction (windage).

B) *Core losses* (in armature core and teeth) due to: a) hysteresis, b) eddy currents.

C) *Copper losses*: a) in the armature winding; in the windings connected in series with the armature winding, viz., the commutating pole winding, compensation winding, etc.; b) in the field circuit winding.

D) Losses in the brush and ring contact layer.

The additional losses are the losses in the steel and copper which occur in the machine as a result of secondary processes of electromagnetic nature. The additional losses are classed as: eddy current losses due to stray magnetic fields in the windings and massive metal parts of the machine, surface losses in the steel and pulsation losses in the teeth, losses in the equalising connections, etc.

7-3. Mechanical Losses

A. Losses in friction bearings. According to the general law of friction these losses are expressed as follows:

$$P_{\text{bearing}} = k_{fr} F_{jr} v_{jr} = k_{fr} \bar{f}_{jr} d_{jr} l_{jr} v_{jr} \quad (7-1)$$

Here

k_{fr} —the coefficient of friction;

F_{jr} —the total journal pressure;

\bar{f}_{jr} —the specific journal pressure, i. e., the pressure per unit of the journal surface projected onto a surface parallel to the shaft axis;

d_{jr} , l_{jr} —journal diameter and length respectively;

v_{jr} —journal peripheral speed.

In the MKSA system the pressure F_{jr} may be expressed in newtons and the speed v_{jr} in metres per second. If we express the pressure in kilograms, then in the right-hand part of the formula (7-1) it is necessary to introduce the conversion factor 9.81.

Oil is used as bearing lubrication. When stationary, the oil between the friction parts is squeezed out and the journal comes into direct contact with the metal of the bearing lining.

When the shaft rotates the oil is entrained by the journal and creates in the tapered space between the shaft surface and the bearing lining a high pressure which maintains the shaft in a suspended condition, so that a thin layer of oil appears between the friction surfaces.

If the friction is to be of an entirely fluid nature it is very important that a film be produced to cover up the irregularities on the friction surfaces.

A number of investigations (Tower, Dettmar and others) have shown that for speeds of $v_{jr}=0.5$ to 4 m/sec the fluid friction coefficient may be expressed as:

$$k_{fr} = \frac{C v_{jr}^{0.5}}{\bar{f}_{jr} d_{jr}} \quad (7-2)$$

Here

C is a constant depending on the grade of the oil and the bearing clearance;

ϑ_{jr} —the temperature of the bearing $^{\circ}\text{C}$.

If the speed $\vartheta_{jr} > 4$ m/sec, the coefficient of friction increases progressively slower in respect to the speed and at $v_{jr} \geq 10$ m/sec already does not depend on the speed. In this case

$$k_{fr} = \frac{C'}{f_{jr} \vartheta_{jr}}, \quad (7-3)$$

where C' is a constant.

By considering formulas (7-2) and (7-3) the following three laws of friction may be established:

1) The coefficient of friction k_{fr} is inversely proportional to the specific pressure f_{jr} when $\vartheta_{jr} = \text{const}$ and $v_{jr} = \text{const}$;

2) The coefficient of friction is inversely proportional to the temperature ϑ_{jr} when $f_{jr} = \text{const}$ and $v_{jr} = \text{const}$;

3) For $f_{jr} = \text{const}$ and $\vartheta_{jr} = \text{const}$ the coefficient of friction is variably dependent on the speed v_{jr} : at speeds up to 4 m/sec, $k_{fr} = v_{jr}^{0.5}$, at speeds $v_{jr} \geq 10$ m/sec— $k_{fr} = \text{const}$.

Substituting the value k_{fr} in equation (7-1), we obtain for friction losses in bearings the following expressions:

$$p_{bearing}(v_{jr} \leq 4) = \frac{C}{\vartheta_{jr}} d_{jr} l_{jr} v_{jr}^{1.5} \quad (7-4a)$$

and

$$p_{bearing}(v_{jr} \geq 10) = \frac{C'}{\vartheta_{jr}} d_{jr} l_{jr} v_{jr}. \quad (7-4b)$$

If the losses $p_{bearing}$ are expressed in watts the diameter and length of journal in cm and the speed in m/sec, then as an average $C=26$ and $C'=19.6$.

From the expression for bearing losses (7-4) an important deduction may be made, that the losses $p_{bearing}$ do not depend on the specific pressure and, hence, do not depend on the machine load, since according to the first law of friction $k_{fr} f_{jr} = \text{const}$. This allows us to determine the no-load machine losses and then assume that for any given speed of rotation these losses maintain their value at all loads while the bearing continues to work with fluid friction.

B. Losses in antifriction bearings. These include ball-bearings used in small-output machines and roller bearings used in average-power machines. In intermediate power machines it is common practice to use a roller bearing only on the side opposite to the driving side.

In comparison with friction-type bearings the ball and roller types have several valuable advantages: a much smaller coefficient of friction (about 10 to 15 times less), smaller dimensions, which permit a decrease in axial length, and less maintenance required, etc.

Losses in ball and roller bearings are estimated by using the formula:

$$p_{\text{bearing}} = k_{fr} \frac{F}{D_c} v_{jr} \quad (7-5)$$

Here,

F —load on bearing ring;

D_c —diameter of circle, drawn through the centres of the balls or roller axes;

v_{jr} —speed at the journal periphery.

If F is expressed in kg, D_c in cm and v_{jr} in m/sec, then for ball-bearings $k_{fr}=0.001$ to 0.002 , and for roller bearings $k_{fr}=0.002$ to 0.003 .

C. Brush friction losses ($p_{br,fr}$). Consider k_{fr} as the coefficient of friction of brush against commutator or ring; f_{br} —specific brush pressure; S_{br} —contact surface of all brushes with commutator or ring; v_c —speed at commutator or ring periphery. Then,

$$p_{br,fr} = k_{fr} f_{br} S_{br} v_c \quad (7-6)$$

f_{br} is generally expressed in kg per sq. cm; S_{br} —in sq. cm and v_c —in m/sec; in this case at the right-hand side of formula (7-6) it is necessary to introduce the conversion factor 9.81 so as to obtain $p_{br,fr}$ in watts.

Based on experimental results for carbon brushes we have: $k_{fr}=0.2$ to 0.3 for the commutator and 0.15 to 0.20 for contact rings; $f_{br}=0.15$ to 0.25 kg per sq. cm, but in special machines, such as, for example, traction motors f_{br} may be of a higher value, up to 0.5 kg per sq. cm.

D. Ventilation losses (p_v). Electrical machines with high electrical and magnetical loadings dissipate a considerable amount of energy in the form of heat within the small volumes of active materials with relatively small exposed cooling surfaces. In this case it is necessary to boost up the ventilation and increase the coefficient of heat dissipation of the machine.

For machines with a built-in fan we have:

$$p_v = k_v V v^2 \quad (7-7)$$

Here,

V is the quantity of ventilating air;

v —speed at the external circumference of fan.

If V is expressed in m^3/sec and v —in m/sec , then $k'_v = 1.1$. Since the quantity of air V is proportional to the cube of speed v , the ventilation losses are also proportional to the cube of speed and the cube of the machine r.p.m. n .

For machines with an external ventilator

$$p_v = k'_v \frac{H}{\eta_v} V. \quad (7-8)$$

Here, H is the pressure; for low-speed machines ($v = 15 \text{ m}/\text{sec}$) $H = 30$ to 50 mm water ; for high-speed machines $H = 50$ to 100 mm water ; η_v —efficiency of the fan, viz., approximately 0.5 for low-speed machines and 0.25 to 0.30 for high-speed machines of the turbogenerator type. If V is expressed in m^3/sec then $k'_v = 9.81$.

E. Total mechanical losses (p_{mech}). Adding together all friction losses and ventilation losses, we obtain:

$$p_{mech} = p_{bearing} + p_{br} + p_v. \quad (7-9)$$

7-4. Principal Core Losses

A. Kinds of principal core losses. In service the active steel parts of the electrical machines are subjected to periodic magnetic reversals which are of two kinds. The first kind called *alternating* magnetic reversals is typical for transformers in which the flux density is practically uniformly distributed over the active core cross-section and varies sinusoidally with time. Almost similar conditions are met with in d. c. and a. c. armature teeth. The second kind of magnetic reversals called *rotatory* occur in d. c. machine cores rotating in the constant with time field of the main poles.

In both cases the losses in the steel core comprise: a) *hysteresis losses*; b) *eddy current losses*. Only short information on these losses is given in this textbook, since the physical concept of this phenomenon is described in *Theoretical Fundamentals of Electrical Engineering* courses. Data pertaining to electrical steel sheet was given in the Introduction.

B. Hysteresis losses (p_h). Hysteresis losses per unit mass in the case of alternating reversals may be expressed by the empirical formula suggested by Steinmetz:

$$p_h = C_h f B^{\alpha}. \quad (7-10)$$

Here C_h —a constant depending on the grade of steel;

f —reversal frequency;

B —maximum value of flux density and

α —experimentally determined exponent of the flux density B .

A mean value of $\alpha=2$ is taken for alloyed steels and flux density is accepted in the range of 0.8 to 1.6 wb per sq. m.

Rotatory reversals are also the cause of hysteresis losses in steel. The nature of the rotatory reversal phenomenon is evidently more complicated than that of the alternating reversals. It may be assumed that with rotatory reversals the losses p_h at

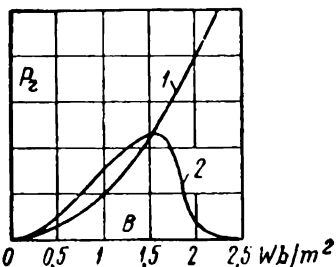


Fig. 7-1. Hysteresis losses for alternating (1) and rotatory (2) magnetising reversals in steel

first grow with an increase of flux density approximately up to the value of $B \approx 1.6$ wb/sq. m, and then with a further increase in flux density an abrupt fall occurs. In Fig. (7-1) the curve 1 depicts the relationship $p_h = f(B)$ for alternating reversals and curve 2 for rotatory reversals.

Since the flux density in the armature core is usually less than 1.6 wb/sq. m, the hysteresis losses originating in the electrical machines with rotatory reversals are calculated by formula (7-10), but an experimentally established correction factor is introduced averaging 1.8.

correction factor is introduced averaging 1.8.

C. Eddy current losses. When steel is subjected to magnetic reversals e.m.f.s are created in it in the direction defined by the conventional right-hand rules. The currents established by these e.m.f.s, termed eddy currents, flow in the same direction. In machines of conventional design these currents are not utilised. Causing loss of energy, they contribute to the heating of the steel and decrease the efficiency of the machine. To minimise the detrimental effect of these currents, the armature is assembled of electrical steel sheets of small thickness (usually 0.5 mm), insulated from each other and arranged in the plane perpendicular to the machine axis (Fig. 7-2).

When calculating eddy current losses we make the following assumptions: a) the steel sheet thickness Δ is insignificant compared with its width and length, b) the flux density varies sinusoidally and is uniformly distributed along the sheet thickness, in other words, we disregard the screening effect of the eddy currents originating in the sheet, and c) the magnetic permeability of

steel and its resistivity remain constant. In this case the e.m.f. induced in the sheet may be assumed as proportional to the magnetic reversal frequency and flux density B , viz., $e_{ed} = fB$; on the other hand, $i_{ed} = \frac{e_{ed}}{r}$, where $r = \text{const.}$

Hence the eddy current losses per unit mass are expressed as:

$$p_{ed} = i_{ed}^2 r = C_{ed} f^2 B^2, \quad (7-11)$$

where C_{ed} is a constant, depending on the steel grade and sheet thickness.

D. Total losses in steel. Formulas (7-10) and (7-11) are usually expressed as follows:

$$p_h = \sigma_h \left(\frac{f}{100} \right) B^2. \quad (7-12)$$

and

$$p_{ed} = \sigma_{ed} \left(\frac{f}{100} \right)^2 B^2. \quad (7-13)$$

Here the losses p_h and p_{ed} are expressed in W/kg, the flux density B —in wb/sq. m; the factors σ_h and σ_{ed} are given in Table 7-1.

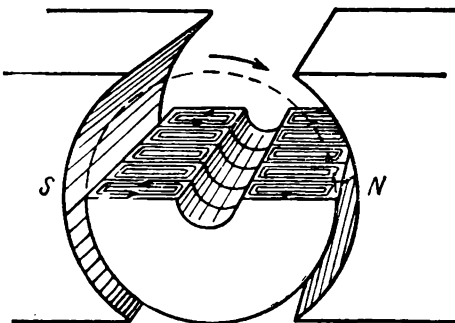


Fig. 7-2. Eddy currents in steel sheets of the armature rotating in a magnetic field

Table 7-1

Values of Factors σ_h and σ_{ed}

Type of alloyed steel	Sheet thickness, mm	σ_h	σ_{ed}
Low- and average-alloyed steel	1.0	4.4	22.4
	0.5	4.4	5.6
	0.35	4.7	3.2
High-alloyed steel	0.50	3.0	1.2
	0.35	2.4	0.6

Hence, the total losses per 1 kg of mass of steel are:

$$p_{st} = p_h + p_{ed} = \sigma_h \left(\frac{f}{100} \right) B^2 + \sigma_{ed} \left(\frac{f}{100} \right)^2 B^2. \quad (7-14)$$

When total losses in steel are calculated it is a common practice to use the figure for the specific losses originating in one kilogramme mass of steel of given grade at a frequency of $f = 50$ c/s and with a sine-wave flux density $B = 1$ wb/sq. m.

Besides this the State Standard 802-54 includes data of specific losses for $B=1.5$ wb/sq. m and 1.7 wb/sq. m, the latter figure only for cold-rolled grain-oriented steel (see Introduction, Table 1-2). In further discussions we shall use as a base for loss computations $B=1$ wb/sq. m.

The total losses in the steel of a given part of the machine at any frequency and flux density may be expressed as:

$$p_{st} = p_{[1/50]} \left(\frac{f}{50} \right)^{\beta} B^2 G_{st}. \quad (7-15)$$

Here:

$p_{[1/50]}$ are the specific losses for $B=1$ wb/sq.m and $f=50$ c/s;

f —frequency of magnetic reversals;

β —exponent averaging for low-alloyed steels $\beta=1.5$, for high-alloyed steels $\beta=1.2$ to 1.3 ;

B is the calculated flux density for a given part of the machine;

G_{st} —mass (weight) of the given part in kg.

E. Practical formulas for estimation of losses in steel. Practice has proved that the actual losses in steel of a manufactured machine are always larger than those calculated by formulas (7-12) and (7-13). This can be explained by the effect of the processing and assembling of the active steel sheets, i. e., increase of hysteresis losses due to "hammer-hardening" of the sheets during stamping and cutting processes; increase of eddy current losses due to forming of burrs when assembling the stacks or due to damage of sheet insulation when compressing the stacks under excessive pressure, etc.

Measures that could diminish the effect of these technological factors are: cleaning the sheets of burrs in special machines, annealing the stampings in a hydrogen atmosphere, adhering to the stipulated pressures when pressing the stacks, etc.

The increase of losses in steel due to technological factors cannot be calculated. Therefore in formulas (7-12) and (7-13) correction factors established by experimental means are introduced. Thus losses in the steel of d. c. machines may be calculated by formulas:

a) for the armature core:

$$p_{st.a} = \left[2\sigma_h \frac{f}{100} B_a^2 + 2.3\sigma_{ed} \left(\frac{f}{100} B_a \right)^2 \right] G_{st.a}; \quad (7-16)$$

b) for the armature teeth:

$$p_{st.t} = \left[1.2\sigma_h \frac{f}{100} B_{t.av}^2 + 3\sigma_{ed} \left(\frac{f}{100} B_{t.av} \right)^2 \right] G_{st.t}. \quad (7-17)$$

Here,

σ_h and σ_{ed} are coefficients from Table 7-1;

2 and 2.3 are coefficients taking into account increase of losses for rotatory magnetic reversals, and also due to non-uniform distribution of flux density through the volume of steel subjected to magnetic reversal;

1.2 and 3 are factors taking into account increase of losses due to the "hammer-hardening" effect during stamping and also due to non-sine-wave flux density variation;

B_a and $B_{t.av}$ are flux densities in wb/m² in the armature core and average flux density in the teeth;

G_{ma} and G_{mt} are weights of mass of armature core and tooth, respectively.

When calculating the total losses in steel it is possible to use the formulas:

$$p_{st.a} = (2.4 \text{ to } 4.0) p_{1/50} \left(\frac{f}{50}\right)^{\beta} B_a^2 G_{st.a}; \quad (7-18)$$

$$p_{st.t} = (1.7 \text{ to } 2.0) p_{1/50} \left(\frac{f}{50}\right)^{\beta} B_{t.av}^2 G_{st.t}. \quad (7-19)$$

Here (2.4 to 4.0) and (1.7 to 2.0) are factors taking into account the increase of total losses in the armature core and teeth; $\beta=1.2$ to 1.5.

7-5. Principal Copper Losses

A. Losses in the armature copper. Let us calculate the losses in the d. c. machine armature copper. Let i_a be the current flowing in one path, $2a$ the number of winding current paths, r'_a the resistance of one path, $I_a = i_a 2a$ and $r_a = \frac{r'_a}{2a}$ are then the armature current and armature winding resistance. Then,

$$p_{cop.a} = i_a^2 r'_a 2a = \left(\frac{I_a}{2a}\right)^2 r'_a 2a = I_a^2 \frac{r'_a}{2a} = I_a^2 r_a. \quad (7-20)$$

Let, further, ρ_{15} be specific resistance of copper at a temperature $\theta_0 = 15^\circ \text{C}$, N —number of armature winding conductors, l_{con} —length of a half-turn of one winding, S_{con} —cross-section area of conductor, θ_a —temperature of armature winding in service, α —copper temperature coefficient numerically equal to an increase in resistance of a 1-ohm conductor when the temperature increases by 1°C ; for ordinary ranges of temperature varia-

tion used in electrical machine construction, the average for $\alpha = 0.004$. Then,

$$r'_a = \varrho_{15} \frac{N l_{con}}{2a S_{con}} [1 + \alpha (\vartheta_a - \vartheta_0)].$$

Hence,

$$p_{cop.a} = \left(\frac{I_a}{2a}\right)^2 \varrho_{15} \frac{N l_{con}}{S_{con}} [1 + \alpha (\vartheta_a - \vartheta_0)]. \quad (7-21)$$

If l_{con} is expressed in cm and S_{con} —in sq. mm, then

$$\varrho_{15} = \frac{1}{5,700} \text{ ohm mm}^2/\text{cm at } \vartheta_0 = 15^\circ \text{C.}$$

According to State Standard 183-41 the losses in the electrical machine copper are reduced to the temperature $\vartheta_a = 75^\circ \text{C}$. Then,

$$p_{cop.a} = \left(\frac{I_a}{2a}\right)^2 \frac{N l_{con}}{4,600 S_{con}}. \quad (7-22)$$

With sufficient accuracy it may be assumed that $l_{con} = l + 1.4\tau + (2 \text{ to } 3)$, where l —armature length and τ is the pole pitch, expressed in cm.

The formula (7-22) may be expressed differently, viz.:

$$p_{cop.a} = \left(\frac{i_a}{S_{con}}\right)^2 \frac{N l_{con} S_{con}}{4,600} = j_a^2 \frac{N l_{con} S_{con} \gamma_{cop}}{4,600 \gamma_{cop}}.$$

Here, $j_a = \frac{i_a}{S_{con}}$ is the current density in the armature winding, expressed in A/sq. mm;

$\gamma_{cop} = 8.9$ —specific weight of copper and

$N l_{con} S_{con} \gamma_{cop} = G_{cop.a}$ —mass of armature winding copper.

If we express l_{con} in dm and S_{con} in sq. dm, then after conversions we obtain:

$$p_{cop.a} = j_a^2 \frac{G_{cop.a} \times 10^5}{4,600 \times 8.9} = 2.4 j_a^2 G_{cop.a}, \quad (7-23)$$

where, $G_{cop.a}$ is expressed in kg.

Losses in copper of other windings may be determined by formulas similar to formulas (7-22) or (7-23).

B. Field losses (p_{exc}). According to State Standard 183-55 the field losses contain losses in the field winding proper and the losses in the field rheostats, if they are necessary for machine operation in rated conditions.

Therefore,

$$p_{exc} = U_{exc} i_{exc}. \quad (7-24)$$

Where,

U_{exc} —the voltage across the field terminals;

i_{exc} —current in the field circuit.

C. Losses in the brush contact (p_{br}). If ΔU_{br} is the contact voltage drop per pair of brushes of different polarity and $I_a = 2ai_a$ —the armature current, then the losses in the brush contact may be determined by formula:

$$p_{br} = \Delta U_{br} I_a. \quad (7-25)$$

The values for ΔU_{br} are given in Table 6-1. According to State Standard 183-41 the voltage drop in the brush contact is assumed constant and for brushes of each polarity constitute: 1V for carbon and graphite brushes and 0.3 for metal-carbon brushes. Therefore, formula (7-25) may be written in concordance with brush grade as:

$$p_{br} = 2 \times (0.3 \text{ to } 1.0) I_a. \quad (7-26)$$

7-6. Additional Losses

Additional losses p_{ad} develop both in the steel and in the copper of the electrical machines. Some kinds of additional losses originate already at no-load, others only under load.

Here we shall consider only d.c. machines; for machines of other types the necessary information is given in the corresponding chapters.

At no-load the additional losses are created: a) in the main and commutating pole cores and in the yoke because of longitudinal flux pulsations due to armature tothing (Fig. 3-11); b) in main pole shoes due to magnetic flux cross oscillations (Fig. 3-10); c) in the armature winding due to non-uniform distribution of the main magnetic field in the armature slot (Fig. 7-3). This field may easily be resolved into a longitudinal field which creates in the winding a normal e. m. f. and a cross field which creates eddy currents in the armature winding conductors. The magnitude of losses due to eddy currents depends on the form and cross-sectional dimensions of the conductor and on the degree of non-uniformity of field distribution; with load these losses are almost invariable.

Additional losses in a machine on load originate: a) in the armature core due to the distortion of the main magnetic field as an effect of armature reaction (in machines without compensation windings); b) in coils undergoing commutation when the leakage flux coupled with the coil varies according to variation of current in the coil section from $+i_a$ to $-i_a$.

Non-uniform distribution of current density over the conductor cross-section occurs in this case and additional losses appear in the armature winding, attaining a magnitude which is the greater, the larger the number of conductors arranged in the slot along its height, the greater the height of conductor h_{con} and the more frequent the magnetic reversals f . An analysis

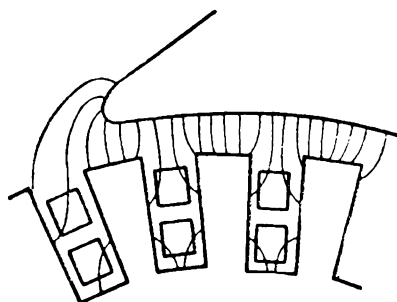


Fig. 7-3. Distribution of field in the armature slots

shows, that with a double layer winding at $f=50$ c/s the critical conductor height, beyond which a sudden increase in additional losses begins, is $h_{con.crit} \leq 10$ mm; c) in the brush contact due to a non-uniform distribution of current density under the brush with curvilinear commutation; d) in equalising connections if used.

These additional losses either entirely defeat all attempts of calculation or may be calculated only with large approximations. Therefore the State Standard 183-55 accounts for additional losses in d. c. machines without compensation windings at rated load by assuming them as one per cent of useful output, if the machine works as a generator, or one per cent of the input power if as a motor; for compensated d. c. machines 0.5 per cent is assumed.

With load change, the additional losses vary proportionally to the square of the current.

7-7. Total Losses in D.C. Machines and Their Efficiency

Knowing all the losses in the separate parts of the machine — mechanical losses p_{mech} , losses in the steel p_{st} , losses $p_{cop.a}$ in the armature winding copper and in windings connected in series with it,¹ brush losses p_{br} , and additional losses p_{ad} , we may determine their total:

$$\sum p = p_{mech} + p_{st} + p_{cop.a} + p_v + p_{br} + p_{ad}. \quad (7-27)$$

If P_1 is the power delivered to the machine, P_2 — the output of the machine, then

$$P_1 = P_2 + \sum p \quad (7-28a)$$

¹ P_{exc} losses in the (excitation) field circuit.

or

$$P_2 = P_1 - \sum p. \quad (7-28b)$$

The efficiency of a machine generally is expressed as a percentage. In this case

$$\eta = \frac{P_2}{P_2 + \sum p} \times 100 = \frac{P_1 - \sum p}{P_1} \times 100 = \left(1 - \frac{\sum p}{P_1}\right) \times 100. \quad (7-29)$$

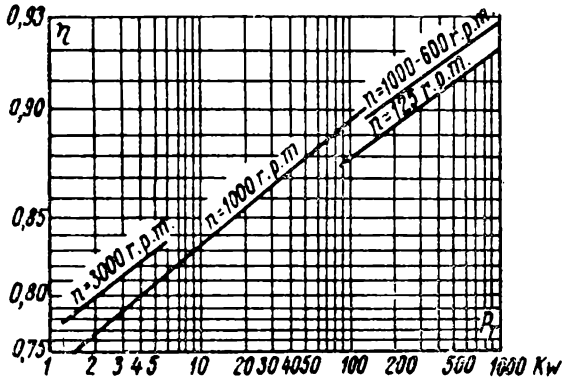


Fig. 7-4. Efficiency curves of a d.c. machine

In Fig. 7-4 the efficiency curves are given in relation to the rated power of the machine.

Chapter Eight

DIRECT-CURRENT GENERATORS

8-1. Preliminary

Modern electric stations generate practically only 3-phase alternating current electrical energy. A large part of this energy is used as alternating current in industry, for lighting and for domestic needs. In cases when industrial needs make it necessary or when it is of greater advantage to use direct current (for chemical and metallurgical plants, electric traction, etc.) it is generally obtained by means of converting a.c. to d.c. with the help of convertors of the ionic or machine types. In the latter case wide

use has been made of such installations as motor-generator units in which an a. c. motor is coupled to a d. c. generator on a common shaft. As primary sources of energy d. c. generators are used mainly in self-contained plants such as automobiles, and airplanes, for electric arc welding, train car lighting, in submarines, etc.

Thus the field of d. c. generator utilisation is sufficiently wide and correspondingly multiform are the requirements pertaining to its output, voltage, speed, reliability, service periods, etc. Here we shall consider only the fundamental properties of d. c. generators, not discussing any of their special performances.

8-2. Classification of D.C. Generators According to Method of Field Excitation

In accordance with the method of excitation d.c. generators are divided into:

- A) separately excited generators and
- B) self-excited generators.

Generators of the separately excited type are classified as: a) generators excited by electromagnetical means and b) generators with permanent magnets.

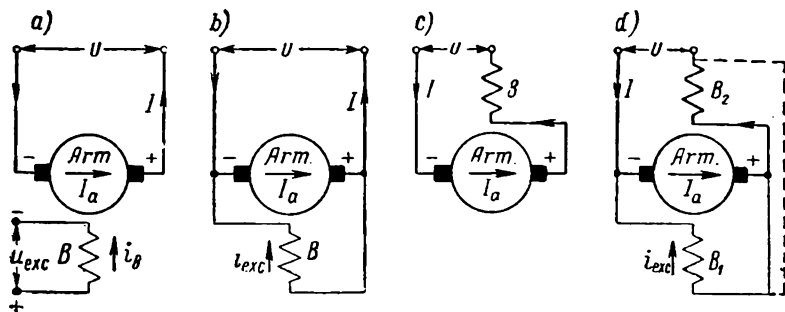


Fig. 8-1. D.c. generator circuit diagrams

As the latter have a limited application, further discussion will deal only with the former type.

Generators with self-excitation may be divided in accordance with type of field winding connection into: a) generators with shunt or parallel excitation, b) generators with series excitation, c) generators with mixed or compound excitation.

Fig. 8-1, *a, b, c, d* shows the various circuit diagrams for generators with separate, shunt, series and compound excitation. Here *A* is the armature; *B*—the field winding; *U* and *U_{exc}*—the voltages across the generator terminals and excitation field circuit; *I_a* is the armature current; *I* is the current delivered by the generator to the circuit; *i_{exc}* is the excitation current.

For a separate excitation generator $I_a = I$ and in the general case $U_{exc} \neq U$. For a shunt generator $I_a = I + i_{exc}$ and $U_{exc} = U$. For a series generator $i_{exc} = I$, i. e., the excitation of the generator depends on the load. The compound generator has two excitation windings, viz., parallel *B₁* and series *B₂*, the m.m.f.s of which may be cumulative or subtractive. In all cases, as much as 1 to 3 per cent of rated power is utilised for generator excitation.

8-3. The Energy Conversion Process in the D.C. Generator

The fundamental process taking place in a generator of any type and in a d.c. generator in particular is the conversion of mechanical energy utilised in the form of rotation, into electrical energy. For this purpose the generator is coupled to some prime mover, for instance an internal combustion engine, which brings it into rotation with speed *n*.

Let us consider the process of energy conversion by using as an example a generator with separate excitation, running at constant speed, i. e., with $n = \text{const.}$ With separate excitation the power P_{exc} , necessary to cover the excitation circuit losses, is not a part of the power P_1 delivered to the generator from the prime mover (Fig. 8-2). When the energy is converted, part of the power P_1 is spent on covering mechanical losses p_{mech} and losses in steel p_{st} , the remainder is converted into electromagnetic energy defined by the electromagnetic power $P_a = E_a I_a$. Thus,

$$P_a = E_a I_a = P_1 - (p_{mech} + p_{st}). \quad (8-1)$$

The useful output $P_2 = U I_a$ delivered by the generator to the circuit is less than the power P_a by the loss value in the copper

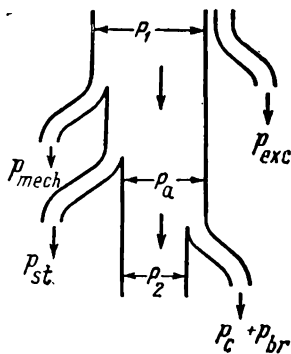


Fig. 8-2. Energy diagram of a d.c. generator with separate excitation

of the armature circuit $p_{cop} = I_a^2 R_{cop.a}$ and brush contact losses $p_{br} = \Delta U_{br} I_a$, where $R_{cop.a}$ is the resistance of the series windings constituting the armature circuit and ΔU_{br} —the contact pressure drop per pairs of brushes. We do not take into account separately the additional losses arising when the machine is working, but include part of them into the steel losses p_{st} and part into the copper losses p_{cop} .

Thus,

$$UI_a = P_2 = P_a - (p_{cop} + p_{br}) = E_a I_a - (I_a^2 R_{cop.a} + \Delta U_{br} I_a). \quad (8-2)$$

The electromagnetic power $P_a = E_a I_a$ is the main link which couples the mechanical power P_1 delivered to the generator and the useful electrical power $P_2 = UI_a$ which is delivered to the power supply network.

8-4. Equation of Generator E.M.F. at $n = \text{const}$

Dividing both parts of the equation (8-2) by I_a we obtain the generator e.m.f. equation in the form:

$$U = E_a - (I_a R_{cop.a} + \Delta U_{br}), \quad (8-3a)$$

or in the form of

$$E_a = U + (I_a R_{cop.a} + \Delta U_{br}). \quad (8-3b)$$

For simplification the sum $I_a R_{cop.a} + \Delta U_{br}$ is often represented in the form

$$I_a \left(R_{cop.a} + \frac{\Delta U_{br}}{I_a} \right) = I_a R_a.$$

In this case

$$E_a = U + I_a R_a. \quad (8-4)$$

It may be seen from this equation, that for $n = \text{const}$ the e. m. f. E_a has two components, one— U , is impressed on the generator terminals and serves the external circuit connected to the generator, the other— $I_a R_a$, overcomes the resistance of the generator and is usually termed the *voltage drop in the generator armature*.

8-5. The Electromagnetic Torque of the Generator

Assume that the prime mover creates a torque M_1 on the generator shaft, bringing the generator into rotation with some constant speed n (Fig. 8-3). Now if the generator is excited an

e. m. f. is induced in conductor a of the armature, located under the north pole and directed towards us; the current i_a in the conductor a flows in the same direction.

Between the magnetic field and the conductor with current i_a cutting the field there arises a force of electromagnetic interaction f_x . Assuming the flux density B_x of the same magnitude along the whole length of the conductor l' , located in the plane perpendicular to the direction of the magnetic field lines, we obtain

$$f_x = B_x l' i_a.$$

Since the field lines pass into the armature surface at 90° the force f_x creates on the generator shaft a torque

$$M_x = f_x \frac{D_a}{2} = B_x l' i_a \frac{D_a}{2}.$$

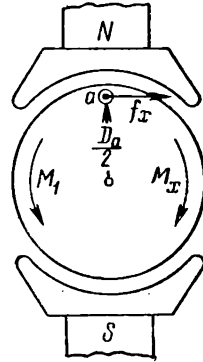


Fig. 8-3. Generator electromagnetic torque

To determine the direction of this torque, it is sufficient to superpose the main magnetic field on the field created by the current in conductor i_a (Fig. 8-4, *a*). The resultant field is shown in Fig. 8-4, *b*. It may be seen that the force f_x is in

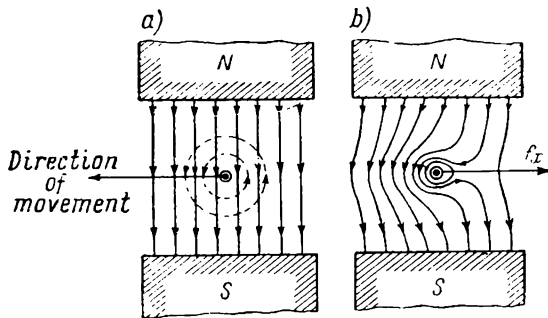


Fig. 8-4. Map of superposed fields

opposition to the direction of armature rotation and hence, the electromagnetic torque of the conductor M_x acts against the torque of the prime mover M_1 , i. e., in respect to the latter it is a braking torque. This deduction, being of a general nature, is true for any conditions of the machine operating as a generator.

The real machine has under each pole $\frac{N}{2p}$ conductors; therefore, the electromagnetic torque of the generator created by all conductors in a machine with $2p$ poles will be:

$$M_a = 2p \sum_1^{\frac{N}{2p}} M_x = 2pl' i_a \frac{D_a}{2} \sum_1^{\frac{N}{2p}} B_x.$$

With a sufficiently large number of conductors the summated value $\sum_1^{\frac{N}{2p}} B_x$ is equal to the average value of flux density B_{av} multiplied by the number of conductors per one pole pitch, i. e.,

$$\sum_1^{\frac{N}{2p}} B_x = B_{av} \frac{N}{2p}.$$

Taking into account that

$$B_{av} = \frac{\Phi}{\tau l'} = \frac{\Phi}{\frac{\pi D_a l'}{2p}} = 2p \frac{\Phi}{\pi D_a l'},$$

and $i_a = \frac{I_a}{2a}$, we will obtain for the electromagnetic torque the expression:

$$M_a = 2pl' i_a \frac{D_a}{2} N \frac{\Phi}{\pi D_a l'} = \frac{l}{2\pi} \frac{p}{a} N I_a \Phi. \quad (8-5)$$

This expression may be rewritten as

$$M_a = \frac{1}{2\pi} \left(N \frac{I_a}{a} \right) (p\Phi), \quad (8-6)$$

i. e., the electromagnetic torque of the generator is proportional to the flux of all p pairs of poles of the machine ($p\Phi$) and the current of the entire armature winding $\left(N \frac{I_a}{a} \right)$.

In a manufactured machine p , N and a are given values. In this case the formula for the torque may be rewritten in a simplified form:

$$M_a = C_m I_a \Phi, \quad (8-7)$$

where

$$C_m = \frac{p}{2\pi} \frac{N}{a}.$$

The expression for electromagnetic torque may be obtained also from the equation for the electromagnetic power $P_a = E_a I_a$, where $E_a = \frac{p}{a} n N \Phi$.

According to the general rule the torque $M_a = \frac{P_a}{\omega}$, where $\omega = 2\pi n$ is the angular speed of rotation. Therefore,

$$M_a = \frac{P_a}{\omega} = \frac{E_a I_a}{2\pi n} = \frac{\frac{p}{2} n N \Phi I_a}{2\pi n} = \frac{1}{2\pi} \frac{p}{a} N I_a \Phi.$$

In the MKSA system the flux is expressed in webers, the torque in newton-metres. If the flux Φ is expressed in maxwells, and the torque M_a in kilogramme-metres, then a conversion factor $\frac{10^{-8}}{9.81}$ is introduced into the R. H. side of formula (8-5).

8-6. Generator Torque Equation

Besides the braking electromagnetic torque M_a at the generator shaft there is also the no-load braking torque M_o corresponding to the power P_o that has to be delivered to the generator on no-load to cover no-load losses $P_{mech} + P_{st}$. According to the general rule

$$M_o = \frac{P_o}{\omega} = \frac{P_o}{2\pi n}. \quad (8-8)$$

At $n = \text{const}$ the *prime mover torque* M_1 and the *generator braking torque* $M_1 = M_a + M_o$ should be mutually balanced, i. e., they should be equal in magnitude and opposed to each other. Hence, for $n = \text{const}$ we have:

$$M_1 = -M_{gen} = -(M_a + M_o). \quad (8-9)$$

Usually M_a and M_o denote the components of the prime mover torque M_1 , each of which balances the corresponding generator torque. In this case

$$M_1 = M_a + M_o. \quad (8-10)$$

The torque equation for the case when $n \neq \text{const}$ is discussed further when considering the machine operating as a generator.

8-7. The Fundamental Characteristics of a D. C. Generator

Properties of generators are analysed with the help of characteristics which give the relationship between the fundamental magnitudes that determine the operation of the generator. These magnitudes are: 1) voltage across the generator terminals U ;

2) excitation current i_{exc} ; 3) armature current I_a ; 4) speed of rotation n .

Since generators generally operate at constant speed, the main group of characteristic curves is plotted for $n = \text{const.}$ Of the other three magnitudes the most important is voltage U as it defines the generator properties in respect to the power circuit to which the generator delivers power. Therefore, the fundamental characteristics are:

1. *Load characteristic* $U = f(i_{exc})$ for $I = \text{const.}$ In the case when $I = 0$ the load characteristic becomes the *magnetisation or no-load saturation curve*, which is of major importance for evaluating the generator and plotting the other characteristic curves.

2. *External characteristic* $U = f(I)$ with constant resistance of excitation circuit $R_{exc} = \text{const.}$

3. *Regulation characteristic* $i_{exc} = f(I)$ with $U = \text{const.}$ In the particular case when $U = 0$, the regulation characteristic becomes the *short-circuit characteristic* $i_{exc} = f(I_{sh})$.

There are also other characteristics besides the above numbered five fundamental characteristics, as, for instance, characteristics for variable speeds of rotation but these are of auxiliary use.

We shall consider the generator characteristics in relation to method of excitation as the main factor that determines the generator properties.

8-8. Characteristics of the Separately Excited Generator

Separate excitation is still widely used in low-voltage generators (4-24 V), in high-voltage generators (above 600 V) in large-output machines, or where a wide range of voltage regulation is required, etc.

A. No-load characteristic: $U_0 = f(i_{exc})$, $I = 0$ and $n = \text{const.}$ The connection diagram for plotting this characteristic curve is shown in Fig. 8-5. The notations are the same as in Fig. 8-1; the rheostat r_{reg} should be so selected, that the current i_{exc} may be regulated over a wide range; Sw is a knife switch which in this case opens the armature circuit.

When plotting the characteristic curve, the brushes should be on the geometrical neutral both in machines with commutating poles and without them. Since a machine has always a sufficient residual magnetic flux, then with $i_{exc} = 0$ the voltage $U'_0 = \text{OA}$ across the generator terminals (Fig. 8-6) is obtained. Generally $U'_0 = (2 \text{ to } 3)$ per cent of the rated voltage U_n .

When the current i_{exc} varies from $i_{exc}=0$ to maximum value $+i_{exc.m}=0c$ the voltage U_0 increases according to curve 1 to a value $+U_{0m}=Cc$. Generally $U_{0m}=(1.1 \text{ to } 1.25)U_n$.

On no-load the armature of the separately excited generator is connected only to a voltmeter which has a relatively large resistance; therefore, it may be assumed that

$$U_0 = E_0 = C_e n \Phi = C'_e \Phi.$$

Thus the relationship $U_0 = f(i_{exc})$ repeats to a certain scale the relationship $\Phi = f(i_{exc})$, i. e., it represents the *magnetisation characteristic* of the machine.

Let us now change the current i_{exc} from the value $+i_{exc.m}=0c$ to the value $i_{exc}=0$ and then reversing the current in the excitation circuit continue the variation of current i_{exc} in the range from $i_{exc}=0$ to $-i_{exc.m}=0d$. The curve 2 thus obtained in the first quadrant lies above curve 1 due to the increased magnitude of the residual magnetic flux.

If we were to repeat the procedure of changing the excitation current but in the reverse order from $-i_{exc.m}=0d$ to $+i_{exc.m}=0c$ we would obtain curve 3 which together with curve 2 forms a hysteresis loop, that determines the property of the steel of the poles and yoke. The curves 2 and 3 are termed the *descending* and *ascending branches* of the no-load characteristic curve. Drawing the middle line 4 between the two branches we obtain the so-called *calculated no-load characteristic curve*. It should be borne in mind, that the variation of current may be carried out only in one direction, as otherwise we will pass over to other magnetisation curves bearing no relation to our test. The lower part of the no-load curve is practically a straight line. This can be explained by the fact that for small excitation currents almost the entire m.m.f. is utilised for conducting the magnetic flux through the air-gap, i. e., through a medium of constant magnetic permeability. Further, as the current i_{exc} and the flux increase, the steel of the machine becomes saturated and we get first the medium-saturated part or the *knee* of the no-load curve and then the heavily saturated part of it. Point N, which corresponds to rated voltage U_n usually lies on the knee of the curve since, when a machine operates on the straight-line part of the curve the voltage becomes unstable and when working

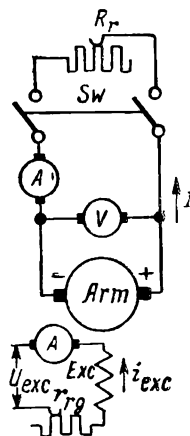


Fig. 8-5. Connection diagram for plotting characteristics of a generator with separate excitation

on the saturated part of the curve voltage regulation becomes restricted. Thus, the no-load characteristic curve allows us to judge of the saturation of the generator magnetic circuit for rated working

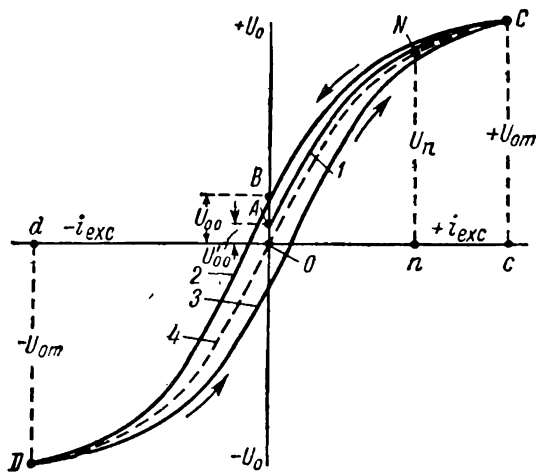


Fig. 8-6. No-load characteristic of a separate excitation generator

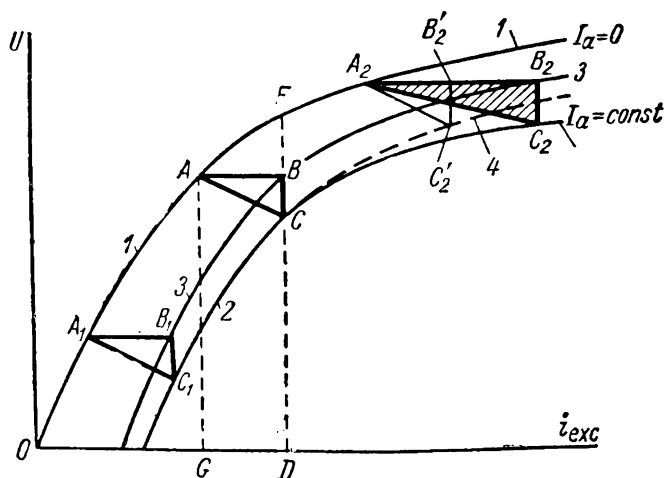


Fig. 8-7. Load characteristic of a separate excitation generator

conditions (the degree of saturation is considered in § 2-12). From subsequent discussion it will be clear, that the degree of saturation greatly affects the performance of machines.

B. Load characteristics: $U = f(i_{exc})$ for $I = \text{const}$ and $n = \text{const}$. Here and further we shall assume that the brushes are in the normal working position on the commutator. In this case, when the generator is loaded with current I , a voltage drop occurs across the generator terminals due to: a) voltage drop $IR_{am} + \Delta U_{br} = IR_a$ and b) armature reaction. Therefore the load characteristic curve passes below the no-load curve, and the larger the current I , the lower it lies.

In Fig. 8-7 the curves 1 and 2 depict the no-load and load characteristics. If we add the voltage drop IR_a to the voltage magnitudes of the load curve, we shall obtain the *internal load characteristic* $U + IR_a = E_a = f(i_{exc})$ for $I = \text{const}$ and $n = \text{const}$ (curve 3).

The load curve plotted together with the no-load curve permits the construction of the so-called d. c. generator *characteristic triangle*. This triangle allows on one hand to judge of the influence of the voltage drop and armature reaction on the generator voltage, and on the other, may be utilised for the construction of the generator external and regulation characteristics.

The characteristic triangle is plotted in the following manner.

Through an arbitrarily chosen point D on the abscissa axis a straight line is drawn parallel to the ordinate axis up to the intersection with curves 2, 3, and 1 in points C , B and F . By construction the segment $CB = IR_a$. At no-load we would have for the same excitation current $i_{exc} = OD$, the voltage $U_0 = DF$; therefore, the full voltage drop at the generator terminals CF when carrying a load current I is greater than the voltage drop $CB = IR_a$ by the value of segment BF caused by armature reaction. On the other hand, at no-load the e. m. f. $E_a = DB$ is obtained for an excitation current OG , less than OD by segment $DG = OD - OG$. Hence, the armature reaction of m. m. f. value, expressed by the excitation current scale is equal to DG . To plot the characteristic triangle ABC , it is sufficient to draw through point B a straight line $BA = DG$ parallel to the abscissa axis.

When $I = \text{const}$ the side $BC = IR_{am} + \Delta U_{br}$ remains constant irrespective of the excitation current i_{exc} magnitude. But the second side AB , corresponding to the armature reaction m.m.f. will remain constant only if it is possible to disregard the effect of saturation on the armature reaction value. From Chapter 4 it can be seen, that if the machine is not saturated, the cross armature reaction does not, practically, affect the performance of the machine (see Fig. 4-7, a, curve 3); therefore side AB of the triangle ABC is determined, in fact, only by the direct-axis armature reaction. But, as saturation increases, the effect of the cross armature reac-

tion becomes more and more pronounced and side AB accordingly begins to grow. Segment B_2B_2' that represents the difference between segment A_2B_2 corresponding to a saturated magnetic circuit and segment $A_2B_2' = A_1B_1$ corresponding to a non-saturated circuit, thus represents the demagnetising m. m. f. of the cross armature reaction. If the machine remains unsaturated with larger values of current i_{exc} , then we could obtain the load characteristic curve by shifting the triangle ABC parallel to itself so that the apex A stays on the no-load curve (the broken line 4 in Fig. 8-7).

Generally, load characteristics are plotted for two values of load current, for instance, for $I = \frac{1}{2} I_n$ and $I = I_n$. As in the case of plotting the no-load curve the current should be changed only in one direction.

C. External characteristics: $U = f(I)$ with $R_{exc} = \text{const}$ and $n = \text{const}$. The external characteristic curve is plotted by using connection scheme in Fig. 8-5 with knife-switch P closed. The voltage U_{exc} across the field circuit terminals is assumed constant; hence

$$i_{exc} = \frac{U_{exc}}{R_{exc}} = \text{const.}$$

According to the State Standard 183-55 *the rated variation in the electrical generator voltage is the change of voltage across the generator terminals (when operating separately from the other generators) with change of load from rated value to zero and with rated r. p. m. retained; for separately excited machines, in addition, the rated excitation current is stipulated, and for self-excited stipulated machine calculated working temperature and non-varying resistance of the field winding circuit.*

The variation in voltage is expressed as the per cent of rated voltage U_n .

Let us agree to express voltage U , load current I and excitation current i_{exc} as fractions of the rated values of these magnitudes, assuming that $U_n = 1$, $I_n = 1$ and $i_{exc.n} = 1$.

To plot the external characteristic we run the generator at rated speed and set up such an excitation current $i_{exc.n}$ that for $I = I_n = 1$ we would have $U = U_n = 1$ (Fig. 8-8). Then we throw off the load gradually down to no-load. The voltage of the generator increases according to curve 1 because with the decrease of load the voltage drop in armature IR_a and the armature reaction also decreases. At no-load $U_o = OA$. Hence,

$$\Delta U = \frac{OA - OB}{OB} \times 100 = \frac{U_o - U_n}{U_n} \times 100. \quad (8-11)$$

Since it may be assumed that $R_a = \text{const}$, the relationship $IR_a = f(I)$ is depicted in Fig. 8-8 by the straight line 2. Curve 3, which represents the relationship $U + IR_a = E_a = f(I)$ is called the *internal characteristic curve* of the generator.

The external characteristic of a generator with separate excitation may be plotted by using the no-load curve and the characteristic triangle, if it be assumed that the sides of this triangle vary proportionally to current I .

It follows from the plotting of the characteristic triangles in Fig. 8-7, that the apexes A, A_1, A_2 , etc., lie on the no-load characteristic, and the sides BC, B_1C_1, B_2C_2 are drawn parallel to the ordinate axis. From this follows the method of constructing an external characteristic for a generator with separate excitation.

Let, in Fig. 8-9, the curve OA_nA_o represent the generator no-load characteristic. As before, we shall assume that $U_n=1, I_n=1$. The characteristic triangle $A_nB_nC_n$ for a current $I_n=I$ we plot on the diagram so, that the apex A_n lies on the no-load curve, while sides A_nB_n and B_nC_n are parallel, the former to the abscissa axis, the latter to the ordinate axis. This defines the position of point C_n , corresponding to voltage $U_n=1$. Extending side B_nC_n of the triangle up to the intersection with the abscissa axis at point C_k , we find the rated excitation current of the generator $i_{exc.n} = OC_k = 1$, corresponding to its rated performance. Extending the same side B_nC_n up to the intersection with the no-load curve at point A_o , we will obtain the generator voltage no-load $U_o = C_nA_o$, corresponding to the excitation current $i_{exc} = \text{const}$. Point C_n we shall project to point D_n on the L. H. side of the ordinate axis, corresponding to current $I_n=1$, and point A_o to point D_o on the ordinate axis.

To obtain the intermediate points of the external characteristics, for example, the point for current $I = \frac{1}{2}I_n$, it is necessary to repeat the construction, dividing in half each of the $A_nB_nC_n$ triangle sides.

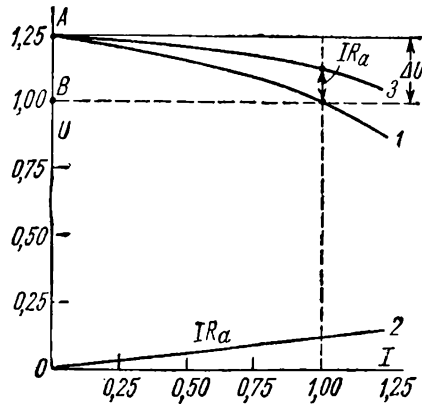


Fig. 8-8. External characteristic of a separate excitation generator

Alternatively, it is possible to divide the hypotenuse $A_n C_n$ in half at point G and move segment $C_n G$ along the straight line $C_n A_o$ into the position occupied by segment $C_1 A_1 = \frac{1}{2} A_n C_n$. After this we project point C_1 to point D_1 corresponding to current $I = \frac{1}{2} I_n$ and then draw through points D_o , D_1 and D_n the external characteristic curve.

This method of construction may be used only within a certain range of current values I , while the assumption that the sides of the characteristic triangle ABC vary proportionally to current

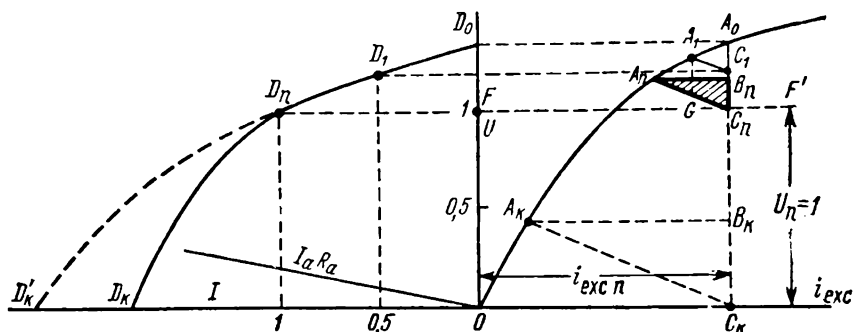


Fig. 8-9. Plotting the external characteristic of a separate excitation generator

I holds true. With a considerable increase of current the ABC triangle sides begin to grow faster, than the current I . This case will be discussed further in p. E.

D. Regulation characteristic: $i_{exc} = f(I)$, $U = \text{const}$ and $n = \text{const}$.

Since with $i_{exc} = \text{const}$ the voltage U across the generator terminals is reduced with an increase in current I and vice versa (Fig. 8-8), to maintain the voltage U constant in magnitude it is necessary to increase the excitation current with an increase in load and reduce it when the load is decreased. In the first case we follow the ascending branch of the magnetisation curve (Fig. 8-6), in the second—the descending branch. Accordingly the regulation curve is of the form depicted in Fig. 8-10. The middle curve, traced by a broken line between the ascending and descending branches, is assumed as the *practical regulation characteristic*.

The regulation characteristic may be plotted similar to the external characteristic by using the no-load curve and the characteristic triangle. For this purpose we draw the line DC in Fig.

8-11 parallel to the abscissa axis at a distance $OD = U_n = 1$ from the latter. Having plotted the characteristic triangle $A_n B_n C_n$ for one, say, the rated current value I_n , we must position this triangle so, that the apex A lies on the no-load characteristic, while the apex C_n is on the straight line DC ; this determines the excitation current $i_{exc} = Oa$ necessary for establishing the voltage U_n . By projecting point a from the abscissa axis downwards corresponding to current I_n we obtain point N of the regulation characteristic for nominal load.

The other points of the regulation characteristic are plotted

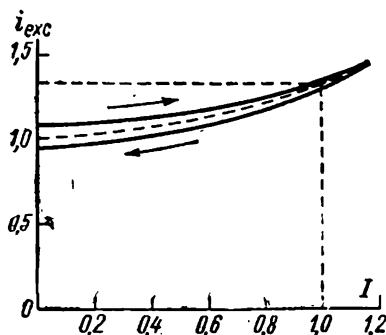


Fig. 8-10. Regulation characteristic of a separate excitation generator

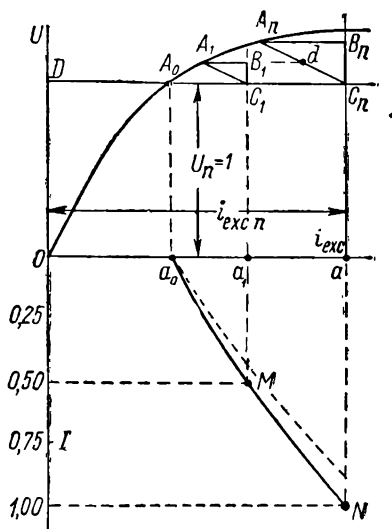


Fig. 8-11. Plotting the regulation characteristic of an external excitation generator

in the same manner, for example, point M for $I = \frac{1}{2} I_n$, on the condition that all the sides of the characteristic triangle vary proportionally to current I . For no-load we have $i_{exc,0} = Oa_0$ and we plot the regulation characteristic through points N , M and a_0 .

Under real machine operating conditions the armature reaction grows faster than the current I and to maintain the voltage $U = \text{const}$ a larger current i_{exc} is necessary. Therefore, the real regulation characteristic passes somewhat above the one plotted, as shown by the broken line in Fig. 8-11.

E. Short-circuit characteristic: $I_{sh} = f(i_{exc})$, $U = 0$ and $n = \text{const}$. To plot this characteristic, the generator should be run at a rated speed with the circuit closed only through an ammeter. In this case the resistance of the external generator

circuit may be disregarded and it is then possible to assume that $U=0$. Then from the e. m. f. generator equation [formula (8-3b)] we have:

$$E_a = I_{sh}R_{am} + \Delta U_{br} = I_{sh}R_a, \quad (8-12)$$

i. e., when a generator is short-circuited its e. m. f. E_a is equal only to the voltage drop in the armature winding and brush contact.

When $I_{sh} \approx I_n$ the e. m. f. E_a does not generally exceed several per cent of the rated voltage. In these conditions it may be assumed that the generator magnetic circuit is non-saturated and that the no-load characteristic curve for this section represents a straight line (line 1 in Fig. 8-12). If it were possible to disregard the

change in resistance of brush contact and assume that $R_a = \text{const}$, the short-circuit characteristic curve would also be a straight line. Actually, it departs a little from a straight line, but in most cases it is possible to neglect these deviations.

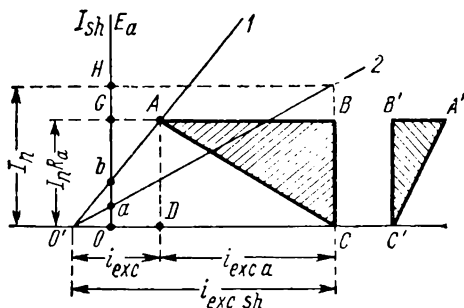


Fig. 8-12. Plotting the characteristic triangle

As the machine has a sufficient residual magnetic flux, in conditions when $i_{exc} = 0$ in the armature circuit there appears a short-circuit current $I_{sh.0} = Oa$ corresponding to e. m. f. $E_a = Ob$. Then the generator is excited so that the direction of the excitation field coincides with the direction of the residual magnetic field. The short-circuit current is generally brought up to values $I_{sh} = (1 \text{ to } 1.25) I_n$ and the data obtained are used to plot the short-circuit characteristic (straight line 2 in Fig. 8-12).

The initial branch of the no-load characteristic and the short-circuit characteristic make possible the construction of the characteristic triangle for some value of the rated current, say, I_n . For this purpose we extend the straight lines 1 and 2 up to the intersection with the abscissa axis at point O' , which we assume as the new co-ordinate origin. Let us lay off on the ordinate axis to the I_{sh} current scale the line $OH = I_n$ and determine on the short-circuit characteristic curve the segment $O'C = i_{exc, sh}$ which represents the full m.m.f. of the short circuit for $I_{sh} = I_n$ scaled to the excitation current i_{exc} . This m. m. f.

should be sufficient a) to compensate the armature reaction and b) to create the e. m. f. $E_a = I_n R_a$. Assuming the resistance R_a a known quantity, we lay off on the ordinate axis segment $OG = E_a = I_n R_a$ and determine on the no-load curve the excitation current i_{exc} , $O'D$, necessary for the creation of the e. m. f. E_a ; then segment $DC - O'C - O'D = i_{exc, sh} - i_{exc} = i_{exc, a}$ represents the m. m. f. of excitation which compensates the armature reaction when current $I_{sh} = I_n$. The triangle ABC with sides $BC = I_n R_a$ and $AB = i_{exc, a}$ is the characteristic triangle of the generator for a given short-circuit current.

Since during short-circuit performance the generator magnetic circuit is practically non-saturated, it may be assumed that the cross armature reaction does not cause any demagnetising effect and therefore side AB corresponds only to the m. m. f. of direct-axis armature reaction, which is created in the generator when the brushes are shifted from neutral in the direction of armature rotation (§ 4-4). When the brushes are on the neutral there is no direct-axis armature reaction, and therefore the side $AB \approx 0$. If the brushes are shifted against armature rotation, then the direct-axis armature reaction renders a demagnetising effect, and the side $B'A'$ moves to the R.H. side of triangle side $B'C' = BC$ (Fig. 8-12, *b*).

It must be noted that if, when plotting the short-circuit characteristic, current $I_{sh} \leq I_n$, then in large-output d. c. generators with accelerated commutation the phenomenon of self-excitation of the machine may often be noticed, explained by the magnetising effect of the commutation armature reaction; this may bring about a large increase in current I_{sh} and heavy sparking at the commutator. To prevent this it is common practice to use a temporary small coil with a magnetic action opposed to the generator main m. m. f.

When $I_{sh} > I_n$ the sides of the characteristic triangle ABC begin to grow faster than they would with direct proportionality to current I_{sh} . Side AB grows as a result of: a) large saturation of the tooth zone under the trailing edge of pole due to which the demagnetising effect of the cross armature reaction m. m. f. abruptly increases, and b) the commutation armature reaction is of demagnetising action in respect to the main field (§ 5-12), i. e., in the same direction as the cross armature reaction.

The side $BC = I_{sh} R_{am} + \Delta U_{br}$ of the characteristic triangle begins to grow faster than the current I_{sh} because due to disturbed commutation and appearance of sparking at the commutator, the voltage drop increase in the brush contact ΔU_{br} is much ahead of current I_{sh} increase.

From the above mentioned it follows that the actual short-circuit current I_{sh} depicted in Fig. 8-9 by segment OD_{sh} should be smaller than the current I_{sh} shown in the same figure by the segment OD'_{sh} plotted on the assumption that the sides of the characteristic triangle vary directly as the current I_{sh} .

8-9. Characteristic Curves of Shunt Generators

Shunt generators are the most widely used types of d. c. generators, because they do not need any special feed source for excitation and provide a stable voltage in the normal load range.

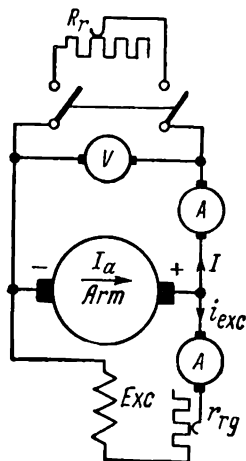


Fig. 8-13. Shunt generator connection diagram

A. Conditions of self-excitation. The shunt generator operates according to the connection scheme for self-excitation in Fig. 8-13 and does not need a separate d. c. power source for its excitation. For sustaining the self-excitation in a generator it is necessary, that there should exist in it a small (2 to 3 per cent of rated value) residual magnetisation flux Φ_{resid} . If after closing the excitation circuit we run the generator at some speed, for example, at the rated speed, then a small voltage would appear at its terminals, approximately 2 to 3 per cent of U_n and a small current starts flowing through the excitation circuit which sets up an additional magnetising flux Φ_o . Depending on direction of current in the excitation winding the flux Φ_o may be either opposed to flux Φ_{resid} or concurrent. The generator becomes

self-excited only when both fluxes are concurrent; in other words, the process of self-excitation of the generator can take place only in one direction, it being determined by the direction of flux Φ_{resid} .

With both fluxes concurrent the resultant excitation flux is increased; this leads to an increase in e. m. f. induced in the armature, and this in turn builds up a further increase in current and consequently in excitation and so on.

Let us consider the limits of the process of self-excitation. We shall assume that the generator operates on no-load, i. e., $I=0$.

For the case of self-excitation the equation for e. m. f. in the excitation circuit may be rewritten as follows:

$$u_0 = i_{exc} R_{exc} + \frac{d(L_{exc} i_{exc})}{dt} \quad (8-13a)$$

or

$$u_0 - i_{exc} R_{exc} = \frac{d(L_{exc} i_{exc})}{dt}. \quad (8-13b)$$

Here u_0 is the alternating voltage across the generator terminals and, hence, across the excitation circuit terminals;

R_{exc} —resistance and

L_{exc} —the inductance of this circuit.

If $R_{exc} = \text{const}$ the voltage drop $i_{exc} R_{exc}$ varies as the current i_{exc} . Graphically this is depicted by a straight line 1 in Fig. 8-14 inclined at an angle α to the abscissa axis.

Here

$$\tan \alpha = \frac{i_{exc} R_{exc}}{i_{exc}} = R_{exc}. \quad (8-14)$$

Hence, to each R_{exc} value corresponds a separate straight line, emerging from the co-ordinate origin at an angle defined by formula (8-14). In the same Fig. 8-14, the curve 2 gives the no-load characteristic. The segments of the ordinate between curves 2 and 1 give us the difference

$$u_0 - i_{exc} R_{exc} = \frac{d(L_{exc} i_{exc})}{dt}$$

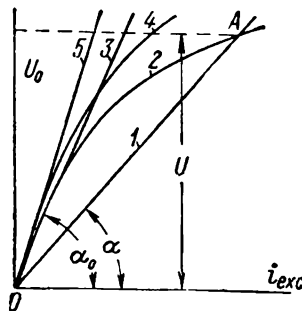


Fig. 8-14. Conditions for self-excitation of a shunt generator

and serve as a measure of the rate of the self-excitation process taking place. Obviously this process will terminate when the difference $u_0 - i_{exc} R_{exc}$ becomes equal to zero, or in other words when the characteristics 1 and 2 intersect. Hence, the steady value of current i_{exc} is determined by the point of intersection A of the characteristics 1 and 2.

If we further increase the resistance R_{exc} , i.e., angle α , then point A will slide along the no-load curve towards point O. For some resistance R_{exc} , which is termed the *critical resistance*, the straight line 1 will become a tangent to the initial part of the no-load characteristic (the straight line 3 in Fig. 8-14). In these conditions the generator practically fails to excite.

Since for a given scale of voltage U_0 and current i_{exc} the slope of the no-load characteristic depends on the armature r. p. m.,

then obviously, to each speed corresponds one critical resistance R_{exc} . Thus, for instance, for the no-load characteristic 4 which corresponds to a high speed of rotation the critical resistance is determined by the straight line 5.

B. No-load characteristic: $U_0 = f(i_{exc})$, $I = 0$ and $n = \text{const}$. Since the shunt generator is self-excited only in one direction, the generator no-load characteristic may be plotted also only in one direction (Fig. 8-15). There is actually no difference between the branches of the no-load characteristics of the generators

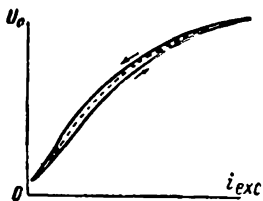


Fig. 8-15. No-load characteristic of a shunt generator

with separate and shunt excitation since the current flowing through the armature in the latter case $I_a = i_{exc}$ does not exceed 1 to 3 per cent of the generator rated current and therefore cannot cause any noticeable change in the voltage across its terminals.

C. Load characteristics: $U = f(i_{exc})$, $I = \text{const}$ and $n = \text{const}$. The load characteristics plotted both for schemes with separate and shunt excitation are practically coincidental, since an increase in

current I_a by the value of the excitation current does not in the latter case perceptibly influence the generator voltage compared with the former case.

D. External characteristic: $U = f(I)$ for $R_{exc} = \text{const}$ and $n = \text{const}$. The external characteristic of a shunt generator, just as that of the separate excitation generator, should make apparent the effect of load change on generator voltage without any regulation of the excitation current by means of a rheostat, i.e., for $r_{exc} + r_{reg} = R_{exc} = \text{const}$. Therefore, for separate excitation $i_{exc} = \frac{U_{exc}}{R_{exc}} = \text{const}$, and for shunt

excitation $i_{exc} = \frac{U_{exc}}{R_{exc}} = \frac{U}{R_{exc}} \equiv U$. When a change in load

takes place, for example, an increase, the voltage across the terminals of a generator with separate excitation decreases due to the effect of two causes—armature reaction and voltage drop in the armature circuit IR_a . In the case of a shunt generator, to the two above a third cause may be added—the decrease of excitation current i_{exc} in direct proportion to voltage U , which causes an additional voltage drop in relation to the voltage of the separately excited generator (curves 1 and 2 in Fig. 8-16, a).

This third cause also explains the difference between the external characteristics of the separately excited and shunt genera-

tors. If we were to gradually decrease the resistance of the external circuit R_c , then with separate excitation the current I will grow continuously and attain its maximum value at $R_c=0$, i. e., when the generator is short circuited. In the case of shunt excitation the current I will increase only to some critical value I_{crit} that generally does not exceed the rated current more than 2 to 2.5 times, and then it begins to drop (the broken-line part of curve 1 in Fig. 8-16, a). This may be explained as follows. When the resistance R_c decreases the current I tends to grow but the three factors mentioned above, that cause a voltage drop at the generator terminals, act in the opposite direction. While the machine is

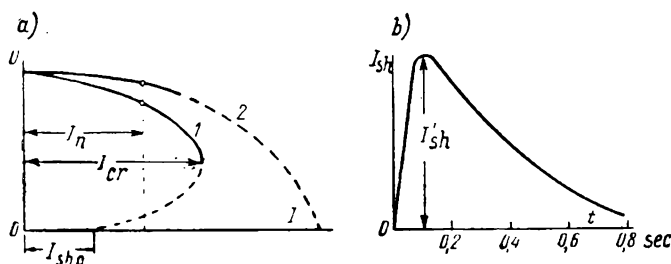


Fig. 8-16. External characteristic of a shunt generator (a) and curve of change of sudden short circuit current (b)

sufficiently strongly saturated and its magnetic system remains adequately stable, the first factor continues to predominate and the current increases. Then as the machine passes into a more and more unsaturated state (the linear part of the no-load characteristic) the factors that cause the voltage drop become the predominating ones. The current I_{sh} , after attaining the value I_{crit} begins to decrease and at short-circuit conditions obtains the value $I_{sh}=0$ defined only by the residual magnetisation flux, since for this particular condition $U=0$ and $i_{exc}=0$.

The external characteristic in Fig. 8-16, a is obtained by gradually varying the currents and voltages. But in actual working conditions *sudden short circuits* are possible, i. e., a comparatively very fast transition to such a state. Since a machine possesses a certain amount of stored electromagnetical energy, the decrease in its magnetic flux and its corresponding e. m. f. occurs with a certain time delay. Therefore, the current of a sudden short circuit may still manage to grow during a period 0.1 to 0.2 seconds to a magnitude exceeding the rated value 8 to 12 times, after which it falls rather abruptly (Fig. 8-16, b). With such an abrupt change of current, a large braking torque is created at

the generator shaft, and heavy sparking occurs at the commutator, which may become a flashover. Sudden short circuit¹ of shunt generators, especially for the large-output units, is dangerous and therefore they should be protected by high-speed circuit breakers.

The plotting of an external characteristic curve for a shunt generator is carried out in the same manner as for the separately excited generator but with a stipulated condition that the current i_{exc} varies as the voltage U ; accordingly the relationship $i_{exc} = f(U)$ in Fig. 8-17 is depicted by the straight line OA_0 , drawn from the co-ordinate origin at an angle α to the abscissa axis,

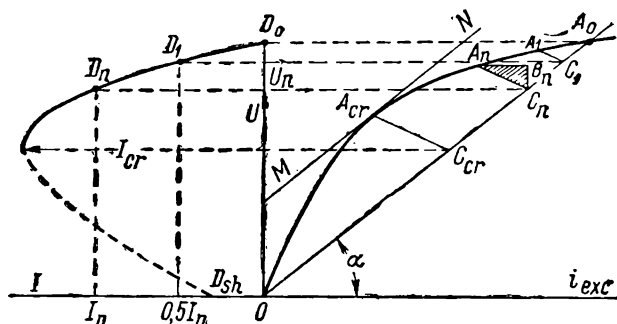


Fig. 8-17. Plotting the external characteristic for a shunt generator

$\tan \alpha$ being equal to R_{exc} [formula (8-14)]. The characteristic triangle ABC is located between the no-load characteristic and the straight line OA_0 .

To the left of the ordinate axis in Fig. 8-17, an external characteristic is plotted for points $I=0$, $I=\frac{1}{2}I_n$ and $I=I_n$ with the assumption, that the sides of the characteristic triangle vary directly as the current I . To obtain the critical current value I_{crit} it is necessary to draw the line MN as a tangent to the no-load curve, parallel to the straight line OA_0 and at the point of tangency A_{crit} draw the straight line $A_{crit}C_{crit}$ parallel to the hypotenuse A_nC_n of the characteristic triangle for current $I=I_n$. Then,

$$I_{crit} = I_n \frac{A_{crit}C_{crit}}{A_nC_n}.$$

¹ Sudden short-circuit phenomenon of d. c. generators are discussed in greater detail in the book of M. P. Kostenko *Electrical Machines. Special Section*

If the current I_{crit} greatly exceeds the rated current, then the phenomena described above in § 8-8, E occur which tend to limit the current I_{crit} .

The rated change in voltage is determined as above in § 8-8, C and is calculated with the help of formula (8-11).

E. Regulation characteristic: $i_{exc} = f(I)$, $U = \text{const}$ and $n = \text{const}$. If we plot the regulation curve for a generator, first with separate excitation, and then in the same conditions also with shunt excitation, there will be no difference between both the curves; this directly follows from the construction in Fig. 8-11.

F. Short circuit characteristic: $I_{sh} = f(i_{exc})$, $U = 0$ and $n = \text{const}$. The short-circuit characteristic curve cannot be plotted for self-excitation because in this case the voltage U and hence the excitation current i_{exc} are equal to zero.

8-10. The Series Generator

For the series generator the current $I_{exc} = I_a = I$ (Fig. 8-18). Therefore the no-load generator characteristic curve, and also its load and short-circuit characteristics may be plotted only when using the separate excitation connection scheme (Fig. 8-5). The characteristics are the usual curves for separately excited

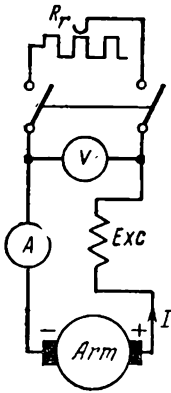


Fig. 8-18. Series generator circuit diagram

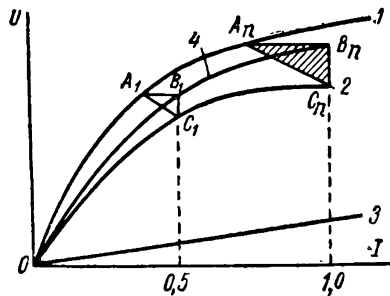


Fig. 8-19. Plotting an external characteristic for a series generator

generators (§ 8-8). Using the no-load and short-circuit characteristics it is possible to construct the characteristic triangle by the method described above in § 8-8, E, the triangle then being used for further plottings.

Since a series generator running with constant speed has only two variables, viz., U and I , this generator has in fact, only one characteristic, i. e., the external curve $U=f(I)$ for $n=\text{const}$.

In Fig. 8-19 curve 1 represents the no-load characteristic curve, curve 2—the external characteristic of the series generator, curve 3—the voltage drop $IR_a=f(I)$ and curve 4—the internal characteristic of the generator $E_a=U+IR_a=f(I)$. The difference between the curves 1 and 4 is due to armature reaction.

For the rated value of current $I_n=1$ the triangle $A_nB_nC_n$ is the characteristic triangle of the generator. Moving it parallel to itself so that point A remains on the no-load curve and then varying the sides of the triangle in proportion to current I it is possible to plot the external characteristic of the series generator.

Since the voltage U of a series generator varies abruptly with load, these generators are rarely used.

8-11. Compound Generator

The compound generator, having both a shunt and series field windings, combines the properties of both types of generators. The connection scheme of a compound generator may be

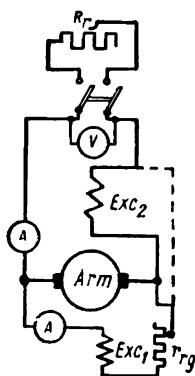


Fig. 8-20. Compound generator circuit diagram

accomplished either with a short shunt, as shown by the continuous line in Fig. 8-20, or with a long shunt shown in the same diagram by the broken line. The difference between both types of windings is practically nil, since the resistance of the series winding and accordingly the voltage drop across the terminals is very small.

Usually the field windings are so connected that the series winding aids the shunt winding, i. e., the m. m. f. s are added up. When connected in this manner the machine is said to be a cumulative compound generator. The machine in which the series field winding opposes the shunt is called a *differentially* compounded generator and is used in some special cases, as, for instance, some types of welding generators. In a cumulative compound generator the main role is played by the shunt winding, whereas the series winding is designated to compensate the m. m. f. of armature reaction and the voltage drop in the armature circuit

for a definite load. By these means therefore, automatic regulation of the generator voltage within a definite range of load currents may be attained.

Knowing the characteristics of the shunt and series excitation generators it is easy to explain the performance of a compound generator. Thus, for instance, the no-load characteristic of a compound generator $U_0 = f(i_{exc})$ for $I=0$ and $n=\text{const}$ does not differ in any respect from the corresponding characteristic of the shunt generator, since in this case the current in the series field winding is equal to zero.

The load characteristics of the compound generator $U = f(i_{exc})$ for $I = \text{const}$ and $n = \text{const}$ have the same form as the corresponding shunt generator characteristics, but with a sufficiently strong series winding the curves may lie above the no-load characteristics (Fig. 8-21). This property of the compound generator load characteristic follows from the method of its construction when using the no-load characteristic and the characteristic triangle ABC . Since the series winding produces a magnetising effect proportional to the armature current, the effect of the winding may be taken into account as the magnetising armature reaction for which the corresponding side AB of the characteristic triangle is positioned to the right of side $BC = IR_a$ (Fig. 8-12, b). If we move the triangle ABC parallel to itself so that its apex A slides along the no-load curve, the apex C then would trace the load curve in the same manner as in the case of the separately-excited generator.

By varying the ABC triangle sides proportional to the current I it is possible to plot a series of load characteristics, for example, for values $I = I_n$ and $0.5 I_n$.

By using the no-load characteristic and characteristic triangle it is also possible to plot the external characteristic of the compound generator $U = f(I)$ for $r_{exc} + r_{reg} = R_{exc} = \text{const}$ and $n = \text{const}$. The plotting procedure for this curve does not differ in principle

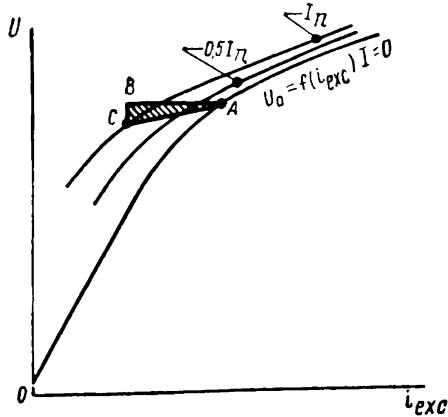


Fig. 8-21. Plotting the compound generator load characteristics

from that of the shunt generator external characteristic curve in Fig. 8-17.

Let, for example, $I = 0.5I_n$. From the co-ordinate origin we draw a straight line OA which expresses the relationship $i_{exc} = \frac{U}{R_{exc}} \equiv U$ for a given value of $r_{exc} + r_{reg} = R_{exc}$ (Fig. 8-22). The characteristic triangle $A_1B_1C_1$ corresponding to current $I = 0.5I_n$ we set at the co-ordinate origin and then move it parallel to itself along the straight line OA until it occupies the position

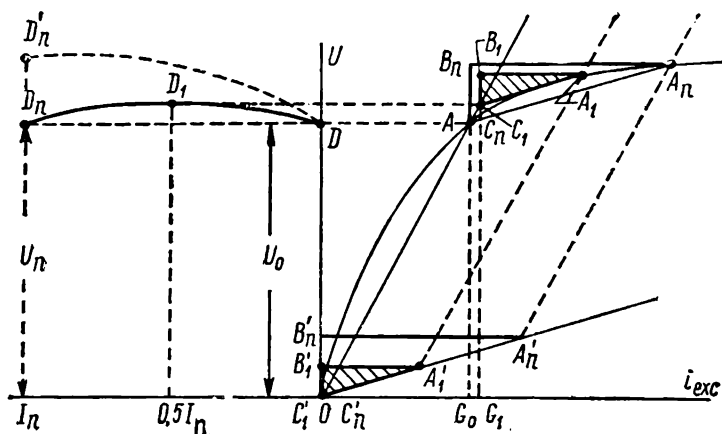


Fig. 8-22. Plotting the external characteristics of a compound generator

of triangle $A_1B_1C_1$ with the apex A_1 on the no-load curve and apex C_1 on the straight line OA (the hatched area in Fig. 8-22). The ordinate G_1C_1 then determines the voltage across the generator terminals for the load current $I = 0.5I_n$. In the same manner the plotting is carried out for current $I = I_n$ (triangles $A_nB_nC_n$ and $A_nB_nC_n$).

The series winding may be so designed that point C_n of the triangle $A_nB_nC_n$ coincides with point A , i. e., so that the voltage at nominal load I_n is equal to the voltage at no-load U_0 . Projecting points A, C_1, C_n (the latter coincides with point A) to points D, D_1, D_n corresponding to currents $I = 0, 0.5I_n, I_n$ and so on to the left of the co-ordinate axis and then joining points D, D_1, D_n , etc., into a smooth curve, the desired external characteristic of the compound generator is obtained.

To be able to maintain constant voltage across the electric energy consumer's terminals it is necessary to compensate the voltage drop in the line. In this case the series winding excitation is strengthened in such a manner that the external characteristic obtains the form of curve $D_0D'_n$, depicted by a broken line in Fig. 8-22.

With a differential connection of the field windings the construction of the compound generator external characteristic is carried out in the same way as for a shunt generator.

Generators with a cumulative connection of the field windings are used in those cases when it is necessary to automatically maintain the voltage at the generator terminals particularly when sudden changes of load current occur. The differential connection of field windings is used in some types of welding generators, where an abrupt drop of the external characteristic curve is a necessary feature.

Compound generators are usually weakly saturated, since only in that case will the flux created by the series field winding be almost proportional to the current in this winding.

In these conditions a series field winding is the one most effective.

Chapter Nine

PARALLEL OPERATION OF D.C. GENERATORS

9-1. General Considerations

All d. c. electric stations and converter substations generally employ several d. c. units so as to provide the necessary standby and provide for a varying load schedule in the most advantageous conditions of machine operation.

To provide parallel operation of generators two methods of connection are available:

a) The *series connection*, when potential points of different signs are connected, as, for example, the "plus" of one generator with the "minus" of the other;

b) The *parallel connection*, when points of like potential sign are connected.

Here only parallel connection of generators will be discussed as the series connections are comparatively rare in practice, mainly in higher voltage installations, as, for example, in electric railway substations with amplidyne converter plant.

9-2. Parallel Operation of Shunt Generators

A. Connection for parallel operation. Assume one of the generators in Fig. 9-1, for instance, generator *I* is already working under load, producing at the bus-bar voltage *U*.

To connect to the same bus-bar generator *II*, two conditions should be satisfied, viz.:

a) The "plus" and "minus" terminals of the generator to be paralleled should be joined with the like terminals of the common bus-bar and

b) The e. m. f. of the generator to be paralleled should be practically equal to the voltage *U*.

To fulfil these conditions, the following has to be carried out. Generator *II* is run at the required speed and then, without exciting it, one of the knife-switches, for example, the left one, is closed. If a voltmeter is attached across the open knife-switch, it will measure the voltage *U* (the influence of the residual field of generator *II* being disregarded).

Let us start to excite generator *II*. If its polarity does not coincide with the polarity of the bus-bar, then both generators are in series (the signs "plus" and "minus" for this case in the scheme are placed in brackets), and the voltmeter measures the sum $U + E_{aII}$. In this case obviously the generator must not be connected to the buses, as this would correspond to the short-circuiting of both machines.

If, on the contrary, the polarity of the connected generator coincides with the polarity of the bus-bars, the voltmeter shows this by decreasing its indications since the difference $U - E_{aII}$ is being measured. When this difference becomes zero, the right-hand knife-switch may be closed thus connecting generator *II* to the bus-bars.

If the generator *II* e. m. f. E_{aII} is exactly equal to power supply voltage *U*, then, from the main equation of generator e. m. f. [formula (8-4)] it follows, that the generator *II* current

$$I_{II} = \frac{E_{aII} - U}{R_{aII}} = 0.$$

To load the generator *II*, it is necessary to increase the mechanical power delivered to it from the prime-mover. This may be effected either by direct positioning of the speed regulator of the generator prime-mover thus increasing its speed or by increasing the excitation current i_{excII} of generator *II*. In the latter case the following process takes place: when current i_{excII} in-

creases, the e. m. f. E_{aII} increases correspondingly and current I_{II} starts to flow in the generator II ; for a given position of the prime-mover regulator the speed of the unit will begin to decrease but that will bring about regulator action which then restores the former speed with unit II output increased.

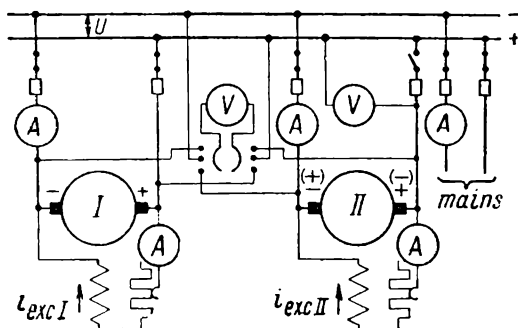


Fig. 9-1. Circuit diagram for parallel operation of shunt generators

B. Parallel operation of generators in conditions of external characteristic performance. Assume for simple argument, that the outputs of generators I and II are equal, i. e., $P_I = P_{II}$, and that their prime-movers possess the same mechanical characteristics.

Let the curves 1 and 2 in Fig. 9-2 represent the external characteristics of generators I and II , operating independently with the same no-load voltage $U_0 = 0$, and the curve 3 represent the total external characteristic $U = f(I_c) = f(I_I + I_{II})$, where $I_c = I_I + I_{II}$ is the current delivered by the generators to the power circuit. If the generators operate in parallel, then with an increase of load the voltage across the both generators should decrease by the same value $\Delta U = U_0 - U = OF - OD = OF - aA$. To be able to determine the currents I_I and I_{II} of each generator, it is sufficient to draw from point A a straight line parallel to the abscissa axis until it intersects with curves 1 and 2 at points B and C ; then $I_I = DC = Oc$ and $I_{II} = DB = Ob$. We observe then that currents I_I and I_{II} are not equal, current I_{II} being larger than I_I ($I_{II} > I_I$).

This deduction may be generalised, viz., a generator with a gently sloping (or hard) external characteristic curve, i. e., with the smaller voltage drop on load takes a larger load current, than the generator with a drooping external characteristic.

Thus, to ensure a more uniform distribution of load between generators of equal output operating without voltage regulation, it is necessary that their external characteristics be identical. To provide with change of load a redistribution of current proportional to the rated outputs of generators with various outputs their relative external characteristics $U = f\left(\frac{I}{I_n}\right)$ should coincide.

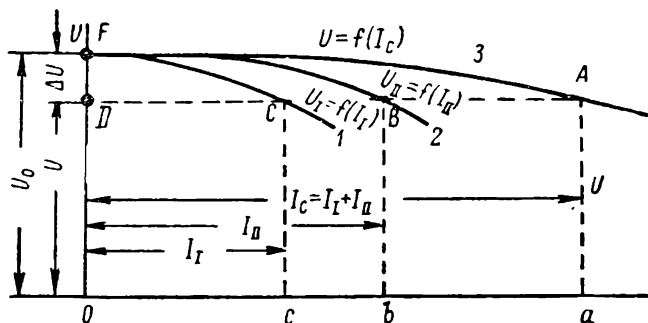


Fig. 9-2. Distribution of load between shunt generators

C. Distribution and retransfer of load. From the fundamental equation for d. c. generator e. m. f. we have:

$$E_{aI} - I_I R_{aI} = E_{aII} - I_{II} R_{aII} = U.$$

If R_c is the resistance of the external circuit then:

$$U = (I_I + I_{II}) R_c.$$

Solving these equations in respect to currents I_I and I_{II} we obtain:

$$I_I = \frac{E_{aI}(R_c + R_{aII}) - E_{aII}R_c}{R_c(R_{aI} + R_{aII}) + R_{aI}R_{aII}}, \quad (9-1)$$

$$I_{II} = \frac{E_{aII}(R_c + R_{aI}) - E_{aI}R_c}{R_c(R_{aI} + R_{aII}) + R_{aI}R_{aII}}. \quad (9-2)$$

Hence,

$$U = \frac{R_c(E_{aI}R_{aII} + E_{aII}R_{aI})}{R_c(R_{aI} + R_{aII}) + R_{aI}R_{aII}}. \quad (9-3)$$

It follows from the formulas (9-1), (9-2) and (9-3) that for given resistances R_{aI} , R_{aII} and R_c the distribution of load currents between the generators depends on the e.m.f. E_{aI} and E_{aII} , or, in other words, on generator speeds n_I and n_{II} and on their resultant fluxes Φ_I and Φ_{II} ($E = C_e n \Phi$).

These formulas show, that if we were to vary the excitation of only one generator, both currents I_I and I_{II} and the voltage U would change. If it is desired to redistribute the loads between the generators with $U = \text{const}$ it is necessary to reverse simultaneously the rotation or excitations of both generators, so that the sum $E_{aI} R_{aII} + E_{aII} R_{aI}$ in the numerator of the fraction in formula (9-3) remains without change.

If we want to stop one of the generators, say, generator I , we have first of all to decrease its excitation and simultaneously increase the excitation of generator II until current I_I drops to zero. With a further decrease in excitation of generator I the difference $E_{aI} - U$ becomes negative and the current $I_I = \frac{E_{aI} - U}{R_{aI}}$ changes its direction in respect to e. m. f. E_{aI} . Physically this means that machine I starts to work as an electric motor.

In this case two motors would be operating on one shaft, viz., a prime-mover and an electric motor, which may cause damage to the unit. Therefore, in generator schemes undervoltage automatic circuit-breakers are provided which switch off the generator, as soon as its current falls below a given value or reverses its sign.

9-3. Parallel Operation of Compound Generators

The electric circuit diagram of compound generators connected for parallel operation is shown in Fig. 9-3. Its main feature is that points 1 and 2 where the series winding is connected to the armature terminals of like sign are joined together by an *equaliser conductor*.

The necessity for such a conductor may be explained as follows. Let us assume, that the speed of rotation of one of the generators, say generator I , has increased by an insignificant value, and in accordance with this the e. m. f. E_{aI} of the generator has also increased. Let us further assume, that the shunt winding of generator I creates flux Φ_1 , and the series winding—flux Φ_2 , the flux $\Phi_2 = C_2 I_I$. In this case,

$$I_I = \frac{E_{aI} - U}{R_{aI}} = \frac{C_e n (\Phi_1 + \Phi_2) - U}{R_{aI}} = \frac{C_e n (\Phi_1 + C_2 I_I) - U}{R_{aI}},$$

hence,

$$I_I = \frac{C_e n \Phi_1 - U}{R_{aI} - C_e C_2 n}.$$

As the denominator in this formula is small, then with an increase of $E_{aI} = C_e n \Phi_1$, the current I_I will increase by a much

greater per cent value, according to which the flux Φ_2 created by the series winding will also be increased. Because of this the E_{a1} will increase still further and cause a still further increase in I_1 , which again causes a further increase of E_{a1} and so on. The result of this will be such an increase in current I_1 , that generator I not only takes on the entire circuit load but will also force the second generator to start performing as a motor in conditions when the shunt and series windings are connected in opposition to each other. A heavy impact of load on the first generator may bring about a decrease in speed of the prime-mover coupled to it,

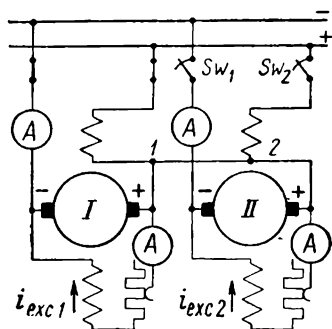


Fig. 9-3. Key diagram for parallel operation of compound generators

the consequence being that the entire load will be transferred to the second generator while the first generator will start performing as a motor. Then the prime-mover of the first generator will again increase its speed and then it will again take on the entire load and so on. Thus, a *transient state* may arise with a periodic throw-over of load current from one generator to the other, making stable generator operation impossible.

If an equalising conductor is joined to the circuit the series field windings of the generator become connected in parallel (Fig. 9-3).

Therefore, their currents are of the same ratios determined by the resistances of these windings. If, for some reason or other, the current in the series winding of one generator increases, the current in the other generator series winding is increased proportionally. Accordingly, there is a simultaneous increase of e. m. f. and load currents of both generators and transient fluctuations will not take place. In such conditions parallel operation of compound generators becomes quite stable and in principle is the same as the operation of shunt generators.

There are, nevertheless, some peculiarities when connecting compound generators for parallel operation, this being accomplished by two different methods.

The first method employed is as follows: making sure of correct polarity of the generator to be connected, for example, of generator II , we regulate its voltage until the bus-bar value is attained and then at once close both knife-switches P_1 and P_2 . In this case the current I_1 in the generator I series winding, after the

generator is connected to the bus-bars, branches off into the series windings of both generators: part of this current, for example, $\frac{1}{2}I_p$, passing into the generator *II* series winding, while the current of the generator *I* series winding decreases to a value $\frac{1}{2}I_p$. Because of this the e. m. f. of generator *I*, and therefore its load current will decrease, while the e. m. f. and current of generator *II* correspondingly increase. As in this case $E_{aI} + E_{aII} \approx \text{const}$, the power circuit voltage at the instance of connection of the generator *II* will not change, but the more rapid and the larger the degree of redistribution of load, the more pronounced and intense will be the mechanical impact at the prime-mover shafts. This method of connection is used at power stations where illumination is the predominating load.

The second method consists in closing knife-switch P_2 prior to connecting generator *II* to the bus-bars and regulating the voltage of the generator to be connected so that it becomes equal to bus-bar voltage U . If after this we should close knife-switch P_1 , the connected generator will not take on load and therefore there will be no impact. The drawback of this method, however, is that directly after closing switch P_2 the voltage at the bus-bars begins to drop rather noticeably because of the decrease of current in the operating generator series winding.

Chapter Ten

DIRECT CURRENT MOTORS

10-1. Reversibility Principle of Electrical Machines

Consider a machine operating as a generator and attached to a supply circuit (buses) with a constant voltage $U = \text{const}$ and developing an electrical torque M_g (Fig. 10-1). We already know (§ 8-6), that this torque is a braking torque in respect to the prime-mover torque M_1 that causes rotation of the generator shaft. For this case $I_a = \frac{E_a - U}{R_a}$ [formula (8-4)].

Let us decrease the generator e. m. f. E_a by reducing the r. p. m. or the flux Φ . With a large decrease in e. m. f. E_a it may become lower than the power circuit voltage U . In this case the armature current I_a will change its sign, i. e., flow in the direction opposite to the initial direction (Fig. 10-1, *b*); but since voltage $U = \text{const}$, the direction of current i_{exc} in the field winding and there-

fore the polarity of the main poles do not change. Corresponding to this the electromagnetic torque M_a will change its sign, i.e., if the machine was working previously as a generator and developing a braking torque converting mechanical power into electrical output, it would now work as an electric motor developing

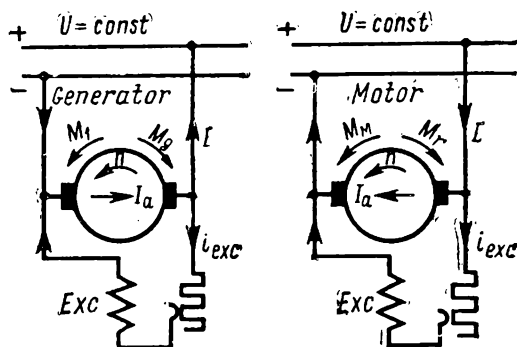


Fig. 10-1. Transfer of shunt machine from generator operation conditions to motor operation conditions

a torque M_a by overcoming the resistance torque at the shaft M_r , and converting electric power into mechanical power; still it continues to run in the former direction and retains former pole polarity. When we switch off the prime-mover we obtain a normal shunt motor scheme (Fig. 10-1, *b*).

This principle of machine reversibility was suggested as early as 1833 by Lentz. Shown above, as an example, for a shunt machine it may be extended to other types of d. c. machines and also to a. c. machines.

10-2. Classification of D.C. Motors

The d. c. motors are classified by the same method as the generators, i. e., according to the method of field winding connection in relation to the armature. Thus we have motors of: a) shunt, b) series and c) compound types.

All these types of motors are widely used and although in compliance with diverse requirements for the various drives employed they have a very wide performance range, nevertheless the energy process on which their performance is based and expressed by the equations of e.m.f. and torque is the same.

10-3. The Energy Process and Energy Diagram of D.C. Motors

We shall examine the energy process with the help of an energy diagram taking as an example a shunt motor (Fig. 10-2). The motor is assumed to be in steady-state operation, i. e., $n = \text{const.}$ If P_1 is the total electrical input to the motor from the power circuit, U —the voltage across the motor terminals, I_a —the armature current, and i_{exc} —the excitation current, then

$$P_1 = U(I_a + i_{exc}). \quad (10-1)$$

Part of this energy is used to cover losses in the field circuit, viz., $P_{exc} = U i_{exc}$ and losses in the armature circuit $p_{cop.a} + p_{br} = I_a^2 R_{cop.a} + \Delta U_{br} I_a = I_a^2 R_a$. The remaining part of the power is converted into electromagnetic power $P_a = E_a I_a$, which in its turn is converted into the full mechanical power P_{mech} . Hence,

$$P_a = P_{mech} = E_a I_a = U(I_a + i_{exc}) - U_{exc} i_{exc} - (p_{cop.a} + p_{br}) = U I_a - I_a^2 R_a. \quad (10-2)$$

The useful mechanical power P_2 delivered by the motor, differs from the power P_a by power P_0 , required to cover losses in the armature steel p_{st} and the mechanical losses p_{mech} , i. e.,

$$P_2 = P_a - P_0 = P_{mech} - (p_{st} + p_{mech}). \quad (10-3)$$

In all other types of motors the energy process is similar.

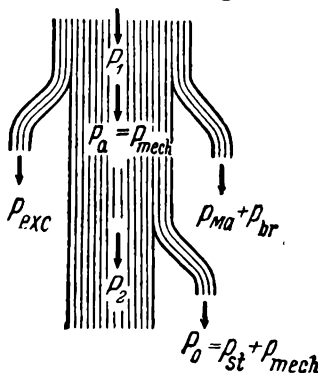


Fig. 10-2. Shunt motor energy diagram (p_{ma} stands for $p_{cop.a}$)

10-4. Equation for Motor E.M.F.

Let us assume that a constant voltage is impressed across terminals $A-B$ of a motor in Fig. 10-3. For the polarity of the poles given in the figure and direction of current I_a in the armature (the armature winding is shown by one conductor), at the motor shaft an electromagnetic torque M_a is created, directed counter-clockwise. We shall assume that under the effect of this torque the motor begins to run in the direction of torque M_a with constant speed n . Applying the right-hand rule we will find that

in the armature conductor (i. e., winding) an e. m. f. e_a is induced which is directed against the impressed voltage U . This deduction may be generalised, i. e., it may be extended to any type of performance of a machine working as a motor. Because of the above-mentioned property the e.m.f. e_a induced in the motor armature winding is named the counter or back e.m.f.

In the general case the motor works in transient conditions, with the armature current i_a , counter e.m.f. e_a and r. p.m. continuously changing. In these conditions an e.m.f. of self-induction— $L_a \frac{di_a}{dt}$ appears in the armature circuit where L_a is the armature

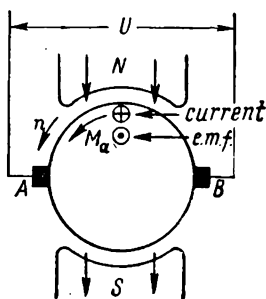


Fig. 10-3. Motor torque M and e.m.f. E_a

circuit inductance. Taking into account the direction of e.m.f. e_a in relation to voltage U , according to Kirchhoff's second law we have:

$$U + (-e_a) - L_a \frac{di_a}{dt} = i_a R_a$$

or

$$U = e_a + L_a \frac{di_a}{dt} + i_a R_a. \quad (10-4)$$

The voltage U may be considered as the effect of the supply circuit in respect to the motor. In the right-hand part of the equation (10-4) there are three components of this voltage, each of which is mutually balanced with the corresponding opposing action (reaction) of the motor in relation to the circuit, viz.: the components e_a and $L_a \frac{di_a}{dt}$ are balanced correspondingly by the e.m.f. $(-e_a)$ and $(-L_a \frac{di_a}{dt})$, while the component $i_a R_a$, usually called the voltage drop, is balanced by the e.m.f. $(-i_a R_a)$, originating due to the opposition which the current i_a meets when flowing through a resistance R_a . From this point of view the equation (10-4) may be considered as the equation of e.m.f. equilibrium for any performance conditions of the motor.

In the specific case when the motor operates in steady-state conditions and therefore $n = \text{const}$, the e.m.f. of self-induction disappears altogether and equation (10-4) assumes the form of:

$$U = E_a + I_a R_a, \quad (10-5)$$

where E_a and I_a are the respective e.m.f. and current corresponding to steady-state conditions.

The equation (10-5) will be very widely used in further discussions.

10-5. Motor Torque Equation

In the general case the following torques act on the motor shaft: 1) the electromagnetic torque M_a ; 2) the static resistance torque M_r , set up by the static forces of the electric power unit and reduced to motor angular speed, and 3) the dynamic torque M_j , which appears with any change in speed of motor or unit and due to the moment of inertia J of all the rotating masses coupled to the motor armature.

The electromagnetic torque of motor, just as the electromagnetic torque of the generator, is set up as a result of interaction of the main field and the current in the armature winding and therefore differs from the generator moment only in sign. According to formulas (8-6) and (8-7) deduced previously, we have:

$$M_a = \frac{1}{2\pi} \left(N \frac{I_a}{a} \right) (p\Phi) = C_m I_a \Phi. \quad (10-6)$$

For simplicity the subscript a of symbol M_a will further be omitted.

The static resistance torque is defined by the properties of the driven machine and depends on the nature of the industrial process. In many cases the static torque during the work process remains practically constant, as, for example, in the case of hoisting a load by a crane. In other cases it varies with speed (fans, propeller shafts), length of travel (for example, when using winders in deep mines and so on).

The static torques are discerned as: A) *reactive* and B) *potential or active*.

To the reactive torques belong static torques due to friction or cutting, for instance, of metal or wood, or due to tensioning and twisting of inelastic bodies as, for instance, yarn or thread. *These torques are always in opposition to the motor torque, i. e., always impede the movement of the electrical unit and therefore represent retarding torques.* To these torques also belongs torque M_0 , created within the motor proper by all forms of friction and losses in the armature steel. Due to the fact that in a motor operating at no-load only this torque is manifest, it is referred to as the *motor no-load torque*.

The active static torques include torques due to weight, compression, tension and torsion of elastic bodies. Contrary to the reactive torques these *static active torques retain their signs when armature rotation is reversed*, i. e., for one rotation direction they may act in opposition to motor torque M and therefore be braking torques, but with the reversed rotation these torques are con-

current with torque M ; therefore, they are driving torques. Thus, for instance, the torque created by the load of the hoisting machine retains its sign both for the lifting and lowering of the load, but in the first case it retards the load movement and in the latter case assists its movement.

In further discussion we shall consider first the cases when the static torque is a braking torque in respect to the motor torque, and then additionally the cases when it is a driving torque.

Irrespective of the kind of static torque, it may be represented as the sum of two torques, the no-load torque M_0 which, as was already mentioned, is created by friction and losses in steel of the motor proper and torque M_2 set up by all external, in respect to the motor, elements of the power unit. Hence,

$$M_r = M_0 + M_2. \quad (10-7)$$

Moment M_2 will be referred to as the *useful braking torque*, since it corresponds to the useful power P_2 developed at the shaft of the motor.

The motor dynamic torque is expressed in the general case as $M_j = \frac{d(J\omega)}{dt}$. But in electromechanical engineering the most important is the case when $J = \text{const.}$ For this condition

$$M_j = J \frac{d\omega}{dt}. \quad (10-7a)$$

Depending on whether the speed $\omega = 2\pi n$ increases or decreases the dynamic torque may be positive or negative, i. e., create at the motor shaft either a positive or negative resistance torque.

The relationship between motor torque M and the total resistance torques at the shaft $M_r + M_j$ ensues from the condition of their being mutually balanced, in other words, *for any condition of operation the torques M and $M_r + M_j$ should be equal in magnitude, but oppositely directed*, i. e.,

$$M = C_m I_a \Phi = -(M_r + M_j). \quad (10-8)$$

Generally, it is not the resistance torques that are meant here, but the *components* of the torque, each of which is in equilibrium with the corresponding resistance torque. Then,

$$M = C_m I_a \Phi = M_r + M_j. \quad (10-9)$$

From the equation of motor torque it directly follows that if for some reason torque M exceeds torque M_r , then a positive dynamic torque appears on the motor shaft and the speed of the motor begins to grow. When $M < M_r$, the process is reversed.

For steady-state working $n=\text{const}$. In this particular case we have:

$$M = C_m I_a \Phi = M_r = M_0 + M_z. \quad (10-10)$$

The equation of torques (10-9) together with the equation of e.m.f. (10-5) are of very great importance for analysing the processes taking place in electrical machines.

10-6. Motor Characteristics

The properties of all motors and in particular d. c. motors are defined as an aggregate of the following characteristics: A) starting, B) performance and mechanical, C) braking, D) regulation.

The starting characteristics define the operation of starting from the moment the motor begins running to the moment when steady-state operation is established and include: a) the starting current I_{start} generally defined by the ratio $\frac{I_{start}}{I_n}$; b) starting torque

M_{start} , defined by the ratio $\frac{M_{start}}{M_n}$; c) time of start t_{start} ; d) the efficiency of operations defined by the amount of energy consumed during the start; e) cost and reliability of starting equipment.

The performance characteristics are those that give the relations of n , M and η as functions of the power P_z or current I_a for $U=U_n=\text{const}$ and constant resistance in the armature and field circuit.

Of major importance for industrial drive mechanisms are the *mechanical characteristics* which represent the relation $n=f(M)$ for conditions of constant voltage and resistance in the armature and field circuits as described above. These also include the braking characteristics.

The regulation characteristics define the properties of motors when their speed is controlled. These include:

a) the regulation range given by the ratio $\frac{n_{max}}{n_{min}}$;

b) efficiency of regulation from point of view of initial cost of equipment and maintenance; c) mode of regulation continuous or stepped; d) simplicity of control apparatus and methods.

As we shall find out from further discussion, the d. c. motors possess versatile and diverse regulation characteristics and for this reason are indispensable in installations where wide-range control of speed is necessary.

10-7. Methods of Starting D.C. Motors

The following methods of motor starting are commonly used:

- A) direct connection to supply circuit (non-rheostatic start);
- B) starting by means of a rheostat connected to the armature circuit (rheostatic start);
- C) starting by means of a special starting unit.

In further discussion only the fundamental starting characteristics are considered mainly in relation to type of motor excitation.

10-8. Non-Rheostatic Start of Motor

Compared with other methods the non-rheostatic method of motor starting has the advantage of the apparatus and starting operations being the most simple. But in this case it is necessary to take into consideration the large current inrush at the initial starting period. This may cause:

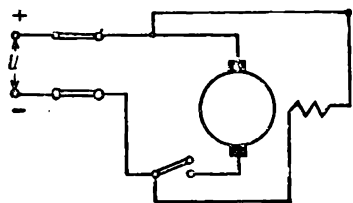


Fig. 10-4. Motor circuit diagram for non-rheostatic starting

- a) considerable sparking at the commutator and even flashovers;
- b) complication of operation of protecting and measuring apparatus in the armature circuit;
- c) the power circuit of the motor should be properly calculated, otherwise a large voltage drop may occur;
- d) a large dynamic moment is created on the motor shaft which has

to be taken into consideration when designing the transmission drive, as otherwise the driven machine may be destroyed.

The simplest case of a non-rheostatic start of a shunt motor will first be considered, it being connected to the circuit without load ($M_z=0$, Fig. 10-4). To simplify the analysis the following assumptions are used: a) the supply circuit voltage $U=\text{const}$; b) the motor is preliminarily excited; c) the armature reaction does not change the motor magnetic flux Φ or, in other words, the starting takes place with $\Phi=\text{const}$; d) the no-load torque M_0 due to losses in the motor may be disregarded, i. e., $M_r=0$. If ω is the angular speed of armature rotation, then $e_a=k_1\omega\Phi$ and the equation for e. m. f. s and moments [formulas (10-4) and (10-8)] may be rewritten as:

$$U = L_a \frac{di_a}{dt} + i_a R_a + k_1 \omega \Phi \quad (10-11)$$

and

$$M = k_1 i_a \Phi \approx M_j = J \frac{d\omega}{dt}. \quad (10-12)$$

From the latter equation we get:

$$\omega = \int k_1 \frac{i_a \Phi}{J} dt = k_1 \frac{\Phi}{J} \int i_a dt. \quad (10-13)$$

Substituting this value of ω in the equation for e. m. f. we find:

$$U = L_a \frac{di_a}{dt} + i_a R_a + \frac{k_1^2 \Phi^2}{J} \int i_a dt = L_a \frac{di_a}{dt} + i_a R_a + \frac{1}{C_a} \int i_a dt. \quad (10-14)$$

The equation (10-14) fully corresponds to the connection of a circuit with parameters R_a, L_a, C_a , on to an impressed constant supply voltage U . In this case

$$C_a = \frac{J}{k_1^2 \Phi^2} \quad (10-15)$$

represents the equivalent "capacity" of the armature, with the e. m. f. e_a acting at its terminals.

By differentiating the formula (10-14) with respect to time we have:

$$L_a \frac{d^2 i_a}{dt^2} + R_a \frac{di_a}{dt} + \frac{1}{C_a} i_a = 0. \quad (10-16)$$

The characteristic equation may be expressed as:

$$L_a \alpha^2 + R_a \alpha + \frac{1}{C_a} = 0. \quad (10-17)$$

The roots of this equation

$$\alpha_{1,2} = -\delta \pm \sqrt{\delta^2 - \omega_0^2},$$

where

$$\delta = \frac{R_a}{2L_a} = \frac{1}{2T_a} \quad \text{and} \quad \omega_0^2 = \frac{1}{L_a C_a}.$$

In the case when $\delta > \omega_0$, the roots of the characteristic equation are real and consequently aperiodic conditions of variation of the values i_a, e_a and n are obtained. The same takes place for the limiting case when $\delta = \omega_0$. If, for instance, $\delta < \omega_0$ then the roots of the characteristic equation are complex values and the conditions that cause the variation of the values i_a, e_a and n are of an oscillatory nature.

Fig. 10-5, *a* is a representative oscillogram of a non-rheostatic start for a Elektrosila Works ПН-85-type d. c. motor for $U = 0.53U_n$ with the following data: $R_a = 0.17$ ohm, $L_a = 0.0071$ henry,

$n=850$ r. p. m., with a gyration torque $GD^2=6$ kgm², where G is the weight of all rotating parts in kg, D is the armature diameter in metres.

A similar oscillogram is represented in Fig. 10-5, *b* for a ПН-45-type motor for $U \approx U_n$ with the following data: $R_a=0.69$ ohm, $L_a=0.0131$ henry, $GD^2=0.405$ kgm², $n=1,650$ r. p. m. It may be seen that in the former case the start is of an aperiodic and in the latter case of an oscillatory nature.

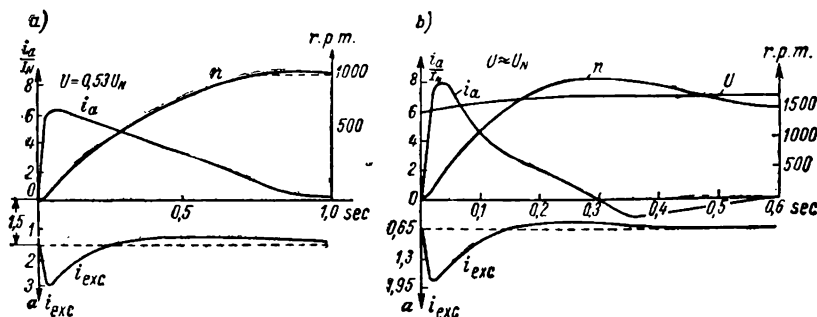


Fig. 10-5. Oscillograms for non-rheostatic starting of d.c. motors:
a — for aperiodic conditions; *b* — for oscillatory conditions

Today it is possible to accomplish non-rheostatic starts of motors with ratings up to 6 kW, with current surges exceeding the rated value 6 to 8 times. If the motor is started idle, the time of acceleration to rated speed is $t_n=0.1$ to 0.3 seconds; therefore the armature winding is heated only to a few degrees. It is possible to increase the range of non-rheostatic start application by using a high-speed automatic breaker which opens the armature circuit when the current reaches a stipulated limiting value and then recloses the circuit with a decrease in the current. Thus, the process of motor acceleration is accomplished by delivering one or several pulses across the armature terminals.

10-9. Rheostatic Starting Method. Starting Rheostats

To decrease the current inrush when starting a motor, a starting rheostat is inserted into the armature circuit. Depending on the assigned duty and conditions of operation the starting rheostats are made of different materials and of diverse design. For d.c. motor starting, practically only metal rheostats with air

or oil cooling are used with two or three terminals, both simple and combined types with manual, automatic or semi-automatic control, etc.; for starting induction wound-rotor motors especially those of the higher ratings mostly liquid rheostats are used.

Let us consider the process of rheostatic starting of a shunt motor with a three terminal starting rheostat consisting of four sections (Fig. 10-6,a); the rheostat connection scheme is depicted in Fig. 10-6,b. There are six contacts of which the first one is idle, the next four are intermediate contacts and the last one is the working contact. Besides, the rheostat is fitted with a copper segment *D* to the terminal *B* of which one end of the field winding is connected. Before starting the motor switch *Sw* should be opened and the handle of the rheostat set on the idle contact 0.

To start the motor, switch *Sw* is first closed and the handle shifted to contact 1; the motor is excited and in the armature circuit there appears the first current surge determining the top limit of the starting current I_{start1} . Since at the first instant of the starting process the motor e. m. f. $E_a = C_e n \Phi = 0$ the current

$$I_{start1} = \frac{U}{R_a + \Sigma R_{start}},$$

where ΣR_{start} is the resistance total of all resistors.

Assume, that the armature reaction does not affect the motor magnetic flux, i. e., that the start takes place when $\Phi = \text{const.}$ Since the resistance of the starting rheostat is relatively large, the inductance of the armature circuit is of secondary significance; therefore in the e.m.f. equation [formula (10-11)] the member $L_a \frac{di_a}{dt}$ may be disregarded. The current I_{start1} corresponds to the initial starting torque $M_{start1} = C_m I_{start1} \Phi$.

If this torque is greater than the static torque M_r , the motor will start with some acceleration and develop a counter e.m.f. proportional to *n* (curve *a* in Fig. 10-7). In accordance with this

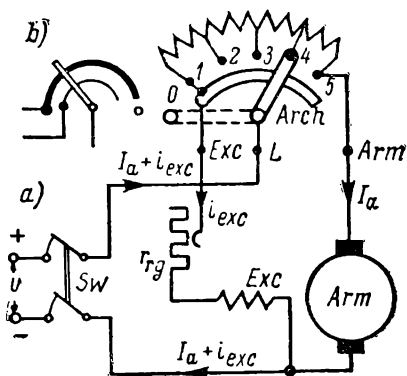


Fig. 10-6. Diagram of connecting starting rheostat into shunt motor circuit

the starting current and the starting torque proportional to it will decrease along curve *A*, on the same diagram.

When the starting current decreases to the value I_{start2} the rheostat arm is shifted to contact 2, thus shunting the resistor R_1 of the first section. With proper choice of the latter the starting current will again rise to I_{start1} , after which the speed of the motor will grow along curve *b* and current and torque will drop along curve *B*. The process then continues in the same order (curves *a-b-c-d-f* and *A-B-C-D-F* in Fig. 10-7) until the entire rheostat is cut out, after which the motor will work in a steady-state condition with current I and speed n .

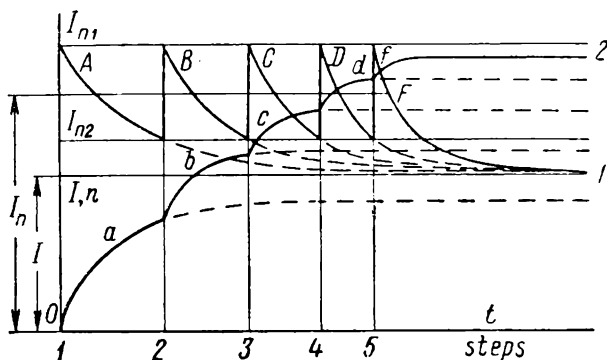


Fig. 10-7. Rheostatic starting of motor, $I_n = I_{start}$

If the rheostat arm be left continuously on one of the intermediate contacts, then with $M_r = \text{const}$ the process of changing of speed and current would be defined by the broken lines which are the continuations of the corresponding thick lines.

It should be taken into consideration, nevertheless, that starting rheostats are not designed for continuous operation in the armature circuit. To control the motor speed regulation rheostats of special design are used in the armature circuits.

Since, with other conditions being equal, the starting moment is proportional to the flux Φ , to facilitate the starting, it is generally carried out with the regulation rheostat cut out of the field circuit ($r_{reg} = 0$) and, consequently, with the highest possible value of current excitation and flux Φ .

For the same reasons it is necessary to arrange the field circuit so that the excitation current does not depend on the current in the armature circuit, and, in particular, on the manipulations of the starting rheostat.

The upper and lower limits of the starting current are chosen—the former from conditions for limiting the starting current and ensuring reliable commutation, the latter from the condition for providing on the motor shaft the necessary dynamic moment. Usually $I_{start 1} = (1.75 \text{ to } 1.5) I_n$ and $I_{start 2} = (1.3 \text{ to } 1.1) I_n$. The starting current here is the mean value $I_{start} = (1.5 \text{ to } 1.3) I_n$. The number of resistor sections at present is greatly limited, only 1 to 2 steps being used. This allows us to obtain a light-weight rheostat design, but the starting process is then of an abruptly stepped nature.

When the motor is cut off from the circuit, it is essential that the excitation circuit is not interrupted, since the electromagnetic energy stored in the excitation winding may lead to the creation of an arc and bring about a voltage surge in the interrupted circuit. To avoid this, contact 1 of the starting rheostat is electrically connected with the copper segment *D*; in this case when the switch *S* is out, the field circuit remains closed through the starting rheostat and motor armature.

The starting procedure for series and compound motors is practically the same as for the shunt motors, but there are some special features, discussed further in §§ 10-15 and 10-18.

10-10. Starting Motors with the Help of Special Units

With large motors the starting rheostats become bulky and considerable loss of energy in them takes place especially with frequent starts. Therefore in some installations it becomes necessary to resort to non-rheostatic methods of starting by means of varying the voltage delivered to the motor at starting. These methods include starting by means of a booster machine or by employing a generator-motor connection; starting battery-fed motors by subdividing the voltage; connection of two or more motors in series is the method widely employed in electric traction.

The generator-motor system is especially widely used. It is discussed further, since it is intended not only for starting the motor but also for controlling its speed.

10-11. Motor Performance Characteristics

1. *Shunt motor performance characteristics:* n , M , $\eta = f(I_a)$ with $U = U_n = \text{const}$ and $i_{exc} = \text{const}$. The motor circuit diagram is given in Fig. 10-8. Here: *F* are the fuses or automatic circuit breakers, r_{reg} —the regulation rheostat in the armature circuit.

When plotting the performance characteristics the rheostat r_{reg} is cut out (position 1 in Fig. 10-8). In this case the power circuit voltage U is impressed directly across the motor terminals. We shall assume $U = U_n$.

The rheostat r_{reg} in the field circuit should be adjusted so, that the motor develops the rated power P_n at rated values of voltage U_n , current I_n and r. p. m. n_n . In this position the rheostat r_{reg} must remain all the time without any change, so that $i_{exc} = \text{const}$.

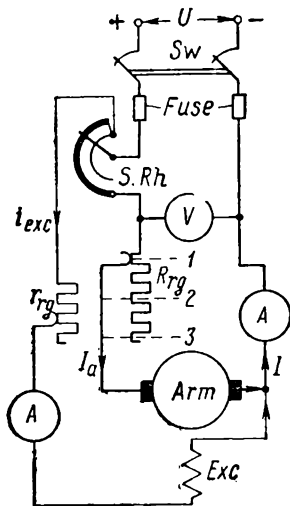


Fig. 10-8. Shunt motor circuit diagram

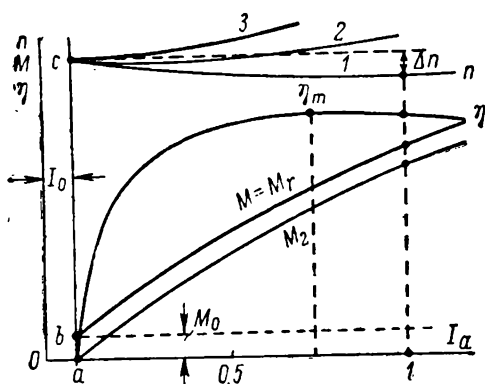


Fig. 10-9. Performance characteristic curves for shunt motor

The performance characteristics of the shunt motor are shown in Fig. 10-9. Let us agree to express the current I_a as a fraction of the rated current I_n , assuming $I_n = 1$. To explain the characteristic curves we shall use the equations of e. m. f. s and torques for steady-state operation conditions [formulas (10-5) and (10-10)].

A. Speed (external) characteristics: $n = f(I_a)$, $U = U_n = \text{const}$ and $i_{exc} = \text{const}$. According to the e.m.f. equation we have:

$$U = E_a + I_a R_a = C_e n \Phi + I_a R_a,$$

hence

$$n = \frac{U - I_a R_a}{C_e \Phi}. \quad (10-18)$$

Since it has been assumed that $U = U_n = \text{const}$ and $i_{exc} = \text{const}$, the shunt motor speed is influenced only by two factors of the second order, viz., the voltage drop $I_a R_a$ and armature reaction. With increase of load current I_a the voltage drop increases, and

the motor r.p.m. decreases accordingly. Conversely, with the brushes set normally the armature reaction demagnetises the motor and consequently tends to increase its speed. Thus the factors mentioned above in respect to motor speed are in opposition and the form of the speed characteristic is determined by the resultant effect of both of the factors.

In Fig. 10-9 the curves 1, 2, 3 depict the shunt motor speed characteristics for three cases: a) when the voltage drop $I_a R_a$ dominates (curve 1); b) when the factors mentioned above are practically balanced (curve 2) and c) when the armature reaction is predominant (curve 3). In all cases it should be borne in mind that with an increase of load the demagnetising effect of armature reaction increases not proportional to current I_a but much faster. Therefore all speed characteristic curves have a convexity towards the abscissa axis though usually this convexity is almost unnoticeable.

The usual form of shunt motor speed characteristic is the so-called *drooping speed characteristic* (curve 1 in Fig. 10-9). According to State Standard 183-55, *the rated change in shunt motor speed Δn_n with rated voltage across its terminals is the change when the load varies from rated load to no-load expressed as a percentage of the rated speed n_n .*

If n_0 is the speed at no-load, then

$$\Delta n_n = \frac{n_0 - n_n}{n_n} \cdot 100. \quad (10-19)$$

Usually $\Delta n_n = 2$ to 8 per cent, the smaller figure pertaining to motors of larger rating.

The form of the speed characteristic is related to the question of the degree of performance stability of the shunt motor in relation to the electrified drive unit. This is discussed in detail in § 10-12.

The slight dependency of shunt motor speed on the load is one of the most unique properties of this type of motor. Such a speed characteristic is often called a *stiff* characteristic.

B. Torque characteristic: $M = f(I_a)$, $U = U_n = \text{const}$ and $i_{exc} = \text{const}$. According to the torque equation for steady-state conditions of operation we have:

$$M = C_m I_a \Phi = M_0 + M_z = M_r.$$

For no-load $M = M_0 = C_m I_0 \Phi = ab$ (Fig. 10-9). If the excitation flux Φ would remain constant complying to $i_{exc} = \text{const}$, the torque characteristic $M = f(I_a)$ would represent a straight line emerging from point b . In reality the flux Φ somewhat decreases with an

increase in current I_a due to the demagnetising effect of the cross armature reaction. Therefore the torque characteristic increases somewhat slower than the current I_a . The characteristic curve of the useful torque $M_2 = f(I_a)$ should pass below the characteristic curve $M = f(I_a)$ at a distance equal to the value of the no-load moment M_0 . Since both the speed and the flux of a shunt motor remain practically constant when the performance curves are plotted, it may be assumed that

$$M_0 = \frac{P_0}{2\pi n_0} = \frac{p_{m0} + p_r}{2\pi n_0} \approx \text{const}$$

and that consequently, the characteristic curve of the useful torque M_2 passes from point a on the abscissa axis ($M_2 = 0$) parallel to the characteristic curve of the torque $M = f(I_a)$.

C. Motor Efficiency: $\eta = f(I_a)$ for $U = U_n = \text{const}$ and $i_{exc} = \text{const}$. According to formula (7-29, c) we have:

$$\begin{aligned} \eta &= \left(1 - \frac{\Sigma p}{P_1}\right) \cdot 100 = \left(1 - \frac{\Sigma p}{U(I_a + i_{exc})}\right) \cdot 100 = \\ &= \left(1 - \frac{p_0 + p_{exc} + I_a^2 R_{am} + \Delta U_{br} I_a p_{add}}{U(I_a + i_{exc})}\right) \cdot 100. \end{aligned} \quad (10-20)$$

It should be recalled that in this formula: p_0 are the no-load losses, i. e., the mechanical losses and losses in the steel core; $p_{exc} = U_{exc} i_{exc}$ —the losses in the excitation circuit; $I_a^2 R_{am}$ —the losses in the windings constituting the armature circuit; $\Delta U_{br} I_a$ —the losses in the brush contact; p_{add} —the additional losses, which amount, according to § 7-6, B, to 1.0 to 0.5 per cent of the motor input for rated value of current I_a .

Since for the conditions considered $n \approx \text{const}$, $i_{exc} = \text{const}$, $\Phi \approx \text{const}$, it is possible to assume that $p_0 + p_{exc} = \text{const}$; the resistance R_{am} is reduced to the temperature 75°C ; hence $I_a^2 R_{am} \equiv I_a^2$; the additional losses p_{add} also vary proportionally to I_a^2 ; for carbon brushes $\Delta U_{br} = 2\text{V}$; hence, $\Delta U_{br} I_a \equiv I_a$.

Disregarding the current i_{exc} in the denominator of formula (10-20), we find the first derivative $\frac{d\eta}{dI_a}$ and equate it to zero; then the condition for maximum shunt motor efficiency may be written as:

$$p_0 + p_{exc} = I_a^2 R_{am(75^\circ)}, \quad (10-21)$$

i. e., the motor efficiency attains its maximum value η_m at such a load when the constant losses are equal to the variable losses which depend on the square of current I_a .

By appropriately distributing the losses, the maximum efficiency may be obtained for a given load. In Fig. 10-9 the value η_m is obtained when $P_2 = 0.75 P_n$. The efficiency curve possesses a typical form, viz., it grows rapidly in the range from $I_a = 0$ up to $I_a = \frac{1}{4} I_n$; when $I_a = \frac{1}{2} I_n$ it reaches a value close to the maximum value, and then in the range of load change from $I_a = \frac{1}{2} I_n$ up to $I_a = I_n$ it remains almost constant. The efficiency η for small motors is usually from 75 to 85 per cent, for average- and large-power ratings $\eta = 85$ to 94 per cent.

2. *Performance characteristics of series motors:* n , M and $\eta = f(I_a)$, $U = U_n = \text{const.}$ The diagram of the motor is shown in Fig. 10-10. The symbols are the same as in Fig. 10-8.

A. Speed characteristic: $n = f(I_a)$ for $U = U_n = \text{const.}$ Since the series motor excitation current is equal to the armature current I_a and varies simultaneously with it, the magnetic flux Φ of the series motor in contrast to that of the shunt motor depends on the load, this being its specific feature.

From the e. m. f. equilibrium equation (10-5) we may obtain the same speed formula as for a shunt motor:

$$n = \frac{U - I_a R_a}{C_e \Phi}. \quad (10-22)$$

While a series motor is running the change in the motor main flux is of first importance, whereas voltage drop $I_a R_a$ and the armature reaction are secondary factors, the voltage drop tending to decrease and the armature reaction tending to increase the speed of rotation (assuming the brushes in the normal position).

For small and average loads the magnetic circuit of the motor may be assumed as non-saturated; in this case $\Phi \equiv I_a$ and hence,

$$n = \frac{U - I_a R_a}{C_e I_a} = \frac{U}{C_e I_a} - \frac{R_a}{C_e}, \quad (10-23)$$

i. e., the speed characteristic of a non-saturated series motor follows a hyperbola curve (the broken line in Fig. 10-11; current $I_n = 1$). As the current increases the motor becomes more and more saturated and the speed of the motor begins to change, although

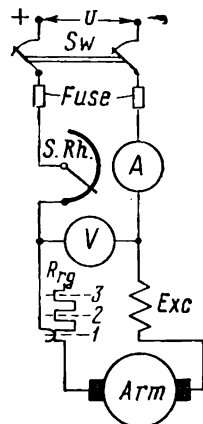


Fig. 10-10. Series motor circuit diagram

by a smaller degree compared with the former hyperbolic nature of change (the continuous line in Fig. 10-11). Special attention should be paid to the fact, that with a large decrease in load the motor begins to build up a very great speed called the runaway speed. At no-load $\Phi \approx 0$ and, according to formula (10-23), the

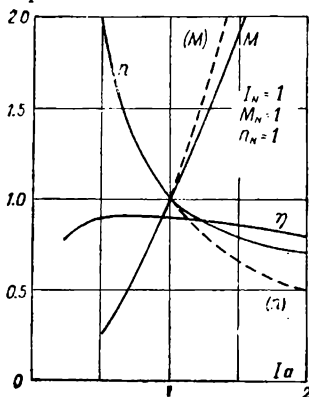


Fig. 10-11. Series motor performance characteristics

speed attains a magnitude which is dangerous because of the mechanical damages ensuing: tearing of binding wires, damage to armature winding, etc. Because of this a series motor should be set in such conditions of operation, as to exclude the possibility of starting without load or on no-load.

According to State Standard 183-55, series motors should be able to withstand without any damage a speed increase of 20 per cent above rated maximum speed, but not less than 50 per cent above rated speed.

Since the speed of a series motor varies in a very wide range, the nominal variation of speed according to the Standard is defined as the variation in speed when changing from rated load to one-quarter rated load, with $U = U_n = \text{const}$. Variation in speed is expressed as a percentage of rated speed. Thus, for a series motor we have:

$$\Delta n = \frac{n [I_a P_n]^{-n_n}}{n_n} \cdot 100. \quad (10-24)$$

The sharply defined relationship between the speed of a series motor and its load is its specific feature. Such a speed characteristic is often referred to as a *soft* characteristic.

B. Torque characteristic: $M = f(I_a)$ for $U = U_n = \text{const}$. Since the torque $M = C_m I_a \Phi$, then for a weak saturation of steel $\Phi \propto I_a$ and $M \propto I_a^2$, i. e., the torque characteristic curve of a series motor represents here a parabola. With an increase in current I_a the motor becomes more saturated, and the torque curve, compared with the parabola, grows more slowly (Fig. 10-11).

The unique property of the series motor, i. e., of being able to develop a greater torque than the one proportional to the current, is of great importance, especially for difficult starting conditions and in the case of overloads. The power in this case grows but less pronounced than its torque, since with an increase in power the speed of the motor decreases. In a shunt motor, on the contrary,

for which $n \approx \text{const}$, the power and the torque increase almost in direct proportion.

C. Motor efficiency. With a change in load all the series motor losses also begin to vary. However, design calculations have proved that the sum of the mechanical losses and losses in steel with load change but slightly. This is mainly due to the fact that with an increase in current I_a the flux densities increase, whereas the speed of rotation decreases. Therefore we may, as with the shunt motor, divide the losses occurring in the series motor into constant and variable losses (see § 10-11,1). Correspondingly, we may make a deduction in respect to the maximum value of efficiency as made pre-

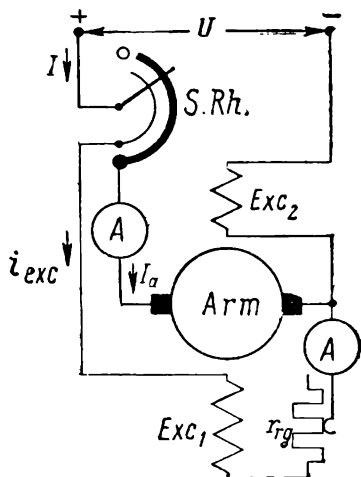


Fig. 10-12. Simplified circuit diagram for compound motor

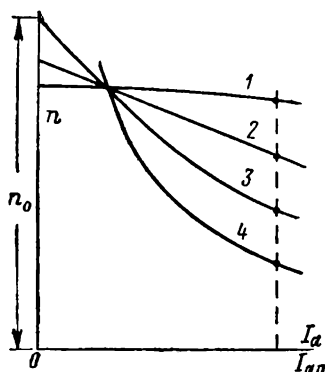


Fig. 10-13. Speed characteristics for compound motor

viously, viz., that it is obtained with the load when $p_0 = I_a^2 R_{am} (75^\circ)$.

3. *Performance characteristics of compound motors.* The scheme of the motor is given in Fig. 10-12. The series field winding may be connected in respect to the shunt winding either cumulatively or differentially.

When the field windings are connected cumulatively, their m.m.f.s. are added up increasing the flux Φ_1 , established by the shunt field winding, by the magnitude Φ_2 .

Therefore the expression (10-18) for motor speed assumes the form:

$$n = \frac{U - I_a R_a}{C_e (\Phi_1 + \Phi_2)} \quad (10-25)$$

With an increase in armature current I_a the resultant flux starts to increase, but to a lesser degree than in the case of a series motor. Therefore depending on the ratio of the fluxes Φ_1 and Φ_2 the compound motor speed characteristics may have the form either of curve 2 or curve 3 in Fig. 10-13, both occupying the intermediate position between the speed characteristics 1 and 4 of the shunt and series motors. A similar intermediate position is occupied by the torque characteristics (not shown in Fig. 10-13).

With a drooping speed characteristic (curve 3 in Fig. 10-13) the shunt field winding limits the excessive speed increase created when the load is removed since in this case flux Φ_1 remains, and it determines the no-load rotation speed n_0 .

For a differentially connected field windings we have:

$$n = \frac{U - I_a R_a}{C_e (\Phi_1 - \Phi_2)}. \quad (10-26)$$

Usually with an increase of load the shunt motor speed drops somewhat (curve 1 in Fig. 10-9). By choosing the proper number of turns of the series winding, it is possible with a compound generator to obtain the same speed characteristics and the same degree of performance stability as for a shunt motor (curves 2 and 3 in Fig. 10-9).

When starting a compound motor with a field winding differentially connected the series field flux may markedly weaken the resultant motor flux and thus complicate the starting procedure. To avoid this, the series winding of such motors is closed on itself during the entire starting period.

10-12. Mechanical Characteristics of D.C. Motors: $n=f(M)$

1. *General.* The main parts of an electrical drive unit are the power unit and the electric motor which communicates the required motion to the power unit. To obtain co-ordinated operation of both of these elements a definite relationship must be set up between the motor mechanical characteristics and the power unit characteristics both for steady-state and transient conditions. The relationship between these characteristics determines the stability of operation of the unit.

2. *Stability conditions for the electrical drive unit.* It is assumed that the motor torque M and the resistance torque M_r set up by the power unit at the motor shaft are given by curves 1 and 2

in Fig. 10-14 which intersect at point A . For convenience in this case the mechanical characteristics are plotted not as the usually applied relationship $n=f(M)$ but as $M=f(n)$. If the speed of rotation n changes, say, for example, it decreases from value $n_1=Oa$ to value $n_2=Ob$, then a positive dynamic moment $M_d=M-M_r=bd-bc=cd$ would originate on the motor shaft under the influence of which the motor speed will increase until it regains its former value n_1 . In the opposite case the process will be reversed. Hence, for given unit operation conditions, A is the point of its stable operation. In the general case stable operation of the electrical unit is provided for the condition when

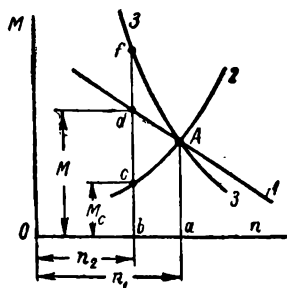


Fig. 10-14. Condition for stability of motor operation

$$\frac{dM}{dn} < \frac{dM_r}{dn}. \quad (10-27)$$

Now assume that the relationship $M_r = f(n)$ has the form of curve 3 in Fig. 10-14. In this case a decrease in speed will cause the appearance on the shaft of a negative dynamic moment $M_j = df$,

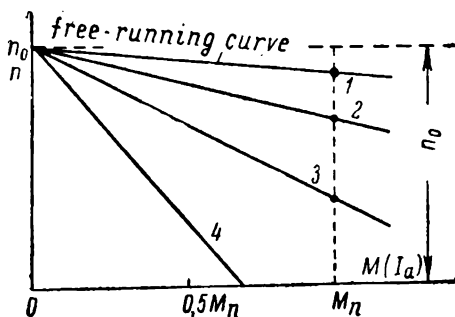


Fig. 10-15. Mechanical characteristics for shunt motor

under the effect of which the speed of the motor will decrease still more causing a further increase of the negative moment M , and so on. Therefore in these conditions motor performance becomes unstable. In the general case non-stable operation of the unit will take place for the condition when

$$\frac{dM}{dn} > \frac{dM_r}{dn}. \quad (10-28)$$

3. *Mechanical characteristics of the shunt motor: $n=f(M)$, $U=U_n=\text{const}$, $i_{exc}=\text{const}$, $\Sigma R_a=\text{const}$.* In the general case, the motor armature circuit may contain an additional regulating resistor R_{reg} (Fig. 10-8); for this case the e. m. f. of the motor will be:

$$U = E_a + I_a(R_a + R_{reg}) = C_e n \Phi + I_a(R_a + R_{reg}), \quad (10-29)$$

and therefore

$$n = \frac{U - I_a(R_a + R_{reg})}{C_e \Phi}, \quad (10-30)$$

or, as it follows from the torque equation $I_a = \frac{M}{C_m \Phi}$ then

$$n = \frac{U}{C_e \Phi} - \frac{M(R_a + R_{reg})}{C_e C_m \Phi^2} = n_0 - \Delta n. \quad (10-31)$$

Here $n_0 = \frac{U}{C_e \Phi}$ is the speed at no-load, if the very small voltage drop magnitude $I_a R_a$ is neglected; Δn is the decrease in speed corresponding to moment M and armature circuit resistance $R_a + R_{reg}$.

Assume that for $i_{exc} = \text{const}$, the flux $\Phi = \text{const}$. In this case the mechanical characteristics of the shunt motor represent straight lines the slope of which in respect to the abscissa axis is determined by the relationship $\frac{\Delta n}{n_0} = \frac{I_a(R_a + R_{reg})}{U}$; in Fig. 10-15 four mechanical characteristics are shown corresponding to the resistors $R_{reg} = 0$; $2.5 R_a$; $5 R_a$ and $10 R_a$. The mechanical characteristic for $R_{reg} = 0$ is called the *free-running characteristic*; since $M = C_m I_a \Phi$ then with $\Phi = \text{const}$ the mechanical characteristic is virtually the speed characteristic in Fig. 10-9 without the armature reaction taken into account. In this connection we shall deal with the problem of shunt motor stability in relation to the form of its speed characteristic.

Fig. 10-16, *a* and *b* shows the drooping (mechanical) characteristics $n = f(I_a) = f(M)$ for $M_r = \text{const}$ and for $M_r = n^2$. In both cases $\frac{dM}{dn} < \frac{dM_r}{dn}$, i. e., motor operation is stable. And conversely, if the motor speed n increases with an increase in current I_a or in the corresponding torque M , then stable performance is possible only in some special cases (Fig. 10-16, *d*) whereas, for instance, with $M_r = \text{const}$ (Fig. 10-16, *c*) it is impossible; physically this may be explained by the fact that if, for example, current I_a increases, this will cause an increase in speed n , which in its turn will cause an increase in current I_a and so on.

From the above discussion it follows, that to provide stable operation in all cases *shunt motors should normally have both drooping speed and drooping mechanical characteristics*. In modern extensively utilised¹ shunt motors the demagnetising effect of the ar-

¹ Note. The term "extensively utilised" here and further applies to large parameter values taken per unit value such as current loading, large flux density, higher temperature rise, etc. — *Tr.*

mature reaction may affect the motor speed more than the voltage drop in the armature circuit, rendering in many cases operation of the motor unstable. To compensate for the effect of armature reaction the motor is furnished with a series field winding, called the stabilising winding with a small number of turns joined *cumulatively* to the shunt field winding. All but two of the many ПН-types of shunt motors made at the Elektrosila Works (ПН-400 and ПН-550 types) are of this design.

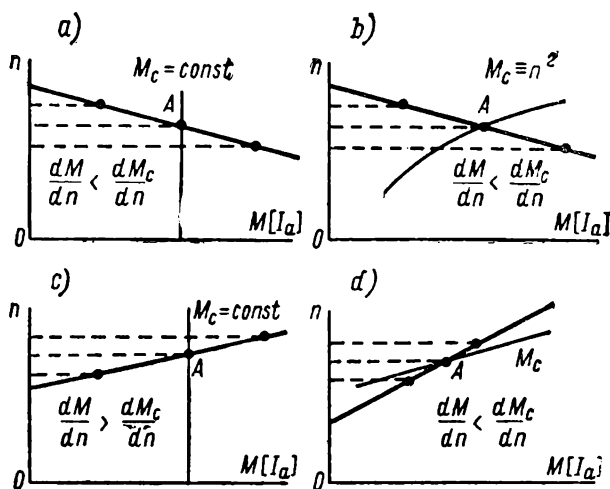


Fig. 10-16. Steady-state operation conditions of shunt motor for various mechanical characteristics of motor and power unit (M_c is the same as M_r)

4. *Mechanical characteristics of the series motor:* $n=f(M)$ with $U=U_n=\text{const}$ and $R_{reg}=\text{const}$. Since with change of load the saturation of steel in a series motor varies within a wide range, its mechanical characteristic may be expressed analytically in a simple form only for some particular case, when the machine is non-saturated and the field $\Phi \equiv I_a$. In this case $M = C_m I_a^2$; hence $I_a = C_m'' \sqrt{M}$, and since

$$n = \frac{U - I_a(R_a + R_{reg})}{C_e \Phi},$$

then

$$n = \frac{U - I_a(R_a + R_{reg})}{C_e' I_a} = C_e'' \frac{U}{\sqrt{M}} - C, \quad (10-32)$$

i. e., the mechanical characteristic of the non-saturated series motor is of a hyperbolic nature.

Fig. 10-17 shows the mechanical characteristics of a series motor plotted for various resistances R_{reg} , introduced into the

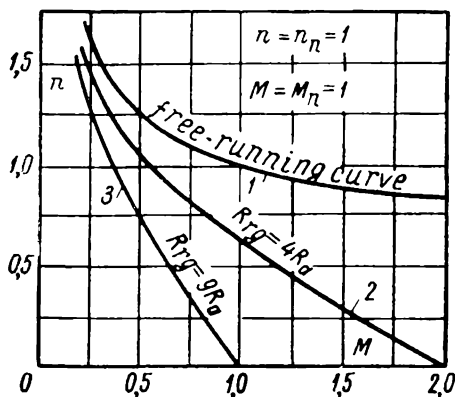


Fig. 10-17. Mechanical characteristics of series motor

armature circuit. The curve 1 plotted for $R_{reg} = 0$ is termed the *natural mechanical characteristic*. In the lower part of the curve where the motor is already saturated the curve noticeably differs from a hyperbola.

Since the series motor possesses a drooping mechanical characteristic its operation is practically always a stable one.

10-13. Braking Characteristics of D.C. Motors

1. *Types of braking*. In a number of installations electrical braking of motors is of most vital importance. Braking action is possible:

- A) With return of energy to the power circuit, otherwise called regenerative braking;
- B) By plugging of motors;
- C) With dynamic braking.

2. *Regenerative braking*. In the case of the shunt motor regenerative braking takes place when the machine, working as a motor, is forced by the power drive to run at a speed exceeding the no-load speed n_0 . The e. m. f. $E_a = C_e n \Phi$ then exceeds that of

the supply circuit voltage and therefore the current $I_a = \frac{U - E_a}{R_a}$ will reverse its sign; accordingly the torque developed by the machine will also change its sign, i.e., the machine will begin to operate as a generator connected in parallel to the power circuit. The elements of the mechanical characteristics 1 and 2 that pertain to regenerative braking are the continuation of the corresponding motor characteristics and are arranged in the second quadrant (Fig. 10-18).

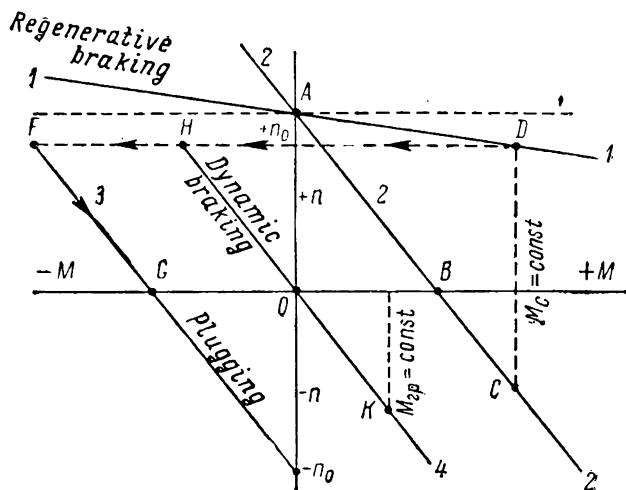


Fig. 10-18. Mechanical characteristics of shunt motor for braking conditions (here M_c is the same as M_r and $M_{rp} = M_{load}$)

With the series motor the case is somewhat more complicated, since the motor cannot be made to change from motor operation to regenerative braking operation by just simply increasing its speed. With an increase in speed the flux Φ will decrease and the counter e.m.f. E_a may become close in value to the power circuit voltage U but cannot exceed it. Therefore the regenerative braking of a series machine may be carried out by conversion of its field to shunt excitation and to the corresponding shunt motor performance (see previous discussion). Regenerative braking of series motors is widely used in electrical traction.

3. *Plugging.* This type of braking may be realised by two methods: a) when the power drive forces the machine to rotate in the direction opposite to that in which the machine develops the torque

and b) by reversing rotation by means of changing direction of the current in the motor armature.

The first case may be illustrated, for example, by the case when a sufficiently large resistor R_{reg} is inserted into the armature circuit of a motor lifting a load. Consider first the braking process in a shunt motor assuming that the torque $M_r = \text{const}$. When the resistor R_{reg} is connected motor conditions change from those defined by the free-running mechanical characteristic 1 (Fig. 10-18) to those defined by characteristic 2 corresponding to the resistance R_{reg} . If at the instant when the resistor is connected the current I_a is limited to such an extent that the motor torque $M = C_m I_a \Phi$ becomes less than the static moment M_r , a negative dynamic moment M_d appears on the motor shaft [see formula (10-9)] and the motor speed is retarded. In this case, the e.m.f. E_a decreases and the current $I_a = \frac{U - E_a}{\Sigma R_a}$ grows; consequently the torque

M increases. This process of parallel decrease of speed n and increase of torque M will continue until M becomes equal to M_r ; in this case $M_d = 0$ and further change of speed ceases. For sufficiently large values of R_{reg} and M_r , the motor may stall while retarding (point B of characteristic curve 2 in Fig. 10-18) and then start to run in the opposite direction. The steady drop in the load is determined by point C in which the characteristic curve 2 intersects with the straight line $M_r = \text{const}$.

For the performance considered power $P_{el} = UI_a$ is delivered from the supply circuit to the motor and $P_{mech} = E_a I_a$ from the mechanism shaft, the sum $P_{el} + P_{mech} = UI_a + E_a I_a = I_a^2 (R_a + R_{reg})$, i. e., it is completely spent in the resistances of the armature circuit.

A similar process takes place also when braking a series motor. With the armature rotation reversed the machine may start functioning as a generator with self-excitation. But with the values of resistance R_{reg} actually introduced into the armature circuit to limit the current, the possibility of self-excitation of the machine is practically nil.

Braking by reversing the current (plugging) is used when it is desired to rapidly stop, for example, a crane trolley. To accomplish this the polarity at the armature terminals is reversed, this consequently bringing about the reversal of the current. Assume as before that $M_r = \text{const}$ and $i_{exc} = \text{const}$. Immediately after switching the armature will continue to rotate in the same direction as before, utilising the kinetic energy of the moving masses of the power drive. For these conditions the sign of the e. m. f. E_a does not change, but the sign of the circuit voltage

U is reversed in respect to E_a . Hence,

$$I_a = \frac{-U - E_a}{R_a + R_{reg}} = -\frac{U + E_a}{R_a + R_{reg}},$$

where R_{reg} is the additional resistance introduced into the armature circuit to limit the current I_a value. Thus, the sign of the current I_a is reversed and on the motor shaft appears a braking moment $-M = C_m (-I_a) \Phi$.

Immediately after switching the motor operation is determined by point F (Fig. 10-18), which corresponds to torque $-M$ and speed n the motor had prior to the switching. Under the action of the braking moment $-M$ the motor begins to slow down and a decrease in e. m. f. E_a , current I_a and torque M takes place accordingly. Motor operation follows the characteristic curve 3 and with an adequately chosen resistance R_{reg} may stall (point G of the characteristic curve 3 in Fig. 10-18), and then start to run in the direction of moment $-M$, i. e., opposite to the initial direction. If this is undesirable, then the motor is cut out of the circuit at the instant when $n=0$.

A similar process takes place when braking a series motor.

4. *Dynamic braking.* When dynamic braking is employed for a shunt motor, its armature is cut off from the power circuit and a load resistance R_{load} is switched across it, the current in the excitation circuit being left unchanged. The machine begins to work as a generator with separate excitation, utilising the kinetic energy stored in the unit. Since in this case $U=0$, the equation of the mechanical characteristic of the machine according to formula (10-31) will be:

$$n = \frac{M (R_a + R_{load})}{C_e C_m \Phi^2}.$$

This equation corresponds to a straight line passing through the origin of the co-ordinates system from the second quadrant to the fourth. The process of braking takes place as follows. Assume that the machine is operating as a motor, its performance being determined by point D on the characteristic curve 1 (Fig. 10-18). Immediately after the machine is transferred to dynamic braking the speed of the machine does not change (practically) and hence the e. m. f. $E_a = C_e n \Phi$ also does not undergo any change. But the current I_a is reversed, since for a motor $I_a = \frac{U - E_a}{R_a}$, while for a generator

$I_a = \frac{-E_a}{R_a + R_{load}}$. Therefore a braking torque $-M$ appears on the machine shaft and machine operation is determined by point

H (Fig. 10-18), corresponding to this torque and the initial speed n .

After that the speed drops following the characteristic curve 4, and may become equal to zero and then the machine will begin to run in the reverse direction ($-n$), for example, under the effect of the load being lowered. The steady speed of lowering the load is determined by point K in which the characteristic 4 intersects with the straight line of torque M_{load} , created by the load, M_{load} being constant.

The dynamic braking of a series motor may be executed in the same way as of the shunt motor, i. e., with separate excitation. But this type of performance is wasteful due to large consumption of energy for the excitation.

The braking performance of a self-excited series machine has the disadvantage, that with small speeds the machine does not excite at all, and after attaining a certain speed the process of self-excitation proceeds very violently and large braking torques may appear on the machine shaft, which may cause damage to the unit.

10-14. Speed Control Characteristics of D.C. Motors

From the point of view of speed regulation d. c. motors have several very valuable advantages, which make them in many cases indispensable.

Here we shall discuss, mainly, the range of speed regulation and efficiency of the regulation procedure, considering other problems (start period, starting apparatus, etc.) only in passing.

In compliance with formula (10-29) we have:

$$n = \frac{U - I_a(R_a + R_{reg})}{C_e \Phi} \quad (10-33)$$

From this formula it follows, that the speed of a d.c. motor may be regulated:

- A) by varying the power circuit voltage U ;
- B) by varying the voltage drop in the armature circuit $I_a(R_a + R_{reg})$ and
- C) by varying the field flux Φ .

Methods B and C are available in any installation with a constant supply circuit voltage; method A is possible only in special installations that permit control of the power supply voltage.

10-15. Motor Speed Regulation by a Rheostat in the Armature Circuit

1. *Shunt Motor.* The scheme of the motor is depicted in Fig. 10-8. The rheostat R_{reg} in the armature circuit should be so chosen that speed regulation in the specified range may be realised. Assume that during the regulation procedure the circuit voltage and excitation current remain constant, i. e., $U = \text{const}$ and $i_{exc} = \text{const}$. Assume also that the static moment $M_r = M_o + M_z$ does not depend on motor speed, i. e., $M_r = \text{const}$. For steady-state operation conditions prior to regulation we have [formula (10-5)]:

$$I_{a1} = \frac{U - E_a}{R_a} = \frac{U - C_e n \Phi}{R_a}.$$

Now let resistance R_{reg} be introduced into the armature circuit by shifting the movable contact of the regulation rheostat from position 1 into position 2 or 3. Assume that the mechanical inertia of the motor rotating parts and of the power drive are relatively so large that a change in motor speed n during the time element Δt just after the introduction of the rheostat may be neglected. The armature circuit current is then reduced to:

$$I'_a = \frac{U - C_e n \Phi}{R_a + R_{reg}} = I_{a1} \frac{R_a}{R_a + R_{reg}}.$$

Such a decrease in armature current involves a decrease in motor torque $M = C_m I_a \Phi$ proportional to the ratio $\frac{I'_a}{I_{a1}}$, if armature reaction be neglected and it is assumed that for $r_{exc} = \text{const}$ the flux $\Phi \approx \text{const}$. Consequently on the motor shaft appears a *negative* dynamic moment $M_j = M - M_r$ [formula (10-9)], under the action of which the motor slows down. But a decrease in speed promotes a proportional decrease in counter e.m.f. $E_a = C_e n \Phi = C_e n$ and a corresponding increase in current I_a , proportional to the difference $U - C_e n$. This process of decrease in n and counter e. m. f. E_a and a collateral increase in current I_a will continue until the current I_a and also the torque M attain their initial values ($I_{a2} = I_{a1}$ and $M_2 = M_1$ —Fig. 10-19). Since in this case $M_j = 0$ the motor will start the new steady performance when $n_2 < n_1$, and

$$\frac{n_2}{n_1} = \frac{U - I_{a1}(R_a + R_{reg})}{U - I_{a1}R_a}.$$

From the above it follows, that: a) the power delivered to the motor from the supply circuit $P_1 = UI_a$ remains unchanged; b) the

useful motor power $P_2 = M_2 2 \pi n$ decreases proportional to n and corresponding to this the efficiency of the unit $\eta = \frac{P_2}{P_1}$ decreases in the same degree; c) cooling conditions become aggravated since with the copper losses constant, the quantity of cooling air decreases approximately proportional to the speed n ; d) commutation conditions are somewhat better due to a decrease in e. m. f. e_r [formula (5-20)].

If the motor moving parts possess a relatively small inertia, then the entire process takes place as described above, but the

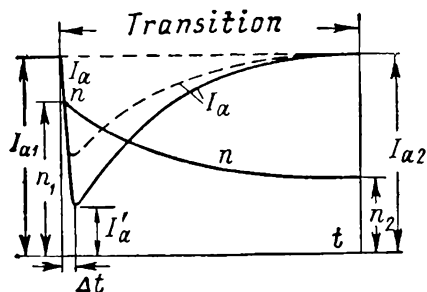


Fig. 10-19. Shunt motor speed regulation by means of rheostat in armature circuit

inrush of current I'_a after introducing the resistance R_{reg} will be less (the broken line in Fig. 10-19), because simultaneously with a decrease in current I_a a certain decrease in speed n takes place.

2. *Series motor.* The process of speed regulation of this type of motor by means of a rheostat in the armature circuit is more complicated because simultaneously with a change of current I_a the excitation current also changes. To investigate the nature of the process, it is sufficient to examine two limiting cases: a) when the magnetic system of the motor is extremely heavily saturated and b) when it is unsaturated. In the first case, the conditions for regulating the speed of a series motor are the same as for the case of the shunt motor considered above, since with a highly saturated series motor it may be assumed that $\Phi \approx \text{const}$. In the second case $\Phi \propto I_a$. If we shall base further discussion on the moving system having a sufficiently large mechanical inertia we may write the e.m.f. equation for an element of time Δt , immediately following the introduction of the rheostat as:

$$U = C_e' I'_a + I'_a (R_a + R_{reg}),$$

and

$$I'_a = \frac{U}{C_e' n + (R_a + R_{reg})}.$$

Before introducing the rheostat we have:

$$I_{a1} = \frac{U}{C_e' n + R_a}.$$

Hence,

$$I'_a = I_{a1} \frac{C_e n + R_a}{C_e n + (R_a + R_{reg})}.$$

Since $C_e n$ exceeds R_a ten times and more, in the non-saturated series motor a current inrush is much less than in the saturated motor. The process of regulation takes place as in the shunt motor, i. e., for $M_r = \text{const}$,

$$I_{a2} = I_{a1} \quad \text{and} \quad \frac{n_2}{n_1} = \frac{U - I_{a1}(R_a + R_{reg})}{U - I_{a1}R_a}.$$

The appraisal of this method of regulation is the same as that discussed above.

If the resistance torque, created by the drive on the motor shaft, depends on the speed n (for example, in the case of a fan $M_r \propto n^2$), the process of speed regulation takes place as in the case of a constant torque, but in this case the current I_{a2} , becoming steady after the introduction of resistance R_{reg} , does not attain its former value I_{a1} , corresponding to a smaller torque on the motor shaft; the speed also decreases at a smaller rate than with $M_r = \text{const}$, in accordance with the smaller voltage drop $I_a(R_a + R_{reg})$.

10-16. Motor Speed Regulation by Variable Excitation

A. Shunt motor. As before we assume that $U = \text{const}$ and $M_r = \text{const}$. The resistance in the armature circuit $R_{reg} = 0$.

Let us further assume that when the rheostat r_{reg} (Fig. 10-8) is introduced, we have decreased the excitation current from the value i_{exc1} to value i_{exc2} , and the flux Φ from value Φ_1 to value Φ_2 . Assume as before that at the instant following the introduction of the rheostat the change in speed n may be neglected. If I_{a1} and I'_a are armature currents before and after the introduction of the rheostat, then

$$I_{a1} = \frac{U - E_a}{R_a} = \frac{U - C_e n_1 \Phi_1}{R_a} \quad \text{and} \quad I'_a = \frac{U - C_e n_1 \Phi_2}{R_a},$$

hence

$$\frac{I'_a}{I_{a1}} = \frac{U - C_e n_1 \Phi_2}{U - C_e n_1 \Phi_1}.$$

It follows from this formula that if, as usual, $E_a = (0.90 \text{ to } 0.96)U$, a given change in flux Φ will correspond to a many times larger change in armature current I_a . Let, for example, $\Phi_2 = 0.8\Phi_1$,

and $E_a = 0.92 U$; then

$$\frac{I'_a}{I_{a1}} = \frac{1 - 0.8 \times 0.92}{1 - 0.92} = 3.3,$$

i. e., when the flux Φ decreases only 20 per cent the current I_a increases at the beginning more than threefold. With greater relative values of E_a the current I_a inrush during the first period are of even greater magnitude.

Corresponding to the much greater increase in current I_a compared with a decrease in flux Φ the motor torque increases in proportion $\frac{C_m I'_a \Phi_2}{C_m I_{a1} \Phi_1}$; since, according to the stipulation, the static resistance

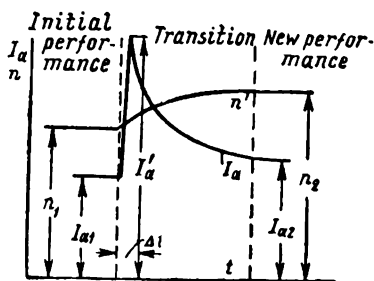


Fig. 10-20. Shunt motor speed regulation by means of rheostat in field circuit

torque $M_r = \text{const}$, then on the motor shaft a positive dynamic moment M_j will appear under the influence of which the speed of the motor begins to grow. In proportion to this increase in speed the counter e.m.f. of the motor E_a increases and the current I_a decreases. This process of speed increase and simultaneous decrease in current I_a continues until the torque M becomes equal to the resistance torque M_r ; for these conditions $M_j = 0$ and the motor begins to operate in new

steady-state conditions, determined by the new value of current I_{a2} and new value of speed n_2 . According to formulas (10-10) and (10-5), we have:

$$I_{a2} = \frac{M}{C_m \Phi_2} \quad \text{and} \quad n = \frac{U - I_{a2} R_a}{C_e \Phi_2}.$$

The change in current I_a and speed n when $U = \text{const}$ and $M_r = \text{const}$ is shown graphically in Fig. 10-20. As a result, the motor input $P = U (I_a + i_{exc})$ practically increases proportionally to current I_a ; the output $P_2 = M_2 \times 2\pi n$ increases in proportion to speed; with such simultaneous increase in input and output the motor efficiency changes but very little. This method therefore allows a smooth and efficient regulation of shunt motor speed. But, at the same time: a) commutation conditions become noticeably worse

due to both greater motor speed and increase in current I_a and, consequently, also an increase in loading A ; b) armature cooling conditions are somewhat impaired since the losses in the armature winding copper increase faster than the amount of ventilating air; c) the degree of motor operation stability is decreased; since the main field is weakened, and the armature reaction is increased. Therefore a shunt motor, designed to operate in varying speed conditions, for example, 1:2 or 1:3 speed changes must be specially calculated to provide the mechanical, commutational and thermal conditions required.

Transients, i. e., periodic fluctuations of speed in respect to some mean value may occur with a heavily weakened magnetic field, especially if the brushes in machines with commutating poles are somewhat shifted against motor rotation, i. e., where conditions of demagnetising may arise. In this case of special importance is the effect of the demagnetising armature reaction. Assume that $M_r = \text{const}$. If, for instance, the current I_a abruptly increases, the demagnetising effect of the armature reaction may lead to such a weakening of the magnetic flux of the motor, that notwithstanding the increase in current I_a , the motor torque $M = C_m I_a \Phi$ will be less than the static torque M_r ($M < M_r$).

A negative dynamic torque will appear on the motor shaft and the motor will slow down. In this case the current I_a decreases and simultaneously the effect of the armature reaction will diminish, i. e., the flux begins to grow. If in this case the product $I_a \Phi$ will grow, then for some value of these factors the torque M will become equal to torque M_r and then exceed it. At the motor shaft a positive dynamic torque will appear and the speed of the motor will begin to increase; the load current I_a will begin to grow and the process of speed fluctuation may reoccur.

The mathematical analysis of this phenomenon shows that in relation to the motor parameters the following kinds of speed variation may prevail: a) aperiodic attenuated, b) periodic attenuated, c) periodic steady-state with an oscillation frequency $f = 10$ to 50 cycles per minute and d) periodic or aperiodic increasing.

To eliminate speed fluctuations, the magnetic system of the motors, in which these fluctuations may be expected (for example, motors with wide speed range obtained by means of weakening of main field) should be adequately calculated.

B. Series motor. There are two main methods of speed regulation of the series motor by means of varying the field flux Φ : a) shunting or tapping of field winding and b) shunting of armature winding (Fig. 10-21).

a) *Regulation of speed by shunting the field winding.* Assume $U = \text{const}$, $M_r = \text{const}$ and that the current I_a is given for non-shunted motor operation, i. e., for open knife-switch (or automatic switch)

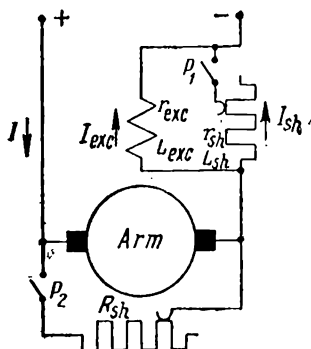


Fig. 10-21. Circuit diagram for speed regulation of series motor

P_1 working position. When the switch P_1 is closed the motor operation conditions change abruptly but since the field winding possesses considerable electromagnetic inertia, the flux linkage of this winding and also the magnetic flux Φ_1 , created by it, and the excitation current tend to remain without change. Therefore, at the instant immediately after shunting, the current in the armature winding increases by the current value in the shunt I_{sh1} and the armature current

is then $I'_a = I_{exc1} + I_{sh1} = I_{a1} + I_{sh1}$. Therefore $M' = C_m \Phi_1 (I_{a1} + I_{sh1}) = C_m \Phi_1 I'_{a1} > M_r$ and on the shaft of the

motor there appears a positive dynamic moment $M_j = M - M_r$, which causes the motor to develop greater speed.

If we disregard the small voltage drop in the armature circuit, the equation of e. m. f. may be written as $U = C_e n \Phi$; from this it may be seen, that with an increase of n the flux Φ decreases and, hence, the current I_{exc} also decreases; this will bring about a decrease of current in the shunt I_{sh} (the law of branching circuits) and the current in the armature $I_a = I_{exc} + I_{sh}$ (Fig. 10-22). This process of change in speed parallel with change in currents I_{exc} and I_a continues until the current in the armature and the excitation

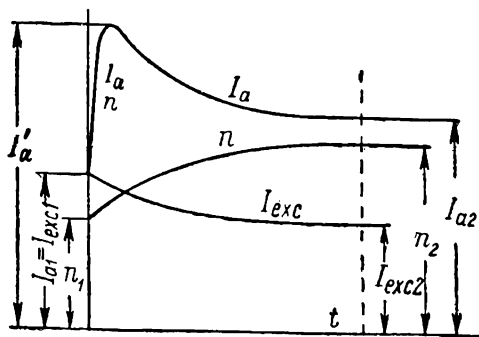


Fig. 10-22. Series motor speed regulation by means of field shunting

flux obtain such new values as I_{a2} and Φ_2 , for which $M = C_m I_{a2} \Phi_2 = C_m I_{a1} \Phi_1 = M_r$. In this case $M_j = 0$ and the motor starts to work in a new steady-state condition with a speed $n_2 = n_1 \frac{\Phi_1}{\Phi_2}$ (Fig. 10-22).

Corresponding to current I_{a2} the motor input $P_1 = UI_{a2}$ also increases. The useful power $P_2 = M_2 2\pi n$ also increases, the efficiency remaining almost without change, but with some relationships between the various losses it may even increase; in other respects the evaluation of this regulation method for the series motor is the same as in the corresponding case of the shunt motor (§ 10-16-1).

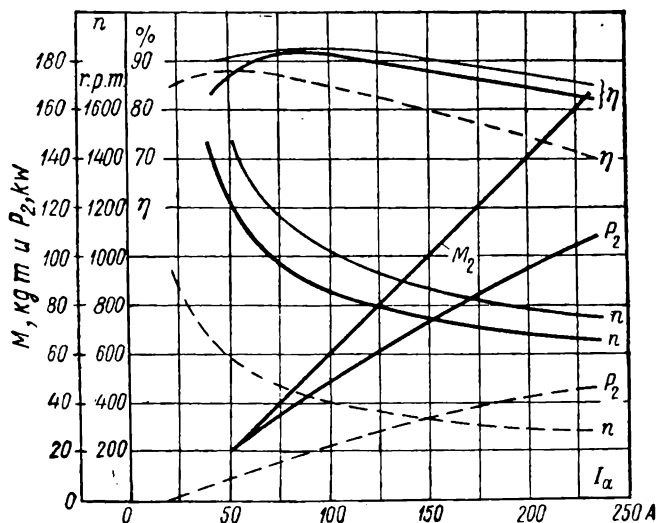


Fig. 10-23. Performance characteristics of ДТН-60-type traction motor for $U=550$ V, $U=275$ V and $k_{reg}=50\%$

This speed regulation method is widely used in electrical traction. The factor $k_{reg} = \frac{I_{exc}}{I_a}$ is termed the *regulation factor*. Usually the shunting resistance is made adjustable so that $k_{reg}=75$ per cent, 61.5 per cent, and 50 per cent are available but in many cases the field is weakened even more. Fig. 10-23 shows the characteristics of the traction (tramway) motor ДТН-60 of the Moscow Dynamo Works with a 60 kW one-hour rating, 500 V, 800 r. p. m.; the thick lines depict the curves for $U=550$ V without shunting of the field, the thin lines depicting curves for $U=550$ V with a 50 per cent regulation factor and the broken line curves are for $\frac{1}{2}U=275$ V without field weakening.

When the traction motor is in service, the current collector sometimes loses contact with the overhead wire. In this case the motor runs for some time without current and is then reconnected

to the circuit. If the field winding is shunted only by an active resistance, the current will pass only through the shunting resistance immediately after the contact with the overhead wire is restored due to the large inductance of the winding. The motor will not develop any counter e. m. f. and the starting current may exceed the permissible limit. To avoid this the shunting resistance is made inductive so that the distribution of current between the field winding and the shunt during the transient process would approximate the distribution of current during steady state conditions.

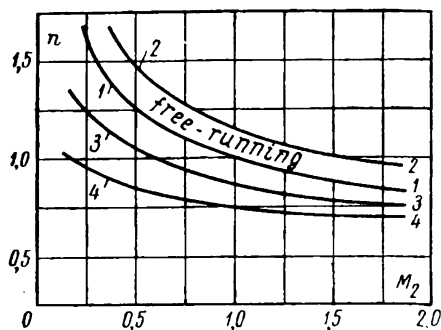


Fig. 10-24. Mechanical characteristics of series motor for different methods of speed regulation

b) *Regulation of speed by shunting the armature winding.* When the armature winding is shunted (Fig. 10-21), the switch P_1 is open and the switch P_2 is closed. The course of reasoning remains the same, but the difference in this case is that some time immediately after shunting the excitation current does not change but the current in the armature decreases

by the amount of current that branches off into the shunting resistance; due to this a negative acceleration torque appears and the motor begins to slow down.

At the end of the process the current in the armature will be less than the initial current, while the field current, and consequently the current from the mains increases. Accordingly the motor input P_1 increases, whereas the useful power $P_2 = M_2 \times 2\pi n$ decreases. It follows, that this method of series motor speed regulation is very wasteful. Therefore, it is used only in those cases when the cost of energy is not an essential factor and where, as for instance in foundries, it is required for a short time to greatly decrease the motor speed. In some installations the speed is regulated by this method in the range of 1 : 5 and even more.

Compared in Fig. 10-24 are the mechanical characteristics of a series motor for various methods of speed regulation plotted in per unit values ($M_n = 1$ and $n_n = 1$): curve 1 is the free-running characteristic, curve 2—the characteristic for a 50 per cent shunted field winding, the curves 3 and 4—the characteristics for the armature winding shunted by two different resistances.

10-17. Motor Speed Regulation by Varying the Voltage Applied to the Circuit

In the cases when the motor is designed for operation in conditions of a wide-range variation in speed, the most efficient method of speed regulation from the point of view of motor utilisation and service reliability, is the method of varying the voltage across the terminals with separate excitation, which allows to obtain the full value of flux Φ at all speeds. In the case when it is possible to provide smooth change of voltage at the motor terminals from zero to maximum, it is possible not only to attain wide-range, efficient and smooth motor speed regulation but also non-rheostatic starting without losses in the starting resistors.

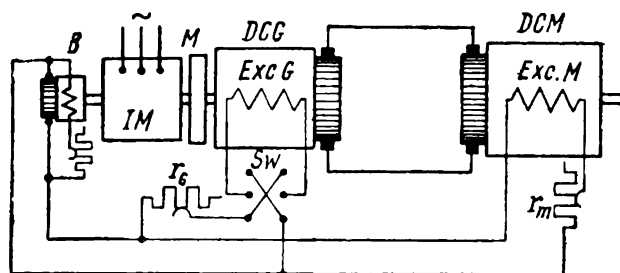


Fig. 10-25. Electrical circuit diagram of a Ward-Leonard (generator-motor) unit system

The most typical of such systems are: A) the Ward-Leonard system, otherwise known as the generator-motor system and B) the Leonard-Ilgner system otherwise known as the generator-motor and flywheel system.

One of the possible Ward-Leonard circuit diagrams is shown in Fig. 10-25. Here *IM* is the three-phase induction motor, coupled to the shaft of the d. c. generator *DCG* and thus forming a system designed for conversion of a. c. into d. c. energy; *DCM* is the drive d. c. motor and *B*—the exciter feeding the d. c. motor and the generator excitation circuits.

In the general case the d. c. generator may feed several d. c. motors if they operate in similar conditions. Constant speed synchronous motors are used instead of an induction motor, especially in case of large or average outputs.

Sometimes a separate excitation unit comprising a small induction motor and an exciter generator is used.

To start the motor, we decrease by means of a rheostat r_g the generator excitation current and consequently the feed voltage of the motor so as to adequately limit the motor starting current and at the same time allow it to start with a certain acceleration.

Hence, no starting rheostat will be necessary, the energy losses during the starting period are reduced and control is simplified since it is carried out with the help of rheostat r_g instead of a cumbersome starting rheostat.

Speed regulation for the Ward-Leonard system is carried out for a given current I_a , for example, $I_a = I_n = \text{const}$. In this case a change in speed from zero to the lowest limit is carried out with constant flux Φ_m of the d. c. motor by means of increasing the generator voltage U_G . In these conditions the motor torque $M = C_m I_a \Phi_m = \text{const}$, and the power $PM = M2\pi n \equiv n$ or, since

$$n \equiv \frac{U_G - I_a R_a}{C_e \Phi M} \approx C U_G,$$

then $PM \equiv U_G$, i. e., the motor rating varies as the voltage U_G across the generator terminals.

A further increase of speed is carried out with constant generator voltage $U_G = \text{const}$ by means of decreasing the motor flux Φ_m . Under these conditions the motor output is $PM = U_G I_a = \text{const}$ and the torque $M = \frac{PM}{n}$.

Thus, the first stage of speed regulation is carried out with constant torque, the second—with constant power. To illustrate these considerations, in Fig. 10-26 are shown curves 1 and 2 of torque M and rating P of a 5,200 kW reversing motor. Up to $n = 50$ r. p. m. the speed is regulated at constant torque and from 50 to 120 r. p. m. at constant power. The curves 3 and 4 give the limiting or, in other words, the *switching-out* values of torque and rating.

Lately, in very large rolling-mill installations (5,000-10,000 kW) with a great number of reversals per unit of time (12-20 per minute) the so-called *quadratic motor-generator system* has been widely employed in which the d. c. generator and motor each have a special exciter, the control of the installation being carried out by varying the current in the exciter field circuit. This considerably simplifies and facilitates control, since the output of the exciter does not exceed 2 to 3 per cent of the main motor

rating. At the present time special d. c. machines, the so-called amplidynes, are becoming widely used as exciters for the Ward-Leonard systems. These amplidynes allow to automate the work of the installation and thus increase its efficiency.

The Ward-Leonard system allows rapid starting and reversing of the drive motor without losses in the rheostats of the main circuit. To carry out reversing it is sufficient to reverse the excitation current of the d. c. generator with the help of switch S_w (Fig. 10-25).

Braking of the motor is also carried out by regulating the generator voltage. In this case, if we rapidly decrease the excitation of the generator, and make its e. m. f. less than the e. m. f. of the motor, the latter begins to work as a generator and returns the braking energy to the power circuit through the generator, which in this case works as a motor that forces the a.c. drive motor to work as a generator.

If during generator-motor system (GM) operation, abrupt peaks of current appear then a flywheel is mounted onto the drive motor shaft which stores energy during the period of increasing motor speed and returns it with a decrease of speed (in Fig. 10-25 the flywheel is shown by broken lines). For the generator-motor-flywheel (GMF) system, only the induction-type motor is used as the drive motor since a synchronous motor runs at constant speed and therefore does not allow to utilise the energy of the flywheel.

The GMF system allows to equalise the load and greatly decrease the current peaks in the a. c. supply circuit. Thanks to the flywheel an induction motor may be chosen of less rating than the d. c. motor. Thus, for driving a conventional bloom mill a reversible d. c. motor of 5,300 kW is installed, whereas the a. c. motor rating is only 3,700 kW.

The GM and GMF systems are widely used in industry as rolling-mill drives, for paper-making machinery, crane motors, helm control, etc.

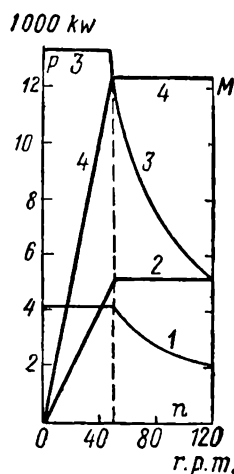


Fig. 10-26. Characteristics of a reversing rolling mill motor fed from a Ward-Leonard system

Chapter Eleven

FUNDAMENTAL AND SPECIAL TYPES OF D.C. MACHINES AND THEIR FUTURE DEVELOPMENT

11-1. Preliminary

Central power stations generate electric energy in the form of three-phase current of commercial frequency. Some branches of industry (for example, aluminium smelting, some chemical processes, etc.) however work only with direct current; in many other cases (rolling mills, etc.) direct current has a number of advantages compared with alternating current. According to a great diversity of requirements of various consumers, d. c. machines are made in an extremely wide power range, from several watts to thousands of kilowatts, and voltages ranging from a few volts to thousands of volts, and speeds with the most diverse service characteristics. It is impossible to cover in this book the entire field of d. c. machines. Therefore here we shall describe only machines of special types which are of interest both from the theoretical and manufacturing point of view.

11-2. Fundamental Types of D.C. Machines

A. Normal types of machines. The ПН type of d. c. machines of small and average capacity manufactured at present in the U.S.S.R. are known for their high efficiency.

Table 11-1 gives the main data of the ПН type d. c. machines. At present a new range of d. c. normal machines is being developed.

B. Traction generators and motors. For converting a. c. into d. c. as a rule, mercury arc rectifiers are employed in modern traction substations. But in some special cases it is preferable to use machine units. Typical in this respect are the units used in the mountain pass substations of the Transcaucasian railway, each consisting of a synchronous motor and two 1,000 kW, 1,500 V, 667 A compound generators in series.

Traction electric motors are used for hauling rolling stock of diverse types of service: urban, suburban and trunk-line electrified railways, water transport, industrial and mine transport,

etc. Accordingly the d. c. traction motors are made for various ratings and voltages, from 1.5 to 5 kW, 80 to 110 V for battery trucks and mining battery locomotives and from 275 to 630 kW, 750 to 1,650 V for the main-line electric locomotives and with diverse regulation and brake characteristics.

Traction-motor working conditions or ratings are distinguished as *continuous* and *one-hour ratings*.

According to the State Standard 2582-50, the continuous rating of a traction machine is the greatest power P_{∞} developed by a motor on the shaft or by the generator at its terminals with which the machine may work continuously in conditions of normally functioning ventilation and with closed commutator inspection hatches while not exceeding the permissible temperature limits for the various parts stipulated by the standard.

Accordingly, the one-hour rating of the traction machine is the power P_h developed by the machine during one hour for the same, as in the case above, ventilation requirements and demands in respect to the ultimate temperature rise.

The continuous and one-hour motor ratings correspond to continuous and one hour values for current and speed— I_{∞} , I_h , n_{∞} and n_h . In modern, adequately ventilated motors, such as traction motors for main-line electric locomotives, the ratios $P_{\infty} : P_h = 0.85$ to 0.90 and $n_{\infty} : n_h = 1.05$ to 1.1 .

Compared with the stationary types of machines the working conditions of the traction electric motors are much more strenuous, since the overall dimensions of the motor are limited by the driving wheels diameter and the railway track gauge; furthermore, motor operation takes place in conditions of frequent starts with high values of rolling stock acceleration accompanied by abrupt changes of voltage across the motor terminals, and also of current and speed; dynamic impact on motor is also possible causing, in particular, vibration of the brushes and brushgear thus disturbing their normal operation and other trouble.

Thus working conditions of the traction motor are very strenuous especially in the commutational, mechanical and thermal respects.

To improve the traction motor, many new developments have been introduced of late, such as increase of commutating pole m. m. f. in relation to the m. m. f. of the armature reaction up to 140-160 per cent (instead of 115-130 per cent for stationary machines), making the commutating poles of sheet steel, introduction of a non-magnetic gasket between the pole-core and yoke, use of better grades of brushes and brush-holders of special design, improvement of commutator production technology, etc.

Main Data for Some Types of the

Types of machine	Power, kW speed, r.p.m.						
	Motor				Generator		
ПН-5	$\frac{1.0}{2,800}$	$\frac{0.75}{2,000}$	$\frac{0.52}{1,450}$	$\frac{0.3}{960}$	$\frac{1.0}{2,930}$	$\frac{0.67}{2,300}$	$\frac{0.37}{1,450}$
ПН-10	$\frac{2.4}{2,800}$	$\frac{1.6}{2,000}$	$\frac{1.0}{1,420}$	$\frac{0.65}{980}$	$\frac{2.2}{2,860}$	$\frac{1.35}{2,000}$	$\frac{0.85}{1,450}$
ПН-17.5	$\frac{3.7}{2,850}$	$\frac{2.7}{2,100}$	$\frac{1.75}{1,450}$	$\frac{1.0}{1,000}$	$\frac{3.1}{2,860}$	$\frac{2.1}{2,100}$	$\frac{1.3}{1,460}$
ПН-45	$\frac{7.0}{2,500}$	$\frac{5.6}{2,200}$	$\frac{4.4}{1,500}$	$\frac{2.5}{1,000}$	—	$\frac{5.4}{2,100}$	$\frac{3.3}{1,460}$
ПН-85	—	—	$\frac{9.0}{1,500}$	$\frac{5.6}{1,000}$	—	$\frac{11.3}{1,900}$	$\frac{6.8}{1,460}$
ПН-100	—	$\frac{15.0}{1,560}$	$\frac{10}{1,090}$	$\frac{5.8}{780}$	$\frac{18.0}{2,000}$	$\frac{13.3}{1,460}$	$\frac{7.8}{980}$
ПН-145	—	$\frac{21.0}{1,500}$	$\frac{13.5}{1,050}$	$\frac{8.5}{780}$	$\frac{25}{2,000}$	$\frac{16.2}{1,460}$	$\frac{11.0}{980}$
ПН-290	—	$\frac{46.5}{1,500}$	$\frac{29}{1,000}$	$\frac{18}{750}$	—	$\frac{23}{970}$	$\frac{16}{750}$
ПН-400	—	—	$\frac{42}{950}$	$\frac{29}{740}$	—	$\frac{70}{1,470}$	$\frac{37}{970}$
ПН-550	—	—	$\frac{60}{980}$	$\frac{30}{600}$	—	$\frac{88}{1,470}$	$\frac{48}{970}$
ПН-1000	$\frac{130}{1,170}$	$\frac{105}{960}$	$\frac{70}{750}$	$\frac{55}{630}$	—	—	$\frac{80}{970}$
ПН-1320	$\frac{170}{1,250}$	$\frac{130}{980}$	$\frac{88}{720}$	$\frac{68}{560}$	—	—	$\frac{100}{975}$
ПН-1750	$\frac{200}{1,150}$	$\frac{165}{970}$	$\frac{115}{750}$	$\frac{80}{550}$	—	—	$\frac{130}{970}$

Notes: 1. All dimensions are in mm.

Table 11-1

ПН D. C. Motor Range

2_p	D_a	l_a	Z	h_t	b_t	K	D_c	l_c	$\delta/\delta_{compote}$	Weight, kg
2	98	90	14	18.5	11.8	56	64	46	$\frac{0.6}{1.0}$	39
2	118	110	18	23.2	10.95	$\frac{54}{72}$	80	45	$\frac{0.8}{1.0}$	60
2	130	118	20	24.2	10.5	$\frac{60}{80}$	80	45	$\frac{0.8}{1.5}$	72
4	160	100	29	26.2	8.5	87	125	50	$\frac{1.0}{2.5}$	98
4	185	160	31	28.2	9.7	93	125	$\frac{62}{50}$	$\frac{1.0}{3.0}$	160
4	245	$\frac{80}{120}$	—	—	—	—	—	—	—	251
—	—	—	35	36.2	8.5	139	170	85	$\frac{1.5}{3.0}$	290
4	295	140	33	36.2	10.8	$\frac{99}{131}$	200	115	$\frac{2.0}{4.0}$	495
4	340	$\frac{140}{185}$	42	42	$\frac{6.9}{9.0}$	$\frac{125}{167}$ 209	250	$\frac{115}{150}$	$\frac{3.0}{5.0}$	$\frac{800}{920}$
4	410	200	$\frac{50}{46}$ 42	41	$\frac{10.6}{11.6}$ 11.6	$\frac{150}{184}$ 125	300	$\frac{273}{236}$ 158	$\frac{4.5/7.35}{4.5/7.7}$ 4.6	1,410
4	475	165	$\frac{70}{63}$ 53	46	$\frac{8.5}{9.4}$ 11.2	$\frac{140}{125}$ 159	350	$\frac{310}{190}$ 190	$\frac{4.5/8.5}{4.5/10.0}$ $\frac{4.5/9.85}{4.5/9.85}$	1,690
4	475	220	$\frac{58}{70}$ 62	46	$\frac{10.3}{8.5}$ 9.7	$\frac{116}{140}$ 248	—	$\frac{310}{310}$ 190	$\frac{4.5/10}{4.5/10.5}$ $\frac{5.0/9.5}{5.0/9.5}$	2,000

2. All values refer to 230 V for generators and to 220 V for motors.

The conventional type of traction motor is the series motor. Its working characteristics are shown in Fig. 10-23. But from the thirties of the current century, compound motors with prevailing series excitation have found wide use. Such motors facilitate the introduction of regenerative braking of trains, but are somewhat heavier and cost more than the series type.

K. I. Shenfer invented in 1929-31 a very interesting voltage booster machine for non-rheostatic control of electric trains. A short description of this machine is given below in § 11-3.

C. Low voltage machines. These machines include the following types: a) generators for electrolysis installations with outputs 160-550 kW, 75-80 V, 2,140 to 6,500 A; b) welding generators for electric-arc welding with 25 to 50 V and various values of welding current. A description of one of these generators, made in the U.S.S.R. at the Elektrik Works is given in § 11-3; c) generators for galvanoplastics and galvanising with outputs of 3 to 30 kW, 6 to 12 V, 250 to 5,000 A, made with a double commutator, which may be connected in parallel (for 6 V) or in series (for 12 V); d) fractional horsepower machines for 30 to 500 W, and for 24 to 30 V, used in automobiles, tractors, aeroplanes, etc.¹

The fractional h. p. motors include universal motors (the YM series) rated from 5 to 55W, used for industrial purposes and in domestic appliances (vacuum-cleaners, mincing machines, etc.). The motors can work both from 110 V d. c. and from 127V a. c. They are fitted with two poles and have a conventional d. c. machine armature winding connected to a commutator. The motor magnet system is assembled of electrical sheet steel punchings. The stator consists of two field windings connected in series with the armature: one is used for d. c., the other for a. c. feed. Thus the universal motor is a machine with series excitation, and therefore the speed falls abruptly with increase of load.

D. High-voltage d. c. machines. These machines are mainly used for radio installations as generators. At the present time such machines are being built for outputs of 3 to 150 kW and voltages from 7.5 to 30 kV. The largest generator of this kind has been made for 150 kW, 15 kV, 850 r. p. m. The high-voltage generators have in most cases a conventional pole system construction, one or two commutators (on both sides of the armature) and correspondingly one or

¹ To illustrate one such machine the following data of a shunt motor are given: 250 W, 27 V $\pm 10\%$, 15 A, 5,000 r. p. m.; outside diameter $D_{out} = 97$ mm, $D_a = 55.4$ mm; full length of motor $l_m = 161$ mm, $l_a = 30$ mm, $2p = 4$; no composes, $\delta = 0.25$ mm, wave armature winding; $Z = 19$, $S = 57$, $w_c = 3$, $B\delta = 0.48$ wb.m², $A = 123$ A/cm, $i_{exc} = 0.6$ A; $D_c = 36$ mm, $l_c = 17$ mm, $K = 57$; $\eta = 67.5\%$, $G = 3$ kg.

two armature windings, a large number of skewed slots per pole pitch (to limit voltage pulsations at the brushes as much as possible), thicker insulation between the commutator bars (up to 1.5 to 2.5 mm because the potential difference between two adjacent commutator bars in such machines may reach 250 V and higher values), special devices for flashover protection, etc. High-voltage generators of larger output are of special design, i. e., with distributed field winding, magnetic wedges in the slots, etc. All high-voltage generators have external excitation.

E. Motors and generators of maximum power. The highest possible power d. c. machines with average voltages are those made for rolling mills motors. Somewhat less is the output of the genera-

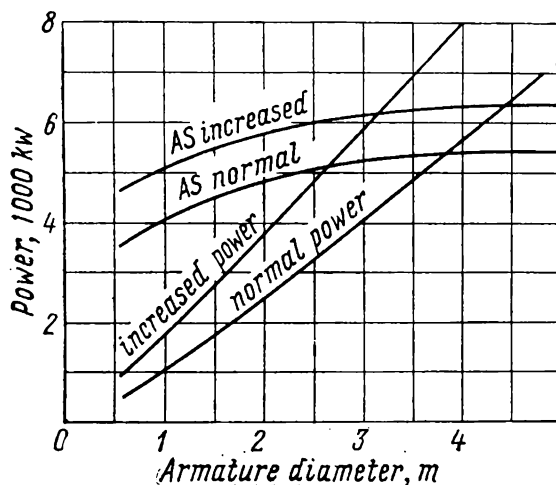


Fig. 11-1. P_{lim} and $A_{lim} = f(D_a)$ for d.c. compensated machines

tors for the rolling mills, the voltages being the same. Typical in this respect is the rolling-mill installation, manufactured by the Elektrosila Works which consists of a 5,150 kW, 750 V, 50/120 r. p. m. rolling-mill motor and two generators each of 3,000 kW, 750 V, 375 r. p. m. comprising the converting installation of the motor. The maximum power both of the normal and larger output types for the d. c. compensated machines and their permissible loadings are given in Fig. 11-1 in relation to the armature diameter D_a . Here it must be noted that modern electrical drive schemes include many industrial electronic devices and also communication and high-frequency techniques have also found

wide use. This means that the study and design of the high-power machines cannot be separated from its working scheme.

Generators used for the electrochemical industry are made with outputs of the same order but for smaller voltages and for very heavy currents. Thus at one aluminium plant 4,550 kW, 350 V, 13,000 A, 300 r.p.m. generators were installed while another uses ten motor-generators of 10,000 kW each. Incidentally, such generators nowadays are successfully substituted by mercury arc rectifiers.

11-3. Special Types of D.C. Machines

A. The homopolar machine. The idea of the homopolar or non-commutator d. c. machine is illustrated in Fig. 11-2. Imagine a disk, rotating in the magnetic field of the magnet $N-S$, consisting of a series of sectors, one sector being shown in the

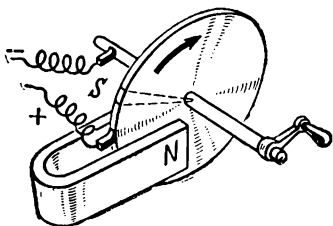


Fig. 11-2. Homopolar machine operation principle

figure by broken lines. Each sector may be considered as a conductor, the apex of which lies on the disk axis and the base on the periphery of the latter. By using the right-hand (right-palm) rule we may find that in this conductor an e. m. f. is induced which all times has one direction—in our case from the disk axis to its periphery. The same may be repeated in respect to any other of the conductors. If the

brushes are closed onto an external circuit a potential difference appears and a constant current will flow between the brushes set on the shaft and the disk periphery. [Bibl. 57, 58]

This fundamental idea attained some development during the first decade of the current century in connection with the attempts to avoid commutation difficulties which were becoming more and more acute as the customer requirements pertaining to d. c. machines became more rigid. But practice has, nevertheless, shown that a homopolar machine has no outstanding advantages over the d.c. commutator machine. Therefore, at present it is used mainly where large currents of low voltage are required as, for example, in the chemical industry. At the beginning of the 30s one homopolar machine was built for 150,000 A, 7.5 V, 514 r. p. m.

In the U.S.S.R. a homopolar machine was developed in 1939 by engineer B. V. Kostin, which tested as a generator showed an output of 7.5 kW at 3 V, 2,500 A, 4,000 r. p. m. and worked successfully.

B. Elektrik Works type welding generator. Welding generators should satisfy the following main requirements: 1) be able to endure the short-circuit conditions which occur when the welder short-circuits the electrodes (as, for example, at the instant of striking the arc); 2) provide a more or less constant value of current for an alternating arc resistance (alternating arc length). The stipulated conditions are met with by the external characteristic of the welding generator having a sharply drooping nature. To obtain this specific characteristic various types of welding generators are used. In the U.S.S.R. the Elektrik Works have started mass production of welding generators with the so-called third brush.

The circuit diagram of a modernised welding generator of the ПС-300 M type is shown in Fig. 11-3. The rated values of the generator are: $U_n = 35$ V, $n = 1,450$ r. p. m., $I = 260$ A for a 100 per cent duty cycle and $I = 340$ A for a 65 per cent duty cycle (a 100 per cent duty

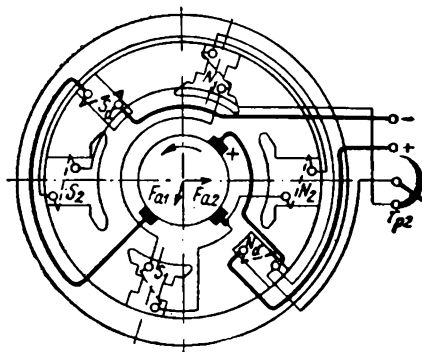


Fig. 11-3. Welding generator put out by Elektrik Works

cycle is the full working period, including intervals). The generator armature is made the usual way. The magnet system consists of four main poles and two commutating poles. The poles N_1-S_1 , somewhat displaced in respect to the vertical and furnished with grooves to increase their magnetic saturation, are called the *main* poles, the poles N_2-S_2 arranged horizontally are called the *cross* poles. The field windings of the main and cross poles are each connected in parallel between the positive brush and the additional brush D in such a way that two adjacent main poles—one main and one cross pole—are of the same polarity.

Therefore, the machine is actually a two-pole machine in which each pole is split into two parts. The excitation current is regulated only in the cross poles excitation circuit by means of the rheostat r_{reg} . With load a m. m. f. of armature reaction will be created which may be resolved along the axes of the main and cross poles into the following components: F_{a1} , magnetising the main poles and F_{a2} , demagnetising the cross poles. The magnetising effect of the F_{a1} m. m. f. tells very little on the main poles, since due to the grooves, they are heavily saturated.

For this reason the voltage impressed on the field winding and due chiefly to the main poles, varies but little with load change. On the contrary, with an increase of load current I the m. m. f. F_{a2} will considerably demagnetise the cross poles thus obtaining the drooping external characteristic required for welding (Fig. 11-4). The welding current is controlled within limits of 80 to 400 A.

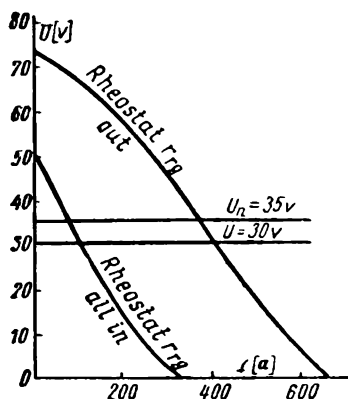


Fig. 11-4. External characteristics of the welding generator put out by the Elektrik Works

C. Exciters for synchronous turbogenerators. Synchronous machines and in particular synchronous turbogenerators are excited by direct current. The feed source is a d. c. generator exciter, which possesses several special characteristics. The armature of the exciter is usually arranged on the protruding end of the rotating part (i. e., rotor) of the turbogenerator, but for units of very large output the exciter is designed as a separate machine, joined by a coupling with the turbogenerator rotor. In both cases the exciter is a high-frequency machine, since in

the U.S.S.R. turbogenerators rotate at a speed of 3,000 r. p. m. Such a machine is sensitive to vibrations, works in difficult commutation conditions and requires intensive ventilation. An exciter of improved design with rated values 300 kW, 400 V, 750 A, 3,000 r. p. m. was developed at the Elektrosila Works for a 100,000 kW turbogenerator with hydrogen cooling. The exciter is a four-pole totally enclosed motor, with commutating poles and a compensation winding. The exciter armature uses a simple lap winding with equaliser connections. The end connections are fastened with the help of heavy bronze bandings. The commutator is of considerable length and fixed with the help of a ring.

The exciter is separately excited from a special sub-exciter with an output of 1,5/6 kW, 115 V, 13/52 A, the top figures corresponding to the continuous rating and the lower to the transient conditions of operation.

The cooling of the exciter unit including the sub-exciter is carried out by means of closed cycle ventilation; for this purpose two chambers with air-coolers are provided inside the base plate.

To eliminate the necessity of a drive the exciter is made as a separate machine with pedestal friction bearings and connected

to the turbogenerator rotor with the help of a flexible coupling.

The longitudinal and transverse cross-sections of the exciter is shown in Fig. 11-5, *a, b*. The main calculation data of the exciter is $D_a=440$ mm, $l_a=310$ mm, $D_c=300$ mm, $l_c=380$ mm; the base-plate dimensions are $2,550 \times 1,200$ mm, the full height of the exciter, including the height of the plate, is 1,480 mm.

D. The amplidyne. The amplidyne is a machine in which the cross-field principle is employed. At the present time the amplidyne is widely used in many diverse systems of electrified drives with continuous control. This amplidyne acts as an automatic continuous-action regulator of one or, in the general case, several values, governing the work of the electric drive—voltage, current, speed of rotation, etc. [Bibl. 63—67]

The circuit diagram of the amplidyne is shown in Fig. 11-6. On a commutator of a conventional d. c. machine armature two pairs of brushes are arranged—one pair on the longitudinal axis A_1-A_2 , and the other pair of brushes on the transverse axis A_3-A_4 , both of which are short-circuited. The stator is fitted with: a) two or, in the general case, several control windings C , one of which serves to create an excitation flux Φ_1 , the other one (or several) joined to the circuit from which it is desired to obtain the signal affecting the work of the amplifier machine; b) a compensation winding CW , which is to compensate as completely as possible the m. m. f. of the armature created by current I_1 along the direct axis; c) the winding of the commutating poles along the longitudinal axis (commutating poles are, as a rule, not used along the cross-axis); d) a series winding SW , is often inserted into the short-circuited loop, acting along the cross-axis.

From the design standpoint the stator of the amplidyne is made with a distributed winding, as shown in Fig. 11-7.

The work principle of the amplidyne consists in the following. Let us feed a small power $P_1=U_1 I_1$ into the winding C_1 , which creates a flux Φ_1 . When the armature rotates in this flux, a small e. m. f. E_2 arises in the short-circuited brush loop A_3-A_4 , which nevertheless creates a considerable current I_2 , since the resistance of this loop is very small. This current I_2 may in certain conditions create a relatively large flux Φ_2 in accordance with which a considerable e. m. f. E_3 is created and a large current I_3 may flow in the brush A_1-A_2 circuit. Since the m. m. f. created by this current is compensated by the m. m. f. of winding CW the resultant field flux remains equal to flux Φ_1 and, therefore, does not depend on current I_3 , and consequently does not depend on the generator output.

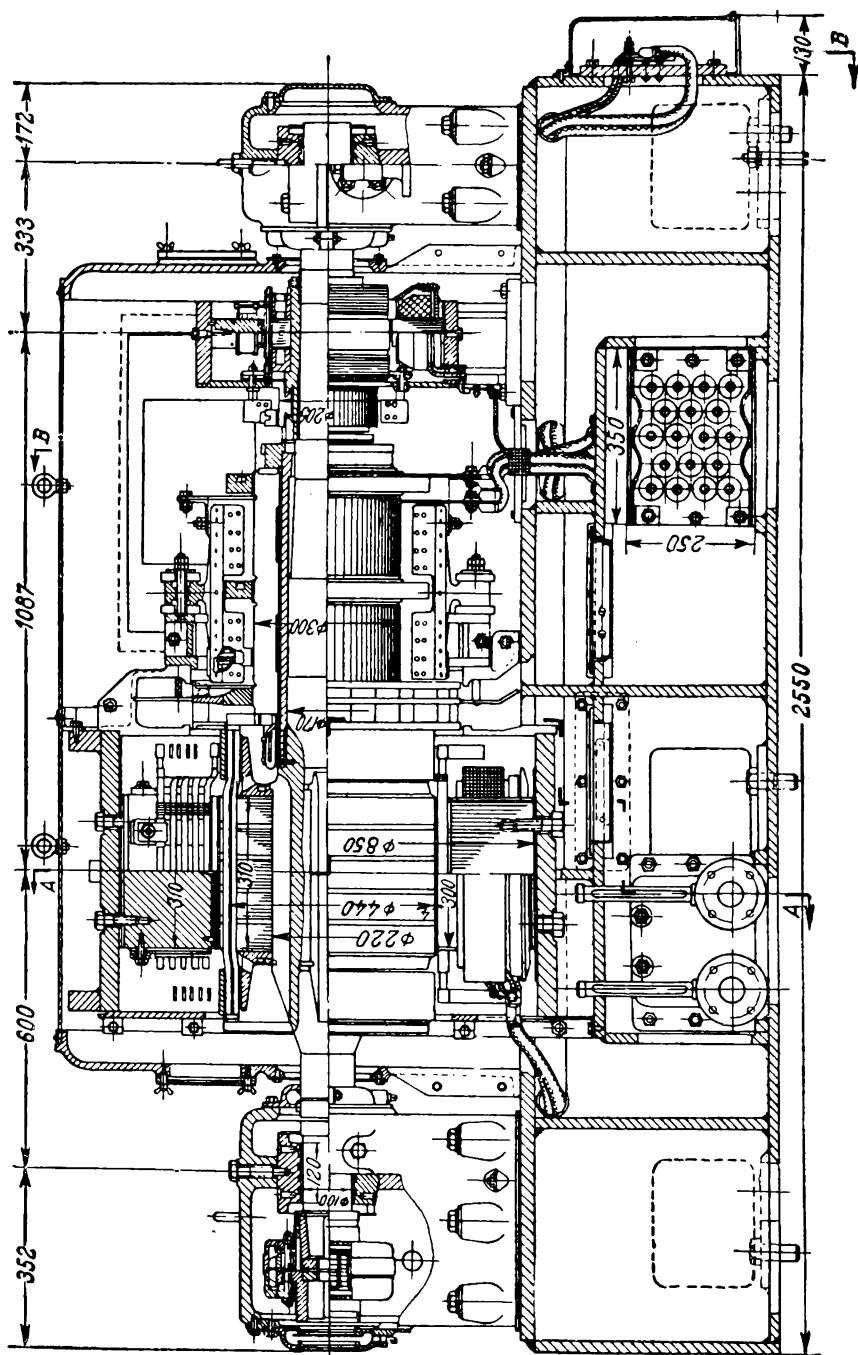


Fig. 11-5a. Axial cross-section of a turbogenerator exciter

To provide maximum efficiency of amplidyne operation the following properties are essential: a) a high amplification factor k_{ampl} , b) small time-constants and c) a sufficient stability of operation.

a) *Amplification factor.* From the previous discussion it follows, that the power is amplified in two stages: during the first stage the power $P_1 = U_1 I_1$ is amplified to the power $P_2 = E_2 I_2$ and during the second—power $P_2 = E_2 I_2$ is amplified to power $P_3 = U_3 I_3$. The ratio

$$k_{ampl} = \frac{P_3}{P_1} = \frac{P_2 P_3}{P_1 P_2} = k_{ampl1} k_{ampl2}, \quad (11-1)$$

is called the *power amplification factor* of the amplidyne.

Let Λ_1 and Λ_2 be the permeances along the direct and cross axes. Then the field flux along the direct axis $\Phi_1 \equiv I_1 \Lambda_1$; the e.m.f. $E_2 \equiv n \Phi_1 \equiv n I_1 \Lambda_1$; the current $I_2 = \frac{E_2}{R_{a2}}$; when $R_{a2} = \text{const}$, $I_2 \equiv E_2 \equiv n I_1 \Lambda_1$; the flux $\Phi_2 \equiv I_2 \Lambda_2 \equiv n I_1 \Lambda_1 \Lambda_2$ and, therefore, $E_3 \equiv n \Phi_2 \equiv n^2 I_1 \Lambda_1 \Lambda_2$. If R is the resistance of the external

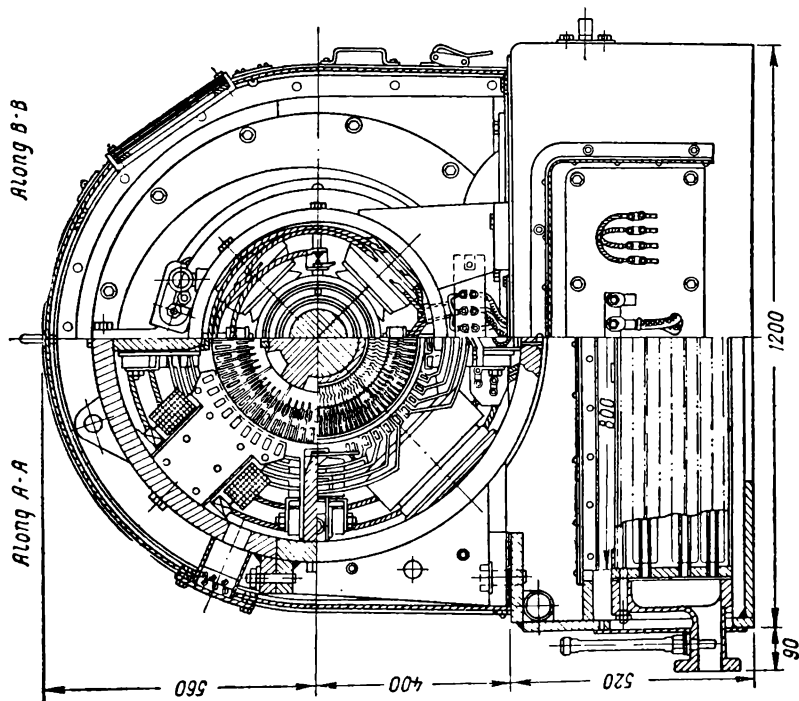


Fig. 11-5b. Cross-section of a turbogenerator exciter

circuit, which is energised by the amplidyne then

$$I_s = \frac{E_s}{R_{as} + R} = \frac{n^2 I_1 \Lambda_1 \Lambda_2}{R_{as} + R};$$

and the power delivered by the amplidyne to the external circuit is:

$$P_s = I_s^2 R = \frac{R}{(R_{as} + R)^2} (n^2 I_1 \Lambda_1 \Lambda_2)^2.$$

Since $U_1 = I_1 R_1$, where R_1 is the resistance of the field winding, according to formula (11-1), we will have:

$$k_{ampl} = \frac{R}{(R_{as} + R)^2 R_1} (n^2 \Lambda_1 \Lambda_2)^2. \quad (11-2)$$

This deduction is made without taking into account the commutation armature reaction. In amplidynes without commutating poles along the cross-axis, the m. m. f. of the commutation armature reaction F_{com} may several times exceed the m. m. f. of excitation F_1 and

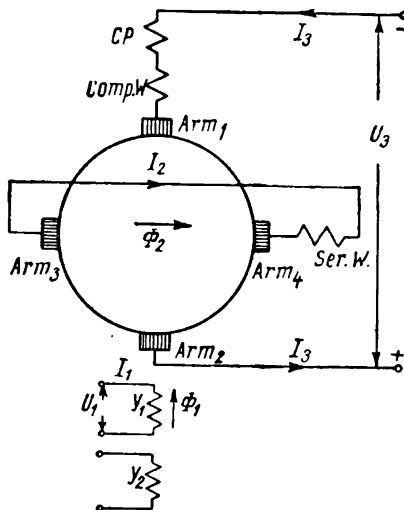


Fig. 11-6. Amplidyne circuit diagram

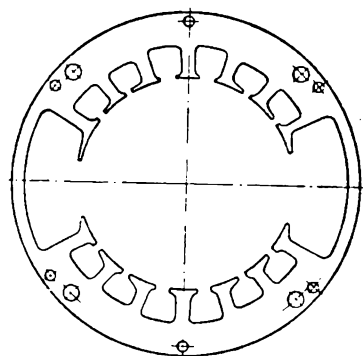


Fig. 11-7. Amplidyne stator steel sheet punching

thus greatly influence the work of the amplifier. This feature distinguishes the amplidyne from the conventional d. c. machines in which the m. m. f. F_{com} more often plays a less important role. In Fig. 11-8 the broken lines 1 and 3 show the curves $I_s = f(n)$ and $E_s = f(n)$ in which the commutation armature reaction is not taken into account while the continuous lines 2 and 4 are the curves in which the armature reaction is taken into account. Thus, the amplification factor depends less on the speed of rota-

tion than it follows from the formula (11-2). On the other hand the larger the permeances Λ_1 and Λ_2 , the larger the factor k_{ampl} ; to provide the necessary magnitudes of these values much smaller flux densities are allowed in the amplidyne than in conventional d. c. machines, and as small as possible air-gaps are made at both the axes of the machine. Evidently the factor k_{ampl} depends also on the external circuit resistance R . Both for an open external circuit, i. e., for $R = \infty$, and for a short-circuited amplidyne, i. e., for $R = 0$, the amplification factor $k_{ampl} = 0$.

Usually the amplification factor $k_{ampl} \leq 10,000$, the factor k_{ampl1} always being much smaller than k_{ampl2} ; thus, for example, with $k_{ampl} = 8,000$, $k_{ampl1} \approx 40$ and $k_{ampl2} \approx 200$. In certain special cases the factor k_{ampl} attains the order of 100,000.

b) *Amplidyne time-constants.* For no-load performance of the amplidyne we have two time constants, viz., for the excitation circuit, $T_1 = \frac{L_1}{R_1}$ and for the cross-field circuit $T_2 = \frac{L_2}{R_2}$; here L_1 and L_2 are the inductances of the corresponding circuits. If the amplidyne works under load, it is necessary also to take into account the time-constant of the operation circuit $T_3 = \frac{L_3}{R_3}$. In many schemes using the amplidyne, the response of the latter, i. e., the speed of its reaction to a given signal, is of major importance. To ensure this the inductances L_1 and L_2 for given values of R_1 and R_2 should be as small as possible. As it is known, the inductance $L = \omega \Phi_{(i=1a)}$, but $\Phi_{(i=1a)} = \omega \Lambda$, where Λ is the permeance along the flux path $\Phi_{(i=1a)}$. Hence,

$$L_1 = \omega_1^2 \Lambda_1 \quad \text{and} \quad L_2 = \omega_2^2 \Lambda_2.$$

Therefore, smaller values of L_1 and L_2 are obtained for smaller values of Λ_1 and Λ_2 . Comparing this deduction with what was previously said about the amplification factor, it may be seen that,

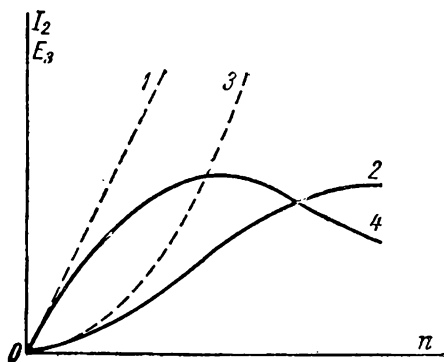


Fig. 11-8. Curves $I_2 = f(n)$ and $E_3 = f(n)$: broken lines — without taking into consideration commutation armature reaction; continuous lines — with the latter taken into account

by increasing k_{ampl} at the expense of increase of Λ_1 and Λ_2 , we simultaneously increase the amplidyne time-constants, i. e., decrease its response; and vice versa, a larger response of the amplidyne corresponds to less amplification capability. It is possible to show that the maximum amplidyne response is obtained when $T_1 = T_2$. Usually $T_1 = 0.05$ to 0.2 sec.

c) *Amplidyne operation stability.* The analysis shows, that transient conditions of the amplidyne are always of an oscillatory nature. In the case when compensation is incomplete the oscillatory process is damped while in the case of overcompensation a steady oscillatory process is created which may disturb normal amplidyne operation.

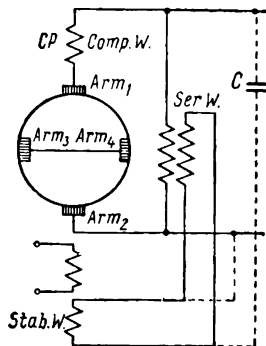


Fig. 11-9. Amplidyne stabilising connections

To avoid self-excitation, the amplidyne is furnished with a special, so-called stabilising winding, arranged along the longitudinal axis and connected to the terminals of the amplidyne via a capacitor or stabilising transformer (Fig. 11-9). If across the working terminals A_1 - A_2 the voltage $U_s = \text{const}$, the current cannot pass through the stabilising winding but with a change in U_s , the capacitor C or the corresponding secondary winding Sec. W starts to feed the stabilising winding Stab. W. In this case the m. m. f. of the stabilising winding tends to increase the voltage U_s when the m. m. f. decreases and to decrease U_s when the m. m. f. increases. This relationship between the voltage U_s and the action of the stabilising winding is called feed-back action. In this case the feed-back is carried out for the first derivative of the voltage U_s .

In the case of undercompensation the stability of amplidyne operation depends on the relationship between the time constants T_1 , T_2 and T_s . An analysis of this shows that the stability of operation becomes the less, the closer these values are to each other and vice versa.

When the amplidyne works on load, currents I_2 and I_3 distributed as shown in Fig. 11-10 flow through the armature winding. Assuming $2a=2$, we may see that in the first and third quadrants the resultant current is equal to $\frac{1}{2}(I_2 - I_3)$, and in the second and fourth quadrants to the sum $\frac{1}{2}(I_2 + I_3)$. Therefore, the current, which

determines the losses in the armature winding, is

$$I_a = \sqrt{\left[\frac{1}{2}(I_2 - I_3)\right]^2 \times 2 + \left[\frac{1}{2}(I_2 + I_3)\right]^2 \times 2} = \sqrt{I_2^2 + I_3^2} \quad (11-3)$$

The nature of the amplidyne external characteristic curve $U_3 = f(I_3)$ for $n = \text{const}$ and $I_1 = \text{const}$ depends to a great extent on

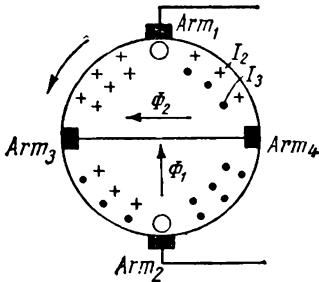


Fig. 11-10. Distribution of currents in amplidyne armature winding

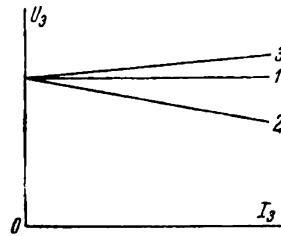


Fig. 11-11. External characteristics for amplidyne: $U_3 = f(I_3)$ with $n = \text{const}$ and $I_1 = \text{const}$

the degree of armature compensation. In Fig. 11-11 the curves 1, 2 and 3 depict the external characteristics of the amplidyne, for the cases of full compensation, undercompensation and overcompensation. Usually the degree of compensation is so established as to obtain the external characteristic corresponding to curves 1 and 2, since operation in conditions of overcompensation is of an unstable nature.

As it was already mentioned above, the amplidyne is used in diverse drive schemes for various purposes. In Fig. 11-12 a scheme is shown which permits to maintain in the generator G armature circuit a constant current. Here 1 is the amplidyne winding, creating the m. m. f. F_1 , 2—the control winding which is connected to the armature circuit of the generator to be controlled and creating the m. m. f. F_2 , opposed to the m. m. f. F_1 . With an increase of generator current I_G , the opposing effect of winding 2 increases and in accordance with this the following values decrease: the direct-axis flux, the voltage across the amplidyne output and the cur-

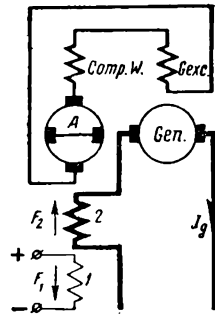


Fig. 11-12. Circuit diagram of a d. c. generator with amplidyne

rent in the generator G field winding; as a result the current I_G is brought almost to its former value. For the given scheme the regulation of current I_G may be achieved within a $\pm (2 \text{ to } 3)$ per cent error.

Amplidyne are built for outputs up to 40 kW. To illustrate the above considerations the following design data for the АГ-3-type amplidyne are given: 2.5 kW output at 125 V, 20 A, 1,450 r. p. m.; external diameter—340 mm, internal diameter—186 mm, armature diameter—185 mm, internal armature diameter—55 mm, $2p=2$; armature length—140 mm, number of axial ventilation ducts 12, each 14 mm in diameter; the stator is fitted with four control windings; the commutator dimensions: $D_c=125$ mm, $l_c=62$ mm, $K=93$ bars, steel grade E1AA=0.5, brushes 10×12.5 mm of the $\Theta\Gamma$ grade.

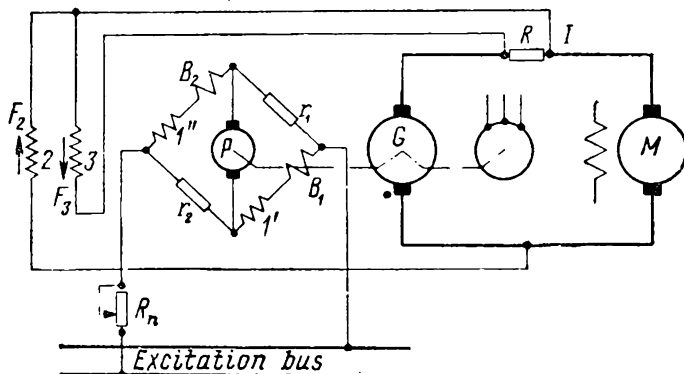


Fig. 11-13. Amplidyne connected to Ward-Leonard unit

E. Electrical machine regulator (EMR). To serve the same purpose as the amplidyne, i. e., automatic control of industrial processes, an electric machine regulator was suggested. In design it is a conventional d. c. machine with several field windings. Fig. 11-13 shows its scheme as a speed regulator employing the principle of counter e. m. f. Here G is a generator driven by a three-phase motor; M is a d. c. motor, fed by generator G ; R is the machine regulator, coupled to the same shaft as the generator (it may also be driven by a small separate induction motor) and connected into the bridge scheme; B_1 and B_2 are two parallel branches of the generator G excitation winding; I' and I'' are two parallel branches of the electric machine-regulator self-excitation winding; 2 and 3 are the control windings. The field windings B_1 and B_2

of generator G and windings I' and I'' of the regulator are connected into the arms of a balanced bridge according to the diagram shown in the drawing. [Bibl. 68]

Winding 2 is connected across the motor terminals, its m. m. f. $F_2 \equiv U_m$; winding 3 is connected across the resistance R and its m. m. f. $F_3 \equiv I$. For steady-state operation conditions the m. m. f. F_1 of the windings I' and I'' and the m. m. f. F_3 are concurrent, but in opposition in respect to F_2 , the sum being $F_1 + F_3 = F_2$. Hence, the resultant m. m. f. of the regulator is equal to zero, its e. m. f. also practically equaling zero, since the magnet system of the regulator is made of special steel with minimum residual magnetism (0.4 per cent instead of the usual 2-3 per cent) and minimum hysteresis effect. Now, let us assume, that we have changed, say, decreased, the resistance R_n ; the m. m. f. F_1 will increase, and in the armature circuit of the regulator there will appear an initial e. m. f. under the influence of which the self-excitation will begin. Thus a small initial pulse brings about a considerable change in generator G field current and consequently in speed of the motor M . If, furthermore, with a given resistance R_n the motor braking torque changes, say, increases, then the current I will tend to increase and the speed n —to decrease; but at the same time the m. m. f. F_3 will also increase and this will lead to such an increase of excitation current and generator G e. m. f. at which the speed remains without change. Electrical machine regulators are made for powers up to 1 kW; in the generator-motor system these regulators allow regulation of speed of the motor in the range of 1 : 120 and in many cases successfully compete with the amplidyne.

F. The K. I. Shenfer type d. c. converter. The d. c. converter invented by K. I. Shenfer in 1929, often called the *metadyne*, is a special regulator machine, which makes available non-rheostatic starting of an electric train with a wide range of speed regulation and braking down to very small speeds. [Bibl. 69, 70] The circuit diagram of the converter is shown in Fig. 11-14. Here is shown a converter running with constant speed and representing a d. c. ma-

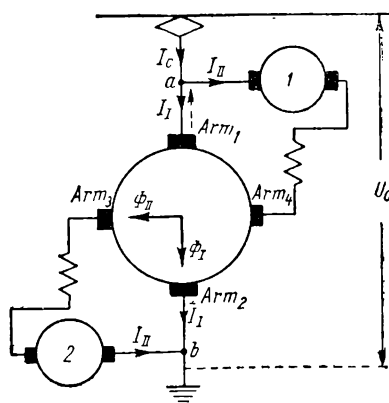


Fig. 11-14. Electrical circuit diagram of Shenfer d. c. converter

chine with two pairs of brushes arranged along the direct and cross axes (brushes A_1-A_2 and A_3-A_4), 1 and 2 are traction motors connected between points a and b in series with the brushes A_3-A_4 , i. e., in the circuit of the cross current I_{II} ; between these points lies the direct current I_I circuit. Thus, we have two parallel branches, one along the direct axis, the other along the cross axis, the currents I_I and I_{II} creating fluxes Φ_I and Φ_{II} in the converter armature along the corresponding axes.

Neglecting for simplicity the voltage drop in the current circuit I_I we have:

$$U_c \approx E_I \approx C_{eI} n_{conv} \Phi_{II} \approx C'_{eI} n_{conv} I_{II}. \quad (11-4)$$

Here U_c is the circuit voltage, n_{conv} —converter speed. Assume that $U_c = \text{const}$ and $n_{conv} = \text{const}$. Then $\Phi_{II} = \text{const}$ and consequently, $I_{II} = \text{const}$.

It follows then, that notwithstanding a change in the speed of traction motors 1 and 2, the current I_{II} remains practically constant in magnitude for the conditions stipulated above.

On the other hand,

$$I_{II} = \frac{(U_c + E_{II}) - 2E_{a.m.}}{R}. \quad (11-5)$$

Here E_{II} is the e. m. f. created in the converter armature winding by flux Φ_{II} ; $E_{a.m.}$ is the counter e.m.f. of each of the traction motors 1 and 2; R is the total resistance of the circuit with current I_{II} .

Assume as before, that $U_c = \text{const}$ and $n_{conv} = \text{const}$. Then $E_{II} = C_{eII} n_{conv} \Phi_I \approx C'_{eII} I_I$ and $E_{a.m.} = C_{e.m} n_m \Phi_m = C'_{e.m} n_m$ and the equation (11-5) may be written as follows:

$$(U_c + C'_{eII} I_I) - I_{II} R = 2C'_{e.m} n_m.$$

From this formula it may be seen, that the current I_I depends on the speed of rotation of the traction motors. If the voltage drop $I_{II} R$ is neglected then at the starting of motors when $n_m = 0$, we have

$$I_I = -\frac{U_c}{C'_{eII}}; \text{ physically this means, that the current } I_I \text{ flows from}$$

the converter to the power circuit (the broken arrow in Fig. 11-14); therefore the current flowing from the circuit will be $I_c = I_{II} - I_I$. Corresponding to the negative direction of current I_I the e. m. f. E_{II} acts in opposition to voltage U_c , thus playing the role of a starting rheostat; hence, for the starting period

$$I_{II} = \frac{U_c - E_{II}}{R}.$$

As the traction motors develop speed the current I_1 gradually decreases in absolute value and for some definite speed n_m reverses its sign, and accordingly the sign of the e. m. f. E_{11} will also change; in these conditions we have:

$$I_{11} = \frac{U_c + E_{11}}{R} \text{ and } I_c = I_{11} + I_1.$$

Thus, the Shenfer converter is a unique d. c. transformer, which transforms the energy of a constant magnitude voltage U_c and varying current I_1 into the energy of the varying in magnitude voltage $U_c \pm E_{11}$, and constant in magnitude current I_{11} .

To regulate the speed of the traction motors two control windings energised from special exciters are arranged on the K. I. Shenfer converter stator. Of major importance is the winding arranged along the brush axis A_3-A_4 , i. e., in the cross direction (Fig. 11-15). The flux Φ_{contr} created by the winding should be in opposition to the flux Φ_{11} , so that the resultant flux along the axis will be $\Phi_{11} - \Phi_{contr} = \Phi_{11 \text{ result}}$. Then formula (11-4) may be rewritten as:

$$U_c \approx E_1 = C_{e1} n_{conv} (\Phi_{11} - \Phi_{contr}) = C_{e1} n_{conv} \Phi_{11 \text{ result}}.$$

For $U_c = \text{const}$ and $n_{conv} = \text{const}$ the resultant flux should also have a constant magnitude, i. e., $\Phi_{11 \text{ result}} = \Phi_{11} - \Phi_{contr} = \text{const}$. Hence it follows that with every change in flux Φ_{contr} corresponding to the current in the control winding I_{contr} a change will take place also in flux Φ_{11} , current I_{11} and corresponding speed of the traction motor.

Tests of a 50 kW d. c. converter working in a common circuit with a compound motor were carried out at the U.S.S.R. Electrical Engineering Institute and have shown that it may be successfully used in a number of cases, and in particular for electric locomotive control.

G. Machines with permanent magnets. In the early thirties of the current century new materials were produced for making permanent magnets; these were alloys of iron with other metals. Of great practical interest is the aluminium-nickel steel, i. e., an alloy of iron with aluminium (11 to 16 per cent) and nickel (28 to 24 per cent). In comparison with the former materials utilised—

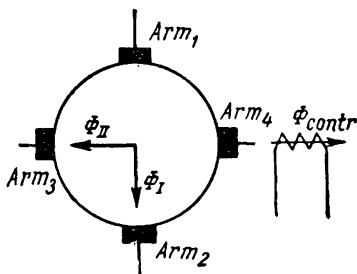


Fig. 11-15. Converter control winding arranged at the quadrature axis

chromium and tungsten steel—the aluminium-nickel steel possesses approximately 10 times more coercive force and has 9 to 10 times more magnetic energy.

Permanent magnets differ from electrical magnets by their low permeability. Thus, for instance, for aluminium-nickel steel $\mu = 8$ to 10, whereas for the electromagnets the value μ is several hundred times larger.

The work of a generator with permanent magnets may be likened to the operation of a generator with separate excitation and $i_{exc} = \text{const}$. But it should not be overlooked that permanent magnet machines in some conditions may partially lose their magnetism under the effect of armature reaction.

D. c. machines with permanent magnets are commercially very small machines as, for example, tachogenerators. But it has been proved that permanent magnet d. c. machines with an output of several kilowatts are quite feasible.

SECTION TWO

TRANSFORMERS

Chapter Twelve

FUNDAMENTALS AND CONSTRUCTION ELEMENTS OF TRANSFORMERS

12-1. Progress in Transformer Engineering

It was already mentioned in the Introduction that the pioneers of transformer engineering were the Russian electrical engineers P. N. Yablochkov, I. F. Usagin and M. O. Dolivo-Dobrovolsky who had developed a three-phase transformer for purposes of electrical energy transmission. Beginning with the 90s of the previous century the initial dry-core type of transformer was gradually substituted by the oil-immersed type. The breakdowns that first took place due to inability to protect the oil from air oxidation were practically completely eliminated with the introduction of oil conservators that came to be widely used from the middle of the first decade of the current century.

The development of transformers was greatly influenced by using silicon alloyed steel usually called the transformer steel. It is sufficient to mention that during the period from 1904 to 1911 the weight of steel used for the 20 kVA oil-immersed transformer has been reduced more than twofold, and the weight of copper almost by 40 per cent for the same or even higher efficiency. Later on a further reduction in the weight of transformer active materials took place and at the present time grain-oriented cold-rolled steels have opened up new vistas.

Since there exists a large number of transformer types, we shall here limit ourselves only to a short description of the power transformer, as it is of great interest in connection with the tremendous developments of electrical power transmission systems.

During the period from 1905 to 1940 the consumption of electric energy in industrially developed countries is being doubled approximately every 8 to 10 years. Power plant capacity and the ratings of the power units, including transformers, grew accordingly. By 1930 there was developed a 100,000 kVA three-phase, five-

leg transformer and by 1936—a three-phase transformer bank rated $3 \times 65,000 = 195,000$ kVA with a conventional fan cooling system and $3 \times 80,000 = 240,000$ kVA with air-blast cooling. Quite recently several transformer banks rated $3 \times 123,500$ kVA have been completed for the Kuibyshev Hydroelectric Station on the Volga River.

Concurrently with the development of long-distance power transmission lines which made available the utilisation of low-grade fuel and especially water sources, the transformer voltages grew from 110 kV in 1907 to 220 kV in 1921, 287.5 kV in 1937 and 400 kV in 1952. The 400 kV voltage is used to transmit electric energy from the Lenin Power Station on the Volga to Moscow and the 500 kV from the Volgograd Hydroelectric Station to Moscow.

The manufacture and maintenance of high-power transformers have brought up a number of important and difficult problems of transformer construction among which are: a) increase of transformer efficiency, b) cooling of transformer, c) overvoltage protection of transformers.

The problem of power transformer efficiency is of great practical import considering that the energy generated at the power station is subjected to three- and often to fourfold transformation before it gets to the consumer. To increase the efficiency of a transformer methods of its calculation and construction techniques must be constantly perfected and the design improved by introduction of new, higher grade materials or utilising the old ones more efficiently.

The problem of transformer cooling can be solved in various ways. At first the tanks of small-size transformers were made of corrugated iron and in large-capacity transformers internal water cooling of the oil was widely used. But such transformers did not give sufficiently reliable service and were eventually replaced by transformers with tanks fitted with heat-dissipating external tubes for capacities up to 2,000 kVA and radiator-type tanks with natural cooling for transformers up to 7,500 kVA and with air-blast cooling in transformers of larger capacity. Prior to the Second World War centralised air-blasting from one or two ventilators for each transformer was practised, but at present each radiator is cooled separately with the help of small-capacity ventilators mounted onto them (see below Fig. 12-15).

After the first high-voltage lines were built there has been an exceptional interest in problems of transformer overvoltage protection. Research has shown that some of the protection measures as, for instance, the strengthening of end coil insulation are insufficient, whereas other devices, such as, for example, protective

reactors are useless. Therefore, way back in the middle of the first decade of the current century the idea of the so-called *non-resonating* or *lightning-proof* transformer originated in which the voltage is distributed along the winding more or less uniformly, independent of transformer duty. In 1929 a lightning-proof transformer was developed with complete capacity protection and then in 1937 a transformer with partial capacity protection was built at the Moscow Transformer Works. At the present time this protective device is used on all Soviet transformers built for 110 kV and higher voltage.

Along with the development of a fundamental type of power transformer, a series of the same transformers but with special characteristics was also developed. Since the mid-twenties the *three-circuit transformers* (see below, Chapter 22) became widely distributed. On the other hand, the interconnected power systems demanded transformers with *voltage regulation under load*, both in magnitude and in phase (the so-called longitudinal and cross regulation). In connection with wide development of electrometallurgical and electrochemical plants, new types of powerful transformer for furnaces and rectifying installations were developed. For the welding operations—arc, contact, butt, etc.—new types of welding transformers were also developed.

From the above discussion it follows that transformer construction has reached a high level of development capable of satisfying all requirements.

12-2. Fundamental Definitions

The transformer is a static electromagnetic device designed for transformation of one (primary) alternating current system into another (secondary) with other characteristics, in particular, other voltage and current.

As a rule the transformer consists of: a) the core assembled of sheet transformer steel and b) two or, in the general case, more than two, windings coupled electromagnetically, and in the case of the autotransformer, also electrically.

The transformer with two windings is called the *two-winding* transformer; the transformer with three or more windings the *three-circuit* or *multicircuit* winding. According to the kind of current, transformers are distinguished as single-phase, three-phase and multiphase. A *multiphase transformer winding* is one where all phases of the windings of the same voltage are connected together according to stipulated schemes. The transformer winding to which the energy of the alternating current is delivered is called

the *primary winding* or the *primary*; the other, from which energy is received is called the *secondary winding* or the *secondary*. In accordance with the name of the winding, all values pertaining to the primary as, for example, power, current, resistance, etc., are also called primary and those pertaining to the secondary—the secondary values.

The winding connected to the circuit with the higher voltage is called the *high-voltage winding* (H.V.), the winding connected to the circuit of the least voltage value is called the *low-voltage winding* (L.V.). If the secondary voltage is less than the primary, the transformer is called a *step-down* transformer, and if more—a *step-up* transformer.

A *transformer with tappings* is one the windings of which are fitted with special taps for changing its transformation ratio.

To avoid the detrimental effect of the ambient air on winding insulation and improve cooling conditions of the transformer its core together with the windings assembled on it is immersed into a tank filled with transformer oil. Such transformers are called *oil* transformers. Transformers not immersed in oil are called *dry* transformers.

12-3. Basic Types of Transformers

The more important types of transformers are the following:

A) Power transformers for transmission and distribution of electric energy;

B) Power transformers for special purposes: i. e., for furnaces, rectifier units, welding, etc.;

C) Induction regulators for the regulation of voltage in distribution circuits;

D) Autotransformers for transforming voltage within a small range, for starting a. c. motors, etc.;

E) Instrument transformers—for connecting to a circuit measuring instruments;

F) Test transformers to carry out tests under high voltage.

Thus, the field of transformer use is tremendously wide. But in all cases the fundamental processes determining the work of a transformer, and also the methods of studying the phenomena in a transformer are essentially the same. Therefore, when we speak of a transformer we will have in view its *basic type*, viz., the *single- and three-phase two-winding power transformer*. The description of some special types of transformers is given in Chapter 22.

12-4. Transformer Ratings

The rated (nominal) values of a transformer—power, voltage, frequency, etc.—are given in the works nameplate, which should always be arranged so as to be accessible. But the term “rated” (nominal) may also be applied to values not indicated on the nameplate as, for example, rated efficiency, rated temperature conditions of the cooling medium, etc.

The *rated (nominal) conditions* of the transformer are the conditions given in the nameplate.

The *rated power* of the transformer is the power at the secondary terminals, indicated in the nameplate and expressed in kilovoltamperes.

The *rated primary voltage* is the voltage indicated in the transformer nameplate; if the primary is provided with tapplings, the rated tapping voltage is specially noted.

The *rated secondary voltage* is the voltage across the transformer secondary terminals on no-load and with rated voltage across the primary; if the secondary has branches, then its rated voltage is specially indicated.

The *rated currents of the transformer*, primary and secondary, are the currents indicated in the nameplate of the transformer and calculated by using the corresponding rated values of power and voltage. In this case due to the fact that transformer efficiency is very large, it is assumed that the rated power of both windings is equal. Let, for instance, the rated power of a three-phase transformer $P_n = 100$ kVA, the rated primary and secondary voltages $U_{1n} = 6,000$ V and $U_{2n} = 230$ V. Then

$$I_{1n} = \frac{P_n}{\sqrt{3}U_{1n}} = \frac{100 \times 10^3}{\sqrt{3} \times 6,000} = 9.63 \text{ A}$$

and

$$I_{2n} = \frac{P_n}{\sqrt{3}U_{2n}} = \frac{100 \times 10^3}{\sqrt{3} \times 230} = 251 \text{ A}.$$

The standard rated frequency in the U.S.S.R. is 50 c/s.

The curve for the voltage, e. m. f. and current may be assumed practically sine-wave if none of its ordinates a (Fig. 12-1) differs from the corresponding ordinate b of the fundamental sine-

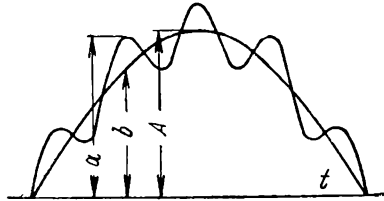


Fig. 12-1. A practically sine-wave curve

wave more than 5 per cent of the amplitude A of the fundamental sine-wave, i. e., if the difference

$$\frac{a-b}{A} \times 100 \leq 5 \text{ per cent.}$$

The three-phase system of voltages and currents may be assumed as practically balanced, if, when resolving it to systems of vectors of positive and negative sequence, the value of the negative sequence vectors does not exceed 5 per cent of the values of the positive sequence vectors.

12-5. Basic Construction Elements of Transformers

The transformer consists of the following main parts: a) core, b) winding, c) oil tank, if it is an oil-immersed transformer, and d) bushings.

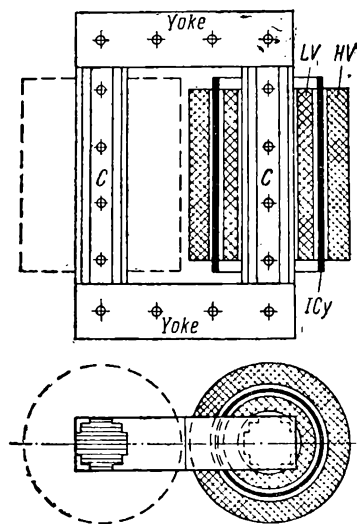


Fig. 12-2. Core of a single-phase core-type transformer with concentric winding

A. Core. The transformer core is the steel system which forms the magnetic circuit with all parts pertaining to its construction. According to type of core the transformers are distinguished as:

a) *Core-type transformers*, in which the windings envelope the legs of the core, and

b) *Shell-type transformers*, in which the windings are partially enveloped by the core.

Independent of type, the cores are all assembled of sheets of special, the so-called transformer, steel 0.35 or 0.5 mm thick. At the present time two main grades of transformer steel are used: a) *hot-rolled* and b) *cold-rolled*. The latter has better magnetic properties in the direction of roll (Fig. 1-2), but requires special methods of core assembly (for details see below, § 13-4).

To insulate the steel sheets paper 0.03 mm thick and oil lacquer are used. Paper insulation is much cheaper than the lacquer, but its heat-conducting and heat-resisting properties and mechanical strength are worse. Besides, the paper insulation occupies too large a percentage of the cross-section of the stack. Due to this in large-

capacity transformers, where these disadvantages are very essential, lacquer insulation is preferred.

As a rule, the cores of large-capacity power transformers (of more than 100 kVA) are assembled of 0.5 mm steel sheets, since such a construction is less labour-consuming than with 0.35 mm sheets.

The cores of single-phase and three-phase core transformers with their windings are shown schematically in Figs. 12-2 and

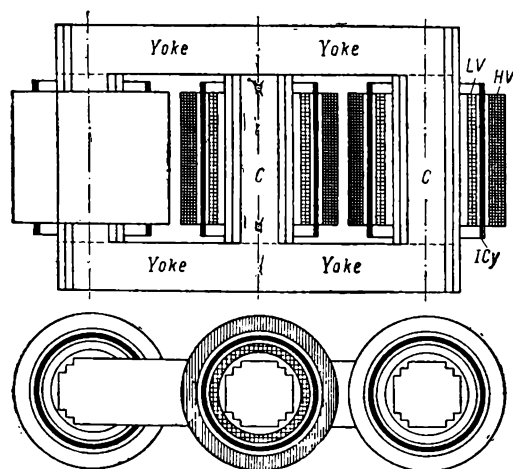


Fig. 12-3. Core of a three-phase, three-leg transformer with concentric winding

12-3. Here $C-C$ are the legs, $Y-Y$ —the top and bottom yokes, LV —the low-voltage, and HV —the high-voltage windings; IC_y —the insulation cylinder between the windings.

In transformers of very large capacity the core consists of three main legs on which the windings are arranged, and two additional cores—at the sides—without windings (Fig. 12-4). This arrangement allows to decrease the height of the yoke (since the leg flux is allowed to branch off), and consequently also of the core, at the expense of a small increase in its length; this facilitates transportation of transformers by rail.

The core is attached to the yoke either by a *butt joint* or by *interleaving* (the so-called *butted* and *interleaved* constructions). With a butt construction the legs and yoke are first assembled separately and then joined with the help of fastenings. Such a core construction facilitates the mounting of the winding onto

the legs, since to fulfil this it is sufficient to remove the top yoke.

By the interleaving method the entire core is assembled complete (Fig. 12-5); therefore, to mount the winding on the leg, the top

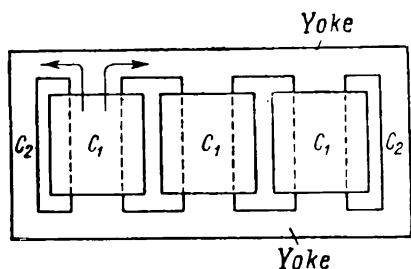


Fig. 12-4. A three-phase, five-leg transformer

yoke has to be dismantled and after the winding is set—again assembled. Thus, the second method is more complicated than the first, but on the other hand it has several valuable advantages, viz.:

1. When the core is interleaved the clearances in the joints of the sheets of the legs and yokes may be minimum since the sheet layers overlap at the butt. With butt

assembly an insulation gasket 0.5 to 1 mm thick has to be inserted between the leg and yoke to avoid creation of eddy currents at the joint (Fig. 12-6) with the consequent large increase of additional losses which may lead even "to a fire in the steel"

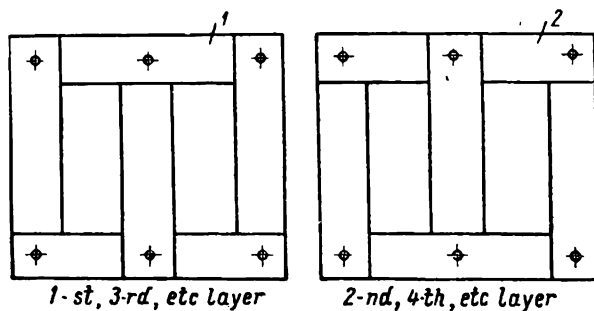


Fig. 12-5. Core assembly by interleaving

due to an excessive rise of temperature at the butt. Elimination of gasket in the interleaved construction allows a decrease in no-load current.

2. When the core is assembled by interleaving, its mechanical stability is noticeably increased, whereas the butt construction requires relatively heavy fastenings for the proper conjunction of legs and yokes. Therefore the weight of the fastenings in the interleaved construction is much less than that for the butt-type assembly. According to the Moscow Transformer Works data, the weight of

the fastenings in a 5,600 kVA, 35 kV transformer was initially 21.5 per cent of the weight of the active core steel for the butt construction and this was decreased to 8 per cent when the interleaved construction was introduced.

Due to these advantages, the interleaved core method has been accepted in the U.S.S.R. for power transformers of all capacities. Therefore, in further discussions we shall deal only with this type of core construction.

The cross-section of the leg is a stepped polygon inscribed into a circle with a diameter D_0 (Fig. 12-7, *a*, *b*, *c*). This is done for better utilisation of the space inside the circle. The number of steps n_{step} depends on the diameter D_0 : with $D_0 \leq 100$ mm $n_{step} = 4$, with $D_0 = 100$ to 500 mm it equals 5 to 6, and for D_0 up to 1,000 mm, $n_{step} = 9$ to 10. Fig. 12-7, *a* shows a five-stepped leg joined with the help of pins.

In transformers of average and large capacity with a leg diameter $D_0 \geq 350$ mm to provide better cooling of the steel core it is divid-

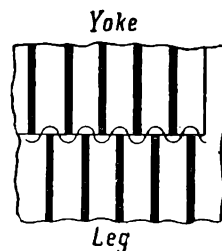


Fig. 12-6. Appearance of eddy currents at butting ends when insulating gasket is absent

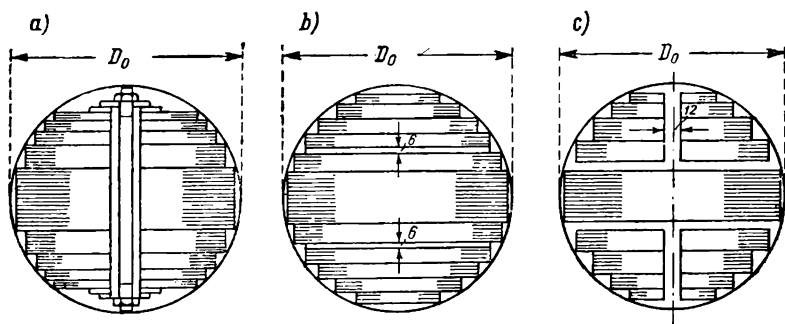


Fig. 12-7. Stepped-core:

a — without cooling ducts; *b* — with axial cooling ducts; *c* — with axial and transverse ducts

ed into packets separated by longitudinal oil ducts 6 mm wide (Fig. 12-7, *b*). In transformers of very large capacity with diameter of leg $D \geq 800$ mm, additional lateral ducts 10-12 mm wide (Fig. 12-7, *c*) are made. In this case the transformer core consists of two separate frames.

The active cross-section of the yoke is made either equal to the cross-section of the leg or increased by 5 to 10 per cent so as to reduce losses in the yoke steel and the no-load current.

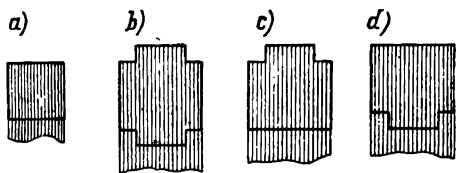


Fig. 12-8. Power transformer yoke cross-sections

For technological reasons the cross-section of the yoke is of a more simple form than the core cross-section, even though in this case the magnetic flux becomes unequally distributed along the cross-sections of these parts, and this leads to the creation of additional losses in the steel. In the U.S.S.R. rectangular-shaped, cross-shaped and T-shaped yokes are used (Fig. 12-8, *a, b, c, d*).

The yoke with a cross-section shown in Fig. 12-8, *a* is used in transformers of comparatively small capacity; the yoke in Fig. 12-8, *b, c* is used for average-capacity transformers.

The T-shape yoke with the shelf downwards (Fig. 12-8, *d*) is used in large-capacity transformers.

If the leg is furnished with ducts, the ducts in the yoke should coincide with these ducts to provide unhindered circulation of the oil.

The core of a single-phase shell-type transformer is shown in Fig. 12-9. The leg is arranged in the middle, and the yokes along both sides of the leg, partially enveloping the winding. The cross-section of the yokes is approximately one-half the section

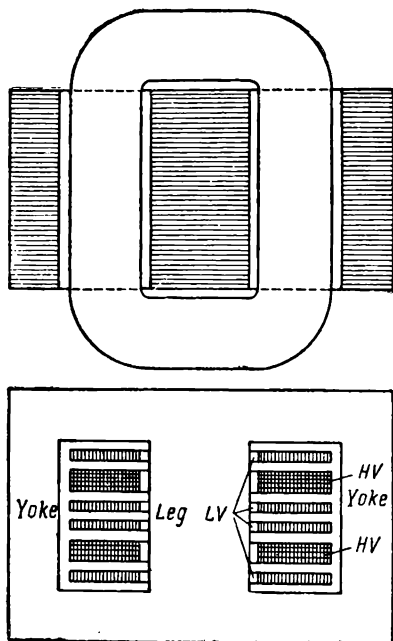


Fig. 12-9. Shell-type transformer cores with sandwich winding

of the leg corresponding to the leg flux branching off into two parts. The leg is rectangular in shape with a side ratio of approximately 1 : 2. Practice has shown that core transformers,

as compared with shell transformers, are much simpler in design, permit of easier assembly and insulation of the windings, especially for high voltage, and besides they are mechanically more stable in short-circuit conditions. Therefore, at the present time the shell-type is used only when making some special power transformers as, for example, the furnace type. In future discussions we shall consider only transformers of the core type.

Independent of type of core, the active steel and all fastening parts excluding the clamping pins, should be earthed. For this purpose they are connected to the tank, the number and locations of the earthing connections being determined by the core construction.

B. Transformer windings. The transformer windings should comply to a number of requirements of which the most important are the following: 1) the winding should be efficient both as regards initial cost, with the market availability of copper taken into consideration and from the point of view of the efficiency of the transformer in service; 2) the heating conditions of the windings should meet standard requirements, since departure from these requirements towards allowing higher temperatures would drastically shorten the service life of the transformer; 3) the winding should be mechanically stable in respect to forces arising when sudden short circuits of the transformer occur; 4) the winding should have the necessary electrical strength in respect to over-voltages.

These requirements are often mutually contradictory. Thus, for example, with a larger current density in the winding less copper is used, but copper losses become larger and therefore the efficiency of the transformer is lower. Larger temperature rises allowed in the winding decrease the overall dimensions of the transformers, but shorten its service life, etc. Therefore modern transformer winding design, especially of the high-voltage transformers, is the result of long-term development and service tests.

According to arrangement the high- and low-voltage windings are distinguished as:

1) *concentric*, i. e., windings which in each cross-section represent circles with a common centre, and

2) *sandwiched*, in which parts of the high- and low-voltage windings alternate along the height of the leg.

The concentric winding is shown schematically in Figs. 12-2 and 12-3. The low-voltage winding is usually located closer to the leg since it is much easier to insulate it from the core than the high-voltage winding.

The main types of concentric windings are:

- a) The *cylindrical layer winding*;
- b) The *helical winding* and its modifications;
- c) The *continuous winding*.

The cylindrical layer winding. If the cross-section of a turn does not exceed 8 to 10 mm², the cylindrical winding is made multilayer of round wire; for larger turn cross-section the winding is made of rectangular cross-section wire, usually double-layer (Fig. 12-10). The winding layer is made up of turns helically wound

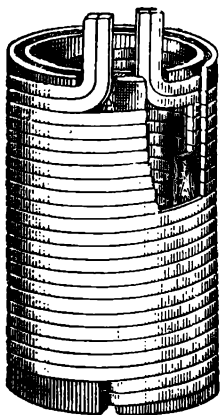


Fig. 12-10. Cylindrical double-layer winding

round a cylinder the turns close to each other. Hence, the height of the winding is the height of the layer. The rectangular wire may be wound either *flatwise* or *edge-wise*. In the former case the larger side of the wire is arranged in the axial direction, in the latter case—in the radial direction of the winding. If the cross-section of the turn exceeds 40-45 mm² then a turn is made of several single conductors, which are placed close to each other along the height of the layer, so that they all occupy the same position in relation to the leakage field.

To improve the cooling of the winding layers ducts 5 to 8 mm wide are left between them (the bigger figure relating to larger capacity transformers).

Cylindrical windings are used mainly for small-capacity transformers up to 560 kVA.

Coil layer windings made of round wire were formerly widely used for transformer construction in the U.S.S.R. but have been almost completely substituted by the cylindrical winding, it having proved less labour-consuming.

The helical windings. These are distinguished as: a) the *simple helical winding*, in which as in the cylindrical winding the turns are helically wound, but in which a duct is left 4.5 to 6 mm wide between two adjacent turns along the height (Fig. 12-11, a), and b) *semi-helical winding*, in which every two turns, excluding the end turns, are joined into one coil without a duct (Fig. 12-11, b).

One turn of the helical or semi-helical winding consists of a row of parallel conductors rectangular in cross-section, arranged in the radial direction of the winding flatwise and close to each other. For a more uniform distribution of current between the parallel branches, *transposition* of the conductors is used. Fig.

12-12 shows the scheme for the transposed turns of the helical winding in three places along its height: in the middle—the so-called middle transposition *A* and two group transpositions *B*, made so that the winding is divided along the height of the winding into four parts, approximately equal.

The number of parallel conductors in one turn of a helical winding is usually from 6 to 20. The helical winding is widely used for windings of low-voltage transformers of average and especially of large capacity.

The continuous winding. High-voltage transformers—for 35 kV and higher—employ the continuous-type winding, which differs

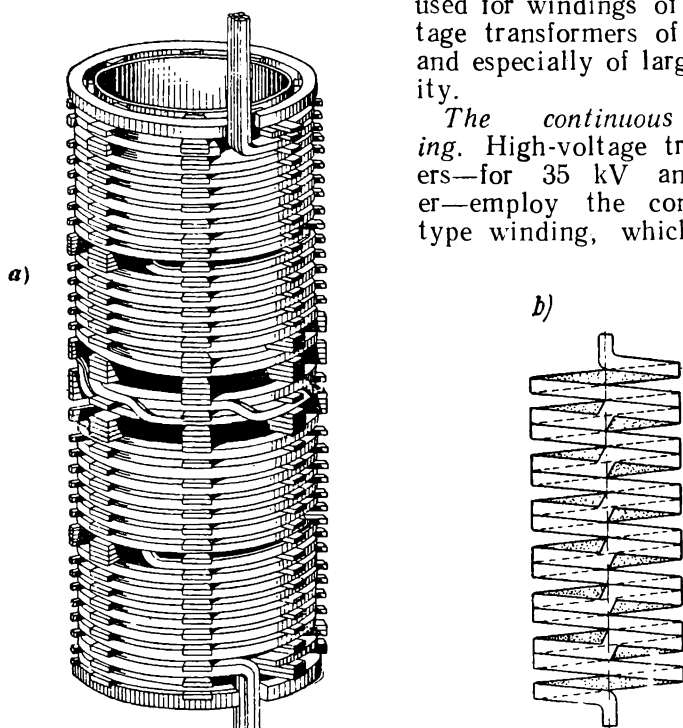


Fig. 12-11. Helical winding:
a — simple; b — semi-helical

from the helical windings in that it consists of a row of flat coil or disks, separated by ducts (Fig. 12-13). The unique and most valuable feature of the continuous winding is that its coils are connected together without soldering, by means of a special method of sandwiching one of the coils into each coil pair. If a winding turn contains several parallel conductors, transposition of conductors is used as in the case of the helical winding.

When the continuous winding serves as a HV winding, tapings are made for the regulation of the transformation ratio in the range of $\pm 5\%$ or $2 \times (\pm 2.5\%)$.

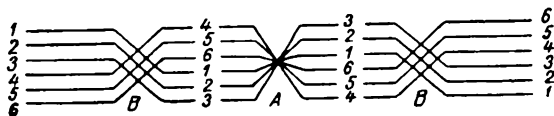


Fig. 12-12. Diagram of transposition of turns for a simple helical winding

Of special importance is the problem of insulating the windings, since they are very often subjected to considerable overvoltages, in relation to which the windings should possess the required electrical strength. This question is discussed in detail in the chapter on overvoltages.

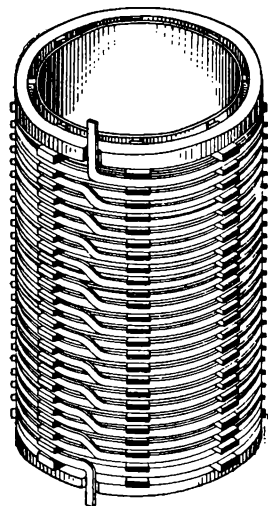


Fig. 12-13. Continuous winding

The *sandwich winding* is shown schematically in Fig. 12-9. Here the HV and LV windings are alternately arranged so that the LV winding coils are nearer to the yoke. Sandwich windings are employed mainly in shell-type transformers. Compared with the concentric windings they have many disadvantages: they are more labour-consuming in manufacture, less stable in respect to short circuits and are more difficult to insulate from each other and from the yoke. This is the reason why the main type of transformer construction is the core type with a concentric winding.

C. The transformer oil tank. At the present time the oil-immersed transformer is the most important type. In this design the transformer proper or the *removable part*, i.e., the core with the windings mounted onto it, is immersed into a tank filled with oil. When the oil gets heated it begins to circulate inside the tank, thus providing natural cooling of the transformer.

The design of the tank is closely related to the thermal rating of the transformer. Usually the power transformer tank is of an oval shape. It should be able to withstand internal

excess pressure of 0.5 atm. The tank is mounted on a trolley with rollers which are calculated for the full weight of the transformer.

Cooling conditions of transformers are the more difficult, the larger the capacity of the transformer. Therefore, the construction of the tank is changed accordingly, viz.:

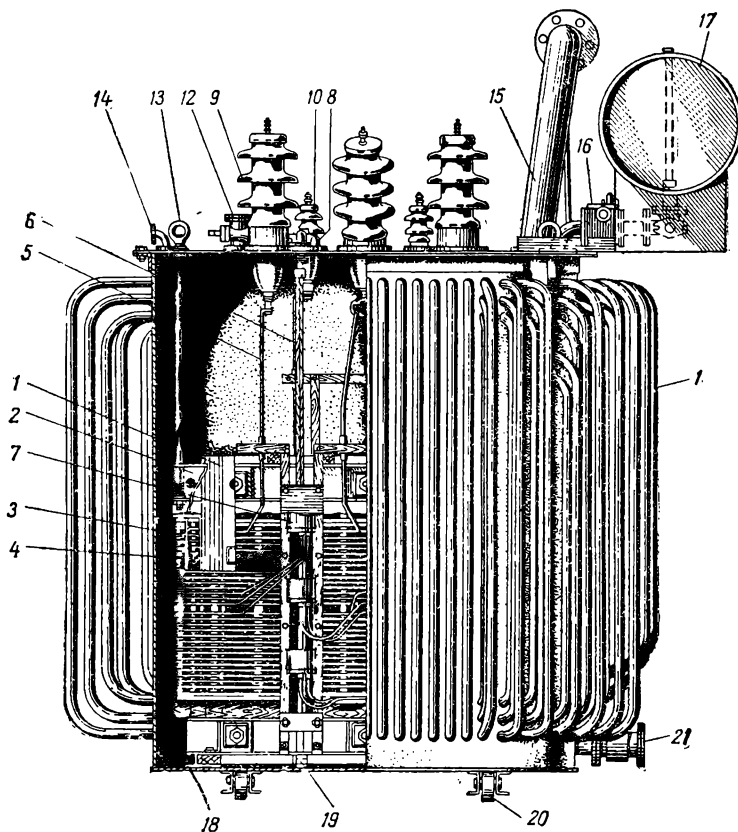


Fig. 12-14. Transformer with a pipe-radiator tank

1 — Laminated magnet circuit core; 2 — Channel iron clamping the yoke; 3 — Low-voltage winding; 4 — High-voltage winding; 5 — High-voltage tapping; 6 — Low-voltage tapping; 7 — Triple change-over switch for high-voltage winding control tappings; 8 — Change-over switch operating mechanism; 9 — HV bushing (insulator); 10 — LV bushing (insulator); 11 — Pipe-radiator tank; 12 — Oil priming valve; 13 — Lifting lug; 14 — Branch pipe for vacuum pump connection; 15 — Exhaust pipe; 16 — Gas relay; 17 — Oil conservator; 18 — Support beam at tank bottom; 19 — Vertical bolt for tightening channels clamping the yoke; 20 — Rollers; 21 — Oil draining cocks

a) Transformers of very small capacity up to about 30 kVA have *smooth tanks*, which are the simplest type of tanks.

b) For transformers of large capacity up to about 3,000 kVA, tanks with *pipe radiators* are used, where pipes 50 mm in diameter arranged in one to three rows are welded into the tank walls (Fig. 12-14). The formerly used tanks of corrugated iron are not used nowadays since, compared with the pipe-radiator type, they are mechanically weaker and do not cool so efficiently.

c) Transformers with a capacity up to 10,000 kVA have a *cooling radiator system* with natural cooling connected to the tank walls. The radiator consists of two collector boxes—top and bottom—

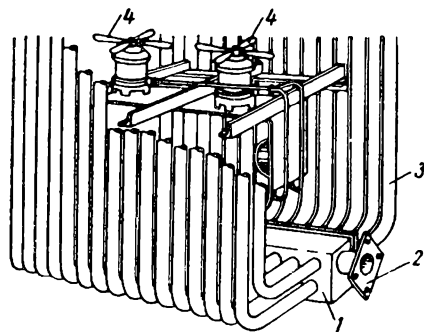


Fig. 12-15. Double pipe-radiator with separate fans

(1 in Fig. 12-15) which are fixed to the tank walls with the help of flanges 2 and into which pipes 3, 50 mm in diameter and 2 mm thick, are welded in two rows. The pipes are located either on one side of the collector box making a *single radiator*, or on both sides of it, the *double radiator*. The radiators are arranged in respect to the tank walls either tangentially or radially. In most cases the system of radial double radiators is used.

d) For transformers with capacities from 10,000 kVA and higher *air-blast cooling of the radiators* is used. At first, a *centralised system of blast cooling* was widely used employing one or two ventilator units. Practice has proved that such a system is less efficient than a system with *individual cooling* of radiators with the help of one or two 150 to 200 watt ventilator mounted on each radiator (4 in Fig. 12-15).

In transformers, used at hydroelectric plants, cooling of the oil by water in oil-coolers is used. In this case the oil is mechanically circulated by means of a special pump unit. Transformers with this method of cooling are of smaller size compared with the conventional type.

D. The tank cover. The tank cover is an essential part of the tank construction. A number of parts are arranged on the cover of which the most important are: a) the bushings for the LV and HV windings; b) oil-expansion chambers in transformers of 100 kVA and higher; c) exhaust (protection) pipe for transformers with a capacity of 1,000 kVA and higher.

For transformers up to 35 kV air- or oil-filled porcelain insulators are used. Fig. 12-16 shows a 35 kV, 275 A outdoor-type in-

ulator. In 110 kV and higher voltage transformers oil-filled insulators are used with a series of concentrically set paper-bakelite cylinders arranged inside them (Fig. 12-17). The dimensions and weights of the insulators grow rapidly with an increase in voltage; thus, for example, the full height of insulators for the 110, 150 and 220 kV transformers is 2,500, 3,080 and 4,490 mm respectively; the weights of the insulators are accordingly 340, 720 and 1,750 kg.

The oil-expansion chamber and the exhaust pipe are shown in Fig. 12-14. The oil-expansion chamber is a cylindrical vessel of sheet steel mounted above the tank cover and connected to it by a pipe. The level of the oil in the oil-expansion chamber should ensure that in all cases the tank is completely filled with oil. Since the surface of the oil in the oil-expansion chamber is much less than the oil in the tank, and the temperature of the oil in the oil-expansion chamber is much lower than in the top part of the tank, the process of oxidation of the oil when it comes into contact with the ambient air is slower; thus a sufficiently reliable protection of the oil and the insulation of the transformer is attained.

Between the oil-expansion chamber and the tank a gas relay is installed (16 in Fig. 12-14), which gives warning of any fault originated in the transformer and if the fault is dangerous, the relay disconnects the transformer from the circuit.

To protect the tank from damage possible with short circuits due to creation of gas in the tank and an abrupt increase in pressure, an exhaust pipe is introduced. It is of steel, usually an oblique cylinder, connected to the tank and covered from above by a glass disc; at a certain pressure the glass disc is pressed out and the gases together with the oil are exhausted from the tank.

E. Transformer oil. For better insulation and better cooling of the active part of the transformer, the latter is filled with mineral transformer oil. The naphta oil used in the U.S.S.R. has the

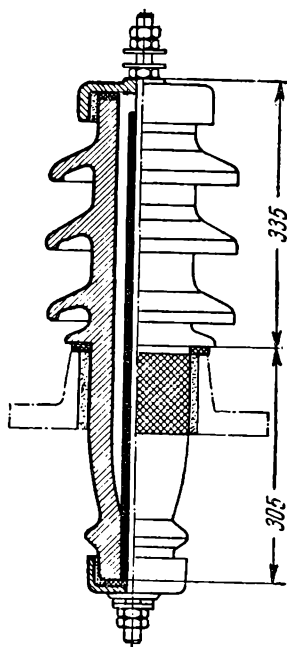
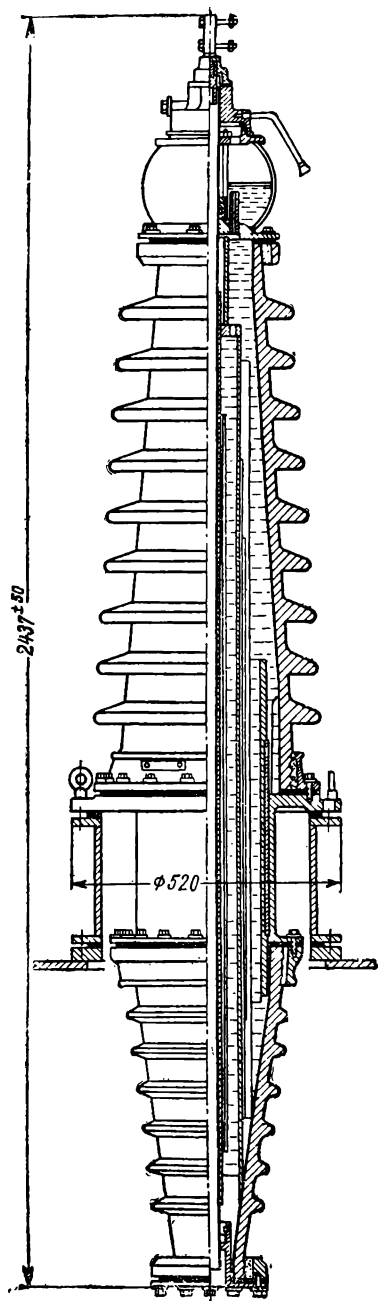


Fig. 12-16. Oil-filled bushing for 35 kV



following specifications (service oil is assumed); specific gravity (at $+20^{\circ}\text{C}$ in respect to water at $+4^{\circ}\text{C}$) not exceeding 0.895; electrical strength 20 to 35 kV/mm; thermal capacity 1,790 to 1,870 W/kg. degree; flash point temperature not below 135°C ; freezing temperature -35°C ; the coefficient of volume expansion 0.069 per cent per 1°C .

Along with the valuable properties indicated above, transformer oil has two main disadvantages: 1) it is inflammable and 2) its fumes in some conditions create together with air explosive mixtures. Therefore, in public buildings, mines, workshops, etc., dry transformers or those filled with special non-inflammable and explosion-proof liquids are preferred as, for example, pyranol which has attained wide use in the U.S.A., *sovtol* which has been developed in the U.S.S.R., its insulation and cooling properties close to the properties of mineral transformer oil, but non-oxidising and resistant to chemical action.

At the same time *sovtol* has a number of disadvantages: its cost is high, it is very sensitive to all kinds of contamination; requires replacement of some grades of materials used in transformer-building and when effected by the electrical arc (as, for in-

Fig. 12-17. Oil-filled bushing for 110kV

stance, in cases of breakdowns in the transformer) produces the hazardous gas HCL. From all points of view, therefore, the dry transformer, made of cold-rolled steel, with a glass-fibre insulation based on a heat-resisting impregnating compound is of great interest. Nevertheless, the oil-immersed transformer, filled with ordinary mineral transformer oil remains the main type of power transformer.

Chapter Thirteen

PHYSICAL CONDITIONS OF TRANSFORMER OPERATION

13-1. Principle of Operation

Transformer operation is based on the principle of electromagnetic interaction of two or, in a general case, of any number of circuits stationary in respect to each other. Fig. 13-1 shows the circuit diagram of a single-phase two-winding transformer. If a voltage from an a. c. power circuit is impressed across the $A-X$ terminals of one of the windings then, due to the action of the magnetic flux linking the two windings, an alternating e. m. f. will be set up in the secondary and a current will flow feeding power consumers connected to the $a-x$ secondary terminals.

In this way a. c. power is transmitted from the primary to the secondary circuit.

To enhance the electromagnetic linkage between windings a laminated core assembled of electrical sheet steel is provided. In order to convert (transform) a primary voltage and a primary current into a secondary voltage and secondary current it is necessary first to calculate and then arrange the primary and secondary windings.

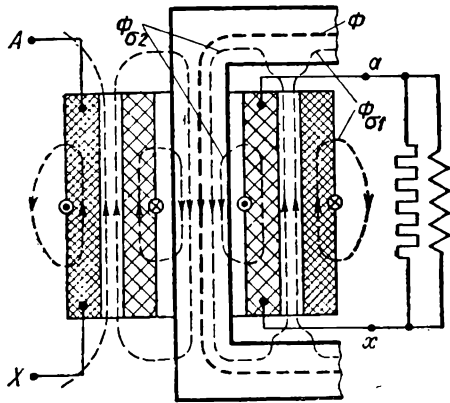


Fig. 13-1. Circuit diagram of transformer on load

13-2. M.M.F. and E.M.F. Transformer Equations

An analysis of transformer operation for any conditions is based on the primary and secondary e. m. f. equations and on the m. m. f. equation.

Consider u_1 as the instantaneous value of a voltage impressed across the $A-X$ terminals of a transformer primary from a power supply with a frequency f ; i_1 , and i_2 are the instantaneous values of currents in the primary and secondary.

The currents i_1 and i_2 create the primary and secondary m. m. f.s $i_1\omega_1$ and $i_2\omega_2$, where ω_1 and ω_2 are respectively the numbers of series-connected turns of the primary and secondary windings.

According to the second Kirchhoff law, when applied to the magnetic circuits, we have:

$$i_1\omega_1 + i_2\omega_2 = i_0\omega_1 \quad (13-1)$$

or

$$i_1\omega_1 = -i_2\omega_2 + i_0\omega_1. \quad (13-2)$$

Here $i_0\omega_1$ is the magnetising component required to establish a flux in the transformer core, the instantaneous value of which is denoted as Φ_t . The flux Φ_t is uniformly distributed over the transformer core cross-section and is linked with all turns both of the primary and secondary windings (the heavy broken line in Fig. 13-1). This flux is of fundamental import and is, therefore, referred to as the main flux.

The main flux produces the following e. m. f.s in the transformer primary and secondary.

$$e_1 = -\omega_1 \frac{d\Phi_t}{dt} = -\frac{d\Psi_{10}}{dt} \quad (13-3)$$

$$e_2 = -\omega_2 \frac{d\Phi_t}{dt} = -\frac{d\Psi_{20}}{dt}. \quad (13-4)$$

Here Ψ_{10} and Ψ_{20} are flux linkages corresponding only to the main flux Φ_t .

Besides, the m.m.f.s $i_1\omega_1$ and $i_2\omega_2$ establish the *primary* and *secondary leakage fluxes*, Φ_{o1} and Φ_{o2} (the thin broken lines in Fig. 13-1), it being assumed that the primary leakage flux Φ_{o1} is created only by current i_1 and linked only with the primary, while the secondary leakage flux Φ_{o2} is created only by current i_2 and linked only with the secondary. Since the leakage fluxes are distributed chiefly in non-magnetic medium with a constant permeability (oil, air, copper, etc.), it may be assumed that the leakage inductances $L_{o1} = \text{const}$ and $L_{o2} = \text{const}$. Correspondingly, the

leakage e.m.f.s created by the leakage fluxes in the transformer primary and secondary are:

$$e_{s1} = -L_{s1} \frac{di_1}{dt} \quad (13-5a)$$

and

$$e_{s2} = -L_{s2} \frac{di_2}{dt}. \quad (13-5b)$$

According to the second Kirchhoff law we have for the primary e.m.f. the following equation:

$$u_1 + e_1 + e_{s1} = i_1 r_1, \quad (13-6)$$

where r_1 is the primary active resistance.

The equation (13-6) may be rewritten as:

$$u_1 = -[e_1 + e_{s1} + (-i_1 r_1)]. \quad (13-7)$$

Written in this form, the e.m.f. equation is the *e.m.f. equilibrium equation* according to which the voltage u_1 is considered to be the action of the power circuit in respect to the transformer primary, the sum $e_1 + e_{s1} + (-i_1 r_1)$ being the opposing action of this winding in respect to the power circuit. The effective (active) and counteracting e.m.f.s at any instant must be equal in value, but opposite in direction; the e.m.f.s e_1 and e_{s1} are created electromagnetically while the e.m.f. $(-i_1 r_1)$ represents the opposing action encountered by current i_1 when flowing in a conductor with a resistance r_1 . Let us agree to call the e.m.f. $(-i_1 r_1)$ the counteracting e.m.f. of the active resistance, or in short the e.m.f. of resistance r .

Substituting in equation (13-7) the expressions for e_1 and e_{s1} [formulas (13-3) and (13-5a)] and opening the brackets, we obtain

$$u_1 = \frac{d\Psi_{10}}{dt} + L_{s1} \frac{di_1}{dt} + i_1 r_1 = \frac{d\Psi_1}{dt} + i_1 r_1. \quad (13-8)$$

Here Ψ_1 is the full primary flux linkage established both by the main flux and by the leakage flux Φ_{s1} of this winding.

The middle part of the equation (13-8) represents the algebraic sum of three voltage components each of which is in mutual equilibrium with the corresponding e. m. f.

In the secondary there acts the e. m. f. e_2 established by the main flux Φ_1 , the e. m. f. e_{s2} established by the leakage flux Φ_{s2} and e. m. f. of the resistance $-i_2 r_2$. The algebraic sum of all these e. m. f.s

forms the voltage u_2 across the secondary terminals counter-balanced by the secondary power circuit reaction.

Thus,

$$e_2 + e_{s2} + (-i_2 r_2) = u_2, \quad (13-9)$$

or, substituting with the expression for e. m. f.s e_2 and e_{s2} [formulas (13-4) and (13-5b)],

$$0 = \frac{d\Psi_{20}}{dt} + L_{s2} \frac{di_2}{dt} + i_2 r_2 + u_2 = \frac{d\Psi_2}{dt} + i_2 r_2 + u_2. \quad (13-10)$$

Here, Ψ_2 is the full flux linkage of the secondary established both by the main flux and the leakage flux Φ_{s2} of this winding. If it is possible to neglect the usually small losses in the core steel and to assume that the permeability of the steel is constant, the flux linkages Ψ_1 and Ψ_2 of the transformer windings may be rewritten as

$$\Psi_1 = L_1 i_1 + M_{12} i_2 \text{ and } \Psi_2 = L_2 i_2 + M_{21} i_1, \quad (13-11)$$

where L_1 and L_2 are the full primary and secondary inductances corresponding to the total flux linked with the appropriate winding, $M_{12} = M_{21} = M$ are the self-induction of the windings.

Substituting for the values Ψ_1 and Ψ_2 in the right-hand sides of the equations (13-8) and (13-10), we obtain

$$u_1 = L_1 \frac{di_1}{dt} + M \frac{di_2}{dt} + i_1 r_1 \quad (13-12)$$

and

$$0 = L_2 \frac{di_2}{dt} + M \frac{di_1}{dt} + i_2 r_2 + u_2. \quad (13-13)$$

13-3. Transformation Ratio of Transformer E.M.F.

The coefficient of transformation of the e. m. f. of a transformer (often called simply the transformation ratio) is the relation of the e. m. f.s induced in the primary and secondary of a transformer by the main magnetic flux Φ_t . Thus,

$$k = \frac{e_1}{e_2} = \frac{-w_1 \frac{d\Phi_t}{dt}}{-w_2 \frac{d\Phi_t}{dt}} = \frac{w_1}{w_2}. \quad (13-14)$$

The transformation ratio is a concept of a very great importance both in transformer theory and for service purposes.

13-4. M.M.F. and E.M.F. Equations for Sine-Wave Variation of Voltages and Currents

If the voltages, e. m. f.s and currents are sine functions of time, the effective values of these functions may be represented by complex quantities \dot{U} , \dot{E} and \dot{I} . Then the m. m. f. equations (13-1) and (13-2) may be rewritten as

$$\dot{I}_1 \omega_1 + \dot{I}_2 \omega_2 = \dot{I}_0 \omega_1 \quad (13-15a)$$

or

$$\dot{I}_1 \omega_1 = -\dot{I}_2 \omega_2 + \dot{I}_0 \omega_1. \quad (13-15b)$$

Here \dot{I}_0 is the effective value of the magnetising current. Correspondingly, the e.m.f. equations (13-6) and (13-7) may be written as:

$$\dot{U}_1 + \dot{E}_1 + \dot{E}_{s1} = \dot{I}_1 r_1 \quad (13-16)$$

or

$$\dot{U}_1 = -[\dot{E}_1 + \dot{E}_{s1} + (-\dot{I}_1 r_1)]. \quad (13-17)$$

For the secondary [formula (13-9)] we have:

$$\dot{E}_2 + \dot{E}_{s2} + (-\dot{I}_2 r_2) = \dot{U}_2. \quad (13-18)$$

With a sine-wave variation of current, the instantaneous value of the primary leakage e.m.f. is:

$$\begin{aligned} e_{s1} &= -L_{s1} \frac{di_1}{dt} = -L_{s1} \frac{d(I_{1m} \sin \omega t)}{dt} = \\ &= -I_{1m} L_{s1} \omega \cos \omega t = -I_{1m} x_1 \cos \omega t. \end{aligned}$$

Thus, the leakage e.m.f. e_{s1} lags on current i_1 by 90° . Its effective value expressed in complex form will be:

$$\dot{E}_{s1} = -j\dot{I}_1 x_1. \quad (13-19)$$

Correspondingly, for the secondary we have:

$$\dot{E}_{s2} = -j\dot{I}_2 x_2. \quad (13-20)$$

Here x_1 and x_2 are leakage reactances of the primary and the secondary windings.

Substituting the expressions for \dot{E}_{s1} and \dot{E}_{s2} into the formulas (13-16), (13-17) and (13-18), we have:

$$\dot{U}_1 + \dot{E}_1 - j\dot{I}_1 x_1 = \dot{I}_1 r_1 \quad (13-21)$$

or

$$\begin{aligned}\dot{U}_1 &= -(\dot{E}_1 - j\dot{I}_1 x_1 - \dot{I}_1 r_1) = -\dot{E}_1 + \dot{I}_1(r_1 + jx_1) = \\ &= -\dot{E}_1 + \dot{I}_1 Z_1;\end{aligned}\quad (13-22)$$

for the secondary

$$\begin{aligned}\dot{E}_2 - j\dot{I}_2 x_2 - \dot{I}_2 r_2 &= \dot{E}_2 - \dot{I}_2(r_2 + jx_2) = \\ &= \dot{E}_2 - \dot{I}_2 Z_2 = \dot{U}_2\end{aligned}\quad (13-23a)$$

or

$$\dot{E}_2 = \dot{I}_2 Z_2 + \dot{U}_2. \quad (13-23b)$$

In these equations $Z_1 = r_1 + jx_1$ and $Z_2 = r_2 + jx_2$ are the impedances of the transformer primary and secondary; the components $\dot{I}_1 Z_1$ and $\dot{I}_2 Z_2$ are usually called the voltage drop in the transformer primary and secondary respectively.

The e.m.f. equations (13-22), (13-23a) and (13-23b) are widely used in transformer theory.

The e.m.f. equations (13-12) and (13-13) may be similarly rewritten, viz.:

$$\dot{U}_1 = j\omega L_1 \dot{I}_1 + j\omega M \dot{I}_2 + \dot{I}_1 r_1 \quad (13-24)$$

or

$$0 = j\omega L_2 \dot{I}_2 + j\omega M \dot{I}_1 + \dot{I}_2 r_2 + \dot{U}_2. \quad (13-25)$$

For power transformer operation analysis, the equations (13-24) and (13-25) are used comparatively seldom (see Chapter 22), since the self-inductances and mutual inductances of such transformers are values which vary within a relatively wide range.

13-5. The Reduced Transformer

Since, in the general case, $\omega_2 \neq \omega_1$, then $E_2 \neq E_1$ and $I_2 \neq I_1$. In accordance with the different e. m. f. s and currents, the parameters of windings, i. e., their resistances and reactances, also are different. This often hampers the quantitative estimation of processes taking place in a transformer and plotting of the vector diagrams particularly in case of large transformation ratios. In order to avoid these difficulties, a method is used in which *both windings of the transformer are reduced to the same number of turns*. Usually the secondary is referred or reduced to the primary. For this purpose the secondary, having w_2 turns, is recalculated for an equivalent winding with the same number of turns w_1 as the primary, provid-

ed that in the process of reducing the secondary to the primary the energy process in the transformer and, consequently, the operating conditions of the primary are not affected.

All values pertaining to the reduced secondary are called *reduced* or *referred* values and are denoted by the same symbols as the actual values, but with a prime ('), i.e., E'_2, I'_2, r'_2 , etc.

A. The reduced secondary e. m. f. E'_2 . In order to obtain E'_2 , it is necessary to modify the e. m. f. E_2 by the ratio between the number of turns w_1 and w_2 of the primary and the secondary, i. e., in proportion to the transformation ratio $k = \frac{w_1}{w_2}$.

Hence,

$$E'_2 = \frac{w_1}{w_2} E_2 = k E_2 = E_1. \quad (13-26)$$

The leakage e. m. f. $E_{\sigma 2}$ of the transformer secondary is modified in the same proportion.

B. The reduced secondary current I'_2 . When reducing the secondary to the primary, its total power must remain without change, i. e., $E'_2 I'_2 = E_2 I_2$. Hence

$$I'_2 = \frac{E_2}{E'_2} I_2 = \frac{1}{k} I_2, \quad (13-27)$$

that is, to obtain I'_2 , it is necessary to modify current I_2 inversely as the transformation ratio.

C. The reduced secondary resistance r'_2 . Since, when reducing the secondary to the primary, the powers do not change, the copper losses in the real and the reduced windings must be equal. Hence,

$$I_2'^2 r'_2 = I_2^2 r_2,$$

and

$$r'_2 = \left(\frac{I_2}{I'_2} \right)^2 r_2 = k^2 r_2, \quad (13-28)$$

i. e., in order to obtain r'_2 , the resistance r_2 must be changed in proportion to the square of the transformation ratio. Physically this means that when changing (for example, increasing) the number of secondary turns k times, the length of the winding is increased k times but its cross-section, assuming current density constant, decreases k times, and consequently the resistance of the winding increases k^2 times.

D. The reduced secondary leakage reactance x'_2 . The reactance of any circuit is $x = \omega L = 2\pi fL$, where L is the circuit inductance. As it is known, L is defined by the sum of the flux linkages established by a current of 1A flowing through a circuit with the circuit turns ($\sum w\Phi_{(i=1A)}$). If the number of turns is increased k times, then with a constant permeability, the flux $\Phi_{(i=1A)}$ also increases k times, and, consequently, $L = wk\Phi_{(i=1A)}$ is increased k^2 times.

Thus

$$x'_2 = \left(\frac{w_1}{w_2}\right)^2 x_2 = k^2 x_2, \quad (13-29)$$

that is, in order to obtain x'_2 , it is necessary to modify x_2 and also r_2 in proportion to the square of the transformation ratio.

E. The reduced impedance of the secondary winding and the secondary circuit. Since $Z_2 = r_2 + jx_2$, then

$$Z'_2 = r'_2 + jx'_2 = k^2 Z_2. \quad (13-30)$$

If Z_r is the resistance of the power circuit fed from the transformer secondary, then in analogy with Z'_2 we have:

$$Z'_r = k^2 Z_r. \quad (13-31)$$

13-6. M.M.F. and E.M.F. Equations for the Reduced Transformer

In a reduced transformer, the m. m. f. equation becomes

$$I_1 w_1 + I'_2 w_1 = I_0 w_1 \quad \text{or} \quad I_1 w_1 = -I'_2 w_1 + I_0 w_1.$$

Cancelling both parts of these equations by w_1 , we have

$$I_1 + I'_2 = I_0 \quad (13-32a)$$

or

$$I_1 = -I'_2 + I_0. \quad (13-32b)$$

The e. m. f. equations are written as:

$$U_1 = -\dot{E}_1 + I_1 Z_1, \quad (13-33)$$

and

$$\dot{E}'_2 - I'_2 Z'_2 = \dot{U}'_2 \quad (13-34a)$$

or

$$\dot{E}'_2 = \dot{E}_1 = I'_2 Z'_2 + \dot{U}'_2. \quad (13-34b)$$

13-7. Transformer Equivalent Circuit

The analytical and graphical investigation of transformer operation is simplified if the actual transformer in which the windings are coupled electromagnetically be substituted by a circuit, the elements of which are joined together only electrically. In the gen-

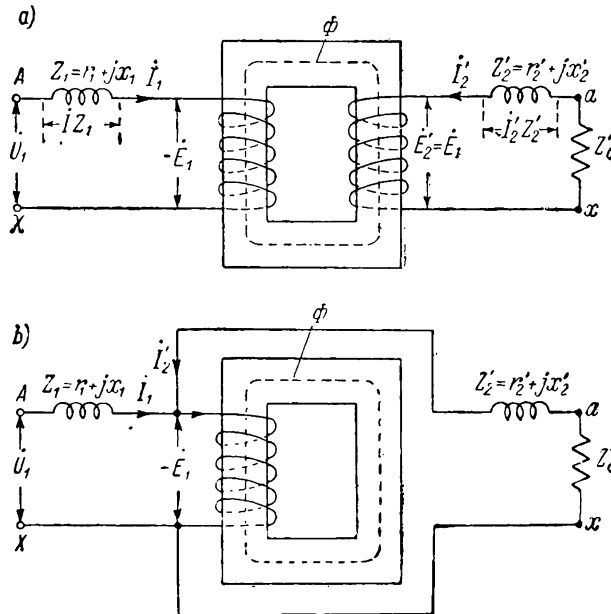


Fig. 13-2. Reduced transformer circuits

eral case this problem may have several solutions, i. e., we may have several different transformer equivalent circuits, but each should satisfy the fundamental e. m. f. and m. m. f. equations of the transformer.

In transformer theory only the so-called T-type equivalent circuit is used. The second kind of the equivalent circuit, the L-circuit, is of greater importance in induction machine theory (Part II).

According to equations (13-32), (13-33), and (13-34) the circuit of a reduced transformer is of the type shown in Fig. 13-2,a. Each winding of such an equivalent transformer consists of two series-connected coils, one of which—without leakage and copper losses—is wound on the transformer core, while the other

represents a coreless reactor having the active resistance and reactance of the appropriate winding.

Since in a reduced transformer $\omega_2 = \omega_1$, both windings of the transformer may be combined into one winding (Fig. 13-2,b), through which flows a magnetising current $\dot{I}_0 = \dot{I}_1 + \dot{I}_2$. In this case, the combined winding represents a magnetising circuit that produces the main magnetic flux Φ closing inside the transformer core. The power utilised in this winding is determined by losses in the steel core p_r .

The relationship between the voltage $-\dot{E}_1$ across the magnetising circuit terminals and the current in the circuit \dot{I}_0 may be expressed as follows:

$$-\dot{E}_1 = \dot{I}_0 Z_m = \dot{I}_0 (r_m + jx_m), \quad (13-35)$$

where $Z_m = r_m + jx_m$ is the impedance of the magnetising circuit;

$$r_m = \frac{p_r}{I_0^2} \text{ and } x_m = \omega M.$$

If U'_2 is the voltage across the terminals of the line fed by the transformer secondary, and Z'_r is the impedance of this line, then

$$\dot{U}'_2 = \dot{I}'_2 Z'_r.$$

Then from equation (13-34b), for the transformer secondary circuit, we find:

$$\dot{I}'_2 = \frac{\dot{E}'_2}{Z'_2 + Z'_r} = \frac{\dot{E}_1}{Z'_2 + Z'_r}.$$

Consequently,

$$\dot{I}_1 = -\dot{I}'_2 + \dot{I}_0 = \frac{-\dot{E}_1}{Z'_2 + Z'_r} + \frac{-\dot{E}_1}{Z_m},$$

and hence

$$-\dot{E}_1 = \dot{I}_1 \frac{1}{\frac{1}{Z_m} + \frac{1}{Z'_2 + Z'_r}}. \quad (13-36)$$

Substituting this value of $-\dot{E}_1$ into equation (13-33) for the primary e.m. f., we obtain

$$\dot{I}_1 = \dot{U}_1 \frac{1}{Z_1 + \frac{1}{\frac{1}{Z_m} + \frac{1}{Z'_2 + Z'_r}}} = \frac{\dot{U}_1}{Z_e}. \quad (13-37)$$

Here

$$Z_e = Z_1 + \frac{1}{\frac{1}{Z_m} + \frac{1}{Z'_2 + Z'_r}} \quad (13-38)$$

is the equivalent resistance of the transformer *T-type equivalent circuit* (Fig. 13-3). A transformer may be represented as a combi-

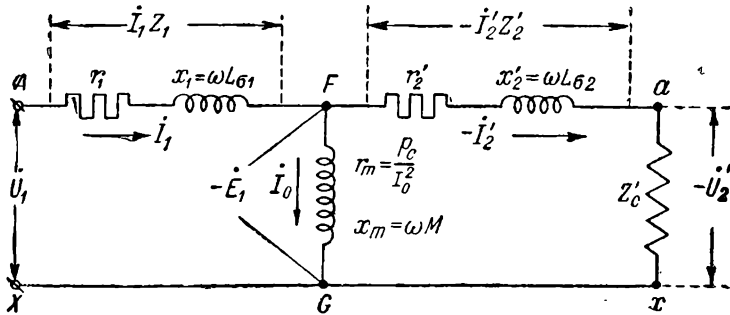


Fig. 13-3. T-type equivalent circuit
(Here $Z_c = Z_r$, $P_c = P_r$)

nation of three branches: *primary* with impedance Z_1 and current I_1 , *magnetising* with impedance Z_m and current I_0 , and a *secondary* branch with impedance $Z'_2 + Z'_r$ and current I'_2 . The distribution of the currents I_1 , I_0 and I'_2 must satisfy the m.m.f. equation $\dot{I}_1 = \dot{I}'_2 + \dot{I}_0$ [formula (13-32b)].

Since according to (13-34b):

$$\dot{E}'_2 = \dot{E}_1 = \dot{I}'_2 Z'_2 + \dot{U}'_2,$$

we have

$$-\dot{E}_1 = -\dot{I}'_2 Z'_2 - \dot{U}'_2, \quad (13-39)$$

i. e., the voltage $-E_1$ across the terminals FG of the secondary circuit is the geometrical sum of the voltage drop $-\dot{I}'_2 Z'_2$ in the secondary due to current $-\dot{I}'_2$ and voltage $-\dot{U}'_2$ across the terminals of the external power circuit.

Chapter Fourteen

TRANSFORMER ON NO-LOAD

14-1. Preliminary

No-load operation of a transformer is the condition when the transformer primary is connected to an a.c. power line with a frequency f , while the secondary is open.

The investigation of no-load conditions is of great importance because it permits by means of computation and experimental methods to determine the following fundamental transformer values: a) the transformation ratio, b) the no-load current and c) the no-load losses.

From the following it will be seen that the no-load condition is of particular value in combination with short-current conditions, since the data for these conditions allow to determine the transformer efficiency, i.e., one of the most important factors in the operation of a power transformer. On the other hand, superposing one condition upon the other, we can obtain any intermediate working condition of the loaded transformer, and this increases the theoretical importance of these conditions when they are in mutual combination.

We shall begin the study of no-load operation with the more simple single-phase transformer, and then show the characteristic features of this condition for the case of a three-phase transformer.

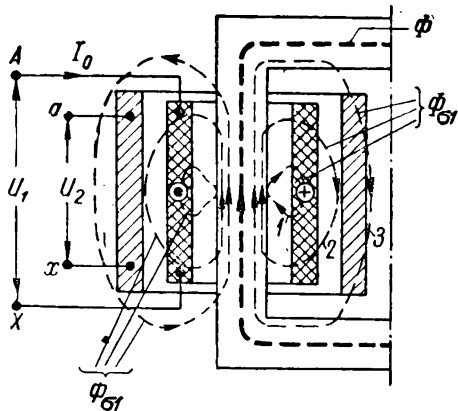
14-2. No-Load Operation of a Single-Phase Transformer

Let us impress across terminals $A-X$ of the transformer primary an alternating voltage u_1 from a power circuit with a frequency f . The terminals $a-x$ of the secondary are open and therefore the secondary current is zero (Fig. 14-1).

Due to voltage u_1 , a no-load current i_0 will flow through the primary giving rise to a m.m.f. $= i_0 \omega_1$, where ω_1 is the number of series-connected turns of the primary. The m.m.f. $i_0 \omega_1$ produces a magnetic flux, the simplified map of which for a concentric winding of a core-type transformer is shown in Fig. 14-1. The predominant part of the flux lines closes through the core and, being linked with both windings, constitutes the main magnetic flux Φ . The other part of the flux, usually much smaller, passes chiefly through a non-magnetic medium and is linked mainly with the

primary (lines 1 and 2 in Fig. 14-1), but partially it may become linked with the secondary (line 3 in Fig. 14-1). The lines 1, 2 and 3 together will be regarded as the primary leakage flux Φ_{s1} linked only with the primary.

When the transformer operates on no-load, no-load losses will appear in it comprising mainly the losses in the steel. These losses are covered by the no-load power P_0 consumed by the transformer from the power circuit.



14-3. No-Load Operation of an Elementary Transformer

Fig. 14-1. Flux map of a transformer at no-load

In conventional transformers the leakage flux for no-load operation is negligible (generally less than 0.25 per cent of the main flux). Equally the losses in the steel make up for only a fraction of one per cent of the transformer rated power (see below, § 16-5). Therefore, we shall first study the no-load operation of so-called *elementary transformer*, i. e., of a transformer without leakage and without losses in the winding copper and core steel ($r_1=0$, $x_1=0$, $P_0=0$). Such a method of preliminary simplifying the problem permits separation and the study first of the substance of a process or phenomenon and then, if needed, to introduce the necessary corrections.

When analysing no-load conditions of operation of an elementary transformer, we proceed from the voltage u_1 being impressed across the transformer primary and then by using the equilibrium equation of the primary e. m. f. establish the relationship between the voltage u_1 and e. m. f. e_1 produced by the main flux of the transformer; then we determine the relationship between the e. m. f. and the main flux, proceeding from the electromagnetic induction law and, finally, using the magnetic circuit law, find the magnetising current $i_{0\mu}$ required for producing the main flux.

A. The e. m. f. e_1 . Since in an elementary transformer $r_1=0$ and $L_{s1}=0$, the equilibrium equation of the primary e. m. f.

[formula (13-7)] becomes

$$u_1 = -e_1, \quad (14-1)$$

i. e., in an elementary transformer the impressed voltage and the e. m. f. induced in the primary are in mutual equilibrium at every instant.

In accordance with present practice we shall assume that the voltage u_1 delivered to the transformer is a sine function of time. In this case

$$u_1 = U_{1m} \sin \omega t = U_1 \sqrt{2} \sin 2\pi f t, \quad (14-2)$$

where U_{1m} is the amplitude of the supply voltage, U_1 its effective value and $\omega = 2\pi f$ the angular frequency.

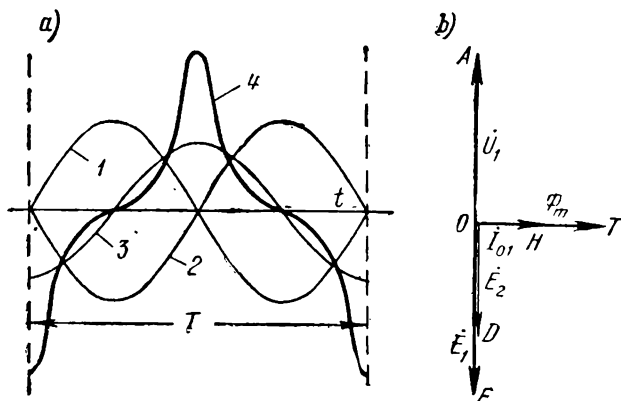


Fig. 14-2. E.m.f. and current diagrams of elementary transformer:

a — in rectangular co-ordinates; b — vector form

In Fig. 14-2,a, the voltage u_1 and the e. m. f. e_1 are represented by curves 1 and 2 having the same amplitudes and displaced in respect to each other by 180° ; thus, it may be said that a curve of the e. m. f. e_1 is the *mirror image of the curve u_1* in respect to the abscissa axis. On these grounds, the e. m. f. e_1 is often referred to as the *counter e. m. f.*

By analogy with the expression for u_1 , we have:

$$e_1 = E_{1m} \sin (\omega t - \pi) = E_1 \sqrt{2} \sin (\omega t - \pi). \quad (14-3)$$

In Fig. 14-2,b, curves 1 and 2 are represented by vectors $\overline{OA} = -\overline{OF} = -\overline{E}_1$ for the instant, when $u_1 = U_{1m}$.

B. The main magnetic flux Φ . According to formula (13-3),

$$e_1 = -\omega_1 \frac{d\Phi_1}{dt} = E_1 \sqrt{2} \sin(\omega t - \pi),$$

where Φ_1 is the instantaneous value of the main flux.

Integrating both sides of the equality, we have:

$$\int d\Phi_1 = -\frac{E_1 \sqrt{2}}{\omega_1} \int \sin(\omega t - \pi) dt,$$

and then

$$\Phi_1 = \frac{E_1 \sqrt{2}}{\omega \omega_1} \sin\left(\omega t - \frac{\pi}{2}\right). \quad (14-4)$$

The constant of integration may be assumed to be zero, since for steady-state conditions of operation there is no constant-direction flux in the transformer core.

From equation (14-4) it follows that with sine-wave impressed voltage *the magnetic flux of an elementary transformer is also a sine function of time, the flux leading the primary e.m.f. by an angle $\frac{\pi}{2}$* , i. e., by a quarter of a cycle, or, which is the same, *the primary e.m.f. lags on the flux by an angle $\frac{\pi}{2}$* (curve 3 in Fig. 14-2, a, and vector $\overline{OT} = \Phi_m$ in Fig. 14-2, b).

Formula (14-4) may be represented as:

$$\Phi_1 = \Phi_m \sin\left(\omega t - \frac{\pi}{2}\right), \quad (14-5)$$

where

$$\Phi_m = \frac{E_1 \sqrt{2}}{\omega \omega_1} = \frac{E_1 \sqrt{2}}{2\pi f \omega_1} = \frac{E_1}{\pi \sqrt{2} f \omega_1} \quad (14-6)$$

is the amplitude of magnetic flux. From this we obtain the fundamental for transformer theory expression of the magnitude of the effective primary e. m. f.:

$$E_1 = \pi \sqrt{2} f \omega_1 \Phi_m = 4.44 f \omega_1 \Phi_m. \quad (14-7)$$

From this formula it follows that with a given frequency f and a number of turns ω_1 , the $E_1 = C_e \Phi_m$, i. e., *the flux Φ_m is directly proportional to the e. m. f. E_1 .*

The secondary is permeated by the same flux Φ_m . Therefore the effective value of the secondary e. m. f. is expressed by analogy to formula (14-7), as:

$$E_2 = \pi \sqrt{2} f \omega_2 \Phi_m = 4.44 f \omega_2 \Phi_m, \quad (14-8)$$

where w_2 is the number of the series-connected secondary turns. The e. m. f. \dot{E}_2 , and the e.m.f. \dot{E}_1 lag in phase on flux Φ_m by an angle $\frac{\pi}{2}$ (vector OD in Fig. 14-2, *b*).

The ratio

$$k = \frac{E_1}{E_2} = \frac{w_1}{w_2}, \quad (14-9)$$

as also the ratio $\frac{e_1}{e_2}$ [equation (13-14)], is referred to as *the transformation ratio of a transformer e. m. f.*, or simply as the *transformation ratio*.

It is common practice to determine the transformation ratio as the ratio of the greater e.m.f. value to the smaller e.m.f. value irrespective of which of the windings is the primary.

From expressions (14-7) and (14-8) for the e.m.f., we determine one of the most important values characterising the transformer and its properties, viz., the e. m. f. per turn:

$$E_{tm} = \frac{E_1}{w_1} = \frac{E_2}{w_2} = \pi \sqrt{2} f \Phi_m = 4.44 f \Phi_m. \quad (14-10)$$

C. The magnetising current $i_{0\mu}$. According to the law of the magnetic circuit, $\Phi_t = \frac{i_{0\mu} w_1}{R_u}$, where $i_{0\mu} w_1$ is the m. m. f. induced by the magnetising current $i_{0\mu}$; R_u is the core reluctance which comprises the steel reluctance and the core joints reluctance. If the transformer core steel is saturated, which is usual for power transformers, the curve shape of the current $i_{0\mu}$ and its amplitude depends on the degree of steel saturation. When we speak of the core steel, we shall have in view, as before, only hot-rolled steel. According to its magnetisation curve (Fig. 1-2), it may be assumed that the transformer steel is not saturated approximately up to a flux density of 0.8 wb/m^2 ; for this zone it may be assumed that the magnetising current is proportional to the flux density. The flux densities from 0.8 to 1.3 wb/m^2 correspond to the knee of the magnetisation curve, i.e., to a medium-saturated steel, and the flux densities above 1.3 wb/m^2 correspond to various degrees of steel saturation.

Fig. 14-3 shows the magnetising current curve $i_{0\mu} = f(t)$ plotted with the help of the magnetisation curve for the transformer sheet steel. Two points are taken on the flux density sine-curve $abcd$: point b for flux density $B_m = 1 \text{ wb/m}^2$ and point c for maximum flux density $B_m = 1.45 \text{ wb/m}^2$. The sequence of the plotting is shown in the figure by arrows ($b-f-g-h-k$ and $c-l-m-n-p$). By connecting a

number of such points, we may obtain the curve $akpd$ of the magnetising current $i_{0\mu}$ for the elementary transformer.

It is evident that, with a sine-wave flux, the no-load current of a transformer with saturated steel is non-sinusoidal (curve 4 in Fig. 14-2,a). The $i_{0\mu}$ curve may be resolved into a series of harmonics (Fig. 14-3). Since this curve is symmetrical in respect to the abscissa axis, the harmonic component series contains only odd order harmonics—the first, the third, the fifth and so on with amplitudes I_{m1} , I_{m3} , I_{m5} , etc. The first harmonic component of the

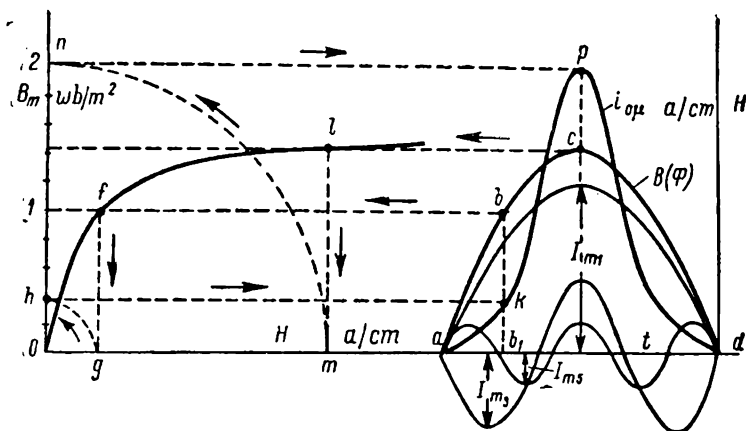


Fig. 14-3. Plotting of curve $i_{0\mu}=f(t)$ and harmonic resolution

magnetising current is in phase with the main flux and thus lags on the primary voltage by 90° . Of the higher current harmonics the most pronounced is the third. From the following discussion it will be seen that for some winding connections this harmonic renders considerable influence on three-phase transformer operation (§ 16-1). The higher order harmonics are much less pronounced than the third, and their influence may, therefore, be neglected.

The percentage content of the higher order harmonics in a no-load current curve is the larger the higher the flux density amplitude.

In Fig. 14-4 the ratio $\frac{I_{m3}}{I_{m1}}$ is determined by curve 1 and, correspondingly, the relation $\frac{I_{m5}}{I_{m1}}$ —by curve 2. The curves have been plotted for E4 grade hot-rolled steel. It may be seen that for the flux densities of the order of 1.4-1.45 wb/m², usually avail-

able in a power transformer core, the ratio $\frac{I_{m3}}{I_{m1}}$ attains 50 per cent, i.e., the curve for no-load operation acquires a noticeable peaked form.

Knowing the harmonic amplitudes in the no-load current curve, we can determine the effective value of this current by means of the well-known formula:

$$I_{0\mu} = \sqrt{\left(\frac{I_{m1}}{\sqrt{2}}\right)^2 + \left(\frac{I_{m3}}{\sqrt{2}}\right)^2 + \left(\frac{I_{m5}}{\sqrt{2}}\right)^2 + \dots} \quad (14-11)$$

Since the no-load current has a non-sine wave shape the vector diagram depicts only the first harmonic of this current $\vec{I}_{01} = \vec{OH}$ (Fig. 14-2,b) since vector diagrams can show values of only one periodicity. Thus the no-load diagram, in respect to the no-load current, is approximate; this should be kept in mind both in this case and when plotting diagrams later. But in practice approximate constructions are usually based on equivalent sine-wave no-load current having an effective value $I_{0\mu}$ [formula (14-11)].

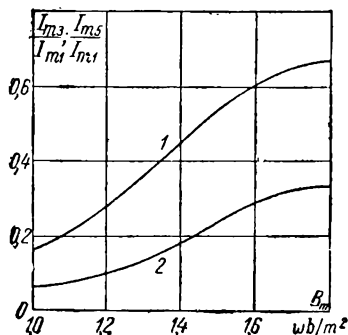


Fig. 14-4. Relationships I_{m3}/I_{m1} and $I_{m5}/I_{m1} = f(B_m)$ for transformer at no-load

Since the current I_{01} lags 90° on the voltage U_1 , the active power of this harmonic is zero; the power of the higher harmonics is also zero, their periodicity differing from the periodicity of the voltage U_1 . Consequently, the active power consumed by an elementary transformer from the power supply circuit is equal to zero, as it should be expected, since the losses in an elementary transformer were assumed to be zero.

14-4. No-Load Operation of a Commercial Single-Phase Transformer

Let us introduce corrections for the leakage and losses which were neglected in the case of an elementary transformer. The leakage flux of the primary produces in it a leakage e.m.f. and the losses during no-load operation of the transformer are compensated by power P_0 delivered to the transformer from the power circuit. In a single-phase transformer $P_0 = U_1 I_{0a}$, where I_{0a} is the effec-

tive value of the no-load current active component. Thus the no-load current of the real transformer has two components: a) the magnetising component with the effective value $I_{0\mu}$, which produces the main magnetic flux Φ and is in phase with it (Fig. 14-5) and b) the active component I_{0a} which is in quadrature with the former component. Substituting the real magnetising current curve shown in Fig. 14-3 for an equivalent sine-wave with the same effective value $I_{0\mu}$ as the real curve, and adding geometrically the components $I_{0\mu}$ and I_{0a} we obtain the current

$$I_0 = \sqrt{I_{0\mu}^2 + I_{0a}^2}.$$

As a rule, the current $I_{0a} < 10\%$ of the current I_0 ; and therefore it renders a negligible (often less than 0.5 per cent) effect on the no-load current value. Equally small is the angle α of lag of the flux Φ on the current I_0 , this angle often referred to as *the magnetic lag angle*.

The shape and phase of the no-load current are somewhat more affected by the current I_{0a} . We shall further deal only with hysteresis loss because in a transformer made of hot-rolled transformer sheet these losses amount to about 85 per cent of the power P_0 (at $f=50$ c/s). A broadened hysteresis loop is shown in Fig. 14-6. Each given flux density value B corresponds to the different no-load current values on the ascending and descending branches of the hysteresis loop. The no-load current curve was plotted here by the method shown in Fig. 14-3. Resolving the curve into a harmonic series, we find that the flux Φ lags on the first harmonic of the current i_{01} by an angle α_2 (Fig. 14-6).

By substituting the real curve of the no-load current for an equivalent sine-wave we may write the primary e. m. f. equation in the symbolic form, since all the values defining the no-load operation vary with time sinusoidally. According to the equation (13-22) we have:

$$U_1 = -\dot{E}_1 + \dot{I}_0 Z_1. \quad (14-12)$$

In accordance with the e.m.f. equation (14-12), a vector diagram of transformer no-load operation may be plotted.

Draw the vector of the main magnetic flux Φ_m in the positive direction of the abscissa axis (Fig. 14-7). The vector of the e. m. f. E_1 lags on the vector of the flux Φ_m by 90° . The vector of the second-

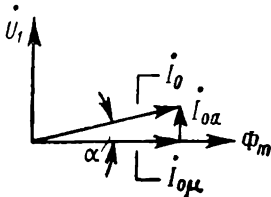


Fig. 14-5. Transformer no-load current component

ary e. m. f. E_2 is in phase with E_1 . The vector of the current I_0 is plotted by drawing its magnetising and active components, in the same way as in Fig. 14-5. The vector $\dot{E}_{c1} = -jI_0 x_1$ lags

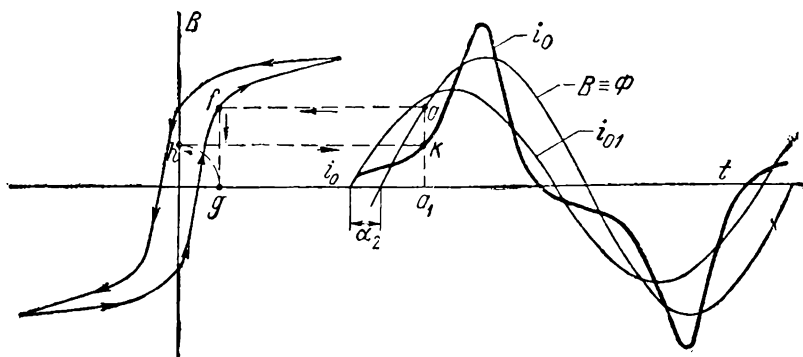


Fig. 14-6. Effect of hysteresis on no-load current curve

on the current vector I_0 by 90° ; the vector $-I_0 r_1$ is in antiphase with the current I_0 . To plot the vector of the voltage U_1 , it is necessary to add together geometrically the voltage components $-E_1$, $I_0 r_1$ and $jI_0 x_1$, each of which is equal in value to the corresponding e. m. f., but of opposite direction (or sign).

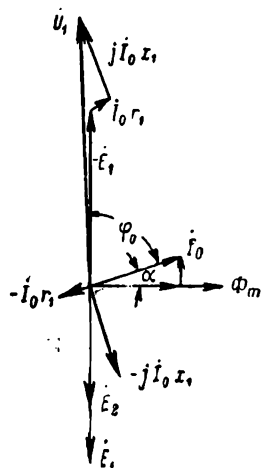


Fig. 14-7. Vector diagram of a transformer on no-load

In Fig. 14-7 the vectors $I_0 r_1$ and $jI_0 x_1$ are depicted, for clarity's sake, to a greatly enlarged scale in comparison with the e. m. f. E_1 . In power transformers, the voltage drop at no-load is usually less than 0.5 per cent of U_1 .

14-5. No-Load Transformer Losses

On no-load, the following losses occur in the transformer: 1) the losses in the copper of the primary $p_{cop1} = I_0^2 r_1$; 2) the main losses in the core steel p_{st0} ; and 3) the additional no-load losses p_{add0} .

The power P_0 consumed by a transformer on no-load is used entirely to cover the no-load losses. Hence it may be assumed that

$$P_0 = p_{cop1} + p_{st0} + p_{add0}. \quad (14-13)$$

Calculations show that the losses $p_{cop1} = I_0^2 r_1$ may be neglected since, even in low-power transformers with a relatively large current I_0 and resistance r_1 , this loss is usually less than 2 per cent of the total no-load losses. It may, therefore, be assumed that

$$P_0 = p_{st0} + p_{add0} = p_{st}, \quad (14-14)$$

i. e., the no-load power is practically utilised entirely as losses in the steel.

A. The main losses in core steel. These losses consist of hysteresis and eddy-current losses and may be estimated according to the formulas given in § 7-4.

It has been mentioned already that transformer cores are assembled of special transformer steel sheets 0.5-0.35 mm thick. The characteristics of this steel, both hot- and cold-rolled, and the magnetisation curves are given in the Introduction, Fig. 1-2.

At the present time, cold-rolled steel (E 310, E 320, E 330 grades) is being more and more used for transformer construction, since in comparison with the hot-rolled steel it is of greater permeability and has smaller specific losses. However, it is distinctly anisotropic, i. e., its high magnetic properties are observed only in the direction of roll, whereas in the direction across the roll the properties of the steel are much worse. The hot-rolled steel core designs are, therefore, not suitable for the cold-drawn steel cores. Special designs were required in which, however, the core assembling process becomes more complicated and labour-consuming. For small-power single-phase transformers spiral cores made of cold-rolled steel band without any joints are used (see Fig. 22-21).

B. The additional no-load losses. The main losses of these types are: a) losses in the sheets due to structural changes during mechanical working; b) losses in joints and pins due to uneven distribution of magnetic flux density; c) loss in construction components, i. e., in bolts, beams, clamping yokes, in the transformer tank, etc.; d) losses in the high-voltage transformer insulation.

The additional no-load losses cannot be precisely calculated. Therefore the transformer no-load losses are calculated by using tabulated data for the specific losses which already contain additional no-load losses. Investigations show that in transformers made of hot-rolled steel, all types of the no-load additional losses begin to increase sharply with flux density in the core exceeding 1.5 wb/m². The same investigations show that for usual flux densities in the transformer core, i.e., 1.45-1.47 wb/m², the addi-

tional losses p_{add} amount to 15-20 per cent of the main loss p_{st0} . Consequently,

$$p_{st} = p_{st0} + p_{add} = (1.15 \text{ to } 1.20) p_{st0}. \quad (14-15)$$

14-6. The Effect of Voltage-Curve Shape on Steel Losses

The previous discussion is the case when the curve of the voltage across a transformer is a sine function of time. The curves of the e.m.f. e , and flux Φ_t of a single-phase transformer therefore are sine-wave shaped (Fig. 14-2). With a non-sinusoidal voltage u , the shapes of the e.m.f. and flux curves change. In the general case, $\Phi_t = -\int e dt$, i.e., the flux is an integral function of the e.m.f. Hence, with an acute-shaped curve of the voltage and of the e.m.f., the flux curve has a flattened shape (see below Figs. 16-2 and 16-3) and vice versa. In the first case, the maximum value of the flux density B_{max} decreases, and in the second case it increases. The steel losses change accordingly, but differently for the hysteresis and for the eddy-current losses. Consider the losses in steel for a stipulated value of the voltage U , or—what is practically the same—of the e.m.f. E_1 , and for a given frequency f . With a non-sine curve shape of the e.m.f. E_1 , we have

$$E_1 = 4k_e f \omega_1 \Phi_m, \quad (14-16)$$

where k_e is the e.m.f. curve shape factor. Consequently,

$$\Phi_{max} = B_{max} = \frac{E_1}{k_e} = \frac{U_1}{k_e}.$$

As we know (Chapter 7), the hysteresis losses $p_h = B_m^2$, i. e., $p_h = \left(\frac{U_1}{k_e}\right)^2$; the eddy-current losses $p_{edd} = k_e^2 B_m^2$, i. e., $p_{edd} = U_1^2$. It follows therefore that *for a given effective value of the e. m. f., the hysteresis loss varies inversely as the square of the e. m. f. curve shape factor, whereas the eddy-current losses do not effect the curve shape*. Since the main losses in the transformer steel are the hysteresis losses, it may be assumed approximately that the total steel losses $p_{st} = \left(\frac{U_1}{k_e}\right)^2$. For a peaked e. m. f. curve the factor $k_e > 1.11$ and for a flattened shape curve $k_e < 1.11$; thus the steel losses in the first case decrease, and in the second case—increase, compared with losses in the case of a sine-shaped e. m. f. curve.

14-7. No-Load Transformer Equivalent Circuit

In accordance with the circuit in Fig. 14-3, the equivalent circuit of a transformer at no-load is as shown in Fig. 14-8,a. The no-load transformer diagram corresponding to this circuit is shown in Fig. 14-8,b.

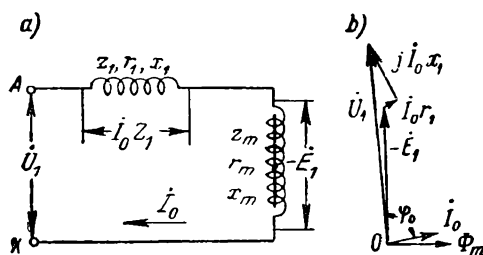


Fig. 14-8. Equivalent circuit and vector diagram of transformer on no-load

14-8. No-Load Transformer Test

The test is performed according to the scheme in Fig. 14-9. The voltage is usually fed to the low-voltage side of the winding. The primary and secondary voltages, U_1 and U_2 , the current I_0 and the power P_0 are measured by means of voltmeters V_1 and V_2 , ammeter A and the wattmeter W ; the frequency-meter F serves for frequency control. Applying a sine-wave voltage at rated frequency and then varying it within certain limits, we obtain the no-load data according to which the curves I_0 and $P_0 = f(U_1)$ may be plotted. In accordance with the rated voltage $U_n = 1$, the rated values for the no-load current I_{0n} and power P_{0n} (Fig. 14-10) are determined. With these data, we may determine the no-load transformer parameters.

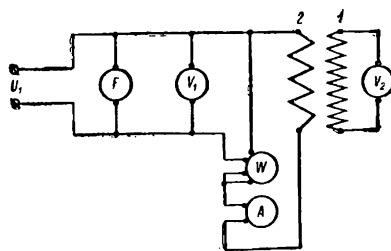


Fig. 14-9. Circuit for testing transformer on no-load

ters. From the scheme in Fig. 14-8,*a* it follows (for brevity the sign n is omitted)

$$\frac{\dot{U}_1}{I_0} = Z_0 = Z_1 + Z_m = (r_1 + jx_1) + (r_m + jx_m) = r_0 + jx_0. \quad (14-17)$$

In power transformers the resistances r_1 and x_1 are negligibly small compared with the r_m and x_m resistances (hundreds of times less). Without introducing any considerable error, we may assume that

$$\begin{aligned} \frac{\dot{U}_1}{I_0} &= Z_0 = r_0 + jx_0 \approx \\ &\approx Z_m = r_m + jx_m. \end{aligned} \quad (14-18)$$

If by calculation or experiment we determine the core steel losses p_{st} , then

$$r_m = \frac{p_{st}}{I_0^2}, \quad (14-19)$$

and hence

$$\begin{aligned} x_m &= \\ &= \sqrt{Z_m^2 - r_m^2} = \sqrt{\left(\frac{U_1}{I_0}\right)^2 - \left(\frac{p_{st}}{I_0^2}\right)^2}. \end{aligned} \quad (14-20)$$

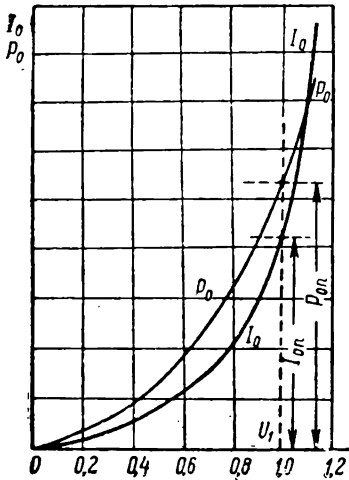


Fig. 14-10. Curves for I_0 and $P_0 = f(U_1)$

The no-load transformer test serves for determining the transformation ratio k of a transformer. Since, at no-load, $U_1 \approx E_1$ and $U_{20} = E_2$, then

$$k = \frac{E_1}{E_2} \approx \frac{U_1}{U_{20}}. \quad (14-21)$$

According to the State Standard 3484-54, the transformation ratio should be determined for all winding taps and for all phases at a lowered voltage. For large transformers with capacities exceeding 560 kVA, the impressed voltage usually amounts to several per cent of the rated voltage; for low-power transformers, this value is equal to a fraction of the rated voltage.

Chapter Fifteen

CLASSIFICATION OF MAGNETIC SYSTEMS AND WINDING CONNECTIONS FOR THREE-PHASE TRANSFORMERS. E.M.F.s OF THREE-PHASE TRANSFORMERS

15-1. Classification of Three-Phase Transformer Magnetic Systems

According to core design three-phase transformers may be distinguished as: a) transformers *with coupled magnetic systems* and b) transformers *with independent or quasi-independent magnetic systems*.

Fig. 15-1 shows a three-leg transformer with a coupled magnetic system. The characteristic feature of the transformer in Fig. 15-1 is the asymmetry of its magnetic system, since the lengths of the magnetic circuit of the core legs A , B and C are not equal: the length of the magnetic circuit in the middle leg B is shorter than that in the outside legs A and C . All three circuits converge at the nodes O_1 and O_2 . If Φ_A , Φ_B and Φ_C are the magnetic flux amplitudes in legs A , B and C , then according to the first Kirchhoff law in its application to magnetic circuits, we have for each node

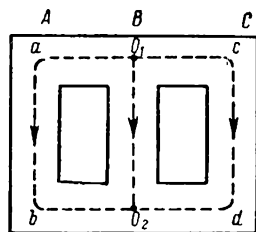


Fig. 15-1. Magnetic circuit of three-leg transformer

$$\dot{\Phi}_A + \dot{\Phi}_B + \dot{\Phi}_C = 0. \quad (15-1)$$

Let us assume that we consider an elementary transformer ($r_1=0$, $x_1=0$, $p_{st}=0$) fed by a sine-wave symmetrical voltage. In this case the voltages \dot{U}_A , \dot{U}_B , \dot{U}_C and the fluxes $\dot{\Phi}_A$, $\dot{\Phi}_B$, $\dot{\Phi}_C$ form regular three-ray stars, each flux vector lagging behind the corresponding voltage vector by a 90° angle (Fig. 15-2).

When the flux Φ_A passes along section O_1abO_2 (Fig. 15-1) a magnetic potential drop equal to $\Phi_A(R_{leg} + 2R_y)$ occurs, where R_{leg} is the leg reluctance and R_y is the reluctance of each half of the upper and lower yoke. Correspondingly, for the leg C we have $\Phi_C(R_{leg} + 2R_y)$. In leg B , the magnetic potential drop is $\Phi_B R_{leg}$. If F_A , F_B and F_C are the m. m. f. amplitudes corresponding to the fluxes Φ_A , Φ_B and Φ_C , then according to the second Kirchhoff law when

applied to magnetic circuits we have:
for the circuit $a-b-O_2-O_1$

$$\dot{\Phi}_A(R_{leg} + 2R_y) - \dot{\Phi}_B R_{leg} = \dot{F}_A - \dot{F}_B;$$

for the circuit $c-d-O_2-O_1$

$$\dot{\Phi}_C(R_{leg} + 2R_y) - \dot{\Phi}_B R_{leg} = \dot{F}_C - \dot{F}_B.$$

Besides, in systems without a neutral wire, the geometrical sum of currents and hence of the m.m.f.s in the three phases should be zero, i. e.,

$$\dot{F}_A + \dot{F}_B + \dot{F}_C = 0.$$

Solving these equations in regard to \dot{F}_A , \dot{F}_B and \dot{F}_C , we obtain:

$$\begin{aligned} \dot{F}_A &= (R_{leg} + 2R_y)\dot{\Phi}_A + \\ &\quad + \frac{2}{3}R_y\dot{\Phi}_B; \end{aligned} \quad (15-2a)$$

$$\dot{F}_B = R_{leg}\dot{\Phi}_B + \frac{2}{3}R_y\dot{\Phi}_B; \quad (15-2b)$$

$$\begin{aligned} \dot{F}_C &= (R_{leg} + 2R_y)\dot{\Phi}_C + \\ &\quad + \frac{2}{3}R_y\dot{\Phi}_B. \end{aligned} \quad (15-2c)$$

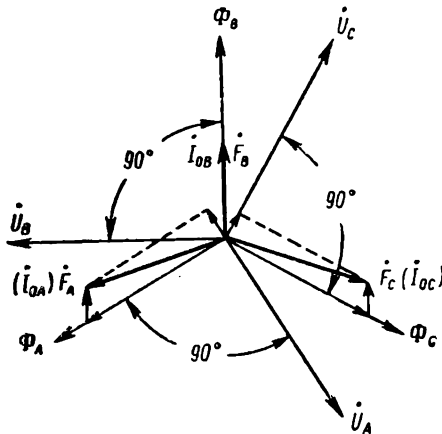


Fig. 15-2. Current diagram of three-leg transformer on no-load

From the equation (15-2b) it follows that the m. m. f. F_B depends only on the flux Φ_B , and, therefore, vector F_B is in phase with the flux vector Φ_B . On the contrary, the m.m.f.s F_A and F_C represent the geometrical sums of two m. m. f.s of which one is in phase with the given flux, while the other is in phase with the flux Φ_B . The vector of the m. m. f. F_A lags on the flux vector Φ_A by some angle, and the m.m.f. vector F_C leads the flux vector Φ_C by the same angle. Thus, the m.m.f.s F_A , F_B and F_C and, therefore, the magnetising currents I_{0A} , I_{0B} and I_{0C} form asymmetrical systems in which $F_A = F_C > F_B$ or, correspondingly,

$$I_{0A} = I_{0C} > I_{0B}$$

(the solid lines in Fig. 15-2).

The no-load current asymmetry is manifest mainly in low-power transformers, where the yoke plays a relatively greater role.

Here $I_{0A} \approx I_{0C} = (1.2 \text{ to } 1.5) I_{0B}$. In large-power transformers, the asymmetry is substantially smoothed out. According to State Standard 401-41, the no-load current I_0 is assumed to be the arithmetic average of the currents I_{0A} , I_{0B} and I_{0C} . As the current I_0 is small (3 to 8 per cent of I_n) the asymmetry of the no-load currents, even in low-power transformers, is no longer manifest even at a very small load.

Since the current I_{0B} lags on the voltage U_B by 90° , the B -phase power is equal to zero; the C -phase power is positive, because the projection of current I_{0C} upon the direction of vector U_C is positive; the A -phase power is equal to the C -phase power in magnitude and is of the opposite sign, since the current I_{0A} projection upon the vector U_A direction is negative. Thus, on no-load, in the three-leg transformer the phases C and A exchange power, but the full power of the transformer on no-load is equal to zero, as it ought to be, since we consider an elementary transformer. The uneven distribution of power at no-load, as well as the current asymmetry, is of minor importance, since this power amounts usually only to 1 per cent of the transformer rated power.

An example of a three-phase transformer with an independent magnetic system is the *three-phase transformer bank* or, otherwise, a *banked transformer* (see below, Fig. 16-1) which represents three identical single-phase transformers, the windings of which are in a certain manner connected together.

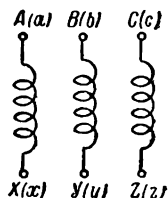
A shell-type transformer may serve as an example of a transformer with a practically independent magnetic system. We shall confine all further discussions to the three-leg transformer and a three-phase transformer bank.

15-2. Methods of Connecting Three-Phase Transformer Windings

Each of the three-phase transformer windings, both primary and secondary, may be: a) star connected, b) delta connected and c) zigzag connected. The most important connections are the star and delta winding connections. The zigzag connections are discussed below in § 15-6.

Irrespective of the connection method, the ends of each phase winding in a three-phase system are referred to as the *beginning* and the *end* of a winding. For any one phase winding the choice of the beginning and the end is arbitrary. Let us assume, for example, that the beginning of the first winding is the end point from which we would wind the winding clockwise (R. H. winding, see Fig. 15-3). Then the beginnings of the two other windings would

be those ends from which they may be wound in the same direction as the first winding. Let us agree to designate the beginnings of the high-voltage three-phase transformer winding by the letters A , B and C , and its ends by the letters X , Y and Z ; the beginnings and ends of the low-voltage winding would be, correspondingly, a , b , c and x , y , z . For brevity's sake the phase windings will further be denoted only by the first letters.



15-3. Three-Phase Winding E.M.F.s

Fig. 15-3. Beginnings and ends of three-phase winding

In the general case, the e.m.f.s e_A , e_B and e_C in the phase windings A , B and C are non-sine-wave. Assuming only odd harmonics present and assuming also the initial phase $\psi=0$, we have for the winding A :

$$e_A = E_{m1} \sin \omega t + E_{m3} \sin 3\omega t + E_{m5} \sin 5\omega t + E_{m7} \sin 7\omega t + \dots \quad (15-3a)$$

Correspondingly, for the B and C phases we have:

$$\begin{aligned} e_B &= E_{m1} \sin \left(\omega t - \frac{2\pi}{3} \right) + E_{m3} \sin 3 \left(\omega t - \frac{2\pi}{3} \right) + \\ &+ E_{m5} \sin 5 \left(\omega t - \frac{2\pi}{3} \right) + E_{m7} \sin 7 \left(\omega t - \frac{2\pi}{3} \right) + \dots = \\ &= E_{m1} \sin \left(\omega t - \frac{2\pi}{3} \right) + E_{m3} \sin 3\omega t + E_{m5} \sin \left(5\omega t - \frac{4\pi}{3} \right) + \\ &+ E_{m7} \sin \left(7\omega t - \frac{2\pi}{3} \right) + \dots \end{aligned} \quad (15-3b)$$

and

$$\begin{aligned} e_C &= E_{m1} \sin \left(\omega t - \frac{4\pi}{3} \right) + E_{m3} \sin 3 \left(\omega t - \frac{4\pi}{3} \right) + \\ &+ E_{m5} \sin 5 \left(\omega t - \frac{4\pi}{3} \right) + E_{m7} \sin 7 \left(\omega t - \frac{4\pi}{3} \right) + \dots = \\ &= E_{m1} \sin \left(\omega t - \frac{4\pi}{3} \right) + E_{m3} \sin 3\omega t + E_{m5} \sin \left(5\omega t - \frac{2\pi}{3} \right) + \\ &+ E_{m7} \sin \left(7\omega t - \frac{4\pi}{3} \right) + \dots \end{aligned} \quad (15-3c)$$

From the equations (15-3a), (15-3b) and (15-3c) we may see that: a) the first e. m. f. harmonic in the phases A , B and C constitute a symmetrical three-ray star with a phase sequence $E_{A1} - E_{B1} - E_{C1}$ (Fig. 15-4, a), b) the third e. m. f. harmonics and, accordingly, the harmonics divisible by three, in all three phase windings are

in phase (Fig. 15-4,*b*) and, consequently, irrespective of the winding connection method, are directed, in each phase winding, either from the beginning to its end or in the opposite direction; *c*) the fifth and seventh e. m. f. harmonics, the same as the first harmonic, form symmetrical three-ray stars, but compared with the

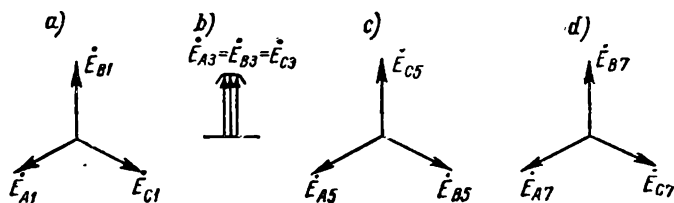


Fig. 15-4. First, third, fifth and seventh e.m.f. harmonics of a three-phase winding

first harmonic, the fifth harmonic has a reverse phase sequence $E_{A5}-E_{C5}-E_{B5}$ (Fig. 15-4,*c*), while the seventh harmonic has the same order as the first harmonic (Fig. 15-4,*d*). In the general case, the harmonics of the $3c+1$ order where c is any even number, have the same phase sequence as the first harmonic obtained at $c=0$, while harmonics of order $3c-1$ have the opposite phase sequence.

15-4. Star-Connected Three-Phase Winding

When a three-phase winding is star-connected either the three beginnings are joined to one common neutral point, leaving the ends free, or the three ends are joined to the neutral leaving the

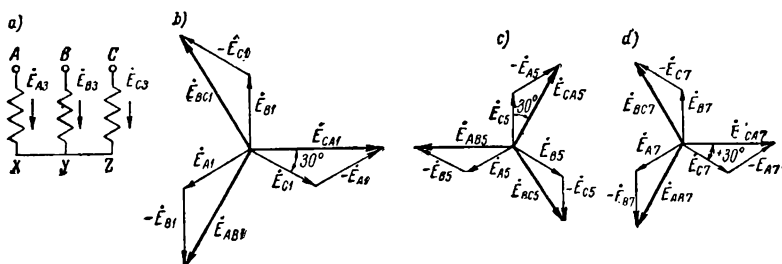


Fig. 15-5. Vector diagrams of e.m.f. for star-connected three-phase winding

beginnings free (Fig. 15-5,*a*). Making the round of any of the three circuits constituting the star, for instance, the circuit $(A \cdot X) - (Y \cdot B)$, we proceed first along winding *A* from its beginning *A* to

the end X , and along winding B from its end Y to beginning B , i. e., we change the direction of the round along winding B in respect to winding A . In this case, the instantaneous values of the line e. m. f.s are

$$e_{AB} = e_A - e_B; \quad (15-4a)$$

$$e_{BC} = e_B - e_C; \quad (15-4b)$$

$$e_{CA} = e_C - e_A. \quad (15-4c)$$

Substituting in these equations for the e. m. f.s e_A , e_B and e_C , we obtain:

$$\begin{aligned} e_{AB} = e_A - e_B &= E_{m1} \sin \omega t - E_{m1} \sin \left(\omega t - \frac{2\pi}{3} \right) + E_{m3} \sin 3\omega t - \\ &- E_{m3} \sin 3\omega t + E_{m5} \sin 5\omega t - E_{m5} \sin \left(5\omega t - \frac{4\pi}{3} \right) + \\ &+ E_{m7} \sin 7\omega t - E_{m7} \sin \left(7\omega t - \frac{2\pi}{3} \right) + \dots = \\ &= \sqrt{3} E_{m1} \sin \left(\omega t + \frac{\pi}{6} \right) + \sqrt{3} E_{m3} \sin \left(5\omega t - \frac{\pi}{6} \right) + \\ &+ \sqrt{3} E_{m7} \sin \left(7\omega t + \frac{\pi}{6} \right) + \dots \end{aligned} \quad (15-4a)$$

accordingly

$$\begin{aligned} e_{BC} = e_B - e_C &= \sqrt{3} E_{m1} \sin \left(\omega t + \frac{\pi}{6} - \frac{2\pi}{3} \right) + \\ &+ \sqrt{3} E_{m3} \sin \left(5\omega t - \frac{\pi}{6} + \frac{2\pi}{3} \right) + \\ &+ \sqrt{3} E_{m7} \sin \left(7\omega t + \frac{\pi}{6} - \frac{2\pi}{3} \right) + \dots \end{aligned} \quad (15-4b)$$

and

$$\begin{aligned} e_{CA} = e_C - e_A &= \sqrt{3} E_{m1} \sin \left(\omega t + \frac{\pi}{6} - \frac{4\pi}{3} \right) + \\ &+ \sqrt{3} E_{m3} \sin \left(5\omega t - \frac{\pi}{6} + \frac{4\pi}{3} \right) + \\ &+ \sqrt{3} E_{m7} \sin \left(7\omega t + \frac{\pi}{6} - \frac{4\pi}{3} \right) + \dots \end{aligned} \quad (15-4c)$$

From the equations (15-4a), (15-4b) and (15-4c) it follows that in the case of a star connection:

a) The harmonics with the order divisible by three disappear in the line voltage; physically this may be explained by the fact that along the paths of each of the two circuits composing the star these harmonics are mutually opposed (Fig. 15-5,a);

b) The line voltages of all $3c+1$ harmonics including the fundamental, i. e., the first harmonic, represent symmetrical three-phase voltage systems of positive sequence with the initial phase

$\psi = +30^\circ$ (Fig. 15-5,b and 15-5,d), and, respectively, the voltages of all $3c - 1$ harmonics represent symmetrical three-phase systems with reversed phase sequence and with the initial phase $\psi = -30^\circ$ (Fig. 15-5,c);

c) The line voltage amplitude of any $3c \pm 1$ harmonic is $\sqrt{3}$ times greater than the phase voltage amplitude of the corresponding harmonic, i. e.,

$$E_{m,l} = \sqrt{3} E_{m,ph}, \quad (15-5)$$

where $v = 3c \pm 1$ is the harmonic order.

When using effective values of the phase and line e. m. f.s, we have the following:

$$E_{ph} = \sqrt{\frac{1}{2} (E_{m1}^2 + E_{m3}^2 + E_{m5}^2 + E_{m7}^2 + \dots)} \quad (15-6)$$

and

$$E_l = \sqrt{\frac{3}{2} (E_{m1}^2 + E_{m3}^2 + E_{m5}^2 + \dots)}. \quad (15-7)$$

It follows from this that

$$E_l = E_{ph} \sqrt{3 \frac{1 + k_{e3}^2 + k_{e7}^2 + \dots}{1 + k_{e3}^2 + k_{e5}^2 + k_{e7}^2 + \dots}}, \quad (15-8)$$

where

$$k_{ev} = \frac{E_{mv}}{E_{m1}} = \frac{E_v}{E_1}. \quad (15-9)$$

Since with a star-connected winding, the phase currents are directly fed to the power circuit, then

$$I_l = I_{ph}. \quad (15-10)$$

As is known from electrical engineering theory, with non-sinusoidal e. m. f.s and currents, the power of the system is equal to the sum of the powers of separate harmonics. Usually, the power of the first or fundamental harmonic is the most important. For this harmonic we have:

$$P_1 = 3 E_{ph1} I_{ph1} \cos \varphi = \sqrt{3} E_{l1} I_{l1} \cos \varphi, \quad (15-11)$$

where φ is the phase angle between the e. m. f. E_{ph1} and current I_{ph1} .

15-5. Delta-Connected Three-Phase Winding

In the case of a delta-connected winding, the beginning of a subsequent phase winding is joined to the end of the previous winding. The connection of windings is possible: a) according to

scheme $(A-X) - (B-Y) - (C-Z) - A$ (Fig. 15-6, *a*) and *b*) according to scheme $(A-X) - (C-Z) - (B-Y) - A$ (Fig. 15-6, *b*).

Let i_{AX} , i_{BY} and i_{CZ} be the instantaneous current values in the phase windings A, B and C , and i_A, i_B, i_C be the instantaneous current

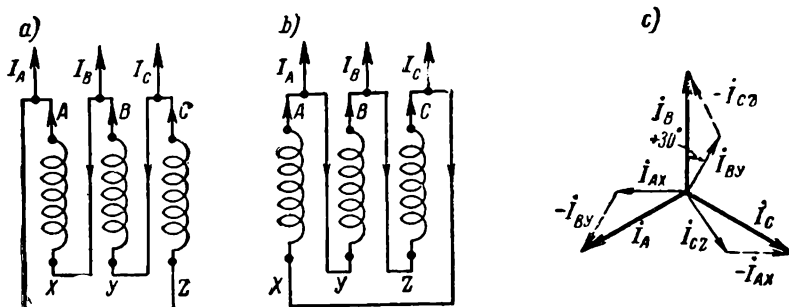


Fig. 15-6. *a* and *b* — delta connections of three-phase winding; *c* — current diagram

values in the lines connected to the beginnings of the windings A, B and C . Then for the scheme in Fig. 15-6, *a* we have

$$i_A = i_{AX} - i_{BY}; \quad (15-12a)$$

$$i_B = i_{BY} - i_{CZ}; \quad (15-12b)$$

$$i_C = i_{CZ} - i_{AX}. \quad (15-12c)$$

The corresponding vector diagram for first current harmonics is depicted in Fig. 15-6, *c* (subscript I in the diagram is omitted). The line current vector leads the phase current vector by 30° , the line current being

$$I_{L1} = I_{ph1} \sqrt{3}. \quad (15-13)$$

In respect to the third harmonic and its multiples, a delta connection is a closed circuit in which all these harmonics act in the same direction—either from the beginning of each phase winding to its end or in the reverse direction. The effective value of harmonics that are multiples of the third is equal to:

$$E_{s\Delta} = \sqrt{E_3^2 + E_6^2 + \dots}. \quad (15-14)$$

The e. m. f. $E_{s\Delta}$ may be measured if we open one of the delta nodes, for instance, node $B-Z$ (Fig. 15-7), and insert a voltmeter in series with the winding.

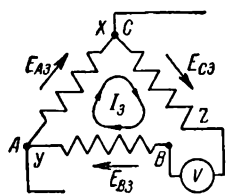


Fig. 15-7. Third e.m.f. and current harmonics for delta-connected windings

Acting around the closed delta circuit, the e. m. f. E_{Δ} produces in it a current I_s , which may be measured if we insert in series with the windings an ammeter instead of the voltmeter. In the line voltages, the e. m. f. E_{Δ} does not appear, since in a closed delta it is fully utilised to balance the voltage drop due to current I_s .

15-6. Zigzag-Connected Three-Phase Winding

The idea of this method is that each phase winding on the low-voltage side is divided into two, most often, equal parts and these parts are placed on different legs (Fig. 15-8,a). The two parts are so connected that their e.m.f.s are geometrically

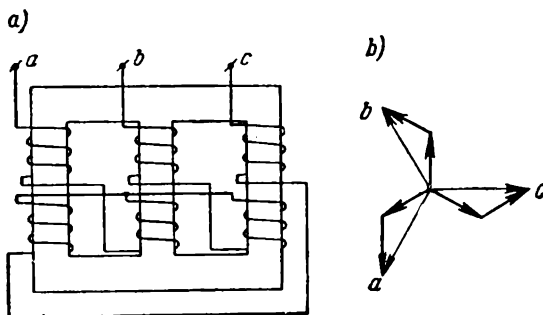


Fig. 15-8. Zigzag connection

subtracted; for this purpose the end of each phase winding half is joined to the end of the other half of the same winding. If in this case the phase windings are divided in half, the resultant e.m.f. of a phase winding is $\sqrt{3}$ times the e.m.f. in each half (Fig. 15-8,b).

The zigzag-connection is used in special transformers, for instance, in transformers for mercury arc rectifiers, discussed in detail in § 22-6.

15-7. Standard Methods of Connecting Three-Phase Transformer Windings

It has been agreed to designate star-, delta- and zigzag-connections by conventional symbols Y , Δ and Z . First, the method for connecting the high-voltage winding is denoted, then the

method for the low-voltage winding, an inclined line being drawn between both notations.

If any winding has a tapped neutral point, the sign 0 is added to the conventional symbol. Thus, the notation Y_0/Δ reads as follows: the high-voltage winding is star-connected and has a tapped neutral, the low-voltage winding is delta-connected.

Connection methods such as Z/Y , Z/Δ and Z/Z are not employed. Hence, the following six methods of connecting three-phase transformer windings are practically possible: 1) Y/Y_0 or Y/Y , 2) Y/Δ , 3) Y/Z or Y/Z_0 , 4) Δ/Y , 5) Δ/Δ and 6) Δ/Z or Δ/Z_0 .

Since any of the windings may be turned "inside out" in respect to the other, for instance, it may be wound in a reverse direction in regard to the former, twelve different methods of connecting the three-phase transformer windings can be obtained. Some of the foreign standards stipulate all these methods, but the U.S.S.R. Standard 401-41 leaves only three, namely: a) Y/Y_0 , b) Y/Δ and c) Y_0/Δ . In further discussions we shall consider only these standard methods of winding connections.

15-8. Winding Diagrams and Connection Groups

The winding connection diagrams for the three-phase two-winding transformers adopted by the State Standard 401-41 are shown in Fig. 15-9. The beginnings and ends of the high- and low-voltage windings are denoted here as stated above (§ 15-2). When plotting these diagrams, line voltages of the high-voltage windings (broken lines in Fig. 15-9) are in all cases depicted as equilateral voltage triangles, with the apexes A , B and C in the lower left corner, upper corner and lower right corner respectively. When we speak of transformer operation, we must foresee the possibility of their being operated in parallel for which only equipotential terminals may be connected. Therefore, indication as to the method of the transformer winding connection alone is not sufficient, it is yet necessary to indicate the phase angle α between the primary and secondary line voltages, in accordance with which the *group* to which the transformer belongs is determined. Let us show that the angle α depends on: a) the direction in which the winding is wound; b) the method of the winding terminal notation, i. e., their marking; c) the method of connecting the three-phase transformer windings.

Let us first make clear the effect of the first two factors, taking a single-phase transformer as an example. Consider the upper transformer winding in Fig. 15-10, a as the transformer primary,

and the lower its secondary. Suppose both these windings are wound in the same direction and the upper terminals have been chosen as the winding beginnings and designated by letters A and a , while the lower terminals marked X and x are the winding ends.

	Winding connections		Vector diagrams		Symbols
	B. H.	H. H.	B. H.	H. H.	
a)					Y/Y_0-12
b)					$Y/\Delta-11$
c)					$Y_0/\Delta-11$

Fig. 15-9. Winding connections of three-phase two-winding transformers (here B. H.=H. V.; H. H.=L.V.)

Since both windings of the transformer are placed on the same leg and are permeated by the same main flux, the e.m.f.s induced in this case at any instant have, in respect to the winding terminals, the same direction, for instance, from the end X to the beginning A in the primary and from the end x to the beginning a in the secondary. In accordance with this, the voltages U_1 and U_2 at the terminals of the primary and of the referred to it transformer secondary windings are in phase and indicated by two vectors \overline{OA} and \overline{Oa} equal in magnitude and of the same direction (Fig. 15-10, b).

If the primary and the secondary are wound in different directions, but retain the same terminal notations as in Fig. 15-10, a, then, as it may be seen in Fig. 15-10, c, the voltages U_1 and U_2

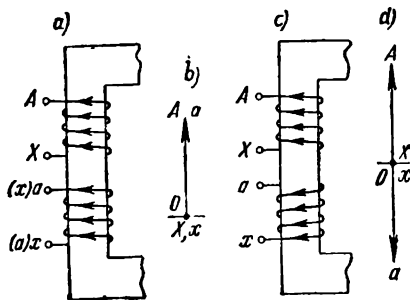


Fig. 15-10. E.m.f. vector angle in relation to winding direction and marking

are of different directions in respect to the primary and secondary terminals, for instance, from X to A in the primary and from a to x in the secondary. Accordingly, the voltages \dot{U}_1 and \dot{U}_2 should be represented by vectors \overrightarrow{OA} and \overrightarrow{Oa} differently directed (Fig. 15-10, d).

We would obtain the same results, if in retaining the same winding method as in Fig. 15-10, a we would change the marking of the secondary by changing positions of its terminal notations (the corresponding letters in Fig. 15-10, a are in brackets). In this case, the primary voltage would be in one direction, for instance, from terminal X to terminal A , while the secondary voltage would be in the other direction, i. e., from terminal a to terminal x .

Thus, considering the primary voltage vector \overrightarrow{OA} as the initial vector, we may say that the vector \overrightarrow{Oa} of the secondary voltage for a single-phase transformer is either in phase with vector \overrightarrow{OA} or in antiphase with it; in the first case the vector \overrightarrow{Oa} is displaced in respect to vector \overrightarrow{OA} by an angle $\alpha=0^\circ$, but in the second case it is displaced by an angle $\alpha=180^\circ$.

Instead of expressing the phase angle between the voltages in degrees, it is more convenient to use the *clock method* of angle designation. With this method vector \overrightarrow{OA} of the primary line voltage is considered as the minute watch hand and set at 12 o'clock. The vector \overrightarrow{Oa} of the secondary line voltage is then considered to be the hour hand and is set on the dial in respect to the position of vector \overrightarrow{Oa} in relation to vector \overrightarrow{OA} . If the vectors \overrightarrow{OA} and \overrightarrow{Oa} are in phase as in Fig. 15-10, b , the hour hand should be set same as the minute hand, at 12 o'clock (Fig. 15-11). The displacement angle between the watch hands is, evidently, zero or, which is the same, $360^\circ=30^\circ \times 12$. Here, the angle 30° represents the angle between two adjacent figures on the clock dial and is regarded as the unit of the dial shift. Thus figure 12 determines the group to which in the given case the transformer belongs.

If the vectors \overrightarrow{OA} and \overrightarrow{Oa} are in antiphase, as shown in Fig. 15-10, d , the hour hand should be set at 6 hours in accordance with the shift angle $30^\circ \times 6=180^\circ$. In this case the transformer group is determined by the figure 6.

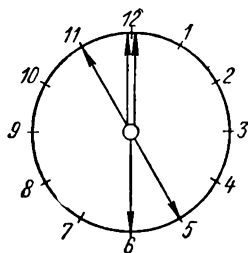


Fig. 15-11. Clock notation of connection groups

Now let us consider the point on three-phase transformer groups. Suppose that both windings of the transformer are star-connected, wound the same direction, and have the same terminal markings. The high-voltage winding will be considered the

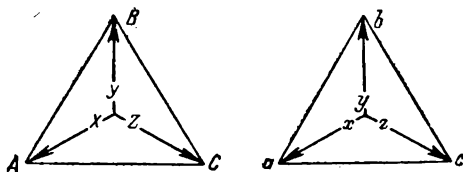


Fig. 15-12. Y/Y-12 connection

primary, the low-voltage winding, the secondary. The systems of the line and phase primary and secondary voltages are supposed symmetrical. Since the secondary in all respects repeats the primary, the star ax , by and cz of the secondary phase voltages and the triangle abc of the secondary line voltages are in phase with the star AX , BY and CZ and the triangle ABC of the phase and line primary voltages (Fig. 15-12). Thus, the phase angle of the secondary line voltage in respect to the primary voltage is zero and, therefore, the transformer belongs to the group Y/Y-12 ($\alpha=0^\circ$ or $\alpha=30^\circ \times 12$).

If we wind the low-voltage winding in the direction opposite to the high-voltage winding direction or change places of the beginnings and ends (but not both simultaneously), then for a star-connection of both windings as before, the voltage triangle abc would turn 180° in respect to the triangle ABC , i. e., by $30^\circ \times 6$ (Fig. 15-13). In this case, the hour hand should be set at 6 hours (Fig. 15-11). Consequently, the given winding connection belongs to the group 6 and is designated as Y/Y-6 or Y/Y_o-6.

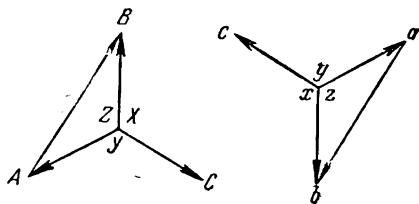


Fig. 15-13. Y/Y-6 connection

Now let us consider the star-delta connection in Fig. 15-9, *b*. Here the low-voltage winding is connected according to the scheme $a-x-c-z-b-y-a$. The sides AB , BC and CA of the voltage triangle ABC represent the line voltages of the high-voltage winding, and the star rays of the same triangle are the phase voltages of this winding. If the high- and low-voltage windings are wound in the

same direction and have the same terminal markings, the phase voltage vectors of both windings coincide. Therefore, when plotting the triangle abc it is necessary to draw from point a (Fig. 15-14), in the lower left angle, the vector \overline{ax} parallel to the vector \overline{AX} , then from the point c , which is to be superposed with the point x , the vector \overline{cz} should be drawn, parallel to vector \overline{CZ} and, finally, from point b , which is to be superposed with point z , the vector \overline{by} should be drawn parallel to the vector \overline{BY} , thereby closing the triangle abc . Comparing the positions of the triangles ABC and abc , for instance, the sides AB and ab , it is evident that the second triangle is turned in respect to the former clock-

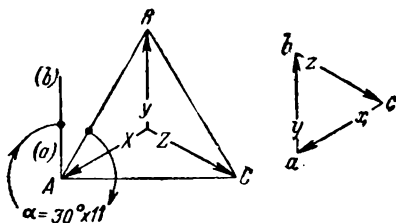


Fig. 15-14. Y/Δ-11 connection

wise by $330^\circ = 30^\circ \times 11$. Consequently, this winding connection belongs to group 11 and its symbol is Y/Δ-11.

If the low-voltage winding is wound in opposition to the high-voltage winding direction or we would change beginnings and ends, the triangle abc would turn in respect to the triangle ABC

by $150^\circ = 30^\circ \times 5$. Hence, such a winding connection gives group 5 and the symbol is Y/Δ-5. It is easy to show that, if we connect the low-voltage winding according to the scheme $a-x-b-y-c-z-a$, then for the same winding direction and terminal marking we would obtain group Y/Δ-1.

The groups 12, 6, 11 and 5 are considered the fundamental groups. From these a number of derivative groups may be obtained. For this purpose it is necessary only to change the place of the low-voltage winding terminals in respect to the high-voltage winding terminals. In Fig. 15-15, a , both windings are star-connected and wound in the same direction, but the terminals a, b, c of the secondary are displaced in respect to the terminals A, B, C of the primary by an angle 120° ; in this case the triangle abc will turn in respect to triangle ABC clockwise by $30^\circ \times 4 = 120^\circ$, i. e., we have the connection group Y/Y-4.

If, observing the same conditions, we displace the terminals a, b, c in respect to terminals A, B, C by 240° (Fig. 15-15, b), we would obtain the connection group Y/Y-8.

In the case, when the low-voltage winding is wound in a direction opposite to the high-voltage winding, we obtain groups 10 and 2 corresponding to groups 4 and 8.

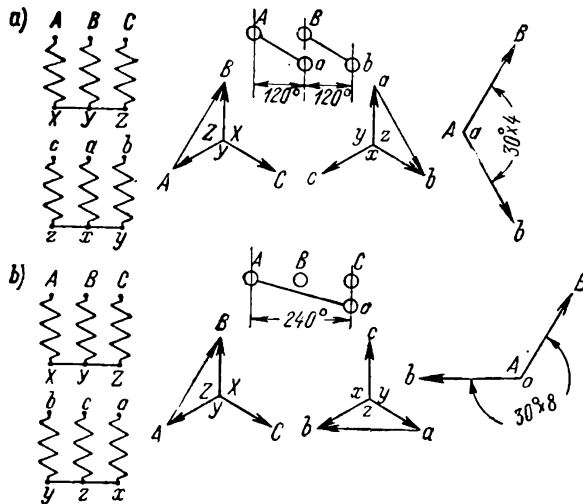


Fig. 15-15. Y/Y-4 and Y/Y-8 connection groups

Thus, in the case of star-star connection, all the even connection groups are obtained. By similar reasoning it is possible to make sure that in the case of star-delta winding connections all the odd connection groups are obtained.

15-9. Application of Various Winding Connection Methods

The connection Y/Y_0-12 is used in cases when the load is of a mixed illumination-power nature. The motors are connected for line voltage of 220 or 380 V, while the lamps are connected between one of the line wires and the neutral wire, i.e., across the voltage $\frac{220}{\sqrt{3}} = 127$ V or $\frac{380}{\sqrt{3}} = 220$ V. Since with a given voltage the current increases in proportion to the power, to avoid difficulties of winding arrangements for large currents, the State Standard 401-41 restricts the maximum transformer power in the case of Y/Y_0-12 connection within the limits shown in Table 15-1. If, in this case, the load is irregular the current in the transformer neutral wire should not exceed 25 per cent of the rated current of the low-voltage winding.

In those cases when the rated secondary voltage exceeds 400 V, the Standard 401-41 stipulates the use of the $Y/\Delta-11$ winding connec-

tion. As will be seen from the following, a delta-connection of one of the two windings renders a valuable positive effect on transformer operation conditions.

Table 15-1

Voltages and Powers of Transformers with Various Winding Connections

Winding connection symbols	Winding voltage		Transformer power, kVA
	high-voltage, kV	low-voltage, V	
Y/Y_0-12	Up to 35 (inclusive) Ditto	230 400	Up to 560 (inclusive) Up to 1,800 (inclusive)
$Y/\Delta-11$	Up to 35 (inclusive)	525 Above 525	Up to 1,800 (inclusive) Up to 5,600 (inclusive)
$Y_0/\Delta-11$	110 and higher 6.3 and higher	3,150 and higher 3,300 and higher	3,200 and higher 7,500 and higher

The last transformer group shown in Table 15-1 pertains chiefly to transmission lines. The winding connection of these transformers by the method of $Y_0/\Delta-11$ provides the possibility of grounding the system on the high-voltage side.

Chapter Sixteen

NO-LOAD OPERATION OF THREE-PHASE TRANSFORMER

16-1. Transformer on No-Load with Y/Y_0-12 Winding Connection

When we investigated no-load operation of a single-phase transformer we saw that, with an impressed sinusoidal voltage, the curves of the primary e.m.f. and of the main flux are sine-shaped, while the current curve contains, in addition to the first harmonic, a strongly pronounced third harmonic (see Fig. 14-3).

Consider a transformer bank consisting of three identical single-phase transformers with a Y/Y_0-12 connection (Fig. 16-1).

The principal difference between no-load operation of such a transformer bank and the no-load operation of a single-phase transformer is that there are *no third harmonics of current in it*.

This follows directly from what was discussed above (§ 15-3). By analogy with formulas (15-3a), (15-3b) and (15-3c) for the third current harmonics we have:

$$i_{oA3} = I_{o3m} \sin 3\omega t; \quad (16-1a)$$

$$i_{oB3} = I_{o3m} \sin 3\left(\omega t - \frac{2\pi}{3}\right) = I_{o3m} \sin 3\omega t; \quad (16-1b)$$

$$i_{oC3} = I_{o3m} \sin 3\left(\omega t - \frac{4\pi}{3}\right) = I_{o3m} \sin 3\omega t. \quad (16-1c)$$

Thus, the third current harmonics, like the third e.m.f. harmonics, are in phase and, consequently, each of these harmonics at any instant is directed either from the beginning of the winding

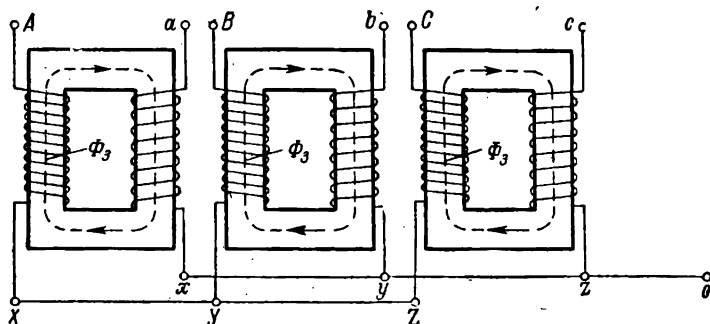


Fig. 16-1. Transformer bank with Y/Y_0-12 winding connection

to its end or in the opposite direction. Therefore, when the windings are star-connected the third harmonic currents drop out of the no-load curve, since at any given instant they are either all directed to the neutral point or from it.

The fifth harmonic currents continue to exist in the no-load curve, but in accordance with the above discussion [formulas (15-3a), (15-3b) and (15-3c)] they have a reversed phase sequence.

The absence of the third harmonic in the no-load current curve distorts the magnetic flux curve. In Fig. 16-2 the curves of the current i_0 and the flux Φ are shown with the third harmonic i_{o3} present in the current i_0 curve (Fig. 16-2, a) and when absent from this curve (Fig. 16-2, b). In the first case the curve of the flux Φ is sinusoidal. The dropping-out of the third harmonic i_{o3} may be represented as the superposition on the i_0 curve in Fig. 16-2, a of a third harmonic current curve oppositely directed,

i. e., $-i_{03}$. Accordingly, onto the sine-wave curve of the flux Φ should be superposed the curve of the flux Φ_3 produced by the current $-i_{03}$ (the thin dotted lines in Fig. 16-2, *b*); the curve of the resultant flux Φ is shown in Fig. 16-2, *b* by a thick broken line.

Since each phase of the transformer has its own separate magnetic system (Fig. 16-1), the magnetic flux Φ_3 closes along the same path as the flux Φ_1 , i.e., along a path with a low reluctance.

Therefore, in a three-phase bank the magnitude of the Φ_3 flux amounts in certain cases to 15-20 per cent of Φ_1 . With a strongly pronounced third harmonic of the flux Φ_3 , the curve of the resultant flux Φ becomes saddle-shaped.

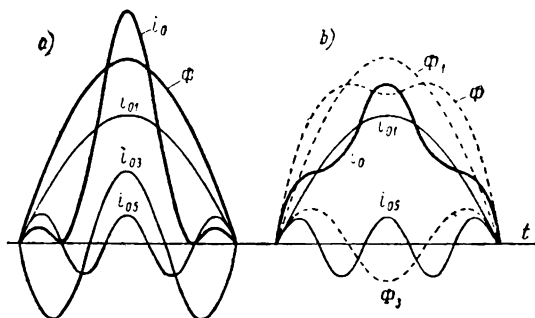


Fig. 16-2. Curves of current i_0 and flux Φ :
a—with third harmonic present in i_0 current curve; *b*—with third harmonic absent in i_0 curve

The flux Φ_3 induces e.m.f.s e_{13} and e_{23} in the transformer primary and secondary windings, and since the flux varies with a frequency $f_3 = 3f$, the e.m.f.s of triple frequency induced by it reach 45-60 per cent of the e.m.f.s e_1 and e_2 . At the same time, as can be seen from the comparison of the e.m.f. curves e_1 and e_{13} (Fig. 16-3), the amplitudes of these harmonics may be added. This increases by the same 45 to 60 per cent the maximum value of phase e.m.f. and by 10 to 17 per cent its effective value ($\sqrt{1^2 + (0.45 \text{ to } 0.60)^2}$). Such an increase in e.m.f. is undesirable and in many cases dangerous. Therefore, for instance, in large-power high-voltage transformers, the connection $Y/Y-12$ in its conventional form is not applied.

In spite of the abrupt change in the *phase* voltage curves the *line* voltages remain sinusoidal, since with star-connected windings the third e.m.f. harmonics disappear in the line voltages (§ 15-3).

The case is different for a three-leg transformer in which the magnetic circuits represent a coupled system. Indeed, the third harmonic fluxes in all three phases, the same as the currents, coincide in time. This means that the third harmonic fluxes at any given instant are equal in magnitude and in the transformer legs are all directed the same way, say, downwards as shown in Fig. 16-4. The third harmonic flux in any one leg, for example, in the first one, cannot close either through the second or through the third leg, because in each of them it encounters the third harmonic flux opposing it. As a result the lines of the third harmonic flux in all three phases fringe from the core and close from yoke to yoke through the air. This path

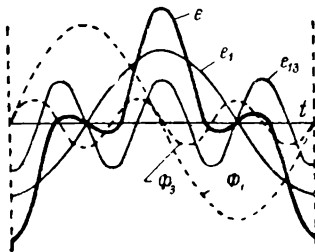


Fig. 16-3. Flux and e.m.f. curves of transformer bank with $Y/Y-12$ winding connection

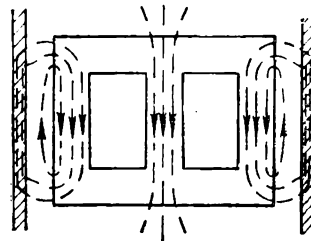


Fig. 16-4. Third harmonic fluxes in a three-legged transformer

has a high reluctance. Hence the third harmonic fluxes are small and with normal steel saturation the phase voltage curves, as a rule, remain practically sine-wave.

The third harmonic fluxes, closing through the air, pulsate with a frequency of $3f$. They naturally tend to follow the path of least resistance utilising for this purpose the tank walls, clamping bolts, etc. As a result of this in the above-mentioned parts appear eddy currents which give rise to local heating which lowers the transformer efficiency.

Investigations have shown that already with flux densities in the leg of the order of 1.4 wb/m^2 losses in the tank amount to about 10 per cent of the losses in the core; when the flux density increases in the leg the losses in the tank grow rapidly, and with a flux density of 1.6 wb/m^2 the losses reach 50-65 per cent of the total core losses.

16-2. Transformer on No-Load with Δ/Y Winding Connection

The transformer primary triangle as we know is a circuit in which all three currents of the third harmonic flow in one direction (Fig. 16-5). But if the third harmonic is present in the no-load current, the curve shapes of the magnetic flux and, accordingly, the shapes of the primary and secondary e.m.f.s approximate a sine-wave (Fig. 16-2), i. e., all the unfavourable phenomena mentioned in the previous paragraph disappear.

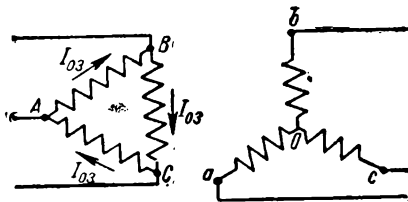


Fig. 16-5. Third no-load current harmonics for Δ/Y winding connection

This represents a very valuable advantage of the Δ/Y winding connection over the Y/Y connection.

16-3. Transformer on No-Load with Y/Δ Winding Connection

The fact that in this case, contrary to the Δ/Y connection, the primary is star-connected and the secondary delta-connected (Fig. 16-6), is of no essential importance. Indeed, with a star-

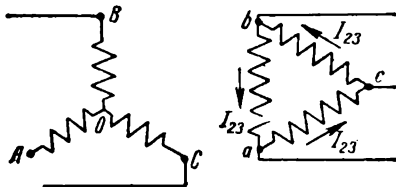


Fig. 16-6. The no-load third current harmonics for Y/Δ winding connection

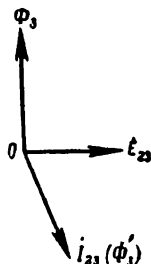


Fig. 16-7. Effect of current I_{23} for Y/Δ winding connection

connected primary the third harmonic drops out of the no-load current curve, and the flux curve assumes a flattened shape (Fig. 16-2, b). The third harmonic of the flux Φ_3 induces in each secondary phase a third harmonic e.m.f. E_{23} lagging on the flux Φ_3 by 90° (Fig. 16-7). The e.m.f. E_{23} produces the cur-

rents I_{23} , closing through the transformer secondary triangle (Fig. 16-6) and lagging on the e.m.f. E_{23} , almost by 90° , since the secondary circuit has a considerable reactance. We see that the current I_{23} is almost in antiphase with the flux third harmonic, i. e., it produces the flux Φ_3 , which practically balances the flux Φ_3 ; owing to this the curves of the resultant flux and, accordingly, the e.m.f.s approximate a sine-wave.

16-4. Y_0/Y_0 -12 Connection with Tertiary Winding

The connection Y/Y -12 is not used for high-power transformers because of the disadvantages discussed previously. But sometimes it is considered advantageous to ground the transformer both on the primary and the secondary sides. In this case the two windings are star-connected, but a so-called *tertiary winding* is built in; it represents an additional delta-connected winding closed on itself (Fig. 16-8). In respect to this tertiary winding the third harmonic flux will act quite similarly and with the same results as with a Y/Δ -11 connection.

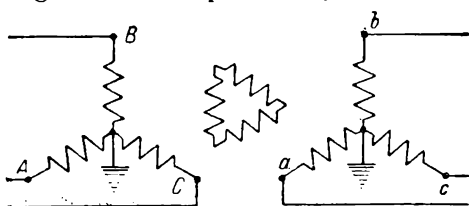


Fig. 16-8. Transformer with tertiary winding

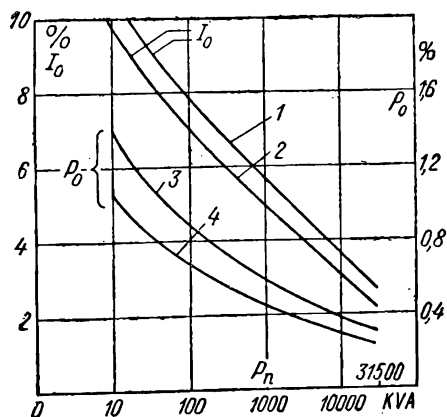


Fig. 16-9. $I_0 = f(P_n)$ and $P_0 = f(P_n)$ curves

expressed as a percentage of I_n , and P_0 as a percentage of P_n . The curves 1 and 3 refer to transformers with voltages of 6 to

The transformers with a tertiary are met with relatively seldom, because, usually, only the high-voltage winding is grounded.

16-5. Characteristic Data for No-Load Transformer Operation

In Fig. 16-9 the curves $I_0 = f(P_n)$ and $P_0 = f(P_n)$ are plotted for a logarithmic scale, the current I_0 being

35 kV, and the curves 2 and 4 to transformers with voltages of 10 to 121 kV. For precise values of the current I_0 and power P_0 , see State Standard 401-41.

Chapter Seventeen

SHORT-CIRCUIT OPERATION OF TRANSFORMERS. MAGNETIC LEAKAGE IN TRANSFORMERS

17-1. Preliminary

A transformer short circuit is a limiting operation condition in which the secondary is closed on itself, and the secondary voltage U_2 consequently equal to zero.

When a short-circuited transformer is fed by a rated voltage applied across its terminals, the short-circuit currents in the transformer windings reach a magnitude exceeding the rated currents of the winding 10 to 20 and more times, since the resistance of the windings are relatively small. Such a short circuit is quite possible in service conditions and may therefore be referred to as the *service* (emergency) short circuit. It is of great danger to the transformer owing both to considerable mechanical forces arising in the transformer and to the possible excessive temperature rise in the winding. The transformer must, therefore, have the necessary mechanical and thermal strength, and its circuit should be provided with a protective device capable of cutting-off the short-circuited transformer from the circuit after a stipulated, usually a very short time period (often less than 1 sec). If the protective device does not function properly the transformer will be seriously damaged.

Another kind of transformer short circuit is the *test of the transformer under short-circuit conditions*, which is carried out with a correspondingly lowered voltage U_{sh} necessary to obtain short-circuit data, namely: a) the impedance voltage and b) the power to be consumed for compensation of the short-circuit losses, since under this condition the transformer does not perform any useful work.

Such a short circuit may be called the *test* short circuit.

Once more it should be noted here that short-circuit conditions, along with no-load conditions, are of utmost importance both in theory and service.

17-2. Impedance Voltage

Suppose that for short-circuit conditions we have lowered the voltage applied to a transformer to the value U_{sh} at which the currents in the transformer windings are equal to the rated values. The voltage U_{sh} expressed as a percentage of the corresponding rated voltage is called *the rated impedance voltage* or simply impedance voltage.

$$u_{sh} = \frac{U_{sh}}{U_n} \times 100.$$

According to the State Standard 401-41, the impedance voltage is reduced to the value corresponding to the rated winding service temperature of 75° C. For three-phase two-winding transformers the stipulated values are given in Table 17-1. From the table it may be seen that the larger the transformer and its voltage the larger is the impedance voltage.

Table 17-1

**Impedance Voltages of Three-Phase Two-Winding Transformers
(according to State Standard 401-41)**

Power, kVA	Rated maximum voltage, kV	u_{sh} , %
5-5,600	6.3 and 10	5.5
50-2,400	35	6.5
3,200-4,200	35	7.0
5,600-10,000	35-38.5	7.5
15,000-31,500	35-38.5	8.0
3,200-60,000	110-121	10.5

The impedance voltage as a value of great importance is always indicated on the nameplate.

17-3. Physical Conditions of Transformer Operation on Short Circuit

Let us apply to the primary terminals of a short-circuited transformer such a sine-wave voltage U_{1sh} for which the primary and secondary currents I_1 and I_2 do not exceed the range close to the rated values. The currents I_1 and I_2 create the primary and secondary m.m.f.s $I_1\omega_1$ and $I_2\omega_2$ interacting with each

other as a result of which the main magnetic flux Φ_{sh} coupled with both transformer windings is created in the transformer core. Besides, the m.m.f.s $I_1\omega_1$ and $I_2\omega_2$ produce the primary and secondary leakage fluxes assuming that each of them is produced only by the given winding and is linked with the turns of this winding alone (Fig. 17-1). The flux Φ_{sh} creates in the transformer primary and secondary the e.m.f.s E_{1sh} and E'_{2sh} , and the leakage fluxes create the e.m.f.s $\dot{E}'_{\sigma 1} = -j\dot{I}_1x_1$ and $\dot{E}'_{\sigma 2} = -j\dot{I}_2x'_2$ (see §§ 13-2 and 13-4). Then, according to formulas (13-22) and (13-23a) the equations of the primary and the reduced secondary e.m.f.s will be written as:

$$\begin{aligned}\dot{U}_{1sh} &= -(\dot{E}_{1sh} - j\dot{I}_1x_1 - \dot{I}_1r_1) = \\ &= -\dot{E}_{1sh} + \dot{I}_1Z_1,\end{aligned}\quad (17-1)$$

$$\dot{E}'_{2sh} - \dot{I}'_2(r'_2 + jx'_2) = \dot{E}'_{2sh} - \dot{I}'_2Z'_2 = 0. \quad (17-2)$$

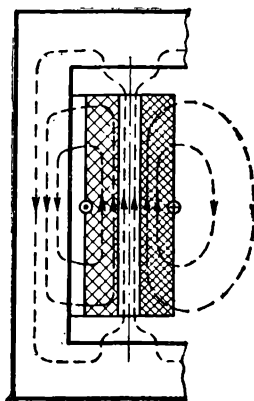


Fig. 17-1. Leakage fluxes in transformer with concentric winding for short-circuit conditions

Since U_{1sh} makes up for only 5-10 per cent of the rated voltage of the corresponding winding (Table 17-1), the main flux in the transformer core Φ_{sh} and the magnetising m.m.f. $F_0 = I_0\omega_1$ required for creating it are so small that they may be neglected. Then according to formulas (13-15a) and (13-15b), the equation of the m.m.f. at short circuit of a reduced transformer may be written as:

$$\dot{I}_1 + \dot{I}'_2 = 0 \quad \text{or} \quad \dot{I}_1 = -\dot{I}'_2. \quad (17-3)$$

Using the equations (17-2) and (17-3), the (17-1) equation may be expressed as:

$$\begin{aligned}\dot{U}_{1sh} &= \dot{I}_1Z_1 + \dot{I}_1Z'_2 = \dot{I}_1[(r_1 + jx_1) + (r'_2 + jx'_2)] = \\ &= \dot{I}_1[(r_1 + r'_2) + j(x_1 + x'_2)] = \dot{I}_1(r_{sh} + jx_{sh}) = \dot{I}_1Z_{sh}.\end{aligned}\quad (17-4)$$

The resistances $r_{sh} = r_1 + r'_2$, $x_{sh} = x_1 + x'_2$ and

$$z_{sh} = \sqrt{r_{sh}^2 + x_{sh}^2}$$

are referred to as the *short-circuit parameters of a transformer*.

17-4. Short-Circuit Diagram of Reduced Transformer

Let $\Phi_{sh.m}$ be the main flux vector on short circuit (Fig. 17-2, a). The e.m.f.s E_{1sh} and $E'_{2sh} = E_{1sh} = OF$ created by this flux lag on the flux $\Phi_{sh.m}$ by 90° . At an angle $\psi_{2sh} = \arctan \frac{x'_2}{r_2}$ to the vector E'_{2sh} is drawn the vector for current I'_2 . The vector of the leakage e.m.f. $E'_{\sigma 2} = -jI'_2 x'_2$ lags behind the current vector I'_2 by a 90° angle; the vector $-I'_2 r'_2$ is in antiphase with

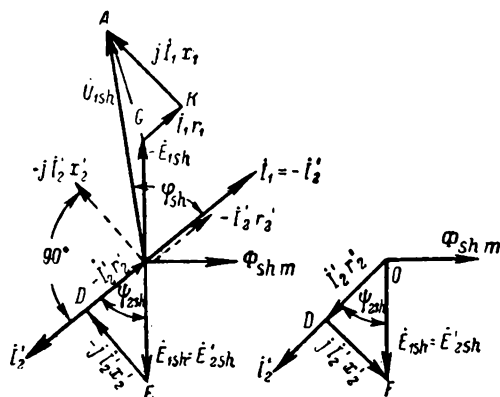


Fig. 17-2. Vector diagram for transformer on short circuit

the current I'_2 . Adding geometrically the secondary e.m.f.s E'_{2sh} , $-jI'_2 x'_2$ and $-I'_2 r'_2$ in accordance with equation (17-2), we obtain a right triangle OFD closed on itself. But the equation (13-23b) may also be used; in this case we plot not the e.m.f.s $-jI'_2 x'_2$ and $-I'_2 r'_2$ but the equal to them in magnitude but reversed vectors of the active and inductive voltage drops in the secondary $jI'_2 x'_2$ and $I'_2 r'_2$ (Fig. 17-2, b).

According to equation (17-3), the current vector I_1 is equal in magnitude to the current vector I'_2 and is in antiphase with it.

The vector of the primary voltage $U_{1sh} = \overline{OA}$ may be plotted the simplest way by using equation (17-1), and using the volt-

age components — $\dot{E}_{1sh} = \overline{OG}$, $\dot{I}_1 r_1 = \overline{GK}$ and $j\dot{I}_1 x_1 = \overline{KA}$. The phase of the current \dot{I}_1 in respect to the voltage U_{1sh} is determined by the angle ψ_{sh} .

17-5. Equivalent Circuit of Transformer on Short Circuit

Solving equation (17-4) with regard to the current \dot{I}_1 we obtain:

$$\dot{I}_1 = \frac{\dot{U}_{1sh}}{Z_1 + Z_2'} \quad (17-5)$$

Hence, the equivalent circuit of a transformer on short circuit represents a circuit to which a voltage U_{1sh} is applied and

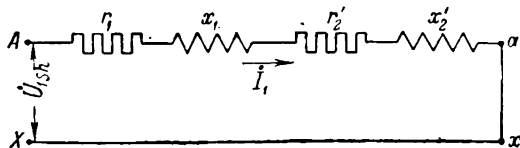


Fig. 17-3. Equivalent circuit of a transformer on short circuit

which consists of series-connected resistances $r_{sh} = r_1 + r_2'$ and reactances $x_{sh} = x_1 + x_2'$ (Fig. 17-3). This circuit may be obtained directly from the circuit in Fig. 13-3, if we exclude the magnetising circuit ($I_0 \approx 0$) and assume that $Z_r' = 0$.

17-6. Transformer Short-Circuit Triangle

The equivalent circuit in Fig. 17-3 permits us to replot the diagram in Fig. 17-2 into a short-circuit triangle notable for its simplicity and clearness.

For this purpose we point the current vector \dot{I}_1 in the positive direction of the ordinate axis (Fig. 17-4), and plot in a conventional manner the voltage drops $\dot{I}_1 Z_1$ and $\dot{I}_2 Z_2'$. The sequence of adding the vectors is arbitrary. Therefore issuing from point O , we may add them in the sequence shown in Fig. 17-4 by the continuous lines. The triangle OBA is referred to as a *short-circuit triangle*. Its sides OB and BA represent the active and reactive components of the voltage u_{sh} called the *active and reactive voltage drops of the transformer*.

From the diagram in Fig. 17-4 it may be seen that

$$OB = I_1 r_1 + I_1 r'_2 = I_1 r_{sh}; \quad (17-6a)$$

$$BA = I_1 x_1 + I_1 x'_2 = I_1 x_{sh}; \quad (17-6b)$$

$$OA = \sqrt{OB^2 + BA^2} = I_1 \sqrt{r_{sh}^2 + x_{sh}^2} = I_1 z_{sh} \quad (17-6c)$$

$$\text{and} \quad \tan \varphi_{sh} = \frac{BA}{OB} = \frac{x_{sh}}{r_{sh}}. \quad (17-7)$$

For practical purposes, the short-circuit triangle is plotted for the current $I_1 = I_n$ and all its sides are expressed as percentages

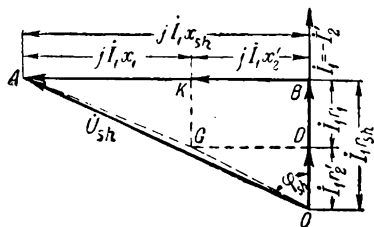


Fig. 17-4. Transformer short-circuit triangle

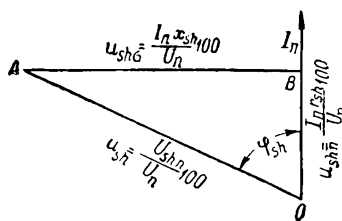


Fig. 17-5. Basic short-circuit triangle

of the rated voltage U_n . In this case we do not need to impart to them a vector form and can omit their designation by arrows (Fig. 17-5). Thus,

$$OB = u_{sha} = \frac{I_n r_{sh}}{U_n} \cdot 100, \quad (17-8a)$$

$$BA = u_{shx} = \frac{I_n x_{sh}}{U_n} \cdot 100, \quad (17-8b)$$

$$OA = u_{sh} = \frac{I_n z_{sh}}{U_n} \cdot 100 = \frac{U_{shn}}{U_n} \cdot 100. \quad (17-8c)$$

The values u_{sha} and u_{shx} are referred to as the *impedance voltage components*, and the triangle OBA in Fig. 17-5 will be called the *fundamental short-circuit triangle*.

17-7. Short-Circuit Losses

Since the main flux on short circuit is small, the losses in the core steel may be neglected, and it may be assumed that the short-circuit rating P_{sh} is expended only to cover the losses in the winding copper p_{cop1} and p_{cop2} , i. e.,

$$P_{sh} = p_{cop1} + p_{cop2}. \quad (17-9)$$

The copper losses consist of:

a) The main losses p_{cop0} determined by the resistances of the windings to the d.c. r_{10} and r_{20} , and

b) The additional losses in the copper due to eddy currents appearing in the winding due to imperfect wire crossings and losses caused by the leakage fluxes in tank walls, etc.

The main losses in the winding copper constitute the major part of the copper losses and are equal to:

$$p_{cop0} = I_1^2 r_{10} + I_2^2 r_{20}. \quad (17-10)$$

The subject of additional losses in the copper is relatively complicated and represents a special problem. The additional losses are usually included in the main losses by increasing the resistances r_{10} and r_{20} up to values $r_1 = r_{10} k_{r1}$ and $r_2 = r_{20} k_{r2}$, where k_{r1} and k_{r2} are the additional loss factors.

Thus,

$$P_{sh} = p_{cop1} + p_{cop2} = I_1^2 r_1 + I_2^2 r_2 = I_1^2 r_1 + I_2^2 r_2 = I_{sh}^2. \quad (17-11)$$

The additional losses depend on the type of winding (concentric or sandwich), on the conductor cross-section (round or rectangular), on the winding type and so on. In normal cases, the values of the factors k_{r1} and k_{r2} equal 1.05 to 1.15, but in some particular cases they may be much greater.

The short-circuit rating, the same as the no-load rating, is of very great importance for service conditions. The value of this rating may be judged by the ratio $\frac{P_{sh.n}}{P_n} \times 100$ where $P_{sh.n}$ is the

Table 17-2

P_n , kVA	$\frac{P_{sh.n}}{P_n} \times 100$ %
5-20	3.7-3
30-240	3-2
320-5,600	2-1
7,500-60,000	1-0.4

short-circuit rating for $I_1 = I_n$ and winding temperature is 75°C . The corresponding figures are given in Table 17-2 based on the State Standard 401-41 data for three- and single-phase two-winding transformers.

If we compare values of the no-load and short-circuit ratings, we should have for standard transformers $P_0 : P_{sh} = 1 : (2.5 \text{ to } 4)$.

The ratio $\frac{P_0}{P_{sh}}$ greatly influences the efficiency curve shape (see § 18-9).

17-8. Determination of Short-Circuit Parameters

To determine short-circuit parameters a short-circuit transformer test is carried out. A short-circuit diagram of a single-phase transformer is shown in Fig. 17-6.

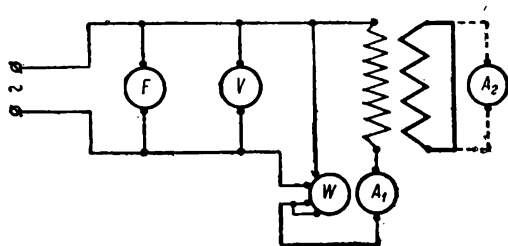


Fig. 17-6. Test circuit diagram for transformer on short circuit

Let U_{sh} , I_1 and P_{sh} be the voltage, current and rating at short circuit; then

$$z_{sh} = \frac{U_{sh}}{I_1}, \quad (17-12a)$$

$$r_{sh} = \frac{P_{sh}}{I_1^2} \quad (17-12b)$$

and

$$x_{sh} = \sqrt{z_{sh}^2 - r_{sh}^2}. \quad (17-13)$$

Knowing the short-circuit parameters, it is possible to determine the voltage u_{sh} and its components u_{sha} , and u_{shx} , viz.:

$$u_{sh} = \frac{I_n z_{sh}}{U_n} \times 100, \quad (17-14a)$$

$$u_{sha} = \frac{I_n r_{sh}}{U_n} \times 100 = \frac{I_n^2 r_{sh}}{U_n I_n} \times 100 = \frac{P_{shn} (w)}{10 P_n (kVA)} \quad (17-14b)$$

$$u_{shx} = \frac{I_n x_{sh}}{U_n} \times 100 = \sqrt{u_{sh}^2 - u_{sha}^2} \quad (17-14c)$$

The u_{sha} and u_{shx} components depend mainly on the rating of the transformer. With an increase in rating the component u_{sha} continuously decreases, whereas the component u_{shx} tends to increase. The result of this is that the ratio $\frac{u_{shx}}{u_{sha}} = \tan \psi_{sh}$ increases relatively fast with the increase of capacity: ratios equal from 1.0 to 2.0 in transformers up to 50 kVA and up to 10 in high-voltage large-capacity transformers.

17-9. Short Circuit of Three-Phase Transformers

Here we shall consider only the case of a three-phase or the so-called *symmetrical short circuit*, when all three phases of a transformer are short-circuited.

Some of the special cases of short-circuiting—single- and two-phase—are considered below.

Contrary to no-load operation, the symmetrical short circuit of three-phase transformers has no specific peculiarities in comparison with the single-phase transformer short circuit. This is explained by the fact that on short circuit, contrary to no-load operation, the core steel is not saturated, hence the currents and loads are symmetrically distributed between the phases, and the e.m.f. curve shapes are not distorted.

On this basis we may extend to the case of a three-phase short circuit all deductions pertaining to the short circuit of the single-phase transformer. It should be remembered that, when carrying out the calculations, we should refer them to one phase only.

17-10. Leakage in Transformers with Concentric and Sandwich Windings

If the m.m.f.s of two transformer windings are precisely balanced, i. e., $\dot{I}_1 w_1 = -\dot{I}_2 w_2$, then the full current $\dot{I}_1 w_1 + (-\dot{I}_2 w_2) = 0$. In this case there is no flux that is linked with both windings, but only the fluxes each linked with its winding, called the leakage fluxes. These conditions very nearly approximate a transformer on short circuit (Fig. 17-1). In the general case $\dot{I}_1 w_1 = -\dot{I}_2 w_2 + \dot{I}_0 w_1$ [formula (13-15b)] or $\dot{I}_1 w_1 - \dot{I}_0 w_1 = (-\dot{I}_2 w_2) = \dot{I}_{11} w_1 = -\dot{I}_2 w_2$, i. e., in this case the leakage fluxes are produced by the currents \dot{I}_{11} and \dot{I}_2 .

This method of leakage determination may easily be applied to the case of a multi-winding transformer.

The leakage phenomenon defines a number of fundamental properties of a transformer both at steady-state operation by affecting a change in secondary voltage, parallel operation conditions, additional losses in the transformer, etc., and at sudden short circuits determining the short-circuit current magnitude and the effects due to it of mechanical and thermal nature. Therefore one of the main problems in transformer theory is the precise determination of the reactance and leakage e.m.f. or, correspondingly, the impedance voltage magnitude u_{sh} .

To calculate the transformer reactance and leakage e.m.f. it is necessary to know the space distribution of the leakage fluxes in the transformer. This distribution is very complicated even for comparatively simple windings and is dependent on their mutual positions and their relative dimensions. Therefore, the reducing method discussed in § 2-4 is used, in which the true complex map of the leakage field is substituted by a calculated mapping which while of maximum simplicity gives the same quantitative results as the true map.

A. Leakage reactance calculation for concentric windings. Let us consider first the simplest case, when the primary and secondary windings represent cylinders of equal height with the same m.m.f. distribution over the winding height, with $i_1 w_1 = i_2 w_2$. Fig. 17-7,a shows the true field leakage mapping for two concentric windings with a large ratio of the axial to radial dimensions (the height of the winding to its width). By the Rogovsky method, this map is substituted by a map shown in Fig. 17-7,b.

Here it is necessary first of all to pay attention to the positions of the centres O_1 and O_2 of the primary and secondary leakage fluxes. If each of the windings existed apart from the other and was surrounded by a homogeneous medium, the flux centre of such a winding would be at the intersection point of the diagonals of the rectangle depicting the winding. But in our case, owing to a lateral thrust of the flux tubes, the leakage flux centres are displaced in opposite directions outwards to the winding edges, remaining at the average height of the latter. It is assumed that all the leakage flux tubes are parallel to the cylinder generatrix and have a calculated length l'_0 . This length is introduced into the calculation of the tube reluctance, whereas the reluctance of the remaining tube part is considered zero. According to theoretical investigations, it may be assumed that approximately

$$l'_0 = \frac{h_{winding}}{1 - \frac{b_1 + b_2 + \delta_{12}}{\pi h_{winding}}} = \frac{h_{winding}}{k_a}. \quad (17-15)$$

Here

- $h_{winding}$ —the height of the winding;
- b_1 and b_2 —the widths of the primary and secondary windings;
- δ_{12} —the clearance between windings and
- k_a —the coefficient of reduction of winding height to calculated length of the leakage field lines.

Since the winding width and clearance are usually small in comparison with $h_{winding}$, for ordinary concentric windings the coefficient $k_s = 0.90$ to 0.97 .

An m.m.f. curve can be plotted for the leakage flux shown in Fig. 17-7, *b*. At centres O_1 and O_2 the m.m.f.s are zero; then the

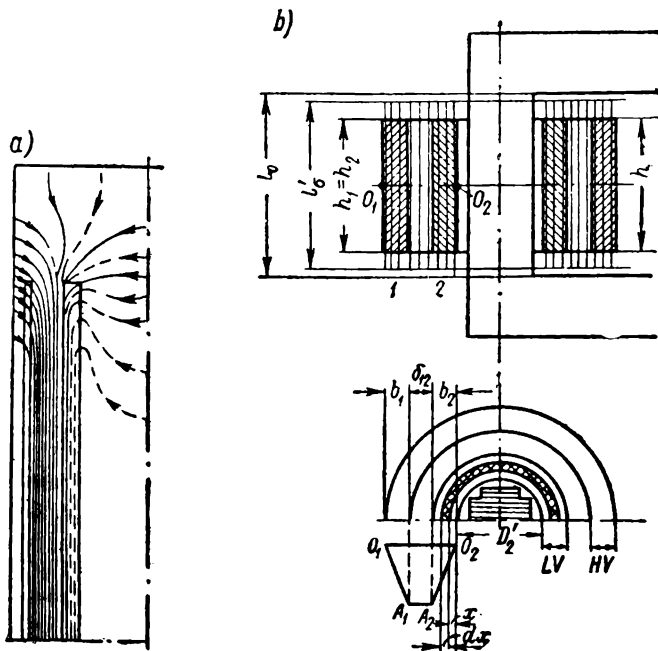


Fig. 17-7. Leakage field of transformer with concentric winding:
a — actual field; *b* — reduced field

m.m.f.s increase proportionally to the distances between tubes of the primary and secondary leakage fluxes and the centre O_1 or, correspondingly, the centre O_2 . In the gap δ_{12} between the windings the m.m.f. does not change, one half of the gap being conditionally considered as filled with primary leakage lines, and the other half by the secondary leakage lines.

Let us calculate the leakage reactance of one of the windings, for example, that of winding 2, assuming that it is reduced to winding 1. The calculation comprises a computation of the inductance L_b over the width of the winding b_2 where the m.m.f. continuously varies and the computation of the inductance

L'_b over the width of $\frac{1}{2} \delta_{12}$ where the m.m.f. remains constant. The inductance sought is $L'_{s2} = L'_b + L'_c$. The calculation procedure is typical and carried out in the following order: a) an elementary tube is singled out and its m.m.f. and flux determined for a current of 1A flowing through the winding; b) the number of flux linkages of all the elementary tubes in the specified limits is calculated.

For the calculation of the inductance $L'_{winding}$ let us single out an elementary tube at a distance x from the inner generatrix of the secondary winding. When $I_2 = 1A$ the m.m.f. of this tube will be:

$$F_x = 1 \times w_1 \times \frac{x}{b_2} = w_1 \frac{x}{b_2}.$$

The reluctance of the same tube will be:

$$R_{\mu x} = \frac{1}{\mu_0} \frac{l'_o}{\pi (D'_2 + 2x) dx},$$

where μ_0 is the permeability of air (oil) and D'_2 is the inner diameter of the secondary winding.

Consequently, the flux $d\Phi_x$ of the singled-out elementary tube and the number of its linkages $d\Psi_x$ will be:

$$d\Phi_x = \frac{F_x}{R_{\mu x}} = \mu_0 w_1 \frac{x}{b_2} \cdot \frac{\pi (D'_2 + 2x) dx}{l'_o}$$

and

$$d\Psi_x = d\Phi_x \left(w_1 \frac{x}{b_2} \right) = \mu_0 \left(w_1 \frac{x}{b_2} \right)^2 \frac{\pi (D'_2 + 2x) dx}{l'_o}.$$

The number of flux linkages over the winding width b_2 for a current of 1A., i. e., the winding inductance will be:

$$L'_b = \int_0^{b_2} d\Psi_x = \mu_0 \frac{w_1^2}{l'_o} \left[\pi \frac{b_2}{3} \left(D'_2 + \frac{3}{2} b_2 \right) \right].$$

The second addend corresponding to the gap width $\frac{\delta_{12}}{2}$, is determined in the same way as the first one, with the only difference that the tube in the gap is created by the entire m.m.f. of the secondary and is linked with all its turns.

Therefore the number of flux linkages over the width $\frac{\delta_{12}}{2}$ will be:

$$\begin{aligned} L'_s &= \int_0^{\frac{\delta_{12}}{2}} d\Phi_x \omega_1 = \int_0^{\frac{\delta_{12}}{2}} \mu_0 \omega_1^2 \frac{\pi (D'_2 + 2b_2 + 2y)}{l'_s} dy = \\ &= \mu_0 \frac{\omega_1^2}{l'_s} \pi \frac{\delta_{12}}{2} \left(D'_2 + 2b_2 + \frac{\delta_{12}}{2} \right). \end{aligned}$$

It may be assumed with a sufficient approximation that the sums $D'_2 + \frac{3}{2} b_2$ and $D'_2 + 2b_2 + \frac{\delta_{12}}{2}$ each represent the average diameter D_{2av} of the secondary. Then the secondary inductance will be:

$$L'_{s2} = \mu_0 \frac{\omega_1^2}{l'_s} \pi D_{2av} \left(\frac{b_2}{3} + \frac{\delta_{12}}{2} \right) = \mu_0 \omega_1^2 \cdot \frac{C_{2av}}{l'_s} \left(\frac{b_2}{3} + \frac{\delta_{12}}{2} \right),$$

where $C_{2av} = \pi D_{2av}$ is the average length of a secondary winding turn.

If we make the same calculations for the primary we will obtain:

$$L_{s1} = \mu_0 \omega_1^2 \frac{C_{1av}}{l'_s} \left(\frac{b_1}{3} + \frac{\delta_{12}}{2} \right),$$

where $C_{1av} = \pi D_{1av}$ is the average length of the primary turn.

Therefore the leakage inductance of both windings will be:

$$\begin{aligned} L_s &= L_{s1} + L'_{s2} = \mu_0 \omega_1^2 \frac{C_{av}}{l'_s} \left(\delta_{12} + \frac{b_1 + b_2}{3} \right) = \\ &= \mu_0 \omega_1^2 \frac{C_{av} k_s}{h_{winding}} \delta'. \end{aligned} \quad (17-16)$$

Here $C_{av} = \frac{C_{1av} + C_{2av}}{2}$ represents the average length of turn in both windings, and $\delta' = \delta_{12} + \frac{b_1 + b_2}{3}$ is the so-called *reduced* clearance between windings.

Since $x_{sh} = x_1 + x'_2 = 2\pi f (L_{s1} + L'_{s2}) = 2\pi f L_s$ the reactance of a transformer is

$$x_{sh} = 2\pi \mu_0 f \omega_1^2 \frac{C_{av} k_s}{h_{winding}} \delta'. \quad (17-17)$$

Accordingly, the reactive component of the impedance voltage [formula (17-8b)] is:

$$\begin{aligned}
 u_{sh} &= \frac{I_n x_{sh}}{U_n} \cdot 100 = \mu_0 2\pi f I_n \frac{w_1^2}{U_n h_{winding}} \frac{C_{av} k_s}{\omega_1^2} \cdot \delta' \cdot 10^2 = \\
 &= \mu_0 2\pi f (U_n I_n) \frac{1}{U_n^2} \cdot \frac{C_{av} k_s}{h_{winding}} \cdot \delta' \cdot 10^2 = \\
 &= \mu_0 2\pi f \frac{P_n k_{leg}}{E_{turn}^2} \cdot \frac{C_{av} k_s}{h_{winding}} \cdot \delta' \cdot 10^2. \quad (17-18)
 \end{aligned}$$

Here P_n is the transformer rating expressed in VA; E_{turn} is e.m.f. per turn; k_{leg} is a factor indicating the rated power per one leg; for single-phase transformers in which the winding is usually placed on two legs (Fig. 12-2), $k_{leg} = \frac{1}{2}$; for three-phase transformers, where the winding is usually wound on one of the legs, $k_{leg} = \frac{1}{3}$.

Ordinarily, the rating P_n is expressed in kVA and the dimensions in cm. Since, besides, $\mu_0 = 4\pi \times 10^{-9}$, then

$$u_{sh} = 0.79 f \frac{P_n k_{leg}}{E_{turn}^2} \frac{C_{av} k_s}{h_{winding}} \delta' \times 10^{-2}. \quad (17-19)$$

The formula (17-19) is of very great importance, since it relates the value u_{sh} with a great number of values on which the transformer design is based.

B. The calculation of the leakage inductance of sandwich windings. The above calculations of u_{sh} for concentric windings may be applied with certain alterations to calculate u_{sh} for sandwich windings.

The sandwich winding is shown schematically in Fig. 17-8, *a*. The high- and low-voltage windings consist of the same number of coils with one coil of the low-voltage winding divided into two half-coils disposed in the upper and lower parts of the winding. The centres, around which the leakage flux lines are formed, are shown by heavy dots. This actual leakage flux mapping is substituted with a reduced mapping (Fig. 17-8, *b*), in which all the flux lines shown by broken lines are perpendicular to the leg axis (cf. the flux map in Fig. 17-7, *b*) and have a calculated length of l'_0 . The distribution curve of the m.m.f. of the winding under consideration is given in Fig. 17-8, *c*. Since the m.m.f. curve is symmetrical in respect to the ordinate axis, the sandwich winding in Fig. 17-8, *a* is termed *symmetrical*. The entire winding may

be divided into n series-connected groups each consisting of two half-coils of high- and low-voltage windings. The m.m.f. curve of each group repeats the m.m.f. curve of a concentric winding in Fig. 17-7, *b*. Therefore, when determining the inductance of a sandwich winding we may proceed from the same

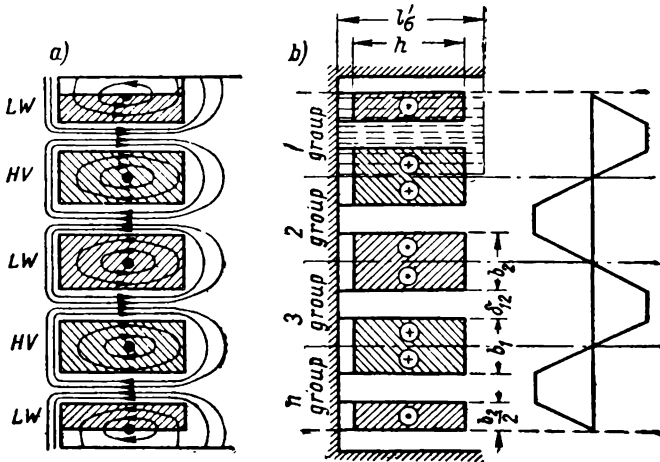


Fig. 17-8. Leakage field and m.m.f. of transformer with sandwich winding

formulas (17-16) and (17-17) which were deduced for a concentric winding, on the condition that the sandwich winding is considered as a winding consisting of n series-connected groups with $\frac{w_1}{n}$ turns in each winding. In this case, according to formula (17-18) we have:

$$L_s = \mu_0 \left(\frac{w_1}{n} \right)^2 n \frac{C_{av} k_s}{h_{winding}} \delta'. \quad (17-20)$$

Hence,

$$u_{shs} = 0.79 f \frac{P_n k_{leg}}{E_{turn}^2} \times \frac{C_{av} k_s}{h_{winding} n} \delta' \times 10^{-2}. \quad (17-21)$$

For sandwich windings the factor $k_s = 1 - \frac{b_1 + b_2 + \delta_{12}}{\pi h_{winding}}$ is usually within the range of 0.65-0.80.

Chapter Eighteen

TRANSFORMERS ON LOAD

18-1. Preliminary

The main object of this chapter is a) to show the applicability of the *superposition method* according to which any transformer load condition may be obtained by means of mutual superposition of no-load and short-circuit conditions, and b) to give methods for the calculation of secondary voltage changes and of the transformer efficiency with the help of suitably simplified equivalent transformer circuits.

18-2. Elementary Transformer on Load

The basic circuit diagram of a single-phase transformer working on a certain load is shown in Fig. 18-1. Let us first discuss the operating conditions of an elementary transformer, assuming

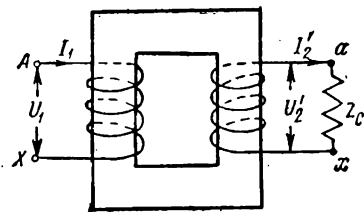


Fig. 18-1. Basic circuit for transformer on load

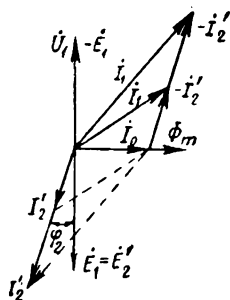


Fig. 18-2. Current diagram of elementary transformer

the secondary is referred to the primary. Since in an elementary transformer we neglect the voltage drop, we always have in it $\dot{U}_1 = -\dot{E}_1$, irrespective of load (Fig. 18-2). Assuming the voltage U_1 constant, we shall have at all loads the same value of the counter e.m.f. E_1 . In accordance with this, *the main flux Φ_m , the current I_0 and the magnetising m.m.f. $F_0 = I_0 \omega_1$ are also independent of the load*, i. e., they retain the same value for any transformer condition.

If we will load a transformer, then from the m.m.f. equation [formula (13-32b)] we have:

$$\dot{I}_1 = \dot{I}_0 + (-\dot{I}'_2), \quad (18-1)$$

i. e., with a loaded transformer, the *primary current* \dot{I}_1 represents the *geometrical sum of two components*, namely, of a constant in value *magnetising current* \dot{I}_0 giving rise to the main flux Φ and of a *load current* $(-\dot{I}'_2)$ the m.m.f. of which balances the m.m.f. produced by the secondary current \dot{I}'_2 .

Fig. 18-2 shows how current \dot{I}_1 changes with a change in current \dot{I}'_2 (angle φ_2 is assumed to be given).

18-3. Real Transformer on Load

The analysis of the operation of a real transformer is based as before on the e.m.f. and m.m.f. equations. Here and in further discussions we shall assume that the transformer has been reduced. Then, [formulas (13-33), (13-34) and (13-32)]:

$$\dot{U}_1 = -\dot{E}_1 + \dot{I}_1 Z_1, \quad (18-2)$$

$$\dot{E}'_2 - \dot{I}'_2 Z'_2 = \dot{U}'_2, \quad (18-3)$$

or

$$\dot{E}'_2 = \dot{U}'_2 + \dot{I}'_2 Z'_2 \quad (18-4)$$

and

$$\dot{I}_1 = -\dot{I}'_2 + \dot{I}_0. \quad (18-5)$$

In accordance with these equations we plot the vector diagrams of a transformer on load.

In Fig. 18-3, *a* a diagram is plotted with the reactive load predominant. The vector of the main flux Φ_m is drawn in the positive direction along the abscissa axis; to create this flux the magnetising current \dot{I}_0 is required, the vector of which leads on the flux Φ_m vector by a small angle (see Fig. 14-5). The e.m.f.s \dot{E}_1 and $\dot{E}'_2 = \dot{E}_1$ produced by the flux Φ_m lag on it by 90° . The current \dot{I}'_2 lags on the e.m.f. \dot{E}'_2 by an angle ψ_2 , determined both by the type of external load and by the inherent resistance of the secondary. According to the m.m.f. equation (18-5), the current $\dot{I}_1 = -\dot{I}'_2 + \dot{I}_0$.

The e.m.f. equation (18-3) can be used to plot the secondary voltage vector $\dot{U}'_2 = OC$. In this case it is necessary to add geome-

trically the e.m.f. $E'_2 = \overline{OF}$, the leakage e.m.f. $E'_{s2} = -j\dot{I}'_2 x'_2 = \overline{FD}$ and the resistance e.m.f. $-I'_2 r'_2 = \overline{DC}$ (Fig. 18-3, a).

On the other hand, equation (18-4) may be utilised to determine the e.m.f. E'_2 ; in this case the voltage $\dot{U}'_2 = \overline{OC}$ and the secondary voltage drops $\dot{I}'_2 r'_2 = \overline{CD}$ and $j\dot{I}'_2 x'_2 = \overline{DF}$ (Fig. 18-3, b) are added together geometrically.

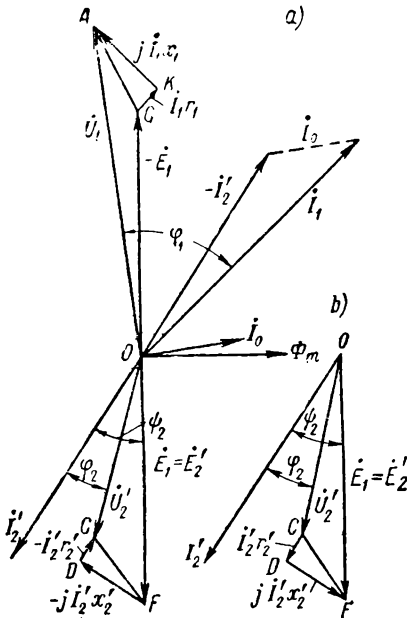


Fig. 18-3. Vector diagram of transformer on inductive load

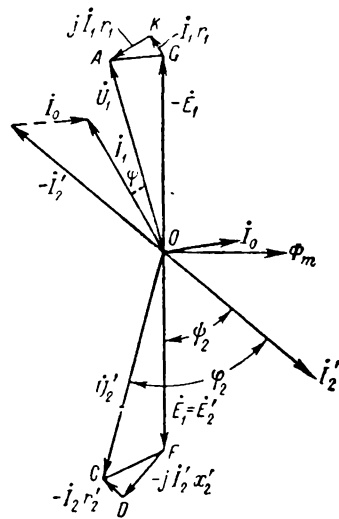


Fig. 18-4. Vector diagram of transformer on capacitive load

The angle φ_2 between the vectors U'_2 and I'_2 depends on the kind of the transformer external load.

The primary voltage vector $\dot{U}_1 = \overline{OA}$ is plotted, according to equation (18-2), by using the three voltage components: $-\dot{E}_1 = \overline{OG}$, $\dot{I}_1 r_1 = \overline{GK}$ and $j\dot{I}_1 x_1 = \overline{KA}$, each of which is balanced by the corresponding e.m.f.

The angle φ_1 between vectors \dot{U}_1 and \dot{I}_1 determines the active power $U_1 I_1 \cos \varphi_1$ delivered to the transformer from the power circuit.

The vector diagram of the transformer for a capacitive load is plotted in Fig. 18-4 without special explanations, since the methods are the same as before.

18-4. Vector Diagrams of the Equivalent Transformer

Fig. 13-3 shows an equivalent transformer circuit, between the elements of which there exists only an electric connection. In a somewhat simplified form this equivalent circuit is reproduced in Fig. 18-5, *a*. The vector diagrams in Fig. 18-5, *b* and *c* are plotted in accordance with this circuit. When plotting, we shall assume the secondary voltage U'_2 , the secondary current I'_2 and the power factor $\cos \varphi_2$ of the secondary line as given values.

The vector of the secondary voltage $-U'_2 = OC$ is superposed with the positive ordinate axis direction. The vector of the load component of the primary current lags on the vector of the voltage $-U'_2$ or leads it by an angle φ_2 . Adding geometrically the voltages $-U'_2$ and voltage drops in the secondary $-I'_2(r'_2 + jx'_2)$ we find the vector of the primary voltage component $-E_1 = OG$; the vector of the main flux Φ_m lags on $-E_1$ by 90° , and the vector of the magnetising current I_0 leads the vector of the flux Φ_m by a small angle. The primary current vector $I_1 = -I'_2 + I_0$. In order to plot the primary voltage vector $\dot{U}_1 = \overrightarrow{OA}$ it is necessary to add the components of this voltage $-E_1$ and $I_1(r_1 + jx_1)$.

18-5. Simplified Vector Diagrams of the Transformer

The diagrams in Fig. 18-5, *b* and *c* are only of theoretical significance, mainly because x_1 and x'_2 cannot be determined separately and also because the triangles AKG and QDC of the primary and secondary voltage drops are oriented in the diagrams differently.

In order to simplify the diagram and make it practical, the power transformers operating on load in conditions near to rated load, the current I_0 is neglected, i. e., it is assumed that $I_1 = -I'_2$. In modern transformers, the current ratio $\frac{I_0}{I_n} \times 100 = 3$ to 8 per cent. This is a rather large figure, but since the currents I_1 and $-I'_2$ are added geometrically, the error is considerably decreased. Besides, it takes place only with primary voltage drop

which within the range of normal loads is a second-order value compared with the voltage U_1 (3-5 per cent of the latter).

With this assumption the equivalent circuit of a transformer becomes as shown in Fig. 18-6. The scheme represents a simple circuit consisting of series-connected impedances: $Z_1 = r_1 + jx_1$, $Z_2 = r_2' + jx_2'$, $Z_c = r_c + jx_c$. In accordance with this simplified equivalent circuit, are plotted the simplified vector diagrams

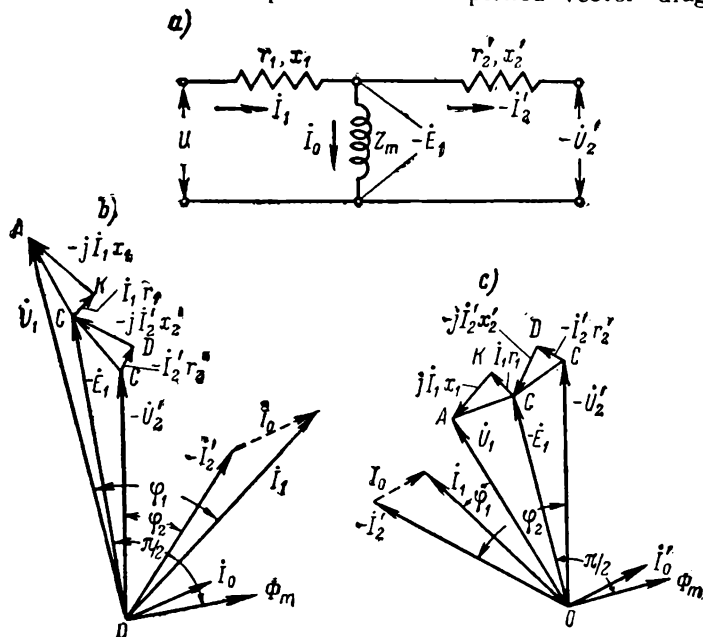


Fig. 18-5. Equivalent circuit and the vector diagrams of transformer operating on inductive and capacitive loads

for the inductive and capacitive loads in Fig. 18-7, *a* and *b*. The vector of the current I_1 is drawn in the positive direction of the ordinate axis. The voltage drop vectors $I_1 r_2'$, $j I_1 x_2'$, $I_1 r_1$ and $j I_1 x_1$ form right-angle triangles CDG and GKA with parallel sides which may be added in the sequence shown in the figure by the heavy lines. It follows from the diagram that vector $CB = I_1(r_1 + r_2') = I_1 r_{sh}$ and vector $BA = j I_1(x_1 + x_2') = j I_1 x_{sh}$. Thus, the triangle ABC is the short-circuit triangle (Fig. 17-4), one side of which is in phase with current I_1 and determines the active voltage drop in the transformer, and the other side leading current I_1 by 90° determines the

inductive voltage drop in it. If we assume as given the voltage U_1 , current I_1 , and kind of load, i. e., the angle φ_2 , then, as seen from the diagram, the secondary voltage is obtained by plotting

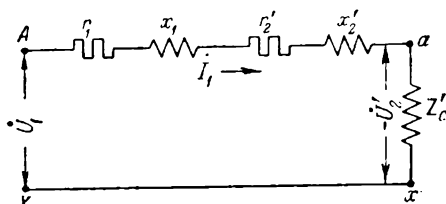


Fig. 18-6. Simplified equivalent circuit of transformer

adjacent to vector \dot{U}_1 the short-circuit triangle ABC with the apex C of the triangle lying on the line drawn at an angle φ_2 from point O to the ordinate axis. Consequently, the secondary voltage $-\dot{U}_2' = \overline{OC}$

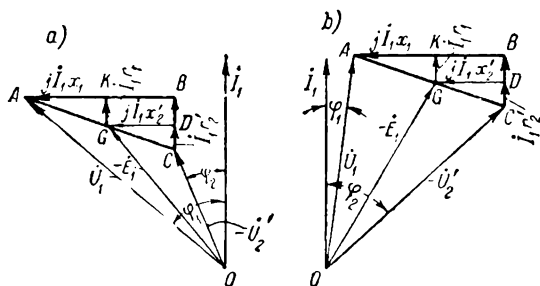


Fig. 18-7. Simplified vector diagrams of an equivalent transformer:

a — on inductive load; *b* — on capacitive load

may be considered as the result of superposing short-circuit conditions, determined by the short-circuit triangle ABC on the no-load conditions determined by vector \overline{OA} .

18-6. The Relationship $U_2' = f(\cos \varphi_2)$

The easiest way to carry out the geometrical plotting of vector $\overline{OC} = -\dot{U}_2'$ is as follows. The triangle ABC is moved downwards parallel to itself until it occupies the position of triangle $OB'C'$ (Fig. 18-8). From point O a line is drawn at an angle φ_2 to the

Consequently,

$$\Delta U = u_{sha} \cos \varphi_2 + u_{shs} \sin \varphi_2 + \frac{(u_{shs} \cos \varphi_2 - u_{sha} \sin \varphi_2)^2}{200} \quad (18-7)$$

The last addend in this formula is usually small. Therefore, where there is no need for particular accuracy it may be assumed that

$$\Delta U = u_{sha} \cos \varphi_2 + u_{shs} \sin \varphi_2. \quad (18-8)$$

We have here determined ΔU for a rated load. For any other load defined by the loading factor $k_{load} = \frac{P_2}{P_n}$, the voltage drop varies practically as the k_{load} [formula (18-8)].

From the above it follows that, for given short-circuit parameters, the voltage drop depends on the kind and magnitude of the load.

18-8. Transformer External Characteristics

The external transformer characteristic is called the relationship $U_2 = f(I_2)$ for $U_1 = \text{const}$ and $\cos \varphi_2 = \text{const}$ (Fig. 18-10). With $I_2 = I_{2n}$, $\cos \varphi_2 = 0.8$ and values of $u_{sh} = 5.5$ to 10.5 per cent, the voltage drop $\Delta U = 5$ to 8 per cent.

18-9. Transformer Efficiency

The efficiency η of a transformer as of any machine is the ratio of the output P_2 expressed in active power units, i. e., in kW or W to the input P_1 expressed in the same units as P_2 . Thus,

$$\eta = \frac{P_2}{P_1} \text{ or } \eta = \frac{P_2}{P_1} \cdot 100\%. \quad (18-9)$$

Since the efficiency of a power transformer is very high (in large transformers more than 99 per cent), the *direct method of determination* of the efficiency by means of actual measurement of the powers P_1 and P_2 is impracticable, since the inevitable errors when measuring the powers P_1 and P_2 would result in a large error in the estimated efficiency.

In this respect, undoubtedly more advantageous are the *indirect*

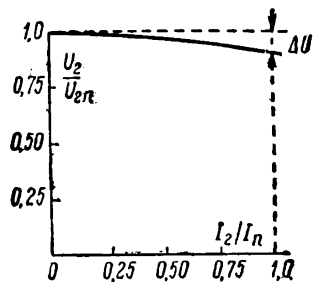


Fig. 18-10. External characteristic of transformer

methods of efficiency determination when one power is expressed by means of the other and the losses.

Let p_{st} be the losses in the steel, and p_{cop} the losses in the winding copper. Then

$$P_1 = P_2 + p_{st} + p_{cop}$$

and

$$\eta = \frac{P_2}{P_2 + p_{st} + p_{cop}} \cdot 100\% = \left(1 - \frac{p_{st} + p_{cop}}{P_2 + p_{st} + p_{cop}}\right) \cdot 100\%. \quad (18-10)$$

While determining all these magnitudes, we introduce a number of simplifying assumptions which inevitably lead to some errors, but which: a) simplify efficiency determination and b) give quite satisfactory final results, since the permissible errors are inherently small and belong to the second order values and in part mutually compensate each other.

The output P_2 in (18-10) will be called transformer *calculated output*. It is determined by means of formula:

$$P_2 = k_{load} P_n \cos \varphi_2, \quad (18-11)$$

where k_{load} is the load factor of a transformer.

The calculated output is of an arbitrary nature and does not coincide with the true output of a transformer in service. Let us recall (§ 12-4) that the rated secondary voltage of a transformer is called the voltage at no-load, i. e., $U_{2n} = U_{20}$. Consequently, the rated output of a transformer on the secondary side is $U_{20} I_{2n}$. The true output of a transformer with a current I_{2n} is $P_2 \equiv U_2 I_{2n}$, where U_2 is the true secondary voltage when the transformer is in operation. Hence, the calculated output of a transformer differs from the true output to the same extent as the voltage U_{20} differs from voltage U_2 .

Of the same conditional nature is the determination of p_{st} and p_{cop} .

Assume that a transformer operates at a rated primary voltage $U_1 = U_{1n} = \text{const}$ and a rated frequency $f = f_n = \text{const}$.

We have seen above [equation (14-4)] that for no-load $p_{st} \approx P_o$. On the other hand, for a given frequency f the loss $p_{st} \equiv B^2 \equiv E_1^2$. But $E_1 = -(\dot{U}_1 - \dot{I}_1 Z_1)$. Therefore the variation of the e.m.f. E_1 depends on the voltage drop in the transformer primary, i. e., with an inductive load the e.m.f. E_1 decreases with an increasing load, but increases with a capacitive load (Fig. 18-8). Consequently, with an inductive transformer load the losses in the steel will be less, compared with the no-load losses while with a capacitive load they may be more. Usually, if the load variation occurs within the normal range, the e.m.f. variation does not exceed $1.5 = 4$

per cent. Thus, the losses in the steel may change by 3-8 per cent. Such a small variation may be practically neglected, and for given operating conditions of a transformer the steel losses may be assumed as independent of the load, i. e.,

$$p_{st} = P_0 = \text{const.} \quad (18-12)$$

The output values P_0 for power oil transformers at rated voltages and frequencies are given in the State Standard 401-41.

Equally, the short-circuit power P_{sh} does not quite accurately define the copper losses during transformer operation on load. Indeed, if we, while maintaining the secondary current constant, change from short-circuit conditions to operation on load, the primary current will change, since $\dot{I}_1 = -\dot{I}_2' + \dot{I}_0$. With an inductive load the current I_1 will thus increase, and the losses in the copper of the primary will correspondingly also increase; with a capacitive load the reverse takes place (Fig. 18-5, *a* and *b*). Thus, by neglecting the current I_0 , we decrease the actual copper losses in the case of an inductive transformer load and increase the losses for a capacitive load. However, since the influence of current I_0 is very small, then this third assumption, like the two former ones, has almost no effect on transformer efficiency, the more so as it partially compensates for the error allowed when determining losses in the steel.

The values of the short-circuit power P_{sh} at rated currents in the windings and for $t=75^\circ\text{C}$ are given in the State Standard 401-41.

If the load makes up a k_{load} part of the rated value, it is assumed that the currents in the transformer winding vary in the same degree. In this case the correction for the winding temperature variation is not introduced. Hence

$$p_{cop} = k_{load}^2 P_{sh}. \quad (18-13)$$

Then the transformer efficiency in a general form is written as follows:

$$\eta = \left(1 - \frac{P_0 + k_{load}^2 P_{sh}}{k_{load} P_n \cos \varphi_2 + P_0 + k_{load}^2 P_{sh}} \right) \times 100. \quad (18-14)$$

Since with a given $\cos \varphi_2$ the only variable in the equation (18-14) is the load factor k_{load} , we may determine the value of this factor at which the transformer efficiency attains a maximum. It is then sufficient to take the first derivative of η for the variable k_{load} , and equate it to zero. Having performed this operation, we obtain:

$$P_0 = k_{load}^2 P_{sh}, \quad (18-15)$$

i. e. the efficiency reaches a maximum at such a load for which the losses in the copper are equal to the losses in the steel or in other words, the variable losses are equal to the constant losses.

18-10. Numerical Example

Determine the efficiency of a three-phase transformer at 100 kVA, 6,000/230 V, 50 c/s for $k_{load} = 1/4, 2/4, 3/4$ and $4/4$ and $\cos \varphi_2 = 0.8$. The no-load losses $P_0 = 0.6$ kW, the short-circuit losses $P_{sh} = 2.4$ kW (according to the State Standard).

The calculated data are given in Table 18-1.

Table 18-1

$$\eta = f(P_2)$$

k_{load}	$P_2 = k_{load} \cdot P_n \cos \varphi_2$, kW	P_0 , kW	$k_{load}^2 P_{sh}$, kW	$P_0 + k_{load}^2 P_{sh}$, kW	$P_2 + P_0 + k_{load}^2 P_n \cos \varphi_2$, kW	η , %
1/4	20	0.6	0.15	0.75	20.75	96.4
2/4	40	0.6	0.6	1.2	41.2	97.1
3/4	60	0.6	1.35	1.95	61.95	96.85
4/4	80	0.6	2.4	3.0	83.0	96.4

From the table it may be seen that already at 1/4 of the rated load the transformer efficiency is very high. According to (18-15) we find that the efficiency attains a maximum at

$$k_{load} = \sqrt{\frac{P_0}{P_{sh}}} = \sqrt{\frac{0.6}{2.4}} = \frac{1}{2}.$$

Chapter Nineteen

UNBALANCED CONDITIONS IN THREE-PHASE TRANSFORMERS

19-1. Preliminary

In the case of unequal currents in the phase windings additional phenomena occur in the transformer usually of adverse nature which lead to the distortion of line and phase voltages, additional losses in the steel and windings, considerable local overheating, etc. [Bibl. 15 b, 73 b].

These phenomena attain their maximum effect during unbalanced short circuits, since these are the limiting cases of an unbalanced load. Moreover, the conditions of unbalanced short cir-

cuits are of considerable interest in respect to actual service and from this point of view they should be studied first.

Several unbalanced short-circuit conditions are distinguished but here we shall consider only three of the most significant, viz.:

a) The single-phase short circuit in the case of the Y/Y_0 -12 winding connection;

b) The single-phase short circuit for the case of Δ/Y_0 -11, mainly to show the effect of various winding connections and

c) The two-phase short circuit for the Y/Δ -11 winding connection.

19-2. Symmetrical Component Analysis

The main method used for the analysis of unbalanced operating conditions of electrical machines and transformers is the method of symmetrical components, the substance of which is assumed to be known from electrical engineering theory.

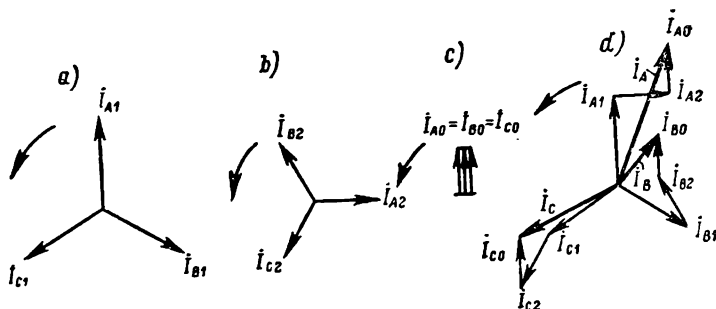


Fig. 19-1. Current systems:

a — positive; b — negative; c — zero; d — resultant

Any unbalanced three-phase system may in the general case be resolved into three symmetrical systems: those of positive, negative and zero sequences of phases or, in short, into the positive, the negative and zero sequences.

In Fig. 19-1, a, b, c and d are shown all the three symmetrical current systems and the non-symmetrical resultant system.

With conventional counter-clockwise vector rotation, the positive system of currents forms a symmetrical star of vectors $i_{A1}—i_{B1}—i_{C1}$ following each other in the alphabetic order.

Correspondingly, the negative current system forms another symmetrical star of vectors following each other in the order $i_{A2}—i_{C2}—i_{B2}$ the sequence being opposite to the alphabetic order.

The zero system of currents consists of three current vectors \dot{I}_{A0} , \dot{I}_{B0} , \dot{I}_{C0} which are equal and in phase.

According to Fig. 19-1, *d* we have,

$$\dot{I}_A = \dot{I}_{A1} + \dot{I}_{A2} + \dot{I}_{A0}, \quad (19-1a)$$

$$\dot{I}_B = \dot{I}_{B1} + \dot{I}_{B2} + \dot{I}_{B0} \quad (19-1b)$$

and

$$\dot{I}_C = \dot{I}_{C1} + \dot{I}_{C2} + \dot{I}_{C0}. \quad (19-1c)$$

Consider the current vector \dot{I}_{A1} as the initial vector. Then the current vectors \dot{I}_{B1} and \dot{I}_{C1} may be written as

$$\dot{I}_{B1} = a^2 \dot{I}_{A1} \quad \text{and} \quad \dot{I}_{C1} = a \dot{I}_{A1}. \quad (19-2)$$

Here a is the so-called *turn operator*, i. e., a multiplier indicating that the given vector is to be turned in respect to the initial vector by an angle of $120^\circ = \frac{2}{3}\pi$ in the direction of vector rotation.

In magnitude

$$a = -0.5 + j \frac{\sqrt{3}}{2} = e^{+j\frac{2\pi}{3}} = e^{-j\frac{4\pi}{3}}. \quad (19-3)$$

Consequently,

$$a^2 = -0.5 - j \frac{\sqrt{3}}{2} = e^{+j\frac{4\pi}{3}} = e^{-j\frac{2\pi}{3}}; \quad (19-4)$$

$$a^3 = 1 \quad (19-5a)$$

and

$$1 + a + a^2 = 0. \quad (19-5b)$$

Accordingly, for the negative sequence we have

$$\dot{I}_{B2} = a \dot{I}_{A2} \quad \text{and} \quad \dot{I}_{C2} = a^2 \dot{I}_{A2}. \quad (19-6)$$

For the zero system of currents

$$\dot{I}_{A0} = \dot{I}_{B0} = \dot{I}_{C0}. \quad (19-7)$$

Substituting these current values into the equations (19-1a), (19-1b) and (19-1c), and solving them for currents \dot{I}_{A1} , \dot{I}_{A2} and \dot{I}_{A0} we obtain:

$$\dot{I}_{A1} = \frac{1}{3} (\dot{I}_A + a \dot{I}_B + a^2 \dot{I}_C), \quad (19-8a)$$

$$\dot{I}_{A2} = \frac{1}{3} (\dot{I}_A + a^2 \dot{I}_B + a \dot{I}_C), \quad (19-8b)$$

$$\dot{I}_{A0} = \frac{1}{3} (\dot{I}_A + \dot{I}_B + \dot{I}_C). \quad (19-8c)$$

19-3. Assumptions Used for Unbalanced Short-Circuit Analysis

When analysing unbalanced short-circuit conditions it will be assumed that:

- a) the bus-bars that feed the transformer are of infinite capacity and in accordance with this the system of primary line voltages U_{AB} , U_{BC} , and U_{CA} remains balanced irrespective of transformer operating conditions;
- b) the secondary is reduced to the primary and
- c) the no-load current $I_0=0$.

19-4. Single-Phase Short Circuit of Transformer with Y/Y_0 Connected Windings

Assume that the phase a is short-circuited, and phases b and c are open (Fig. 19-2). In accordance with this we have an unbalanced system of secondary currents $I_a=I_{sh1}$, $I_b=0$ and $I_c=0$.

Suppose for simplicity $r_{sh}=0$ and the current I_{sh1} lags on $E_a=E_A$ by 90° (Fig. 19-3).

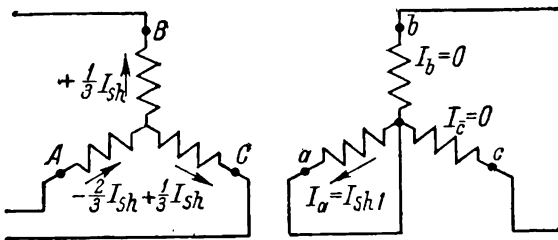


Fig. 19-2. Single-phase short-circuit with Y/Y_0-12 connected windings

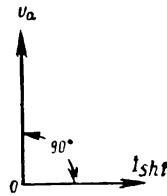


Fig. 19-3. Current of a single-phase short-circuit for $r_{sh}=0$

Using equations (19-8a), (19-8b) and (19-8c), let us resolve the unbalanced system of secondary currents into three symmetrical systems: the positive sequence \dot{I}_{a1} , \dot{I}_{b1} , \dot{I}_{c1} ; negative sequence $-\dot{I}_{a2}$, \dot{I}_{c2} , \dot{I}_{b2} and zero sequence $-\dot{I}_{a0}$, \dot{I}_{b0} , \dot{I}_{c0} (Fig. 19-4). Each of these currents of any system equals to $\frac{1}{3} I_{sh1}$.

To systems of positive and negative sequence in the secondary correspond to similar current systems in the primary. But there is

no zero system in the primary because this winding has no neutral brought out. In this case, then, $\dot{I}_A + \dot{I}_B + \dot{I}_C = 0$ and, therefore, according to [formula (19-8c)],

$$\dot{I}_{A0} = \frac{1}{3}(\dot{I}_A + \dot{I}_B + \dot{I}_C) = 0.$$

Thus, a single-phase short circuit of a Y/Y_0 connected transformer may be considered as the result of the superposition of three operating conditions, viz.: of two symmetrical conditions of a three-

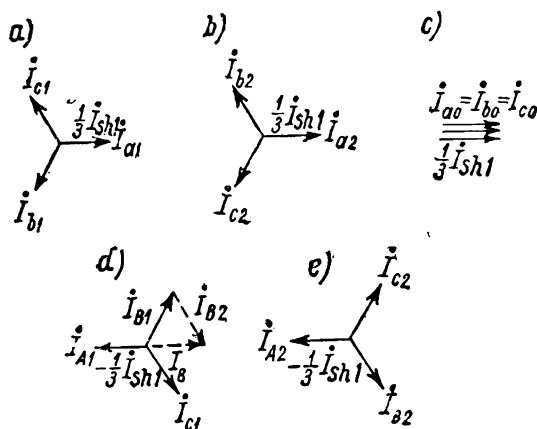


Fig. 19-4. Resolution of a single-phase short-circuit current with Y/Y_0 -12 connected windings

phase short circuit with positive and negative current systems and the third, the single-phase current condition in the secondary winding.

The positive and negative current systems create normal three-phase systems within the range of each of which the primary and secondary m.m.f.s are mutually balanced. Therefore, the primary and secondary currents are shown in Fig. 19-4, *a*, *d* and in 19-4, *b*, *e* in antiphase and of the same magnitude, since the secondary, according to the condition, is reduced to the primary.

Adding geometrically currents of positive and negative sequences in the primary phases (the addition of currents \dot{I}_{B1} and \dot{I}_{B2} in phase *B* is shown in Fig. 19-4, *d* by a broken line), we obtain:

$$\dot{I}_A = \dot{I}_{A1} + \dot{I}_{A2} = -\frac{2}{3} \dot{I}_{sh1}, \quad (19-9)$$

$$\dot{I}_B = \dot{I}_{B1} + \dot{I}_{B2} = \frac{1}{3} \dot{I}_{sh1} \quad (19-10a)$$

and

$$I_c = I_{c1} + I_{c2} = \frac{1}{3} I_{sh1}. \quad (19-10b)$$

Both three-phase current systems have the same equivalent circuit with short-circuit impedance $Z_{sh} = Z_1 + Z'_2$ (Fig. 19-5) similar to the equivalent circuit in Fig. 17-3. This may be explained

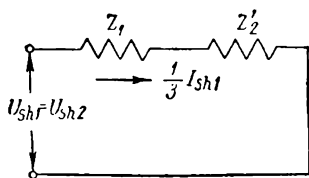


Fig. 19-5. Equivalent circuit for currents of positive and negative sequence

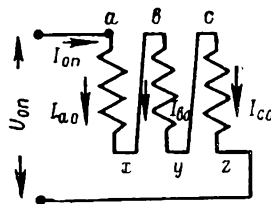


Fig. 19-6. Zero sequence currents ($0n$ is same as $0s$)

by the transformer being a device in which, contrary to rotating electrical machines, the sequence of phases whether $A-B-C$ or $A-C-B$ is of no importance.

The zero system currents I_{a0} , I_{b0} and I_{c0} flowing only in the secondary winding are equal and in phase; hence, they must all flow through the winding in one direction, i. e., from the beginning of the phase windings to their ends or in the opposite direction. Accordingly, we may visualise the secondary phase windings as series-connected, following the circuit $(a-x)-(b-y)-(c-z)$ thus forming a circuit through which flows the current

$$I_{0s} = I_{a0} = I_{b0} = I_{c0} = \frac{1}{3} I_{sh1}$$

from the source of the single-phase current with rated frequency and a voltage U_{0s} (Fig. 19-6).

Corresponding to this scheme, we have:

$$I_{0s} = \frac{U_{0s}}{3Z_{0s}}, \quad (19-11)$$

where $Z_{0s} = r_{0s} + jx_{0s}$ is the zero sequence impedance. Flowing through the windings, the current $I_{0s} = \frac{1}{3} I_{sh1}$ produces three m.m.f.s equal and in phase $\dot{F}_{0s} = I_{0s} \omega_1 = \frac{1}{3} I_{sh1} \omega_1$. The effect of this m. m. f. depends entirely on the nature of the transformer magnetic

system. In a three-legged transformer, the m.m.f.s F_{0s} , being oriented the same direction in all three legs (in Fig. 19-7, the m.m.f.s F_{0s} are all directed upwards), act along each leg pair circuit in opposition and create a single-phase flux Φ_{0s} , which closes from one yoke to the other in the medium surrounding the transformer (the thin broken lines in Fig. 19-7).

Since the reluctance of this medium is high, the flux Φ_{0s} for a given value of current I_{0s} is relatively small. On the contrary, in

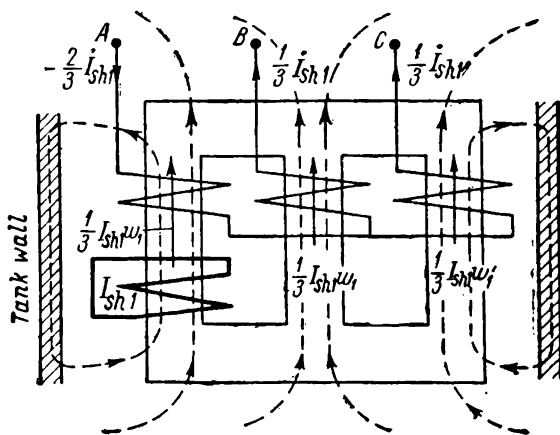


Fig. 19-7. Single-phase flux in three-leg transformer with Y/Y_0 connected windings

a transformer bank, the flux Φ_{0s} closes through the core of each of the single-phase transformers, i. e., along the path of the main flux (Fig. 19-8); therefore, even a very small current I_{0s} —about the order of the no-load current—creates a flux Φ_{0s} comparable in value to the main flux of a transformer.

In order to show the effect of the flux Φ_{0s} , the diagram in Fig. 19-9 is plotted. Here ABC is the triangle of the primary line voltages $\dot{U}_{AB} = \overline{AB}$, $\dot{U}_{BC} = \overline{BC}$ and $\dot{U}_{CA} = \overline{CA}$; point O is the neutral point of both windings; $\overline{OA} = \dot{U}_A$, $\overline{OB} = \dot{U}_B$ and $\overline{OC} = \dot{U}_C$ are the phase voltages for a balanced load.

Since, according to assumption, the transformer is fed from infinite bus-bars, the potentials of points A , B , and C are given beforehand and do not depend on transformer operating conditions.

The current I_{sh1} and, consequently, the current $I_{os} = \frac{1}{3}I_{sh1}$ lags on the voltage U_A of the short-circuited phase by 90° ($r_{sh}=0$).

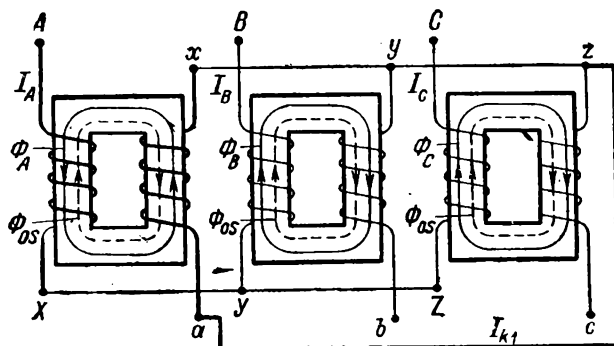


Fig. 19-8. Single-phase flux in transformer bank with Y/Y_0 connected windings

The flux Φ_{os} produced by the m.m.f. $I_{os}\omega_1 = \frac{1}{3}I_{sh1}\omega_1$ is in phase with current I_{sh1} and induces into each phase winding of the transformer an e.m.f. E_{os} lagging on flux Φ_{os} by 90° . When summing

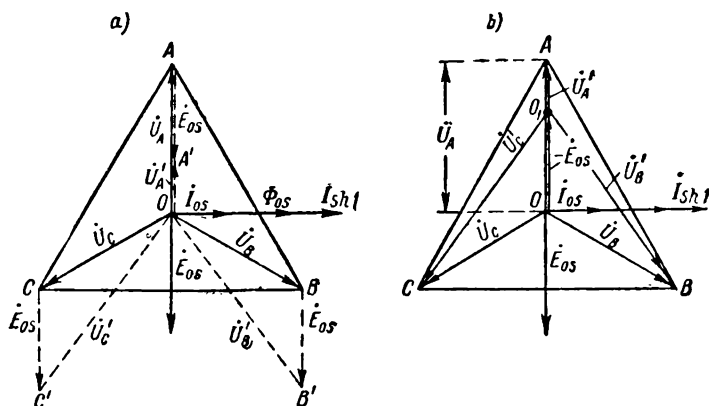


Fig. 19-9. Effect of single-phase flux Φ_{os} on Y/Y_0 connected windings

with the voltages U_A , U_B and U_C , the e.m.f. E_{os} tends to change the potential of points A , B and C in the manner shown in Fig. 19-9, *a* by the broken lines. But, as it was indicated above the potentials of these points are fixed. Therefore the action of the

e.m.f. E_{os} is in displacing the neutral point by the value of the e.m.f., i. e., E_{os} (Fig. 19-9, *b*). It may be seen that E_{os} decreases the phase voltage of the short-circuited phase *A* and increases the phase voltage of two other windings. In this case with a three-legged transformer having a coupled magnetic system, the displacement of the neutral point is restricted (Fig. 19-9, *b*) in accordance with the limited value of the flux Φ_{os} (Fig. 19-7). Conversely, in transformers that have independent magnetic systems, i. e., the shell-type, the five-legged, and the bank-type, the flux Φ_{os} reaches values commensurable with the magnitude of the main flux Φ already at current values $I_{os} \approx I_0$, i. e., at a negligible unbalanced load. In this case the neutral point in Fig. 19-9, *b* practically coincides with point *A*; accordingly, we have the following phase winding voltages, $U'_A = 0$ and $U'_B = U'_C = U_l$. Such a distortion of phase voltages is entirely inadmissible, and therefore transformers with an independent magnetic system are never employed in Y/Y_0 systems.

19-5. Diagram of Single-Phase Short Circuit of Transformer with Y/Y_0 Connected Windings

In plotting this diagram, we shall as before neglect the active resistances. In this case $Z_{sh} = jx_{sh}$ and $Z_{os} = jx_{os}$.

The diagram is given in Fig. 19-10, where the phase voltages U_A , U_B and U_C , the current I_{sh1} and the e.m.f. E_{os} are plotted as in

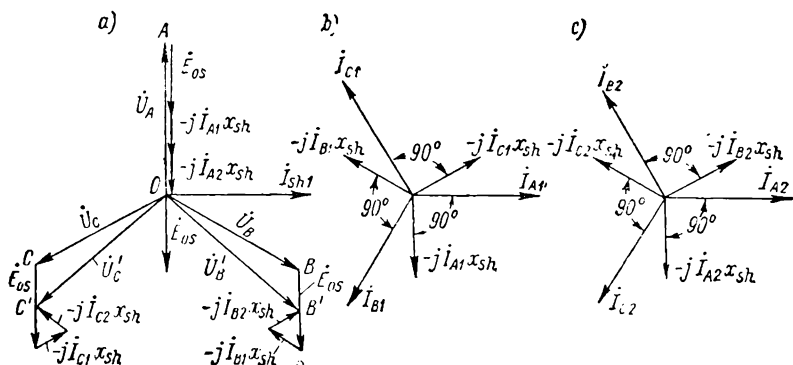


Fig. 19-10. Single-phase short-circuit diagram for transformer with Y/Y_0 connected windings

Fig. 19-9. The currents of the positive and negative sequence produce leakage e.m.f.s— $j\dot{I}_{A1}x_{sh}$, $-j\dot{I}_{A2}x_{sh}$, etc., shown in Fig. 19-10, *b* and *c*, according to each phase current.

Since phase *A* is short-circuited, the e.m.f.s acting in this phase are mutually balanced.

Consequently,

$$\dot{U}_A + \dot{E}_{os} - j\dot{I}_{A1} x_{sh} - j\dot{I}_{A2} x_{sh} = 0.$$

The phase windings *B* and *C* are not short-circuited. Therefore there exist voltages \dot{U}'_B and \dot{U}'_C across their terminals, in accordance with which the e.m.f. equations for these windings are written as

$$\dot{U}_B + \dot{E}_{os} - j\dot{I}_{B1} x_{sh} - j\dot{I}_{B2} x_{sh} = \dot{U}'_B$$

and

$$\dot{U}_C + \dot{E}_{os} - j\dot{I}_{C1} x_{sh} - j\dot{I}_{C2} x_{sh} = \dot{U}'_C.$$

The geometrical summation of the e.m.f. vectors corresponding to the equations written above is shown in Fig. 19-10, *a* (the leakage e.m.f.s scale is approximately twice reduced).

If we were to take into account the active resistances of the winding, then for phase *A* we have:

$$\dot{U}_A + \dot{E}_{os} - \dot{I}_{A1} Z_{sh} - \dot{I}_{A2} Z_{sh} = 0. \quad (19-12)$$

The e.m.f. \dot{E}_{os} is determined from the diagram in Fig. 19-6, viz.:

$$\dot{E}_{os} = \frac{1}{3} \dot{U}_{os} = -\dot{I}_{os} Z_{os} = -\frac{1}{3} \dot{I}_{sh1} Z_{os}.$$

Besides $\dot{I}_{A1} = \dot{I}_{A2} = \frac{1}{3} \dot{I}_{sh1}$. Consequently,

$$\dot{U}_A - \frac{1}{3} \dot{I}_{sh1} Z_{os} - \frac{1}{3} \dot{I}_{sh1} Z_{sh} - \frac{1}{3} \dot{I}_{sh1} Z_{sh} = 0,$$

and hence,

$$\dot{I}_{sh1} = \frac{3\dot{U}_A}{Z_{os} + 2Z_{sh}}. \quad (19-13)$$

Here $U_A = U_{ph} = \frac{U_l}{\sqrt{3}}$; the impedance Z_{sh} is determined from short-circuit tests, while for determining Z_{os} a special test is carried out.

19-6. Determination of Zero-Sequence Resistance

Here we shall discuss only a three-legged transformer as the only one used in Y/Y_0 circuits. To determine the transformer impedance Z_{os} it is necessary to connect one of the windings, in parallel or series, leaving the other winding open (Fig. 19-11 shows only the series connection of the windings). Having measured the

voltage, the current and the power per phase, $U_{os\ ph}$, $I_{os\ ph}$ and $P_{os\ ph}$, we obtain the following equations:

$$z_{os} = \frac{U_{os\ ph}}{I_{os\ ph}}; \quad (19-14a)$$

$$r_{os} = \frac{P_{os\ ph}}{I_{os\ ph}^2} \quad (19-14b)$$

and

$$x_{os} = \sqrt{z_{os}^2 - r_{os}^2}. \quad (19-14c)$$

Experiments have shown that: a) the inductive component of the zero resistance x_{os} is considerably larger than the active component r_{os} so that $z_{os} \approx x_{os}$; b) the values of x_{os} and r_{os} are largely

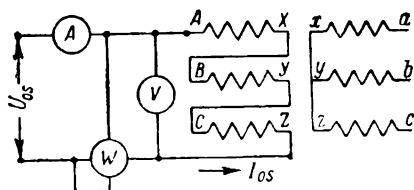


Fig. 19-11. Circuit for determination of z_{os}

affected by the oil transformer tank, through which lines of flux Φ_{os} pass (see Fig. 19-7); c) the impedance z_{os} is much greater than impedance z_{sh} (for clarity the scales in Fig. 19-10, a are not adhered to). For example, when testing a three-phase 100 kVA, 6,300/220 V oil transformer by the scheme assembled on the

low-voltage winding side, the following results have been obtained: a) with the transformer taken out of the tank, $z_{os}=0.20$ ohm, $r_{os}=0.022$ ohm and $x_{os}=0.199$ ohm; b) with the transformer in the tank, $z_{os}=0.31$ ohm, $r_{os}=0.055$ ohm and $x_{os}=0.30$ ohm; c) $z_{sh}=0.028$ ohm, $r_{sh}=0.0127$ ohm and $x_{sh}=0.0248$ ohm.

19-7. Unbalanced Loading of Transformer with Y/Y_0 Connected Windings

If the transformer works with the Y/Y_0 connection then some of the power consumers, for example, motors, are connected to the line voltage, while others, for example, lamps, are connected to the phase voltage (Fig. 19-12, a). With the load unbalanced we shall, as before, resolve the unbalanced current system into three symmetrical systems. If I_{os} is the zero-sequence current in each secondary phase (the currents of the balanced load are not shown in Fig. 19-12, a), then the current $3I_{os}$ flows through

the neutral wire. Suppose $3I_{os} = I_n$, i. e., that $I_{os} = \frac{1}{3} I_n$. The zero point displacement in the line voltage triangles is determined by the ratio $\frac{E_{os}}{U_{n.ph}} \cdot 100 = \frac{I_{os} z_{os}}{U_{n.ph}} \cdot 100$. If we assume that $z_{os} = 10z_{sh}$,

$$\text{then, } \frac{E_{os}}{U_{n.ph}} \cdot 100 = \frac{10}{3} \frac{I_n z_{sh}}{U_{n.ph}} \cdot 100 = \frac{10}{3} u_{sh}.$$

If, for instance,

$$u_{sh} = 5.5 \text{ per cent, then } \frac{E_{os}}{U_{n.ph}} \cdot 100 = 18 \text{ per cent.}$$

But with a transformer on load, the displacement of the neutral depends on the kind of load. Let, for example, as before

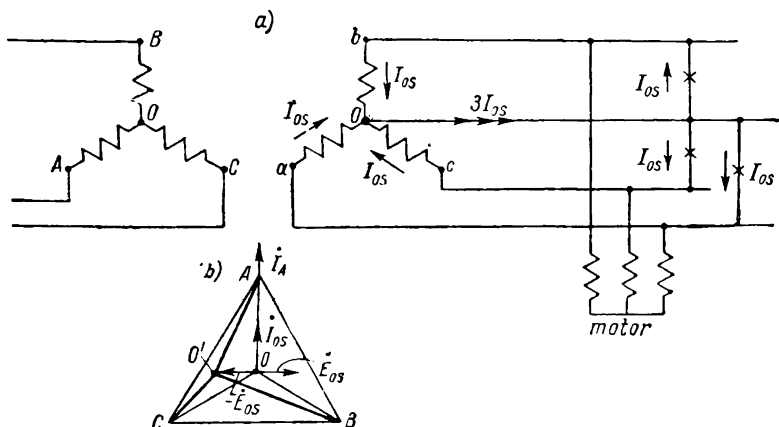


Fig. 19-12. Transformer operation with Y/Y₀ connected windings on unbalanced load

only phase A be on load and the load be purely active. Having carried out the same construction as in Fig. 19-10, b, we obtain the diagram shown in Fig. 19-12, b. In the case considered the phase voltages of the non-loaded phases vary in a wide range, whereas the voltage of the loaded phase varies relatively little.

To ensure the safety of the consumer, the State Standard 401-41 requires that the current in the neutral of a transformer with Y/Y₀ windings connection should not exceed 25 per cent of the low-voltage winding rated current; the phase current should not exceed the rated voltage in any of the phases.

19-8. Single-Phase Short Circuit of Transformer with Δ/Y_0 Connected Windings

When a transformer is working on a single-phase load with the windings Δ/Y_0 connected (Fig. 19-13), as in the case of the Y/Y_0 winding connection transformer there appears a zero sequence

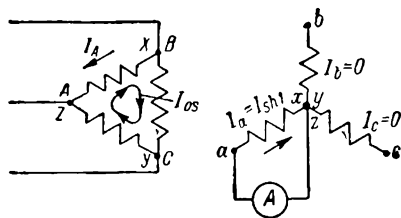


Fig. 19-13. Single-phase short circuit with Δ/Y_0 connected windings

current I_{0s} . But in this case, the current I_{0s} exists not only on the secondary side, but also flows through the circuit of the primary triangle $A-X-B-Y-C-Z$. Thus, currents of all the three sequences flow in both Δ/Y_0 connected windings of the transformer. The m.m.f.s produced by each of these current systems are al-

most balanced, hence the single-phase flux Φ_{0s} , and the shift of the neutral point O created by it though actually existing are nevertheless almost imperceptible. Therefore $I_A \approx I_a = I_{sh1}$, $I_B \approx 0$, $I_C \approx 0$. Phase voltages are distorted considerably less than in the Y/Y_0 system. This deduction may be extended also to a transformer on load, and from this point of view the Δ/Y_0 system has better characteristics than the Y/Y_0 system.

19-9. Two-Phase Short Circuit of Transformer with Y/Y Connected Windings

Let us short-circuit the phase $b-c$, leaving phase a open (Fig. 19-14). In this case $I_a = 0$ and $I_b = -I_c$. Since the neutral point is not tapped, such a current system may be resolved into two current systems—of positive and negative sequences—whereas the zero sequence current I_{0s} is absent ($I_a + I_b + I_c = 0$); accordingly, $\Phi_{0s} = 0$ and $E_{0s} = 0$; thus, the neutral point of this system, contrary to the systems considered before, is not displaced from its position when the transformer is loaded.

In the primary there exist the same two current systems as in the secondary; therefore, in the reduced transformer, $I_A = 0$ and $I_B = -I_C$. Each current system is determined by the three-phase short-circuit impedance $Z_{sh} = r_{sh} + jx_{sh}$. Simplifying, we assume $r_{sh} = 0$ and, consequently, the current I_B is phase-shifted in respect to the voltage $U_{BC} = BC$ by 90° (Fig. 19-15, a). Using equations

(19-8a), (19-8b) and (19-8c), we resolve the unbalanced current system $\dot{I}_B = -\dot{I}_C$ into the positive and negative systems \dot{I}_{A1} , \dot{I}_{B1}

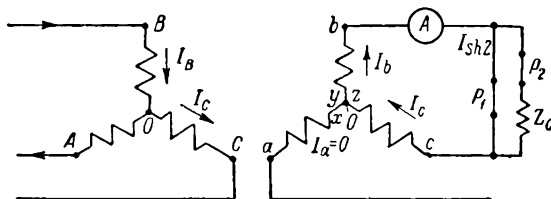


Fig. 19-14. Two-phase short circuit of transformer with Y/Y connected windings

and \dot{I}_{C1} , \dot{I}_{A2} , \dot{I}_{C2} , \dot{I}_{B2} (Fig. 19-15, *b* and *c*). Omitting the intermediate steps we find:

$$\dot{I}_{B1} = \frac{\dot{I}_B}{\sqrt{3}} e^{-j\frac{\pi}{6}}; \quad (19-15a)$$

$$\dot{I}_{B2} = \frac{\dot{I}_B}{\sqrt{3}} e^{+j\frac{\pi}{6}}; \quad (19-15b)$$

$$\dot{I}_{C1} = \frac{\dot{I}_C}{\sqrt{3}} e^{+j\frac{\pi}{6}}; \quad (19-16a)$$

$$\dot{I}_{C2} = \frac{\dot{I}_C}{\sqrt{3}} e^{-j\frac{\pi}{6}}. \quad (19-16b)$$

Each of these currents produces a corresponding leakage e.m.f. lagging 90° on the current.

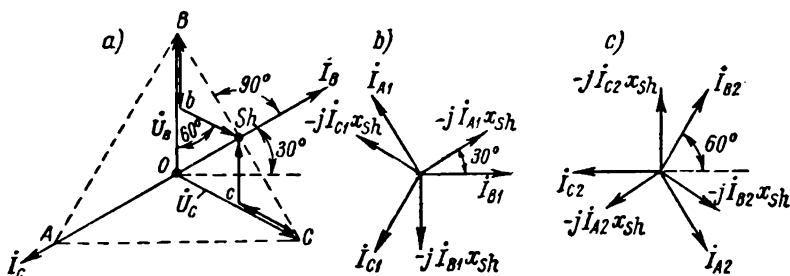


Fig. 19-15. Two-phase short-circuit diagram of transformer

When the circuit (*b-y*)-(*c-z*) is short-circuited, we have for the primaries of the *B* and *C* phases

$$\dot{U}_B - \dot{U}_C + (-j\dot{I}_{B1}x_{sh}) + (-j\dot{I}_{B2}x_{sh}) + (-j\dot{I}_{C1}x_{sh}) + (-j\dot{I}_{C2}x_{sh}) = 0.$$

Substituting into this equation the values of currents \dot{I}_{B1} , \dot{I}_{B2} , \dot{I}_{C1} , \dot{I}_{C2} , we find, after carrying out the usual operations, that

$$\dot{I}_B = \dot{I}_{sh2} = -j \frac{\dot{U}_B - \dot{U}_C}{2x_{sh}}, \quad (19-17)$$

i. e., the current \dot{I}_B which is the current \dot{I}_{sh2} of the two-phase short circuit lags by 90° on the line voltage $\dot{U}_B - \dot{U}_C$ and is equal to $\frac{U_l}{2x_{sh}}$.

Hence,

$$I_B = I_{sh2} = \frac{U_l}{2x_{sh}} = \frac{U_{ph} \sqrt{3}}{2x_{sh}}. \quad (19-18)$$

The same result may be obtained graphically (Fig. 19-15, a). Current I_{B1} produces the e.m.f. $-j\dot{I}_{B1}x_{sh} = \overline{Bb}$ that is in antiphase with the e.m.f. \dot{U}_B ; the current I_{B2} produces the e.m.f. $-j\dot{I}_{B2}x_{sh} = \overline{bk}$ equal to the e.m.f. \overline{Bb} and leading it by an angle 60° corresponding to the 60° angle between vectors \dot{I}_{B1} and \dot{I}_{B2} . Therefore the e.m.f. triangle Bbk is an isosceles triangle with the angle $Bbk = 120^\circ$ and the triangle Obk is an equilateral triangle. Thus $Bb = \frac{OB}{2} = \frac{U_{ph}}{2}$ and, consequently,

$$Bb = I_{B1} x_{sh} = \frac{I_B}{\sqrt{3}} x_{sh} = \frac{U_{ph}}{2},$$

hence,

$$I_B = I_{sh2} = \frac{U_{ph} \sqrt{3}}{2x_{sh}}. \quad (19-19)$$

19-10. Unbalanced Loading of Transformer with Y/Y Connected Windings

Let us open the switch P_1 in Fig. 19-14. In this case the transformer works on a circuit with the impedance Z_c , and the currents $I_a = I_A = 0$, $\dot{I}_b = -\dot{I}_c$ and $\dot{I}_B = -\dot{I}_C$. Since the zero sequence current $I_{0s} = 0$, the neutral point of the system is not displaced. Consider current \dot{I}_B in phase with the line voltage $U_{BC} = BC$ (practically an active load). According to the condition, the potential of the points A , B and C are stipulated, and, consequently, the phase primary voltages do not change with load. In order to

obtain the secondary phase and line voltages it is possible, without carrying out the resolution of the unbalanced two-phase current system, to add geometrically the vector \overline{OB} to the e.m.f. vectors $-\dot{I}_B r_{sh}$ and $-j\dot{I}_B x_{sh}$ and vector \overline{OC} to the e.m.f. vectors $-\dot{I}_C r_{sh}$ and $-j\dot{I}_C x_{sh}$ (Fig. 19-16). In the case considered the phase voltage $U_B = OB'$ increases, while the voltage $U_C = OC'$ decreases, the secondary line voltages being distorted. But when $I_B = I_n$ the voltage variation does not exceed the impedance voltage value u_{sh} , i. e., the change remains within the range of several per cent.

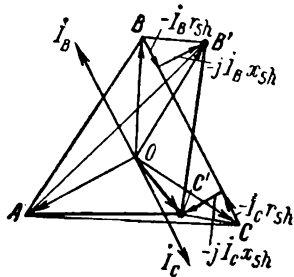


Fig. 19-16. Voltage diagram for two-phase transformer load

19-11. Transformer Operation with Open-Delta Connection

To obtain the open delta, it is sufficient to connect two single-phase transformers to the primary circuit as shown in Fig. 19-17, *c*. Let us compare operating conditions of transformer groups with closed and open delta. Let us suppose that a) the primary line voltages U_{AB} , U_{BC} and U_{CA} form a symmetrical system and do not depend on transformer load; b) the secondary is reduced to the primary; c) the no-load current $I_0 = 0$; d) with closed a delta (Fig. 19-17, *a*) the load is active and uniformly distributed; e) the voltage drops in the transformer so far are not taken into account.

Then the diagram of voltages and currents for the *closed* delta will have the form shown in Fig. 19-17, *b*. Here the vectors U_{AB} , U_{BC} and U_{CA} represent a symmetrical system of primary line voltages. At the same time these vectors also represent phase primary voltages U_{AX} , U_{BY} , U_{CZ} . With an active load, the phase currents I_{AX} , I_{BY} and I_{CZ} are in phase with their corresponding phase voltages, and the line currents represent the geometrical difference of two phase currents, viz., $I_B = I_{AX} - I_{BY}$, $I_C = I_{BY} - I_{CZ}$ and $I_A = I_{CZ} - I_{AX}$. The same arrangement of voltages and currents is observed in the secondary winding and in the secondary power circuit.

Let us now see how the operating conditions change when the primary and secondary deltas are opened (the phase *BY-by* is eliminated). Since as stipulated, the primary line voltages U_{AB} , U_{BC} and U_{CA} , and the corresponding phase voltages U_{AX} and U_{CZ} do not change, then in compliance with the e.m.f.

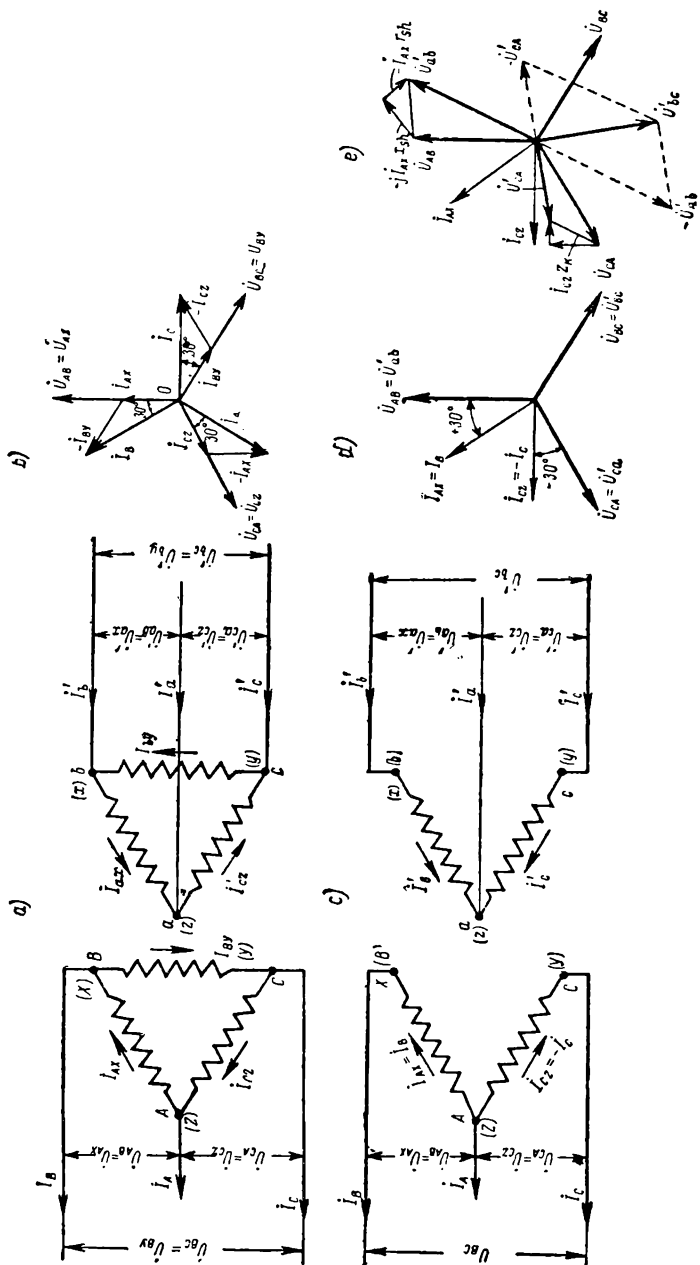


Fig. 19-17. Transformer open-delta operation

equilibrium condition, neither the primary e.m.f.s of the A - X and C - Z phases nor the magnetic fluxes required to create these e.m.f.s may change. When there are no voltage drops, the voltage $U'_{ab} = U_{AB}$ and $U'_{ca} = U_{CA}$, i. e., the secondary voltages U'_{ab} and U'_{ca} also do not undergo change, in magnitude or in phase. Since $\dot{U}'_{ab} + \dot{U}'_{bc} + \dot{U}'_{ca} = 0$ and, consequently, $\dot{U}'_{bc} = -(\dot{U}'_{ab} + \dot{U}'_{ca})$, the voltage \dot{U}'_{bc} as also the voltages \dot{U}'_{ab} and \dot{U}'_{ca} does not undergo any changes (Fig. 19-17, d).

Thus, if there are some consumers in the secondary circuit, then with open delta and absence of voltage drops they remain under the same voltage as with closed delta. Therefore the secondary and accordingly the primary line currents remain without change, while the phase currents change both in magnitude and in phase. Having compared current distribution for open and closed delta in Fig. 19-17, a and 19-17, b , we observe that currents I_{AX} in phases A - X of a closed and open delta flow in one direction, while the current I_{CZ} in the phase C - Z of the open delta changes its sign in respect to current I_{CZ} for a closed delta. Therefore, in an open delta $\dot{I}_{AX} = \dot{I}_B$ and $\dot{I}_{CZ} = -\dot{I}_C$, i. e., the current \dot{I}_{AX} leads the voltage U_{AB} by 30° , with the current \dot{I}_{CZ} lagging on voltage U_{CA} by 30° (Fig. 19-17, d). The capacity of the system in accordance with the above discussed remains without change, since $3U_{ph} I_{ph} = 2U_{ph} I_{ph} \sqrt{3} \cos 30^\circ$. But in this case the transformer windings in a scheme with an open delta prove to be overloaded by current $\sqrt{3}$ times. To avoid overheating of windings it is necessary to lower the current load $\sqrt{3}$ times, i. e., down to $\frac{100}{\sqrt{3}} = 58$ per cent of the rated current of the transformer bank.

The unbalance of the phase currents gives rise to some unbalance in the secondary voltages. Adding together geometrically the voltage vectors U_{AB} and U_{CA} with their corresponding e.m.f. vectors $\dot{I}_{AX} Z_{sh}$ and $\dot{I}_{CZ} Z_{sh}$, we obtain the secondary voltage vectors \dot{U}'_{ab} and \dot{U}'_{ca} (Fig. 19-17, e). The voltage $\dot{U}'_{bc} = -(\dot{U}'_{ab} + \dot{U}'_{ca})$. The unbalance in the secondary line voltages that takes place depends on the magnitude and kind of load and on the short-circuit parameters, i. e., on the u_{sh} value. With $u_{sh} = 5.5$ per cent the open-delta circuit gives practically symmetrical voltages almost up to rated current load value of each transformer.

The operation of the three-legged transformer with open primary and secondary deltas does not differ practically from the operation of the bank just considered above.

Transformer operation with open delta is used on transmission lines when they are just inaugurated, i. e., when they are not yet fully loaded, or when in the case of damage to one of the three transformers of a bank, operation has to be continued with a reduced load. Besides, all measuring transformers are also open-delta connected.

Chapter Twenty

PARALLEL OPERATION OF TRANSFORMERS

20-1. Stipulations for Parallel Operation of Transformers

Because a growing load may make it necessary to increase the kilovolt-ampere capacity of an existing bank by the addition of new transformers in parallel with it, or when it is desirable to supply an important load from several groups of transformers in order to maintain continuity of service despite failure of one of the transformers or its associated circuits, transformers are often operated in parallel. [Bibl. 89]

Parallel-connected transformers will operate in the best conditions, if the following stipulations for parallel transformer operation are observed:

a) The rated primary voltages and the corresponding secondary voltages of all parallel-operating transformers should be equal, i. e.,

$$U_{11} = U_{12} = U_{13} = \dots = U_{1n} \quad (20-1)$$

and

$$U_{21} = U_{22} = U_{23} = \dots = U_{2n}. \quad (20-2)$$

The first stipulation amounts practically to the requirement that all transformation ratios should be equal, i. e., that

$$k_1 = k_2 = \dots = k_n; \quad (20-3)$$

b) Transformers operating in parallel should belong to one group;

c) The active and reactive components of the short-circuit voltage of all transformers must be equal, i. e.,

$$u_{sh\ a1} = u_{sh\ a2} = \dots = u_{sh\ an} \quad (20-4)$$

and

$$u_{sh\ x1} = u_{sh\ x2} = \dots = u_{sh\ xn}. \quad (20-5)$$

The third stipulation practically boils down to a requirement that the impedance voltages should be equal, i.e., that

$$u_{sh1} = u_{sh2} = \dots = u_{shn}. \quad (20-6)$$

If the transformers meet all the above stipulations, all their vector diagrams plotted in per unit values for operation on load coincide (Fig. 20-1). In this case all transformers are loaded in proportion to their rated powers, and the load currents of the transformers may be added arithmetically.

In practice, however, only the second stipulation must unconditionally be fulfilled; the first and third stipulations may be met with certain departures for which some practically permissible limits should be fixed.

20-2. Parallel Operation of Transformers with Unequal Transformation Ratios

A. Parallel operation of two transformers on no-load. Suppose two parallel-connected transformers 1 and 2 satisfy the second and third stipulations, but do not satisfy the first stipulation and also $k_1 < k_2$. To explain the substance of the phenomenon,

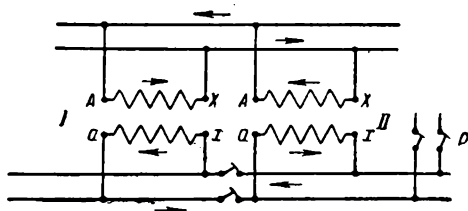


Fig. 20-2. Parallel operation of transformers with unequal transformation ratios

it is sufficient to examine parallel operation of single-phase transformers or of the separate corresponding phases of two three-phase transformers (Fig. 20-2). Let us assume that the primary line voltage equals the rated primary voltages of each of the connected in parallel transformers, i. e., $U_1 = U_{1n1} = U_{1n2}$. Then

$$U_{21} = \frac{U_1}{k_1} > U_{22} = \frac{U_1}{k_2},$$

the vectors $\vec{U}_{21} = \overline{OA}_1$ and $\vec{U}_{22} = \overline{OA}_2$ in this case being in phase (Fig. 20-3). The action of the difference of voltages $\vec{U}_{21} - \vec{U}_{22} = \Delta \vec{U} = \overline{OD}$, in transformers 1 and 2 is such that a circulating current I_{circ} appears, the instantaneous distribution of which in transformers 1 and 2 is shown in Fig. 20-2 by arrows. We may see that in respect to current I_{circ} the transformers 1 and 2 are

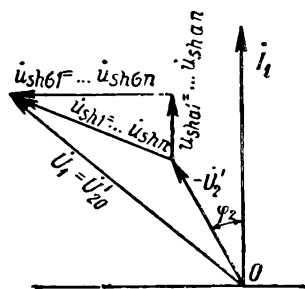


Fig. 20-1. Vector diagram for transformers operating in most favourable conditions

in short-circuit conditions, the current flowing in the transformer windings in opposite directions; in accordance with this, the circulating current is shown in Fig. 20-3 by two vectors:

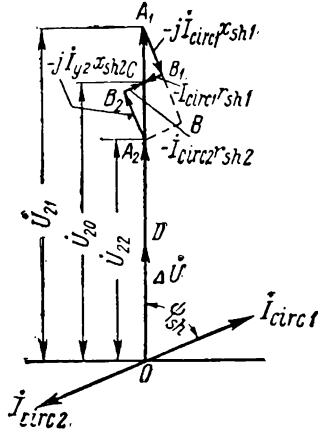


Fig. 20-3. Diagram of voltages and circulating currents of transformer on a no-load and $k_1 < k_2$ (y stands for *circ*)

I_{circ1} in transformer 1 and $I_{circ2} = -I_{circ1}$ in transformer 2. If Z_{sh1} and Z_{sh2} are the short-circuit impedances of transformers 1 and 2, then

$$I_{circ} = \frac{\Delta \dot{U}}{Z_{sh1} + Z_{sh2}} = \frac{\dot{U}_1 \left(\frac{1}{k_1} - \frac{1}{k_2} \right)}{Z_{sh1} + Z_{sh2}} = \frac{\dot{U}_1 \frac{k_2 - k_1}{k_1 k_2}}{Z_{sh1} + Z_{sh2}}. \quad (20-7)$$

To modify this equation, let us assume that $k_1 k_2 = k^2$ and $\frac{U_1}{k} = U_{2n}$. Here k is the average transformation ratio of both transformers and U_{2n} is the average value of the secondary rated voltage. Since $u_{sh1} = u_{sh2}$ and $u_{sh1} =$

$= u_{sh2}$ (the third stipulation), then

$$I_{circ} = \frac{\frac{U_1}{k} \frac{k_2 - k_1}{k}}{Z_{sh1} + Z_{sh2}} = \frac{U_{2n} \frac{k_2 - k_1}{k} \cdot 100}{\frac{Z_{sh1} I_{2n1}}{I_{2n1}} \cdot 100 + \frac{Z_{sh2} I_{2n2}}{I_{2n2}} \cdot 100} = \frac{\Delta k}{\frac{Z_{sh1} I_{2n1}}{U_{2n}} \cdot \frac{100}{I_{2n1}} + \frac{Z_{sh2} I_{2n2}}{U_{2n}} \cdot \frac{100}{I_{2n2}}} = \frac{\Delta k}{\frac{u_{sh1}}{I_{2n1}} + \frac{u_{sh2}}{I_{2n2}}}. \quad (20-8)$$

Here $\Delta k = \frac{k_2 - k_1}{k} \times 100$ is the difference in transformation ratios expressed as a percentage relation to the average value; I_{2n1} and I_{2n2} are the rated values of secondary currents of the transformers 1 and 2.

Usually the current I_{circ} is expressed as per cent of rated current of one of the transformers, for example, of current I_{2n1} in transformer 1. Then

$$I_{circ[0]} = \frac{I_{circ1}}{I_{2n1}} \times 100 = \frac{\Delta k \cdot 100}{u_{sh1} + u_{sh2} \frac{I_{2n1}}{I_{2n2}}} = \frac{\Delta k \cdot 100}{u_{sh1} + u_{sh2} \frac{P_{n1}}{P_{n2}}}, \quad (20-9)$$

where P_{n1} and P_{n2} are the rated powers of transformers 1 and 2.

Let, for example, $\Delta k = 1$ per cent; $u_{sh1} = u_{sh2} = 5.5$ per cent and $\frac{P_{n1}}{P_{n2}} = \frac{100}{100}, \frac{100}{320}$ and $\frac{100}{\infty} = 0$. Then $I_{circ1} = 9.1$ per cent, 14 per cent and 18.3 per cent.

The current I_{circ1} is phase-shifted in respect to ΔU by an angle

$$\psi_{sh} = \arctan \frac{x_{sh1} + x_{sh2}}{r_{sh1} + r_{sh2}}. \quad (20-10)$$

The currents I_{circ1} and I_{circ2} produce in transformers 1 and 2 the e.m.f.s $-j\dot{I}_{circ1}x_{sh1}$, $-\dot{I}_{circ1}r_{sh1}$, $-j\dot{I}_{circ2}x_{sh2}$ and $-\dot{I}_{circ2}r_{sh2}$ geometrically summing with voltage \dot{U}_{21} and correspondingly with \dot{U}_{22} .

If the rated powers of transformers are equal, i. e., $P_{n1} = P_{n2}$, then for $u_{sh1} = u_{sh2}$ (the third stipulation), we have $Z_{sh1} = Z_{sh2}$. In this case the short-circuit triangles A_1B_1C and A_2B_2C are equal in magnitude, and the segment A_1A_2 is divided at point C in two. Thus, in this case the current \dot{I}_{circ1} lowers the voltage \dot{U}_{21} down to the common voltage $\dot{U}_{20} = \overline{OC}$ across the secondary buses, while the current \dot{I}_{circ2} increases the voltage \dot{U}_{22} up to the same value $\dot{U}_{20} = \overline{OC}$. This actually is the role of the circulating voltage.

If the transformers are of different power, for instance, $P_{n1} < P_{n2}$, then for equal voltages u_{sh1} and u_{sh2} the resistances r_{sh} and x_{sh2} are inversely proportional to the powers, i. e., $r_{sh1} > r_{sh2}$ and $x_{sh1} > x_{sh2}$. In accordance with this, the triangle A_1B_1C in Fig. 20-3 becomes larger than the triangle A_2B_2C , but remains similar. Consequently, the point C is displaced downwards along segment A_1A_2 . At the limit, when $P_{n2} \gg P_{n1}$, point C coincides with point A_2 , and the triangle A_1B_1C will occupy the position of triangle A_1BA_2 . In this case $\dot{U}_{20} = \dot{U}_{22} = \overline{OA_2}$.

B. The parallel operation of two transformers on load. Let us assume as before that $k_1 < k_2$, $P_{n1} < P_{n2}$ and that the second and third stipulations of parallel transformer operation are fulfilled.

As the basis for studying the operation condition under consideration we assume the *method of superposition* of two conditions. The circulating current brings the secondary voltage of both transformers to a common voltage \overline{OC} (Fig. 20-3), i. e., to a state when parallel transformer operation takes place in the most advantageous conditions. Therefore, with the appearance of an external load, the external load current is distributed between the transformers in proportion to their rated powers.

Thus, all this takes place as if in each of the transformers there existed two currents, the *circulating current* I_{circ} and load current I_{load} corresponding to the external load. In reality there exists only the resultant current representing the geometrical sum of both currents.

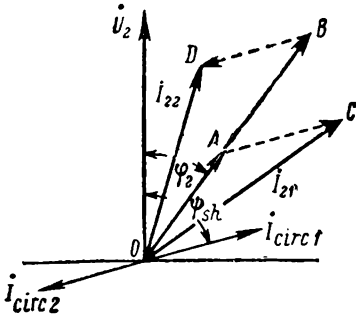


Fig. 20-4. Current diagram for load when $k_1 < k_2$

Since with load the secondary voltages of both transformers decrease practically by the same value, the voltages and accordingly the circulating currents I_{circ1} and I_{circ2} within the usual load range do not depend on transformer operating conditions.

In the part pertaining to the circulating currents, Fig. 20-4 repeats the plotting carried out in Fig. 20-3. The load currents

I_{load1} and I_{load2} of transformers 1 and 2 are represented by vectors \overline{OA} and \overline{OB} for the case when $\frac{OA}{OB} = \frac{I_{load1}}{I_{load2}} = \frac{P_{n1}}{P_{n2}} = \frac{1}{2}$. Vectors \overline{OA} and \overline{OB} are shifted in respect to the voltage vector \vec{U}_2 , for instance, they lag on it by the same angle φ_2 determined by parameters of the external circuit. The resultant currents of transformers 1 and 2 are determined by vectors

$$\overline{OC} = \vec{I}_{load1} + \vec{I}_{circ1} = \vec{I}_{21} \text{ and } \overline{OD} = \vec{I}_{load2} + \vec{I}_{circ2} = \vec{I}_{22}.$$

From the triangles OAC and OBD we have:

$$I_{21} = \sqrt{I_{load1}^2 + I_{circ}^2 + 2I_{load1}I_{circ}\cos(\psi_{sh} - \varphi_2)} \quad (20-11)$$

and

$$I_{22} = \sqrt{I_{load2}^2 + I_{circ}^2 + 2I_{load2}I_{circ}\cos(\psi_{sh} + \varphi_2)}. \quad (20-12)$$

As a measure of transformer loading by the circulating current the following relationships may be used:

$$\frac{I_{21}}{I_{n1}} = \sqrt{1 + \left(\frac{I_{circ}}{I_{load1}}\right)^2 + 2\frac{I_{circ}}{I_{load1}}\cos(\psi_{sh} - \varphi_{sh})} \quad (20-13)$$

and

$$\frac{I_{22}}{I_{n2}} = \sqrt{1 + \left(\frac{I_{circ}}{I_{load2}}\right)^2 + 2\frac{I_{circ}}{I_{load2}}\cos(\psi_{sh} + \varphi_{sh})}. \quad (20-14)$$

From the latter expressions it can be seen that the degree of overload or underload of the transformers depends, first, on the I_{circ} and ψ_{sh} values defined by the transformer parameters, and secondly on the angle φ_2 defined by the external circuit parameters.

In the particular case with an inductive load and $\varphi_2 = \psi_{sh}$ we have:

$$\frac{I_{21}}{I_{load 1}} = 1 + \frac{I_{circ}}{I_{load 1}} \quad (20-15a)$$

and

$$\frac{I_{22}}{I_{load 2}} = 1 - \frac{I_{circ}}{I_{load 2}}. \quad (20-15b)$$

In this case the transformer 1 is overloaded, and the transformer 2 underloaded.

With a capacitive load and $\varphi_2 = -\frac{\pi}{2} + \psi_{sh}$

$$\frac{I_{21}}{I_{load 1}} = \sqrt{1 + \left(\frac{I_{circ}}{I_{load 1}}\right)^2} \quad (20-16a)$$

and

$$\frac{I_{22}}{I_{load 2}} = \sqrt{1 + \left(\frac{I_{circ}}{I_{load 2}}\right)^2}; \quad (20-16b)$$

i. e., both transformers are overloaded.

Let, for instance, $P_{n1} = 100$ kVA, $P_{n2} = 320$ kVA; $\frac{I_{circ}}{I_{n1}} = 0.14$; $\cos \varphi_2 = 0.8$ and $\psi_{sh} = 75^\circ$. Then $\frac{I_{21}}{I_{load 1}} = 1.115$ and $\frac{I_{22}}{I_{load 2}} = 0.955$, i. e., due to the circulating current transformer 1 overloads by 11.5 per cent transformer 2 being underloaded 4.5 per cent.

Hitherto we had assumed $k_1 < k_2$. With an inverse relationship of the transformation ratios the vectors of the circulating currents I_{circ1} and I_{circ2} would exchange their positions (Fig. 20-4). In this case the second, more powerful transformer, would be overloaded but if the same quantitative relationships as above were considered its overload would not exceed 5 per cent, whereas transformer 1 would have been underloaded.

These conditions are more advantageous than the former. True, they may change if the load becomes capacitive, but such a case occurs relatively seldom. Therefore, with the transformation ratios unequal it should be preferred that the transformer of smaller power should have a greater transformation ratio. Since transformers should not be overloaded to avoid overheating,

it becomes necessary to lower the external load so that overloaded transformer could be returned to normal operating conditions. In this case the other transformer will be underloaded, and the system would be less utilised. According to the data given above, transformer 1 is overloaded approximately by 11.5 per cent. Consequently, the external load current should be decreased by the same value so that the full current of the first transformer does not exceed the rated value.

From the above it follows that any significant inequality of transformation ratios is not to be tolerated. According to the State Standard 401-41, for transformers with a transformation ratio under 3 and also for substation auxiliary transformers, $\Delta k \leq 1$ per cent, for all other types of transformers $\Delta k \leq 0.5$ per cent.

20-3. Parallel Operation of Transformers Belonging to Different Groups

If one of the transformers belongs to group 12, and the other one to group 11, the triangles of the secondary line voltages, as we have already seen (Fig. 15-9), are turned 30° relative to each other.

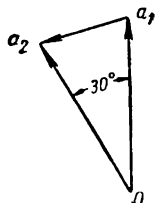


Fig. 20-5. E. m. f. diagram for parallel operation of transformers of different groups

Consequently, between such transformers there always exists a voltage determined by vector $a_1 a_2$ in Fig. 20-5. Since $a_1 a_2 = 2 \times a_1 O \times \sin 15^\circ = 0.52 \times a_1 O = 0.52 a_2 O$, the circulating current in the case of parallel connection of transformers would several times exceed the value of the rated current. Therefore, parallel operation of transformers belonging to different groups is impossible.

If transformers belong to groups 12 and 6 or 11 and 5, they may be used for parallel operation only when the higher or lower voltage winding of one of the transformers would be "turned inside out", i. e., the beginnings and ends of each phase winding would be reversed.

20-4. Parallel Operation of Transformers with Unequal Impedance Voltages

Suppose the first and second stipulations for parallel operation are met, but $u_{sh1} \neq u_{sh2}$. When we speak of short-circuit impedances, it should be remembered that they may differ from each

other both in magnitude and in components. First we shall consider the influence of the second factor. Let us take, for instance, transformers with capacities 10 kVA and 100 kVA. According to State Standard 401-41, the 10 kVA transformer data is $u_{sh}=5.5\%$, $u_{sha}=3.35\%$ and $u_{sh\sigma}=4.36\%$; correspondingly, for the 100 kVA transformer $u_{sh}=5.5\%$, $u_{sha}=2.4\%$ and $u_{sh\sigma}=4.95\%$. Having superposed the hypotenuses of the short-circuit triangles AB_1C and AB_2C we obtain the diagram shown in Fig. 20-6. If we neglect the no-load current, it may be assumed that the current I_{21} is in phase with the component $\overline{CB_1}$, and the current I_{22} is in phase with the component $\overline{CB_2}$; hence, the currents I_{21} and I_{22} are shifted in phase from each other by an angle $\Delta\varphi_{sh} = \varphi_{sh2} - \varphi_{sh1}$, and $I_c = I_{21} + I_{22}$. But, as it is seen from the diagram in Fig. 20-6, even with a relatively large difference between the components u_{sha} and $u_{sh\sigma}$ of the transformers under consideration the angle $\Delta\varphi_{sh}$ is quite small, and it may, therefore, be assumed that the currents I_{21} and I_{22} add arithmetically, i. e.,

$$I_c = I_{21} + I_{22}. \quad (20-17)$$

This deduction is of a sufficiently general nature, i. e., it may be applied to any number of transformers.

Now assume that $u_{sh1} \neq u_{sh2}$. Since for parallel transformer operation the primary and secondary voltages coincide both in magnitude and in phase, the voltage drop in all the transformers must be equal, i. e.,

$$I_1 Z_{sh1} = I_2 Z_{sh2} = \dots = I_m Z_{shm} = \dots = I_n Z_{shn}.$$

Consequently,

$$\begin{aligned} I_1 : I_2 : \dots : I_m : \dots : I_n &= \\ &= P_1 : P_2 : \dots : P_m : \dots : P_n = \\ &= \frac{1}{z_{sh1}} : \frac{1}{z_{sh2}} : \dots : \frac{1}{z_{shm}} : \dots : \frac{1}{z_{shn}}, \end{aligned} \quad (20-18)$$

where $P_1, P_2, \dots, P_m, \dots, P_n$ are the powers of each of the parallel operating transformers.

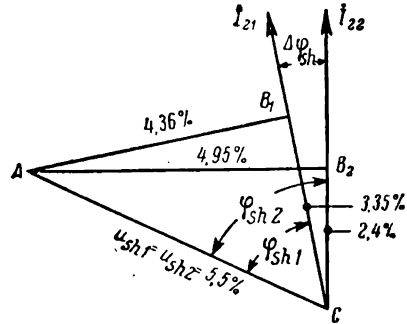


Fig. 20-6. Current diagrams for $u_{sh1} = u_{sh2}$, $u_{sha1} \neq u_{sha2}$, $u_{sh\sigma1} \neq u_{sh\sigma2}$.

From formula (20-18) it follows that

$$\begin{aligned} \frac{P_m}{\sum_1^n P_m} &= \frac{\frac{1}{z_{sh m}}}{\sum_1^n \frac{1}{z_{sh m}}} = \frac{1}{z_{sh m} \sum_1^n \frac{1}{z_{sh m}}} = \\ &= \frac{1}{\frac{I_{n m} z_{sh m}}{U_1} \cdot 100 \cdot \sum_1^n \frac{I_{n m}}{\frac{I_{n m} z_{sh m}}{U_1} \cdot 100}} = \frac{1}{\frac{u_{sh m}}{P_{n m}} \sum_1^n \frac{P_{n m}}{u_{sh m}}} \end{aligned}$$

Thus, the power of the m -th transformer will be

$$P_m = \frac{\sum_1^n P_m}{\sum_1^n \frac{P_{n m}}{u_{sh m}}} \cdot \frac{P_{n m}}{u_{sh m}}. \quad (20-19)$$

Consider, for example, three three-phase oil transformers each for 100 kVA where $u_{sh1}=3.5\%$, $u_{sh2}=4.0\%$ and $u_{sh3}=5.5\%$. The total load is $\sum_1^n P_m = 300$ kVA. According to formula (20-19) we have

$$\sum_1^n \frac{P_{n m}}{u_{sh m}} = \frac{100}{3.5} + \frac{100}{4} + \frac{100}{5.5} = 71.8.$$

Hence,

$$P_1 = \frac{300}{71.8} \cdot \frac{100}{3.5} = 119.5 \text{ kVA}; \quad P_2 = \frac{300}{71.8} \cdot \frac{100}{4} = 104.5 \text{ kVA}$$

and

$$P_3 = \frac{300}{71.8} \cdot \frac{100}{5.5} = 76 \text{ kVA},$$

i. e., the first transformer is 19.5% overloaded and the third 24% underloaded.

By reducing the external load 19.5%, we obtain a new load distribution between the transformers: $P_1=100$ kVA, $P_2=87.2$ kVA and $P_3=63.5$ kVA. In this case the first transformer will be loaded normally, but the two others will be underloaded. Such parallel operation conditions cannot be considered as satisfactory. Therefore the State Standard 401-41 requires that the

transformers designed for parallel operation should allow the impedance voltage u_{sh} to differ from the mean arithmetical value by not more than $\pm 10\%$.

If transformers with different power operate in parallel, it is better if the transformer with smaller power should have a higher u_{sh} voltage. Indeed, on load it will be underloaded, but that is of minor inconvenience, since the underloading of a transformer with small power affects the total power of the system less than the underloading of a large transformer. On the contrary, if the small transformer would have a lower u_{sh} voltage, it would limit the operation of the entire system, since it would be necessary to remove the load from the system so that the small transformer would not become overloaded.

Departures from favourable operating conditions increase with the difference between the power of the transformers operating in parallel. The State Standard 401-41 recommends for parallel-connected transformers that the ratios of maximum to minimum power should not exceed 3 : 1.

Chapter Twenty-One

TRANSIENT PHENOMENA IN TRANSFORMERS

21-1. Classification of Transients

With any change in one or several of the values basic for transformer operation—voltage, frequency, load, etc.—a transition occurs from one steady state to another. Usually this transition lasts only a very short time, but nevertheless it may be accompanied by considerable and dangerous for transformer operation effects, i. e., appearance of very large mechanical stresses between the windings or their parts, extremely distorted distribution of voltages between sections of windings or even between separate turns, excessive overheating of windings, etc. These effects are of particular importance in modern H.V. large-output transformers. Therefore contemporary transformer engineering has developed a number of measures for increasing the mechanical, electrical and thermal strength of the transformers.

Depending on which of the factors—the current or the voltage—determines in the main the transient phenomenon, two major groups of the phenomena are distinguished: a) the overcurrent phenomena and b) the overvoltage phenomena. The investigation of these phenomena is of great practical importance.

21-2. Overcurrents

In their most distinctive form overcurrents arise A) when an unloaded transformer is connected to the power circuit and B) when a short circuit occurs.

A. The starting current. Let us assume the secondary of the transformer open. We knew that for steady-state operation the no-load current of a power transformer does not exceed 10 per cent. But when the transformer is switched in the power circuit with a voltage close to the rated value, current inrushes may be observed many times the no-load rated values. Physically these current inrushes may be explained as follows. With steady no-load operation, the given value of the impressed voltage $u_1 = ab$ (Fig. 21-1) corresponds to a steady-state flux value $\Phi_{steady} = ac$. But if we do not take into account the residual magnetisation

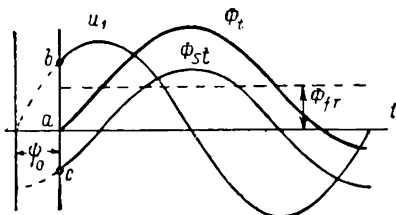


Fig. 21-1. Magnetic fluxes when transformer is switched in

flux, then at the instant of transformer connection to the line, the current i_0 and the flux Φ_0 produced by it must be zero. Therefore, when a transformer is connected to the circuit a free flux Φ_{free} (Φ_{fr}) arises in it of a magnitude to provide $\Phi_{steady} + \Phi_{free} = 0$. If the active resistance of the primary winding system would be zero ($r_1 = 0$), the electromagnetic energy corresponding to the flux Φ_{free} would not dissipate, and the flux Φ_{free} would remain constant in value and sign for an indefinite time (the broken straight line in Fig. 21-1), and would superpose onto the alternating steady-state flux Φ_{steady} . At the instants, when both fluxes pass around the transformer core the same way and, consequently, add arithmetically, the core steel may be much more saturated than on steady-state no-load. In conformance with this the no-load current, determined by means of the transformer magnetisation curve increases accordingly.

In reality $r_1 \neq 0$, and therefore the flux Φ_{free} is gradually damped.

Let us assume that the impressed voltage varies sinusoidally and that it does not depend on the transformer operation conditions. In this case the equation of the e.m.f. for the instant of transformer switch-in may be written as:

$$u_1 = U_{1m} \sin(\omega t + \psi_0) = i_0 r_1 + w_1 \frac{d\Phi_t}{dt}. \quad (21-1)$$

Here ψ_0 is the connection phase, i. e., the phase angle determining the u_1 value at the instant of transformer switch-in (Fig. 21-1).

Since the relationship $\Phi_t = f(i_0)$ is of a complex nature determined by the transformer magnetisation curve, the solution of equation (21-1) is possible only under a simplifying assumption that the flux Φ_t is a linear function of the current i_0 , i. e., $\Phi\omega_1 = L_1 i_0$, where L_1 is the constant inductance corresponding to the entire flux linked with the primary.

The equation (21-1) then assumes the form of:

$$U_{1m} \sin(\omega t + \psi_0) = \frac{\Phi\omega_1}{L_1} r_1 + \omega_1 \frac{d\Phi_t}{dt}$$

or

$$\frac{\Phi_t}{L_1} r_1 + \frac{d\Phi_t}{dt} = \frac{U_{1m}}{\omega_1} \sin(\omega t + \psi_0). \quad (21-2)$$

This equation is solved the usual way. The flux Φ_t is expressed as the sum of two fluxes—of the periodical flux Φ_{steady} corresponding to steady state conditions and of the free flux Φ_{free} corresponding to transient conditions. Thus,

$$\Phi_t = \Phi_{steady} + \Phi_{free}. \quad (21-3)$$

The flux Φ_{steady} lags on the transformer impressed voltage u_1 almost by 90° (Fig. 14-7). Therefore,

$$\Phi_{steady} = \Phi_m \sin\left(\omega t + \psi_0 - \frac{\pi}{2}\right) = -\Phi_m \cos(\omega t + \psi_0), \quad (21-4)$$

where Φ_m is the flux amplitude for steady-state operation.

To determine the flux Φ_{free} we assume the right hand part of equation (21-2) equal to zero and, solving the equation obtained this way, we find:

$$\Phi_{free} = C e^{-\frac{r_1}{L_1} t}, \quad (21-5)$$

where C is the integration constant determined from initial conditions. At the instant the transformer is switched to the line, i. e., for $t=0$, there exists in the core only the residual magnetisation flux $\pm\Phi_{res}$ (Φ_{re}). In this case equation (21-3) may be rewritten as:

$$\Phi_t = \pm\Phi_{res} = -\Phi_m \cos \psi_0 + C,$$

and therefore

$$C = \Phi_m \cos \psi_0 \pm \Phi_{res}.$$

Substituting this value of C into equation (21-5) we find:

$$\Phi_{free} = \Phi_m \cos \psi_0 e^{-\frac{r_1}{L_1} t} \pm \Phi_{res} e^{-\frac{r_1}{L_1} t}. \quad (21-6)$$

Then

$$\Phi_t = \Phi_{steady} + \Phi_{free} = -\Phi_m \left[\cos(\omega t + \psi_0) - \cos \psi_0 e^{-\frac{r_1}{L_1} t} \right] \pm \Phi_{res} e^{-\frac{r_1}{L_1} t}. \quad (21-7)$$

The best conditions for switching in will occur when

$$\psi_0 = \frac{\pi}{2} \text{ and } \Phi_{res} = 0.$$

In this case

$$\Phi_{steady} = -\Phi_m \cos\left(\omega t + \frac{\pi}{2}\right) = \Phi_m \sin \omega t, \quad \Phi_{free} = 0,$$

i. e., immediately established in the transformer is a flux corresponding to the steady-state operation.

The most unfavourable conditions for switching in occur in the case when $\psi_0 = 0$, i. e., when $u_1 = 0$ and the flux Φ_{free} is of opposite sign compared with flux Φ_{steady} (Fig. 21-2). In this case:

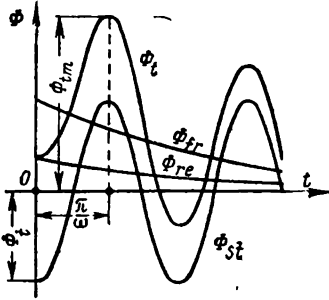


Fig. 21-2. Magnetic fluxes when the transformer is switched in at the instant when $\Phi_{free} = -\Phi_{steady}$

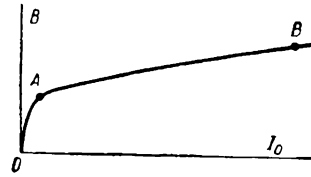


Fig. 21-3. Magnetisation curve

$$\Phi_t = -\Phi_m \cos \omega t + \Phi_m e^{-\frac{r_1}{L_1} t} \pm \Phi_{res} e^{-\frac{r_1}{L_1} t}. \quad (21-8)$$

Usually $\Phi_{res} = (0.2 \text{ to } 0.3) \Phi_{steady}$. In this case after one half period, i. e., when

$$\omega t = \frac{2\pi}{T} \cdot \frac{T}{2} = \pi,$$

we have:

$$\Phi_t = \Phi_m + \Phi_m e^{-\frac{r_1}{L_1} t} + (0.2 \text{ to } 0.3) \Phi_m e^{-\frac{r_1}{L_1} t}.$$

Since, according to previous discussion, $r_1 \ll \omega L_1$, then

$$\varepsilon - \frac{r_1}{\omega L_1} \pi \approx 1$$

and

$$\Phi_{tm} = \Phi_m + \Phi_m + (0.2 \text{ to } 0.3) \Phi_m = (2.2 \text{ to } 2.3) \Phi_m.$$

The magnetising current i_0 required for creating such a flux is determined from the magnetisation curve. The points A and B on the curve in Fig. 21-3 correspond to the normal and double values of the power transformer flux density, i. e., normal and double values of the flux Φ_{steady} . We see that the amplitude of the starting current i_{om} may be many times the amplitude of the steady-state no-load current I_{om} . The oscillographic records indicate that for $B=1.4 \text{ wb/m}^2$ the ratio $\frac{i_{om}}{I_{om}} = 50$ to 80 and with greater flux densities may be as high as 120. If we bear in mind that the current $I_0 = 5\%$ of I_n then it is clear that the starting current may exceed the rated value 4 to 6 times.

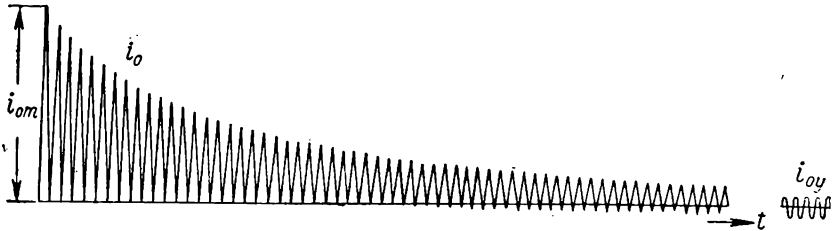


Fig. 21-4. No-load starting current of power transformer

Fig. 21-4 shows a starting oscillogram for $u_1=0$. For comparison, the steady-state no-load current is shown on the right. Since $r_1 \ll \omega L_1$, the starting current attenuates slowly: even one second after the start the current is three times the current i_0 . Complete damping occurs after 6 to 8 sec. But in powerful high-voltage transformers the damping process sometimes takes more than 20 sec.

The starting current does not present a direct danger to the transformer but it may lead to its being tripped out of the power circuit. Therefore, the protection apparatus must be so designed as to avoid the transformer being unduly switched out.

The above discussion pertains to a single-phase transformer. When a three-phase transformer is switched on a more or less considerable current inrush should be expected, since there

will always be a phase, the voltage of which at the starting instant is close to zero.

B. Sudden short-circuit current. When sudden short circuits of a transformer occur and also when testing it on short circuit, the no-load current may be neglected. In this case the equivalent circuit of a transformer represents an elementary electric circuit with a total active resistance of $r_{sh} = r_1 + r'_2$ and a total reactance $x_{sh} = x_1 + x'_2 = \omega L_{s1} + \omega L'_{s2} = \omega L_{sh}$ (see Fig. 17-3), where L_{sh} is the leakage inductance of the transformer. Since the leakage fluxes are distributed chiefly in a non-magnetic medium, $L_{sh} = \text{const.}$ In this case the e.m.f. equation for a sudden short circuit is written in the form of:

$$u_1 = U_{1m} \sin(\omega t + \psi_{sh}) = i_{sh} r_{sh} + L_{sh} \frac{di_{sh}}{dt}. \quad (21-9)$$

Here ψ_{sh} is the connection phase of the transformer on short circuit, similar to the connection phase ψ_0 on no-load (Fig. 21-1).

Solving equation (21-9) in relation to current i_{sh} and assuming that

$\psi_{sh} = \arctan \frac{x_{sh}}{r_{sh}} \approx 90^\circ$, we obtain:

$$\begin{aligned} i_{sh} &= i_{sh, \text{steady}} + i_{sh, \text{free}} = - \frac{U_{1m}}{\sqrt{r_{sh}^2 + (\omega L_{sh})^2}} \cos(\omega t + \psi_{sh}) + \\ &+ \frac{U_{1m}}{\sqrt{r_{sh}^2 + (\omega L_{sh})^2}} \cos \psi_{sh} e^{-\frac{r_{sh}}{L_{sh}} t} = \\ &= -I_{sh} \sqrt{2} \cos(\omega t + \psi_{sh}) + I_{sh} \sqrt{2} \cos \psi_{sh} e^{-\frac{r_{sh}}{L_{sh}} t}. \end{aligned} \quad (21-10)$$

Here $i_{sh, \text{steady}}$ and $i_{sh, \text{free}}$ are the instantaneous values of the steady-state and free short-circuit currents;

$$I_{sh} \sqrt{2} = \frac{U_{1m}}{\sqrt{r_{sh}^2 + (\omega L_{sh})^2}}$$

is the amplitude of the steady-state short-circuit current.

The most unfavourable short-circuit conditions which should be taken into account when designing transformers take place when $\psi_{sh} = 0$, i. e., when $u_1 = 0$; in this case

$$i_{sh} (\psi_{sh} = 0) = -I_{sh} \sqrt{2} \cos \omega t + I_{sh} \sqrt{2} e^{-\frac{r_{sh}}{L_{sh}} t}. \quad (21-11)$$

If the short circuit occurs with a rated voltage across the transformer terminals, then $I_{sh} \sqrt{2} = \frac{100 \cdot \sqrt{2}}{u_{sh}} I_n$, where u_{sh} is the impedance voltage expressed in per cent, and I_n is the rated current.

In the limiting case for $\frac{r_{sh}}{L_{sh}} = 0$, the current i_{free} does not decay (the broken horizontal line in Fig. 21-5), and, consequently, one half-period after the instant of sudden short

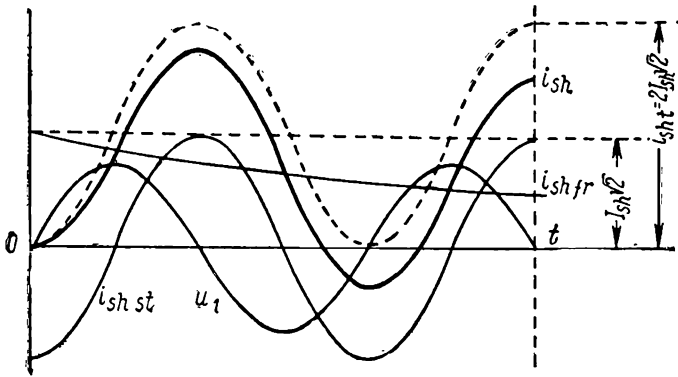


Fig. 21-5. Sudden short-circuit current at $u_1=0$

circuit the amplitude i_{msh} of the sudden short-circuit current attains double the amplitude value of the steady-state short-circuit current, i. e.,

$$\frac{i_{sh.m}}{I_{sh} \sqrt{2}} = k_{sh} = 2.$$

In real transformers the current $i_{sh.free}$ decays the faster the larger the ratio $\frac{r_{sh}}{L_{sh}}$.

In low-power transformers, for which $\frac{r_{sh}}{\omega L_{sh}} = \frac{1}{2}$ to $\frac{1}{3}$, the rate of decay is one or two periods, i. e., $k_{sh} = 1.2$ to 1.3 .

In large-output transformers, where $\frac{r_{sh}}{\omega L_{sh}} \leq \frac{1}{10}$, $k_{sh} = 1.7$ to 1.85 .

21-3. Short-Circuit Thermal Phenomena

Although the short-circuit of a transformer does not usually last very long, nevertheless the temperature of its windings may attain values which may be of danger to the insulation.

At present there are yet no fixed limits for the short-time heating of windings. Temperatures in the range of 200-250°C are considered permissible, but it is better not to exceed the limit set by the first figure. According to approximate calculations, the time t in sec, during which the winding temperature reaches 250°C, is determined by the following formula [6]:

$$t \approx 2.5 \left(\frac{u_{sh}}{j_{av}} \right)^2. \quad (21-12)$$

Here u_{sh} is the impedance voltage, and j_{av} the mean current density in A/mm².

The time required for heating a winding to a limiting temperature usually does not exceed 5 to 25 sec. But the cooling of the winding to the temperature stipulated for operation after the removal of the short circuit often lasts tens of minutes. This is accounted for by the relatively low intensity of the process of heat removal from the winding surface to the surrounding medium.

21-4. Mechanical Stresses Accompanying Sudden Short Circuits

Mechanical stresses $F_1 = -F_2$, arise between conductors, through which the current flows in opposite directions, as is

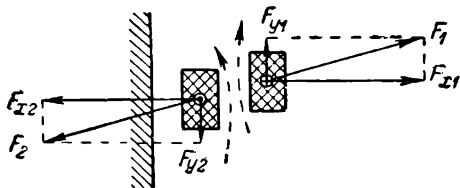


Fig. 21-6. Mechanical stresses in transformer windings

actually the case of a transformer short circuit (Fig. 21-6). Both forces may be resolved into radial components F_{x1} and F_{x2} and axial components F_{y1} and F_{y2} . The former tend to stretch the external winding and to compress the inner winding, while the latter tend to displace both windings in the axial direction. Since with a short circuit $i_1 = i'_2 = i_{sh}$, the forces F_1 and F_2 are proportional to i_{sh}^2 and, consequently, are of an alternating nature.

Besides stresses F_x and F_y between turns of the same winding there are also stresses F_h that tend to compress the winding along its height. [Bibl. 91, 92]

The three typical stresses acting at short circuit are shown in Fig. 21-7, *a*, *b* and *c*. These stresses occur in usual operating conditions too, but then they are small and are not dangerous, whereas in short-circuit conditions they increase hundredfold and may damage the transformer.

To estimate the mechanical stresses accompanying short circuits, we shall base the calculations on the electromagnetic energy of the windings corresponding to the leakage flux.

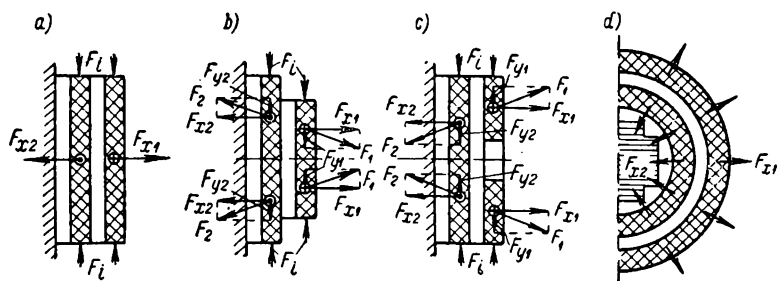


Fig. 21-7. Axial, transverse and internal forces:

a — windings of equal height; *b* — windings shortened on both sides; *c* — tappings at mid-height of a winding; *d* — cross-section of windings

Let i_{sh} be the instantaneous value of the short-circuit current and L_{sh} the leakage inductance of the transformer.

Suppose that during the time dt the current i_{sh} does not change, and that one of the windings under the action of the force F_x is displaced in respect to the second winding the distance dx towards the axis x (Fig. 21-8). In this case mechanical work $dA_x = F_x dx$ is performed. On the other hand, winding displacement gives rise to a change in inductance L_{sh} and, correspondingly, to a change in the electromagnetic energy of the leakage field by the value $dW_x = \frac{1}{2} i_{sh}^2 \frac{dL_{sh}}{dx} dx$. The same winding displacement leads also to a change in full leakage flux by the amount $d\psi_x = i_{sh} dL_{sh} = i_{sh} \frac{dL_{sh}}{dx} dx$ giving rise to an e.m.f. in the winding expressed as

$$e_x = - \frac{d\psi_x}{dt} = - i_{sh} \frac{dL_{sh}}{dx} \frac{dx}{dt}.$$

If, neglecting the voltage drop, we assume the e.m.f. balanced by the voltage u_x , i. e., $u_x = -e_x$ then energy $dW_c = u_x i_{sh} dt = i_{sh}^2 \frac{dL_{sh}}{dx} dx$ is supplied from the power line that feeds the transformer. This energy is spent in accomplishing the work dA_x and in varying the leakage field energy by the amount dW_x , i. e.,

$$dW_c = dA_x + dW_x$$

or

$$i_{sh}^2 \frac{dL_{sh}}{dx} dx = F_x dx + \frac{1}{2} i_{sh}^2 \frac{dL_{sh}}{dx} dx,$$

and hence

$$F_x = \frac{1}{2} i_{sh}^2 \frac{dL_{sh}}{dx}. \quad (21-13)$$

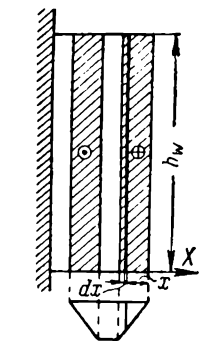


Fig. 21-8. Calculation of mechanical stresses in windings

Let us apply this formula to determine force F_x in the simplest case of a winding shown in Fig. 21-7, a.

According to equation (17-16) we have:

$$L_{sh} = \mu_0 \omega^2 \frac{C_{av} k_s}{h_{winding}} \delta'.$$

Since the winding is displaced in the abscissa-axis direction, i. e., across the width of the duct δ then,

$$\frac{dL_{sh}}{dx} = \frac{dL_{sh}}{d\delta} = \mu_0 \omega^2 \frac{C_{av} k_s}{h_{winding}}.$$

Consequently,

$$F_x = \frac{\mu_0}{2} (i_{sh} \omega)^2 \frac{C_{av} k_s}{h_{winding}}. \quad (21-14)$$

The current i_{sh} reaches maximum at a sudden short circuit at the instant, when $u_1 = 0$. In this case

$$i_{sh} = k_{sh} \frac{100}{u_{sh}} I_{sh.ph} \sqrt{2},$$

where $k_{sh} = 1.5$ to 1.9 for high-power transformers and $k_{sh} = 1.2$ to 1.3 for low-power transformers. Therefore,

$$F_{xm} = \mu_0 \left(\frac{10^2 k_{sh} I_{sh.ph} \omega}{u_{sh}} \right)^2 \frac{C_{av} k_s}{h_{winding}}. \quad (21-15)$$

This equation may be rewritten in a more convenient form, if we assume that $u_{sh} = u_{shx}$ and substitute u_{shx} for the value from (17-18).

In a final form

$$F_{xm} = 14.5 k_{sh}^2 \frac{k_{steady} P_n}{f u_{sh} \delta'} . \quad (21-16)$$

If P_n is expressed in kVA, δ' in cm, and F_{xm} is desired in tons (t), then

$$F_{xm} = 148 k_{sh}^2 \frac{k_{steady} P_n}{f u_{sh} \delta'} . \quad (21-17)$$

Thus, for instance, for one of the transformers manufactured by the Moscow Transformer Works we have

$$P_n = 5,600 \text{ kVA}, U_1 = 35 \text{ kV}, k_{steady} = \frac{1}{3}; f = 50 \text{ c/s};$$

$$u_{sh} = 7.3 \text{ per cent}; \delta' = 6.15 \text{ cm}.$$

For a transformer of this power, $k_{sh} = 1.55$. Then

$$F_{xm} = 148 \cdot 1.55^2 \frac{5,600}{3 \cdot 50 \cdot 7.3 \cdot 6.15} = 295 \text{ tons}.$$

As we have already mentioned, this force which is directed along the axis of the turn both sides of any of its cross-sections tends to tear the outer winding. If ω is the number of turns in a given winding and S the cross-section area, the breaking stress per area unit will be

$$F_{break} = \frac{F_{xm}}{2\pi\omega S} . \quad (21-18)$$

For the representative transformer above $\omega_1 = 571$ and $S_1 = 2.07 \text{ mm}^2$; therefore, $F_{break} = 3.98 \text{ kg/mm}^2$. The permissible value is usually $F_{break} \leq 5$ to 6 kg/mm^2 .

Since in transformers of normal design, the forces F_y and F_h are usually much less than the force F_x , the calculation of these forces is not carried out here.

21-5. Cause and Nature of Overvoltages in Transformers

Any rise of transformer voltage above the maximum operating voltage may be referred to as overvoltage¹. But usually the term "overvoltage" relates to short-term processes, having the nature of separate short pulses of a periodical or aperiodical nature.

¹ Depending on the class of winding insulation, the following maximum operating voltages are stipulated for transformers:

Insulation class	3	6	10	15	20	35	110	154	220
Maximum operating voltage, kv...	3.5	6.9	11.5	17.5	23	40.5	121	169	

The causes of overvoltages may be:

1) *Phenomena of atmospheric nature*, i. e., lightning directly striking transmission lines, electromagnetic induction in lines due to cloud discharges and electrostatic induction due to charged clouds, electrification of line wires by the wind with the participation of fine dust particles, snow, etc.;

2) *Switching processes*: switching in, switching off, rapid changes of load, etc., accompanied by sudden changes of electromagnetic energy in the system;

3) *Processes of an emergency nature*, i. e.: short circuits, fall-outs, repetitive earthing arcs, etc.

The nature of the processes in a transformer accompanying overvoltage depends on the electromagnetic wave form. These are distinguished as: a) *simple* (Fig. 21-9, a) and *complex* (Fig. 21-9, b) *aperiodic waves*, the former being more often observed during atmospheric overvoltages, and b) *periodic waves* (Fig. 21-9, c) observed during switching processes.

Investigations have shown that: a) overvoltages due to switching exceed the rated phase voltage 2 to 5 times; b) the overvoltages of emergency nature exceed it 7-8

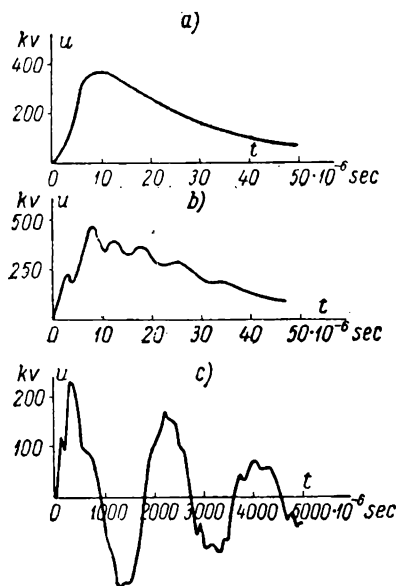


Fig. 21-9. Overvoltage surge waves

times; and c) the overvoltages due to atmospheric causes exceed it 7-12 times. *Overvoltages exceeding the normal operating voltage of a line $2\frac{1}{2}$ times are considered as safe; if they exceed it $3\frac{1}{2}$ times they are already regarded as dangerous.*

Overvoltages that reach the transformer terminals may be restricted by some protective device. Much more dangerous are the overvoltages which occur inside a transformer when an electromagnetic wave is distributed along the winding and when the voltages between separate coils and even separate turns of the winding may many times exceed the normal voltage between them for steady-state operation of the transformer. Experience proves that the turns nearest to the transformer terminals

are those most often damaged but, generally speaking, the overvoltages and corresponding insulation breakdowns may take place at any point of the winding depending mostly on its characteristics. An insulation breakdown results in considerable damage to the transformer and to the disturbance of normal service of the installation. From this point of view it is clear why the overvoltages in transformers have been the object of numerous investigations and observations.

But it should be borne in mind, however, that the processes accompanying overvoltage wave propagation in a transformer are of an extremely complex nature and cannot be fully mathematically analysed. A number of simplifying assumptions are necessary which make it possible to reduce the phenomenon to its relatively simple form and make clear its basic properties. Nevertheless, the results obtained have allowed to make a number of valuable deductions and serve as an impetus to the development of new viewpoints on overvoltage phenomena and in particular help to develop the new, so-called, surgeproof-type transformers.

21-6. Transformer Equivalent Circuit for Overvoltages

We shall consider only the simple case of overvoltages in a transformer when there is but one high-voltage transformer winding onto which an overvoltage wave surges from the line terminal A (Fig. 21-10), the other terminal X (the neutral) being either insulated or earthed.

With steady-state operation the current flows practically only through the transformer winding, encountering in passing active and inductive resistances. But with overvoltage the entire picture radically changes. Indeed, the processes connected with overvoltages take place with extreme rapidity and affect the transformer as oscillatory processes of very high frequency.

In this case the inductive resistance of the transformer becomes very large, whereas the capacitive resistance decreases. As the limiting case, it may be assumed that with overvoltage the current flows only through the capacitive resistances, utilising for this purpose the capacity K of a given part of the winding, for

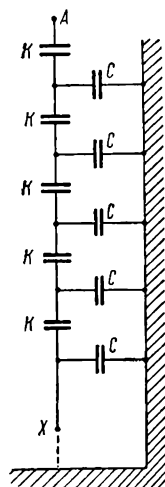


Fig. 21-10. Simplified equivalent circuit of H.V. winding for wave process in transformer

instance, of a coil, in respect to an adjacent part and the winding to ground capacitance C . For simplicity, the capacity between separate windings is not taken into account. In this case the equivalent circuit of a transformer is as shown in Fig. 21-10. Here A is the line terminal of the high-voltage transformer winding, and X —the end terminal which may be earthed or insulated.

Since the capacities K are series-connected, the capacity along the winding is

$$K_{winding} = \frac{1}{n} K, \quad (21-19a)$$

where n is the number of winding elements (coils).

The capacitances to earth C are connected in parallel, therefore the capacity of the winding in respect to earth is

$$C_{earth} = nC. \quad (21-19b)$$

The capacitances $K_{winding}$ and C_{earth} may be substituted by one equivalent or so-called *input capacitance*

$$C_{input} = \sqrt{K_{winding} C_{earth}}. \quad (21-19c)$$

When analysing the processes occurring in a transformer during overvoltages, we shall proceed from the assumption that the transformer is hit by an infinitely long wave with a rectangular front. As is known, an overvoltage wave propagates along a line with a velocity $v = \frac{1}{\sqrt{LC}}$, where L and C are the inductance and capacitance per unit length of a line; for aerial lines this velocity is near to the velocity of light propagation. One of the fundamental characteristics of a line is its so-called characteristic impedance $z = \sqrt{\frac{L}{C}}$; for aerial lines $z \approx 350-450$ ohms; for cable lines, owing to their considerably greater capacity $z \approx 50$ ohms. The characteristic impedance of transformers is several times that of the aerial lines; it varies depending on the nature or frequency of the oscillations.

As is known, when the overvoltage wave passes from a circuit with a smaller characteristic impedance, in our case from the line, into a circuit with higher characteristic impedance, the transformer, the voltage at the transformer terminals increases and in the extreme case may be doubled (Fig. 21-11, *a* and *b*). The time interval, during which the voltage U_0 across the input terminal of a transformer increases to double value $2U_0 = U$, is very short, of the order of 0.1 microsecond. During this time,

i. e., practically instantaneously, the capacitive circuit of a transformer (Fig. 21-10) is charged, and the picture of initial voltage distribution along a winding is created. This picture may greatly differ from the voltage distribution in a winding for steady-state conditions.

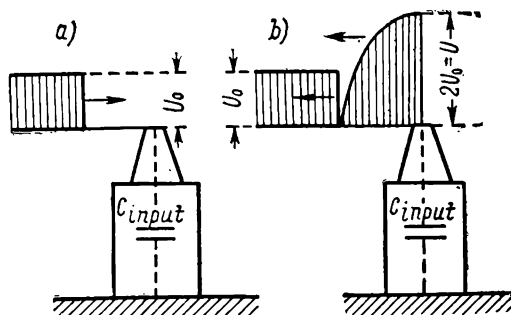


Fig. 21-11. Reflection of wave with rectangular front

Since during subsequent development of the process the winding represents a complex combination of capacitances and inductances, the transition from the initial state to equilibrium occurs as an oscillatory process gradually decaying due to the active resistance of the winding and the conductivity of the insulation.

21-7. Initial Voltage Distribution Along Transformer Windings

Consider the circuit in Fig. 21-10, assuming that the end X of the winding is earthed. If there are no capacities to earth ($C=0$), all capacitances K would be series-connected to each other, and the same current would flow through the entire circuit. With equality of capacitances K we would obtain a uniform voltage distribution along the winding, i. e., the same as during steady-state operation. Such a distribution is shown in Fig. 21-12, *a* by the sloping straight line connecting points M and N which correspond, accordingly, to the input terminal of a winding with impressed voltage U , and to the end having a zero potential.

Conversely, if there are no capacitances K ($K=0$), the current would flow from the line into the earth only through the first capacitance C , next to the winding beginning. Physically this means that all the voltage is concentrated on the first turn which is, therefore, highly overstressed. In Fig. 21-12, a such a distribution is shown by a vertical straight line connecting point M with the co-ordinate origin.

The actual voltage distribution along the winding lies between those two limiting distribution pictures. Let us find the nature of the voltage distribution for a particular case. Suppose the

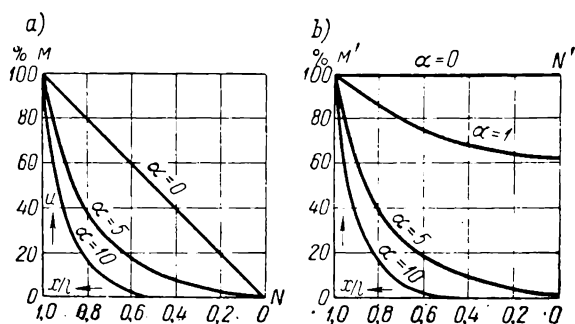


Fig. 21-12. Voltage distribution at initial moment in transformers:

a — with earthed neutral; b — with isolated neutral

high-voltage winding consists of $n=5$ links and that $K=C$ (Fig. 21-13, a). Let U_1, U_2, \dots, U_5 be the voltages at the terminals of the condensers C , the elements and their corresponding capacitances being counted from X winding end to its beginning A . Then

$U_1 = \frac{q_1}{C} = \frac{q}{C}$, where $q_1 = q$ is the charge in the first, from the winding end, condenser C . Since the condensers C and K are series-connected, the charge $q^I = q$. In this case the voltage $U_2 = \frac{q_2}{C}$, but since $U_2 = U_1 + \frac{q^I}{C} = \frac{q}{C} + \frac{q}{C} = \frac{2q}{C}$, $q_2 = 2q$. Correspondingly, $q^{II} = q_2 + q^I = 2q + q = 3q$. Now we can determine the charge q_3 , namely: $U_3 = \frac{q_3}{C}$ or $U_3 = U_2 + \frac{q^{II}}{C} = \frac{2q}{C} + \frac{3q}{C} = \frac{5q}{C}$; consequently, $q_3 = 5q$. Continuing further the calculation of the charges we obtain the chain circuit shown in Fig.

21-13, b) where $q^{III} = q_3 + q^{II} = 5q + 3q = 8q$, $q_4 = q^{III} + q_3 = 13q$, $q^{IV} = q_4 + q^{III} = 21q$, $q_5 = q^{IV} + q_4 = 34q$ and $q^V = q_5 + q^{IV} = 55q$.

More detailed mathematical analysis shows that the voltage along the chain, substituting the winding, is distributed according to the law of hyperbolic functions, the potential u_x in re-

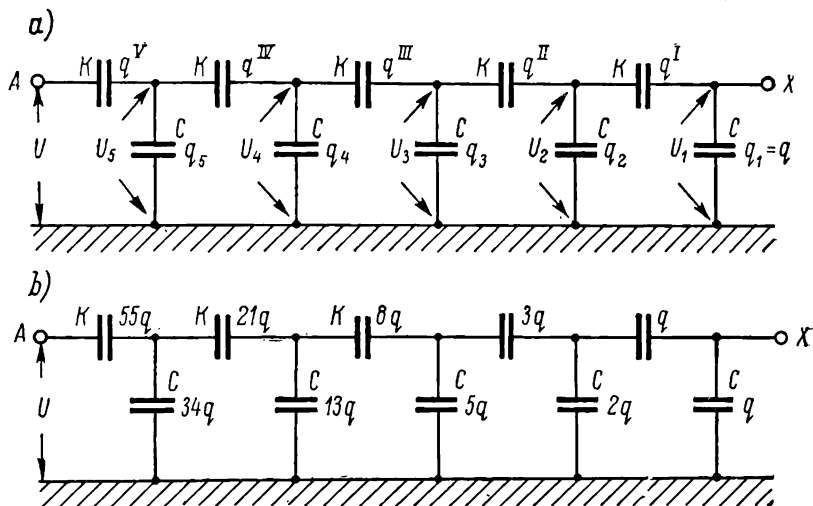


Fig. 21-13. Initial voltage distribution along transformer winding

spect to the earth at any point at a distance x from the winding end is determined by the expressions:

a) in the case of an earthed neutral

$$u_x = \frac{U \operatorname{sh} \frac{\alpha x}{l}}{\operatorname{sh} \alpha}; \quad (21-20)$$

b) in the case of an isolated neutral

$$u_x = \frac{U \operatorname{ch} \frac{\alpha x}{l}}{\operatorname{ch} \alpha}. \quad (21-21)$$

Here U is the voltage across the transformer output terminals (Fig. 21-11, b); $\alpha = \sqrt{\frac{C_3}{K_{winding}}}$; l is the full length of the transformer winding. In modern transformers $\alpha = 5$ to 15; therefore the ex-

pressions (21-20) and (21-21) give, practically, the same picture of initial voltage distribution for the both considered cases, i. e., both for the earthed and for the isolated neutral (Fig. 21-12, *a* and *b*). In the particular case considered above we have

$$C_s = 5C, K_{winding} = \frac{K}{5} = \frac{C}{5} \text{ and } \alpha = \sqrt{\frac{C_s}{K_{winding}}} = 5.$$

It is easy to prove that the voltage distribution curve corresponding to the chain circuit in Fig. 21-13, *b*, practically coincides with the curve for $\alpha=5$ plotted according to formulas (21-20) or (21-21) in Fig. 21-12, *a* and *b*.

To calculate the electric strength of a winding it is necessary to know the voltage gradient between two adjacent winding elements (coils or turns). From the curves in Fig. 21-12, *a* and *b* it may be seen that at the first instant the maximum voltage gradient is at the beginning of a winding, on the first turns, i. e., at $x=l$. The magnitude of this gradient is determined

by the first derivative $\frac{\partial u_x}{\partial x}$. Determining the value of this derivative from expressions (21-20) and (21-21) and taking into account that for $\alpha \geq 3$ we have $\tan \alpha \approx \cotan \alpha \approx 1$, we obtain in both cases:

$$\left[\frac{\partial u_x}{\partial x} \right]_{x=l} = \frac{U}{l} \alpha. \quad (21-22)$$

The first multiple gives the value of the voltage gradient for uniform voltage distribution along the winding, while the second multiple indicates that at the initial moment of time the winding elements nearest to the output terminal *A* are stressed by a voltage $\alpha=10$ to 15 times more than for uniform voltage distribution. This makes it necessary to take steps to protect the winding insulation from breakdown.

21-8. Transfer Process and Final Voltage Distribution

The voltage distribution curves for $\alpha=10$ shown in Fig. 21-12, *a* and *b* correspond to the initial moment of the process, i. e., to $t=0$. After this begins the transfer process at the termination of which—after a sufficient interval—the voltage wave is uniformly distributed along the winding. In the case of an earthed neutral the finite voltage distribution is depicted by the sloping line *MN* in Fig. 21-14, *a*, while with an isolated neutral the entire winding acquires at the final moment of time the same po-

tential depicted in Fig. 21-14, *b*, by the straight line $M'N'$ parallel to the abscissa axis. As it was already stated above, the transition from the initial to the final voltage distribution is accomplished in the form of oscillations occurring in time and in space. The analysis of the process at this stage is of considerable complexity, since it is necessary to take into account the relationships existing between the winding parts which cannot be expressed by any simple law. [Bibl. 73b, 93—97]

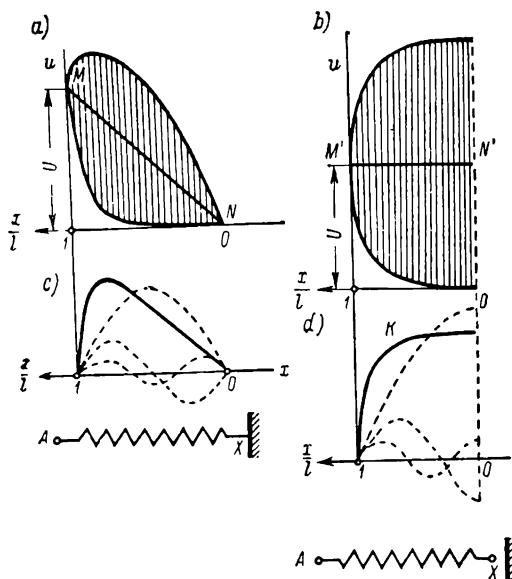


Fig. 21-14. Transient phenomena in transformer:
a and *c* — with earthed neutral; *b* and *d* — with isolated neutral

Depending on one or another assumption made in reference to the mentioned relations we obtain an expression for the process law of the oscillations occurring in a transformer winding. With the most simple assumptions, the expression sought for is obtained as an integral of a differential equation in partial derivatives of not lower than the fourth order. A detailed analysis gives the following results: *a*) the process taking place in a winding is a periodical process which decays according to the law of the exponential function; the voltage varies in space in the coordinate x , i. e., along the winding length, and with time at each point of the winding; *b*) the final voltage distribution

(lines MN and $M'N'$ in Fig. 21-14, a and b) may be considered as axes in reference to which the oscillatory process takes place; the limits of possible oscillations lie in the shaded regions in Fig. 21-14, a and b ; c) the difference between the final and initial voltage distributions may be expanded into a series of harmonics, and for transformers with an earthed neutral a series is obtained consisting of one, two, three, etc., half-waves (Fig. 21-14, c); for transformers with an isolated neutral we obtain a

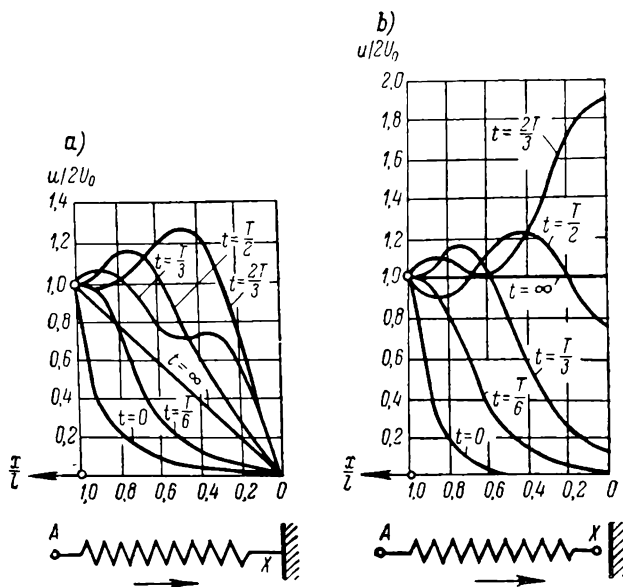


Fig. 21-15. Voltage distribution along winding at different instants:

a — with earthed neutral; b — with isolated neutral

series consisting of $\frac{1}{4}$, $\frac{3}{4}$, $\frac{5}{4}$, etc., waves (Fig. 21-14, d); with time the higher harmonics pulsate with a frequency f_n proportional to the order of the harmonic n .

The voltage harmonics of different orders propagate along the winding with different velocities; therefore, the wave that has penetrated the winding will be continuously distorted. Fig. 21-15, a for an earthed and Fig. 21-15, b for an isolated neutral show exemplary distribution of voltage along a winding at different instants, the time on the curves being indicated in fractions of the oscillation period from the moment of the establish-

ment of the initial voltage distribution. Besides, the analysis leads to the deduction that the characteristic impedance of a transformer winding is not a constant value, but represents a function of the harmonic order. In respect both to wave deformation and the characteristic impedance, a transformer greatly differs from a transmission line, along which the wave propagates almost without any distortion, the line having a constant characteristic impedance for all waves and pulses.

The more complex phenomena occurring when a transformer is hit by an aperiodical pulse of any form may be considered in a similar way. If the pulse represents a high-frequency oscillation, there is the danger of resonance between the pulse of the given frequency and any one of the harmonics. As a result it may be assumed that considerable voltage gradients are possible both between the transformer winding at a given point and the earth and between adjacent winding parts. In each of these cases the transformer may be heavily damaged and put out of service for a long time.

21-9. Transformer Overvoltage Protection

There are two kinds of transformer protection from overvoltages—external and internal. The object of the external protection is to render sufficiently harmless the wave hitting the transformer, by lowering its crest value and making it flatter. The external protection includes: the proper choice of the transmission line route, the arrangement of earthing cables, different kinds of arresters and also the co-ordination of the insulation of the whole system by means of special spark gaps called *co-ordinators* in a manner that ensures that the winding insulation is the strongest in the entire system.

The reactive coils and capacities employed in the past for protective purposes are not used today, since experience has shown and the subsequent analysis confirmed that the efficiency of such a protection is insufficient.

Internal transformer protection from overvoltages includes: 1) the necessary *reinforcement of the input and output coil insulation*, where, as discussed above, maximum voltage gradient can be expected; 2) capacitive protection of transformers.

Today, all power oil transformers for voltages up to 38.5 kV inclusive made in the U.S.S.R. have overvoltage protection only in the form of a fortified end-coil insulation for the high-voltage winding. The normal coils of such transformers have a

0.5 mm insulation on both sides, whereas the coils with a fortified insulation have correspondingly a 1.4 mm insulation. Since in this case heat removal is hindered, the current density in coils with a reinforced insulation is 20 to 30 per cent less than in the normal coils. The number of coils with reinforced insulation amounts to 5-7 per cent of the total number of winding coils.

In transformers for 110 kV and more along with end coil insulation, fortifying capacitive protection is used so that overvoltage pulses are distributed along the winding approximately in the same manner as the final voltage distribution, i.e., sufficiently uniform. Aggressive oscillatory processes cannot take place in such a winding, and, consequently, excessive voltage gradients between winding elements are also impossible. Transformers provided with such protection are referred to as *non-resonating or lightning-proof*.

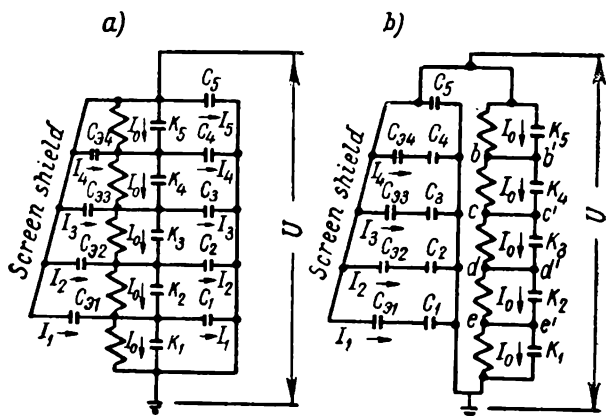


Fig. 21-16. Equivalent circuits for non-resonating transformer

The idea of capacitive protection consists in the following. If a winding could be made so that the earth capacitance $C_{earth}=0$, we would have $\alpha = \sqrt{\frac{C_{earth}}{K_{winding}}} = 0$; in this case, as seen from the curves in Fig. 21-12, *a* and *b*, the distribution voltage along the winding becomes uniform immediately, i. e., from the instant the overvoltage wave arrives at the transformer. It is physically impossible to eliminate the transformer to earth capacitances, but it is possible to compensate the currents required for charge-

ing these capacitances by the current flowing from the power circuit through a system of shielding protective capacities C_{screen} connected to the winding.

These protective capacities may be of various design. Fig. 21-16, *a* shows a system with an earthed neutral in which the protective capacitance is accomplished in the form of a special *shielding screen* (C_s) made of an insulating material with a metalised surface and connected to the line end of the winding. With an appropriate choice of protective capacities, the current required for charging any given earth capacitance, for instance, the current I_2 for charging the earth capacitances C_2 , is delivered directly through the protective capacitance $C_{screen2}$, bypassing the chain of series-connected capacitances K between coils K . Therefore, the circuit in Fig. 21-16, *a* may be substituted by the circuit in Fig. 21-16, *b*. Its left part consists of capacitances and, consequently, represents a non-resonating system. The right-hand part of the same circuit is constituted by two parallel branches one of which consists of a number of series-connected inductances, while the other consists of the same number of series-connected between coil capacitances. All the links of each chain are identical; therefore each link of each chain has the same voltage, and the current of given magnitude flows in each chain throughout its entire length. In the bridge connections bb' , cc' , etc., there is current flow, i.e., everything is as if the two chains were electrically independent of each other. Thus, the right-hand part of the circuit as also the left-hand part, represents a nonresonating system.

The capacitive protection in the form of shielding screens complicates the transformer design. Therefore at the Moscow Transformer Works (MTW) a unique system of partial capacitive protection was developed (by S. I. Rabinovich, S.Y. Kronhaus, A. M. Chertin and A. G. Perlin). Schematically this protection system is

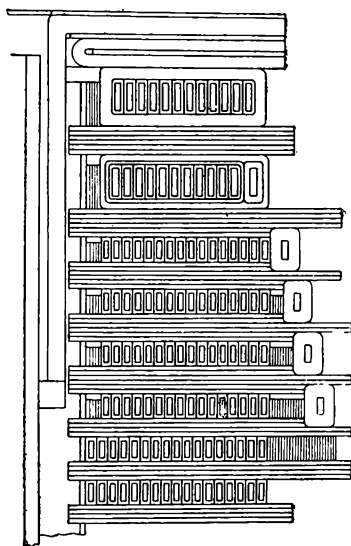


Fig. 21-17. H.V. winding protection by means of capacitive screens

shown in Fig. 21-17. The protective devices consist of: a) a coil with 3.5 to 5 mm fortified insulation on each side; b) a coil with the same fortified insulation as for coil (a) and with a capacitive screen fixed to the coil; c) four coils with normal insulation each protected by a capacitive screen.

The coils with fortified insulation are made of conductors 1.5-2 times larger in cross-section than the other coils corresponding to less permissible current density.

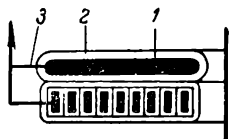


Fig. 21-18. Capacitive ring:

1 — capacitive ring 2 — capacitive ring insulation;
3 — connection to input lead

The capacitive screens are made of copper conductors of the same cross-section as the coil they protect and are connected to the line end of the winding, i.e., they have line potential. The screen conductor is reliably insulated from the coil with a 5 mm insulation on each side. The distance between the coil and the conductor determines the required value of the protective capacity. The capacitive screen must be open-circuited (to avoid forming of a turn

closed on itself) and covers the coil approximately over $\frac{2}{3}$ of its circumference.

Since the voltage gradients attain maximum at the input coil, it is most important to distribute the voltage between turns of this coil as uniformly as possible. For this purpose in modern large-power transformers, in addition to capacitive screens, a *capacitive ring* is used which may be made of pressboard and represents a washer 8-10 mm thick with rounded edges wound with a copper band and externally insulated (Fig. 21-18). The copper band is connected by means of a special cable with the line and neutral ends of the winding. The capacitive ring, as also the capacitive screen, must be electrically open.

Service experience indicates that transformers protected in the way described above are stable against the most dangerous of their kind, atmospheric overvoltages; therefore such transformers are often referred to as lightning-proof transformers.

For the same purpose of transformer protection from overvoltages is used also a multi-layer cylindrical winding (Fig. 21-19). In this design the capacitance between layers $K_{winding}$ is considerably larger than layer-to-earth capacitance C_{earth} . Conse-

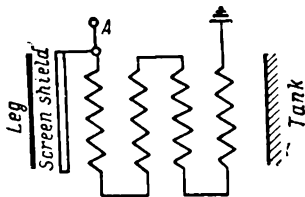


Fig. 21-19. Circuit diagram of a screened multilayer winding

quently, the factor $\alpha = \sqrt{\frac{C_{earth}}{K_{winding}}}$ is small, and the initial voltage distribution differs but little from the steady-state distribution. To equalise the capacitance between layers and to eliminate the winding-to-bar capacitance, one or two cylindrical screens may be used according to diagram in Fig. 21-19.

Chapter Twenty-Two

SPECIAL TYPES OF TRANSFORMERS

22-1. General

There are a great number of special types of transformers. These include: a) autotransformers, b) three-winding transformers, c) high-power transformers with voltage regulation under load, d) induction regulators made as induction machines (see Part II), e) instrument transformers, f) furnace transformers, g) welding transformers, h) transformers for mercury rectifiers, i) test transformers; etc.

Transformers may also be used for frequency multiplication, for changing the number of phases, as reactors for various purposes, etc. Recently there have been developed portable transformers, dry-type transformers of relatively large capacity, non-inflammable oil transformers, wound-core transformers, etc. Here we shall discuss briefly only the most widely used special-type transformers.

22-2. Autotransformers

An autotransformer is such a transformer, in which one part of the winding belongs simultaneously to the primary and secondary systems. As the ordinary transformers, autotransformers may be step-down and step-up, single-phase and three-phase. Fig. 22-1, *a* and *b* shows circuits of a step-down autotransformer, and Fig. 22-1, *c* shows a step-up autotransformer circuit.

Consider the operation of a single-phase step-down autotransformer (Fig. 22-1, *a*). The primary voltage $U_1 = U_{AX}$ is impressed across the terminals of the primary *AX*; the secondary is a part of the primary between terminals *a* and *x*, the terminal *x* coinciding with terminal *X*.

The no-load performance of an autotransformer ($I_2=0$) does not differ from the corresponding operation of an ordinary trans-

former. Since the voltage U_{AX} across an autotransformer is uniformly distributed between the primary turns, the secondary voltage will be:

$$U_2 = U_{ax} = \frac{U_{AX}}{\omega_{AX}} \omega_{ax} = \frac{U_{AX}}{\frac{\omega_{AX}}{\omega_{ax}}} = \frac{U_{AX}}{k_a} = \frac{U_1}{k_a}, \quad (22-1)$$

where $k_a = \frac{\omega_{AX}}{\omega_{ax}}$ is the transformation ratio of an autotransformer.

In case of a step-up autotransformer (Fig. 22-1, c) we have

$$U_2 = U_{AX} = k_a U_1.$$

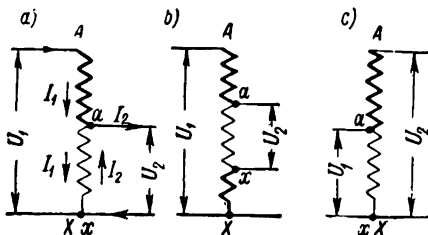


Fig. 22-1. Circuit diagrams of step-down and step-up transformers

When the autotransformer is short-circuited the current I_1 flows from the primary circuit, and a current I_2 flows in the conductor closing the terminals $a-x$.

If the windings $A-X$ and $a-x$ were electrically separated as in an ordinary transformer, then neglecting the magnetising current we would have [according to formula (13-15a)]:

$$I_2 \omega_{AX} + I_2 \omega_{ax} = 0,$$

or

$$I_1 + \frac{1}{k_a} I_2 = 0. \quad (22-2)$$

In an autotransformer the current I_1 flows only through a part of the winding $A-a$, whereas in the common part of the winding $a-x$ flows a current I_{ax} representing the geometrical sum of currents I_1 and I_2 .

Consequently,

$$I_{ax} = I_1 + I_2 = -I_1 (k_a - 1) = I_2 \left(1 - \frac{1}{k_a}\right). \quad (22-3)$$

From this it follows that in a step-down autotransformer the current I_{ax} flows in the common part of the winding $a-x$ in a direction opposite to that of current I_1 and in concordance with the current I_2 .

Let us compare the short-circuit parameters of an ordinary transformer and of an autotransformer. The former we shall designate by the usual signs, the latter by subscript a .

The copper losses in an ordinary transformer amount to $I_1^2 r_1 + I_2^2 r_2$. In an autotransformer the current I_1 flows only through section $A-a$ the active resistance of which is equal to:

$$r_{[Aa]} = r_1 \frac{w_{Aa}}{w_{AX}} = r_1 \frac{w_{AX} - w_{ax}}{w_{AX}} = r_1 \left(1 - \frac{1}{k_a}\right). \quad (22-4)$$

Hence

$$p_{cop [Aa]} = I_1^2 r_{Aa} = I_1^2 r_1 \left(1 - \frac{1}{k_a}\right). \quad (22-5)$$

The winding section $a-x$ plays the role of the secondary with current I_{ax} amounting to $1 - \frac{1}{k_a}$ part of current I_2 of an ordinary transformer. Assuming the same current density, it is possible to change in the same proportion the cross-section area of this part of the winding in accordance with which the active resistance of this part varies inversely to this proportion. Then

$$p_{cop [ax]} = I_{[ax]}^2 r_{[ax]} = I_2^2 \left(1 - \frac{1}{k_a}\right)^2 \frac{r_2}{1 - \frac{1}{k_a}} = I_2^2 r_2 \left(1 - \frac{1}{k_a}\right). \quad (22-6)$$

Comparing the formulas (22-5) and (22-6), we may see that an autotransformer may be considered as an ordinary transformer with active primary and secondary resistances decreased $1 - \frac{1}{k_a}$ times, i.e.,

$$r_{sh. a} = r_{sh} \left(1 - \frac{1}{k_a}\right). \quad (22-7)$$

Correspondingly,

$$P_{sh. a} = P_{sh} \left(1 - \frac{1}{k_a}\right). \quad (22-8)$$

The weight of copper in the autotransformer windings varies in the same proportion, i.e., $G_{cop. a} = G_{cop} \left(1 - \frac{1}{k_a}\right)$, since at the part $A-a$ the cross-section of the autotransformer winding compared with the ordinary transformer is the same but $1 - \frac{1}{k_a}$ times shorter, and at the part $a-x$ it has a length as the transformer secondary, but of $1 - \frac{1}{k_a}$ times smaller cross-section.

The same deduction as for the active resistance may be made in respect to the reactance of the autotransformer, i.e.,

$$x_{sh. a} = x_{sh} \left(1 - \frac{1}{k_a}\right). \quad (22-9)$$

Consequently, the short-circuit voltage of the autotransformer is

$$u_{sh. a} = u_{sh} \left(1 - \frac{1}{k_a}\right). \quad (22-10)$$

Thus in comparison with an ordinary transformer all the sides of the short-circuit triangle of an autotransformer are $1 - \frac{1}{k_a}$ times smaller, while the short-circuit currents are correspondingly larger.

The power $P_1 = U_1 I_1$ delivered to the autotransformer is transferred to the secondary partially in the form of electromagnetic power P_{12} corresponding to the winding part $A-a$, and partially in the form of electric power P_e corresponding to the $a-X$ part of the winding. Consequently,

$$P_{12} = U_{Aa} I_1 = (U_1 - U_2) I_1 = P_1 \left(1 - \frac{1}{k_a}\right) \quad (22-11)$$

and

$$P_e = P_1 - P_{12} = P_1 \frac{1}{k_a}. \quad (22-12)$$

The conditions of the autotransformer operation on load may be obtained by means of mutual superposition of the no-load and short-circuit operating conditions. The load diagram of the autotransformer has, therefore, the same form as in the case of an ordinary transformer (Fig. 18-3, 18-4), but corresponding to a smaller impedance voltage $u_{sh.a}$ and copper losses $P_{sh.a}$, the autotransformer voltage varies less, and its efficiency is higher than in the ordinary transformer. From formulas (22-9) and (22-10) it follows that this difference depends on the factor k_a . For $k_a = 1$ the losses $P_{sh.a}$ and the weight $G_{cop.a}$ would be zero, but in this case point a would coincide with point A and the entire electric energy input of the autotransformer would be transferred to the secondary without any transformation. On the other hand, with large values of k_a the difference between an autotransformer and a transformer is smoothed out. For $k_a = 2$ the autotransformer has little advantage, since the consumers fed by the autotransformer need protection from overvoltage and since the high- and low-voltage windings are electrically interconnected. For this reason $k_a = 1.25$ to 2 is usually preferred.

Autotransformers are used for starting synchronous and induction motors as voltage dividers in various testing and laboratory circuits and also with transmission lines and distributing networks.

Fig. 22-2, *a* and *b* shows the direct and inverse schemes of a three-phase starting oil autotransformer. According to the State Standard 3211-46, the starting autotransformers should have three steps of secondary voltage, namely, 0.55, 0.64 and 0.73 of the primary voltage U_1 , in case of the direct schemes, and 0.27, 0.36, and 0.45 of U_1 , for the inverse scheme. The voltages 0.64 and 0.36 at the middle step are considered as the rated voltages. The rated load duty of a starting autotransformer is the

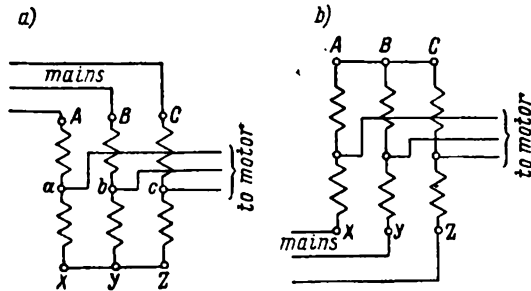


Fig. 22-2. Circuit diagrams of starting autotransformers:

a — direct circuit; *b* — inverse circuit

two-minute rating with a current corresponding to the name-plate power. The temperature rise of the starting autotransformer windings measured by the resistance method should not exceed 135°C . The cooling period of an autotransformer following removal of load is from 4 to 6 hours.

The autotransformers used for transmission lines and networks are made for high voltage and power. Thus, for example, the voltage of a transmission line now in service in the U.S.A. was increased from 150 kV to 220 kV. In another case when carrying out power station modernisation an 11 kV generator was connected to a 22 kV network via a 66,667 kVA autotransformer. The efficiency of large autotransformers reaches 99.7 per cent.

22-3. Three-Circuit Transformers

A. General. When a line with a voltage U_1 feeds simultaneously two other lines with different voltages U_2 and U_3 , it is possible, instead of using two transformers with voltages $\frac{U_1}{U_2} = \frac{U_1}{U_3}$ to install one transformer with two separate secondaries and, conse-

quently, with two secondary voltages. Such a transformer with voltage $U_1/U_2/U_3$ is called the *three-circuit* transformer and is at present widely used in transformer substations. [Bibl. 15b, 85, 98, 99]

In the general case there may be any number of transformer circuits, but here we shall discuss only the three-circuit transformer since it is the most important one.

According to the State Standard 401-41, the three-circuit power transformers are made: a) as three-phase transformers for capacities

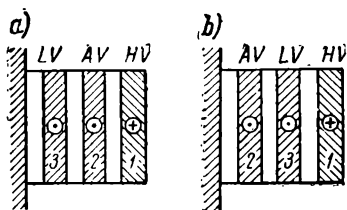


Fig. 22-3. Winding arrangement diagram for a three-circuit transformer

ties from 5,600 kVA to 31,500 kVA with the upper limit of rated voltage 121 kV for the highest voltage winding (H. V.), 38.5 kV for the average-voltage winding (A. V.) and 11 kV for the low-voltage winding (L. V.); b) as single-phase transformers for capacities from 5,000 kVA to 40,000 kVA with the same voltages of the H. V. and A. V. windings and with the upper

limit of 15.75 kV for the L. V. winding. It should be, however, noted that at present large three-circuit transformers for 220 and 400 kV are being manufactured in the U.S.S.R.

According to the standard mentioned previously, the windings of three-phase three-circuit transformers are $Y_0/Y_0/\Delta$ -12-11 or $Y_0/\Delta/\Delta$ -11-11 connected.

The rated power of a three-circuit transformer is the power of the winding with the greatest capacity, i.e., actually the power of its primary. Table 22-1 gives the rated power values of the average- and low-voltage windings, the low-voltage winding power assumed as 100 arbitrary units.

Table 22-1

Rated Powers of the Windings in Per Cent of Rated Power of a Three-Circuit Transformer

Windings		
Low-voltage	Average-voltage	High-voltage
100	100	100
100	66.7	100
100	100	66.7
100	66.7	66.7

From a design standpoint two methods of arrangement of the high-, medium- and low-voltage windings are assumed shown in Fig. 22-3, *a* and *b*. From now on we shall designate the three windings HV, AV, LV by figures 1, 2 and 3 correspondingly.

B. Physical conditions of three-circuit transformer operation.

In a three-circuit transformer, as in the two-winding transformer, there exist:

a) The main flux or the mutual induction flux Φ , linked with all three transformer circuits and

b) the leakage fluxes, the map or picture of which is more complex than that of a two-winding transformer, since not only leakage fluxes each closing round each single winding but also the leakage fluxes enveloping each two windings (Fig. 22-4) are taken into account.

The action of the main flux is characterised by the mutual inductances M_1 , M_2 and M_3 , and the leakage fluxes—by inductances $L_{\sigma 1}$, $L_{\sigma 2}$, $L_{\sigma 3}$, $L_{\sigma 12}$, $L_{\sigma 21}$, $L_{\sigma 13}$, $L_{\sigma 31}$, $L_{\sigma 23}$ and $L_{\sigma 32}$.

When analysing the operation of the three-circuit transformer we assume that both secondaries are referred to the primary both in the number of turns and the power, since in a three-circuit transformer the powers developed in the windings 1, 2 and 3 may be different in the general case (Table 22-1).

Thus,

$$\omega_1 = \omega_2 = \omega_3 = \omega$$

and

$$P_{n1} = P_{n2} = P_{n3} = P_n.$$

Besides, as in the case of the two-winding transformer, we shall assume that all the values varying with time are sine-wave and that the steel permeability $\mu = \text{const}$. In these conditions

$$M_1 = M_2 = M_3 = M, \quad \dots \quad (22-13)$$

$$L_{\sigma 12} = L_{\sigma 21}; \quad L_{\sigma 13} = L_{\sigma 31}$$

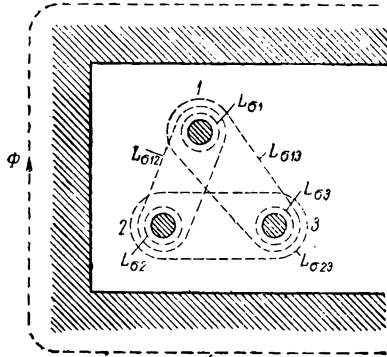


Fig. 22-4. Leakage flux diagram of a three-circuit transformer

and

$$L_{o23} = L_{o32}. \quad (22-14)$$

For simplicity sake we shall write all reduced (referred) values without primes.

C. M.m.f. equation of a three-circuit transformer. Similar to equation (13-32a) for the m.m.f. of a two-circuit transformer, we have

$$\dot{I}_1 + \dot{I}_2 + \dot{I}_3 = \dot{I}_0, \quad (22-15)$$

where \dot{I}_0 is the transformer no-load current.

In three-circuit transformers $\dot{I}_0 = 2.5$ to 3.5 per cent of \dot{I}_n ; therefore, we may neglect it and write the m.m.f. equation in a simplified form:

$$\dot{I}_1 + \dot{I}_2 + \dot{I}_3 = 0. \quad (22-16)$$

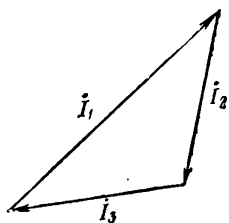


Fig. 22-5. Three-circuit transformer current diagram

The current diagram corresponding to this equation is shown in Fig. 22-5.

D. The first form of a three-circuit transformer e.m.f. equation. In accordance with the flux picture in Fig. 22-4, we have:

a) The full inductances of windings 1, 2 and 3:

$$L_1 = M + L_{o1} + L_{o12} + L_{o13}; \quad (22-17a)$$

$$L_2 = M + L_{o2} + L_{o21} + L_{o23}; \quad (22-17b)$$

$$L_3 = M + L_{o3} + L_{o31} + L_{o32}. \quad (22-17c)$$

b) The full mutual inductances of windings 2 and 3 in respect to winding 1 are determined by the sums $M + L_{o21}$ and $M + L_{o31}$ correspondingly;

c) The mutual inductances of windings 1 and 3 in respect to winding 2 and, correspondingly, of windings 1 and 2 in reference to winding 3 are determined by sums $M + L_{o12}$, $M + L_{o32}$, $M + L_{o13}$ and $M + L_{o23}$.

Then the e.m.f. equations of a three-circuit transformer will be:

$$\begin{aligned} \dot{U}_1 = & \dot{I}_1 r_1 + j \dot{I}_1 \omega (M + L_{o1} + L_{o12} + L_{o13}) + \\ & + j \dot{I}_2 \omega (M + L_{o21}) + j \dot{I}_3 \omega (M + L_{o31}); \end{aligned} \quad (22-18a)$$

$$\begin{aligned} -\dot{U}_2 = & \dot{I}_2 r_2 + j \dot{I}_2 \omega (M + L_{o2} + L_{o21} + L_{o23}) + \\ & + j \dot{I}_3 \omega (M + L_{o32}) + j \dot{I}_1 \omega (M + L_{o12}); \end{aligned} \quad (22-18b)$$

$$\begin{aligned} -\dot{U}_3 = & \dot{I}_3 r_3 + j \dot{I}_3 \omega (M + L_{o3} + L_{o31} + L_{o32}) + \\ & + j \dot{I}_1 \omega (M + L_{o13}) + j \dot{I}_2 \omega (M + L_{o23}). \end{aligned} \quad (22-18c)$$

Here r_1, r_2, r_3 are the active resistances of windings 1, 2 and 3.

In the expressions (22-18a), (22-18b) and (22-18c) all the subscripts are in a definite order; of two adjacent subscripts the first belongs to the winding, the current of which is proportional to the corresponding e.m.f. component, and the second refers to the winding, the coupling of which is then taken into account.

Let us subtract from equation (22-18a) first the equation (22-18b) and then the equation (22-18c) and substitute into the obtained differences the current values $I_1 = -(I_2 + I_3)$ from the m.m.f. equation (22-16).

Then,

$$\dot{U}_1 - (-\dot{U}_2) = \overline{\Delta U}_{12} = -\dot{I}_2(r_1 + r_2) - \dot{I}_3 r_1 - j\dot{I}_2 \omega(L_{\sigma 1} + L_{\sigma 12} + L_{\sigma 2} + L_{\sigma 23}) - j\dot{I}_3 \omega(L_{\sigma 1} + L_{\sigma 32}). \quad (22-19a)$$

and

$$\dot{U}_1 - (-\dot{U}_3) = \overline{\Delta U}_{13} = -\dot{I}_3(r_1 + r_2) - \dot{I}_2 r_1 - j\dot{I}_3 \omega(L_{\sigma 1} + L_{\sigma 12} + L_{\sigma 2} + L_{\sigma 32}) - j\dot{I}_2 \omega(L_{\sigma 1} + L_{\sigma 23}). \quad (22-19b)$$

These equations are true for any operating condition of a three-circuit transformer. Let us refer them once to short-circuit conditions between windings 1 and 2, with the winding 3 open and, consequently, $I_3 = 0$, and the second time to the short circuit between windings 1 and 3 and $I_2 = 0$.

In the first case the equation (22-19a) is rewritten as:

$$\begin{aligned} \Delta \dot{U}_{12} &= -\dot{I}_2(r_1 + r_2) - j\dot{I}_2 \omega(L_{\sigma 1} + L_{\sigma 12} + L_{\sigma 2} + L_{\sigma 23}) = \\ &= -\dot{I}_2 r_{sh12} - j\dot{I}_2 x_{sh12}. \end{aligned} \quad (22-20a)$$

In the second case we have:

$$\begin{aligned} \Delta \dot{U}_{13} &= -\dot{I}_3(r_1 + r_2) - j\dot{I}_3 \omega(L_{\sigma 1} + L_{\sigma 12} + L_{\sigma 2} + L_{\sigma 32}) = \\ &= -\dot{I}_3 r_{sh13} - j\dot{I}_3 x_{sh13}. \end{aligned} \quad (22-20b)$$

The equations (22-20a) and (22-20b) are quite similar to the equations for a short-circuited reduced two-winding transformer, if it is assumed that

$$\omega(L_{\sigma 1} + L_{\sigma 12} + L_{\sigma 2} + L_{\sigma 23}) = x_{sh12} \quad (22-21)$$

and

$$\omega(L_{\sigma 1} + L_{\sigma 12} + L_{\sigma 2} + L_{\sigma 32}) = x_{sh13}. \quad (22-22)$$

By analogy from short-circuit conditions of windings 2 and 3 for $I_1 = 0$, we have:

$$\omega(L_{\sigma 2} + L_{\sigma 21} + L_{\sigma 3} + L_{\sigma 31}) = x_{sh23}. \quad (22-23)$$

Returning to equations (22-20a) and (22-20b), we assume that the sum $L_{\sigma 1} + L_{\sigma 2} = L_{\sigma 1} + L_{\sigma 2}$ is the equivalent leakage inductance of winding 1 and that, correspondingly, the product

$$\omega(L_{\sigma 1} + L_{\sigma 2}) = \omega(L_{\sigma 1} + L_{\sigma 2}) = x_1 \quad (22-24a)$$

is the equivalent leakage reactance of this winding.

Similarly,

$$\omega(L_{\sigma 2} + L_{\sigma 1}) = \omega(L_{\sigma 2} + L_{\sigma 1}) = x_2 \quad (22-24b)$$

and

$$\omega(L_{\sigma 3} + L_{\sigma 12}) = \omega(L_{\sigma 3} + L_{\sigma 12}) = x_3, \quad (22-24c)$$

where x_2 and x_3 are the equivalent leakage reactances of the 2 and 3 windings.

Then the equations (22-20a) and (22-20b) acquire the form of:

$$\begin{aligned} \Delta \dot{U}_{12} &= -\dot{I}_2(r_{sh12} + jx_{sh12}) - \dot{I}_3(r_1 + jx_1) = \\ &= -(\dot{I}_2 Z_{sh12} + \dot{I}_3 Z_1) \end{aligned} \quad (22-25)$$

and

$$\begin{aligned} \Delta \dot{U}_{13} &= -\dot{I}_3(r_{sh13} + jx_{sh13}) - \dot{I}_2(r_1 + jx_1) = \\ &= -(\dot{I}_3 Z_{sh13} + \dot{I}_2 Z_1). \end{aligned} \quad (22-26)$$

The equations (22-25) and (22-26) are the basic equations of three-circuit transformer operation. We see that: a) the voltage drops ΔU_{12} and ΔU_{13} depend on the currents \dot{I}_2 and \dot{I}_3 in both secondaries and b) the measure of mutual effect of windings 2 and 3 is the complex impedance Z_1 .

E. The second form of three-circuit transformer equations. Equations (22-25) and (22-26) may be modified, if in the first we introduce $\dot{I}_3 = -(\dot{I}_1 + \dot{I}_2)$ and into the second $\dot{I}_2 = -(\dot{I}_1 + \dot{I}_3)$.

In this case we have:

$$\Delta \dot{U}_{12} = -\dot{I}_2 Z_{sh12} + \dot{I}_1 Z_1 + \dot{I}_2 Z_1 = \dot{I}_1 Z_1 - \dot{I}_2 (Z_{sh12} - Z_1)$$

or, since $Z_{sh12} - Z_1 = Z_2$ then

$$\Delta \dot{U}_{12} = \dot{I}_1 Z_1 - \dot{I}_2 Z_2. \quad (22-27)$$

Correspondingly,

$$\begin{aligned} \Delta \dot{U}_{13} &= \dot{I}_1 Z_1 + \dot{I}_3 Z_1 - \dot{I}_2 Z_{sh13} = \dot{I}_1 Z_1 - \dot{I}_3 (Z_{sh13} - Z_1) = \\ &= \dot{I}_1 Z_1 - \dot{I}_3 Z_3, \end{aligned} \quad (22-28)$$

where

$$Z_3 = Z_{sh13} - Z_1.$$

F. The equivalent circuit of a three-circuit transformer. With the equations (22-27) and (22-28), as the base, it may be seen that the equivalent circuit satisfying these equations is a three-ray star of impedances Z_1 , Z_2 and Z_3 (Fig. 22-6). The circuit corresponds to one phase of a three-circuit transformer, and the point N of the scheme determines not the electric, but the electromagnetic coupling between windings 1, 2 and 3 similarly to point F of the equivalent circuit of a two-winding transformer (see Fig. 13-3).

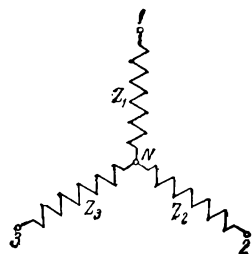


Fig. 22-6. Three-circuit transformer equivalent circuit

G. Three-circuit transformer parameters. These parameters are determined, as in a two-winding transformer, from the no-load and short-circuit tests.

a) *The no-load test.* According to the three windings of a transformer, three no-load tests may be made from which we obtain:

1) Three transformation ratio values, viz.:

$$k_{12} = \frac{U_1}{U_2}; \quad k_{13} = \frac{U_1}{U_3}; \quad k_{23} = \frac{U_2}{U_3} = \frac{\frac{U_2}{U_1}}{\frac{U_3}{U_1}} = \frac{k_{12}}{k_{13}};$$

2) Three values of no-load current; if the powers of the windings are not equal, these currents are recalculated and expressed as the per cent of the rated current of the winding with the greatest power;

3) The no-load losses. The same in all three cases.

It follows that it is practically sufficient to carry out only one no-load test and determine two transformation ratios for instance of k_{12} and k_{13} , after which the ratio k_{23} may be calculated.

b) *Short circuit of a three-circuit transformer.* As in the case of no-load operation, three short-circuit tests may be carried out, viz.:

- 1) Between windings 1 and 2 with winding 3 open;
- 2) Between windings 1 and 3 with winding 2 open;
- 3) Between windings 2 and 3 with winding 1 open.

From these tests, the same as for a two-winding transformer, the parameters of each winding pair may be determined, namely:

$$Z_{sh12}; \quad r_{sh12} = r_1 + r_2; \quad x_{sh12} = x_1 + x_2; \quad (22-29a)$$

$$Z_{sh13}; \quad r_{sh13} = r_1 + r_3; \quad x_{sh13} = x_1 + x_3; \quad (22-29b)$$

and

$$Z_{sh23}; \quad r_{sh23} = r_2 + r_3; \quad x_{sh23} = x_2 + x_3. \quad (22-29c)$$

Solving these equations, we obtain:

$$r_1 = \frac{r_{sh12} + r_{sh13} - r_{sh23}}{2}; \quad x_1 = \frac{x_{sh12} + x_{sh13} - x_{sh23}}{2}; \quad (22-30a)$$

$$r_2 = \frac{r_{sh12} + r_{sh23} - r_{sh13}}{2}; \quad x_2 = \frac{x_{sh12} + x_{sh23} - x_{sh13}}{2}; \quad (22-30b)$$

$$r_3 = \frac{r_{sh13} + r_{sh23} - r_{sh12}}{2}; \quad x_3 = \frac{x_{sh13} + x_{sh23} - x_{sh12}}{2}. \quad (22-30c)$$

It should be recalled that the parameters x_1 , x_2 and x_3 represent equivalent leakage reactances of windings 1, 2 and 3 determined by sums $L_{\sigma 1} + L_{\sigma 23}$, $L_{\sigma 2} + L_{\sigma 13}$ and $L_{\sigma 3} + L_{\sigma 12}$ equations (22-24a), (22-24b), (22-24c).

The active resistances r_{sh12} , r_{sh13} and r_{sh23} , as well as the resistances r_1 , r_2 and r_3 , practically do not depend on the mutual arrangement of the 1, 2 and 3 windings, i. e., of the HV-, AV- and LV windings. But the leakage reactances of the windings and therefore also the impedance voltages depend, as is known, on the distance between them (§17-10, A). The standard arrangement of windings of the three-circuit power transformers is shown in Fig. 22-3, *a* and *b*. The impedance voltage values corresponding to these two diagrams are given in Table 22-2 in accordance with the State Standard 401-41.

Table 22-2

Impedance Voltages of Three-Circuit Power Transformers as Per Cent of Rated Voltage

Windings	HV-AV	HV-LV	AV-LV
Impedance voltage according to diagrams in Fig. 22-3, <i>a</i> . . .	10.5	17	6
Impedance voltage according to diagrams in Fig. 22-3, <i>b</i> . . .	17	10.5	6

H. The vector diagram of a three-circuit transformer. According to the e.m.f. equations (22-25) and (22-26) or (22-27) and (22-28), three-circuit transformer vector diagrams may be plotted. For this purpose we plot first the current triangles OAB (Fig. 22-7, *a* and *b*), assuming that the currents I_2 and I_3 are given both by magnitude and phase in respect to the voltages

U_2 and U_3 . To obtain the voltage vector U_1 , the vectors of voltages $-U_2$ and $-U_3$ should be added geometrically to the voltage drop vectors according to equations (22-25) and (22-26) (Fig. 22-7,a) or equations (22-27) and (22-28) (Fig. 22-7,b).

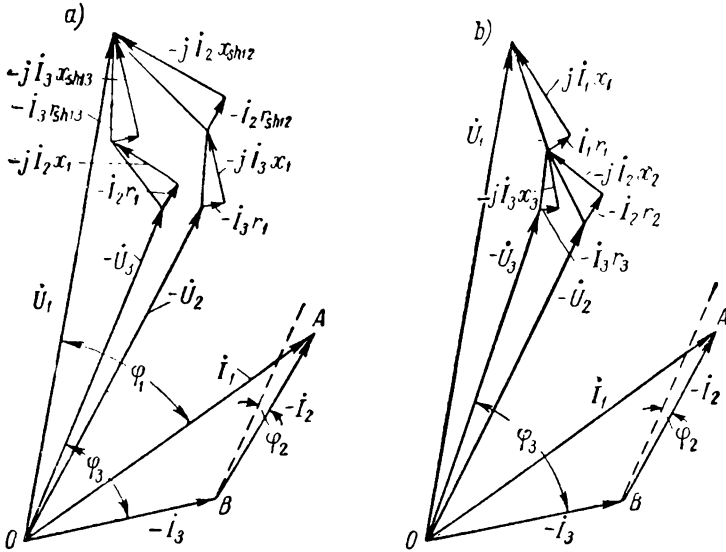


Fig. 22-7. Three-circuit transformer vector diagrams

I. Determination of voltage variation by computation. Let us determine the voltage variation for rated values of the currents I_2 and I_3 . By analogy with a two-winding transformer, using the diagram in Fig. 22-7,a, let us project all the voltage drop vectors once onto the direction of the current I_2 vector and onto the direction perpendicular to it, and then onto the direction of current I_3 vector and onto the direction perpendicular to it.

Let us introduce the notations:

$$\frac{I_2 r_{sh12}}{U_1} \cdot 100 = u_{sh.a12}; \quad (22-31a)$$

$$\frac{I_2 x_{sh12}}{U_1} \cdot 100 = u_{sh.s12}; \quad (22-31b)$$

$$\frac{I_2 r_1}{U_1} \cdot 100 = u_{sh.a1}; \quad (22-32a)$$

$$\frac{I_2 x_1}{U_1} \cdot 100 = u_{k.a1}; \quad (22-32b)$$

$$\frac{I_3^2 r_{sh13}}{U_1} \cdot 100 = u_{sh.a13}; \quad (22-33a)$$

$$\frac{I_3^2 x_{sh13}}{U_1} \cdot 100 = u_{sh.o13}; \quad (22-33b)$$

$$\frac{I_3^2 r_1}{U_1} \cdot 100 = u_{sh.a3}; \quad (22-34a)$$

$$\frac{I_3^2 x_1}{U_1} \cdot 100 = u_{sh.o3}. \quad (22-34b)$$

Then the voltage variation as a percentage of the rated value of U_1 may be expressed as:

$$\begin{aligned} \Delta U_{12} = & \frac{U_1 - U_3}{U_1} \cdot 100 = U_{sh.a12} \cos \varphi_2 + u_{sh.o12} \sin \varphi_2 + \\ & + u_{sh.a3} \cos \varphi_3 + u_{sh.o3} \sin \varphi_3 + \\ & + \frac{(u_{sh.o12} \cos \varphi_2 - u_{sh.a12} \sin \varphi_2 + u_{sh.o3} \cos \varphi_3 - u_{sh.a3} \sin \varphi_3)^2}{200}; \end{aligned} \quad (22-35)$$

$$\begin{aligned} \Delta U_{13} = & \frac{U_1 - U_3}{U_1} \cdot 100 = u_{sh.a13} \cos \varphi_3 + u_{sh.o13} \sin \varphi_3 + u_{sh.a2} \cos \varphi_2 + \\ & + u_{sh.o2} \sin \varphi_2 + \\ & + \frac{(u_{sh.o13} \cos \varphi_3 - u_{sh.a13} \sin \varphi_3 + u_{sh.o2} \cos \varphi_2 - u_{sh.a2} \sin \varphi_2)^2}{200}. \end{aligned} \quad (22-36)$$

J. The efficiency of a three-circuit transformer. Let P_1 , P_2 , P_3 be the rated powers of the transformer windings, k_1 , k_2 , k_3 —the load factors in fraction of a unit; $\cos \varphi_2$ and $\cos \varphi_3$ —the power factors for loads $k_2 P_2$ and $k_3 P_3$, P_0 —the no-load losses. Then the efficiency of a three-circuit transformer as a percentage will be expressed as:

$$\begin{aligned} \eta = & \left[1 - \frac{P_0 + m(k_1 I_1)^2 r_1 + m(k_2 I_2)^2 r_2 + m(k_3 I_3)^2 r_3}{k_2 P_2 \cos \varphi_2 + k_3 P_3 \cos \varphi_3 + P_0 + m(k_1 I_1)^2 r_1 + m(k_2 I_2)^2 r_2 + m(k_3 I_3)^2 r_3} \right] \times \\ & \times 100. \end{aligned} \quad (22-37)$$

Here m is the number of phase windings.

The efficiency of the three-phase and single-phase power three-circuit transformers corresponding to maximum losses and $\cos \varphi = 1$ is within the limits of 98.25 to 99.25 per cent.

22-4. Transformers with Voltage Regulation Under Load

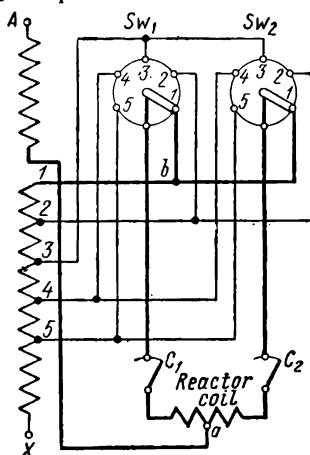
It was already mentioned in § 12-2 that all power transformers are provided with tappings for voltage regulation of transformer disconnected from the primary and secondary circuits. But during the operation of a large-capacity energy system it

is necessary sometimes to redistribute both the active and reactive currents between the different elements of the system by means of voltage regulation at the corresponding points. This is done with the help of special transformers with stepped voltage regulation under load by varying the transformation ratio. The usual voltage regulation range is ± 10 per cent but in some cases it may reach ± 15 per cent and more. [Bibl. 19a, 73b]

The transition under load from one voltage step to the other must be performed without breaking the working circuit. Such a stepped voltage regulation may be accomplished in two ways: a) by means of varying the number of transformer winding turns and b) by means of a special booster transformer with a variable transformation ratio inserted into main transformer circuit.

Fig. 22-8 shows a circuit of the first kind. Here $A-X$ is the winding of a single-phase transformer or one winding of a three-phase transformer; K_1 and K_2 are contactors; Sw_1 and Sw_2 are switches. In normal conditions, the contactors C_1 and C_2 are closed, and switches Sw_1 and Sw_2 are set on the same contacts, for instance, 1-1 (position 1 in the table under the figure). At the midpoint a of the reactor coil, the current branches off and flows parallel along both (left and right) halves of the circuit to point b and further into the winding. In this case the m.m.f.s of both reactor halves are opposed owing to which the reactance of the reactor is small.

To change the transformation ratio we open contactor C_1 and send the load current along only the right-hand half of the circuit via the contactor C_2 and switch Sw_2 ; then we move the handle of the switch Sw_1 from contact 1 to contact 2 and again close contactor C_1 . The part of the winding between contacts 1 and 2 is closed through reactor coil which serves, thus, as a short-circuit current-limiting device; the short-circuit current appears in the switched part of the winding. The same is done with the right-



Position	①					②
Switch Sw_1	1	1	2	2	2	2
Switch Sw_2	1	1	1	1	1	2
Contactor K_1	•	•	•	•	•	•
Contactor K_2	•	•	•	•	•	•

• Contactor closed

Fig. 22-8. Voltage regulation circuit under load by means of changing transformer winding tapings ($K_1=C_1$ and $K_2=C_2$)

hand part, and the regulation procedure is thereby completed. The complete sequence of the procedure is indicated in the table under Fig. 22-8. In the case of the circuit in Fig. 22-8, the switching device is connected to the winding circuit in series and should be, therefore, calculated for its rated current and voltage. In some cases, however, it is advisable to isolate the apparatus from the power line. This is achieved with the help of two additional transformers, viz., a series transformer inserted into the line and a regulating transformer which serves for feeding the former.

Each of the additional transformers is rated at a power which

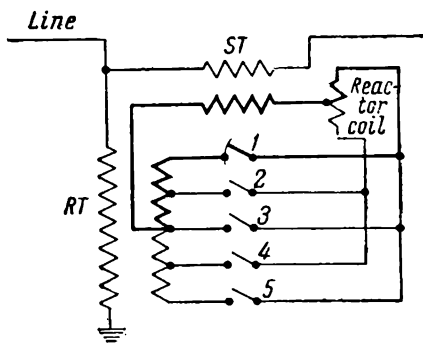


Fig. 22-9. Voltage regulation circuit under load by means of a booster transformer

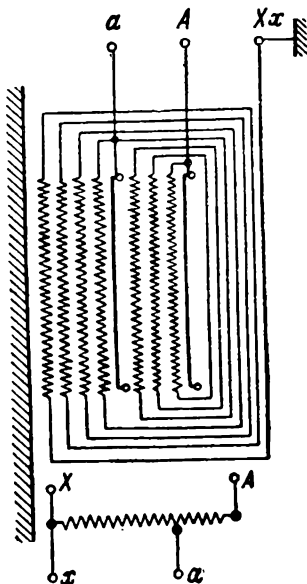


Fig. 22-10. Circuit diagram of an autotransformer protected against overvoltage

matches the voltage regulation range. The corresponding circuit for one phase is shown in Fig. 22-9. Here RT is the regulating transformer; ST is the series transformer; 1, 2, 3, 4, 5 are the contactors. During operation only one contactor, for instance 1, is closed. The current flows along the circuit shown by the solid lines, utilising the upper half of the reactor; in this case an inductive voltage drop occurs in the reactor half which may be, however, neglected if the reactor is properly calculated. During the switching procedure we close contactor 2 without opening contactor 1; the reactor coil then acts as a limiter of the short-circuit current in the part of the winding between contactors 1 and 2. Then we open contactor 1 and complete thereby the switching procedure.

Non-inductive current-limiting resistors are often used instead of reactors. But unlike the reactor, the non-inductive current limiter is utilised only during the period of closing the contactors of the switched part of the winding.

A 40,500 kVA three-phase, three-circuit transformer with voltage regulation under load on the high-voltage winding side at 110 kV was built at the Moscow Transformer Works. For limiting the short-circuit current in the switching part, a reactor was used instead of the previously contemplated active resistance. Medium- and low-capacity transformers are provided with automatic or manual control apparatus. In the U.S.A. voltage regulation is often accomplished with the help of autotransformers which in service have proved reliable. In order to protect the autotransformer from overvoltage, its winding is provided with two protective screens—external and internal—the latter located at the connection point of both parts of the autotransformer (Fig. 22-10).

22-5. Transformers with Continuous Voltage Regulation

It is more difficult to accomplish continuous regulation of transformer voltage than by stepped regulation. That is why these transformers are made for relatively small power, mainly for special purposes. The continuous voltage regulation is attained in many different ways, for instance, by displacing the yoke in respect to one or both of the windings; with the help of a movable iron-core reactor; by displacing one winding in respect to the other and the magnetic core. In 1927, V. A. Andronov patented the first design of a regulating autotransformer after which analogous constructions appeared in other countries. The autotransformer winding is wound on its core in one layer and usually of non-insulated wire. Brushes of special design slide over the winding, the brush width providing smooth passage from turn to turn without breaking the circuit. To limit the short-circuit currents appearing in this case within the winding turns covered by the brush, the latter may be made of a series of contacts connected together through active resistances, or made of carbon so that the transverse resistance of the brush is sufficient to limit the short-circuit current, and the longitudinal resistance would not cause an excessive voltage drop when the load current is flowing through it. The selected number of winding turns ensures from 0.5 to 1 V per turn and, hence, practically continuous voltage regulation.

In 1948, the Moscow Electromechanical Works Gosteasvet began the production of the autotransformers with continuous voltage regulation under load both of single-phase 20 kVA, 220 V, and three-phase for 25 to 260 kVA, 127-380 V. The power and voltage given above are rated values and correspond to the upper limit; the regulated voltage may be stepped down to zero, and the load power varies as a function of the secondary voltage; the efficiency of such autotransformers may vary within the range of 0 to 98 per cent.

22-6. Transformers for Mercury Arc Rectifiers (Rectifier Transformers)

The general principles governing the theory and design of power transformers are applicable also to rectifier transformers. The main difference between both types of transformers is that owing to the valve effect of the mercury rectifier, each of its anodes works only during part of a period, in accordance with which operating conditions for the primary and secondary windings of a rectifier transformer are not identical. It is necessary, therefore, to specify some of the definitions for power transformers. [Bibl. 100—104]

1. The rated power of a rectifier transformer is the power of its primary P_1 , since it is this power that is supplied to the transformer from the mains. The rated power of a transformer is expressed in kVA.

2. For the definition of rated primary voltage see § 12-4.

3. The rated secondary voltage of a rectifier transformer is the voltage across the secondary between the neutral (zero) and phase leads of the latter at no-load.

4. The rated primary current I_1 is determined from the rated power and the rated primary voltage of the transformer.

5. The secondary power P_2 of a rectifier transformer is determined as the product of the rated secondary voltage U_2 and the effective value of the secondary current I_2 at full load on the side of the rectified current. The secondary power, as well as the primary, is expressed in kVA.

6. The rated values of the rectified voltage and current are voltage U_{rec} and the current I_{rec} at full load of the rectifier.

7. The typical power of a rectifier transformer is the half-sum of the primary and secondary powers, i.e.,

$$P_T = \frac{1}{2} (P_1 + P_2). \quad (22-38)$$

Let us consider several typical circuits for the alternating current rectification.

A. A three-phase rectifying circuit with transformer windings connected as star-star with tapped neutral. The corresponding circuit diagram is shown in Fig. 22-11, *a*. Let us assume that the inductance of the transformer is zero. In this case each subsequent anode begins to operate at the moment when the preceding anode ceases its operation; correspondingly the rectified voltage curve has the form shown in Fig. 22-11, *b*.

Let $U_{rec\,av}$ be the average value of the rectified voltage, m —the num-

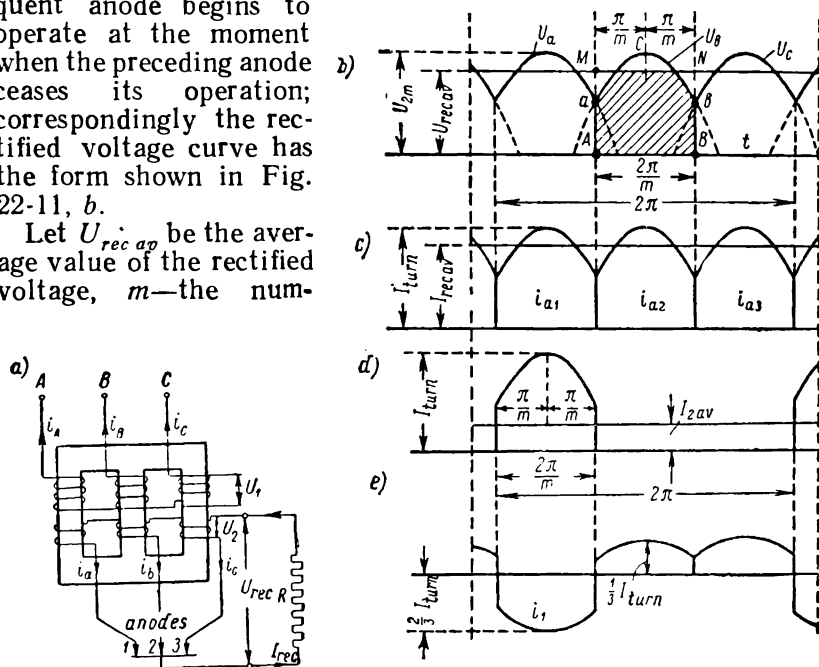


Fig. 22-11. Three-phase rectifier with star-star connected transformer windings and tapped neutral:

a—connection diagram; *b*—rectified voltage; *c*—anode currents; *d* and *e*—currents in the transformer primary and secondary

ber of phases equal to the number of anodes, and let the rectified voltage vary sinusoidally within the range of angle $\frac{2\pi}{m}$. Let us agree to reckon the time from the instant the rectified voltage reaches its maximum value U_{2m} ; then the instantaneous value of the voltage within the range of angle $\frac{2\pi}{m}$ would be $U_{2m} \cos x$; the average value of the rectified voltage (the index *av* here and later on is omitted) is equal to the height *AM* of the rec-

tangle $AMNB$ equivalent to the area $AaCbB$. Hence

$$U_{rec} = \frac{1}{\frac{2\pi}{m}} \int_{-\frac{\pi}{m}}^{+\frac{\pi}{m}} U_{2m} \cos x \, dx = U_{2m} \frac{\sin \frac{\pi}{m}}{\frac{\pi}{m}} = U_2 \sqrt{2} \frac{\sin \frac{\pi}{m}}{\frac{\pi}{m}}. \quad (22-39)$$

If the rectifier is loaded only with active resistance R , the rectified current has the same shape as the rectified voltage (Fig. 22-11,c). Hence, the average value of the rectified current is expressed by a formula similar to formula (22-39), viz.,

$$I_{rec} = I_{rec.m} \frac{\sin \frac{\pi}{m}}{\frac{\pi}{m}}. \quad (22-40)$$

Each phase of the transformer secondary conducts a current only during $\frac{1}{m}$ th of a period (Fig. 22-11,d). The average value of the current in winding is, therefore,

$$I_{2av} = \frac{I_{rec}}{m}. \quad (22-41)$$

Correspondingly, the effective value of the current in the same winding is:

$$I_2 = \sqrt{\frac{1}{2\pi} \cdot \frac{2\pi}{m} I_{rec}^2} = \frac{I_{rec}}{\sqrt{m}}. \quad (22-42)$$

Let us refer the primary to the secondary. In this case $U_1 = U_2$, and the primary current curve in Fig. 22-11,e consists of a part repeating the secondary current curve, but having an amplitude which equals to $\frac{2}{3}$ of the secondary current amplitude, and of two sections of reversed direction with amplitudes $\frac{1}{3}$ of the secondary current amplitude [formulas (19-9), (19-10,a) and (19-10,b), § 19-4]. Then the effective value of the primary current is:

$$I_1 = \sqrt{\frac{1}{2\pi} \times \frac{2\pi}{m} \left[\left(\frac{2}{3} I_{rec} \right)^2 + 2 \left(\frac{1}{3} I_{rec} \right)^2 \right]} = I_{rec} \sqrt{\frac{2}{3m}}. \quad (22-43)$$

The main disadvantage of the star-star connection with a tapped neutral is that the m.m.f.s induced by the primary and secondary currents are not balanced. To prove this it is sufficient

to compare the currents in Fig. 22-11, *d* and *e*. We see that unbalanced m.m.f.s, $\frac{1}{3}$ of $I_{rec.m}$ each, all directed the same way, act in the three transformer legs. These operating conditions of a rectifier transformer are similar to the operating conditions of a star-star connected transformer with tapped neutral for unbalanced load (Chapter 19). As was previously the case, magnetic fluxes appear in the rectifier transformer legs equal in magnitude and direction, which close from one yoke to the other via the air (Fig. 19-7). As a result the neutral point is shifted, and the phase voltages distorted (Fig. 19-12, *b*); the leakage inductances of the transformer and the additional losses are increased.

The connection schemes which do not have this disadvantage are: a) the three-phase bridge scheme, b) the star-double zigzag scheme and c) the star-two reversed stars scheme with an equalising coil.

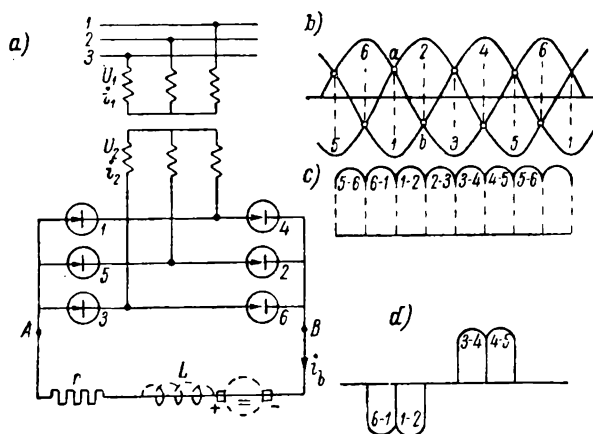


Fig. 22-12. Three-phase bridge circuit:

a — connection diagram; b — transformer secondary phase voltages;
c — rectified voltage; d — transformer secondary phase current

B. The three-phase bridge scheme. The circuit diagram is shown in Fig. 22-12, *a*. In this scheme at any instant two anodes are firing: one belonging to the even group, which has the highest voltage, and the other to the odd group, the voltage of which is the lowest. Fig. 22-12, *b* shows the secondary phase voltages of a transformer. The first and second anodes are firing from point *a* to point *b*, after which the first anode ceases operation and the third anode begins firing so that the second and third anodes are operating, etc. Fig. 22-12, *c* shows the secondary line voltages

obtained as the difference of two corresponding phase voltages in Fig. 22-12,*b*. Since any of the two operating anodes are connected to the secondary line voltage, the same curve may also be considered as the rectified voltage curve, which has, thus, six wave forms. In the absence of inductance, the current curve repeats the voltage curve. A current curve for one phase of a transformer secondary is shown in Fig. 22-12,*d*. Part of the curve under the abscissa axis gives the current in anode 1, operating in turn with anodes 6 and 2, while the curve part above the abscissa axis gives current in anode 4, operating in turn with anodes 3 and 5.

The rectified voltage and current curves in Fig. 22-12,*c* indicate that, in a bridge circuit, the rectified voltage waveforms are smaller than in a three-phase circuit with a tapped neutral. In this respect the bridge circuit is equivalent to a six-phase circuit with a tapped zero. Owing to this, the average value of a rectified voltage may be obtained by means of equation (22-39), assuming that $m=6$ and introducing into it a multiplier $\sqrt{3}$, since the rectified voltage is equal to the secondary line voltage. Hence,

$$U_{rec} = \frac{\sqrt{3}U_2 \sqrt{2} \sin \frac{\pi}{6}}{\frac{\pi}{6}} = 1.35 \sqrt{3} U_2 = 2.34 U_2. \quad (22-44)$$

The average value of the rectified current and the effective value of the current in a transformer secondary are determined by formulas (22-40) and (22-42), if we assume $m = 6$ and take into account that two anodes are conducting simultaneously. Then

$$I_{rec} = I_{rec.m} \frac{\sin \frac{\pi}{6}}{\frac{\pi}{6}}; \quad (22-45)$$

$$I_2 = \frac{2}{\sqrt{6}} I_{rec} = 0.817 I_{rec}. \quad (22-46)$$

The power in the secondary will be

$$P_2 = 3U_2 I_2 = 3 \frac{U_{rec}}{2.34} 0.817 I_{rec} = 1.05 U_{rec} I_{rec}. \quad (22-47)$$

The current in the primary of a reduced transformer operating with a three-phase bridge circuit is equal to the current in the secondary (Fig. 22-12,*d,e*). We have, therefore,

$$P_1 = P_2 = P_T = 1.05 U_{rec} I_{rec}. \quad (22-48)$$

The factor $k_T = \frac{U_{rec} I_{rec}}{P_T}$ is referred to as the utility factor of the transformer. In the given case $k_T = \frac{1}{1.05} = 0.955$, i.e., it is relatively high.

Since with a bridge circuit the currents in the primary and secondary of a transformer are equal, the primary and secondary m.m.f.s are mutually balanced, and the additional single-phase flux in the transformer core is absent. This is a valuable advantage of the bridge circuit.

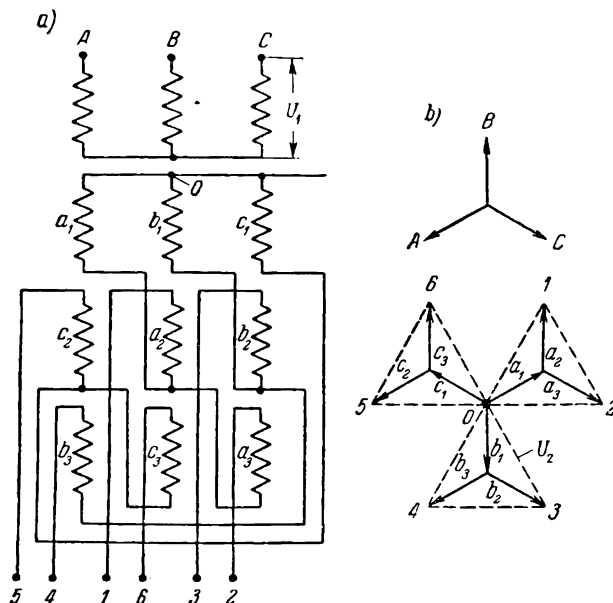


Fig. 22-13. Transformer for mercury rectifier:
a — star-double zigzag connected winding; b — e.m.f. diagram

In installations using large mercury rectifiers two circuits are of principal importance: 1) star-double zigzag and 2) star-two inversed stars with a separating coil.

C. The star-double zigzag circuit (Fig. 22-13,a). The primary of a transformer is connected in star, and each phase of the secondary is divided into three equal parts connected with each other in zigzag. Thus, for instance, the end of the part a_1 , placed on leg A is connected with ends of parts a_2 and a_3 placed on legs B and C. From the neutral O of the secondary a conductor

leads to the cathode of the mercury rectifier, and the winding ends 1, 2, 3, 4, 5, 6 are connected to the corresponding anodes of the rectifier. In Fig. 22-13,*b* the e.m.f. diagram is shown for the transformer in Fig. 22-13,*a*. The secondary is wound in the direction opposite to that of the primary. In accordance with this, the e.m.f. star $a_1-b_1-c_1$ is turned in respect to the star $A-B-C$ by 180° . The e.m.f.s of parts a_2 and a_3 are geometrically subtracted from the e.m.f. of a_1 , since some of the winding parts are connected by their ends; similar is the case for the two other phases. The results of the geometrical subtraction are shown in Fig. 22-13,*b*. As a whole, the voltages $O1, O2, \dots, O6$ between the neutral O and anodes 1, 2, ..., 6 of the rectifier form a symmetrical six-phase system, in which the voltages $O1=O2=\dots=O6=U_2$, where U_2 is the voltage between zero and the output terminal of the transformer. Thus, the circuit in Fig. 22-13,*a* is equivalent to a six-phase circuit; hence according to formula (22-40) we have:

$$U_{rec} = U_2 \sqrt{2} \frac{\sin \frac{\pi}{6}}{\frac{\pi}{6}} = 1.35 U_2. \quad (22-49)$$

The current in the secondary part directly connected to the anode is equal to [formula (22-43)]:

$$I_1 = \frac{I_{rec}}{\sqrt{m}} = \frac{I_{rec}}{\sqrt{6}} = 0.41 I_{rec}. \quad (22-50)$$

The current in the winding part connected to the neutral is a combination of the currents of two anodes, and its effective value is:

$$I'_2 = 0.41 \sqrt{2} I_{rec} = 0.58 I_{rec}. \quad (22-51)$$

Since in the case under consideration $m = 6$, the secondary power will be:

$$P_2 = 6 U_2 I_2 = 6 \frac{U_{rec}}{1.35} 0.41 I_{rec} = 1.81 U_{rec} I_{rec}. \quad (22-52)$$

The primary power is the same as in a bridge three-phase circuit, i.e.,

$$P_1 = 1.05 U_{rec} I_{rec}. \quad (22-53)$$

Consequently, the typical power of the transformer is equal to:

$$P_T = \frac{1}{2} (1.81 + 1.05) U_{rec} I_{rec} = 1.43 U_{rec} I_{rec}. \quad (22-54)$$

Fig. 22-14 shows the external characteristic of a rectifier installation operating in accordance with the scheme in Fig. 22-13, *a*. The characteristic is similar to the external characteristic of an ordinary transformer, but the operation of a rectifier transformer somewhat differs from ordinary transformer operation, since in the secondary of a rectifier transformer flows a constant current component, which increases the leakage fluxes of this transformer and its additional losses.

The star-double zigzag circuit is used in rectifier installations with capacities up to 1,000 kVA. The short-circuit voltage of a rectifier transformer is 4-5 per cent.

D. The star-two inverse stars circuit with an equalising coil

(Fig. 22-15, *a*). The secondary of the transformer winding consists of two stars inverted in respect to each other, with a single-phase reactor coil *RC* inserted between the neutral points O_1 and O_2 . One star feeds the odd group of anodes 1, 3, 5, the oth-

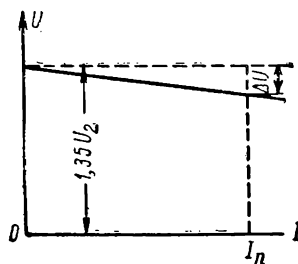


Fig. 22-14. $U_{rec} = f(I_{rec})$ curve for star-double zigzag connection

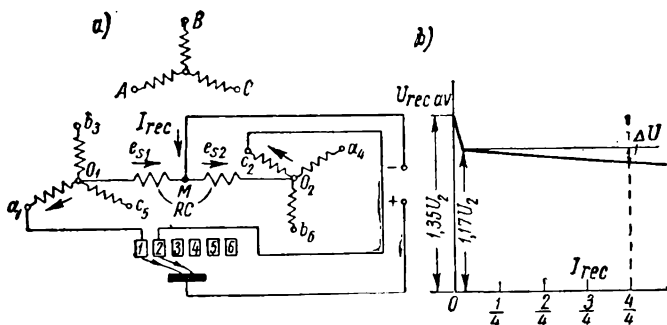


Fig. 22-15.

a — star-double zigzag connection with equalising coil; *b* — external characteristic of rectifier

er feeds the even anode group 2, 4, 6. Having connected mid-point *M* of the coil to the negative pole of the rectified current circuit, we may see that both stars can operate in parallel, one half of the reactance coil being inserted into each star. Let us assume that at a given instant anode 1 has the highest voltage under the action of which current I_{rec} flows in the anode circuit. Since

this current flows in the left-hand half of the reactance coil, the flux produced in it induces the e.m.f.s e_{s1} and e_{s2} in both halves of the coil. With the anode current rising, the e.m.f. e_{s1} has a direction, in which it tends to oppose the increase of current and, hence, lowers the voltage of phase O_1a_1 in respect to point M . On the contrary, the e.m.f. e_{s2} in the right-hand coil half, having the same direction as the e.m.f. e_{s1} , tends to increase the voltage of the phase O_2c_2 in respect to point M . As a result, the voltages of phases O_1a_1 and O_2c_2 are balanced, and hence the reactance coil acts as an equaliser, which forces the anodes 1 and 2 to operate in parallel. If the resistances of both secondary stars of a transformer are equal, the load current will be equally distributed between the two stars. Further these conditions occur for anodes 2-3, 3-4, etc.

The second valuable property of this scheme is that with simultaneous parallel operation of two anodes each is fired 30° earlier than for six-phase operation and is extinguished 30° later. Hence, the anode operates not during one-sixth of the period as in the circuit in Fig. 22-13, but during one-third of it, i.e., in the same manner as in a three-phase rectifier.

The advantage of this circuit is that: 1) it facilitates anode operation and increases the loading capacity of the rectifier, since for any given value of the rectified current I_{rec} approximately one half of current I_{rec} passes into each of the two parallel operating anodes; 2) it permits better utilisation of the transformer, since instead of employing a six-phase circuit the rectifier now uses a three-phase one; 3) it has smaller voltage drop ΔU , or for a given ΔU value a higher impedance voltage, which in certain cases, as, for instance, in traction installations, is of great importance.

Since in the case considered, the rectifier employs a three-phase circuit with a tapped neutral, and, according to previous discussion, each anode conducts one half of the current I_{rec} , from formulas (22-39) and (22-42) it follows:

$$U_{rec} = U_2 \sqrt{2} \frac{\sin \frac{\pi}{3}}{\frac{\pi}{3}} = 1.17 U_2 \text{ and } I_2 = \frac{I_{rec}}{2 \sqrt{3}} = 0.289 I_{rec}.$$

Hence, the power in the secondary winding is equal to:

$$P_2 = 3 U_2 \times 2 I_2 = 3 \frac{U_{rec}}{1.17} 2 \times 0.289 I_{rec} = 1.49 U_{rec} I_{rec}. \quad (22-55)$$

The power in the primary is the same as in the circuit in Fig. 22-13, a, i. e.,

$$P_1 = 1.05 U_{rec} I_{rec}. \quad (22-56)$$

Hence, the power of the standard transformer will be

$$P_T = \frac{1}{2} (1.49 + 1.05) U_{rec} I_{rec} = 1.27 U_{rec} I_{rec}. \quad (22-57)$$

The disadvantage of this circuit is that with a change in load from no-load to about 1 per cent an abrupt voltage change occurs from $U_{rec} = 1.35 U_2$ to $U_{rec} = 1.17 U_2$, i. e., by 15 per cent (Fig. 22-15, *b*). This may be explained by the fact that with very small load currents, the balancing coil does not obtain the magnetising current required for its operation and acts as though switched out of the circuit. In these conditions the rectifier operates as a six-phase rectifier, in which according to formula (22-40) $U_{rec} = 1.35 U_2$. When the current increases more than 1 per cent of the rated value, the coil becomes normally magnetised, and the rectifier begins to operate as a three-phase rectifier in which $U_{rec} = 1.17 U_2$. To smooth out this voltage peak, a ballast resistance is connected to the rectifier which ensures a load of the order of 1 per cent, or a special transformer is used to magnetise the balancing coil.

The impedance voltage of transformers operating with the scheme in Fig. 22-15, *a* amounts to 5-8 per cent; the efficiency of the rectifier transformers is somewhat lower and the weight somewhat larger than for power transformers. The other rectifier transformer parts—tanks, covers, control and protection devices, etc.—are of usual design.

22-7. Test Transformers

For testing materials and for various investigations, voltages may be required of the order of 500 to 2,000 kV at normal commercial frequency. The main equipment for generating such voltages are the test transformers¹. The initial test transformer designs, which differ but little from ordinary power transformer designs, were far from satisfactory. Therefore, special test transformer designs were developed, based on the following principles:

- 1) Forced distribution of high voltage throughout the entire high-voltage circuit, owing to which the potentials of the nodal points of the circuit are fixed in respect to the earth;
- 2) The summary voltage is divided between several transformers connected in series or in cascade;
- 3) The so-called isolating transformers are used as auxiliaries;

¹ For impulse tests with voltages up to 10 MV, the so-called impulse generators employing special capacitor circuits are used.

4) The high-voltage winding is designed as a capacitance-type insulator.

The test transformers may be of both oil-immersed and dry type.

The schemes based on the first principle at the present time have no practical importance. The circuits corresponding to the second principle are shown in Fig. 22-16 and 22-17.

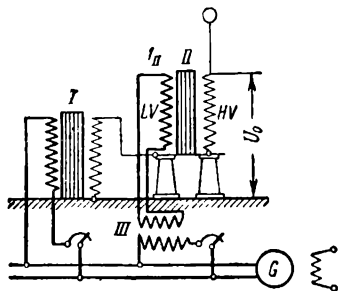


Fig. 22-16. Diagram of test transformer with isolating transformer

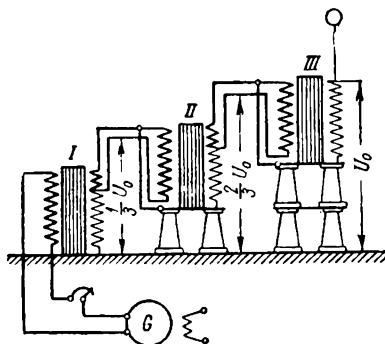


Fig. 22-17. Test transformer diagram with autotransformer type of excitation

The transformers *I* and *II* in Fig. 22-16 are series-connected and each of them is rated at $\frac{U_0}{2}$, half of the total voltage U_0 . The transformer *II* is mounted on insulators which are stressed by a voltage $\frac{U_0}{2}$. In order that the high-voltage winding potential of the transformer *II* be rigidly set in respect to the core of the same transformer, the core and the tank (if it is an oil transformer) are connected to the zero end of the high-voltage winding of the transformer. The excitation of the transformer *II*, the core and tank of which are under potential $\frac{U_0}{2}$ in respect to the earth may be accomplished with the help of the so-called isolating transformer (*III* in Fig. 22-16) with a transformation ratio $k=1$, the insulation between windings of the isolating transformer being calculated for the voltage $\frac{U_0}{2}$. The transformers *I* and *III* are excited by a generator *G*. This principle was used in constructing one of the first installations for 1 MV consisting of three transformers including an isolating transformer.

If the number of series-connected transformers exceeds three, the installation with isolating transformers becomes cumbersome; therefore, at present the principle of cascade excitation of trans-

formers is applied more often, in particular, by connecting them up into an autotransformer scheme (Fig. 22-17). The second and, correspondingly, the third transformer are excited from a part of the high-voltage winding of the preceding transformer (in Fig. 22-17 these winding parts are shown by thick lines). For this purpose, both ends of each exciting winding are led out through a high-voltage insulator to the exciting winding of the subsequent transformer. By using this principle, doubled cascades for voltages up to 2 MV with a grounded middle point may be constructed, the total number of transformers being from four to eight.

However, these cascades have also considerable disadvantages. Since each subsequent transformer obtains energy from the preceding one, the capacity of each of them is different. If, according to the circuit in Fig. 22-17, the capacity of transformer *III* is P , the power of transformer *II* must be $P + P = 2P$, and the power of transformer *I* should be $P + 2P = 3P$; the total installed power is $6P$, whereas the power of the cascade is only $3P$. Besides, with an increased number of stages the total inductance is greatly increased. If, for instance, with one transformer the inductance amounts to 1.25 per cent, with two transformers it is 4 per cent, with three—9 per cent, and with four it amounts to 16.4 per cent. The third disadvantage of a cascade circuit is the non-uniform distribution of impulse voltages throughout the separate stages similar to the distribution of such voltages along the winding of a single transformer. Meanwhile, even routine operation of a cascade (during discharges, etc.) is usually accompanied by over-voltage pulses.

Therefore, some attempts are still being made to construct test transformers for full voltage U_0 in one unit, and such transformers have already been built for voltages up to 1 MV. The transformer is designed similar to the capacitor-type insulators (Fig. 22-18). The high-voltage winding is wound with round wire in one layer onto insulation cylinders. The number of cylinders, their lengths and diameters are so selected that with the end of the winding on the first cylinder of leg *I* connected in series with the beginning of the first cylinder of leg *II*, the end of the first cylinder of leg *II* with the beginning of the second cylinder of leg *I*, and so on, the potential increase from one turn to the other, starting with the

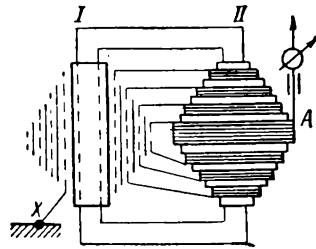


Fig. 22-18. Winding arrangement diagram for test transformer with combined circuit

beginning of the earthed winding of the first cylinder of leg I , should correspond to the distribution of potential according to the winding concentric layer capacitances.

The oil-immersed type of test transformer is relatively bulky and heavy, particularly for high voltages. It is clear that, for instance, the installation in Fig. 22-17 will need a crane to mount and dismount the cascade for maintenance and repairs, and such operations are in this case very labour-consuming.

The important advantage of the dry test transformers is the absence of the extremely bulky and expensive bushings and that, notwithstanding rather large dimensions of the cores and windings, the weight of dry transformers, owing to the absence of tank and oil, is considerably less than the weight of similar oil transformers. If a transformer is made as a capacitance-type transformer, like the one shown in Fig. 22-18, then with a proper design it is dust- and moisture-proof, and the dismantling procedure for repairs is relatively simple. The dry test transformers of the capacitance type may be produced with a voltage up to 1 MV per unit.

22-8. Welding Transformers

Welding transformer may have different designs depending on the nature of the welding operation—arc, butt, seam or spot welding. Here we shall consider transformers for arc welding only.

A welding transformer, the same as a d.c. welding machine, must have a no-load voltage of about 60-70 V sufficient to fire the arc and also a drooping external characteristic. In the simplest case an autotransformer may be used for this purpose, which may give good performance but is unacceptable from the point of view of the welder's safety, since the welder may find himself under full voltage of the power line. Therefore, in practice, the primary in the welding transformers is separated from the secondary windings. For obtaining the requisite external characteristic, welding transformers are provided with a relatively large leakage either in the transformer proper or by adding a separate reactor (Fig. 22-19). The regulation of the welding current may be accomplished: a) in steps, by switching the sections of one or several windings, and b) continuously, by changing the reluctance of the transformer or of the reactor connected to it.

For illustration the data of the CTЭ-34 transformer designed for manual arc welding by the Electric Works is given.

The transformer rated values: $P_n = 30$ kVA, $U_1/U_2 = 220/60$ V, $I_1/I_2 = 147/500$ A, single-phase, 50 c/s, with cycle duration 65 per cent.

The calculation and construction data are as follows: core type; steel E41-05; flux densities: in the leg 1.3 wb/m^2 , in the yoke 1.26 wb/m^2 ; cross-section of the leg—rectangular $93 \times 120 \text{ mm}$; window cycle dimensions: height 274 mm , width 93 mm ; no-load current 3.4 per cent; steel weight 87.5 kg ; e.m.f. per turn 2.98 V ; windings of the cylindrical type, two-layer with a duct between

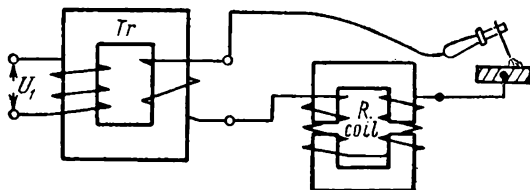


Fig. 22-19. Welding transformer electric diagram for arc welding

the layers; the secondary is of bare copper wire; current densities in the windings with 65 per cent cycle duration: in the primary 2.11 A/mm^2 , in the secondary 3.2 A/mm^2 ; complete winding weight 46.8 kg ; calculated efficiency 93 per cent.

Reactor-regulator: single-phase, 50 c/s, cycle duration 65 per cent, voltage 50 V , e.m.f. per turn 3.57 V , steel E41-05, flux density in the leg 1.18 wb/m^2 , leg dimensions $100 \times 130 \text{ mm}$, cylindrical winding with bare wire $9 \times 12.5 \text{ mm}$, current density 3.48 A/mm^2 .

22-9. Brief Information on Various Types of Transformers

A. Current transformers. The primary of a current transformer consists of one or a small number of turns of relatively large cross-section and is series-connected into the circuit, the current of which is measured (Fig. 22-20). On the contrary, the secondary consists of a great number of turns of relatively small cross-section and is closed through instruments of very small resistance—ammeters, series windings of wattmeters, meters, etc. Thus, the condition, in which a current transformer works, may be regarded practically as a short-circuit condition. For a rated current the flux density in a current transformer core is $B=0.08$ to 0.10 wb/m^2 . Neglecting a very small magnetising current I_0 required for producing such a flux density, $I_1: I_2=w_2: w_1=k$. In reality, however, the current I_0 does exist, and this results first of all in the presence of a "current" error $\Delta_i = \frac{kI_2 - I_1}{I_1} \times 100$ per cent and,

secondly, an angular error, since the current I_0 is shifted in phase with respect to currents I_1 and I_2 .

According to guaranteed error value, current transformers are subdivided into five classes of accuracy, namely 0.2; 0.5; 1; 3 and 10, each class being determined by the value of the maximum current error for the rated current. Current transformers

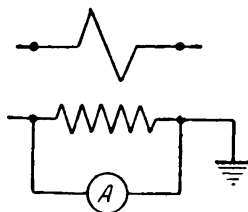


Fig. 22-20. Transformer current diagram

are designed for rated primary currents within the range of 5 to 15,000 A and have, as a rule, a rated secondary current $I_{2n}=5A$ (for indoor installations). Depending on the purpose, the transformers may have various construction features. There are the through-type current transformers resembling in shape a through insulator, the bar-type transformers for large currents with one turn in the primary, the single- or multi-turn laboratory transformers, etc.

For safety the secondary of a transformer must be reliably earthed.

It should be particularly stressed that the secondary must in no case be open while the transformer is switched on for work or be opened during operation. In this case the transformer gets into no-load conditions. The flux density in the steel increases many times compared with the normal value, i. e., up to 1.4-1.8 wb/m² (instead of 0.08-0.1 wb/m²); accordingly the steel losses increase and prolonged operation of the transformer under these conditions inevitably results in core overheating and damaging of the secondary insulation. But the main danger lies in the voltage U_{20} across the open secondary terminals which has abrupt peaks due to a very intense saturation of the steel, owing to which the transformer flux obtains the form of a very flattened curve. The peaks U_{20} in current transformers for large currents reach several thousands of volts and more and are a hazard to the attending personnel. From this it may be seen how important it is to keep the transformer secondary closed on itself or on the instruments.

B. Voltage transformers. The operating conditions of voltage transformers correspond to transformer operating on no-load. The rated secondary voltages of the voltage transformers must be equal to 100, $100/\sqrt{3}$ or $100/3V$, according to the State Standard 1988-43. To keep the permissible transformer error within certain limits, the transformer magnetising current should be limited. For this purpose, the transformer is made of a high-grade and relatively lightly saturated steel ($B \leq 0.6$ to 0.8 wb/m²).

According to permissible error value, voltage transformers are divided into four accuracy classes: 0.2, 0.5, 1 and 3 and are made both in the form of single-phase transformers for rated capacities up to 1,000 VA and in the form of three-phase transformers for capacities up to several kVA.

The design of the voltage transformers manufactured by the Moscow Transformer Works has recently been radically altered. In the new design, shell-type cores and the concentric layer windings of enameled wire are used.

As a result, it became possible to considerably decrease both the weight and dimensions of the transformers. Thus, for instance, the total weight of a single-phase oil-type voltage transformer for 6 kV was reduced from 38.8 to 23 kg, i. e., by 40.5 per cent; for the 35 kV type the weight was reduced from 385 to 230 kg, i. e., by 40 per cent.

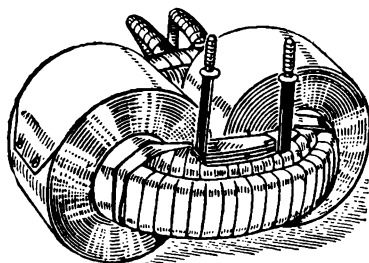


Fig. 22-21. Transformer with wound core

C. Transformers with wound core. A shell-type transformer with a core wound of a cold-rolled steel is shown in Fig. 22-21. Such transformers give a saving in materials by about 15-20 per cent, owing to the absence or to a significant decrease in air-gaps and to a great reduction in steel wastes. The wound-core transformers are manufactured for capacities up to 500 kVA only in the single-phase version, since the three-phase version offers great constructional difficulties.

D. Flame-proof and explosion-proof transformers. The ordinary transformer oil is inflammable, but its vapours mixed with air may produce explosive mixtures. Therefore flame- and explosion-proof transformers became necessary.

The problem allows several solutions. One of them is filling of the tank with a non-inflammable and non-explosive oil. In 1935 in the U.S.S.R. Electrotechnical Institute a liquid non-inflammable dielectric *sovol* was developed; some time later there appeared the less viscous *sovtol*. In 1938 the Moscow Transformer Works manufactured an experimental model of a transformer filled with *sovtol*. Unfortunately, the disadvantages inherent in the *sovtol* (see § 12-5, E) prevented its wide application.

The second possible solution of the same problem is the dry transformer. Absence of oil and the oil installation is its valuable

advantage, but the cooling and insulation conditions are in this case more difficult than with an oil transformer. Great progress was made in the design of efficient dry transformers using cold-rolled steel and heat-resistant insulating varnishes. Thus, for example, while a dry transformer with a 50 kVA capacity in 1938 weighed 557 kg, in 1942 it weighed already 263 kg and in 1944 only 205 kg. At present dry transformers are being manufactured for capacities up to 4,000 kVA and operating voltages up to 15 kV.

The winding copper is covered by glass-fibre or asbestos insulation with a special varnish which can endure continuously 160°C. Each winding is separately impregnated with the heat-resistant varnish and is baked at a high temperature; besides, the entire immersed part of the transformer is impregnated and baked. An average (in resistance) winding overheat of 80°C is permissible, and the temperature of a winding hot spot should not exceed 140-155° at an ambient temperature of 40°C.

The third possible solution of the flame- and explosion-proof transformer problem is an oil-filled transformer, where an inert gas under normal pressure is introduced above the oil. Research has shown that to prevent the oxidation of the transformer oil and the insulation by oxygen dissolved in the oil it is sufficient to use nitrogen. After suitable treatment, the oxygen content in the oil is reduced to a fraction of one per cent, and in service when reliable packings and moisture- and oxygen-absorbing filters are used it does not exceed 1 per cent. The reduction of the oxygen content to 3 per cent makes these transformers flame- and explosion-proof, though they still need supervision and maintenance.

The further development of this type of transformer is the compressed gas transformers, i. e., the transformers with tanks filled only with gas under certain pressure. It is recommended to use either nitrogen or carbon dioxide under pressures up to 40 atm. The main advantage of such transformers is that they may be built for temperatures considerably exceeding ordinary temperatures of the core and winding (300-325°C for the former and 200°C for the latter) if high heat-resistant insulation materials are used. In this case transformer dimensions are reduced to 75 per cent, particularly when higher frequencies of the order of 600-1,200 c/s are used.

TABLE OF SYMBOLS

ENGLISH LETTER SYMBOLS

A

A	Armature loading
At	Ampere-turns
a	Number of armature current paths
a	Turn operator of symmetrical component
a	Displacement of pole axis
$2a$	Number of path pairs
av	Average (quantity)

B

B	Magnetic flux density
B	Maximum flux density
B	Flux density in the air gap
B_a	Flux density in armature core
B_{ax}	Flux density under pole shoe
B_k	Flux density in commutation zone
B_m	Flux density in pole core with pole shoe
B_{sec}	Flux density in section
B_t	Flux density in teeth
$B_{t \cdot av}$	Flux density in tooth
B_x	Flux density in tube path
B_x	Flux density in given section x
B_y	Flux density in yoke
B_1	Flux density under leading pole tip
B_2	Flux density under trailing pole tip
b	Width of pole
b_{add}, b_d	Width of commutating pole shoe
b_b	Width of ventilation duct
b_{br}	Width of brush

b_c	Part of winding over armature periphery
b_c	Width of commutator bar or segment
b_{cz}	Commutation zone dimension
b_o	Slot width
b_{lt}	Width of tooth top over armature periphery
b_x	Average width of tube path
b_1 and b_2	Width of primary and secondary

C

C	Constant depending on oil grade and bearing clearance
C	Capacitance
C_{av}	Average length of turn of the windings
C_e	Machine constant $= p \frac{N}{a}$
C_{earth}	Capacitance to earth
C_{edd}	Constant depending on steel grade and sheet thickness
C_h	Constant depending on steel grade
C_{in}	Input capacitance
C_m	Machine constant $= \frac{P N}{2 a}$
C'	Constant in friction formula
C_{1av}, C_{2av}	Average length of primary or secondary turn
C	Screen
C_s	Shielding screen

D

D_a	Armature diameter
d_{jour}	Diameter of journal
D_c, D_{com}	Commutator diameter
D_2	Internal diameter of secondary winding

E

E	Effective value of electromotive force
-----	--

E	Constant e.m.f.
E_{mc}	E.M.F. amplitude
E_a	E.M.F. at machine terminals
E_a^1	E.M.F. of branch (path)
$E_{a.m}$	Motor counter e.m.f.
E_{1sh}	Primary short-circuit e.m.f.
$E_{s.ph}$	Single phase e.m.f.
$E_1 \left\{ \right.$	E.M.F. of armature winding paths
$E_2 \left\{ \right.$	
E_{tm}	E.M.F. per turn
E_2^1	Secondary leakage e.m.f. reduced or referred to primary
E_{2sh}^1	Secondary short-circuit e.m.f. reduced or referred to primary
e	Instantaneous e.m.f.
e_a	E.M.F. induced in coil section prior to commutation
e_{aq}	E.M.F. of coil section due to cross armature field
e_c	Commutation e.m.f.
e_{edd}	Eddy e.m.f.
e_L	Self induction e.m.f.
e_M	Mutual induction e.m.f.
e_o	Remaining e.m.f.
e_r	Reactive e.m.f.

F

F	Effective value of magneto-motive force
F_a	Armature m.m.f.
F_{ad}	Armature direct axis m.m.f.
F_{aq}	Armature square axis m.m.f.
F_{ax}	M.M.F. along path at distance from mid-line
F_{exc}	M.M.F. of one pole
F_{jour}	Full pressure on journal
F_m	Magnet m.m.f.
F_o	Fundamental or main m.m.f.
$F\delta_o$	Gap m.m.f. for smooth armature
$F\delta_{com.p.}$	M.M.F. per pair of poles for flux between commut. pole and armature

F_1, F_2	Teeth m.m.f.
F_{sto}	Gap and tooth m.m.f. in axial plane of pole
F_{stt}	Gap and tooth m.m.f. in plane x
F_y	Yoke m.m.f.
f	Frequency of magnetic reversals
f	Frequency of power circuit
f	Frequency of a periodic function
f_{br}	Unit pressure on brush
f_{jour}	Unit pressure on journal
f_t	Tooth fluctuation frequency
F_δ	Gap m.m.f.
f_x	Electromagnetic mutual action force

G

G_{ac}	Mass (weight) of armature copper
G_c	Mass (weight) of part of machine
G_{ca}	Mass (weight) of armature core
G_{tc}	Mass (weight) of tooth

H

H	Magnetic field intensity or magnetising force
H	Pressure, mm water column
H_δ	Air gap magnetising force
H_μ	Magnetising force for pole with pole shoe
H_a	Armature core magnetising force
H_{ax}	Armature core magnetising force under pole
H_c	Coercive force
H_{sec}	Magnetising force for section
H_{sx}	Field intensity in given slot cross-section
H_t	Teeth magnetising force
H_y	Yoke magnetising force
h_a	Height of armature core
h_e	Coil height

h_c	Conductor height
h_{c-cr}	Conductor height, critical
h_{exc}	Height of pole core
h_m	Height of magnet
h_t	Height of tooth
h_w	Height of winding

I

I	Effective value of current
I	Current delivered by generator to power circuit
I_a	Current to power circuit or received from circuit
I_a^1	Armature current after introduction of rheostat
I_{a1}, I_{b1}, I_{c1}	Positive sequence currents
I_{a2}, I_{b2}, I_{c2}	Negative sequence currents
I_{a0}, I_{b0}, I_{c0}	Zero sequence currents
I_{0s}	Zero sequence current
$\dot{I}_{A0}, \dot{I}_{B0}, \dot{I}_{C0}$	Zero system of current vectors
I_c	Control current
I_c, I_{arc}, I_y	Circulating current
I_f	Additional excitation or feed current
I_h	Hour rating current
I_l	Line current
I_n	Rated (nominal) current
I_0	No-load current, magnetising current
I_{0a}	Effective value of active no-load component
I_{rec}	Rectified current
I_{ph}	Phase current
I_{sh}	Short-circuit current
I_{sh0}	Short-circuit current when $i_{exc}=0$
I_{start}	Starting current
I_1, I_2	Currents in primary and secondary
\dot{I}_{1s}	Current (vector) creating leakage flux
I_2^1	Current reduced or referred to primary
I_2^1	Load current
$I_{0A3}, I_{0B3}, I_{0C3}$	A, B, C third harmonic

I_{load1}, I_{load2}	Load currents
I_{0u}	Effective value of magnetising component
i	Current in section undergoing commutation
i	Rms value of momentary load current
i	Instantaneous current
i_a	Current in one path
i_c	Additional commutation current
i_{edd}	Eddy current
i_{exc}	Excitation (field) current
i_0	Magnetising current
i_{0m}	Amplitude of starting current
$i_{0\mu}$	Magnetising current
i_{sh}	Current in shunt
$i_{sh.c}$	Additional commutation current when short-circuited loop is opened
$i_1 \}$	Current in windings (primary and secondary)
$i_2 \}$	
i_{03}	No-load current third harmonic
$i_{0A3}, i_{0B3}, i_{0C3}$	No-load current in legs

J

j	Current density
j	Effective value of current density
j_{br}, j_{br2}	Current densities under leading and trailing parts of brush
j	$= \sqrt{-1}$

K

K	Number of commutator divisions (bars or segments)
k	Transformation ratio
k	Average transformation ratio of two parallel working transformers
k_a	Transformation ratio of autotransformer
k_{am}	Amplidyne (power) amplification factor
k_c	Stacking factor
k_f	Coefficient of friction

k_{leg}	Factor indicating part of rated capacity per leg
k_{load}	Load factor = $\frac{P_s}{P_n}$
k_{reg}	Regulation coefficient
k_{tx}	Tooth geometry factor
k_T	Transformer utility factor
k_u	Factor taking into account increase of e.m.f. under poles
K_v	Ventilation coefficient
K_v^1	External ventilator coefficient
Δk	Per cent difference of transformation ratios
k_a	Main pole leakage factor
k_a	Coefficient of reducing winding height to calculation length of leakage field lines
$k_{\delta cp}$	Commutating pole air-gap factor
K_μ	Saturation factor

L

L	Leakage inductance
L	Self-inductance
L_a	Average length of magnetic path in armature
L_b^1	Inductance for width b_s of winding
L_{exc}	Inductance of excitation circuit
L_r	Resultant inductance of coil section
L_s	Inductance of section undergoing commutation
L_s	Self-inductance of coil section undergoing commutation
L_{sc}, L_{sh}	Short-circuit inductance
L_ψ^1	Winding inductance
L_v	Length of magnetic path in yoke
$L_{\sigma 1}, L_{\sigma 2}$	Leakage inductances
l	Armature stack length
l^1	Calculated armature length
l_a	Full armature length
l_{br}	Brush length in machine axial direction

l_{con}	Part of a conductor length cutting through lines of commutating field
l_{con}	Length of half-turn of winding
l_{end}	Overhang, length of end connection
l_{jour}	Length of journal
l_m	Length of pole, axial
l_{tx}	Length of tooth in given section x
l_o^1	Calculated length of leakage tube

M

M	Mutual inductance
M_a	Electromagnetic torque (braking torque)
M_g	Electrical torque
M_j	Motor dynamic torque
M_r	Resistance torque (moment) at shaft
M_{start}	Starting torque
M_o	{ Braking torque for no load (no-load torque of motor)
M_x	
	Electromagnetic torque of conductor
M_1	Torque created by prime-mover at generator shaft
M_2	Useful braking torque
m_o	Number of leakage flux unit tubes

N

N	Number of winding turns
n	Speed, revolutions per minute
n	Number of winding elements (coils)
n_b	Number of ventilation ducts
n_h	One-hour duty speed (r.p.m.)
n_{max}	Maximum r.p.m.
n_{min}	Minimum r.p.m.
n_n	Rated (nominal) speed (r.p.m.)
n_o	No-load speed rotation
n_{∞}	Continuous duty speed (r.p.m.)

Δn_n	Rated (nominal) change of speed (r.p.m.)
P	
P	Power; average power
P_a	Electromagnetic power
$P_{cop,a}$	Losses in armature copper
P_{cop1}, P_{cop2}	Copper losses in primary and secondary
P_e	Electric power
P_{exc}	Power covering excitation losses
P_h	One-hour rating
P_m	Capacity of the m-th transformer in parallel
P_{mech}	Power covering mechanical losses
P_n	Rated (nominal) transformer capacity
P_o	No-load power covering no-load losses
P_{sh}	Short-circuit power
P_{st}	Total losses in steel
P_T	Typical power of transformer = $U_{rec} I_{rec}$
P_{∞}	Continuous rating
P_1	Input
P_2	Output
p	Number of pairs of poles
p_{ad}	Additional losses in steel and copper
p_{add-o}	Additional no-load losses
p_{bear}	Friction bearing losses
p_{br}	Losses in brush contact
$p_{c,a}$	Losses in core of armature
$p_{cop,m}$	Main copper losses
p_{cw}	Losses in winding copper
p_{edd}	Eddy current losses
p_{exc}	Excitation (field) losses
p_{f-br}	Brush friction losses
p_h	Hysteresis loss
p_{mech}	Total mechanical losses
p_s	Losses in armature steel
p_{ta}	Losses in armature teeth
p_v	Ventilation losses
$2p$	Number of poles
R	
R	Resistance
R_e	Resistance of external circuit

R_{load}	Load resistance
R_{reg}	Resistance in series motor
R_{μ}	Reluctance of (magnetic) circuit
$R_{\mu cp}$	Commutating pole reluctance
$R_{\mu \delta}$	Reluctance to commutating flux Φ_c in gap under pole
$R_{\mu \sigma}$	Reluctance to leakage flux
r	Radius
r_a	Resistance of armature path winding
r_{am}	Resistance of armature series-connected windings
r_{br}	Resistance of brush contact
r_{br1}, r_{br2}	Resistance of brush contacts with bars 1 + 2
r_{exc}	Resistance of excitation circuit
r_m	Active resistance of magnetising circuit
r_{os}	Zero-sequence resistance
r_{reg}	Regulation resistance
r_s	Resistance of coil section
r_{sh}	Short-circuit resistance
$r_{sh.a}$	Short-circuit resistance of autotransformer
r_w	Resistance of connection wires
r_1, r_2	Active resistances of primary and secondary
r_2^1	Active secondary resistance reduced (referred) to primary
S	
S	Number of coil sections
S	Area
S_a	Cross-section area of armature core
S_{br}	Surface area of brush
S_{br1}	Surface area of parts of brushes leading on to bar 1 and trailing off bar 2
S_{br2}	
S_c	Cross-section area of conductor
S_m	Cross-section area of pole with shoe

S_s	Cross-section of slot
S_t	Cross-section area of tooth belt or teeth
S_{set}	Cross-section of path
S_{tx}	Cross-section of tooth at x
S_y	Cross-section area of yoke
S_δ	Cross-section area of air gap

T

T	Time constant
T	Period (time) of commutation or period during which coil undergoes commutation
T'	Actual commutation period
T_n	Period during which coil undergoing commutation moves to adjacent brush
t	Tooth width
t_{st}	Starting period of motor
t_1	Tooth pitch over armature periphery

U

U	Voltage across generator terminals
U_n	Rated (nominal) voltage
U	Voltage between two adjacent brushes of different polarity
U_{exc}	Voltage across field terminals
U_l	Line voltage
$U_{n.ph}$	Rated phase voltage
$U_{os.ph}$	Zero-sequence phase voltage
U_{ph}	Phase voltage
U_{rec}	Rectified voltage
U_{sh}	Impedance voltage
$U_{sh.n}$	Rated (nominal) impedance voltage
U_o	Generator voltage at no load
U_{oo}	Generator terminal voltage at no-load and when $i_{exc}=0$
U_1, U_2	Voltage across brushes

U_1, U_2	Primary and secondary voltages
U_{1sh}	Voltage delivered to short-circuited transformer
U_{2m}, U_{1m}	Voltage amplitude (primary and secondary)
ΔU	Voltage difference
ΔU_{br}	Contact voltage drop per pair of brushes
u	Number of section sides in slot
u_o	Alternating voltage at shunt generator terminals
u_{sh}	Per cent impedance voltage
$u_{shy}, u_{sh.a}, u_{shx}$	Per cent components of impedance voltage
u_{max}	Maximum voltage between two adjacent commutator segments

V

V	Quantity of cooling air
v	Speed or rotation
v_a	Speed at armature periphery
v_c	Speed at commutator periphery
v_{jour}	Speed at journal periphery

W

w	Number of turns
w_c	Number of turns of coil section

X

X	Reactance
X_o	Open circuit or no-load reactance
X_{os}	Zero-sequence reactance
X_{sh}	Short-circuit reactance
$X_{sh.a}$	Short-circuit inductance of autotransformer
x	Distance
x_m	Reactance of magnetising circuit

x_1, x_2	Leakage inductance resistance of primary and secondary
------------	--

Y

y	Winding pitch
y_c	Commutator pitch
$y_c \text{ tap}, Y_c \text{ tap}$	Commutator pitch lap winding
y_{cw}	Commutator pitch wave winding
y_p	Potential pitch
y_1	Front pitch
y_2	Back pitch
y_{2l}, y_{1l}	Back and front pitch, lap winding
y_{2w}, y_{1w}	Back and front pitch, wave winding

Z

Z	Impedance
Z_c	Circuit impedance
Z_e	Number of elementary slots
Z_e	Equivalent circuit impedance
Z_m	Impedance of magnetising circuit
Z_{0s}	Zero-sequence impedance
Z_{sh}	Transformer short-circuit impedance
Z_2	Secondary impedance
Z_2^1	Secondary impedance reduced (referred) to the primary

GREEK LETTER SYMBOLS

α	Experimental power index for flux density
α	Angular displacement
α	Temperature coefficient of copper
α'	Calculated pole arc factor
β	Power index for alloyed steel
β	Angle of brush shift

γ	Slot relation factor
γ_c	Specific gravity of copper
Δ	Sheet steel thickness
δ_{av}	Air-gap between armature and commutating pole
δ	Air-gap length
δ_x	Average length of path tube
δ'	Calculated air gap
ε	Part of winding pitch
η	Efficiency of machine
η_v	Ventilator efficiency
v_a	Armature winding temperature
v_{jour}	Bearing temperature °C
v_o	Temperature
λ	Instantaneous flux linkages
λ_{end}	Permeance of end connections
λ_s	Permeance of slot
λ_t	Permeance of tooth
λ_{tube}	Magnetic permeance of tube path
λ_1	Equivalent specific permeance of coil section
λ	Effective value of flux linkages
λ_1	Square axis permeance
λ_2	Direct axis permeance
μ	Permeability
μ_a	Permeability of armature
μ_o	Permeability of free space
μ_{sec}	Permeability of path section
μ_t	Permeability of tooth
μ_y	Permeability of yoke
δ''	Reduced width of gap between windings
v	Order of harmonic
π	Ratio of circumference to circle diameter
δ_{12}	Gap width between windings
ρ	Volume resistivity
ρ_{15}	Volume resistivity at 15°C
σ	Factor used in determination of equivalent air-gap length
σ	Leakage coefficient
σ_{edd}	Eddy losses leakage coefficient
σ_h	Losses leakage coefficient
Σ	Summation sign

Σ	Total losses in machine
τ	Pole pitch
Φ	Main (fundamental) magnetic flux
Φ	Magnetic flux; useful magnetic flux
Φ_c	Control flux
$d\Phi$	Elementary tube flux
Φ_c	Commutating flux in gap under commutating pole
Φ_{cp}	Flux through commutating pole core
Φ_{free}, Φ_{fr}	Free transient flux
Φ_m	Total flux
Φ_m	Magnetic flux amplitude
Φ_m	Flux amplitude, steady state
Φ_0	Main, fundamental or total flux
Φ_{os}	Zero-sequence flux
Φ_{rem}	Remanent magnetisation flux
Φ_{sec}	Flux in section
Φ_{resid}	Residual flux
Φ_{st}	Steady state flux
Φ_{sx}	Flux through slot section x
Φ_t	Total flux of tooth and slot
Φ_t	Transformer flux
Φ_{tube}	Elementary tube flux
Φ_{tx}	Flux through tooth section x
Φ_y	Flux through yoke
Φ_3	Leakage flux
$\Phi_{\sigma 1}$	Leakage flux between poles
$\Phi_{\sigma 2}$	Leakage flux of pole sides
φ	Displacement angle between phase current and voltage
φ_1	Angle between vectors U_1 and I_1
Ψ_{sh}	Short-circuit phase flux linkage
Ψ_{10}, Ψ_{20}	Flux linkages
ω	Angular frequency
$\omega = 2\pi n$	Angular rotation speed

OTHER SYMBOLS

 \vec{A}
 I Vector A
Vector

\equiv	Identically equal to;
	equal by definition
\approx	Approximately equal to
∞	Infinity; continuous rating

UNIT SYSTEM

The following units are given for reference since they are often used in various text-books

Length, mass, time	metre, kilogram, second	m, kg, s
Area, volume	sq. metre, cu metre	m ² , m ³
Density	kilogram per cu metre	kg/m ³
Work and energy	metre-newton=joule	m-N, J
Power	joule per sec=watt	W
Torque	newton-metre	N-m
Pressure	newton per sq. metre	N/m ²
Angle	radian	rad
Velocity: angular	radian per sec	rad/s
linear	metre per sec	m/s
Rotational speed	revolution per sec	r.p.s.
Inertia	kilogram-sq. metre	kg-m ²
Temperature	degree centigrade	°C
Thermal resistivity	watt per metre	
	per sq. metre per	
	deg. C thermal	Ω
Resistivity	ohm per metre	
	per sq. metre	Ω -m
Magnetic flux, linkage	weber, weber-turn	Wb, Wb-T
Magnetic flux-density	weber per sq. metre	Wb/m ²
Magnetomotive force	ampere-turn	AT
Magnetising force	amp.-turn per metre	AT./m
Reluctance	amp.-turn per weber	AT./Wb
Permeance	weber per amp.-turn	Wb./AT
Permeability (abs)	weber per sq. meter	
	per amp.-turn per	
	metre	H./m
Specific magnetic	weber per sq. metre	Wb/m ²
loading		
Specific electric	amp.-conductors per	
loading	metre	AC./m
Current density	amp. per sq. metre	A/m ²

INDEX

A

Active parts, 83
 Additional active resistance, 181
 Additional excitation, 189
 Additional losses, 193
 Additional losses in copper, 366
 Additional no-load losses, 334
 Air-blast cooling, 312
 Air-gap, 37, 45, 47
 Amplidyne, 274, 285
 control winding, 291
 external characteristic, 291
 output, 292
 stability, 290
 time-constants, 289
 Amplification factor, 287
 Analysis of commutation process, 147
 Angle
 electrical, 69
 magnetic lag, 333
 Aperiodic waves, 424
 Arc, commutation, 164
 Armature, 39
 core, 46
 drum-wound, 83
 specific loading, 131
 reaction, 130
 demagnetising reaction, 269
 direct-axis reaction, 134
 quadrature reaction, 134
 slotted drum-type, 39
 smooth, 48
 winding, 39
 Autotransformer 300, 437
 impedance voltage, 440
 no-load performance, 437
 transformation ratio, 438

B

Baffle plate, 181
 Bank, three-phase transformer, 341

Braking

 dynamic, 263
 regenerative, 260
 torque, 209

Bridge circuit, 457

Brush

 characteristics, 181
 carbon-graphite, 186
 contact phenomenon, 167
 contact resistance, 181
 electrographitised, 186
 friction coefficient, 183
 grades, 182
 potential curves, 188
 pressure, 182
 rocker, 41
 yoke, 39, 41

Brushgear, 41

Brush-holder, 40

Brush-holder stud, 42

Bucking, 163

Bushing, oil-filled, 314

Butt commutator, 40

C

Calculated air-gap, 52
 Calculated armature length, 51
 Calculated flux density, 55
 Calculated values, 51
 Calculation of mechanical stresses, 422
 Calculated pole arc coefficient, 50
 Capacitive protection, 434
 Capacitance, input, 426
 Cascade excitation of transformer, 465
 Cathode polarisation of commutator, 168
 Characteristic
 calculated no-load, 213

- compound generator load, 229
 - drooping, 233, 251
 - external, 212, 224
 - impedance, 426
 - internal, 217
 - internal load, 215
 - free-running, 258
 - load, 212, 224
 - magnetisation, 213
 - no-load, 212, 224
 - practical regulation, 218
 - regulation, 212, 218
 - short-circuit, 219
 - speed, 253
 - start equation, 245
 - triangle, 215
 - Characteristics, 211
 - mechanical, 243
 - shunt motor performance, 249
 - shunt motor speed, 251
 - starting, 243
 - Circulating current, 114, 405
 - Class of commutation, 143
 - Classic theory of commutation, 165
 - Classification of motors, 238
 - Clock method of angle designation, 350
 - Coefficient of transformation, 318
 - Coefficient of air-gap, 52
 - Coil
 - bottom layer, 84
 - section, 65
 - ring-type, 68
 - Commutating e.m.f., 146, 155, 172
 - Commutating poles, 38, 171
 - Commutating poles, saturated, 176
 - Commutation, 143
 - accelerated, 150
 - adjustment, 180
 - analysis of process, 147
 - arc, 164
 - armature reaction, 159
 - class of commutation, 143
 - ionic, 168
 - non-sparking, 165
 - period, 165
 - retarded, 150
 - zone, 157, 173
 - Commutator, 39
 - bar, 65
 - butt-type, 40
 - cathode polarisation, 168
 - Commutator
 - disk type, 40
 - divided, 40
 - division, 65
 - double, 40
 - flashover, 163
 - function, 35
 - potential curve, 163
 - Compensation winding, 177
 - Components of torque, 242
 - Compound generator, 228
 - Compound generator, connecting for parallel operation, 236
 - Compound motor, performance characteristics of, 255
 - Conditions for parallel operation, 232
 - Conditions of self-excitation, 222
 - Conditions of symmetry, 113
 - Connection
 - differential, 231
 - for parallel operation, 232
 - Open-delta, 401
 - star-double, zig-zag, 459
 - star-star, 353
 - two inverse stars, 461
 - Contact brush resistance, 181
 - Contact drop potential, 181
 - Coordinators, 433
 - Copper losses, 366
 - Critical resistance, 223
 - Cross-section, 36
 - Cumulative connection, 231
 - Current
 - circulating, 115, 408
 - commutation, 145
 - load, 408
 - specific loading, 58
 - path, 73
 - pulsating, 35
 - rated, 42
 - Curves, brush potential, 188
 - Cycle, 34
- D**
- Dead coils, 104
 - Degree of sparking, 144
 - Differential connection, 231
 - Distortion of main field, 164
 - Distribution of load, 234
 - Drooping external characteristic, 233
 - Drooping speed characteristic, 251
 - Dust zone, 186

E

Efficiency, motor, 252, 255
 Electrical degree, 69
 Electrical radian, 69
 Electrical wear of commutator, 167
 Electromagnetic power, 207
 Elementary slot, 89
 Elementary tube, 45
 Effect of brush width, 158
 E.M.F.
 commutating, 155
 construction of star and poly-
 gon, 98
 creation of, 33
 harmonics, 342
 induced in conductor, 33
 mutual inductance, 146
 pulsating, 35
 pulsations, 37
 reactive, 170
 resultant, 72
 ring armature, 81
 self-induction, 146
 star, 78
 winding, 76
 End of winding, 341
 Energy conversion, 207
 End connections, 83
 Equaliser
 conductor, 235
 design, 123
 equaliser of the second type, 120
 equaliser of the first type, 114
 Equation, e.m.f. equilibrium, 317
 Equation for motor E.M.F., 239
 Equation of equilibrium, 240
 Equipotential surfaces, 48
 Equivalent circuit, T-type, 325
 Equivalent circuit of transformer,
 323
 Equivalent transformer, 323
 Equivalent transformer, vector dia-
 grams, 378
 Evaluation of sparking, 143
 Exhaust pipe, 313
 Excitation, additional, 189
 Exciter, 284
 Experimental adjustment of com-
 mutation, 180
 External characteristic, 216
 External characteristic of series gen-
 erator, 228
 External characteristic of shunt
 generator, 225

F

Field
 coil, 38
 cumulative connection of field
 windings, 231
 main, 38
 map, 49
 poles, main, 37
 Finish of coil section, 65
 flashing, 163
 flashover barriers, 181
 Flux
 commutating, 178
 density, air-gap, 47
 density, calculated, 49
 density, trapezoidal, 50
 linkages, 153
 main, 43
 steady-state, 414
 Fractional pitch, 84
 Frame, 38
 Frame, solid, 38
 Free short-circuit current, 418
 Frequency, 34
 Fundamental characteristics, 212

G

Gap coefficient, 52
 Gas relay, 313
 Generator
 differentially compounded, 228
 e.m.f., 208
 excited, 206
 generator-motor system, 275
 self-excited, 206
 separately excited, 206
 series, 227
 welding, 283
 Geometrical addition of vectors, 94
 Geometrical subtraction of e.m.f.
 vectors, 94
 Group of equalisers, 117

H

Half-coils, 87
 Hard external characteristic, 233
 Harmonic, fundamental, 34
 High-speed automatic breaker, 181
 Hyperbolic mechanical characteris-
 tic, 260
 Hyperbolic nature of characteris-
 tic, 254

- I**
- Impedance
 - characteristic, 426
 - reduced, 322
 - zero sequence, 391
 - Indirect methods of efficiency determination, 384
 - Improving commutation, 171
 - Induction regulator, 300
 - Inductive shunt, 180
 - Insulating screens, 181
 - Interleaved core, assembly, 304
 - Ionic processes, 167
 - Ionisation, 164
 - Ionisation of contact, 168
- K**
- Knee of no-load, 213
- L**
- Leakage
 - coefficient, 43
 - determination, 368
 - e.m.f., 319
 - flux, 43
 - flux, primary, 316
 - flux, secondary, 316
 - inductance of sandwich winding, 373
 - reactance calculation, 369
 - reduced reactance, 322
 - total, 59
 - Leg, cross-section, 305
 - Leonard-Ilgner system, 273
 - Lightning-proof transformer, 434
 - Limit of self-excitation, 222
 - Linear commutation, 148
 - Load, rated, 42
 - Losses
 - additional 193, 203
 - brush friction, 196
 - copper, 366
 - core, 197
 - eddy current, 198
 - field, 202
 - hysteresis, 197
 - losses in antifriction bearings, 195
 - losses in friction bearings, 194
 - losses in steel, 200
 - losses in armature copper, 201
 - no-load additional losses, 334
 - total, 204
 - total losses in steel, 199
 - ventilation, 196
- M**
- Machine
 - high-voltage, 280
 - homopolar, 282
 - low voltage, 280
 - Magnetic circuit, 45
 - Magnetic circuit, basic law, 45
 - Magnetic flux, 43
 - Magnetic flux, useful, 82
 - Magnetic permeability, 45
 - Magnetic permeance, 48
 - Magnetic saturated circuit, 137
 - Magnetic tubes, unit, 47
 - Magnetisation curve, 61, 416
 - Magnetisation curve, ascending branch, 213
 - Magnetisation curve, descending branch, 213
 - Magnetising current, 330
 - Magnetising current, first harmonic component, 331
 - Main losses in core, 334
 - Mapping, 47
 - field leakage, 369
 - reduced, 373
 - Mechanical stresses, 420
 - Mechanical stresses between conductors, 420
 - Mechanical wear of brushes, 167
 - Mechanical wear of commutator, 167
 - Method of superposition, 130, 407
 - Mitigating sparking, 168
 - M.M.F.
 - of air-gap, 51
 - non-compensated, 178
 - Motor
 - torque equation, 241
 - rolling mill, 281
 - multiple closed winding, 65
 - negative current system, 387
- N**
- Neutral
 - geometrical, 33
 - mechanical, 33
 - physical, 137

No-load operation of transformer, 326
 No-load test, 337
 Non-resonating transformers, 434
 Non-symmetry of flux, 119
 Non-symmetry of voltage distribution, 121
 Normal machines, 276

O

Oil
 oil-expansion chamber, 313
 tank, 310
 transformer, 313
 Open delta, 401
 Overcurrent, 414
 Overvoltage, 423, 424, 426
 wave, 426
 transformer protection, 433

P

Parameter, short-circuit, 367
 Partial capacitive protection, 435
 Parallel operation of generators, 231
 Paths, 73
 Periodic waves, 424
 Permanent magnet machines, 295
 Permeance, equivalent specific, 153
 Permeance, specific, 153
 Permeances, method of
 adding specific, 156
 Phenomenon, leakage, 368
 Pigtail, brush, 40
 Pipe radiator, 312
 Pitch
 back, 90, 107
 commutator, 65, 90
 front winding, 89
 potential, 116
 winding, 90
 Plugging, 261
 Plotting of external characteristic, 226
 Pole arc, calculated, 50
 Pole shoe, 38
 Polygon, e.m.f., 73
 Positive system, 387
 Potential over the commutator, 161
 Power
 amplification factor, 287
 electromagnetic, 207

 no-load, 335
 short-circuit, 385
 typical, 454
 Processes during overvoltage, 426
 Property of series motor, 254
 Pulsation of voltage, 74

R

Radian, electrical, 69
 Radiator system, 312
 Rated capacity, 42
 Rated change in speed, 251
 Rated performance, 42
 Rated power of transformer, 301
 Rated voltage variation, 216
 Rated transformer voltage, 301
 Rating, 42
 continuous, 277
 one-hour, 277
 Rectangular front wave, 426
 Rectifier secondary power, 454
 transformer, rectifier, 454
 Rectification alternating current, 35
 Redistribution of load, 235
 Reduced conditions, 50
 Reduced secondary resistance, 321
 Reduced secondary current, 321
 Reduced winding, 321
 Reduction method, 49
 Reflection of wave, 427
 Regulation factor, 271
 Reluctance, 45
 Requirements of symmetry, 117
 Resistance, additional active, 181
 resistance commutation, 147
 Rheostat, speed regulation, 265
 Right-hand rule, 34
 winding, 85
 Riser, 40

S

Saturation of generator circuit, 214
 Saturation coefficient, 61
 Self-excitation of generator, 222
 Series connection of generators, 231
 Series motors, performance characteristics, 253
 Shenfer converter, 293
 Shield bearings, 39
 Shield, frame-head, 39
 Shielding screen, 435

- Shifting of brush, 169
 Short-chord winding, 84
 Short-circuit
 parameters of transformer, 362
 single-phase, 394
 symmetrical, 368
 test, 360
 triangle, 364
 unbalanced, 386
 Shunt motor, mechanical
 characteristics of, 257
 Shunting the armature winding, 272
 Sine-wave, equivalent, 333
 Slot damper, 169
 Soft characteristic, 254
 Coil section undergoing commutation, 146
 Speed characteristic, drooping, 256
 Speed formula for shunt motor, 253
 Speed regulation, 264
 Speed regulation by shunting the field, 270
 Speed regulation by varying circuit voltage, 273
 Speed regulation by varying excitation, 267
 Speed, runaway, 254
 Stability conditions for drive, 256
 Start of winding, 65
 Start, non-rheostatic, 244
 Starting by generator-motor connection, 249
 Starting by subdividing the voltage, 249
 Starting current, 243
 Starting d.c. motors, 244
 Starting rheostat, 247
 Static torque of resistance, 241
 Steady-state short-circuit current, 418
 Steel, cold-rolled, 302
 hot-rolled, 302
 Stepped-core, 305
 Stepped winding, 101
 Stiff characteristic, 251
 Stresses, short circuit, 421
 Structural elements of machines, 37
 Switching processes, 424
 Sudden short circuit, 225
 Sudden short-circuit of transformers, 418
 Symmetrical components, 387
 Superposition method, 375
 Symmetry conditions, 77
- T**
- Tank cover, 312
 Tank, smooth, 311
 Tertiary, 359
 Theory of point contact, 166
 Third harmonic, 355
 Three-circuit transformer, efficiency, 450
 operation, 443
 parameters, 447
 vector diagram, 448
 Top section side, 91
 Torque
 braking, 209
 dynamic, 241
 electromagnetic, 209, 241
 gyration, 246
 motor dynamic, 242
 no-load braking, 211
 prime mover, 211
 static, 241
 static active, 241
 static potential, 241
 static reactive, 241
 starting, 243
 useful braking, 242
 Traction generator, 276
 Traction motor, 276
 Transfer of load, 234
 Transformation ratio, 318
 Transformer
 bank, 354
 banked 341
 calculated output, 384
 cascade excitation, 465
 compressed gas, 470
 connection groups, 348
 core, 306
 core-type, 302
 current, 467
 dry, 300, 437, 466, 470
 efficiency, 383
 elementary, 327
 equations, 316
 equivalent circuit, 323
 explosion-proof, 469
 external characteristics, 383
 furnace, 437
 lightning-proof, 436
 no-load test, 338
 oil, 300
 on load, 375
 operation analysis, 320
 parallel-connected, 404

- power, 300
 - rectifier, 454
 - shell-type, 302
 - step-down, 300
 - step-up, 300
 - surge-proof, 425
 - test, 463
 - three-circuit, 442
 - three-leg, 339
 - three-winding, 437
 - voltage, 468
 - two-winding, 299
 - under short-circuit conditions, 360
 - utility factor, 459
 - welding, 466
 - breaking stress, 423
 - wound-core, 437
 - Transient phenomenon, 413
 - process, 430
 - state, 236
 - voltage distribution, 430
 - Transients, 269, 413
 - Transition characteristic, 138
 - Transition under load, 451
 - Transposition of conductors, 308
 - Triangle, characteristic, 215
 - Tubes, unit, 48
 - Turbogenerator, 284
 - Turn operator, 388
 - Typical power, 454
 - Types of braking, 260
- U**
- Unbalanced loading of transformer, 396, 400
 - Unbalanced short-circuit conditions, 391
 - Unfavourable short-circuit conditions, 418
 - Useful output, 207
- V**
- Vector diagrams, simplified, 378
 - Vector representation, 93
 - Ventilator, 39
 - Ventilation
 - axial system, 39
 - ducts, 39
 - radial system, 39
 - Voltage between adjacent commutator bars, 161
 - Voltage drop
 - active, 364
 - in transformer, 320
 - reactive, 364
 - Voltage gradient, 430
 - Voltage
 - impedance, 361
 - operating, 42
 - rated, 42
 - Regulation under load, 450
 - variation, 381
 - Curve shape effect, 336
- W**
- Ward-Leonard system, 273
 - Wedges, 87
 - Width of commutation zone, 173
 - Winding
 - armature, 39
 - artificially-closed, 104
 - bar, 87
 - characteristics, 129
 - complex lap, 108
 - coil, 87
 - compensation, 177
 - concentric, 307
 - connections, 349
 - cylindrical, 308
 - continuous-type, 309
 - delta-connected, 341, 345
 - double closed, 106
 - double-layer, 84
 - double-reentrant, 105
 - equisectional, 86
 - frog armature, 123
 - formulas, 65
 - helical, 308
 - left-hand, 85
 - lap progressive, 85
 - lap retrogressive, 85
 - multiplex, 109
 - multiplex double-closed, 107
 - multiplex lap, 106
 - multiplex wave, 111
 - pitch, resultant, 106
 - sandwich, 307
 - section, 85
 - single closed, 106, 65
 - single reentrant, 105
 - simple lap 65, 67, 74
 - star connected, 341
 - stepped, 86
 - symmetrical, 77

tertiary, 359
transformer, 307
triple closed, 106
wave retrogressive, 86
wave progressive, 86
zigzag connected, 341

Y

Yoke, 46
cross-section, 306
T-shaped, 306

Z

Zero system of currents, 388
Zigzag-connection, 347
zone, rupturing, 186

BIBLIOGRAPHY

1. Д. В. Ефремов и М. И. Радовский а) История динамомшины. 1934. б) История электродвигателя. 1936. Изд. Ак. Наук СССР, Ленинград.
2. Классики русской энергетики. М. О. Доливо-Добровольский. Избранные труды (о трехфазном токе). Госэнергоиздат, М.—Л., 1948.
3. М. А. Шателен. Русские электротехники. Госэнергоиздат, М.—Л., 1955.
4. К. А. Круг. Основы электротехники. Б-ое издание. т. I и 2. Госэнергоиздат, М.—Л., 1946.
5. Л. Р. Нейман и П. Л. Калантаров. Теоретические основы электротехники. ч. I, II, III. Госэнергоиздат, М.—Л., 1954.
6. P. Janet. Leçon d'électrotechnique générale. T. I.— Généralités.— Courant continu. 1920. T. II.— Alternateurs — transformateurs. 1921. Gauthier-Villars, Paris.
7. A. Mauduit. Machines Electriques. Theorie, Essais et Construction Dunod. Paris, 1922.
8. R. Richter. Electricische Maschinen. а) I Band. Allgemeine Berechnungselemente. Die Gleichstrommaschinen. 1924. б) III Band. Die Transformatoren. 1932. J. Springer, Berlin.
9. L. Graetz. Starkstromtechnik. J. Ambrosius Barth, Leipzig, 1928.
10. М. А. Шателен, В. Ф. Миткевич, В. А. Талвинский и др. СЭТ. Справочная книга для электротехников. т. V. Электрические машины (общая часть).
11. A. Langsdorf. а) Principles of Direct-Current Machinery. 1940. б) Theory of Alternating Current Machinery. 1937. McGraw-Hill, New York.
12. E. Rziha, U. J. Zeidner. Starkstromtechnik. Band I. Siebende Auflage. 1930. Teil I. Achte Auflage. 1951. W. Ernst, Berlin.
13. M. Liwischitz-Garrik, C. Whipple. Electric Machinery. Vol. I. Fundamentals and D-C Machines. Vol. II. A-C Machines. D. Van Nostrand, New York, 1946.
14. Д. А. Завалишин и др. Сборник задач и примеров по электрическим машинам. Госэнергоиздат, М.—Л., 1940.
15. М. П. Костенко. Электрические машины. а) часть общая. 1944. б) часть специальная. 1949. Госэнергоиздат, М.—Л.
16. Л. М. Пиотровский. Электрические машины. Госэнергоиздат, М.—Л., 1949.

17. **А. Е. Алексеев.** а) Тяговые электродвигатели. Госэнергоиздат, М.—Л., 1951. б) Конструкция электрических машин. Госэнергоиздат, изд. 2-ое, М.—Л., 1958.
18. **П. С. Сергеев.** Электрические машины. Госэнергоиздат, М.—Л., 1955.
19. **Г. Н. Петров.** Электрические машины. а) часть 1-ая. Трансформаторы, 1956. б) часть 2-ая. Коллекторные машины постоянного и переменного тока. 1947. Госэнергоиздат, М.—Л.
20. **I. Gheorgiu.** Masini Electrice. Vol. I. Masina de current continuu. Transformatorul. București, 1957.
21. **C. Hawkins.** The Dynamo. Its Theory and Manufacture. Vol. I. 1922. Vol. II. (Continuous Current Dynamos). 1923. Pitman, London.
22. **E. Arnold-la Cour.** Die Gleichstrommaschine. а) Erster Band. Theorie und Untersuchung. Dritte Auflage. 1921. б) Zweiter Band. Konstruktion, Berechnung und Arbeitsweise. Dritte Auflage, 1927. J. Springer, Berlin.
23. **К. И. Шенфер.** Динамо-машины и двигатели постоянного тока. ГОНТИ, М.—Л., изд. 5-ое, 1937.
24. **Д. А. Завалишин.** Машины постоянного тока. ГОНТИ, М.—Л., 1934.
25. **В. А. Толвинский.** Электрические машины постоянного тока. Госэнергоиздат, М.—Л., изд. 2-ое, 1956.
26. **G. Guilbert.** Essais des Machines Electriques. J. Baillière, Paris, 1922.
27. **M. Vidmar.** Wirkungsweise elektrischer Maschinen. J. Springer, Berlin, 1928.
28. **Л. М. Пиотровский и Е. А. Паль.** Испытания электрических машин, часть I. Общая часть и испытание машин постоянного тока. Госэнергоиздат, М.—Л., 1949.
29. **W. Nörnberg.** Die Prüfung elektrischer Maschinen. J. Springer, Berlin, 1940.
30. **Г. К. Жерве.** Промышленные испытания электрических машин. Изд. 2-ое. Госэнергоиздат, М.—Л., 1959.
31. **M. Walker.** а) Specification and Design of Dynamo-Electric Machinery. 1920. б) The Diagnosing of Troubles in Electric Machines. 1921. Longmans Green, London.
32. **M. Pistoya.** Construction et usinage des Machines électriques. J. Bailiere, Paris, 1923.
33. **A. Linker.** Elektromaschinenbau. Berechnung elektrischer Maschinen in Theorie und Praxis. J. Springer, Berlin, 1925.
34. **M. Liwschitz.** Die Elektrischen Maschinen. Band I. Allgemeine Grundlagen. Band II. Berechnung und Bemessung. Teubner, Leipzig und Berlin, 1931.
35. **M. Liwschitz und H. Glückner.** Die Elektrischen Maschinen. Konstruktion und Isolierung. Teubner, Leipzig und Berlin, 1931.
36. **F. Punga.** Vorlesung über Elektromaschinenbau. Darmstadt, 1934.

37. П. С. Сергеев и др. Проектирование электрических машин. Госэнергоиздат, М.—Л., 1950.
38. И. М. Постников. Проектирование электрических машин. Гостехиздат Укр. ССР, изд. 2-е, 1961.
39. В. П. Андреев и Ю. А. Сабинин. Основы электропривода. Госэнергоиздат, М.—Л., 1956.
40. Th. Lehmann. a) Determination graphique des champs magnetiques laplaciens et tourbillonnaires, à lignes de flux planes. 1923, p. 347. b) Spectres ferromagnétiques. 1926, p. 43. *Revue Generale d'Electricité*.
41. R. Richter. Ankerwicklungen für Gleich-und Wechselstrommaschinen. J. Springer, Berlin, 1920.
42. А. Н. Левитус. Лягушечья обмотка электрических машин. *Электричество*, 1932, № 17—18, стр. 836.
43. В. И. Зимин и др. Обмотка электрических машин. Госэнергоиздат, М.—Л., 1954.
44. В. И. Калитвянский. Изоляция электрических машин. Госэнергоиздат, М.—Л., 1949.
45. A. Mauduit. Recherches expérimentales et théoriques sur la commutation dans les dynamos à courant continu. Dunot et Pinet, Paris, 1912.
46. B. Lamme. Theory of Commutation and Its Application to Commutating Pole Machines. Electrical Engineering Papers, p. 201, Westinghouse, Pittsburgh, 1919.
47. L. Dreufus. Die Stromwendung grosser Gleichstrommaschinen. J. Springer, Berlin, 1929.
48. С. В. Хмельницкий. Улучшение коммутации генераторов блуминга путем применения диверторов. *Электричество*, 1945, № 3, стр. 37.
49. В. Т. Касьянов. Регулировка дополнительных полюсов машин постоянного тока. *Электричество*, 1934, № 20, стр. 1; 1935, № 1, стр. 45.
50. А. И. Москвитин. а) Скорость распространения кругового огня по коллектору, *Электричество*, 1934, № 14, стр. 28. б) О способах борьбы с круговым огнем на коллекторе. *Электричество*, 1935, № 18, стр. 36.
51. О. Б. Брон и В. С. Александров. Круговой огонь на коллекторе машин постоянного тока. *Электричество*, 1935, № 3, стр. 3.
52. К. И. Шенфер и С. Б. Юдицкий. а) Коммутация в машинах постоянного тока при толчкообразной нагрузке. *Электричество*, 1935, № 11, стр. 5. б) С. Б. Юдицкий. Коммутация машин постоянного тока. Госэнергоиздат, М.—Л., 1941.
53. М. П. Костенко. а) Расчет влияния насыщения добавочного полюса на характер кривой подпитки. *Электричество* (З. ХЭМЗ), 1936, № 3, стр. 12. б) Основные вопросы коммутации машин постоянного тока. Труды Ленинградского Индустриального Института, 1937, № 2, стр. 3.
54. А. И. Голубев и О. Е. Гольдин. Защита сетей постоянного тока быстродействующими автоматическими выключателями. Госэнергиздат, М.—Л., 1931. *Электричество*, 1938, № 8, стр. 6.
55. М. Ф. Карасев. а) Экспериментальные исследования процесса коммутации электрических машин постоянного тока на специальной модели.

Электричество, 1948, № 7, стр. 37. 6) Коммутация коллекторных машин постоянного тока. Госэнергоиздат, М.—Л., 1955, 1961.

56. **О. Г. Вегнер.** а) О некоторых вопросах коммутации при помощи коллектора и щеток. Труды Ленинградского Индустриального института, 1938, № 7, стр. 25. б) Теория и практика коммутации машин постоянного тока. Госэнергоиздат, М.—Л., 1961.

57. **B. Ugrimoff.** Die unipolare Gleichstrommaschine. J. Springer, Berlin, 1910.

58. **B. Lamme.** Development of a Successful Direct-Current 2000 kW Unipolar Generator. Electrical Engineering Papers. p. 145. Westinghouse, Pittsburgh, 1919.

59. **E. Rosenberg.** Die Gleichstrom Querfeldmaschine. J. Springer, Berlin, 1928.

60. **Б. В. Костин.** Новый униполярный генератор. *Электричество*, 1939, № 2, стр. 33; № 10—11, стр. 108.

61. **S. Bergman.** A New System for D. C. Arc Welding. *AIEE Trans.*, 1931, стр. 678.

62. **Ю. П. Петрунькин.** Электрические генераторы и трансформаторы для дуговой сварки. ОНТИ, М.—Л., 1934.

63. **A. Fisher.** Design Characteristics of Amplidyne Generators. *General Electric Review*, 1940, No. 3, p. 107.

64. **T. Graybeal.** Steady-State Theory of the Amplidyne Generators. *AIEE Trans.*, 1942, p. 750.

65. **J. Bower.** Fundamentals of the Amplidyne Generators *AIEE Trans.*, 1945, p. 873.

66. **Я. С. Эпштейн.** Особенности проектирования амплидинов. *Электричество*, 1945, № 12, стр. 40.

67. **Н. А. Моносзон.** Некоторые особенности теории и проектирования электромашинного усилителя. *Электричество*, 1948, № 9, стр. 13.

68. **E. Harder and C. Valentine.** Static Voltage Regulator for Rototrol Exciter. *AIEE Trans.*, 1945, p. 601.

69. **J. Pestarini.** Les métadynes entre elles et leur dérivés. *Revue Générale d'Electricité*, 1930, T. 27, p. 355, 395; T. 28, p. 813, 854, 900.

70. **К. И. Шенфер.** а) Безреостатное управление тяговыми электродвигателями постоянного тока. *Электричество*, 1940, № 3, стр. 55. б) Новая схема соединения метадина с тяговыми двигателями последовательного возбуждения. *Электричество*, 1941, № 3, стр. 35.

71. **A. Puchstein and T. Loyd.** Alternating-Current Machines. J. Wiley, New York, 1936.

72. **R. Lawrence.** Principles of Alternating Current Machinery. McGraw-Hill, New York, 1940.

73. **Г. Н. Петров и др.** а) Электрические машины, ч. I, 1940. б) Трансформаторы, 1934. Госэнергоиздат, М.—Л.

74. **A. Pen-Tung Sah.** Fundamentals of Alternating-Current Machines. McGraw-Hill, New York, 1946.

75. J. Tarboux. Alternating-Current Machinery. International Text-book, Scranton, 1947.
76. M. Say. The Performance and Design of Alternating Current Machines. Transformers, Three-Phase Induction Motors and Synchronous Machines. I. Pitman, London, Third Edition, 1958-61.
77. Ю. С. Чечет. Расчет электрических машин и трансформаторов. ч. III, Трансформаторы. МАКИЗ, 1927.
78. Ф. И. Холуянов. Трансформаторы однофазного и трехфазного тока. ОНТИ. Энергоиздат, Л.—М., 1934.
79. Л. М. Пиотровский. Трансформаторы. Изд. Кубуч, Ленинград, 1935.
80. M. Vidmar. Die Transformatoren. J. Springer, Berlin, 1925.
81. E. Arnold und S. la-Cour. Die Transformatoren. Ihre Theorie, Konstruktion, Berechnung und Arbeitsweise. Zweite Auflage. J. Springer, Berlin, 1910-23.
82. P. Bunet. Les transformateurs. J. Baillièrre, Paris, 1923.
83. A. Stigant and M. Lacey. The Transformer Book. J. Phillips, London, 1925.
84. M. Vidmar. Der Transformator im Betrieb. J. Springer, Berlin, 1925.
85. Л. М. Пиотровский, С. Б. Васютинский, Е. Д. Несговорова. Испытание электрических машин. Часть II. Трансформаторы и асинхронные машины. Госэнергоиздат, М.—Л., 1960.
86. А. В. Трамбицкий. Расчет трансформаторов. Изд. ГОНТИ, Л.—М., 1938.
87. Л. И. Шницер. Трансформаторы. Основы теории и нагрузочная способность. Госэнергоиздат, М.—Л., 1950.
88. А. В. Сапожников. Конструирование трансформаторов. Госэнергоиздат, М.—Л., 1952.
89. Г. В. Алексеенко. Трансформаторы, параллельная работа трансформаторов. Госэнергоиздат, Л.—М., 1960.
90. Е. Марквардт. а) Об электромагнитном рассеянии, *Электричество*, 1936, № 9, стр. 44. б) Индуктивное рассеяние обмоток трансформатора, *Электричество*, 1936, № 23, стр. 26.
91. W. Moody and A. Boyajian. Mechanical Forces in Transformers. *General Electric Review*, 1927, p. 420.
92. М. С. Либкинд. Механические силы в обмотках трансформаторов. *Электричество*, 1945, № 9, стр. 43; № 12, стр. 47.
93. K. Palueff. Effect of Transient Voltage on Transformer Design. *AIEE Trans.*, 1929, p. 681; 1930, p. 1179; 1931, p. 803; 1932, p. 601.
94. W. Morris and J. Hagenguth. The Non-Resonating Transformer. *General Electric Review*, 1930, p. 558.
95. L. Bewley. Travelling Waves on Transmission Systems. General Electric Co., Pittsfield, 1933.
96. М. В. Липковский. Система нерезонирующих трансформаторов. *Электричество*, 1941, стр. 25.

97. В. А. Карасев. Теория электромагнитных процессов в обмотках. Госэнергоиздат, М.—Л., 1946.

98. A. Boyajian. Theory of Three Circuit Transformers. *AIEE Trans.*, 1924, стр. 508.

99. P. Banet. Calcul et détermination des chutes des tensions des transformateurs à trois enroulements. *Bulletin de la Société Française des Electriciens*. 1931, No. 8, p. 770.

100. А. М. Утевский. Токораспределение в обмотках трансформаторов для ртутных выпрямителей при аварийных режимах. *Электричество*, 1937, № 20, стр. 16.

101. W. Schilling. Die Gleichrichterschaltungen. Ihre Berechnung und Arbeitsweise. Oldenbourg, 1938.

102. М. П. Костенко, Л. Р. Нейман и Г. Н. Блавдзевич. Электрические процессы в системах с мощными выпрямительными установками. Изд. Ак. наук СССР, 1946.

103. M. P. Kostenko et L. R. Neuman. Les Processus électromagnétiques dans les redresseurs puissants et leur relations avec les paramètres du réseau d'alimentations. Conference Internationale des Grands Réseaux Electriques à Haute Tensions (C.I.G.R.E.), Paris, Session, 1948. *Электричество*, 1947, № 1, стр. 7

104. И. Л. Каганов. Электронные и ионные преобразователи. Госэнергоиздат, М.—Л., 1956.

TO THE READER

The Foreign Languages Publishing House would be glad to have your opinion of this book and any suggestions you may have for future publications.

Please send them to 21, Zubovsky Boulevard, Moscow, U.S.S.R.

Printed in the Union of Soviet Socialist Republics

